WILLIAM HUSTRULID

BLASTING PRINCIPLES FOR OPEN PIT MINING

1 GENERAL DESIGN CONCEPTS

BLASTING PRINCIPLES FOR OPEN PIT MINING

BLASTING PRINCIPLES FOR OPEN PIT MINING
VOLUME 1 – GENERAL DESIGN CONCEPTS

Hidden page

Hidden page

BLASTING PRINCIPLES FOR OPEN PIT MINING

Volume 1 – General design concepts

WILLIAM HUSTRULID

Professor Emeritus
Colorado School of Mines, Golden, Colorado, USA

A.A.BALKEMA/ROTTERDAM/BROOKFIELD/1999

Published by
A.A. Balkema, P.O. Box 1675, 3000 BR Rotterdam, Netherlands
Fax: +31.10.413.5947; E-mail: balkema@balkema.nl; Internet site: http://www.balkema.nl

A.A. Balkema Publishers, Old Post Road, Brookfield, VT 05036-9704, USA
Fax: 802.276.3837; E-mail: info@ashgate.com

Complete set of two volumes: ISBN 90 5410 458 9
Volume 1: ISBN 90 5410 459 7
Volume 2: ISBN 90 5410 460 0

Printed in the Netherlands

Contents

Dedication

To the members of my family who have waited patiently in the background while I spent much of our quality time together on this book.

Preface

Proper rock fragmentation is the key first element of the ore winning process. It is a two step activity in the sense that the holes for distributing the explosives within the rock mass must first be drilled (Step 1) as specified by the fragmentation plan. This is then followed by the controlled rubblization (Step 2) of the interlying rock. The resulting product is then picked up and hauled away (Steps 3 and 4). Hence, when considering the structure of a book on Unit Operations in Open Pit Mining it might be considered logical to begin with an integrated treatment of drilling and blasting under the heading of fragmentation. On the other hand most mining books are organized by individual unit operation and the presentation is in the order in which they occur in the mine, i.e.

- Drilling,
- Blasting,
- Loading,
- Hauling.

This is also a very logical sequence from the miners point of view. However, in reviewing the composition of these four unit operations, one rapidly comes to the conclusion that they are a mixture of three apples and an orange. The physical operations of drilling, loading and hauling are very heavily machine-oriented (the apples) whereas blasting is engineering/design/experience oriented (the orange). Today a number of mining and quarrying operations in recognizing this trueism 'farm-out' their blast engineering/design/implementation to a blasting contractor with the required specialized expertise. The in-house expertise is focussed on the three remaining unit operations of drilling, loading and hauling which actually *service* the fourth, blasting. This relationship is shown diagrammatically in Figure 1.

Important in the past and important today, carefully engineered blasting will be an even more important aspect of successful open pit mining in the future as pits become deeper and steeper and quality separation to avoid dilution and ore losses during blasting becomes paramount. Therefore, both mining engineers and mining companies must have a firm grasp of blasting fundamentals and practice whether or not the actual design and implementation is done in-house or by contractors.

In response to this, the originally planned book entitled *Unit operations in open pit mining* has been divided into two books. This book *Blasting principles for open pit mining* deals with both the engineering and the scientific aspects of blasting with special application to open pit mining. In a book under preparation *Unit operations in open pit*

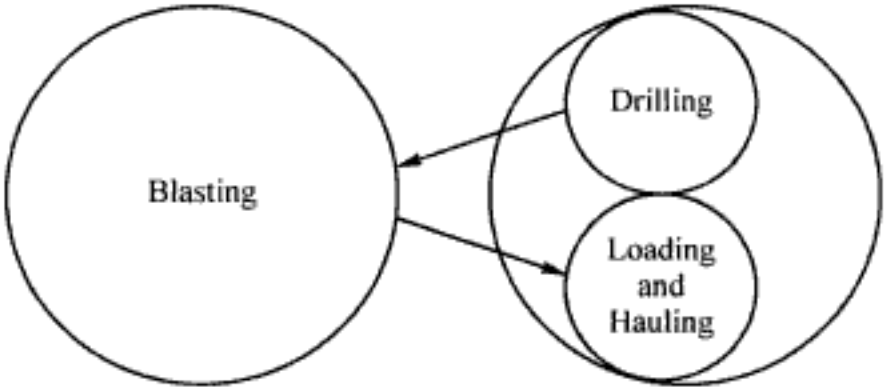

Figure 1.

mining the principles of the machine-based service activities of drilling, loading, and hauling will be presented.

Blasting principles has been divided into two volumes. Volume 1 entitled 'General design concepts' is intended to introduce the reader to the basic engineering concepts and building blocks which make up a blast design. It consists of ten chapters:

- Chapter 1. An historical perspective
- Chapter 2. The fragmentation system concept
- Chapter 3. Explosives as a source of fragmentation energy
- Chapter 4. Preliminary blast design guidelines
- Chapter 5. Drilling patterns and hole sequencing
- Chapter 6. Sinking cut design
- Chapter 7. Bulk blasting agents
- Chapter 8. Initiation systems
- Chapter 9. Environmental effects
- Chapter 10. Perimeter blasting

Volume 2 entitled 'Theoretical foundations' is intended to provide the reader additional depth and breadth for better understanding some of the fundamental concepts involved in rock blasting. It consists of eleven chapters:

- Chapter 11. Fundamentals of explosives
- Chapter 12. Blasting in the absence of a free face
- Chapter 13. The effect of the shock wave
- Chapter 14. Attenuation
- Chapter 15. Spherical charges
- Chapter 16. Cylindrical charges
- Chapter 17. Decoupling
- Chapter 18. Heave
- Chapter 19. The basics of cratering
- Chapter 20. Hydrodynamic-based models
- Chapter 21. Some Russian contributions to rock blasting

In these chapters the author has tried to bridge the gap between theory and practice and to present the underlying concepts in an understandable way. It is hoped that the contained material will provide a basis for engineers to improve (a) their blasting operations as well as (b) their ability to understand the content and potential application of papers appearing in the technical literature. Historically, in spite of the importance of the topic, very few books dealing with the *design* aspects of rock blasting have been written with the mining engineer in mind. The book *The Modern Technique of Rock Blasting* by Langefors and Kihlström first published in 1963 and two more recent related books *Swedish Blasting Technique* by R. Gustafsson and *Applied Explosives Technology* by Stig Olofsson are exceptions.

The series of Blaster's Handbooks published for many years by Dupont and CIL are aimed primarily at blasters with quarrying and civil construction applications. In this regard, the International Society of Explosive Engineers (1998) has recently released an updated and expanded version of original Duport Blasters' Handbook. Although these Handbooks contain much valuable information they are not intended to provide the engineering background.

Recently a number of books have begun to appear aimed at the engineering practitioner. They vary quite widely in both the depth and breadth of their coverage of the subject. The author refers the reader to the extensive 'Blaster's Library' collection of books available through the International Society of Explosives Engineers. The relatively recent book by Atlas Powder Company entitled *Explosives and Rock Blasting* presents in a very readable way a discussion of a number of important topics. The book *Rock Blasting and Explosives Engineering* by Persson, Holmberg and Lee has become something of a standard in the field. Finally the book *Principles of Rock Fragmentation* by George B. Clark is also to be recommended.

In addition the interested reader is directed to the bi-monthly magazine Explosives Engineering published by the International Society for Explosives Engineers as well as the Proceedings of their yearly conference. The International Journal for Blasting and Fragmentation FRAGBLAST published by Balkema has recently begun publication. It comes out on a quarterly basis and is intended to publish papers which bridge the gap between academia and practitioners in the field. FRAGBLAST symposia have also held on a regular basis since 1982 and the proceedings provide a wealth of information regarding blasting.

The mining world is, for better or worse, still bilingual with both English (Imperial) and SI units being used. In this book no attempt has been made to follow one or the other. It is assumed that the reader can make the translation as necessary. The symbols used are consistent within any given chapter but not necessarily between chapters. The author apologizes for any confusion that this may cause but it greatly simplifies the presentation for both the reader and the author.

Although care has been taken to avoid errors both in understanding and presentation, they unfortunately will be present in a work of this magnitude. The author will be pleased if the reader will bring them to his attention so that corrections to future editions may be made.

This book is primarily intended as a text for mining engineering students. However the material contained and the presentation form should make it of value to practicing engineers as well.

REFERENCES

Atlas Powder Company 1987. *Explosives and Rock Blasting.*
Clark, G.B. 1987. *Principles of Rock Fragmentation.* John Wiley & Sons, New York.
Gustafsson, R. 1973. *Swedish Blasting Technique.* SPI, Gothenburg, Sweden.
International Society of Explosive Engineers 1998. Blasters' Handbook, 17th edition. ISEE, Cleveland, Ohio.
Langefors, U. & B. Kihlström 1963. *The Modern Technique of Rock Blasting.* John Wiley & Sons, New York.
Olofsson, S.O. 1989. *Applied Explosives Technology.* Applex, P.O. Box 71, Ärla, Sweden.
Persson, P-A., R. Holmberg & J. Lee 1993. *Rock Blasting and Explosives Engineering.* CRC Publishing Company.

Acknowledgements

This book has, I guess, been in progress for nearly 40 years. It began when, as an undergraduate at the University of Minnesota, I took my first class in surface mining from Professor E.P. Pfleider. He was a very fine teacher and an enthusiastic booster of the mining industry. Through him and Professor Donald Yardley I became hooked on mining. Charles Fairhurst and Tony Starfield together with an energetic band of fellow graduate students provided my formal introduction to drilling and blasting principles. There was a steady stream of the world's best experts in rock mechanics and related topics who visited the department. I had the chance to work with Thomas Atchison, Dave Fogelson and others from the Twin Cities Research Center, USBM during my graduate studies. My first academic position after receiving my PhD in 1968 was in the Mining Department of the Colorado School of Mines. I remember very well, John Reed, the department head, impressing on me the importance of trying to be a 'complete' mining engineer. That has not been an easy task, John, but I have tried and it has been an interesting voyage. The Denver Research Center of the USBM was close to the Mines campus and I had the privilege of working with Leonard Obert, Wilbur Duvall and Harry Nicholls, as well as others you will meet later in the book. As the years have passed I have had the opportunity to come in contact with, and sometimes work with, a number of those who I consider have made major contributions to the field of blasting. To name a few, this group has included Ulf Langefors, George Clark, Richard Ash, Claude Cunningham, Mick Lownds, Frank Chiappetta, Gyn Harries, Keith Mercer, Bob Hopler, Tim Hagan, R.F. Favreau and Dane Blair. Over the years I have had the opportunity to work closely with the Swedish Detonic Research Foundation. Roger Holmberg, Per-Anders Persson, Nils Lundberg and, most recently, Finn Ouchterlony and Shulin Nie have been valuable speaking partners. Dennis Shannon of Cambrian College has, through my participation in his short courses, inspired me to try and package the blasting materials in an industry-understandable form. A person with more enthusiasm for mining is hard to find. The Swedish mining company, LKAB, has been my work place during the last stages of completing this book. The long, cold and dark winters and the cool and sometimes rainy summers coupled with the long vacation periods have presented me with an excellent opportunity of pursuing this hobby of mine. At LKAB my speaking partners have been Ingemar Marklund, Lars Larsson and Carlos Quinteiro. Bernt Larsson and Anders Nordqvist of LKABs daughter company Kimit AB have provided valuable insights and advice. To all of you, I extend my heart felt thanks.

In preparing this book, I have had the opportunity to make some new friends. Iosif Neyman has been a very valuable speaking partner in the development of ideas contained in Chapter 20 on Hydrodynamic Theory. Dale Preece from Sandia National Laboratories has graciously reviewed and provided feedback on the material contained in Chapter 18 regarding the use of his Distinct Motion Code for heave prediction. Ruilin Yang and Stephen Chung, ICI Explosives Canada have provided input on Chapters 18 and 6, respectively. Jim Savely, Inspiration Copper, provided data on their approach to perimeter blasting. John Watson of The Ensign-Bickford Company provided input on shock tube-based electronic blasting caps.

Plenum Publishing Company has very generously permitted the publication of material from articles originally published in Soviet Mining Science. Atlas Powder Company has allowed the publication of some figures from their book Explosives and Rock Blasting. The University of Minnesota Press has kindly allowed publication of the photographs from early Minnesota mining. The Society of Explosive Engineers, the Society of Mining Engineers, The Canadian Institute of Mining and Metallurgy, the Australian Institute of Mining and Metallurgy, and Blasting Analysis International, Inc have all generously allowed me to include materials originally published by them.

Thanks also go to Marianne Snedeker, formerly publications manager of the SME, Denver, Colorado who, some 20 years ago, introduced me to the world of writing mining textbooks.

The picture on the cover is of Boliden Mineral AB's Aitik Mine, Gällivare, Sweden. It was taken by Kurt Eriksson, Profoto AB, Gällivare, Sweden. My thanks are extended to Mr. Eriksson for permission to use his photo. Thanks are also extended to Agne Ahlenius, Mine Superintendent, and to Bo Ringqvist, Area Manager, for the numerous chances to visit and study this world-class operation.

Last, but not least, I want to acknowledge the students who I have had the privilege, pleasure, and challenge of working with over the years. They have been the driving force for me to try and put this material into a readable and hopefully understandable form.

Important Notice – Please Read

This book has been written for use as a textbook by students studying surface rock excavation, in general, and mining engineering, in particular. The focus has been on presenting the principles involved in explosive rock excavation in as logical and easily understood way as possible. Inspite of great efforts made to avoid the introduction of mistakes both in understanding and presentation, this may have inadvertently/unintentionally occurred. The author would be pleased if you, the reader, would bring such mistakes to his attention so that they may be corrected in subsequent editions.

Neither the author nor the publisher shall, in any event, be liable for any damages or expenses, including consequential damages and expenses, resulting from the use of the information, methods, or products described in this textbook. Judgements made regarding the suitability of the techniques, procedures, methods, equations, etc for any particular application are the responsibility of the user, and the user alone. Recognizing that there is still a great deal of 'art' in successful blasting, field evaluation and testing remain an important part of technique, explosive and design selection for a given excavation in a given rock formation.

CHAPTER 1

An historical perspective

1.1 INTRODUCTION

Today's shovel-based, large-scale, open pit mining has its origin, for all practical purposes, just about 100 years ago on the Mesabi Range in Northern Minnesota. As the 21st Century rapidly approaches and we look forward to the developments it will hold for open pit technology, and prior to discussing the 'modern' techniques in use today, it is perhaps well to pause and reflect on the techniques considered 'modern' in earlier times. Specifically the discussion will focus on the unit operations of drilling, blasting, loading and hauling as practiced about 1910 on the Mesabi Range.

The word 'Mesabi', according to Winchell (1920), comes from the Ojibway Indian language and is the name of a fabulous giant who made this district his dwelling place. The various boulders which are so numerous in this area were supposed to have been used by him as ammunition in killing game (Winchell, 1920 and Skillings', 1995).

The first mining claim in the State of Minnesota was staked at Prairie River Falls on the western end of the Mesabi Range by Henry H. Eames in 1866. Although the hard hematite as exposed by the Prairie River cutting through the Range was of good quality, it occurred in rather thin layers (Winchell, 1920). As the years progressed, other discoveries of iron were made along what would become known as the 'Range' but large scale exploration only began in earnest in about 1890. The early prospectors faced great difficulties since the country was a dense, almost trackless forest alternating with vast swamps. Surface indications of ore were almost totally absent. As indicated by Van Barneveld (1913),

'While some of the earliest discoveries were made by chance, the tracing of the Mesabi formations and the discovery of valuable ore bodies is in the main the result of careful study and resolute enterprise, intelligently directed'.

The result of the exploration was the definition of not an orebody, nor a mining district, but a Range of enormous proportions. As can be seen in Figure 1.1, the Range has a length of 110 miles, a width varying from two to 10 miles, and covers an area of about 400 square miles (Gerry, 1912). The Ojibway name 'Fabulous Giant' fits the Range very well indeed.

The Biwabik Mine was the first on the Range (Van Barneveld, 1913) with the original discovery being quite accidental when an uprooted tree exposed the iron ore. This led to systematic prospecting in 1892. The orebody which covered approximately 80 acres lay

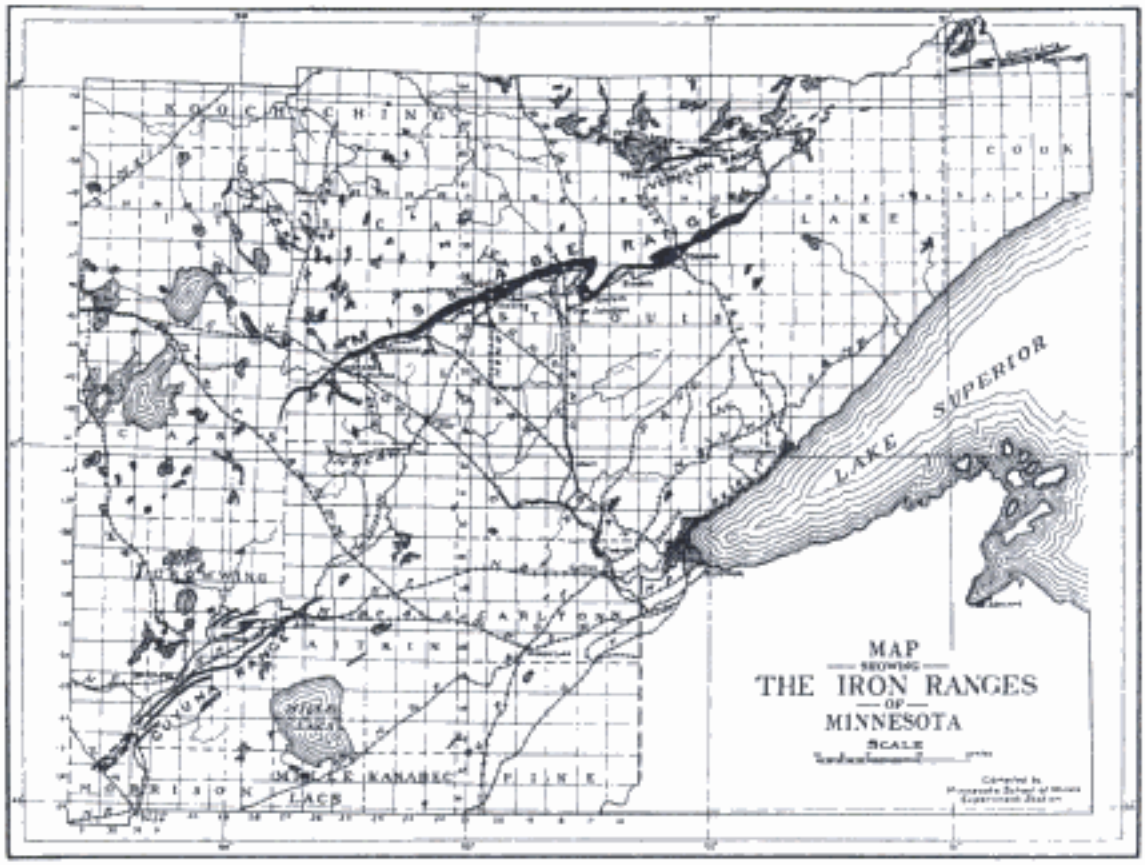

Figure 1.1. The location and extent of the Mesabi Range (Van Barneveld, 1913).

within 20 feet of the surface on the north end and dipped toward the south at 10 degrees. The general thickness of the overburden ranged from 20 to 50 feet with an extreme of 90 feet on the south side. In 1892 the first experiments in mechanical mining were conducted when a small steam driven stripping shovel was hauled in by wagon. In 1893, a contracting company brought in a 27-ton (shovel weight, not capacity) shovel, set it on rails, and stripped several hundred thousand cubic yards of overburden. A shipment of 151, 500 tons of ore was made that year. This heralded the beginning of large scale open pit mining on the Range.

From those rather modest beginnings, steam shovel based mining increased very rapidly. Over the 19 year period from 1892 to 1910, the mines on the Mesabi Range produced a total of 224,905,184 tons of iron ore using the mining techniques which will be now be described as well as some less 'modern'. For the next few minutes of reading settle back and relax. Imagine turning back the clock to 1910 and try to visualize through the text description the mining as it was being carried out at that time.

1.2 MINE DESIGN FACTORS

Nearly the whole region was covered with glacial drift varying in thickness from 25 to 150 feet, with the average thickness being of the order of 100 feet. The Mesabi hematite ore was, for the most part, weathered and soft and lay near the surface in near horizontal

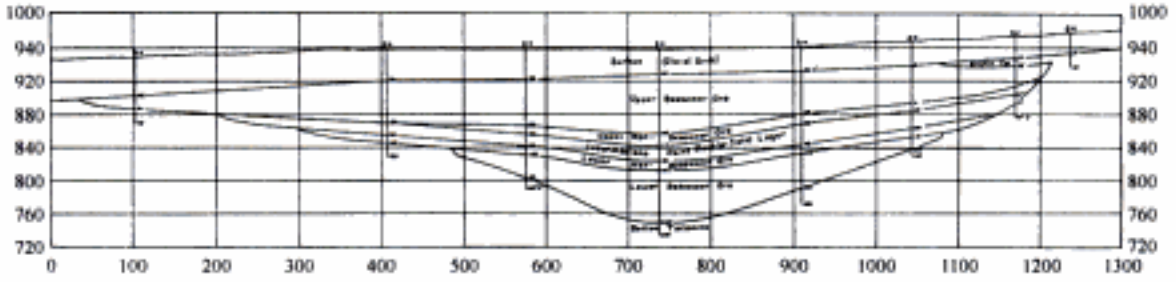

Figure 1.2. A typical cross-section through a Central Mesabi Range iron ore deposit (Van Barneveld, 1913).

or gently dipping beds (Figure 1.2). The overall ore thickness varied from about 50 feet to more than 300 feet. Generally the ore was shipped directly to the steel mills without intermediate processing. To be saleable, the minimum natural iron content (cutoff grade) had to be greater than about 50%. Since the glacial drift had to be first removed or 'stripped' away to expose the iron formations, the exploitation of these deposits depended upon the development of an inexpensive method for moving large volumes of material. Hence the application of steam shovel technology was key.

The planning of a mine on the Range involve a detailed study of the following factors (Van Barneveld, 1913):

1. The proportion of overburden to ore,
2. Location of the best approach for the tracks considering both the stripping and the subsequent ore transportation,
3. Stripping dump locations,
4. Track system,
5. Drainage system,
6. Mechanical equipment selection.

In preparation for mine evaluation and eventual design, exploratory holes were drilled, logged and the results plotted on the maps. The initial exploration holes were usually located about 300 ft apart until the ore was struck (Gerry, 1912). Then the pattern was tightened up to 100 ft squares or even closer. Churn drilling was used down to the ledge rock. The hole was then cased with pipe and a diamond bit used through the taconite and other rock. Drilling in the ore was then continued by churn drilling. The contractors charged \$3 to \$3.50 per foot for churn drilling and \$5 to \$6 per foot for diamond drilling. Using the drilling information the engineer would construct cross-sections and sometimes longitudinal sections to show clearly the positions of the various layers of ore and rock intrusions. On the plan maps, contours showing top of ore, bottom of ore, top of high-grade, etc would be drawn. A 'crest of ore' line would be drawn in plan at some distance outside of the ore holes. The distance would depend upon the open pit 'strength'. A 'toe of stripping' line would then be drawn. This was displaced outward 20ft from the 'crest of ore' line. The 'crest of stripping' line was then constructed allowing a 45° overall slope in the overburden. For estimating the available ore tonnage, an overall slope of 45° was used on the side of the pit intended to carry the track system and an overall slope of 60° on the other sides. Because of the flatter slope on the track side, the pit approach had to be carefully considered from both a stripping and mining viewpoint.

In 1910, for mine planning purposes, the final pit size/economical stripping limits were controlled by one or more of the following relationships:

1. A maximum overall stripping ratio of one yd^3 of overburden stripped for each ton of ore removed.

2. As applied at the final pit boundary, the stripping limit was 2 ft. depth of overburden (glacial till) to 1 ft of ore. Since hard slates and taconites cost from two to three times as much to strip as ordinary glacial till, it was customary when applying these figures to consider 1 ft of such material as equal to 3 ft of overburden.

3. The maximum stripping depth should be less than or equal to 150 ft under all circumstances.

The upper portion of the overburden generally consisted of a few feet of vegetable mold and soil and often contained many granite boulders. The remaining thickness was composed of sand, gravel and boulders. The boulders increased in both size and frequency near the bottom of the overburden. The lower overburden benches often consisted of boulders and compacted clay and other fine material. This had to be loosened before the shovel could make any progress. As the shovel encountered these large boulders in the loosened bank, they were 'chained out' and moved to one side. A regular trail of such boulders was often seen in the 'wake' of the shovel.

Overburden stripping was done using benches about 30 ft in height until approaching the ore when a 'clean up cut' 6 to 10 ft in height was taken. In the ore the benches were from 10 to 25 ft high depending upon the grade of the tracks and the particular part of the orebody being mined. With standard equipment, the width of the cut was 20 to 25 ft.

Whenever possible, stripping was done a season ahead of loading so that pit grades could be conserved and the pit left uncrowded. For smaller pits it was common for all of the stripping to be completed before beginning ore mining.

1.3 THE STEAM SHOVEL

This machine which forms the centerpiece of this technique will, before considering the other unit operations, now be described in some detail. The material used has been largely extracted from the references by Marsh (1920), McDaniel (1913) and Van Barneveld (1913).

The power shovel has been designed to imitate in a mechanical way the motions gone through by a man shovelling (Marsh, 1920). Reduced to the simplest form there are three basic movements. The first, that of advancing the dipper (bucket) into contact with the material to be removed, always occurs in a vertical plane and is called the crowd. In the second movement, the dipper is filled and elevated. This also occurs in a vertical plane and is called hoisting. The third motion in which the loaded dipper is traversed laterally in a horizontal plane is called the swing. Each of the crowd, hoist and swing movements may act independently of one another or two or even all three motions may occur simultaneously or with overlapping motion periods. The two auxiliary movements are propelling and dumping. For convenience in moving from place to place the machine is usually equipped with a self propelling mechanism which drives it backwards (moving-back) or forwards (moving-up). To empty the dipper, the bottom, which is hinged and latched, is tripped thereby permitting the material to fall through.

A standard steam shovel of this era is shown in Figure 1.3. As can be seen the operating machinery and power equipment are placed on the deck of the car-body which, in turn, is supported on two four-wheel standard gage trucks (bogies). The boiler is located at the rear end (Figure 1.4) directly over one set of trucks and the A-frame and boom are

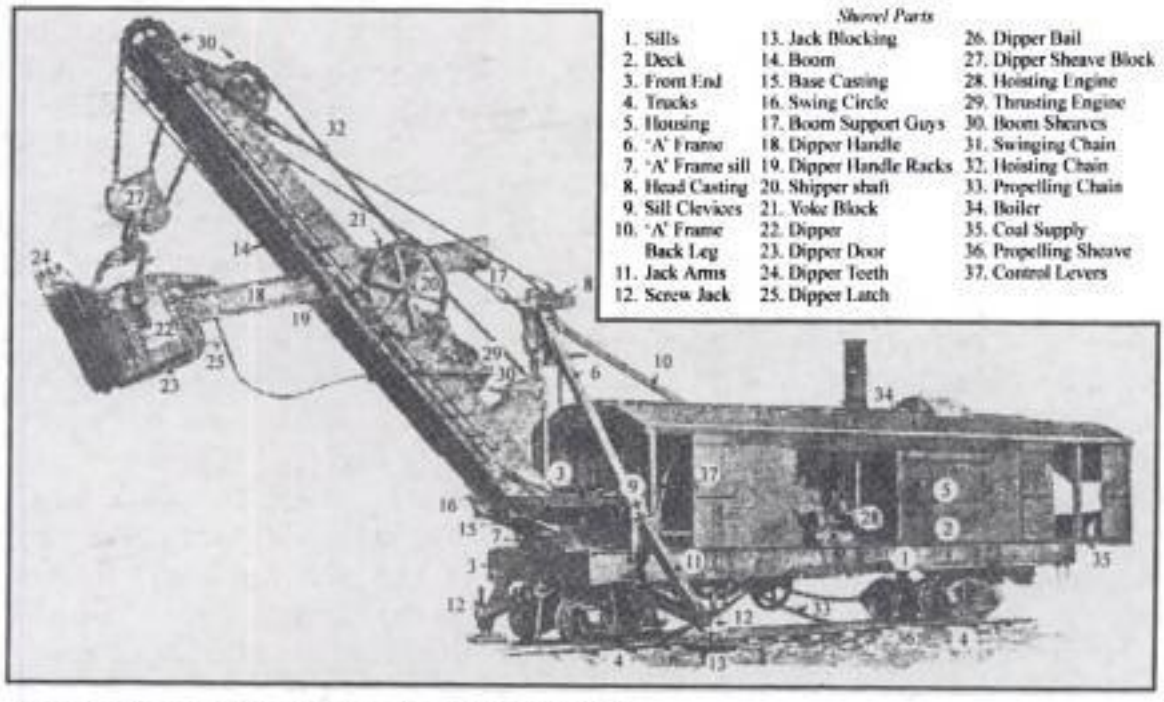

Figure 1.3. A standard type of steam shovel (Marsh, 1920).

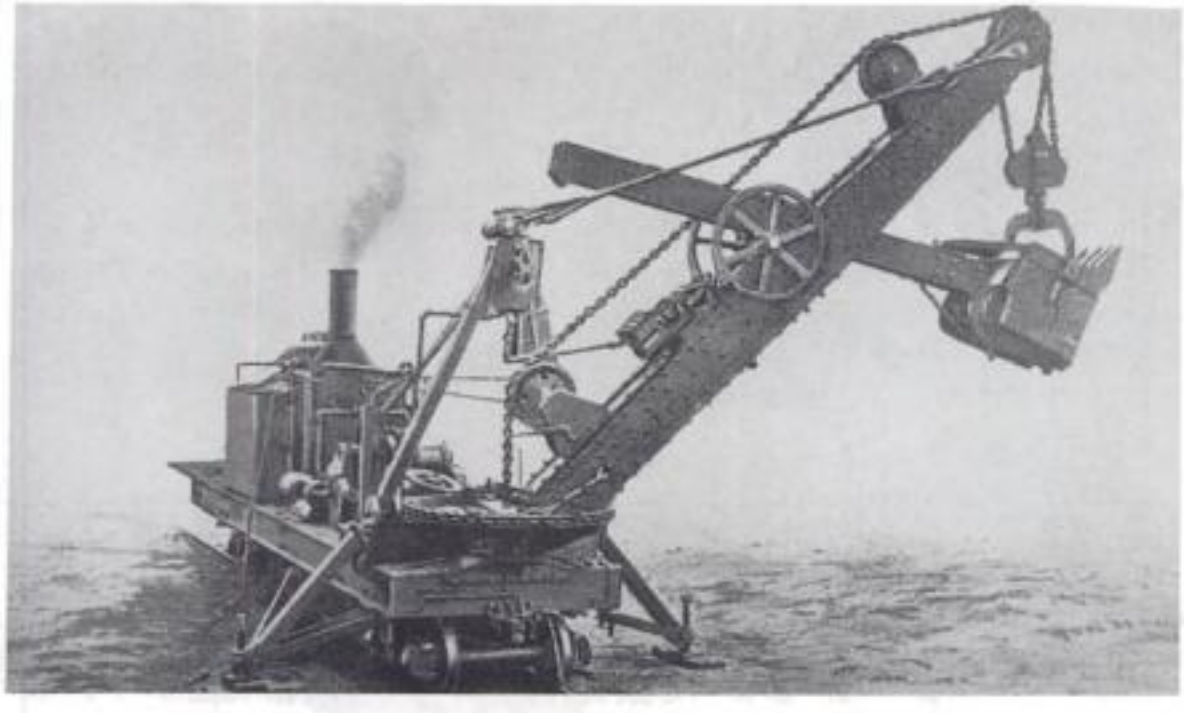

Figure 1.4. The Marion shovel with the housing removed (Van Barneveld, 1913).

at the front end over the other set. The hoisting/swing engines are placed in the middle. Since the car-body is subjected to severe and rapidly repeated strains, it must be constructed very ruggedly and rigidly. The frame (sill), made of steel I-beams and channels well braced both longitudinally and transversely, is topped by a 3-in thick plank floor (deck) of oak or yellow pine. The side to side swinging of the boom, dipper and dipper

handle tends to tip the front end of the car. To prevent this, jack-braces are placed on the sides of the car-body at the feet of the A-frame. The lower ends carry screw jacks which can be easily raised or lowered to get a bearing on the ground surface. The inside axles of both trucks are chain connected to sprocket wheels operated by the engine. This furnishes the propelling power for moving the shovel in either direction along the track.

The base casting which carries a large vertical journal is mounted at the front of the frame. This serves as the pivotal bearing for the rotating turntable, swing circle and the boom. The boom is a simple beam made in two sections which are spaced to allow the free passage of the dipper handle. Constructed of wood reinforced with steel plates or entirely of steel it reaches from 14 to 20 ft above the track/ground level, has a swing radius of 15 to 20 ft and an included swing angle of 180 to 240 degrees. The boom is normally inclined at an angle of 40 degrees above the horizontal. The lower end of the boom rests on the swing circle which pivots around the front end of the platform. The upper (outer) end of the boom is connected to the head casting mounted at the top of the A-frame by boom support guys consisting of steel rods or bars. The A-frame, made of heavy steel bars with timber reinforcement or entirely of structural steel posts, is given a slight inclination forward. It is considerably shorter than the top of the boom. The feet of the posts are supported on each side of the turntable. The back leg, a solid steel tension member connects the top of the A-frame to a point at the rear end of the car, directly over the rear trucks.

The dipper handle is generally made of a single timber of white oak. A toothed rack is fastened to its lower side and the upper edges are reinforced with steel angles or bent plates. The handle which is run in and out by pinions on the shipper shaft is held in contact with the pinions by means of the yoke block. A small, double-cylinder, horizontal type engine placed on the upper side of the boom is used to crowd the dipper into the bank. It operates a set of gears which revolve a shaft on which is set a steel pinion feeding into a steel-toothed rack on the bottom side of the dipper handle.

The scoop shaped dipper is attached to the lower end of the handle. Normally it is slightly wider at the bottom than the top to facilitate the dumping of the muck. The bottom is hinged and held closed by a spring lug-latch on the front side. The craneman empties the dipper by pulling on a light line attached to the latch through a lever.

The car-body supports a framework of timber or steel upon which a sheathing of wood or corrugated steel is applied to form the sides and roof of the car. This is necessary to protect the crew and machinery from climatic conditions and falling rock.

A horizontal, locomotive-type boiler is used. The required coal and water for making steam are stored at the rear of the platform. The hoist/swing engine is either of the vertical type with a single steam cylinder or of the horizontal type with double steam cylinders. The engine supplies power for both hoist and swing. In the design shown in Figure 1.4, there are three drums mounted on one shaft. This shaft is continuously rotated in one direction by a large steel gear driven by a pinion on the engine shaft. The three drums mounted on the shaft are actuated and controlled by friction clutches. The outer two, the swing drums, are reversed and operated by the same lever. A chain passes around the swing circle and is wound around the drums starting from the two ends. During the swing part of the cycle, as the chain on one drum unwinds it is taken up by the other.

The drum in the center is for hoisting. The hoisting chain passes from the hoisting drum to sheaves mounted just below the turntable. The chain then passes over a sheave wheel mounted near the foot of the boom and thence along the boom to the sheave mounted on the upper side of the boom near the end. It then passes around the sheave

wheel located directly at the end of the boom, continues around the sheave wheel contained in the sheave block, continues up over the sheave wheel at the end of the boom a second time and finally is fastened to the sheave block. Rotation of the hoisting drum lets out or draws in the chain and thus lowers or raises the shovel. This hoisting arrangement can be clearly seen in Figures 1.4 and 1.5.

The Atlantic shovel shown in Figures 1.6 and 1.7 was introduced to the Range in 1910. The chain previously used for hoisting has been replaced by a direct wire-rope hoist. The hoisting engine was bolted to the base of the boom and the wire rope passed over one large twin-grooved sheave directly to the dipper back. The steel hoisting rope was made up of two parallel cables whose loads were equalized by passing around a thimble on the dipper. The placing of the hoisting engine on the boom threw a considerable amount of additional weight on the turntable and the front end. It did however make place in the body which was used for an extra large, efficient boiler with its large water tank (Marsh, 1920).

A steam shovel is normally operated by a crew of seven men, the runner, the craneman, the fireman and four pitmen (McDaniel, 1913). The runner/engineer and the craneman directly control the movement of the machine. The runner stands at the set of levers and brakes placed in front of the machinery. He controls and directs the raising and lowering of the dipper, the swinging of the crane and propelling the machine. The craneman controls the operation of the dipper and the dipper handle, regulates the depth of the cut, releases the dipper from the bank, and finally empties it into the car. He is stationed on a small platform on the right side of the crane near the lower end. The fireman keeps the boiler supplied with fuel and water and looks after the oiling of the machinery. The duties of the pitmen who generally are under the direct supervision of the craneman consist of:

- Breaking down of high banks
- Assisting the shovel in loading material lodged too near the machine
- Leveling the surface in front of the machine
- Laying of new track

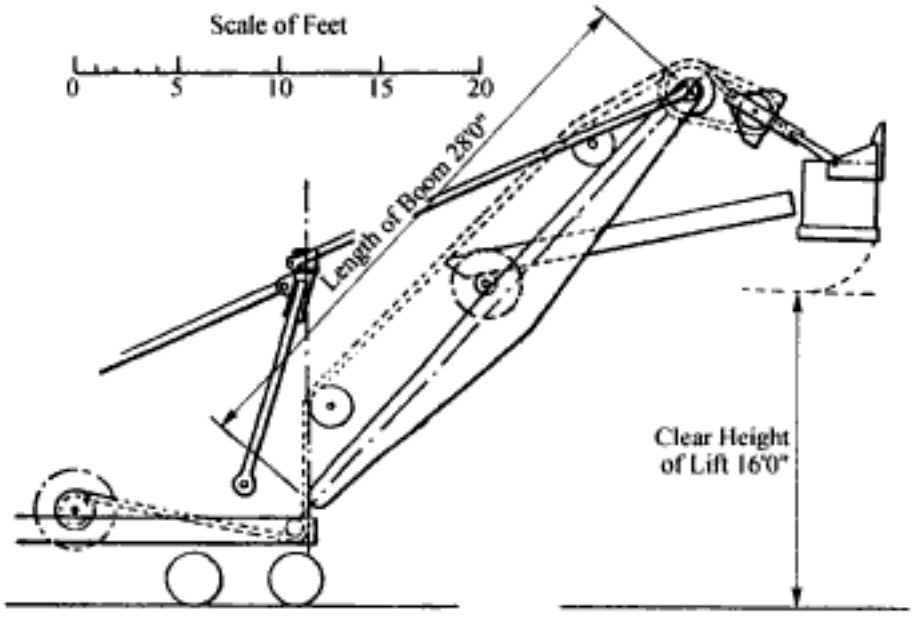

Figure 1.5. Drawing of the front end of a standard shovel showing the hoisting and digging geometry (Van Barneveld, 1913).

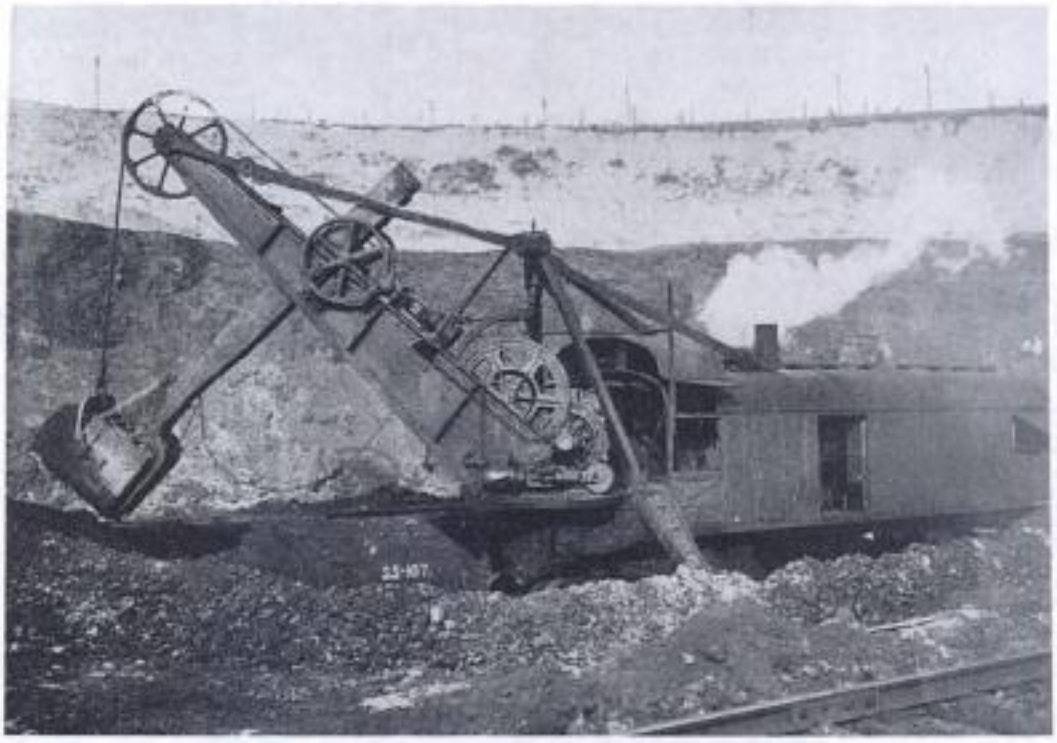

Figure 1.6. General view of the Atlantic Shovel (Van Barneveld, 1913).

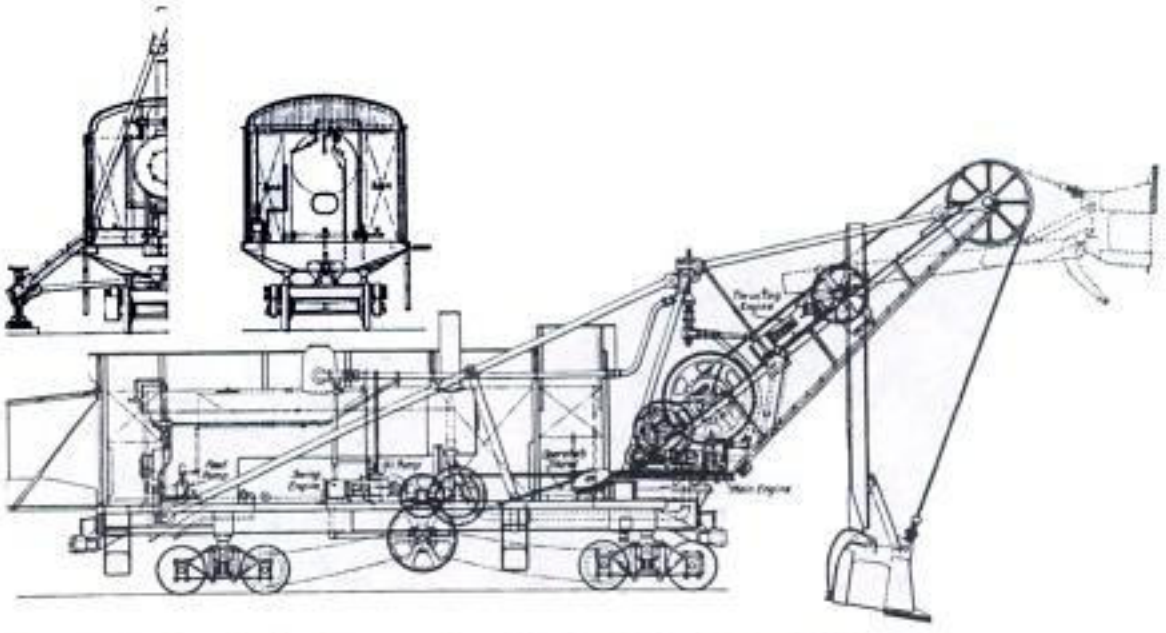

Figure 1.7. Drawing showing the cross-section of the Atlantic Shovel (Marsh, 1920, p. 29).

– Operating the jack braces and blocking
– General service

When the ground is hard, from two to six extra laborers (rock men) are required to break down overhanging material in high banks, drill holes and blast out material, assist in loading the shovel, etc.

McDaniel (1913) has given the following rather vivid and colorful description of the process involved in digging and loading rock using a steam shovel:

'The act of excavation commences with the dipper handle nearly vertical and the dipper resting on the ground, with the cutting edge directed slightly into the earth. The engineer then moves a lever throwing the hoisting drum into gear and starting the engine. The revolution of the hoisting drum winds up the hoisting line and pulls the dipper upward. At the same time the cranesman starts the engine which controls the thrusting of the dipper handle and moves the latter forward as the dipper rises. These two motions must be made smoothly and coordinately or the hoisting engine will be stopped and the whole machine tipped suddenly forward. When the shovel has reached the top of the cut or its highest practicable position, the engineer throws the hoisting drum out of gear and sets the friction clutch with a foot brake, thus bringing the dipper to a stop. Immediately the cranesman releases his brake and reverses the engine which draws back the dipper handle, thus releasing the dipper from the face of the excavation. When the shovel or dipper digs clear of the excavation, it is unnecessary to release it as described in this last motion. The engineer then starts the swinging drums or engine into operation and swings the boom to the side, until the dipper is over the place for dumping. With a foot brake he sets the friction clutch and stops the revolution of the swinging drum or drums. The cranesman then pulls the latch rope, which opens the latch and allows the door at the bottom of the dipper to drop and release the contents. The engineer then releases the friction clutch by the foot brakes and reverses the swinging engine, pulling the boom and dipper back to its position for the next cut. As the boom is swung around, the engineer gradually releases the friction clutch of the hoisting drum and allows the dipper to drop slowly toward the bottom of the cut. When near the point of commencing the new cut and as the dipper approaches the vertical, the cranesman releases the friction clutch on the engine with his foot brake, which regulates the dipper handle. Thus, as the last part of the drop is made by the dipper, it is also brought into the proper position and the length of the dipper arm set for the beginning of the new cut. As the dipper drops into place, the bottom door closes and latches by its own weight. The time required to make a cut and to dump the excavated material varies from one-half minute for loose earth or gravel to three minutes for hard and dense soils. The length of each complete operation depends to a great extent upon the skill and experience of the operators. The motions described above must be coordinated to produce a smooth and harmonious action.'

The Bucyrus Company and the Marion Company supplied most of the steam shovels used on the Range at the time. Some information concerning two of the most common models is given below:

- *Model 91 Marion*
  Working weight = 120 tons
  Dipper = 3 to 5 yd^3
- *Model 95-C Bucyrus*
  Working weight = 107 tons
  Dipper = 3 1/2 to 5 yd^3
  Overall dimensions = 44.2 ft × 10 ft
  Width of cut at 8 ft elevation = 66 ft
  Height from rail to point of boom = 28 ft
  Clearance height (from rail to bottom of dipper door when open) = 17 ft
  Cost = $12,500-$13,000 FOB Milwaukee, Freight = $450

With both these models the boom was located at and rotated about a turntable mounted at the front of the shovel. The dipper was hoisted using a chain as opposed to by wire rope which had just been introduced.

The time consumed in the various motions of the shovel vary with the nature of the material and the height of the bank (Barneveld, 1913). Typical shovel cycle times during stripping might be

Conditions	Cycle times (sec)
Easy digging and/or high banks	20
Difficult digging and/or low banks	40
Average	25-30

The move-up distance was usually 6 ft and required 3 to 5 minutes to accomplish. When working a 30 ft high bank, the shovel would move up about 10 times a shift (about once an hour). This gave the pit men ample time to clean up, lay track ahead of the shovel and get everything ready for the move. Under those conditions a minimum amount of time was consumed in moving up. For banks only 20 ft high the shovel was required to move-up more often (perhaps 15 times per shift). When mining low banks and on clean-up work many more moves were required and hence much shovelling time was lost from the shift. This large variation in operating conditions is reflected by the large percent time distribution ranges applicable for a 10-hour shovel shift shown in the Table 1.1.

Since the advance per move is determined by the fixed length of the extension track segments, the face area (height × width) which the shovel works controls to a high degree the loading efficiencies and costs.

As indicated the shovel is moved-up in 6 foot increments. The 6-foot track extensions have the usual plate connections and bridles found with standard track. As soon the shovel has advanced about 50 ft on such segments, a standard track segment is substituted for these short segments. This process is continued as the shovel moves along the bench. At the end of the cut, the shovel moves back along the standard track to begin the next cut. This standard track then becomes the new loading track used by the locomotive and the cars and the previous loading track is torn up and used in constructing the new shovel track.

Although the ore has been shot, the result of the blast is often mostly a shaking of the bank and the face is rarely thrown down. Sometimes there are masses of ore especially at the top of the bank, which remain almost undisturbed and with enough strength remaining so that they do not fall down or crumble under their own weight. In this case the face is scaled by dragging the dipper across the face with the bottom open so that the ore falls down in front of the shovel. The process is called 'clawing'. In addition to the face di-

Table 1.1. Time distribution for shovel loading (Van Barneveld, 1913).

Shovel activity	Percent time (range)
Actual loading	40 to 75%
'Moving-up'	25 to 5%
Shovel repairs	15 to 10%
Waiting on cars	15 to 5%
Miscellaneous	(that time needed for total to be 100%)

rectly ahead of the shovel, clawing of the side is also done. This results in a vertical face of ore being formed at a distance from the shovel track equal to the extreme reach of the dipper handle. Such a 'clawed' bench situation is shown in Figure 1.8. After loading is completed a small pile of broken but unloadable ore remains in the corner. This is removed with the next pass.

Table 1.2. indicates the supplies consumed by a typical Bucyrus 95-B shovel equipped with a 2 1/2 yd^3 bucket and digging in iron ore (Bucyrus, 1911 and Van Barneveld, 1913).

Typical stripping performances for a 10-hour shift might be

Digging Conditions	Production (yd^3/shift)
Easy	2000
Average	1500
Hard	750-1000

When using shovels for stripping, production rates ranged from 45,000 to 80,000 yd^3/month (52 shifts of 10 hours each). When loading ore the comparative figures were 75,000 to 100,000 long tons (lt) per month. To provide a volume comparison, the loose weight of the ore (tonnage factor) varied from about 13 ft^3/lt for ore running 62% Fe to 17 ft^3/lt for that running 49% Fe. An average value might be 2 lt/yd^3. Assuming an average shovel production of 1500 yd^3/shift and an average shovel labor cost of $30 per shift the average direct labor cost involved in loading would be 2 cents per cubic yard.

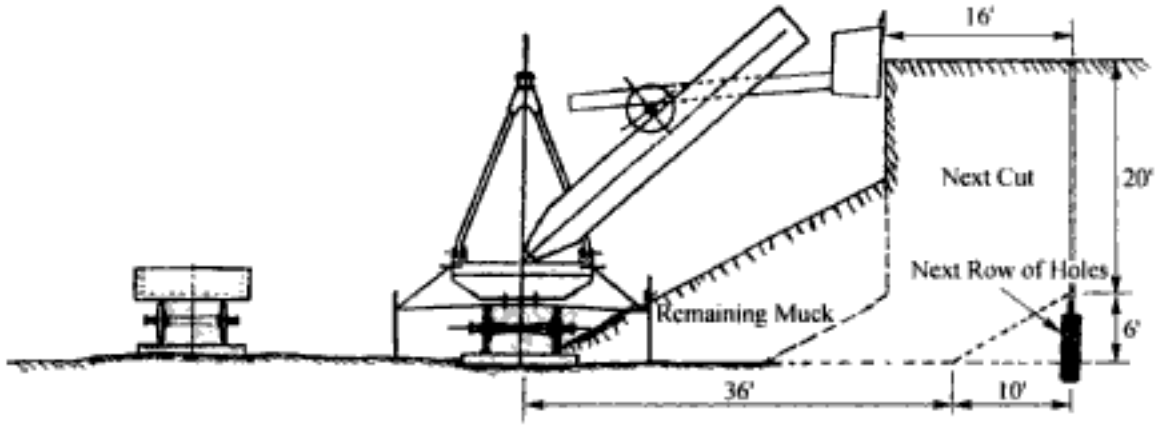

Figure 1.8. A typical cross-section showing the bench geometry when loading ore at the Sellers Pit. (Bucyrus, 1911).

Table 1.2. Supply consumption by a 2-1/2 yd^3 shovel (Van Barneveld, 1913).

Item	Consumption
Coal (per 10 hour shift)	2 1/2 to 3 1/2 tons
Water (per 10 hour shift)	4000-6000 gallons
Lubricants	
Black oil (per 10 hour shift)	1 1/4 to 2 1/2 gallons
Valve oil (per 10 hour shift)	1 1/2 to 2 1/2 gallons
Grease (per 10 hour shift)	1/2 to 1 lb.
Illuminants	
Gasoline (per night)	10 to 15 gallons
Kerosene (per night)	2 1/2 gallons

1.4 HAULAGE

Both ore and waste was hauled by rail (Figures 1.9 and 1.10). The 50 or 60 lb rails (weight per yard) were standard gauge and thus the distance between the rails (as measured between the rail heads) was 56 1/2 inches. The standard side dump overburden car was flat-bottomed and high-set. They were constructed of wood, had two 2-wheel trucks (Fig. 1.8), had a nominal capacity of 7 yd^3 (6 yd^3 actual capacity) and could dump to either side. The dumping was still done by hand although air dump cars of 12 to 16 yd^3 capacities were becoming available. These had the advantage of reduced labor expense as well as less dumping related delays which meant that the cars could get back to the shovel quicker. In stripping, a standard train consisted of up to 12 cars depending upon the grades involved. On the main haulage lines the grades could be as high as 3%. The pit grades could at times be 5% and even up to 7% over short stretches. The haul distance varied greatly but in the largest of pits it could be from two to three miles. The ore was generally loaded directly into 100,000 lb (50 ton) capacity steel cars equipped with two four-wheel trucks. These would eventually be formed into a train going to the port. In the pit two to four cars could form a train in which steep grades were involved and 6 to 8 cars on easy grades.

The majority of the locomotives were steam driven, coal fired, standard gage and weighed from 50 to 60 tons each. In 1910 there were 233 locomotives and 126 steam shovels in active operation on the Range.

Careful dump planning, design and construction were an important part of the haulage system. The first concern in this regard was dump location. Although one might think that the obvious first choice would be to fill in some of the plentiful muskeg swamps of the area, these turned out to be very poor sites. In examining the remaining potential sites,

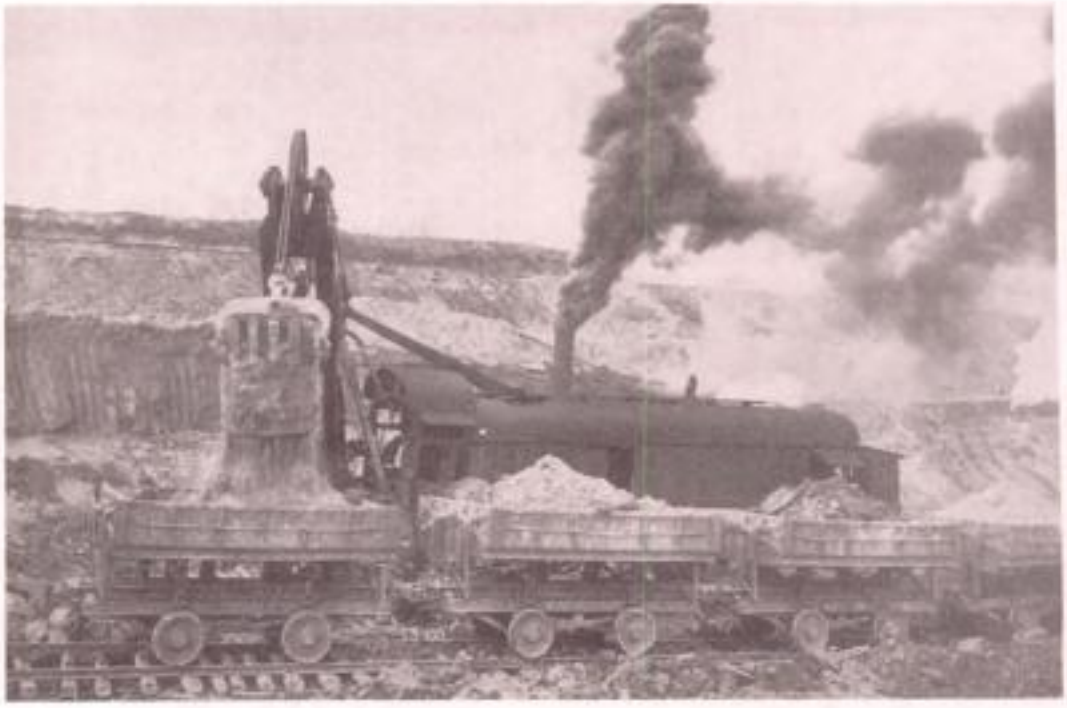

Figure 1.9. Stripping with the Atlantic Shovel (Van Barneveld, 1913).

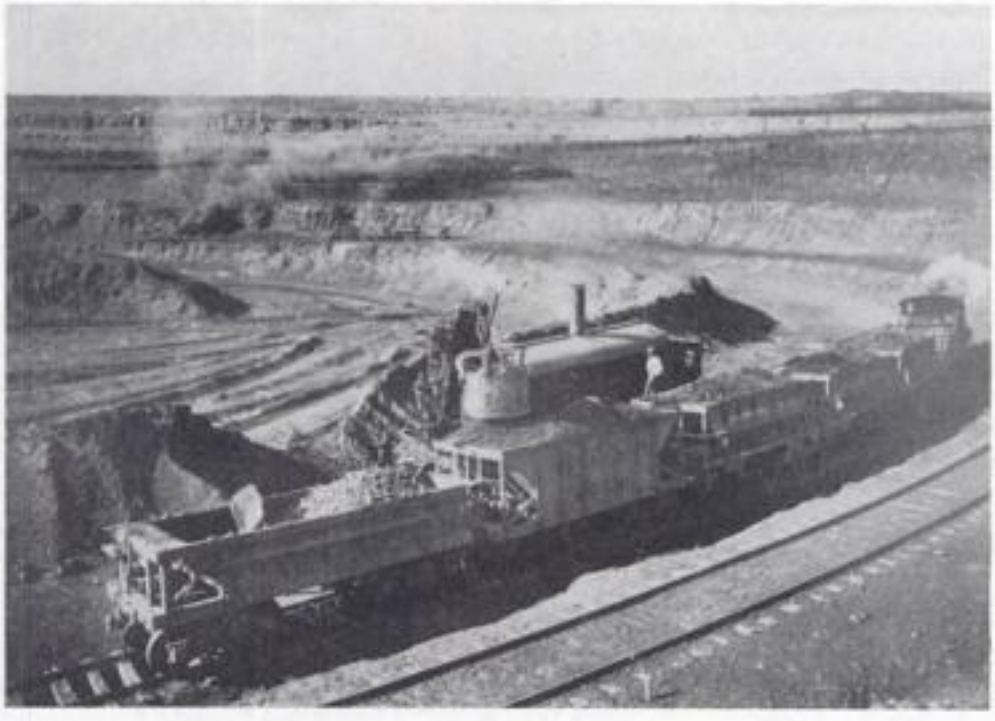

Figure 1.10. Steam shovel mining of ore (Van Barneveld, 1913).

care had to be taken to avoid placing dumps over future orebodies. Based often on bad previous experiences the companies would generally drill a series of exploratory holes to make sure that the proposed dump land did not contain mineable reserves. Since the relief was low, the dumps were built upward in a series of lifts or benches each 20 to 25 feet in height. There were two basic systems of dump building. In the first type, the dump was started by backing the train out of the pit with the locomotive in the rear and the cars in the front. Upon reaching the future dump site, the train would stop and the loads from all the cars would be dumped beside the track where they were parked, with alternate cars being dumped to the same side. The dumping crew would then shovel the rock back towards the center of the road bed while jacking-up the track. This process would continue until the starter dump (appearing much like a long dike) had reached the desired height and length. It could then be expanded to either one or both sides by dumping to the desired expansion direction(s). Upon reaching the desired height with the expansion slice the track would be thrown (moved) sidewise 4 feet. Due to the lower initial compaction of the dumps outer edge compared to an inner position, the outer rail would be elevated sufficiently with respect to the inner to allow for settling under the repeated loading by the trains. The final dumps created in this way could be several thousand feet long and several hundred feet wide.

The second technique of dump building began with the building of a wooden trestle 20 to 25 feet high and the length of the desired dump (1200 to 1400 feet). The trestle was simply an easy way of gaining height and eliminating the successive lifting of the track required by the first method. It carried, however, a price tag of between $2.50 and $4 per lineal foot depending upon the required load carrying capacity. Since it is only temporary (the trestle will eventually be fully encased by the stripping material which will then take over the function of supporting fully loaded trains) it is of light construction being able to carry (support) the weight of the empty train but not the loaded train. Figure 1.11 shows the partially completed starter dump. The locomotive pushes the loaded cars out of the pit as discussed with the previous method. When the first loaded car just passes the transition point between the encased and the exposed trestle, the train is stopped and the car is dumped to one side. The locomotive then advances the train one car length and stops. The second car is then dumped to the opposite side from the first. This process continues with alternate side dumping until the last car has been dumped. At this point the entire line of empty cars is on the trestle but the locomotive remains on the starter dump. The dumping crew shovels the dumped rock toward the center region of the trestle and fills in around the legs. Once this starter dump has been created sidewise expansion occurs in the same way as described earlier.

1.5 DRILLING AND BLASTING

Although drilling machines were available and were used on some parts of the Range, much of the blasthole drilling in 1910 was still being done using hand methods. As will be seen, due to the general softness of the ore and the overburden, the productivities and resulting costs were good which no doubt encouraged maintaining the techniques. In describing these techniques the author has drawn heavily on information originally presented by Fay (1911), EMJ (1912), Anonymous (1913e), Van Barneveld (1913) and Gillette (1916).

In ore, the 15 to 25 ft high benches were sometimes soft enough to be dug by the dipper teeth without any blasting. However, in most orebodies, blasting loosened the existing

rock structure and made loading much easier and more efficient. Vertical blast holes, or so-called 'Top' holes, were placed about 15 to 20 ft back from the crest and about the same distance apart extending along the entire bench to be broken. With regard to the pattern dimensions being used, the rules suggested that the burden and spacing should be about equal and ranged from 1/2 the hole depth to equal to the hole depth depending on the properties of the material (Marsh, 1920). The specific drilling ranged from

– 0.25 to 1.25 ft of hole/yd^3

and the specific charge (powder factor) from

– 0.30 to 0.70 lb of black powder (or 40% dynamite)/yd^3

These top holes were drilled using a 'churn' or 'jumper' drill. A churn drill, as the name implies, used an action similar to that of a butter churn for creating a hole in the rock. The drills were made from 1-in to 1 1/4-in hexagonal, octagonal or round steel bars tipped with 1 1/2-in diameter chisel bits. Often both ends of the steel bars were tipped with bits

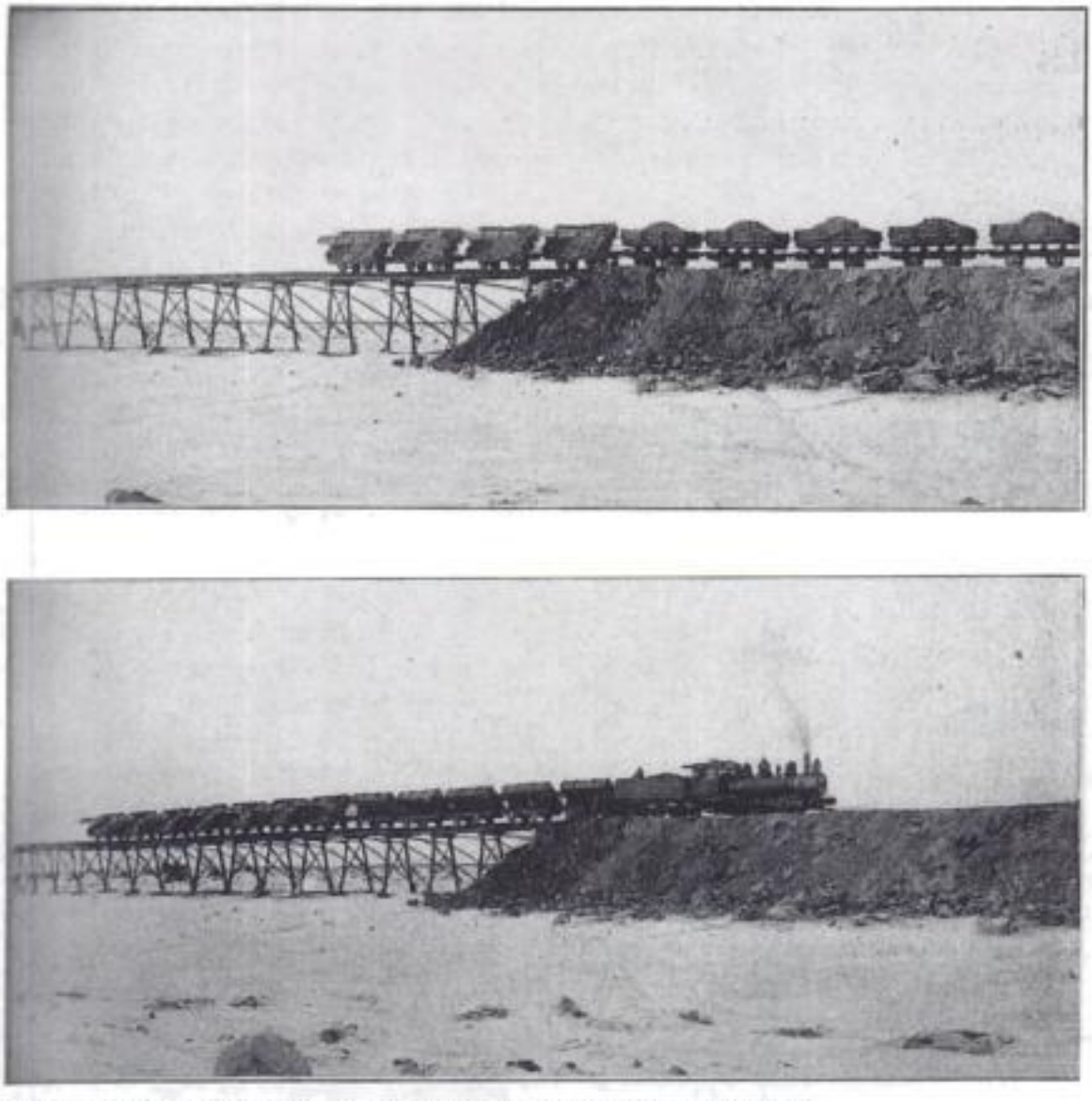

Figure 1.11. Construction of a dump using a starting trestle (Van Barneveld, 1913).

so that the required steel sharpening changes were halved. A 25-ft long rod 1 1/4 in. in diameter weighed slightly more that 100 lbs. In drilling, the rod would be lifted vertically about 2 ft off of the hole bottom by 2 to 4 men (depending upon the hole depth) and then allowed to drop freely. For the case of the 25-ft long rod dropping through 2 ft. the velocity at impact would be 11.3 ft/sec (3.46 m/sec) and the kinetic energy available for rock-breaking about 400 ft-lbs (55.5 N-m). Lifting of the steel is facilitated by means of a heavy iron cross handle or yoke 26 inches long. It was slipped over the steel and fastened in place with a 6-inch wedge. There was one such set of arms for each pair of men. Bit rotation was accomplished simply by the men moving around a 3-foot diameter circular path surrounding the hole.

When the hole was at the required depth (about a foot or two below the desired grade so that there would be no 'tight' ore on the bottom), one or two sticks of 7/8-in × 6 in long 60 percent dynamite would be lowered and shot to 'spring' (enlarge) the hole. The hole was re-opened and now 5 to 15 sticks of dynamite were placed at the bottom of the hole and shot to spring the hole further so that it would eventually hold 2 to 3 kegs (each keg contains 25 lbs) of black powder. About 2/3 of the way through the loading process, a primer consisting of five sticks of 60 percent dynamite tightly wrapped together was prepared. Each primer had two electric caps or two caps and fuses. The remaining powder was then poured into the hole. After the powder was in place the hole was firmly tamped with sand. During cold weather only one hole was shot at a time and the loosened material loaded out before it had the opportunity to freeze. In the summer often 15 to 20 holes would be shot one after the other yielding enough material to keep the shovel busy several days. A gang of 4 men could drill, on average, 100 linear feet of such hole in a 10-hr shift. Assuming an average in place specific gravity for the ore of 4.0 and a 15 ft × 15 ft pattern, there would be 25 long tons per foot of hole. Thus the 4 men could drill out 2500 tons of ore per shift. At a wage of $2/shift/man, the direct labor portion of the drilling would be about 0.3 cents per ton.

Vertical churn drill holes were sometimes also used for breaking overburden. These holes were spaced 15 to 20 ft apart, at a distance of 20 ft back from the previous shovel cut and were 20 to 25 ft deep. They would also be chambered at the bottom. In such material the gang of 4 men would average 40 linear feet of hole in a 10 hour shift.

Normally, however, when blasting benches in overburden, a 'gophering' process was used. In particular it was used (a) in ground so dry and sandy that a vertical hole could not be kept open or (b) when the bench was too high to be drilled from the top. The collar of the hole was located at the base of the bank and the hole inclined downward from the horizontal at an angle of 10 to 20 degrees. These 'gopher' holes were 15 to 25 feet deep and spaced at 15 feet in hard material and high banks and at 25 feet in lower banks and softer material.

The typical set of tools needed for gophering are shown in Figure 1.12. In loose material, the hole was created simply using the ordinary No. 2 round-pointed shovel. The sides of the blade would be turned slightly upward to give a depth of 2 inches and the socket opening enlarged to accept the large 2- to 3- inch end of a peeled sapling (20 to 25 ft long). An ordinary hand auger of small diameter (not shown) was sometimes used to start the hole and remove the first few feet of material. This hole would then be blasted with a few sticks of dynamite. The effect would be to leave a long bootleg 8 to 14 inches in diameter. Since the auger was unwieldy in deep holes, a long pointed moil would next be brought into service. This would be driven a foot or two into the bottom of the hole by

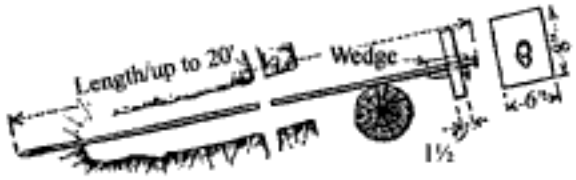

a. Long Moil With Plate and Wedge For Driving it Out of the Hole

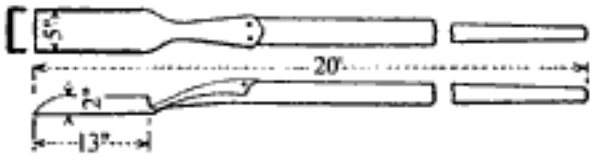

b. Spoon or Shovel

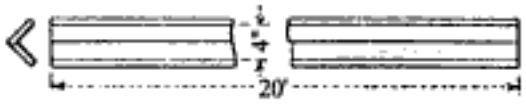

c. Loading Trough

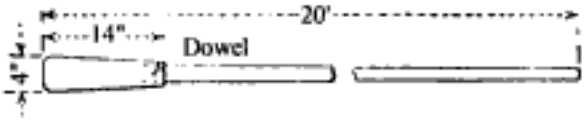

d. Tamping Bar

Figure 1.12. A typical set of Gopher-Hole tools (Anonymous, 1913e and EMJ, 1916).

two men using double jacks. When progress became slow, a perforated plate about 1 1/2 × 6 × 8 in was slipped over the end of the moil and wedged to it, either with two small wedges or with one wedge and a track spike as illustrated. By hitting the head of the wedge(s) with the two doublejacks, the moil could be extracted. During this process, the moil was usually supported on a log, to keep the plate off of the ground. The moil hole was then blasted by inserting a stick or two of powder and exploding with an electric cap. The loose dirt was taken out with the shovel and these alternating processes of drilling, springing and shoveling continued until the desired depth was reached. Hole depth depended both upon the height of the bank and on the width of the cut. The bottom of the hole was then sprung as described earlier with respect to the vertical holes. A final sprung diameter of 10 to 14 inches was desired.

Two techniques were used to place the black powder charge in the sprung gopher hole. The first technique was to feed the black powder into the hole by means of a wooden box or spoon 3in wide by 3 in high (inside dimensions) by 32 in long attached to the end of a 25 ft long pole. In the second technique, a V-shaped trough was constructed of 3/4 × 4-in boards. The powder was poured into the upper end and the trough then given a series of backward and forward motions shaking the powder along the trough to the hole bottom. Copper nails were used in the construction of both the spoon and the trough to avoid setting off the powder from sparks. Tamping of the loose powder using a wooden tamping pole such as shown was an important part of the operation. The priming was done in the same way as described with the vertical holes. Tamping to the hole mouth with loose gravel was essential to contain the energy.

The benches were drilled and blasted by a regular gopher-hole crew consisting of 10 to 30 men (common laborers) working in gangs of two. The time required for drilling such a gopher hole varied from 2 to 12 hours depending on the ground. It was considered good work if the blasted bank came down to the loading track but did not cover it.

As indicated earlier there were many granite boulders of various sizes present in the overburden. The shovel could usually move and load those smaller than 3 feet in diameter. The rest, however, which ranged up to 12 feet in diameter had to be broken by 'block-holing'. Single- or double-jacking was used. In single jacking one man held the 7/8 inch diameter drill steel with one hand while pounding with the other. The weight of the hammer used was commonly 4.5 lbs. In two hand drilling (double jacking), one man held the steel while the other hammered. In three-hand drilling one man held the steel while two men struck the steel. The weight of the hammer in these cases was 10 lbs. For vertical holes water was poured into the hole to hold the cuttings in suspension. The resulting sludge was removed from time to time. Normally single jacking was used and the hole depth was of the range of 1 1/2 to 2 1/2 feet. Depending on the length, 2 to 4 sticks (3/4 in × 7 in long) of 60 percent dynamite were inserted in the completed hole and shot. The powder had to be well rammed and then tamped with a little moist clay. The driller worked on contract with 25 cents being paid per linear foot. Usually he drilled 12 to 15 feet of such hole per day.

1.6 PRODUCTION STATISTICS

Given these semi-mechanized mining techniques, one might question the possible production rates and productivities achievable. Table 1.3 provides the production statistics for some of the larger operations on the Range for the year ending June 30, 1910.

The actual totals for all of the open pit operations on the Range for this period were

- 20,667,751 tons of ore shipped
- 25,902,178 yd^3 of overburden stripped

For this year, the ore from the Mesabi Range supplied 40% of the feed for US pig iron production. This amounted to 17% of the world's supply. A total of nearly 9000 men

Table 1.3. Production from some of the larger Mesabi range operations for the year ending June 30, 1910 (Fay, 1911).

Mine	Stripping (yd^3)	Ore Shipped (lt)
Susquehanna	532,857	275,709
Hull-Rust	2,923,460	3,624,414
Mahoning	568,791	1,552,114
Dale-Uno	1,694,203	–
Sellers	1,356,865	989,503
Rust	1,301,669	–
Morris	1,487,973	1,973,258
Adams	1,260,742	1,739,996
Fayal	247,629	2,023,053
Genoa	1,064,791	1572
Leonard	1,716,407	341,030
Shenango	1,431,789	910,870
Hartley	2,240,649	95,371
Grant	1,002,333	–
Stevenson	82,190	1,378,174
Subtotal	18,912,348	14,905,064

were employed with 4879 in stripping operations and 4054 in ore mining. Although today open pit operations are generally regarded as safer than those conducted underground, the fatality rate was 4.59 per thousand as compared to 3.32 per thousand for the underground mines. The reason for this was that the open pit operations more nearly resembled railroading than mining. That such tonnages could be produced with these techniques speaks well for the miners of that era. Tables 1.4, 1.5, and 1.6 provide an indication of the wages paid, the costs, and the revenues, respectively applicable to mining on the Range at that time.

Table 1.4. Wages ($/10-hr day) Paid on the Mesabi Range in About 1910 (Anonymous, 1910 and Van Barneveld, 1913).

Job Category	Wages
Mining engineer	$3.84
Assistant engineer	2.57
Chemist	3.25
Carpenter	3.12
Mason	3.68
Machinist	3.53
Blacksmith	3.16
Steam shovel operator (Runner)*	5.77
Craneman (helper on shovel)*	4.04
Fireman (on locomotives)	2.50
Locomotive engineer*	4.10
Pitman	2.35
Surface foreman	3.37
Pit foreman	4.13
Rockman (common labor)	2.00
**Bonus Schedule*	
Runner	$25/month of 25 days
Craneman	$20/month of 25 days
Locomotive engineers	$20/month maximum

Table 1.5. Approximate 1910 costs applicable for Mesabi Range ores (Finlay, 1909, Anonymous, 1913a, Marsh, 1920, Van Barneveld, 1913).

1. Stripping costs	
– Glacial drift	$0.30/yd^3
– Paint rock	$0.30/yd^3
– Broken taconite	$0.75/yd^3
– Solid taconite	$1.00/yd^3
2. Ore mining	$0.15/ton
3. Mining, stripping and local overhead charges (ore on cars) but excluding royalty, taxes and extraneous overhead charges.	
– Range	$0.15 to $0.75/ton
– Average	$0.40/ton
– Favorable	$0.30/ton
4. Royalty	$0.40/ton
5. Taxes	$0.10/ton

Table 1.5. Continued.

6. Ore transport costs	
– Train from the Mesabi Range to the Upper Lake Port (Duluth)	$0.80/ton
– Boat transport from Duluth to Lake Erie port	$0.60/ton
– Train from Lake Erie port to Pittsburgh	$0.60/ton
7. Average total cost (insitu to blast furnace)	$2.90/ton

Table 1.6. Prices paid at the Pittsburgh blast furnaces in 1911 (Van Barneveld, 1913).

1. Bessemer ore:
   Price: $4.85/long ton
   Analysis:
   - natural iron = 55%
   - moisture = 10%
   - dried iron = 61.12%
   - dried phosphorus = 0.045%

   Base unit value: 0.0881818 cents/ltu. This is applied to the natural iron content
2. Non-Bessemer ore:
   Price: $4.105/long ton
   Analysis:
   - natural iron = 51.50%
   - moisture = 12%
   - dried iron = 58.52%

   Base unit value: 0.079611 cents/ltu. This is applied to the natural iron content
   (ltu = long ton unit)

1.7 PRODUCTION STRATEGY THEN AND NOW

Successful mining operations are not simply a matter of men, machines and techniques but require well thought through operating strategies for their efficient use as well. According to Van Barneveld (1913) the essential requirements for a successful stripping job were:

1. Proper supervision of the whole job. This means keeping firmly in mind that cooperation all along the line is the key to success.
2. First-class machinery adapted to the work.
3. Facility for quick repairs and thorough upkeep of the plant.
4. Skilled runners (shovel operators) and cranemen, experienced in the particular field, preferably men accustomed to working together.
5. Easy access to the shovel for stripping trains, with the empty train pulling out as the loaded train pulls out.
6. Good track systems with reasonable grades and curves.
7. A good pit crew and a well organized dump gang.

The operating strategy (Van Barneveld, 1913) for these large steam shovel operations (Figs 1.13 and 1.14) was, stated simply, to keep the shovels (the source of supply) going steadily. Maximum efficiency could only be maintained by keeping other operations subservient to the steam shovel. In practical terms, this meant that

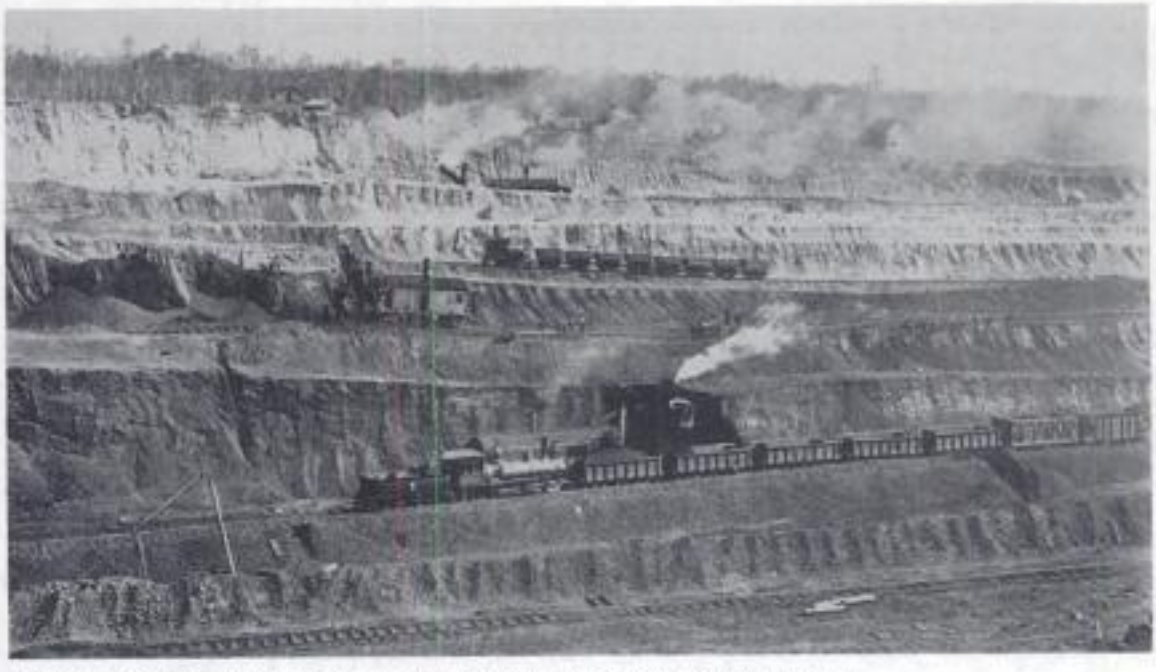

Figure 1.13. Stripping and mining ore at the Stevenson Pit (Van Barneveld, 1913).

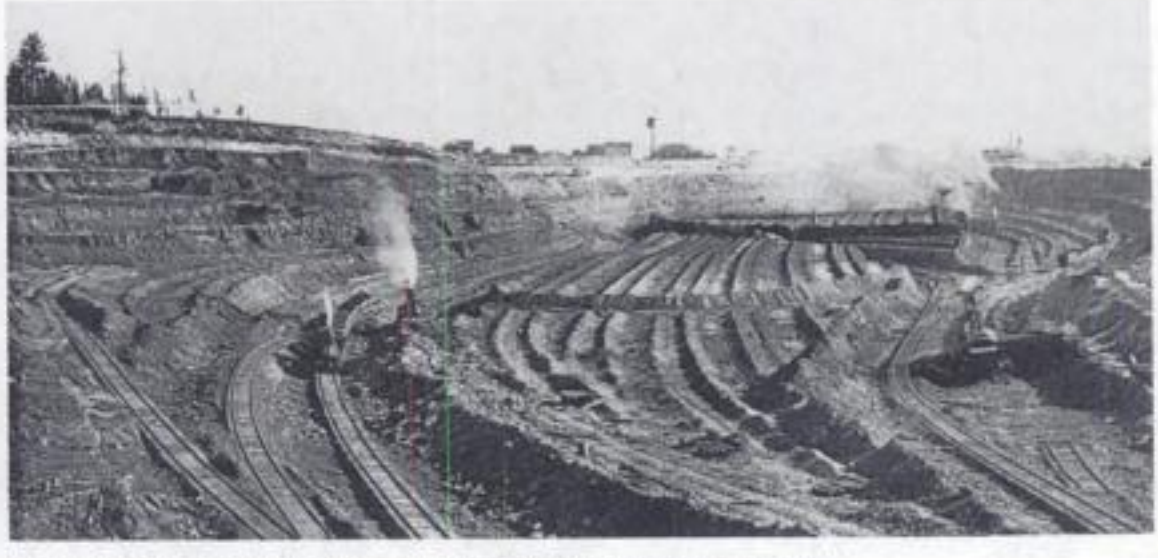

Figure 1.14. An overview of the Mountain Iron Mine (Van Barneveld, 1913).

(a) The shovel should never have to wait on a locomotive. For a properly organized stripping operation half a dozen trains may be waiting at any given time in various places and positions for an available steam shovel.

(b) Since bank blasting was such an important part of the process it should be kept well ahead of the shovel.

(c) Poorly blasted material increased

- The strain on the shovel
- The number of delays and breakdowns
- The repair bill

and caused both direct and indirect reductions in the output.

(d) The blasting efficiency was not measured by minimum powder consumption but rather by a thorough comminution of the bank. This was defined as that which yielded maximum digging and loading efficiency at the shovel with a minimum of repairs.

Today, although the equipment and techniques have significantly changed through time, the operating strategy remains basically the same; keep the loading machine – the source of supply – producing efficiently. If there is waiting to be done, it is by the trucks and not the loader. Fragmentation costs (drilling and blasting) except in the hardest of rock types, still make up a relatively small percentage of the total operating costs. The effects of inadequate fragmentation on the loading/hauling operations remains the same today as in 1910. When considering the overall process of removing ore from insitu and delivering it to the final customer one strives to do that at minimum overall cost. For steam shovel iron mining on the central Mesabi Range in 1910, the apparent 'customer' was the ore car since intermediate processing was often not required. The true customer was in fact the *shovel* since it was simply an extension of the rail car.

For open pit metal mining operations today this is generally *not* the case. The true customer may be a conventional fixed primary crusher, a mobile crusher/conveyor, or even the entire mill itself expressed in terms of throughput demand.

In the future the optimization process will be even more complicated. It will involve identifying the 'real' customer and together specifying the product requirements and then developing a strategy (manpower, machines, techniques and procedures) for satisfying those requirements at a minimum cost.

As indicated in the Preface this book (Volumes 1 and 2) deals only with the unit operation blasting. A companion volume, in preparation, will cover drilling, loading and hauling. Even though, by necessity, the specific technical aspects involved with the different unit operations are covered in different chapters and even in different volumes, the reader must clearly keep in mind their important interdependence.

REFERENCES AND BIBLIOGRAPHY

Anonymous 1910. Wages paid on the Mesabi Range. *The Engineering and Mining Journal* 90(26): 1244. Dec 24.

Anonymous 1912. Open pit mining of Mesabi iron ore. *The Engineering and Mining Journal* 93(19): 938. May 11.

Anonymous 1913a. Iron mining in Minnesota. *The Engineering and Mining Journal* 95(26): 1295. June 28.

Anonymous 1913b. Lake Superior Institute Meeting. *The Engineering and Mining Journal* 96(10): 455-456. Sept 6.

Anonymous 1913c. Open pit mining under difficulties. *The Engineering and Mining Journal* 96(11): 497. Sept 13.

Anonymous 1913d. Choice of mining methods on the Mesabi. *The Engineering and Mining Journal* 96(13): 592. Sept 27.

Anonymous 1913e. Drilling Mesabi gopher holes. *The Engineering and Mining Journal* 96(25): 1169-1170. Dec 20.

Anonymous 1995. The spelling of Mesabi. *Skillings Mining Review* 84(2): 48.

Bucyrus Company 1911. *Handbook of Steam Shovel Work* (First Edition). The Bucyrus Company and Construction Service Company. pp. 5-15, 236-244.

E/MJ 1916. *Details of Practical Mining* (First Edition). Compiled by the editorial staff from the Engineering and Mining Journal. McGraw-Hill Book Company, Inc. New York. 544 pages. pp. 58-63.

Fay, A.H. 1911. Steam shovel work on the Mesabi Range. *The Engineering and Mining Journal*. 91(8): 420-423. Feb 25.

Finlay, J.R. 1909. Cost of pig iron made from Lake Superior ores. *The Engineering and Mining Journal* 87(15): 739-745. April 10.

Gerry, A.L. 1912. Iron mining on the Mesabi Range. *The Engineering and Mining Journal* 94(15): 693-696. Oct. 12.

Gillette, H.P. 1916. *Handbook of Rock Excavation Methods and Cost.* Clark Book Company, New York. pp. 21-39.

Kellogg, L.O. 1914. Notes on Mesabi Range mining practice-I. *The Engineering and Mining Journal* 97(14): 695-699. April 4.

Marsh, R., Jr. 1920. *Steam Shovel Mining* (First Edition). McGraw-Hill Book Company, New York. pp. 1-30, 51-54, 75-82, 93-99, 135-149, 224-226.

McDaniel, A.B. 1913. *Excavation Machinery.* McGraw-Hill Book Company, New York. pp. 43-69.

Van Barneveld, C.E. 1913. *Iron Mining in Minnesota.* Bulletin No.1. Minnesota School of Mines Experiment Station. The University of Minnesota, Minneapolis. pp. 131-153.

Winchell, H.V. 1920. Letter communication with Skillings' Mining Review. Jan 27.

CHAPTER 2

The fragmentation system concept

2.1 INTRODUCTION

In Chapter 1, the historical background to modern large-scale open pit mining systems based upon mining on the Mesabi Range in Minnesota was presented. Today the 2 1/2 to 4 yd^3 dippers used to load the natural ores on the Mesabi Range in 1910 have been replaced with loading machines about 10 times larger. One truck will carry the same amount as 20 of the wagons making up an early stripping train and there have been corresponding changes in the drilling and blasting operations. The ore being mined has changed as well. As opposed to the easily mined natural ores, the taconite currently being mined is some of the hardest rock in the world. However, even though (a) the machinery has grown with the times, (b) the techniques have vastly improved, and (c) hand labor was long ago replaced by machines, the basic operating strategy remains the same – all other unit operations are subservient to the loader and to loading. Although the loader does indeed form the heart of production since it is the source of ore supply, blasting provides the muscle. These muscles must be properly developed and then applied to the proper degree and in the appropriate way for the succeeding operations to be successful. This was probably true then, is true today and will be especially true in the future. If this muscle function is underdeveloped and thereby performs poorly or below capacity so then will all those operations which follow.

Although the endearing term 'powder monkey' has often been used to refer to the person responsible for the blasting in the mine, today it is more likely to be the 'blasting engineer' and in the future the 'fragmentation specialist'. These do not have the same colorful ring as 'powder monkey' but are more fitting descriptions of the background, position and level of responsibility for the person in whose hands depends an important part of the overall mine economy.

This Chapter will provide an overview of the subject of fragmentation engineering and, in particular, the fragmentation system concept in theory and reality. The powerful, versatile explosive muscles with which we have to work will be introduced in Chapter 3.

2.2 MINE – MILL FRAGMENTATION SYSTEMS

The expression 'systems approach', in vogue today, is used to describe the process of system identification, system description, system goal definition and finally system optimization. The concept is that by examining the 'system' as a whole one can often realize cost, productivity, product quality, etc improvements which would not otherwise be achieved by considering the various elements comprising the system singly.

The 'system' to be optimized can be any group of people, machines or other elements that work together to do a certain job or accomplish a certain objective. When the components or sub-systems interact significantly it may be possible to achieve the same final level of performance in many different ways. An enhanced or superior performance level by one sub-system may offset a lesser performance somewhere else along the chain. Once the system and its sub-systems have been defined and the system goal(s) defined then the various means for achieving the final desired result may be studied. These optimization studies, called 'tradeoff studies', suggest how a given result may be achieved in the most economical manner.

The boundaries distinguishing one sub-system (operation) from another in the production chain are often traditional. For example one group may be responsible for drilling, another group responsible for blasting etc. Given this structure, the individual 'operations' or 'sub-systems' are generally often very highly developed and may in fact be 'optimized' within themselves. If, however, these traditional boundaries are flexed (moved) or removed entirely then the new sub-systems formed may, or may not, be optimized. If they turn out to be sub-optimized, this presents an improvement opportunity. In applying a systems engineering approach to an operation one examines both the whole (the system) as well as the individual parts (sub-systems). Special attention is paid to the interface regions. By, at least conceptually, flexing (removing) the current interfaces and forming new groupings, one is in effect required to look concurrently at the forest, various groves of trees, and the individual trees themselves for cost and productivity improvements. Since this often involves a number of well developed practices and even individually 'optimized' sub-systems of long standing the job is not easy but can be highly rewarding.

Consider now how this 'systems approach' might be applied to the system of rock fragmentation by the mine-mill complex. The stated goal will be that of

achieving a prescribed level of fragmentation at minimum cost.

The main mine unit operations are, as shown in Figure 2.1, drilling and blasting, loading, hauling and primary crushing. The latter may or may not be the responsibility of the mine but it will be included as so in this discussion. In Figure 2.2 the drilling and blasting category has been split into the two component parts. A 'Product' box has been inserted between each of the unit operations in Figures 2.1 and 2.2 to represent the seller-buyer action which occurs at hand-off.

As opposed to the mining of natural ores on the Mesabi Range in 1910, most ores today require some type of further treatment before going on to the marketplace. In this case it will be assumed to be a mill which adds value to the mined product by removing at least a major portion of the associated waste products and produces a concentrate which is now sent further. For the purposes of this discussion the mill will be defined as the unit which performs the further mechanical breakdown of the ore. The unit operations included are shown in Figure 2.3. which presents an overview of the entire Mine-Mill fragmentation

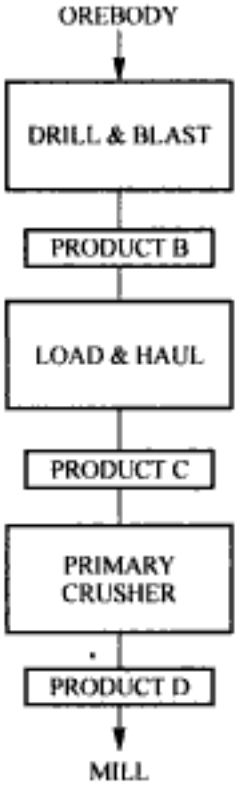

Figure 2.1. Diagrammatic representation of the chain of mine unit operations showing product transfers.

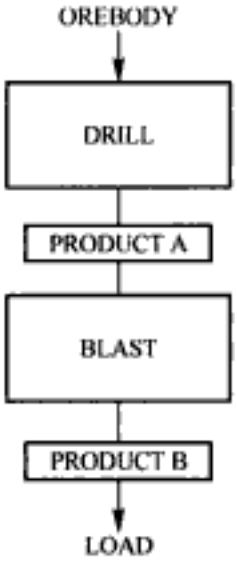

Figure 2.2. The drill-blast portion of the unit operation chain with product boxes added.

system being considered. Further treatment of the mill product, might include flotation, magnetic/electrostatic separation, etc. It is assumed that all mechanical fragmentation activities have been completed by the time the ore leaves the mill. Often the mine and mill fragmentation sub-systems are treated separately and this is denoted by the dashed lines in the figure. If this is the case then the seller-customer representation becomes that shown in Figure 2.4. The product box shown drawn between the two simply indicates that material 'sold' by the mine and 'purchased' by the mill. In closely examining Figure 2.4 one can see that it can be expressed in terms of fragmentation and transportation unit operations. This has been done in Figure 2.5. From this it is clear that when looking to make

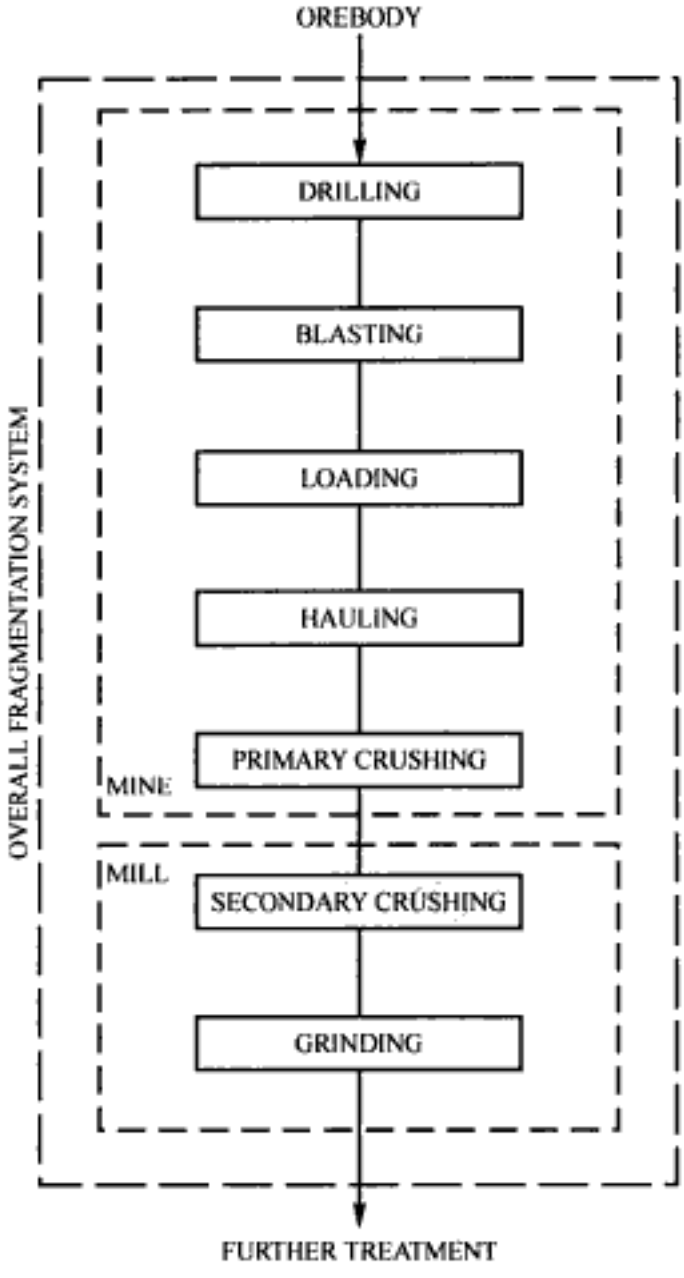

Figure 2.3. Diagrammatic representation of the overall mine-mill fragmentation system and the mine and mill subsystems.

further improvements, a systems study based upon tracking fragmentation is in order. The entire process takes insitu material with a 'particle size' considered to be very large and reducing it down to, for example, –325 mesh (in the case of taconite ore) to facilitate the further treatment. The problem becomes that of deciding where in the system the different stages of size reduction should occur and to which level they should occur since such size reduction is accompanied by the expenditure of increasing amounts of energy per unit volume using processes having different breaking efficiencies. This question of energy requirements in fragmentation will be explored more fully in the following section.

To simplify the discussion the milling portion of the fragmentation chain will be replaced by a product demand requirement (Product D) and the focus will be on that part of the chain traditionally considered the mining responsibility as shown in Figure 2.3. As a way of proceeding one can consider the product specifications or requirements for each product box. If one begins with Product D, the succeeding steps in the process are very energy

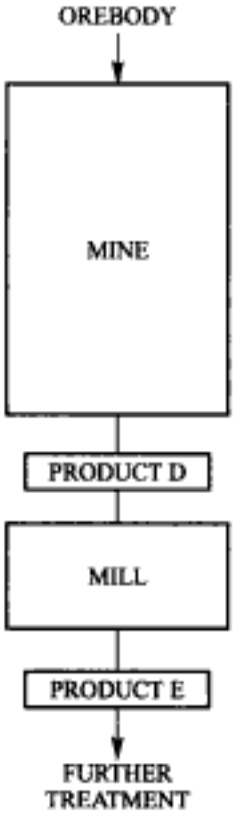

Figure 2.4. The mine-mill system with product boxes added.

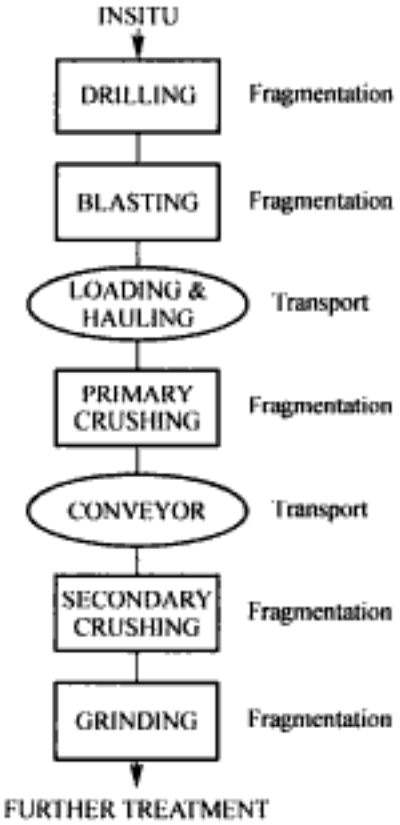

Figure 2.5. The mine-mill system represented as fragmentation and transport unit operations.

demanding and therefore one might like to have as finely crushed feed as possible. On the other hand if autogeneous milling is being used a certain size distribution is also needed for best results and maximum throughput. Thus there could be a desire, if not a demand, for a certain size distribution and average size. The mill requirements on the proceeding steps in the fragmentation process are shown in Figure 2.6. Knowing the reduction characteristics of the primary crusher one could transfer these into the mill requirements placed on Product C which is the feed to the primary crusher. Considering simply the primary crushing operation itself, for high capacity throughput and efficient crushing a feed commensurate with its designed function is required. This primarily means the elimination of oversize which causes bridging. One would ideally like to have material that would pass through without crushing and then this stage could be removed. On the other extreme one wants to avoid particles of such size that 'bridging' occurs because then the throughput is dramatically reduced. Thus there is room for optimization with respect to this unit. With respect to fragmentation, Products B and C are the same except for

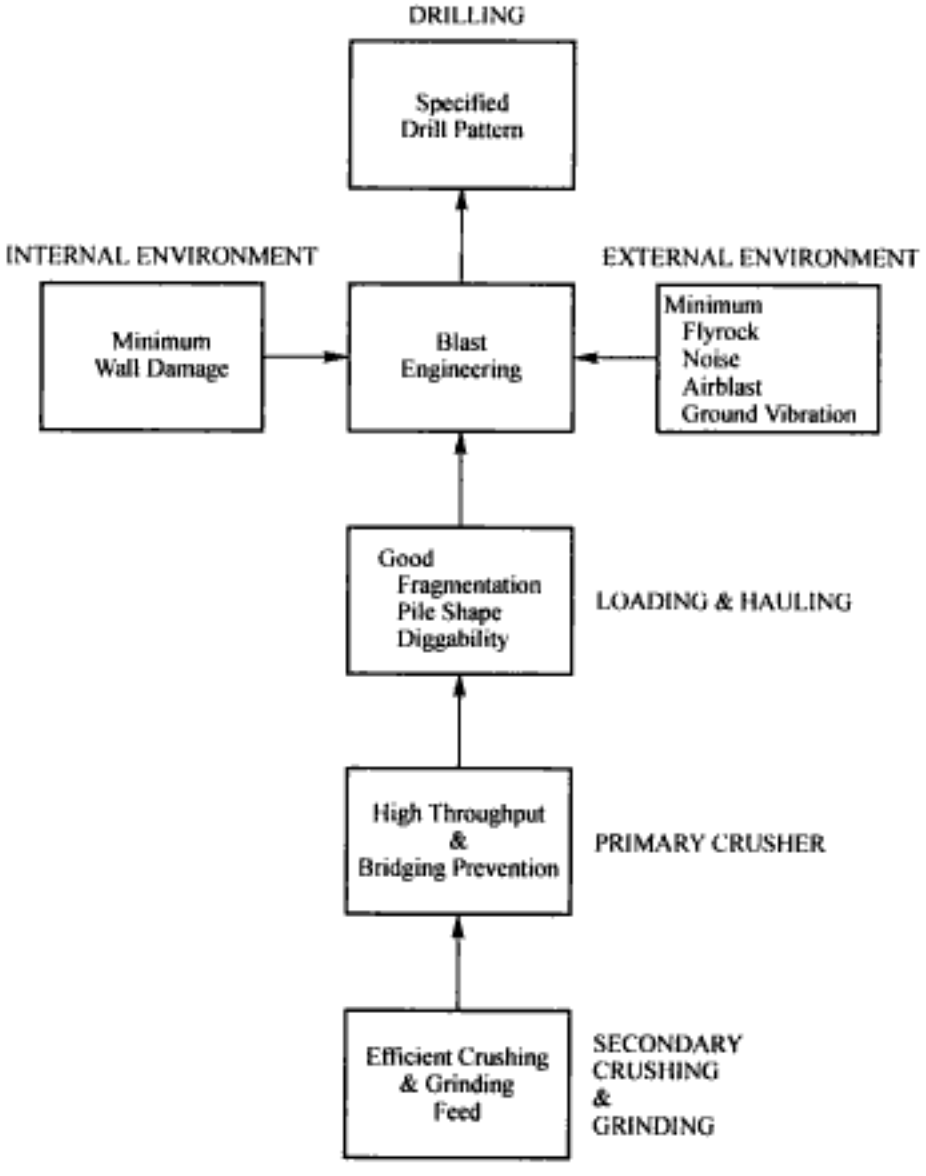

Figure 2.6. The fragmentation requirement flow sheet.

the fragmentation which occurs during the loading process. This will be neglected in this discussion. In addition to those requirements imposed by Products C and D, Product B has specific requirements regarding fragmentation as imposed by transport (loading and hauling). These are:

- Diggability
- Muck pile shape
- Average size and size distribution
- Boulder frequency/size

What about Product A? The Blast Engineering function specifies the hole patterns, and the Drilling function carries out the design. There are also some other factors (constraints) which most be considered. First there are two groups of environmental factors. The external environmental factors are airblast, flyrock, noise and far field ground vibration. These often have limiting values imposed by law. Obviously these also affect the near field mine environment as well but it is not the same type of constraint. The internal environmental factor which does have a direct effect on the mine is unwanted rock damage done by blasting to the remaining wallrock. This constraint does not apply throughout the pit but where it is important, it is important. An ore grade control constraint is sometimes imposed with the desire being that the ore remain more or less in the same place before and after blasting. There are also constraints imposed by limited operating room, bench sizes, equipment or facilities in close proximity, etc. The Blast Engineering box is shown with the different demands imposed upon it in Figure 2.6.

Now there are obviously costs (penalties) and benefits associated with the different demands and some tradeoffs have to be made. However with the factors identified and specified, the blast engineer can begin the design process and weigh the different alternatives.

Figure 2.7 illustrates quite well the many controllable and uncontrollable variables involved in any given blast and the resulting outputs. The logic trail involved in preparing the design are shown in Figure 2.8 with a somewhat simplified version of the design-test-redesign circle given in Figure 2.9. As can be seen the process of engineering a blast is a challenging process involving the marriage of

- Explosive characteristics
- Explosive fracturing phenomena
- Layout geometry
- Rock and rock mass properties
- Timing
- Sequencing

so that the desired degree of fragmentation as required by the down-stream operations as well as the other demands shown in Figure 2.6 are satisfied. The tools required to attack this job are presented in the remaining portions of Volume 1 of this book.

2.3 THE ENERGY REQUIRED IN FRAGMENTATION

There are three common approaches which have been used throughout the years to describe the work done in breaking down a material from one particle size to another using mechanical means. In 1867, Rittinger suggested that the energy (work) required was related to the amount of new surface area created (energy was a function of area). Kick

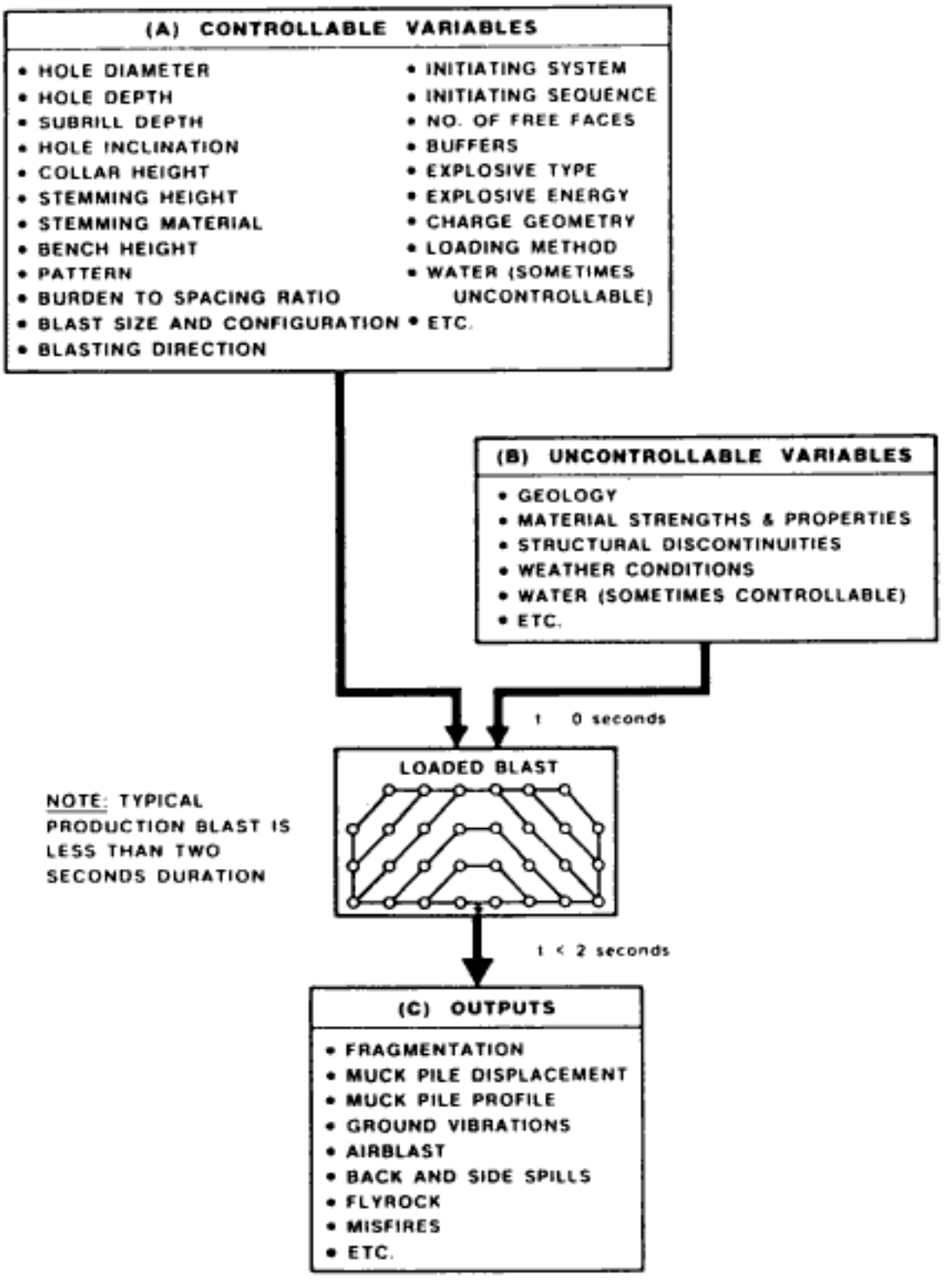

Figure 2.7. Field model illustrating blast design inputs outputs (Atlas Powder Company, 1987).

(1885) on the other hand concluded that it was related to the total strain energy required by the particles to bring them to the point of failure and hence a function of volume. Bond (1952) indicated in his so-called 'Third Law' that since the particle must first be strained to the breaking point (volume dependence) and then new surface is created during failure

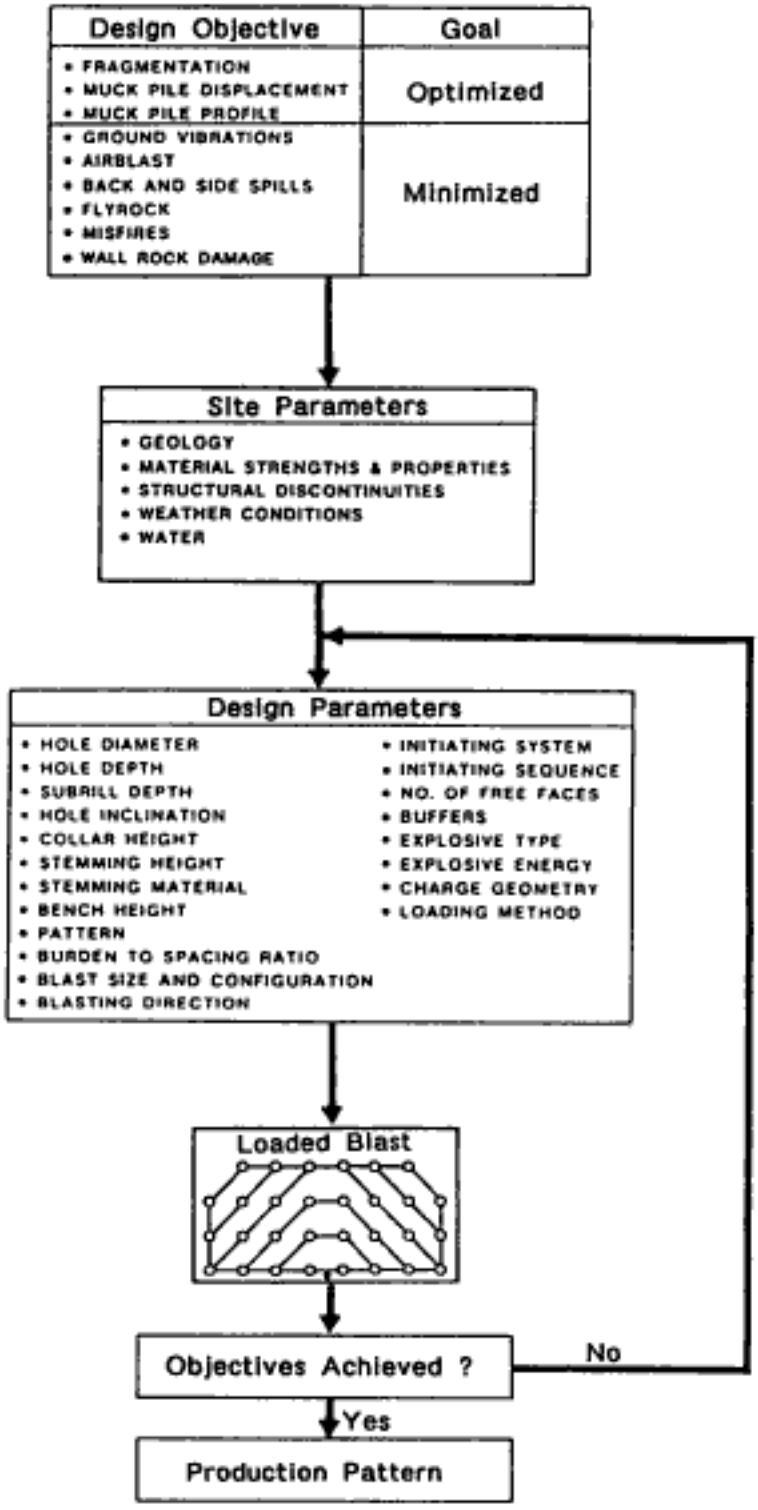

Figure 2.8. Blast design flowsheet logic (modified after Atlas Powder Company, 1987).

(area dependence) that both processes must be involved. Oka (1969) showed that all three of these 'Laws' can be described by the following formula

$$W = K_i[P^{-6/B} - F^{-6/B}] \tag{2.1}$$

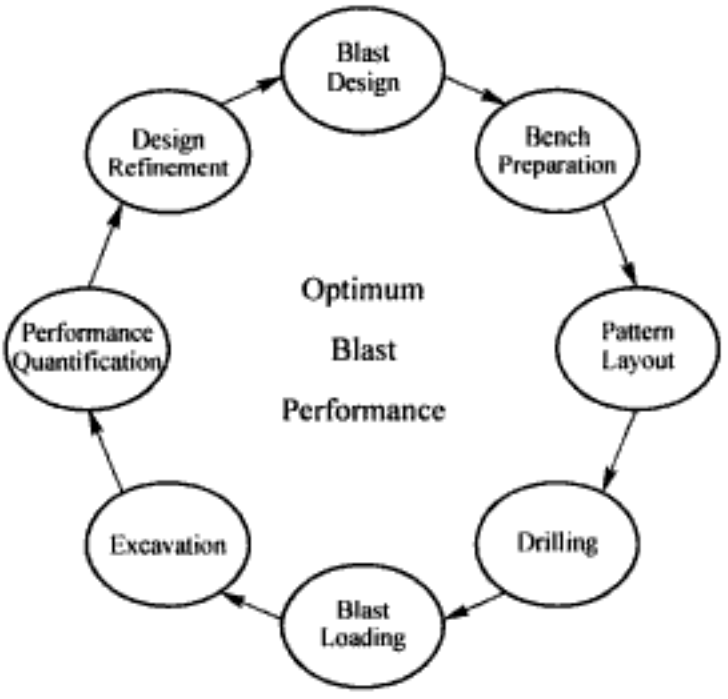

Figure 2.9. The blast design-evaluation-redesign improvement circle (Humphreys, 1995 and Dyno/Wesfarmers, 1993).

where W = total energy (work) required for size reduction from feedsize (F) to product size (P), F = feed diameter, P = product diameter, K_i = constant which is 'Law' dependent, B = infinite (Kick's Law), B = 6 (Rittinger's Law), B = 12 (Bond's Law).

Since this relationship is most easily demonstrated for the Rittinger Law, such an approach will be followed here. The work required according to Equation (2.1) is

$$W = K_R \left[\frac{1}{P} - \frac{1}{F}\right] \tag{2.2}$$

where K_R = the Rittinger constant.

In the beginning of the proof, assume that one begins with a cube of edge length F. In the case of a unit cube, $F = 1$. The surface area (A_F) is

$$A_F = 6\,F^2$$

and the volume (V_F) is

$$V_F = F^3$$

There is just 1 such cube so that the number (N_F) of feed particles involved is

$$N_F = 1$$

If the surface energy per unit area is assumed equal to S, the general expression for the total energy (E) then becomes

$$E = N \times A \times S \tag{2.3}$$

where E = total surface energy, N = no. of particles, A = surface area per particle, S = surface energy/unit area.

Substituting into Equation (2.3) the values appropriate for the feed one finds that

$$E_F = 1 \times 6\,F^2 \times S = 6\,F^2\,S \tag{2.4}$$

Consider now that after crushing the product is made up of particles having a side length P. The surface area (A_P) and the volume (V_P) of each particle are respectively

$$A_P = 6P^2$$

$$V_P = P^3$$

The number (N_P) of product particles is

$$N_P = \frac{V_F}{V_P} = \frac{F^3}{P^3}$$

and the total surface energy (E_P) after crushing is

$$E_P = \frac{F^3}{P^3} \times 6P^2 \times S = \frac{6F^3S}{P} \tag{2.5}$$

The work done (W) is the difference in the surface energies before and after crushing.

Hence

$$W = E_P - E_F = \frac{6F^3S}{P} - 6F^2S = 6SF^3\left[\frac{1}{P} - \frac{1}{F}\right] \tag{2.6}$$

This is the form required. The other formulas can be developed in much the same way.

Today, the Bond Law is probably the most often used:

$$W = K_B\left[\frac{1}{P^{1/2}} - \frac{1}{F^{1/2}}\right] \tag{2.7a}$$

where W = work or energy input to a machine reducing material from a definite feed size to a definite product size. It is expressed in kWh/ton. F = diameter [expressed in microns (10^{-6} m)] of the square hole that will pass 80% of the feed. It is determined from a sieve analysis. P = diameter [expressed in microns (10^{-6} m)] of the square hole that will pass 80% of the product. It is determined from a sieve analysis.

Equation (2.7a) can also be written in the alternate form of

$$W = K_B\frac{F^{1/2} - P^{1/2}}{P^{1/2}F^{1/2}} \tag{2.7b}$$

The constant K_B is expressed using Equation (2.7b) as

$$K_B = W\frac{P^{1/2}F^{1/2}}{F^{1/2} - P^{1/2}} \tag{2.8}$$

and is determined by measuring the amount of energy required to reduce a given feed to a given product. By way of example assume that an input energy of 3 kWh reduces 1 ton of material from a size F = 1600 microns to P = 400 microns. Substituting these values into Equation (2.8) one finds that

$$K_B = \frac{3 \times 400^{1/2} \times 1600^{1/2}}{1600^{1/2} - 400^{1/2}} = 120 \text{ kWh-micron}^{1/2}\text{/ton}$$

Using Equation (2.7a) one can calculate the energy required to go from a feed which is infinite in size (F = infinite) to any given product size P. The energy will be referred to as the total energy or the total work and given the symbol, W_i. Thus

$$W_t = K_B \left[\frac{1}{P^{1/2}} - \frac{1}{\infty^{1/2}} \right] = \frac{K_B}{P^{1/2}} \tag{2.9}$$

For the example,

$$W_t = \frac{120}{1600^{1/2}} = 3 \text{ kWh/ton}$$

Another important special case is the calculation of the amount of energy required to reduce the material from infinite feed size to a product size of 100 microns. This is given the symbol W_i and is the Bond Work Index. Substituting into Equation (2.7a) one finds that

$$W_i = K_B \left[\frac{1}{100^{1/2}} - \frac{1}{\infty^{1/2}} \right] = \frac{K_B}{100^{1/2}} \tag{2.10}$$

Using the example values and solving for W_i one finds that

$$W_i = \frac{120}{100^{1/2}} = 12 \text{ kWh/ton}$$

This Index provides a common basis by which engineers around the world can compare the comminution properties of and the energy requirements for different materials and processes. The total energy (W_t) required to reduce a material from infinite feed size to a product size P_2 can (a) be obtained using Equation (2.9) or (b) by applying Equation (2.8) to calculate the energy required to go to an intermediate size P_1 and then adding the energy needed to go from size P_1 to P_2. The total energy required to go from an infinite size to a product size of 400 microns in the example is

$$W_t = \frac{K_B}{P^{1/2}} = \frac{120}{400^{1/2}} = 6 \text{ kWh/ton}$$

Now as was found earlier, the energy required to go from an infinite feed size to a product size of 1600 microns, was 3 kWh/ton. The measurement made when reducing the 1600 micron material to 400 microns was 3 kWh/ton. Thus the total as expected is 6 kWh/ton.

When taking a total systems approach to the fragmentation process as was discussed earlier in Section 2.2, one must examine both the amount of required input energy and the point at which (and in which form) it should be introduced into the system. In this regard consider the following example in which an approach based upon the Bond Work Index has been applied to a hypothetical blasting and crushing situation. It is based loosely on the Northshore Mine in Minnesota using published data when available and making reasonable assumptions as necessary. Figure 2.10 shows the size distribution of the blasted rock as determined from video films of truck loads of mine run ore (Pastika et al., 1995). Here one can see that the average size was 4.25 ins and the size through which 80% of the material would pass was 9.5 ins. They indicate that in good blasts 80% of the rock is less than 4 ins in dimension. In Bond (1952), Work Index values as calculated from Allis-Chalmers laboratory tests have been presented for samples collected from many mining properties. The values given for Reserve taconite (the predecessor of Northshore Mining) are given in Table 2.1. The Work Index values are given in kWh/ton from infinite feed size to 80% passing 100 microns. This corresponds to about 65% passing 200 mesh. Using all values, the range is from about 11 to 26 kWh/ton with the average being 17. Using

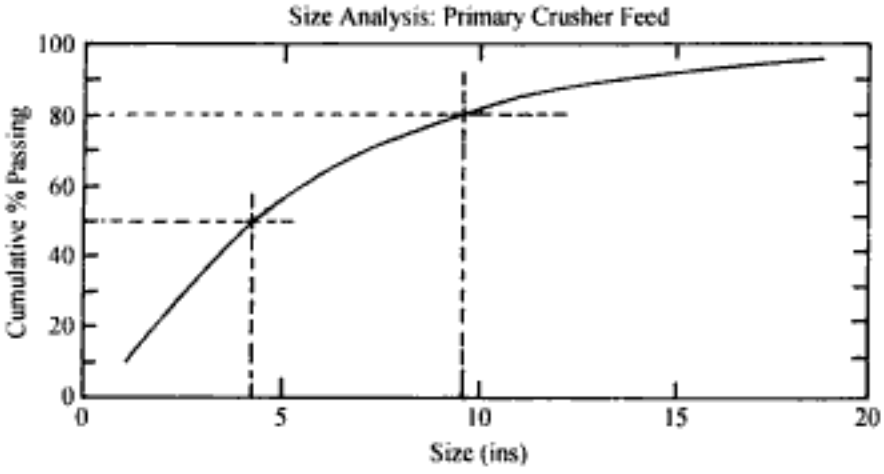

Figure 2.10. Run-of-mine fragment size analysis for the Northshore mine. (Pastika et al., 1995).

Table 2.1. Work index values for Northshore (Reserve) Taconite (Bond, 1952).

Test	Mill type	Spec. gravity	Mesh	Work Index (multiple samples)
1748	Rod		14	16.28, 25.70
2476	Rod		14	18.80, 13.80
2475	Rod		14	18.50, 21.42, 17.75
2159	Impact Crushing	3.50		11.10
1877	"	3.75		14.86, 15.00, 19.28
1748	"	3.07		15.88
1456	"	3.16		16.29
39R	"	3.48		12.07

These work index values have been calculated from laboratory tests conducted by Allis Chalmers. The given values are expressed in kWh/ton for an infinite feed size to 80% passing 100 microns (or about 65% passing 200 mesh).

Equations (2.9) and (2.10) one finds that the total energy required to break the material from infinite (insitu) size to a product of which 80% passes 9.5 ins (0.24×10^6 microns) would be

$$W_t = W_i[\frac{100}{P}]^{1/2} = 17[\frac{100}{24\times10^6}]^{1/2} = 0.35 \text{ kWh/ton}$$

On the other hand the amount of energy required to produce a product with $P = 4$ ins (0.100×10^6) microns would be

$$W_t = 17[\frac{100}{0.100\times10^6}]^{1/2} = 0.54 \text{ kWh/ton}$$

In using this approach the expectation would be that to reduce the product size from 9.5 ins to 4 ins an energy input of 0.19 kWh/ton is required.

It is interesting to compare the energy requirements as calculated using the Bond Work Index with those expended in blasting. An average powder factor of 0.9 lbs/long ton will be used. The energy content/unit weight (E_e) of the emulsion explosive will be assumed to be 93% of that of ANFO or 850 cal/gm. Since 1 calorie is equal to 4.184 Joules, the energy content is

$$E_e = 850 \text{ cal/gm} = 3556 \text{ Joules/gm} = 3.56 \text{ MJ/kg}$$

Since

$$1 \text{ kWh} = 3.6 \text{ MJ}$$

the explosive energy expressed in the same units as electrical energy is

$$E_e = 0.99 \text{ kWh/kg}$$
$$E_e = 0.45 \text{ kWh/lb}$$

Using the powder factor of 0.9 lb/long ton, the total explosive energy per long ton is

$$E_t = 0.9 \text{ lb/lt} \times 0.45 \text{ kWh/lb} = 0.41 \text{ kWh/lt}$$

Since the Bond Work Index value is given in terms of energy/short ton the conversion between short and long ton must be made.

$$1 \text{ short ton} = 2000 \text{ lbs}$$
$$1 \text{ long ton} = 2240 \text{ lbs}$$

hence

$$E_t = 0.41 \times \frac{2000}{2240} = 0.36 \text{ kWh/st}$$

This is of the same order of magnitude as would be calculated using the Bond Work Index. Although this result may simply be fortuitous, it does provide a convenient way for evaluating the amount of explosive energy required to achieve a given fragmentation and compare it with energy being applied through electricity.

It must be noted that nothing has been said about the effectiveness (efficiency) of energy utilization in either process. In the case of the crusher, the electricity is that used to drive the electric motors. In blasting, the theoretical energy of the explosive is used. To perform an actual energy balance, the efficiencies must be known. The approach outlined may, however, be the only practical way to proceed.

In making decisions as to where the energy should be applied to create a certain fragmentation, the cost of energy application enters. The cost of the explosive will be assumed to be \$0.16/lb. Using the energy value/lb determined earlier the explosive cost would be

$$C_e = \frac{\$0.16 / \text{lb}}{0.45 \text{ kWh} / \text{lb}} = \$0.36/\text{kWh}$$

On the other hand, the cost for electrical power is in the range of \$0.05 to \$0.10/kWh depending upon location, demand and other factors. Thus looking simply at energy cost on a kWh basis explosive energy is of the order of 5 times more expensive than electrical energy. However the cost of the system for applying the energy must also be included. It is not fair to examine the energy cost alone. In blasting, additional energy may often be applied to the system by simply increasing the energy of the explosives loaded in the existing holes. However if adding energy to the system requires that new holes be drilled and these filled with explosives then obviously the added energy costs are much higher. In crushing, one has both capital and operating costs to consider. The operating costs involve liner plates, repair/maintenance labor, etc. while the capital costs reflect the investment in

the crushing plant. Hence, in both cases, one must calculate the total real costs involved in energy application expressed in $/kWh and know the energy needed to achieve a certain fragmentation. On that basis the most favorable time and place for energy application can be selected.

2.4 FRAGMENTATION EVALUATION

A critical element in fragmentation system optimization is the development of practical methods for determining the degree of fragmentation. By degree of fragmentation one generally means specifying the average particle size and the distribution of the particles around that mean. Both direct and indirect methods are available for determining the fragmentation. The direct methods include screen analyses, counting boulders, and measuring the pieces directly. The most accurate method of determining fragmentation is obviously to sieve the whole pile. Although this is possible to do for small amounts of material and for very special purposes it is very tedious, time consuming and very costly. This is even more true when measuring the pieces directly. Counting and measuring the boulders (oversize) is a common practice and easily done. It provides information about the extreme tail of the distribution but nothing more.

There are two categories of indirect techniques:

1. Photographic methods
2. Measurement of parameters which can be correlated to the degree of fragmentation.

In applying the photographic technique, the following steps are followed (Rholl et al., 1993b):

1. The photographs are taken with a 35-mm camera, a medium format camera or a video camera.
2. They are then digitized. In the evaluation of the photographs, one can do the digitization by hand or with an automatic image processing program. The hand method is very tedious and time consuming. The scanner screens the image and converts it into an output consisting of x and y coordinates (the intersections of each row and column) and assigns a value corresponding to its shading on the grey scale. This information triple is stored in memory and hence easily accessible for performing further digital evaluations.
3. In the computer technique, special software is used to enhance the rock fragments and to detect the edges. The digitized points are connected to form closed shapes.
4. Once the outlines of the individual rock fragments are defined, the sizes of the individual fragments may be determined.
5. The size of the fragments are related to the minimum screen size through which they would pass.
6. In the final step the fragmentation distribution is calculated.

The accuracy of the photographic assessment technique depends upon controlling the source errors and minimizing their magnitude (Rholl et al., 1993b). Theses errors include:

1. Photographs have limited resolution and rock fragments which are smaller than a certain minimum value will not be observed.
2. Photographs leave a third dimension unexposed.
3. Photographs normally sample only the rock fragments on the surfaces of muck piles.

4. Rock fragments in photographs tend to overlap and may also be cut off at the edges of the photographs.

5. Photographic images can easily be distorted.

6. Image interpretation software can introduce errors, especially in those cases where the surfaces of rock fragments are highly textured.

The principal steps involved in the photographic technique are shown in Figure 2.11. There are also stereo techniques as opposed to the 2-D procedures described above which provide a direct evaluation of 3-D data. However they are time consuming and require high performance, expensive equipment. The photographic technique can be applied to stationary muck faces or muck piles. It can also be used to scan the material as it passes by in haulage trucks or on a conveyor belt. Just (1979) has found that photographs taken of the surface of a muck pile or the digging face are not representative of the whole. Still photographs of the material contained in passing haul trucks does, on the other hand, provide such results. At the Rössing Mine (Hunter et al., 1990) every truck that passes the camera during daylight hours can be sampled in this way. System improvements could include 24 hour photography and capturing live images using video cameras.

Crusher monitoring is one of the techniques which provides an indirect indication of the fragmentation. It includes determining

- Crusher energy consumption
- The type, strength and size of the feed material
- The size of the crushed product
- Crusher throughput

The theory behind this approach has been discussed in Section 2.3.

Another indirect and widely used technique is the monitoring of secondary breaking/blasting costs.

Shovel monitoring is a natural way of following and describing both qualitatively and quantatively fragmentation and fragmentation changes. The diggability or fragmentation indexes developed on the basis of shovel monitoring should incorporate the effects of size distribution, swell factor and muck pile profile. One such monitoring system currently records/produces the following values (Hunter et al., 1990):

- Load time per truck
- Time per dig cycle
- Time waiting for trucks
- Downtime
- Fill angle (arc moved through during the dig motion)
- Swing angle (angle from dig to truck)
- Number of boom jackings and hoists
- Trip outs
- Boom vibration
- Motor voltage, current and energy consumption

These data provide many different possibilities for learning about the effectiveness of the loading operation and identifying improvement possibilities. As Williamson et al. (1983) point out, when developing a degree of fragmentation index it is important to identify a measure which will relate primarily to digging conditions at the face and be insensitive to operator behavior, truck availability, and a variety of other factors which influence

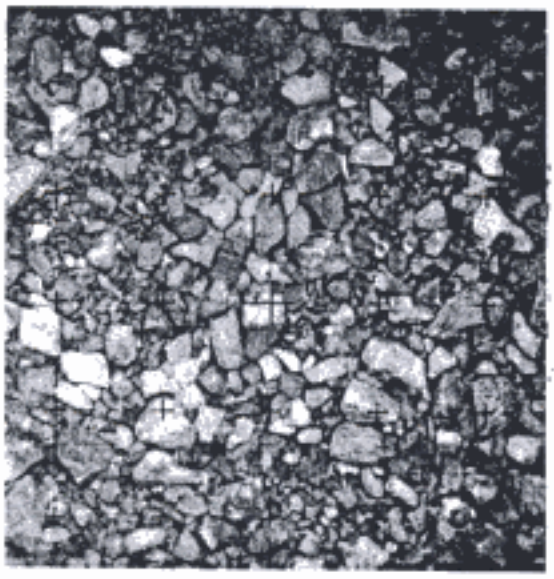

a. Input image for image processing

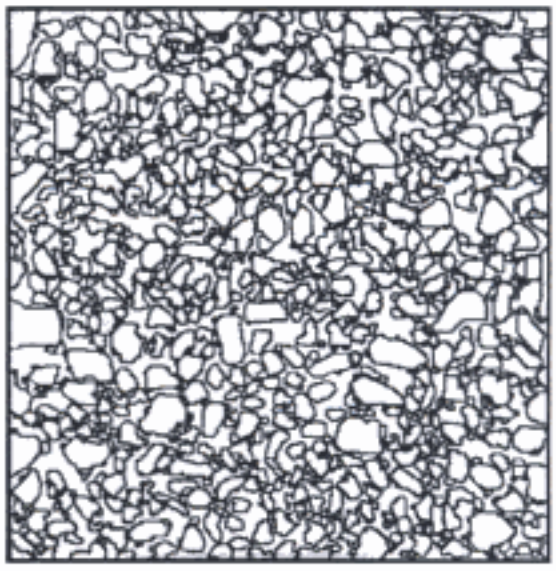

b. Object contours

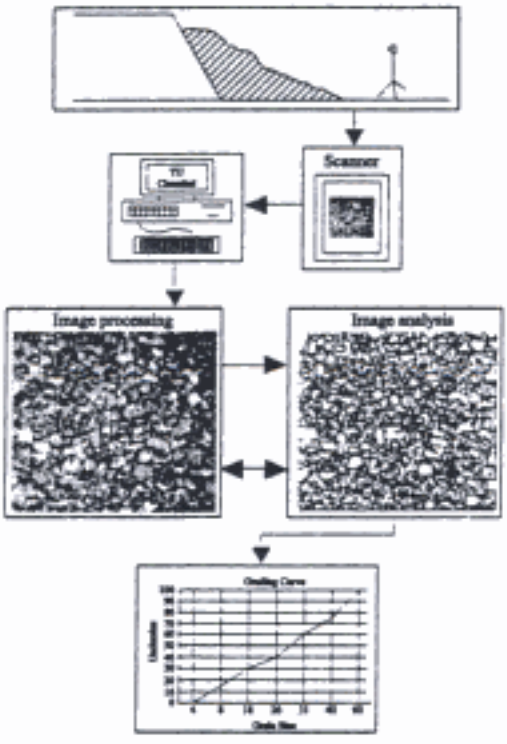

c. Measurement process

Figure 2.11. A fragmentation analysis system (Vogt & Aßbrock, 1993).

productivity. In the shoveling action shown in Figure 2.12 and described earlier in Chapter 1 the dipper is forced into the bank through the use of the crowd action while being lifted with the hoisting movement. The load is then swung and dumped. With respect to focussing on fragmentation conditions and largely eliminating the other factors, only the digging section of the operating cycle is considered. For electric loading shovels the following parameters are easily monitored from the relevant electrical circuits:

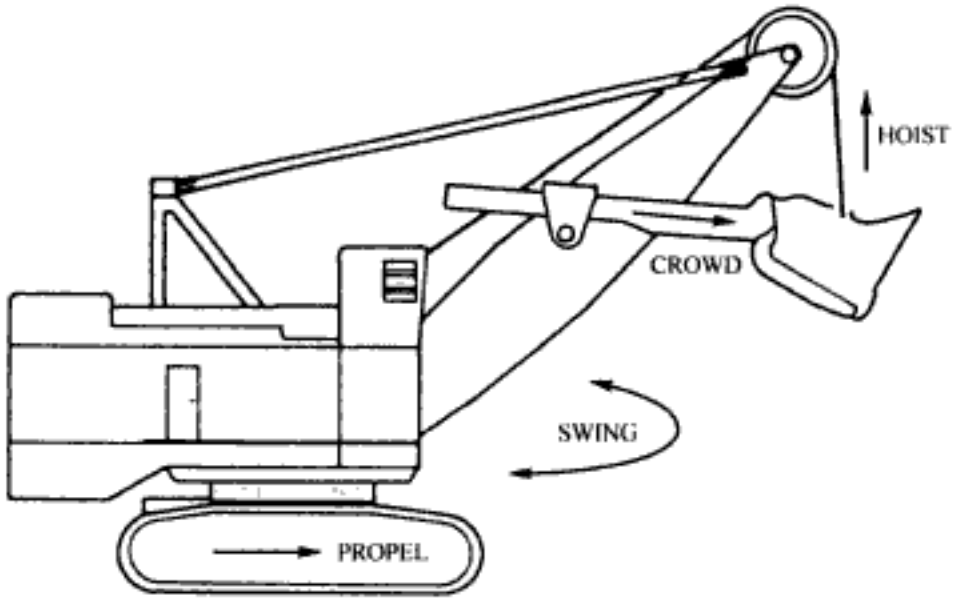

Figure 2.12. The shovel actions involved in the mining process (Williamson et al., 1983).

- Crowd armature voltage and current
- Hoist armature voltage and current
- Dipper trip (dump) relay and the crowd/propel relay.

A number of different indexes have then been developed based upon using these measurements. Three of these are:

- Dig Utilization Index
- Diggability Index
- Boom Vibration Index

Williamson et al. (1983) define the Dig Utilization Index as the ratio of the number of buckets hauled to the total number of digging actions. This gives an indication of the rilling characteristics or tightness of the face as well as the face profile. A related index is the Bucket Fill Factor which is the ratio of the minimum number to the average number of bucket loads per truck observed under the given digging conditions. The Diggability Index (Williamson et al., 1983) is a more complicated index based upon a shape analysis of the crowd motor voltage signals during digging. An alternative index based on the crowd motor power consumption is easily computed from the voltage and current signals. However it has been found to be less sensitive to the fragmentation than the crowd voltage. This index reflects the effects of size distribution and swell factor. The Boom Vibration Index (Hunter et al., 1990) is defined as the number of peaks above a certain threshold recorded by a tilt sensor mounted on the boom during the loading of one truck. It gives a measure of digging conditions, operating characteristics and is a direct measure of loading severity on the boom's mechanical structure.

Figure 2.13 is a flow sheet which shows how the fragmentation and the diggability components are combined at a mining operation to define the overall blast results.

With respect to mean fragment size and distribution there are predictive techniques available based upon the rock type and the explosive/pattern being used. These techniques will be discussed in Chapter 4.

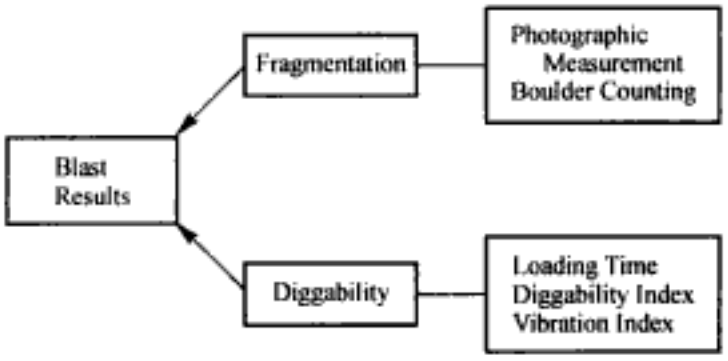

Figure 2.13. The diggability and fragmentation inputs for evaluating blasting results (Williamson et al. 1983).

2.5 OPTIMUM FRAGMENTATION CURVES

2.5.1 *The MacKenzie fragmentation curves*

Some 30 years ago, MacKenzie (1966, 1967) presented his now classic conceptual curves showing the cost dependence of the different mining unit operations

- Drilling
- Blasting
- Loading
- Hauling
- Primary crushing

on the degree of fragmentation. They are presented in their original form in Figure 2.14. As can be seen some of the costs decrease with increasing fragmentation while others increase. By adding the curves together one obtains the overall cost versus degree-of-fragmentation curve presented in the lower part of the figure. It has the form of a saddle indicating that there is a certain degree of fragmentation for which the overall cost is a minimum. In the particular case shown, the base of the saddle is quite broad suggesting that the overall costs change little over a wide fragmentation range. Before discussing the development and application of these curves it is important to understand the logic behind them. Beginning with the loading, hauling and crushing curves the logic, as presented by MacKenzie, is as follows:

Loading
An increase in the degree of fragmentation will give the shovel a higher rate of productivity. At standard operating costs per hour (for all practical purposes independent of the production rate) this will result in lower costs per ton or cubic yard moved. The effect of wear and tear will also decrease, giving lower operating cost per hour.

Hauling
Under similar conditions of haul, lift, size and type of truck and haul road conditions, truck production per hour will increase with greater degree of fragmentation due to faster shovel loading rates and a decrease in bridging (and hence waiting time) at the crusher. There will be a consequent decrease in cycle time. At a standard operating cost per hour, this increase in truck speed or productivity will result in lower unit operating costs.

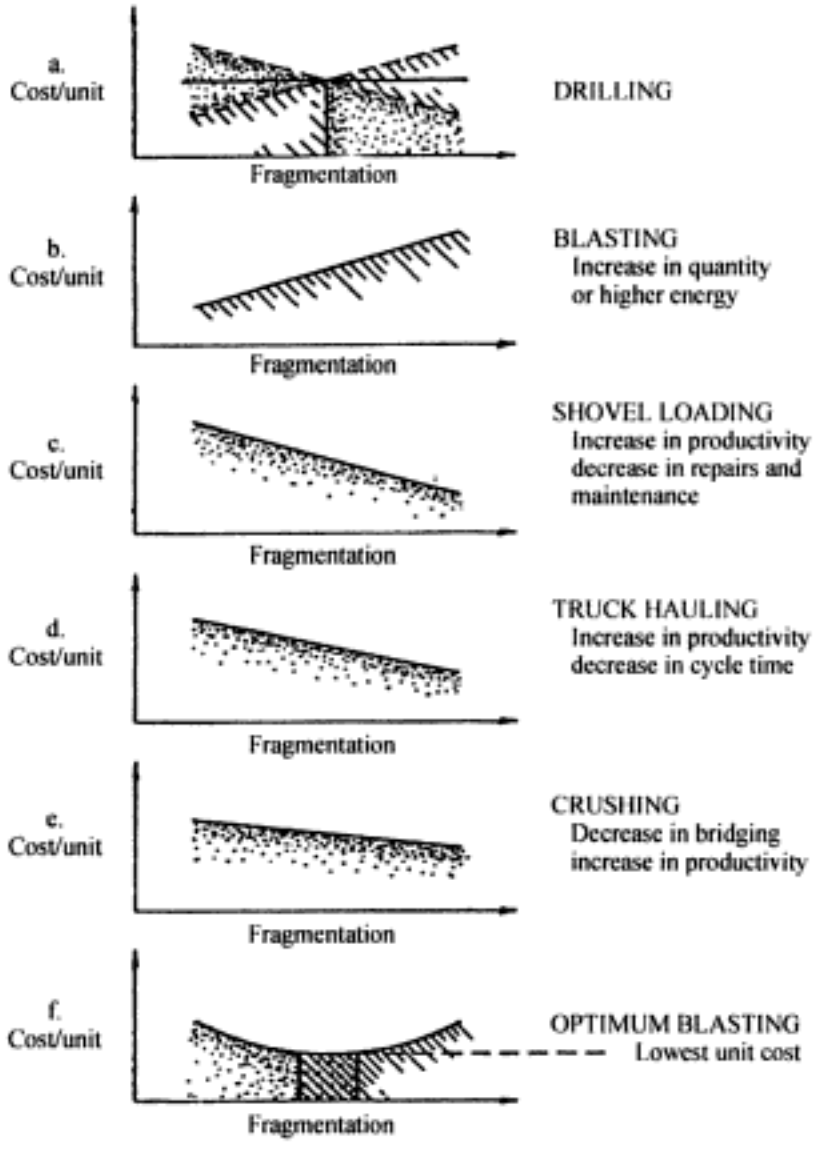

Figure 2.14. The effect of the degree of fragmentation on the individual unit operation costs and on the overall cost (MacKenzie, 1967).

Crushing

An increase in the degree of fragmentation gives lower crushing costs as more material passes through as undersize. Liner costs, repair and maintenance, and bridging time will decrease and the crushing rate per hour will increase. As indicated decreased bridging time also cuts down on truck delay time at the crusher which in turn gives higher truck and shovel productivity. Any increase in degree of fragmentation means less work for the crusher. The % bridging time is one indicator, along with shovel loading rate of this degree of fragmentation.

These have been the easiest to explain since the unit costs always decrease with increasing fragmentation. The same is not true for the drilling and blasting costs. There are many possible combinations which can occur depending upon the particular design. The following explanation has been patterned after that given by MacKenzie.

Blasting

For a given rock type, geologic structure, and firing sequence, an increase in the degree of fragmentation may be achieved by (a) increasing the consumed quantity of a given explosive, (b) changing to an explosive having greater energy content per unit hole volume (higher energy content/ density), or (c) combinations of both.

For blasting case (a) the associated drilling cost would increase if the explosive quantity were to be increased by simply drilling the same diameter drill holes but on a tighter pattern. Thus there would be more drill holes required to blast a given volume. If larger diameter drill holes were substituted and the increased hole volume (explosive quantity) achieved in this way then the rate of increase or decrease would depend upon the comparative drilling cost per foot of hole. For case (b), presuming that the same hole diameter and pattern is used, the drilling costs would remain constant independent of the fragmentation. For case (c) the drilling cost could 1. Remain constant, 2. Increase or 3. Decrease depending upon the situation. If the same fragmentation is desired and a more energetic explosive is substituted for the one currently in use, then the unit drilling cost could decrease due to the possibility of increasing the hole spacing (spreading the pattern).

In his original presentation MacKenzie has explained the drilling dependence as follows:

'Drilling. Generally speaking, for a given type of drilling and of explosive, the cost per cubic yard or ton will remain constant or increase with the degree of fragmentation. If higher energy explosives are substituted, the drilling cost per yard will decrease. The rate of increase or decrease or decrease will be dependent upon the drilling cost per foot.'

Unfortunately, by attempting to present several of the different possible combinations on the same drilling figure (Fig. 2.14a) the close coupling between the drilling and blasting costs is lost and the possibility for confusion arises.

In terms of the practical determination of degree of fragmentation MacKenzie suggested that the most effective evaluation is obtained by using the shovel loading rate, exclusive of all delays. The degree of secondary breaking, high bottom, and bridging delays at the crusher may be used in conjunction with shovel loading rate to achieve a better correlation.

Before discussing some practical applications of the concept, it is perhaps well to present some background information regarding the Quebec-Cartier Mine applicable at about the same time as these papers by MacKenzie were written. Table 2.2 describes the main mining unit operations with particular emphasis on the drilling and blasting whilst Table 2.3 gives the estimated costs and the cost distribution.

The costs in Table 2.3 should help to put the effects associated with cost increases or decreases of the different unit operations into perspective. The changes which were underway in 1967 were to increase the hole size, to expand the pattern and to convert to a metallized slurry explosive. The approach described in his papers was used as a way of evaluating the different options/combinations.

There are numerous ways in which overall cost-degree of fragmentation curves can be used. Two will be discussed here using the MacKenzie results. In the first example it will be assumed that one has an explosive and a drill pattern which yields suitable fragmentation (Pattern A). Due to various reasons one would like to evaluate other alternatives which would yield at least equally good results and hopefully at a lower cost. This case, is shown diagrammatically in Figure 2.15. One does not care at which absolute point on the

Table 2.2. Information regarding the Quebec-Cartier Mine (Pfleider & Weaton, 1968).

1. Ore type: Taconite
2. Drilling
   12 1/4" diameter rotary bits in ore (9 7/8" and 12 1/4" in waste)
   penetration rate = 14.5 ft/hr (16 ft/hr)
3. Blasting
   powder factor = 0.70 lbs/ton
   explosives used: ANFO, slurry, metallized slurry
   bench height = 40 ft
   subgrade = 4 ft
   spacing = 23 ft (24-30 ft)
   burden = 23 ft (24-30 ft)
4. Loading, hauling and crushing

Table 2.3. Estimated direct operating costs and the cost distribution for the Quebec-Cartier Mine (Hammes, 1966).

Unit operation	Cost ($/lt)	Cost (%)
Drilling	0.06	13
Blasting	0.11	23
Loading	0.07	15
Hauling	0.18	38
General	0.05	11
TOTAL	0.47	100

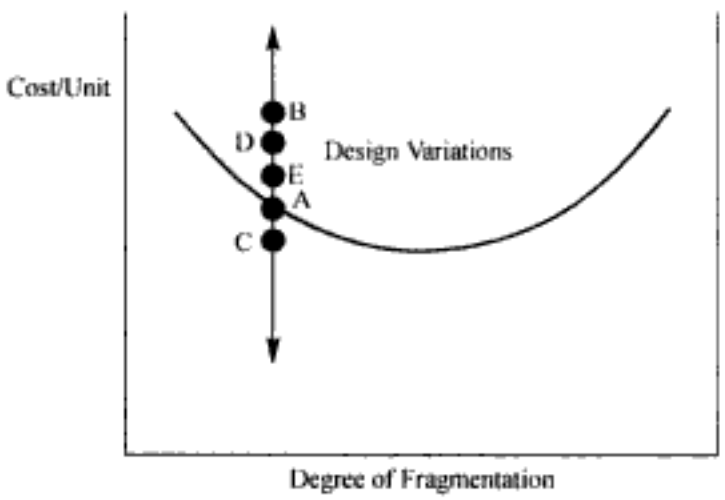

Figure 2.15. Diagrammatic representation of flexing the blast design while maintaining constant fragmentation.

overall curve one is operating but simply that the fragmentation remains more or less the same. Shown superimposed on the curve are the results of four different patterns and from this it appears that Pattern C is an interesting alternative.

Consider the case of the Quebec-Cartier Mine where the drill holes were 9 7/8 inches in diameter and the bench height was 40 ft. These were maintained constant. In the system current at that time, the lower portion of the blasthole was loaded with a bottom charge of a high energy, water resistant, more costly explosive. Then in a second operation, the upper part of the hole was loaded with a column charge consisting of a lower cost, lower en-

ergy, water-sensitive explosive. This two part charge will be denoted as Pattern A. For the square pattern of holes with a hole spacing of 22.5 ft, the fragmentation was considered satisfactory. It will be assumed that the drilling cost for each hole is $220. For Pattern A the explosive cost per hole is $120 and hence the total drilling and blasting cost per hole is $340. Since each hole breaks a volume (V_H) of

$$V_H = \frac{[22.5\text{ ft} \times 22.5\text{ ft} \times 40\text{ ft}]}{27\text{ ft}^3/\text{cy}} = 750\text{ cy}$$

the fragmentation costs are $0.45/cy. It is desired to replace this system by one in which the entire hole is filled with a water resistant explosive in one pass. This is to be done while maintaining current fragmentation and costs. There were four possible explosives to choose between. The costs ($/hole) associated with each are given in Table 2.4.

It is obvious from examining Table 2.4 that the hole spacing must be increased for all of the candidate explosives in order to maintain the current cost/cy. The cost ($/cy) for each of the explosives is shown as a function of the hole spacing (assuming a square pattern) in Figure 2.16. A series of blasting tests were performed with each of the explosives. The hole spacing yielding the same fragmentation as the current pattern was identified. These positions are shown on the figure by the large filled circles. As can be seen, even though the cost per hole is significantly more than that for the current pattern, Explosive C due to its increased breaking ability and the spreading of the pattern yields a lower

Table 2.4. Costs for the different alternatives.

Explosive	Costs ($/hole) Drilling	Explosive	Total
A (current)	220	120	340
B	220	260	480
C	220	275	495
D	220	320	540
E	220	340	560

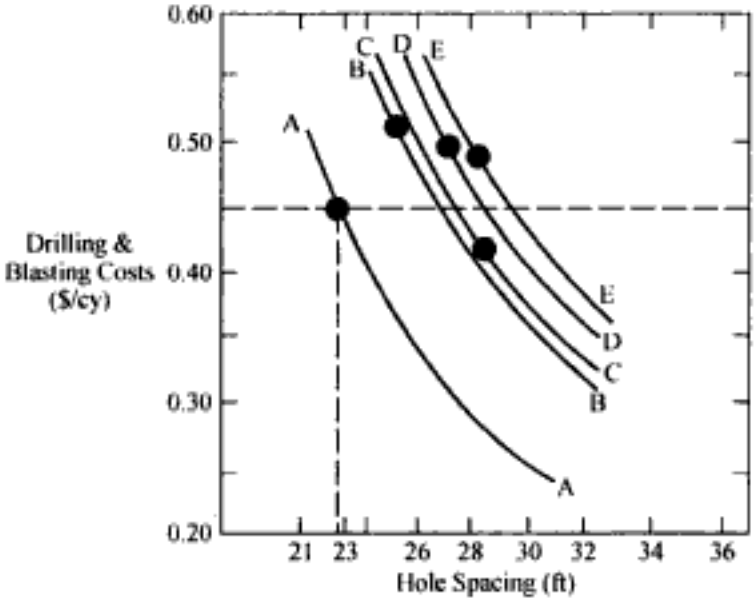

Figure 2.16. Results from the Quebec-Cartier mine when blast design flexing under constant fragmentation conditions.

cost/cy than Explosive A. The decision was made to change to this explosive which turned out to be the metallized slurry. Assuming a specific gravity of 3.3 for the ore, the drilling and blasting cost would be $0.18/lt which is similar to those given in Table 2.3.

A second application of the approach would be that once the explosive and the hole diameter has been chosen, one could flex the pattern by changing the hole spacing and thereby vary the specific charge (the amount of explosive per unit of rock). A common form of specific charge is the so-called powder factor. As the spacing is increased or decreased there should be a corresponding change in the degree of fragmentation observed. Based upon the corresponding economic analyses one's position with respect to the optimum can be determined. This type of test is shown diagrammatically in Figure 2.17. Obviously one could also vary several parameters at the same time (explosive, hole pattern, etc) however then it is much more difficult to identify the cause of the improvement or degradation. The results from test series performed by MacKenzie to select the new explosive and pattern were apparently also used to study the position on the overall cost-degree of fragmentation curve. The results are shown in Figure 2.18. There is good correlation between these actual results and the conceptual curves shown in Figure 2.14. with the possible exception of the blasting. The summary cost curve is as shown in Figure 2.19. The question marks reflect the possible types of curve extension with increasing fragmentation. All would suggest that the current patterns lie on the left flank of the curve and that further improvement is possible.

In summary, this approach to determining the optimum fragmentation makes good sense. Since those costs associated with producing an increase in fragmentation (drilling and blasting) increase while those related to handling the product (loading, hauling and crushing) decrease there should be a certain fragmentation or fragmentation range yielding a minimum overall cost. The fact that the optimum is apparently quite broad is positive in the sense that a pattern lying somewhere in the optimum range would be expected to function nearly equally well when one of the non-controllable inputs such as rock type/rock conditions varies somewhat. The curve would also suggest that once one has a workable design, presumably lying in the optimum range, there is little economic incentive to seek the 'true' optimum. In short, there is reason to establish patterns giving 'satisfactory' results in the different rock types occurring in the open pit but little reason to seek optimums. This obviously simplifies the *production* blast design/layout problem markedly.

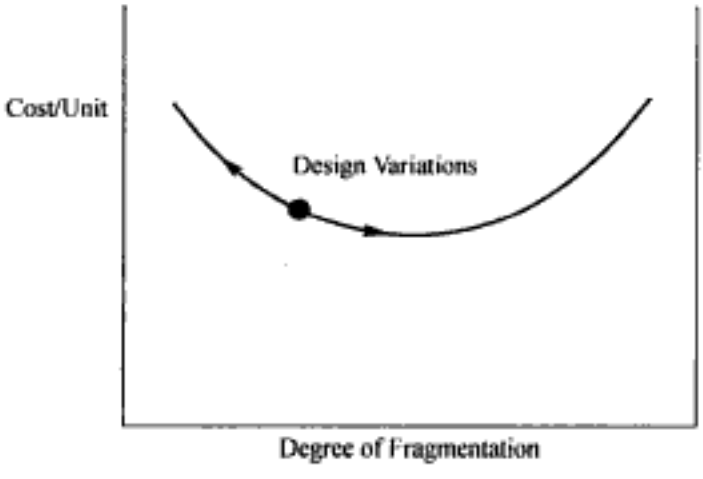

Figure 2.17. Diagrammatic representation of the optimum seeking process.

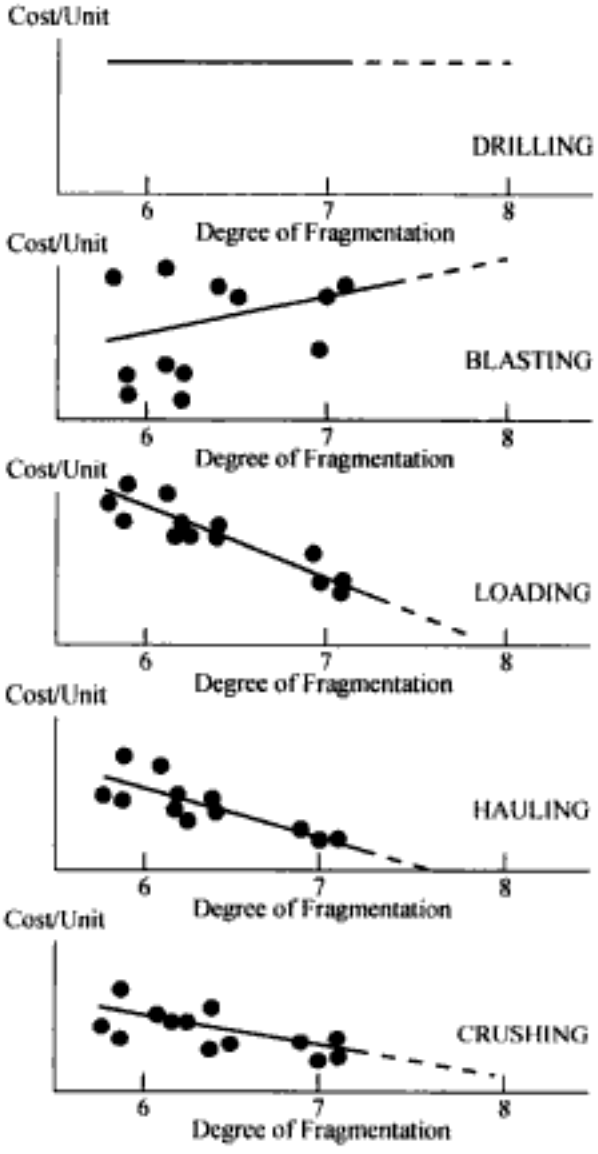

Figure 2.18. Unit costs as a function of the degree of fragmentation for the different unit operations at the Quebec-Cartier mine (MacKenzie, 1967).

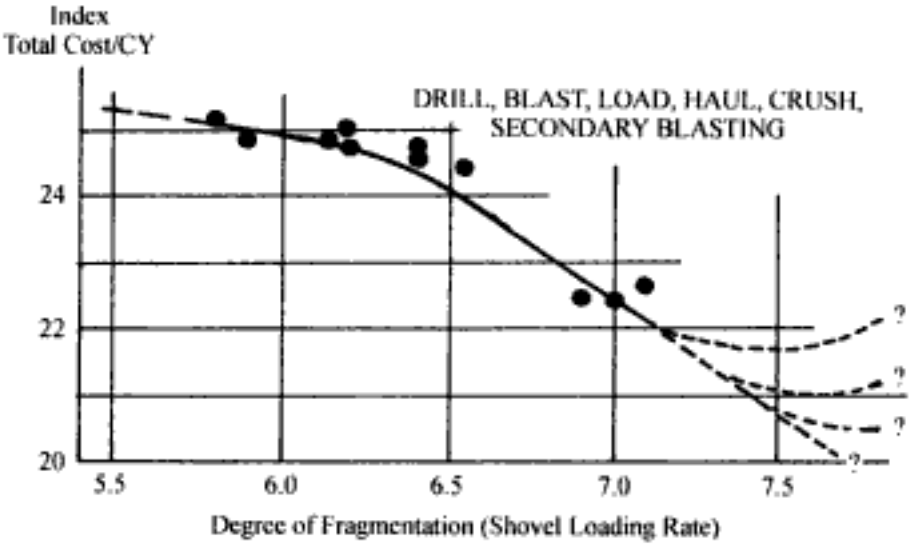

Figure 2.19. Relative total cost versus degree of fragmentation curve for the Quebec-Cartier mine (MacKenzie, 1967).

2.5.2 *The Minntac experience*

There is, unfortunately, very little data available in the technical literature providing practical substantiation of the MacKenzie optimum fragmentation concept and the value of seeking and operating in the optimum region. There are several probable reasons for this. The first of these is that the required data are difficult to obtain especially given the natural variations within a pit. A second reason is that if the 'optimum' region is quite broad with little change in unit cost over a range of reasonable fragmentation conditions then there is little point in seeking out the optimum and operating there. This is probably the case for the soft and even medium strength rock formations especially if one considers only the direct mine related fragmentation costs. For stronger, harder, more abrasive rock formations with a large amount of downstream crushing and grinding, the situation is quite different. This is one explanation why the examples presented in this Chapter all involve the mining and processing of taconite ore which is one of the meanest in those respects in the world. Eloranta (1995) has presented an interesting series of results aimed at evaluating the optimum blast fragmentation point for the Minntac Mine which is located in the central part of the Mesabi Range at Mt. Iron, Minnesota. In 1994, a total of 49,130,952 long tons (lt) of taconite ore were mined and 14,440,418 long tons of taconite pellets shipped (Inspector of Mines, 1995). The weight of one long ton (lt) is 2240 lbs. Using the ore mined and the amount of pellets produced one finds that, on average, 3.4 long tons of taconite ore are required to produce one long ton of pellets. In collecting and presenting his data Eloranta has used the powder factor (defined as the amount of explosive (lbs) used per long ton broken) as the measure of fragmentation. By doing this, he assumes that the degree of fragmentation increases linearly with the powder factor. The explosive used at the Minntac Mine is a blend of ammonium nitrate/fuel oil (ANFO) and emulsion and goes by the generic name of heavy ANFO. The characteristics of this type of explosive will be discussed in detail in Chapter 7. Since the energy content per unit hole volume changes with the relative proportions of the two components, Eloranta has normalized the results by calculating an ANFO equivalent powder factor. Although the powder factor is expressed in terms of lbs/lt of mined ore, some of the results are given in terms of powder cost per long ton of pellets ($/lt). This transformation is easily made knowing the powder factor, the cost of the explosive ($/lb), and the number of ore tons required to produce a ton of pellets.

Minnesota has a typical inland climate with warm summers and cold winters. Thus it might be expected that the seasonal variations would affect the results. Figure 2.20 which is a plot of shovel loading rate (lt/min) versus monthly temperature reveals that this factor must be included when combining results collected during different times of the year. Figure 2.21 is a plot of the shovel loading rate as a function of powder factor with the correction for seasonal variation taken into account. The same type of temperature dependence as was observed for shovel loading (Fig. 2.20) was also observed for the crusher throughput and, in addition, the rate was also adversely affected by the snow depth. Figure 2.22 shows the variation in crusher throughput (as corrected for temperature and snow depth) and the powder factor over the period 1990 to the middle of 1993. As can be seen there is no clear relationship. The crusher throughput has, in general, steadily increased whereas the powder factor has remained more or less constant.

The ore undergoes a large amount of fine crushing and grinding to liberate the magnetite from the waste rock and the plant is by far the major consumer of electrical energy. To try

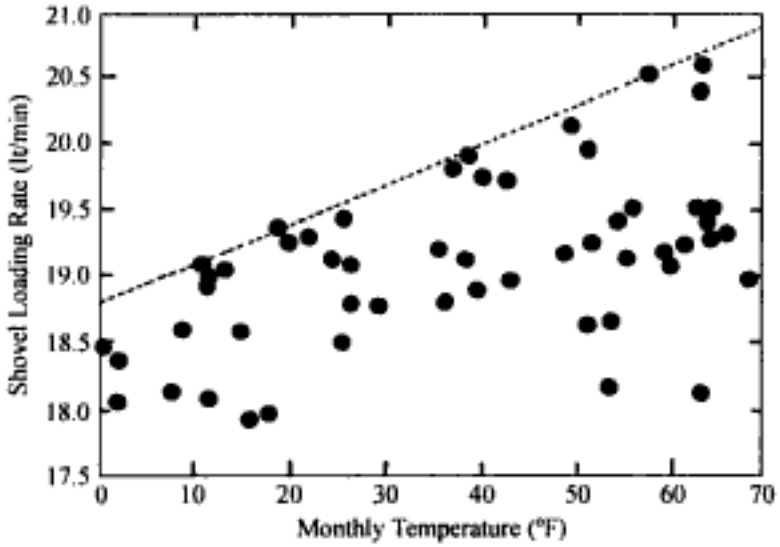

Figure 2.20. The shovel loading rate as a function of monthly temperature (Eloranta, 1995).

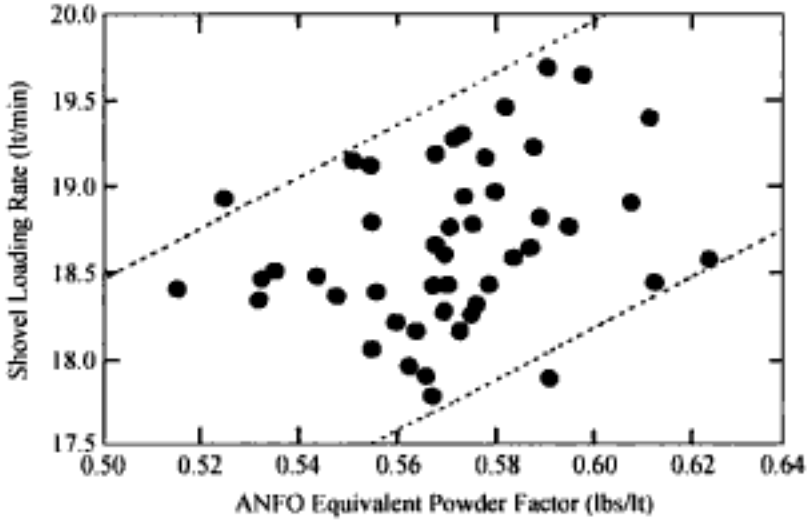

Figure 2.21. Shovel loading rate as a function of powder factor (Eloranta, 1995).

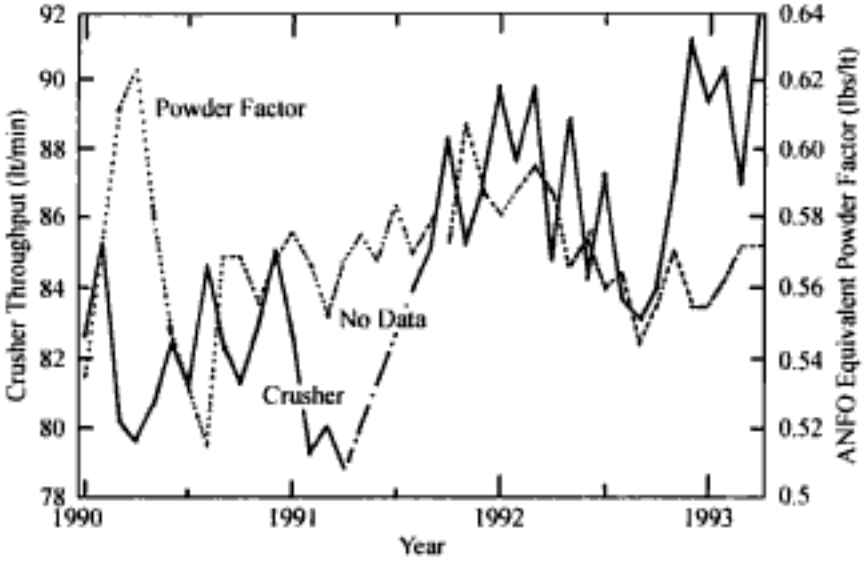

Figure 2.22. An historical view of crusher throughput and powder factor changes at the Minntac mine (Eloranta, 1995).

and assess how the fragmentation in the mine affects the downstream fine grinding costs it is natural to examine the electrical consumption per ton of pellets produced. However as seen in Figure 2.23 this is also strongly temperature dependent and hence this must be taken into account. Furthermore the electrical energy consumption is largely independent of ore grade but the pellet production per long ton of ore is strongly dependent on grade. Thus when considering electrical cost per ton of pellet production ore grade must be included. The relationship between electrical cost (as corrected) and powder cost is given in Figure 2.24.

Other costs associated with fragmentation are those related to the dipper. These have been simply grouped together under the heading of 'teeth' cost with the results shown in Figure 2.25.

Combining the electricity, teeth and powder costs ($/lt of pellets produced) and plotting the result versus powder cost ($/lt of pellets) on obtains the result depicted in Figure 2.26. As with the other plots there is quite a lot of scatter although there does appear

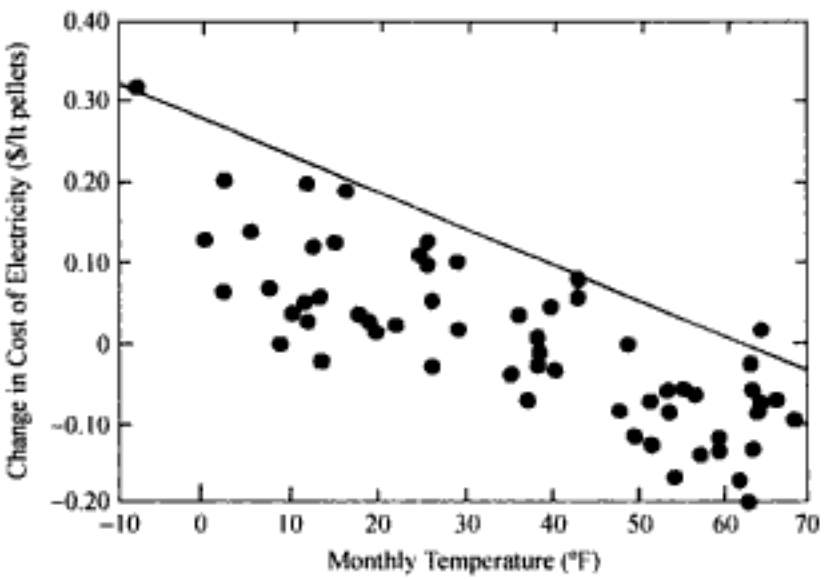

Figure 2.23. Electrical power cost as a function of monthly temperature (Eloranta, 1995).

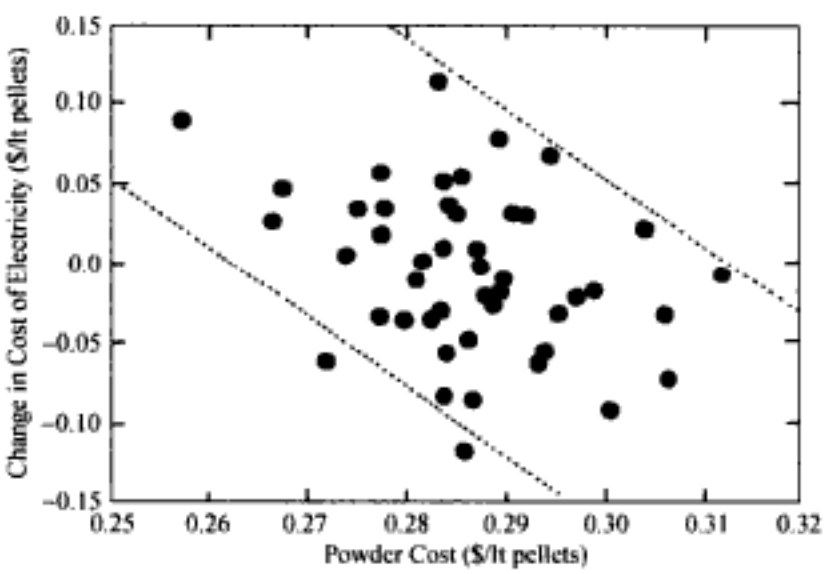

Figure 2.24. Change in electrical cost as a function of powder cost (Eloranta, 1995).

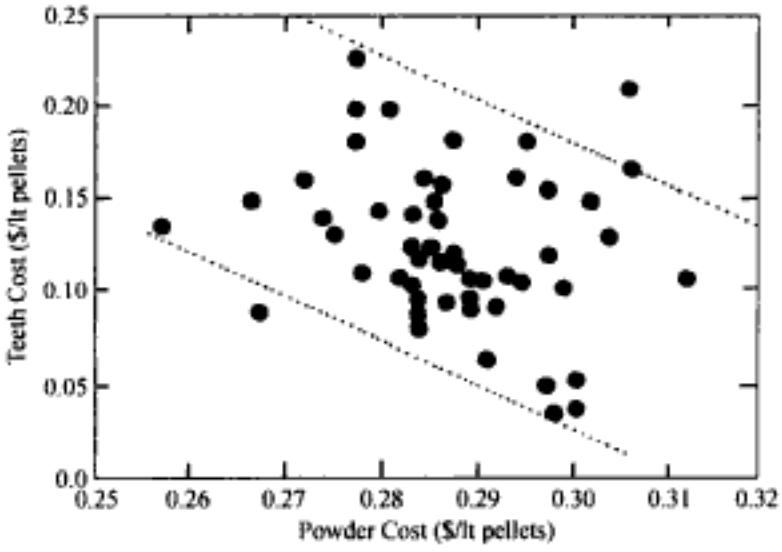

Figure 2.25. Dipper teeth cost as a function of powder cost (Eloranta, 1995).

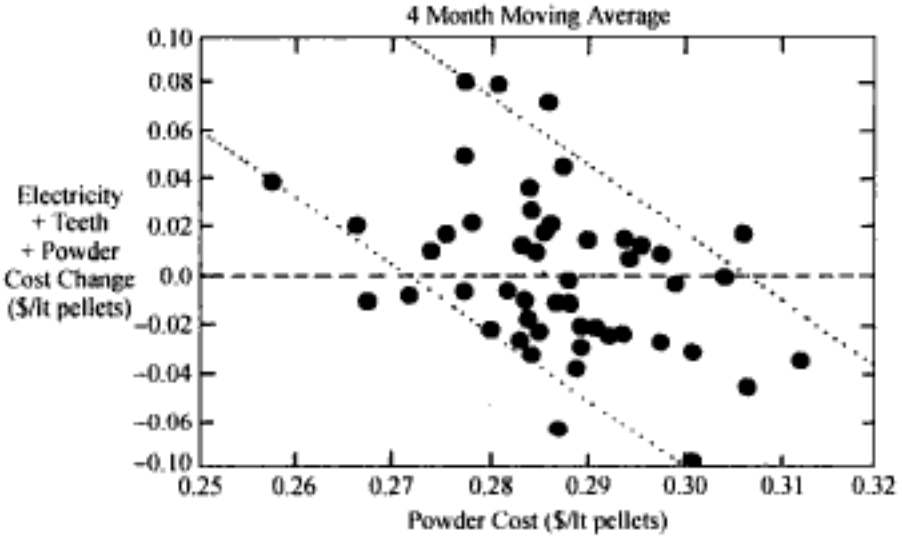

Figure 2.26. The cost of electricity, dipper teeth and explosive as a function of explosive cost (Eloranta, 1995).

to be a trend of decreasing cost with increasing powder factor and by implication increasing degree of fragmentation. Such a trend would suggest that the current blasting is on the left flank of the optimum curve and that there might be merit in increasing the energy going into primary rock breaking. This study shows very clearly the complexity of the problem of data collection and analysis.

2.5.3 *Computer-based information system approach*

It is obvious that there are a great many factors that go into the construction of the overall cost versus degree-of-fragmentation curve. First one must have a good system for evaluating the degree of fragmentation. Some of the various possibilities were discussed in Section 2.4. Of these, those in which the data are captured and processed automatically and directly into quantitative measures such as loading machine operating parameters and/or image processing systems are the most interesting since no intermediate handling or man-

ual data entry is necessary. The second part of the process is to identify and track the relevant costs. The third part is to relate the costs and the degree of fragmentation achieved with the patterns/explosives used. Hunter et al. (1990) have described the computer-based system used by them at the Rössing Uranium Mine to collect and process the information required to construct fragmentation cost versus degree-of-fragmentation curves. It uses the following data bases:

1. Mine Operating Cost Data Base.
2. Drill and Blast Management System

This system contains the records regarding the blast design, operators records of drilling and charging, and routine observations of boulders and digging conditions made by the blast foremen

3. Blast Analysis System

This system contains the surveyed coordinates of each blasthole and the blast outline geometry. It is used for locating the position of the shovel while loading and for correlating the blast results with position within the blast.

4. Management Information System

This system reports on all haul truck and shovel operations using data received via the dispatch system. The information is used in conjunction with shovel monitoring in order to correlate the results with the area in which the shovel is digging. It is also used in conjunction with the Fragmentation Analysis System to identify the source and destination of the material photographed in each truck.

5. Fragmentation Analysis System.

This is a computerized method for analyzing photographs of broken rock for making size distribution (fragmentation) determinations.

6. Shovel Monitoring System.

This is computer system mounted on each shovel which monitors crowd and swing motor voltages/currents, boom tilt and a number of factors which are used to calculate diggability as well as other indexes.

7. Mine Maintenance System.

This system provides data regarding the long term consumption and cost of the major components (boom, crowd gearbox and dipper sticks) affected by digging conditions. For example, severe shock loading occurs when high bottoms and boulders are met while digging.

Even after gathering these data and having them in a manageable form their interpretation is complex because of the great many factors involved.

2.6 FRAGMENTATION SYSTEMS ENGINEERING IN PRACTICE

The Mesabi Range, the Fabulous Giant, is still very much alive today. But times have changed. Where there were more than 100 mines in operation on the Range in 1910, today there are 9. Of these there are 3 which still send to market the natural ores which were the trademark of the Range up until the 1960s. The 1994 natural ore tonnage of slightly more than 500,000 long tons pales in the face of the nearly 21 million long tons sent during 1910. However the total tonnage sent to market from the Range in 1994 was nearly 44 million long tons. The difference between the natural ores and the total tonnage was made

up of a highly processed product in the form of pellets. The iron instead of being contained in the soft, easily worked hematite ore is now in the form of magnetite grains tightly bound in taconite some of the hardest rock known. There are currently 7 mines on the Range producing these pellets from taconite. To produce the pellets nearly 140 million long tons of ore were mined and 30 million cubic yards of waste stripped in 1994. The employment was just about 6000 people. To be economic, the fragmentation system used to liberate the iron first from insitu and then down to the last stages where the individual grains are liberated must be very effective.

This section describes the fragmentation system and strategy employed by the Northshore Mining Company located at the Eastern tip of the Range. The material being mined is the hardest of the taconites. The discussion which follows is based largely upon the papers presented by Pastika (1995) and Indihar (1991).

Northshore Mining Company, a subsidiary of Cleveland Cliffs, Inc., mines approximately 10 million long tons of taconite running 25.8% magnetic iron per year at its Peter Mitchell Mine in Babbitt, Minnesota. Mining began at the property in the early 1950s under the auspices of the Reserve Mining Company, one of the two pioneering large scale taconite operations on the Range. It closed in 1986 due to poor economic conditions. It was reopened in 1990 by Cyprus Minerals and on October 1, 1994 Cliffs Minnesota Minerals Company took over the ownership and the operations. At the mine the ore is drilled, blasted, loaded, hauled and crushed to –4 inch before being shipped 47 miles by rail to the E.W. Davis Works at Silver Bay. A capsule view of the mining as practiced at the Northshore mine with particular reference to the drilling and blasting operations is given in Table 2.6. At the Davis Works the ore is crushed to –3/4 inch, ground to 89% passing 325 mesh, concentrated using magnetic separation and flotation, and finally pelletized in one of two traveling grate furnaces.

Table 2.6. Details of the Northshore mining operation (Pastika et al., 1995).

1. 1994 Production
   - 9,964,610 lt ore mined
   - 3,505,652 lt pellets shipped
   - 281,026 cy waste removed
   - ore to pellets ratio = 2.84
   - average ore grade 25.8% magnetic iron
   - number of employees = 417
2. Taconite ore
   - specific gravity = 3.0 to 4.0 depending on the iron content. Average = 3.35.
   - Moh's hardness = 7.0
   - uniaxial compressive strength = 50-70,000 psi
3. Drilling
   - hole diameter = 16 ins
   - very hard rock tungsten carbide button bits
   - penetration rate = 30 ft/hr
   - bit life = 1300 ft
   - pulldown = 90,000 lbs
   - rotation rate = 80 rpm
4. Loading
   - 13 cy electric shovels
5. Haulage
   - 100 ton capacity trucks

Table 2.6. (continued).

6. Crushing
   - 1-60 in gyratory primary crusher
   - 4-30 in gyratory secondary crushers
   - final product –4 ins.
7. Grinding
   - 89% – 325 mesh
   - 70% – 500 mesh
8. Blasting
   - emulsion explosive, SG = 1.35, cost = $0.16/lb
   - average powder factor = 0.90 lbs/lt
   - average bench height = 45 ft.
   - staggered pattern = 30 ft × 30 ft
   - subdrill = none
   - stemming = 12 ft
   - Primadet detonators
   - 2-2 lb boosters/hole
   - surface lines = 25 grain Primacord
   - rows fired en echelon with 35 ms delays between rows
   - individual hole delays within each row
   - decked charges sometimes used
   - average shot size = 500,000 lt
   - blast security radius = 5000 ft

The process of producing a marketable product from taconite can be broken down into three distinct stages:

- Disassembly
- Separation
- Reassembly

As indicated earlier, in the *disassembly* stage, the ore is

- Drilled, blasted and crushed (coarse crushing) to –4 inches at the mine and then sent to the mill where it is
- Further crushed to –3/4 inches (fine crushing) and then
- Ground (fine grinding) to 89% passing 325 mesh.

Separation is the process of picking the –325 mesh magnetite particles out of the mixture created during disassembly. It is done both magnetically and by flotation. *Reassembly* is the process of putting the iron particles back together in a form and size that can be shipped and utilized by a blast furnace.

For the particularly hard ore at Northshore the relative costs of these three stages as a percentage of the direct costs of producing one long ton of pellets are:

Disassembly	43%
Separation	11%
Reassembly	46%

From this it is obvious that

breaking rock is a major part of the costs involved with producing a final product.

A closer examination of the costs will now be performed beginning with those normally considered as direct mining costs. These are expressed below as a percentage of the total mining cost:

Drilling	14%
Blasting	22%
Pit handling (loading, hauling, misc,)	64%

Drilling and blasting costs, particularly explosive costs, are one of the biggest single line items in any hard rock mining budget. The tendency and practice, at times, has been to minimize mining costs by reducing costs for blasting. When looking at all of the costs associated with the disassembly process, the picture becomes:

Drilling	5%
Blasting	8%
Pit handling	23%
Coarse crushing	8%
Fine crushing	20%
Fine grinding	36%

The pit handling costs have been included as disassembly costs even though no size reduction occurs since the cost of delivering the broken ore to the crusher is a direct function of fragmentation and a major portion of the overall cost at this stage.

From this it is clear that

– Breaking rock gets more expensive downstream

– The entire mining process begins with drilling and blasting and all downstream efficiencies and costs are controlled by effective fragmentation.

To put drilling and blasting costs in perspective, although they stand by themselves as significant line items, they are but a small part of the overall costs. Of further and major importance, drilling and blasting are the first step in the disassembly process and control to a large degree all downstream costs, including in-pit handling. Thus drilling and blasting have a large leverage on overall costs out of proportion to their relative size.

This leverage is increased by the fact that, in addition to any direct downstream savings that can result, better fragmentation also permits major redesigns/changes in the mining process with very high cost-savings potential. If, for example, one could break the rock to –4 inches by blasting one would eliminate the need for both the primary and secondary cone crushers at the mine.

Northshore Mining has based its philosophy of drilling and blasting on the following three fundamental axioms:

1. The whole is not equal to the sum of the parts.

This first axiom simply states that drilling and blasting are part of the overall process and that process must be treated as a total system. The parts of the system are not independent and the total cost of the process cannot be minimized by minimizing the individual parts. Decreased costs for explosives, for example, do not necessarily lower overall costs. Increased spending in one area can be offset by greater savings in other areas.

2. Breaking rock gets more expensive downstream.

This means that, at least up to a point, it is more effective to break rock with explosives than mechanically in crushers or grinding mills. At some point it does become prohibitive to further decrease drill spacing and increase the amount of explosives used to blast the rock. At Northshore, that point due to technical difficulties such as the technical constraints imposed by delay timing accuracies has not yet been found.

3. The entire mining process begins with drilling and blasting and all downstream efficiencies and costs are controlled by effective fragmentation.

This simply means that no matter how efficient or large mining equipment is, it cannot be effective unless the rock can be handled efficiently. Furthermore, because downstream costs are large in comparison, the opportunity exists to save money downstream by better fragmentation from blasting.

When talking to realtors about selling a house it is well known that the three most important factors are: Location, Location and Location. History at Northshore has shown that drilling and blasting efficiency as defined by decreased average and maximum fragment size is also controlled by three important factors: Energy, Energy, and Energy. Specifically fragmentation is controlled by 1. The *total energy* in the shot, 2. The *energy distribution*, and 3. The *energy utilization.*

With regard to the first of the energy factors, total energy, the idea is 'the more, the better' as long as the blasting can be kept under control (the resulting muck pile is satisfactory, etc.).

Since holes are drilled to hold the explosives, the energy in a blast is concentrated in discrete locations. Fragmentation is excellent near the charge and gets worse as the distance away from the energy source increases. The second energy factor, energy distribution, is a particular problem in the upper part of the bench where explosive has been replaced by stemming. Northshore has improved the energy distribution, increased the total energy, and minimized poor fragmentation in the top part of the blasts by placing shallow (8-10 foot) satellite holes with 200 to 300 lbs. of explosive centered between each main production hole.

The third energy factor, energy utilization, is controlled by two factors proper stemming and proper timing between holes and rows. Both are needed to contain the explosion and provide the time needed for the explosives to do their work. It is particularly important that the delay between rows is of sufficient duration to allow each row to move out before the following row fires.

Experience has shown that drilling and blasting must be treated as a system and that any single factor such as hole spacing, powder type or powder factor, or timing alone will not improve results unless all the factors are balanced.

Results have shown that better drilling and blasting practices can produce better fragmentation which in turn has a positive effect on overall costs.

As indicated earlier, the mine closed in 1986 due to adverse economic conditions, was reopened in 1990 and is operating successfully today (1998). For this to occur major cost reductions were needed. The major productivity increases and savings from 1986 to 1994 as expressed as percentages based upon 1994 dollars are as follows:

A. Drilling and Blasting

– 28% decrease in the cost per ton mined.

B. Ore Loading

– 29% productivity increase with the same equipment.

– 33% decrease in the cost per ton mined.

C. Mine Haulage

– 6% increase in productivity.
– 48% decrease in the cost per ton mined.

D. Miscellaneous Pit

– 50% reduction in the cost per ton mined.

E. Coarse Crushing

– 34% increase in crusher productivity (tons crushed/hour).

F. Fine Crushing

– 22% increase in crusher productivity (tons crushed/hour).
– 41% reduction in the electrical cost per ton crushed.

G. Fine Grinding

– 42% reduction in overall grinding costs.

The overall cost to extract and reduce the ore to less than the 325 mesh size needed for separation has decreased by 42% over this period. Improved fragmentation has been achieved even though the overall powder factor (total explosives used per ton of rock) has not changed. The additional drilling for satellite holes has not increased drilling costs appreciably since these holes (a) drill faster than average due to prefracturing of the top of each bench from previous blasts and (b) allow the spacing for the deep holes to be expanded. Hence the improvements to date have been largely achieved through the better distribution and utilization of the explosive energy. Increased costs for drilling and blasting due to general inflation have been more than offset by cost savings brought about by

– Improved operator performance
– Improved maintenance practices
– The utilization of more cost effective explosives

In summary, since 1986 the costs at Northshore to break rock to less than 325 mesh has decreased by 42% and the overall cost to produce a ton of pellets by over 50%. The success has been the result of many factors including good management, an excellent workforce, reduced overhead, cooperation and help from suppliers and numerous changes in operating practices. Improved fragmentation from blasts, however, has been a major factor both directly and indirectly by allowing some of the other changes to be made.

2.7 SUMMARY

In this chapter the dominant role that fragmentation plays in the overall process of extracting the ore from the insitu through to final mineral liberation at the end of the mine-mill processing chain has been described and emphasized. Through the years much has been said about how most if not all of the primary crushing should be done in the pit and that explosive energy is one of the most convenient and inexpensive sources of energy for the miner. Yet there has also been great attention placed upon maintaining as low powder factors as possible since explosive costs can be substantial. Book keeping by unit operation forces each unit operation to focus on cost cutting for that particular operation and to maintain costs at as low a level as possible. However, as was emphasized repeatedly throughout the chapter, a 'low-cost' blasting unit operation may not at all be low cost when

the added costs due to sub-optimizing this one operation continue to incur additional costs for the downstream operations. Today there are many new and powerful tools for evaluating the degree of fragmentation at various stages in the process and for collecting, storing, processing, analyzing and presenting the great amounts of data generated by an operation each day. Thus the possibilities to make the system decisions as to where to set the company's fragmentation resources can be made on a much more solid foundation than ever before. As the costs of the various forms of energy change in the future, one has the opportunity to allocate those energy dollars in the most effective way. To do this one must understand the system, the interactions which occur within the system and the workings of each of the unit operations themselves.

REFERENCES AND BIBLIOGRAPHY

Bond, F.C. 1952. The third theory of comminution. *Mining Engineering* (5): 484-494.

Bond, F.C. 1959. The work index in blasting. *Quarterly of the Colorado School of Mines* 54(3): 77-82.

Callow, M.I. & V.P. Kenyen 1992a. Grinding. Section 25.3.2 in SME *Mining Engineering Handbook*, 2nd Edition (H.L. Hartman, senior ed.), SME (AIME), Littleton, Colo. pp. 2201-2209.

Callow, M.I. & V.P. Kenyen 1992b. Crushing. Section 25.3.2 in SME *Mining Engineering Handbook*, 2nd Edition (H.L. Hartman, senior ed.), SME (AIME), Littleton, Colo. pp. 2184-2201.

Carlsson, O. & L. Nyberg 1983. A method for estimation of fragment size distribution with automatic image processing. *Proceedings of the 1st Int. Symp. on Rock Fragmentation by Blasting.* Luleå, Sweden. pp. 333-345.

Cheimanoff, N.M., R. Chavez & J. Schleifer 1993. FRAGSCAN: A scanning tool for fragmentation after blasting. *Proceedings of the 4th Int. Symp. on Rock Fragmentation by Blasting, Fragblast-4* (H.P. Rossmanith, ed.). A.A. Balkema, Rotterdam pp. 325-330.

da Gama, C.D. 1971. Size distribution general law of fragments resulting from rock blasting. *Trans. SME/AIME.* 50(Dec): 314-316.

da Gama, C.D. 1974. The size of the largest fragment in rock blasting. *Proceedings of the 3rd Int. Congress of the Int Soc. Rock Mechanics.*, Denver. vol iii-B, pp. 1343-1348.

da Gama, C.D. 1983. Use of comminution theory to predict fragmentation of jointed rock masses subjected to blasting. *Proceedings of the 1st Int. Symp. on Rock Fragmentation by Blasting.* Luleå, Sweden. pp. 565-580.

da Gama, C.D. 1990. Reduction of costs and environmental impacts in quarry rock blasting. *Fragblast'90. Proceedings, 3rd Int. Symp. on Rock Fragmentation by Blasting,* Austral. Inst. Min. Metall., Victoria, Australia, pp. 5-8.

da Gama, C.D. & C.L. Jimeno 1993. Rock fragmentation control for blasting cost minimization and environmental impact abatement. Rock Fragmentation by Blasting *Proceedings of the Fourth Int. Symp. on Rock Fragmentation by Blasting, Fragblast-4* (H.P. Rossmanith, ed.). A.A. Balkema, Rotterdam pp.273-280.

Dyno Wesfarmers Ltd/Blast Dynamics, Inc. 1993. *Efficient blasting techniques.* Sanctuary Cove.

Eloranta, J. 1995. The effects of blast fragmentation on downstream processing costs. *Skillings Mining Review.* 84(April 8): 4-6.

Eloranta, J. 1995. Selection of powder factor in large diameter blastholes. *Proceedings, EXPLO '95.* Brisbane. pp. 25-28.

Hadjigeorgiou, J. & M. Scoble 1988. Prediction of digging performance in mining. *Int. Journal of Surface Mining.* 2: 237-244.

Hammes, J.K. 1966 The economics of producing and delivering iron ore pellets from North American taconite type resources. *Proceedings of the 27th Annual Mining Symposium,* Univ. of Minnesota. pp. 9-16.

Hendricks, C., J. Hadjigeorgiou & M. Scoble 1988. Electric mining shovel diggability studies. *Proceedings, Int. Symp. on Mine Planning and Equipment Selection, Calgary.* Nov. pp. 327-333.

Hendricks, C., J. Hadjigeorgiou & M. Scoble 1989. Relationship between fragmentation and diggability performance monitoring of electric shovels as an indicator of blast efficiency. *Proceedings of the 91st Annual General Meeting, CIM.* May.

Hendricks, C., J. Peck & M. Scoble 1990. Integrated drill and shovel performance monitoring towards blast optimization. *Proceedings, 3rd Int. Symp. on Rock Fragmentation by Blasting*, Austral. Inst. Min. Metall., Victoria, Australia, pp. 9-20.

Herbst, A.S. & D.J. Schiller 1988. *Avogadro's Numbers for Engineers, Scientists, Students*. Indelible Ink Publishing Company, Butte, Montana. 97p.

Humphreys, M. & G. Baldwin 1995. Blast optimization for improved dragline productivity. *Explosives Engineering*. 12(5): 13-16, 26-32.

Hunter, G.C., D.A. Sandy & N.J. Miles 1990. Optimisation of blasting in a large open pit mine. *Fragblast '90 Proceedings, 3rd Int. Symp. on Fragmentation by Blasting*, Austral. Inst. Min. Metall., Victoria, Australia, pp. 21-30.

Indihar, M.A & T.L. Barkley 1991. Blasting at Cyprus Northshore Mining Co – A new approach to mining taconite at an old mine. *Proceedings of the 64th Annual Meeting of Minnesota Section AIME and 52th Annual Minnesota Mining Symposium*, Duluth.

Inspector of Mines. 1995. The Annual (1994) Report of the Inspector of Mines. St. Louis County, Minnesota.

Just, G.D. 1979. Rock fragmentation by blasting. *CIM Bulletin* 72(803): 143-148.

Kick, F. 1885. *Das gesetz der proportionalen widerstande und sein anwendung*. Artus Felix. Leibzig.

Langefors, U. & B. Kihlstrom 1963. *The Modern Technique of Rock Blasting*. John Wiley, New York.

MacKenzie, A.S. 1966. Cost of explosives – Do you evaluate it properly? *Mining Congress Journal*. 52(5): 32-41.

MacKenzie, A.S. 1967. Optimum blasting. *Proceedings of the 28th Annual Minnesota Mining Symposium*, Duluth, pp. 181-188.

McDermott, C., G.C. Hunter & N.J. Miles 1989. The measurement of rock fragmentation using image analysis. *Proceedings, Symposium on Surface Mining – Future Concepts*. University of Nottingham, Marylebone Press, Manchester. April 1989. pp. 103-108.

Mol, O., R. Danell & L. Leung 1987. Studies of rock fragmentation by drilling and blasting in open cut mines, *Proceedings, 2nd Int. Symp. on Rock Fragmentation by Blasting*, Keystone, Colorado. pp. 381-392.

Montoro, J.J. & E. Gonzalez 1993. New analytical techniques to evaluate rock fragmentation based on image analysis by computer methods. *Proceedings of the 4th Int. Symp. on Rock Fragmentation by Blasting, Fragblast-4* (H.P. Rossmanith, ed.). A.A. Balkema, Rotterdam. pp. 309-316.

Nie, S-L. & A. Rustan 1987. Techniques and procedures in analysing fragmentation after blasting by photographic method. *Proceedings, 2nd Int. Symp. on Rock Frag. by Blasting*, (W.L. Fourney & R.D. Dick, eds). Keystone, Colo. Aug. Society for Experimental Mechanics. pp 102-113.

Oka, Y. & H. Majima 1969. Energy requirements in size reduction. *Trans. Soc. Min. Eng. (AIME)*, 244(9): 249-251.

Pastika, P.L., M. Indihar & B. Von Wald 1995. Improved fragmentation for mine cost reduction. *Proceedings of the 68th Annual Meeting of Minnesota Section AIME and 56th Minnesota Mining Symposium*, Duluth, pp. 185-192.

Persson, P-A. 1983. Energy in rock fragmentation. *Proceedings of the First Int. Symp. on Rock Blasting by Fragmentation, Luleå, Sweden*, August. pp. 777-788.

Pfleider, E.P. & G.F. Weaton 1968. Iron ore mining. *Section 13.4 in Surface Mining* (E.P. Pfleider, ed.), AIME, NY, pp. 897-927.

Rholl, S.A., S.G. Grannes & M.S. Stagg 1993a. Fragment size distribution assessment using a digital image based measurement system. *Proceedings of the 9th Annual Symp on Explosives and Blasting Research. SEE*, pp. 241-250.

Rholl, S.A., S.G. Grammes & M.S. Stagg 1993b. Photographic assessment of the fragmentation distribution of rock quarry muckpiles. *Proceedings of the 4th Int. Symp. on Rock Fragmentation by Blasting, Fragblast-4* (H.P. Rossmanith, ed.). A.A. Balkema, Rotterdam. pp. 501-506.

Sandy, D.A. 1989. Drill, blast, load and haul practices at Rossing Mine, Namibia. *Trans. IMM.98* (May-Aug): A98-A104.

Skillings, D.N. 1995. North American iron ore industry at 15-year high-production of 99.33 million gross tons in 1995. *Skilling Mining Review*. July 29. 84(30): 20-38.

Stagg, M.S. & R.E. Otterness 1995. Effect of blasting practices on fragmentation: Full-scale results. *Proceedings of the 68th Annual Meeting Minnesota Section SME and 56th Mining Symposium*, Duluth, Minnesota. Jan 24-26. pp. 215-230.

Van Aswegan, H. & C.V.B. Cunningham 1986. The estimation of fragmentation in blast muckpiles by means of standard photographs. *J SAIMM*. 86(12): 469-474.

Villar, J.W. & A.W. Swanson 1992. *Low-grade iron ore: Empire Mine. SME Mining Engineering Handbook, 2nd Edition* (H.L. Hartman, senior ed.). Society for Mining, Metallurgy, and Exploration, Inc. Littleton, Colorado. pp. 1380-1384.

Vogt, W. & O. Aßbrock 1993. Digital image processing as an instrument to evaluate rock fragmentation by blasting in open pit mines. *Proceedings of the 4th Int. Symp. on Rock Fragmentation by Blasting, Fragblast-4* (H.P. Rossmanith, ed.). A.A. Balkema, Rotterdam. pp. 317-324.

Von Rittinger, P.R. 1867. *Lehrbuch der Aufbereitungskunde*, Berlin.

Western Mine Engineering, Inc. 1994. Spokane, Wa. p EP 85.

Williamson, S., C. MacKenzie & H. O'Loughlin 1983. Electric shovel performance as a measure of blasting efficiency. *Proc First Int. Symp on Rock Fragmentation by Blasting*, Luleå, Sweden, pp. 625-635.

Yalum, Y. 1987. A size distribution study of the blasted ore fragments in Shui-Chang Open Pit Mine, China. *Proceedings, 2nd Int. Symp. on Rock Frag. by Blasting*, (W.L. Fourney & R.D. Dick, eds). Keystone, Colo. Society for Experimental Mechanics. pp. 672-676.

CHAPTER 3

Explosives as a source of fragmentation energy

3.1 EXPLOSIVE POWER

An explosion is a type of redox (reduction/oxidation) reaction which takes place over a very short time. Common rusting is an example of a redox reaction which takes place very slowly. The equation describing the rusting process is written below

$$4Fe + 3O_2 \Rightarrow 2Fe_2O_3 + \text{Heat} \tag{3.1}$$

The iron (Fe) is *oxidized* to rust (Fe_2O_3/ferrous oxide) and the oxygen (O_2) is said to be *reduced*.

In explosive terminology the O_2 is the *oxidizing agent* and the Fe is the *fuel*. If one placed sensitive thermocouples on a rusting iron building, an increase in temperature would be found to accompany the process.

A common blasting agent used in open pit mines today is a combination of ammonium nitrate (AN) and No. 2 diesel oil/fuel oil (FO). The combination is called ANFO. Although neither of these components are explosive in themselves, under the proper conditions the mixture can be made to *detonate* (the explosion front will propagate along a column of explosive). Under other conditions, the mixture will simply *deflagrate* (burn) at a very rapid rate.

The chemical reaction for the process is given below

$$3NH_4NO_3 + CH_2 \Rightarrow 7H_2O + CO_2 + 3N_2 + \text{heat} \tag{3.2}$$

In this case, the AN is the oxidizer (it contains the oxygen) and the fuel oil is the fuel. The fuel oil is oxidized and the AN is reduced in a very, very short time. As can be seen, the products are gases at high temperature. The amount of energy liberated in the form of heat is called the heat of explosion and denoted by symbol, Q. For ANFO, Q = 912 calories/gram.

The reaction is carried along the column of explosive at the velocity of detonation (*VOD*) which for ANFO is of the order of 4529 m/second.

Although one knows that the power involved in an explosion is large, it is difficult to visualize just how large simply through the energy release value of 912 calories/gm. To help in this regard, consider a borehole 300 mm in diameter (D) and 8 m in length (L_e) filled with ANFO having a density (ρ_e) of 0.8 g/cm^3.

The column would have a volume (V_e) of

$$V_e = \frac{\pi D^2 L_e}{4} = \pi (0.30)^2 (8)/4 = 0.566 \text{ m}^3 \tag{3.3}$$

containing explosive with a mass (M_e) of

$$M_e = \rho_e V_e = 0.566 (800) = 452 \text{ kg} \tag{3.4}$$

The total energy (E) unleashed would then be

$$E = 912 \text{ kcal/kg} \times 452 \text{ kg} = 412{,}000 \text{ kcal} \tag{3.5}$$

To obtain the energy in kilojoules* one multiplies kilocalories by a factor of 4.184.

$$E = 4.184 \times 0.412 \times 10^6 = 1.72 \times 10^6 \text{ kJ} \tag{3.6}$$

Using a detonation velocity for ANFO of 4529 m/second, the time (t_e) required for the entire column to detonate is

$$t_e = \frac{L_e}{VOD} = 8 \text{ m} / 4529 \text{ m/s} = 1.77 \times 10^{-3} \text{ seconds} \tag{3.7}$$

Thus the power (P_{OW}) generated is

$$P_{OW} = \frac{E}{t_e} = 1.72 \times 10^6 / 1.77 \times 10^{-3} = 0.97 \times 10^6 \text{ MJ/second} \tag{3.8a}$$

or

$$P_{OW} = 3498 \times 10^6 \text{ MJ/hour} \tag{3.8b}$$

By dividing the power expressed in MJ/hour by the factor 3.6 one obtains the power in kW.

$$P_{OW} = 972 \times 10^6 \text{ kW} \tag{3.8c}$$

Since 1 horsepower (hp) is equal to 0.746 kW, the power output expressed in horsepower is

$$P_{OW} = 972 \times 10^6 / 0.746 \cong 1.30 \times 10^9 \text{ hp} \tag{3.8d}$$

The challenge in blast design is to harness this power so that it performs the desired useful work.

3.2 PRESSURE-VOLUME CURVES

An ANFO mixture will detonate when suitably confined (such as in a borehole) and initiated by a high explosive (called a primer) of sufficient intensity. The reaction progresses along the explosive column with a speed equal to the velocity of detonation (VOD). The pressure of the gas directly at the detonation front is called the *detonation* pressure (P_{DET}). For many explosives it may be approximated by

$$P_{DET} \text{ (atm)} = 2.5 \rho_e (VOD)^2 \tag{3.9a}$$

$$P_{DET} \text{ (MPa)} = 0.25 \rho_e (VOD)^2 \tag{3.9b}$$

where ρ_e = density (kg/m^3), VOD = detonation velocity (km/sec), P_{DET} = detonation pressure.

---

*The prefix kilo (k) means 10^3, mega (M) means 10^6 and giga (G) means 10^9 of the unit in question. Thus 1 kcal means 10^3 calories.

The *explosion pressure* (P_e) which denotes the gas pressure applied to the borehole walls just after detonation is approximately one-half of this value.

$$P_e \cong 1/2\ P_{DET} \tag{3.10}$$

To demonstrate how this works, consider the simplified example of a 10 cm diameter borehole 200 cm in length filled with ANFO ($\rho_e = 0.8$ gm/cm^3 and $VOD = 4529$ m/s).

The total volume (V_e) and mass (M_e) of explosive involved are respectively

$$V_e = \frac{\pi}{4} D^2 L_e = 0.01571 \text{ m}^3$$

$$M_e = \frac{\pi}{4} D^2 L_e \rho_e = 12.57 \text{ kg}$$

Using Equations (3.9a) and (3.10), the estimated detonation (P_{DET}) and explosion (P_e) pressures are respectively

$$P_{DET} = (2.5)\ (800)\ (4.529)^2 = 41{,}024 \text{ atm}$$

$$P_e = 20{,}512 \text{ atm}$$

The actual values (see Chapter 11) are

$$P_{DET} = 43{,}943 \text{ atm}$$

$$P_e = 19970 \text{ atm}$$

Although not strictly applicable due to the very high temperatures and pressures involved, relationships based upon ideal gas behavior are very useful in demonstrating basic concepts. A more rigorous treatment of this topic is provided the interested reader in Chapter 11.

If the temperature is maintained constant (isothermal conditions) during the subsequent expansion of the explosive gases with an accompanying decrease in borehole pressure, then the right hand side (nRT) of the Ideal Gas Law

$$PV = nRT \tag{3.11}$$

where P = Pressure (atm), V = volume (l/kg), n = no. of moles of gas (moles/kg), R = universal gas constant = 0.08207 l – atm/(mole – °K), T = temperature (°K) is a constant. Equation (3.11) can be written as

$$PV = \text{constant} \tag{3.12}$$

An alternative form of this pressure-volume relationship familiar to all physics students is

$$P_1 V_1 = P_2 V_2 = P_e V_e \tag{3.13}$$

Knowing that

$$P_e = 19{,}970 \text{ atm}$$

$$V_e = 0.01571 \text{ m}^3$$

the pressure-volume curve shown in Figure 3.1 may be constructed. However the temperature of the explosive gases *does not* remain constant. Initially it is very high (of the order of 2810°K) and then decreases with expansion to near ambient (298°K). A much better approximation to the true P-V curve describing this situation is achieved by assuming that the expansion takes place adiabatically (there is no heat loss).

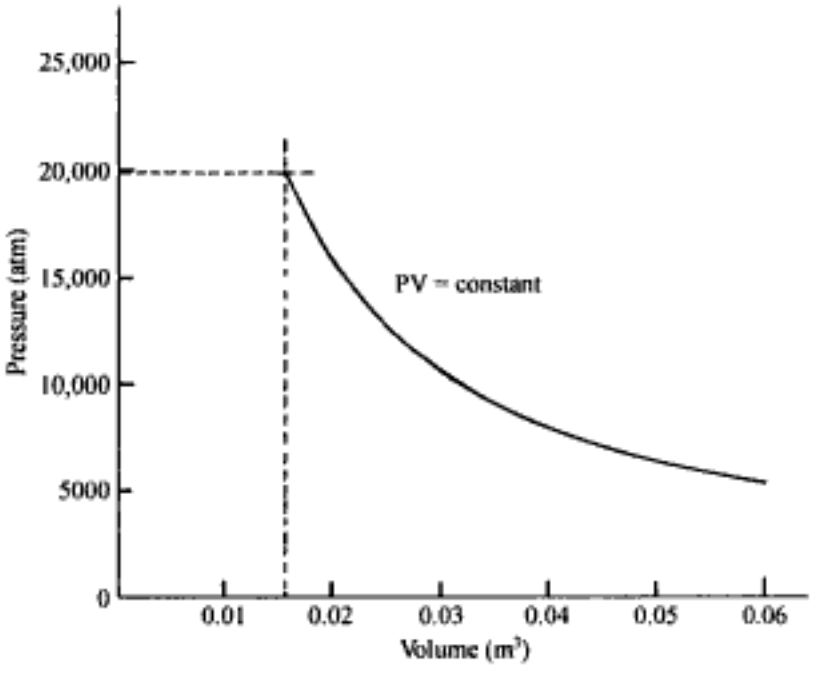

Figure 3.1. The predicted P-V curve assuming isothermal expansion.

The appropriate Ideal Gas Law equation is

$$PV^{\gamma} = \text{constant} \tag{3.14}$$

where γ = ratio of the specific heats.

For ANFO, the appropriate values of γ depend upon the pressure range. For this example the following values (see Chapter 11 for details) will be used:

Region 1: $\gamma = 2.035$ $4500 \text{ atm} \le P \le 19{,}971 \text{ atm}$ (3.15a)

Region 2: $\gamma = 1.631$ $500 \text{ atm} \le P \le 4500 \text{ atm}$ (3.15b)

Region 3: $\gamma = 1.285$ $100 \text{ atm} \le P \le 500 \text{ atm}$ (3.15c)

Region 4: $\gamma = 1.271$ $1 \text{ atm} \le P \le 100 \text{ atm}$ (3.15d)

The pressure-volume relationship for Region 1 (pressure range $P \ge 4500$ atm) is

$$PV^{2.035} = P_1 V_1^{2.035} = \text{constant} \tag{3.16}$$

The value of the constant is obtained by substituting the known values for P_e and V_e

$$P_e = 19971 \text{ atm}$$

$$V_e = 0.1571 \text{ m}^3$$

into Equation (3.16). Thus

$$P_1 V_1^{2.035} = 19{,}970\ (0.01571)^{2.035} = 4.262 \tag{3.17}$$

The equation

$$P_1 V_1^{2.035} = 4.262$$

may now be used to determine the pressure given the volume or vice versa for any point in this Region. In particular it can be used to determine the volume (V_{T1}) at the pressure transition point (P_{T1})

$$P_{T1} = 4500 \text{ atm}$$

Substituting into Equation (3.17) one finds that

$$V_{T1}^{2.035} = 4.262/4500 = 0.0009471$$

$$V_{T1} = 0.03267 \text{ m}^3$$

For Region 2 (pressure range 500 atm ≤ P < 4500 atm) Equation (3.14) becomes

$$PV^{1.631} = P_2V_2^{1.631} = 4500\ (0.03267)^{1.631} = 16.97712 \tag{3.18}$$

At the second transition pressure (P_{T2} = 500 atm) the volume (V_{T2}) is

$$V_{T2}^{1.631} = 16.9771/500 = 0.0339543$$

$$V_{T2} = 0.12568 \text{ m}^3$$

For Region 3 (pressure range 100 atm ≤ P < 500 atm) Equation (3.14) becomes

$$PV^{1.285} = P_3V_3^{1.285} = 500\ (0.12568)^{1.285} = 34.795 \tag{3.19}$$

At the third transition pressure (P_{T3} = 100 atm) the volume (V_{T3}) is

$$V_{T3}^{1.285} = 34.795/100 = 0.347954$$

$$V_{T3} = 0.43975 \text{ m}^3$$

For Region 4 (pressure range (1 atm ≤ P < 100 atm) Equation (3.14) becomes

$$PV^{1.271} = P_4V_4^{1.271} = 100\ (0.43975)^{1.271} = 35.1976 \tag{3.20}$$

When the pressure (P_{T4}) drops to 1 atm, the volume V_{T4} is

$$V_{T4}^{1.631} = 35.1976 / 1.0 = 35.19765$$

$$V_{T4} = 16.473 \text{ m}^3$$

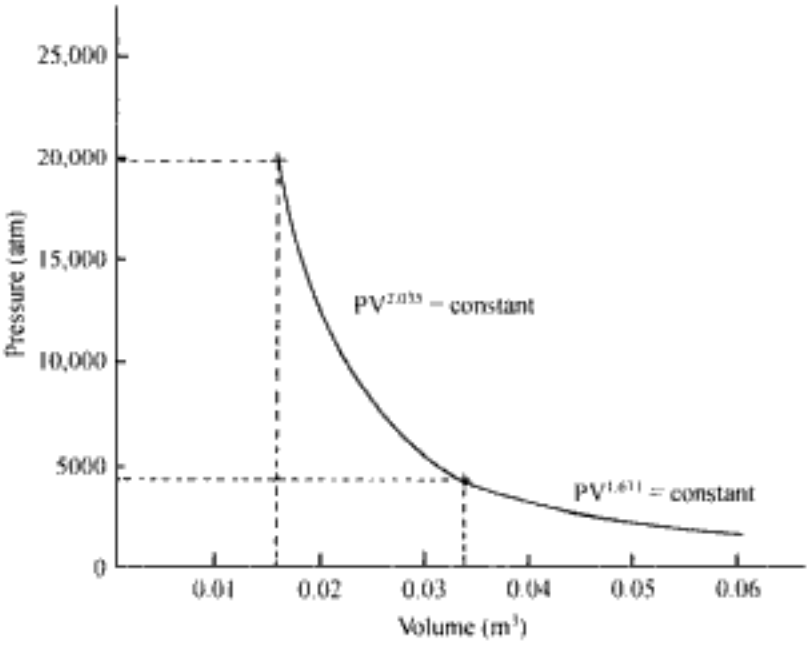

Figure 3.2. The idealized adiabatic P-V curve for ANFO undergoing relatively small expansions.

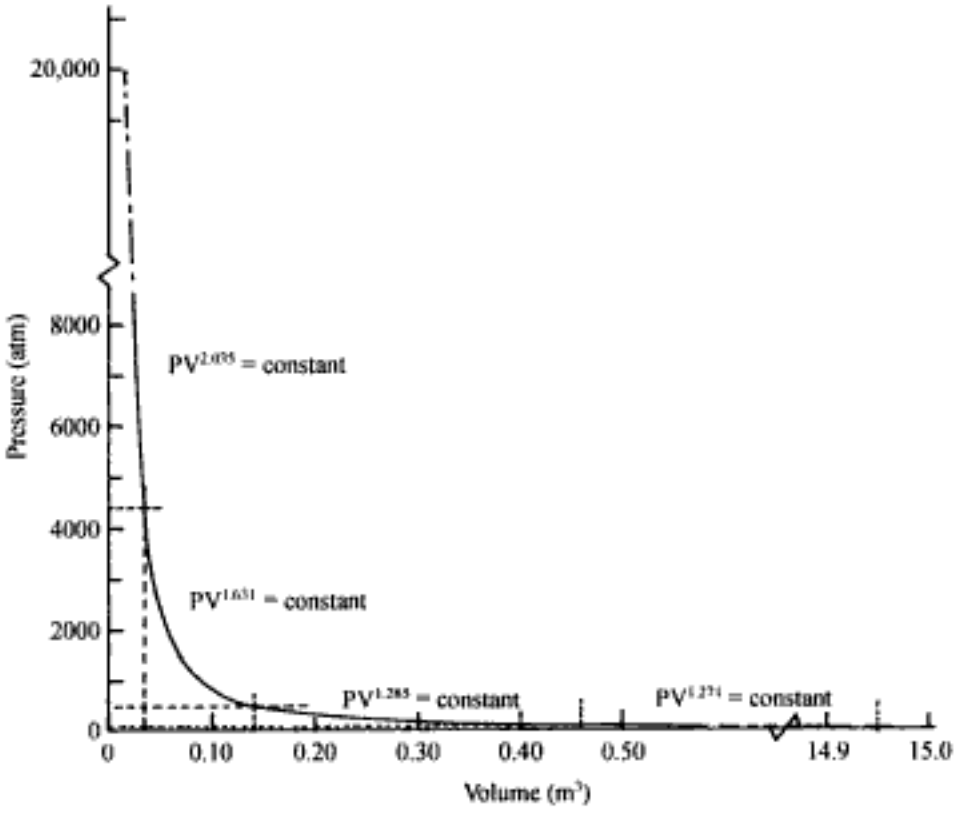

Figure 3.3. The idealized adiabatic P-V curve for ANFO over the entire expansion range.

Using Equations (3.17-3.20) the pressure-volume curve for the entire range can be constructed. Figures 3.2 and 3.3 show the predicted *P-V* curve drawn to two different volume scales.

The amount of expansion work (A) which can be done is given by the area under the curve.

$$A = \int_{V_e}^{V_{T1}} P\,dV + \int_{V_{T1}}^{V_{T2}} P\,dV + \int_{V_{T2}}^{V_{T3}} P\,dV + \int_{V_{T3}}^{V_{T4}} P\,dV \tag{3.21}$$

In this case

$$A = 4.262 \int_{0.01571}^{0.03267} \frac{dV}{V^{2.035}} + 16.977 \int_{0.03267}^{0.12568} \frac{dV}{V^{1.631}} + \\ + 34.795 \int_{0.12568}^{0.43975} \frac{dV}{V^{1.285}} + 35.198 \int_{0.43975}^{16.473} \frac{dV}{V^{1.271}} \tag{3.22}$$

Integrating Equation (3.22) one finds that

$$A = \frac{4.262}{1.035}\left[\frac{1}{0.01571^{1.035}} - \frac{1}{0.03267^{1.035}}\right] + \\ + \frac{16.977}{0.631}\left[\frac{1}{(0.03267)^{0.631}} - \frac{1}{(0.12568)^{0.631}}\right] +$$

$$+\frac{34.795}{0.285}\left[\frac{1}{(0.12568)^{0.285}}-\frac{1}{(0.43975)^{0.285}}\right]+$$
$$+\frac{35.198}{0.271}\left[\frac{1}{0.43975^{0.271}}-\frac{1}{(16.473)^{0.271}}\right] \tag{3.23}$$

The expansion energy is

$$A = 161 + 133 + 66 + 103 = 463 \text{ atm–m}^3$$

This can now be converted into kilocalories by

$$A = 0.0242 \times 10^3 \times 463 = 11{,}205 \text{ kcal}$$

Since there are 12.57 kg of ANFO involved in the explosion the amount of energy released per kilogram calculated using the idealized *P-V* curve described by Equation (3.15) is

$$A = 11{,}205/12.57 = 891 \text{ kcal}$$

It should be recalled that the theoretical energy release is

$$Q = 912 \text{ kcal/kg}$$

and the difference between the two is heat energy (≈ 21 kcal/kg) which remains trapped in the explosive products. The ratio between the amount of useful energy (A) available to the theoretical energy (Q) is called the mechanical efficiency (e).

$$e = \frac{A}{Q} \tag{3.24}$$

In this case it is

$$e = 891/912 = 0.977$$

which means that 97.7% of the theoretical explosive energy could do useful work if released in a controlled way down to a pressure of 1 atm.

3.3 EXPLOSIVE STRENGTH

Although the discussion to this point has focussed on ANFO, there are many other explosive types and variations. When selecting an explosive for a certain application one of the more important characteristics to be considered is 'strength'. Over the years, various ways have been used by manufacturers to measure and describe the strength of their explosives. Today unfortunately there is no standard approach of producing and providing these data. It has become quite common, however, for manufacturers to include *weight strengths* and *bulk strengths* (both *absolute* and *relative*) on their product specification sheets (see Chapter 7).

The weight strength (S_{WT}) is defined as the explosive energy per unit weight (mass). For its calculation, the problem becomes that of defining which 'energy' to use. The simplest is to use the theoretical heat of explosion (Q) calculated based upon the constituents. For ANFO (94.5%/5.5%) the value of Q is

$$Q = 912 \text{ kcal/kg}$$

Hence the weight strength is

$$S_{WT} = 912 \text{ kcal/kg}$$

The bulk strength (S_{BULK}) is defined as the explosive energy per unit volume and has units of kcal/m^3, cal/cm^3, etc. Since the cost per unit volume of hole created in the rock mass by drilling is substantial it is generally desired to pack as much explosive power into this volume as possible. Thus for most applications, the bulk strength is more important than the weight strength. The two are related through the density.

$$S_{BULK} = \rho_e S_{WT} \tag{3.25}$$

For ANFO with a density $\rho = 0.8$ gm/cm^3, the bulk strength is therefore

$$S_{BULK} = 0.8 \times 912 \text{ cal/gm} = 730 \text{ cal/cm}^3 = 730 \text{ kcal/m}^3$$

The 'energy' used in the calculation could also be defined in some other way, i.e. that defined by the *P-V* curve, the gas bubble energy, etc. Manufacturers often publish *relative* weight strength and bulk strength values for their explosives. Most of the time the strengths are relative to ANFO (94.5/5.5) of a given density, diameter and degree of confinement.

Assume for example that a certain explosive has a heat of explosion equal to 890 cal/g and a density of 1.3 g/cm^3. The weight strength of this explosive relative to ANFO is denoted by S_{ANFO}. Since for ANFO the heat of explosion is equal to 912 cal/gm and density is 0.8 gm/cm^3 then for the new explosive the relative weight strength is given by

$$S_{ANFO} = 890 / 912 = 0.9766$$

On the other hand, the bulk strength relative to ANFO denoted by B_{ANFO} is

$$B_{ANFO} = [890 \times 1.3] / [912 \times 0.8] = 1.59$$

One might conclude that for the same hole diameter this explosive would be far superior for fragmenting the rock than ANFO. Unfortunately, there is not necessarily a 1 to 1 correlation between total energy applied and the fragmentation produced.

3.4 ENERGY USE

In rock blasting the energy goes into

- Creating new fractures
- Extending old fractures
- Displacing parts of the rock mass relative to others (loosening)
- Moving the center of gravity forward (heave)
- Undesirable effects: flyrock, ground vibrations, air blast, noise, heat.

Exactly how the energy is partitioned into these different categories depends upon

- The explosive
- The rock/rock mass
- The blast geometry

Some (hard, massive) rock types require the creation of new fractures for adequate fragmentation. The shock energies needed for new fracture generation are associated with high explosion pressures (high detonation velocity and high density).

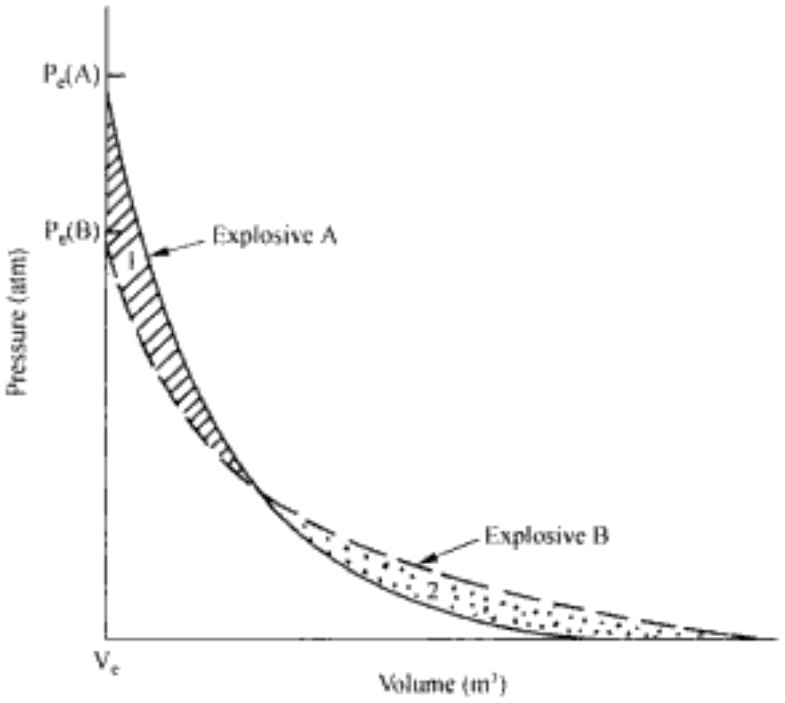

Figure 3.4. Diagrammatic representation of the P-V curves for two explosives with the same energy.

Other rock types which are already cracked depend more upon the heaving/displacing action provided by gas pressures for breaking. This may be best accomplished by an explosive with a lower detonation velocity and density.

Two explosives could have exactly the same total energy (same areas under the curves) but as shown in Figure 3.4 quite different *P-V* curves.

Note that

– Explosive *A* has a much higher peak pressure than explosive *B*
– The total energies of the two explosives are the same (Area 1 = Area 2).
– Explosive *B* maintains a higher gas pressure with expansion than does explosive *A*.

Explosive *A*, termed a high brisance/low gas pressure explosive, would be recommended for use in hard, brittle rocks. Explosive *B*, on the other hand, is a low brisance/high gas explosive for use in softer/more jointed rocks. To properly match explosive/rock/geometry and achieve optimum blasting results, it is therefore important to understand

– The rock mass failure process
– The partitioning of the explosive energy (shock energy/heave energy)
– Explosive-rock interaction.

These will be discussed in succeeding Chapters and particularly in Chapter 12.

3.5 SUMMARY

In the past only a relatively few explosive products with properties lying within a relatively narrow range were available for the fragmentation engineer to choose between. Today the products placed in the holes are many and their properties can be easily varied over the hole length. In addition initiation timing has been markedly improved. Thus the possibilities available to the blast designer are far more than those of a few short years

ago. The challenge facing the mining engineer is how to most effectively use these possibilities. Engineered fragmentation as opposed to 'blasting' or the epitome 'military' blasting will be an even more important aspect of future mining. The following Chapters will further develop the foundations needed for skillfully applying these highly efficient, convenient energy sources so that our fragmentation objectives are met.

REFERENCES AND BIBLIOGRAPHY

AECI Explosives and Chemicals Limited 1981. The strength of explosives. *Explosives Today*. Series 2, No 23, March.

AECI Explosives and Chemicals Limited 1984. Introduction to explosives. *Explosives Today*. Series 2, no 35, 1st Quarter.

AECI Explosives and Chemicals Limited 1988. The historical development of commercial explosives. *Explosives Today*. Series 3, no 1, Sept.

Anonymous 1975. *Programming Your Blast With Gulf Explosives*. Gulf Oil Chemical Company. 47p.

Anonymous *Explosive selection criteria*. Explosives Engineering. Excerpted from Bureau of Mines IC 8925. pp. 19-21.

Ash, R.L. 1963. The mechanics of rock breakage (Part 3) – Characteristics of explosives. *Pit and Quarry*. 56(4): 126-131.

Atlas Powder Company 1987. *Explosives and Rock Blasting*. Maple Press. 662pp.

Bauer, A. & W.A. Crosby 1992. Blasting. Section 6.2.1 in *Surface Mining*, 2nd Edition (B.A. Kennedy, ed.). Society for Mining, Metallurgy, and Exploration, Inc. Littleton, Colo. pp. 540-564.

Brown, F.W. 1956a. Determination of basic performance properties of blasting explosives. Symposium on Rock Mechanics. *Quarterly of the Colorado School of Mines* 51(3): 169-188.

Brown, F.W. 1956b. Simplified methods for computing performance parameters of explosives. *Proceedings. Second Annual Symposium on Mining Research*; (G.B. Clark, editor) Rolla, Missouri, Nov. 12-13 Missouri School of Mines, Bulletin No. 94 pp. 123-136.

Clark, G.B. 1968. Explosives. Section 7.1 in *Surface Mining* (E.P. Pfleider, ed.). AIME. New York. pp. 341-354.

Clark, G.B. 1980. Industrial High Explosives: Composition and Calculations for Engineers. *Quarterly of the Colo School of Mines* 75(1) January, 47pp.

Clark, G.B. 1981. Basic Properties of Ammonium Nitrate Fuel Oil Explosives (ANFO). *Quarterly of the Colo School of Mines* 76(1) January, 32 pp.

Clark, G.B. 1987. *Principles of Rock Fragmentation*. John Wiley & Sons. New York. 610pp.

Cook, M.A. 1958. *The Science of High Explosives*. American Chemical Society Monograph Series, No. 139, Reinhold, New York, 440pp.

Cook, M.H. 1974. *The Science of Industrial Explosives*. Ireco Chemicals. Graphic Service and Supply, Inc, 449pp.

Day, J.T., M.L. Thomas & L.L. Udy 1987. The importance of explosive energy on mining costs. *Proceedings of the 13th Conference on Explosives and Blasting Techniques. SEE*. pp. 131-143.

Dick, R.A. 1968. *Factors in selecting and applying commercial explosives and blasting agents*. USBM IC 8405. 30pp.

Dick, R.A. 1972. *The Impact of Blasting Agents and Slurries on Explosives Technology*. USBM IC 8560. 44pp.

Dick, R.A., D.V. D'Andrea & L.R. Fletcher 1993. Back to basics: The chemistry and physics of explosives. *Explosives Engineering*. 10(5): 33-41.

Dick, R.A., D.V. D'Andrea & L.R. Fletcher 1993. Back to basics: Properties of explosives. *Explosives Engineering*. 10(6): 28-45.

Dick, R.A., L.R. Fletcher & D.V. D'Andrea 1983. *Explosives and Blasting Procedures Manual*. USBM IC 8925. 105pp.

Dowding, C.H. & C.T. Aimone 1992. Rock breakage: explosives. Chapter 9.2 in *SME Mining Engineering Handbook*, 2nd Edition (H.L. Hartman, senior ed.). Society for Mining, Metallurgy, and Exploration, Inc. Littleton, Colo. pp. 722-746.

Drury, F.C. & D.J. Westmaas 1978. Considerations affecting the selection and use of modern chemical explosives. *Proceedings of the 4th Conference on Explosives and Blasting Technique. SEE*. pp. 128-153.

Drury, F.C. 1980. Ammonium nitrate blasting agents from manufacture to field use. *Proceedings of the 6th Conference on Explosives and Blasting Technique. SEE.* pp. 415-429.

E.I. DuPont de Nemours and Co. *DuPont Blasters' Handbook.* 1977 Edition. Wilmington, Del. 494 pp.

Evans, W.B. & D.P. Taylor 1987. Blended ANFO-based explosives. *CIM Bulletin.* 80(905): 60-64.

Harries, G. 1977. Explosives. Chapter 2 of the *Australian Mineral Foundation, Inc.*. Adelaide, 2-6 May.

Harries, G. 1977. Theory of blasting. Chapter 5 of the *Proceedings Drilling and Blasting Technology*, Australian Mineral Foundation Inc. Adelaide, 2-6 May. 65pp.

Harries, G. 1978. Breakage of rock by explosives. *Proceedings of the Rock Breaking Symposium.* Aus. I.M.M., Melbourne Branch, pp. 107-113.

Herbst, A.S. & D.J. Schiller 1988. *Avogadro's Numbers.* Indelible Ink Publishing Company, Butte, Montana.

Holmberg, R. 1977. Computer program for calculation of explosion energies. Report DS 1977: 16, *Swedish Detonic Research Foundation.* 22 pages.

Johansson, C.H. & P.A. Persson 1970. *Detonics of High Explosives.* Academic Press, New York. 330pp.

Lownds, C.M. 1986. The strength of explosives. *The Planning and Operation of Open Pit and Strip Mines* (J.P. Deetlefs, ed.) Johannesburg, SAIMM, pp. 151-159.

Lownds, C.M. 1991. Energy partitioning in blasting. *Proceedings of the 2nd High-Tech Seminar on Blasting Technology, Instrumentation and Explosives Applications*, Blasting Analysis International, Inc., June.

Manon, J.J. 1978a. Explosives: their classification and characteristics. *E/MJ Operating Handbook of Mineral Surface Mining and Exploration* (Richard Hoppe, ed.). E/MJ Mining Informational Services, McGraw-Hill, NY, NY. pp. 152-156.

Manon, J.J. 1978b. The chemistry and phisics of explosives. *E/MJ Operating Handbook of Mineral Surface Mining and Exploration* (Richard Hoppe, ed.). E/MJ Mining Informational Services, McGraw-Hill, NY, NY. pp. 157-166.

Manon, J.J. 1978c. Explosives: The mechanics of detonation. *E/MJ Operating Handbook of Mineral Surface Mining and Exploration* (Richard Hoppe, ed.). E/MJ Mining Informational Services, McGraw-Hill, NY, NY. pp. 167-168.

Manon, J.J. 1978d. Commercial applications of explosives. *E/MJ Operating Handbook of Mineral Surface Mining and Exploration* (Richard Hoppe, ed.). E/MJ Mining Informational Services, McGraw-Hill, NY, NY. pp. 169-171.

Manon, J.J. 1978e. How to select an explosive or blasting agent for a specific job. *E/MJ Operating Handbook of Mineral Surface Mining and Exploration* (Richard Hoppe, ed.). E/MJ Mining Informational Services, McGraw-Hill, NY, NY. pp. 172-183.

Mason, C.N. & W.C. Montgomery. 1978. Aluminum additives impart energy and sensitivity to many explosives. *E/MJ Operating Handbook of Mineral Surface Mining and Exploration* (Richard Hoppe, ed.). E/MJ Mining Informational Services, McGraw-Hill, NY, NY. pp. 184-186.

Mohanty, B. 1981. Energy, strength and performance, and their implications in rating commercial explosives. *Proceedings of the 7th Conference on Explosives and Blasting Technique. SEE*, pp. 293-306.

Paddock, R.C. 1987. A primer on explosives costs. Coal Mining, March. pp. 42-44.

Persson, P-A, R. Holmberg & J. Lee 1994. *Rock Blasting and Explosives Engineering.* CRC Press, Inc. Boca Raton, Florida.

Persson, P-A. 1973. How an explosive can seem expensive and yet shave blasting costs. *E&MJ.* 174(6): 110-113.

Taylor, J. 1952. *Detonation in Condensed Explosives.* Oxford at the Clarendon Press.

Thornley, G.M. & A.G. Funk 1981. Aluminized blasting agents. *Proceedings of the 7th Conference on Explosives and Blasting Techniques. SEE.* pp. 271-292.

Tousley, G.H., Jr. 1976. The professional approach to drilling and blasting operations. Preprint No. 76-F-312. *Soc. of Min. Engrs. of AIME.* For presentation at the 1976 SME-AIME Fall Meeting & Exhibit. (Denver, Colo) Sept. 1-3.

Udy, L.L. & C.M. Lownds 1990. The partition of energy in blasting with non-ideal explosives. *Fragblast '90. Proceedings of the 3rd Int. Symp. on Rock Fragmentation by Blasting*, Brisbane, August. Austral. Inst. Min. Metall., Victoria, Australia, pp. 37-43.

Wright, K.W. 1986. Effective blast round design-selecting the right explosive for the right job. *Mining Engineering.* 38(3): 28-32.

Yancik, J.J. 1969. *Monsanto Blasting Products-ANFO Manual: Its explosive properties and field performance characteristics.* 37pp.

Yancik, J.J. & A.A. Arias 1969. Technique for selection of optimum explosive system: Essential element to achieving optimum blasting. *Presented at the 11th Convention of Mining Engineers, Lima, Peru.* Dec. 28pp.

CHAPTER 4

Preliminary guidelines for blast layout

4.1 INTRODUCTION

In this chapter guidelines which can be used for preliminary blast design will be provided. As a result of feedback from the field, the patterns can be then adjusted/optimized for the actual characteristics of the rock mass – explosive – geometry combination. The blasthole terminology which will be used is shown in Figure 4.1. In bench blasting there is normally a long dimension of the bench and a short dimension. It will be assumed that the rows of blast holes are alined parallel to the long dimension.

The drilled burden (B) is then defined as the distance between the individual rows of holes. It is also used to describe the distance from the front row of holes to the free face. When the bench face is not vertical the burden on this front row of holes varies from crest to toe. The spacing (S) is the distance between holes in any given row. Generally the holes are drilled below the desired final grade. This distance is referred to as the subgrade drilling or simply the sub-drill (J). A certain length of hole near the collar is left uncharged. This will be referred to as the stemming length (T) whether or not it is left unfilled or filled with drill cuttings/crushed rock. The drilled length (L) is equal to the bench height (H) plus the sub-drill (J). The overall length of the explosive column (L_e) is equal to the hole length (L) minus the stemming (T). This column may be divided into sections (decks) containing explosives of various strengths separated by lengths of stemming materials. Sometimes the explosive strength is varied along the hole, i.e. a higher strength bottom charge with a lower strength column charge. As will be seen in the next section, the different dimensions involved in a blast design are not arbitrary but closely related to one another. The selection of one, for example the hole diameter, fixes within rather strict limits, many of the others.

4.2 BLAST DESIGN RATIONALE

This section presents a rationale for the type of geometrical design used in most open pit mines today. Five different design relationships will be introduced. Consider first the plan view (Fig. 4.2) of a bench in which the hole spacing (S) and burden (B) are as shown.

In viewing the figure it can be seen that the hole spacing can be expressed as a constant (K_S) times the burden

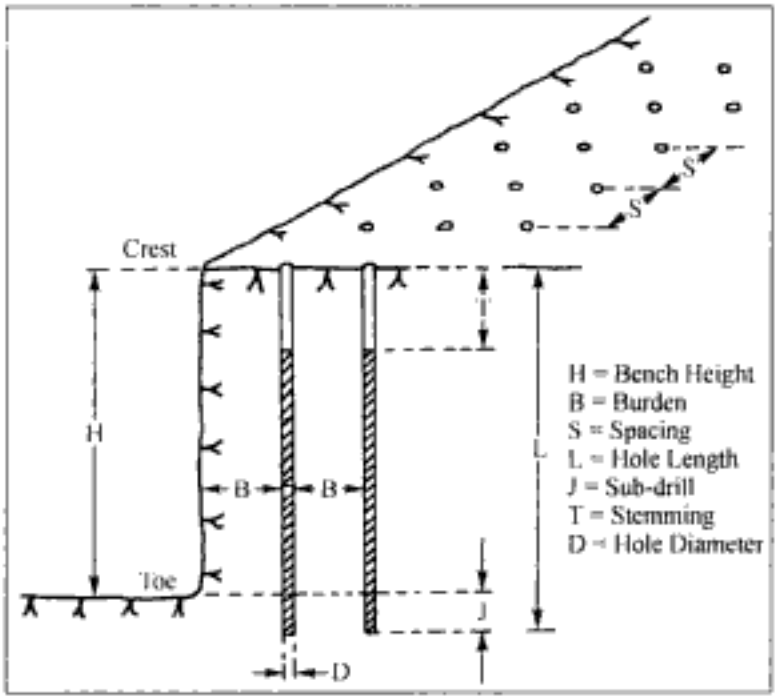

Figure 4.1. An isometric view of a bench showing blast geometry.

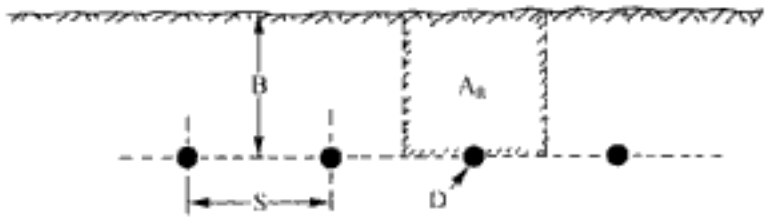

Figure 4.2. Bench plan view of the one row blast layout.

$$S = K_S B \tag{4.1}$$

where K_S = constant relating spacing to the burden.

This is the first of the fundamental design relationships.

Each hole of diameter D can be thought of as having to break its own individual area (A_R) as outlined by the dashed lines, in the figure.

$$A_R = B \times S \tag{4.2}$$

The volume required to be broken by a hole of unit length is

$$V_R = B \times S \times 1 \tag{4.3}$$

A certain amount of explosive energy per unit volume (E_V) must be applied to satisfactorily fragment the rock. The total energy (E_R) required is therefore

$$E_R = V_R \times E_V = B \times S \times E_V \tag{4.4}$$

Combining Equations (4.1) and (4.4) the required energy becomes

$$E_R = K_S B^2 E_V \tag{4.5}$$

Hence the required fragmentation energy is proportional to the square of the burden.

$$E_R \alpha B^2 \tag{4.6}$$

The amount of available explosive energy (E_A) is determined by the explosive volume V_e present in that unit length of borehole

$$V_e = \frac{\pi}{4} D_e^2 \tag{4.7}$$

where D_e = explosive diameter, multiplied by the explosive bulk strength expressed as energy per unit volume (E_e)

$$E_A = \frac{\pi}{4} D_e^2 E_e \tag{4.8}$$

When using packaged explosives and at pit perimeters where perimeter blasting techniques are employed, the charge diameter (D_e) may be less than that (D) of the hole. However, in production blasting using bulk blasting agents, the entire cross-sectional area of the hole is filled with explosive. Thus the hole diameter (D) and the explosive diameter (D_e) are the same. This assumption will be used here.

Thus the available energy is proportional to the square of the hole diameter

$$E_A \alpha D^2 \tag{4.9}$$

Setting the available and the required explosive energies equal to one another one finds that the burden is proportional to the hole diameter.

$$B \alpha D \tag{4.10}$$

Introducing the proportionality constant K_B, the relationship can be written as

$$B = K_B D \tag{4.11}$$

where K_B = constant relating burden to the hole diameter.

This is the second of the fundamental design relationships. The constant K_B, as will be discussed in Section 4.6, incorporates both explosive energy factors and the rock density. The design relationship (4.11) suggests a linear increase in the burden with hole diameter assuming that the same explosive is used (Fig. 4.3).

The toe region (Fig. 4.4) is highly confined and extra explosive energy must be applied to assure adequate fragmentation. This extra explosive energy is generally provided by extending the drill hole below the toe elevation and filling the so-called subdrill length

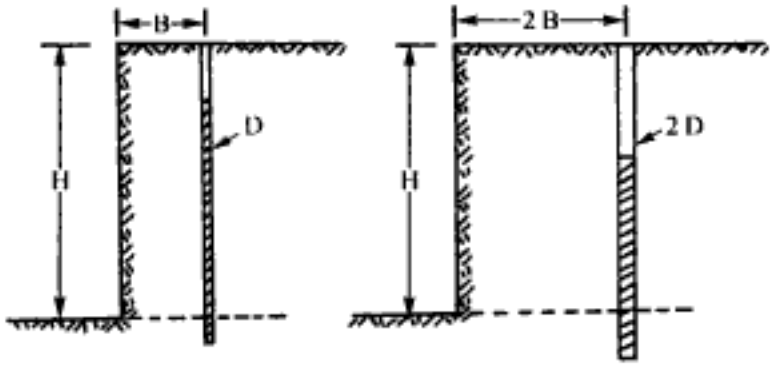

Figure 4.3. Diagrammatic representation showing the effect of hole diameter on burden.

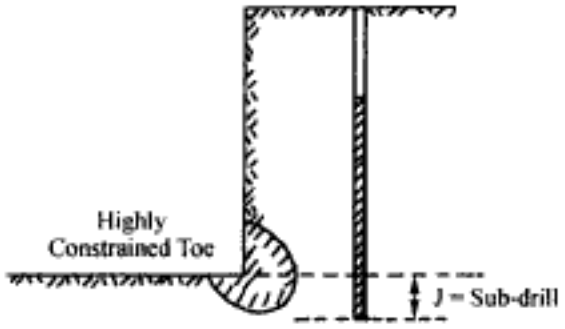

Figure 4.4. The geometrical relationship between the subdrill and the highly constrained toe.

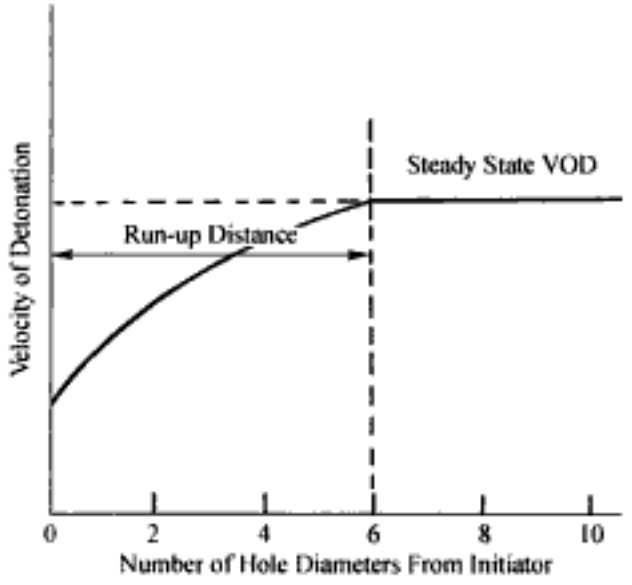

Figure 4.5. The variation of the detonation velocity with distance from the primer (underdriven) AECI, 1987b.

(J), with explosive. There are several different rationales used for selecting the appropriate length. Here an explanation based upon explosive run-up distance will be presented. A second one will be included under the discussion of the stemming length. In Chapter 16 a third approach based upon strain wave superposition will be described. The results are essentially the same with all three techniques.

As will be discussed in more detail in Chapter 8, there is a certain distance (called the run-up distance) characteristic of the initiating system/explosive which the shock wave must travel away from the point of initiation before steady state conditions are reached in the explosive column (Fig. 4.5). To break the confined toe, the borehole pressure should be as high as possible. Since the explosion (borehole wall) pressure (P_e) is proportional to the square of the detonation velocity

$$P_e \alpha (VOD)^2 \tag{4.12}$$

the elevation in the hole at which steady state velocity is reached should not be higher than the bench toe elevation. To be conservative the minimum run-up distance will be assumed to be $6D$.

In addition, the primer is seldom placed directly at the bottom of the blasthole due to the presence of cuttings and water. A normal offset is of the order of $2D$. Therefore, the distance from the drilled end of the hole to the toe elevation (the subdrill distance J) should be

$$J \approx 8D \tag{4.13}$$

As has been shown

$$B \propto D$$

and therefore the subdrill J may be expressed as

$$J = K_j B \tag{4.14}$$

where K_j = constant relating the subdrill distance to the burden.

This is the third of the design relationships. As will be seen later, the burden dimension (B) for most bulk explosives and rock types is of the order of

$$B = (25 \rightarrow 35)\, D \tag{4.15}$$

Using Equations (4.13) and (4.15), one would therefore expect that

$$K_j \approx 0.23 \rightarrow 0.32 \tag{4.16}$$

A typical value used for design is $K_j = 0.3$.

Near the hole collar, the rise of the explosive should be controlled so that the possibility of breaking upward toward the horizontal free surface should be 'as difficult' or 'even more difficult' than breaking, as is desired, toward the vertical free face. This could be satisfied, for example, by the placement of a *spherical* charge capable of breaking burden 'B' at a distance of 'V' below the collar (Fig. 4.6).

The general constraint would be written as

$$V \geq B \tag{4.17}$$

The spherical charge geometry is not a practical one for most surface mining applications. However as will be discussed in a later chapter, there is a practical equivalence in breaking effect between spherical and cylindrical charges. In Figure 4.7 the spherical charge has been replaced by a cylindrical charge of length T_C having the same total weight and effect.

Obviously the degree of 'equivalence' of the charges will depend upon the proximity to the charge. As a first approximation it will be assumed that T_C is linearly related to the distance of interest which in this case is B.

$$T_C = K_{TC} B \tag{4.18}$$

For B large, then T_C is large and vice versa. The general expression for the uncharged hole length (T) may be written as

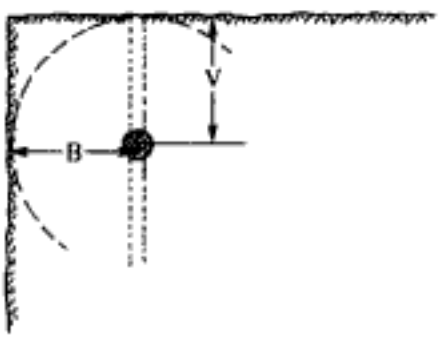

Figure 4.6. Section view showing a spherical charge located near the collar.

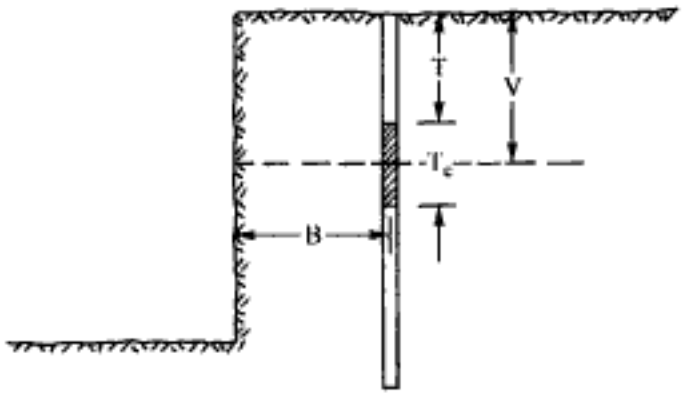

Figure 4.7. Section view showing a short cylindrical change located at the hole collar.

$$T = V - \quad T_C \tag{4.19}$$

If one used the 'as difficult' breaking constraint in Equation (4.17), then

$$V = B$$

Combining Equation (4.18) and Equation (4.19) subject to this condition yields

$$T = B - \quad K_{TC}\, B = \left(1 - \frac{K_{TC}}{2}\right) B \tag{4.20}$$

Equation (4.20) can be simplified to

$$T = K_T\, B \tag{4.21}$$

where

$$K_T = 1 - \frac{K_{TC}}{2} \tag{4.22}$$

This becomes the fourth of the fundamental relationships. The problem is then the determination of K_{TC}.

For bench blasting Langefors & Kihlström (1963) have suggested that the spherical/cylindrical charge equivalence is as shown in Figure 4.8. To explain the significance of the curve, consider a bench containing two vertical side-by-side blastholes. The burden is the same for both. Rather than discussing the collar region which is the subject of this portion, this example will involve the toe region. The reason for this is that the explanation is easier and the principle is the same. Consider a spherical charge of quantity Q_o placed at the toe elevation in one of the holes. In the second blasthole a cylindrical charge with a linear charge concentration of l kg/m of hole is emplaced. The bottom of the charge is at toe elevation and then the column extends upward towards the collar. The length of the elongated charge is expressed in multiples of the burden B. For a cylindrical charge of length B, the total charge would be $B \times l$. From the Figure one can see that at the toe this elongated charge has only the equivalent breaking power of a spherical charge of weight $0.6 \times l \times B$. This is understandable since the energy contained in that part of the elongated charge near the collar must travel a much longer distance to reach the toe and in the process the energy is spread over a much larger volume of rock. The energy density by the time it reaches the toe is much less than that produced by energy which has travelled a shorter distance. For a linear charge of length $0.3B$ the total charge has a mass of $0.3 \times l \times B$. From the curve it is seen that this

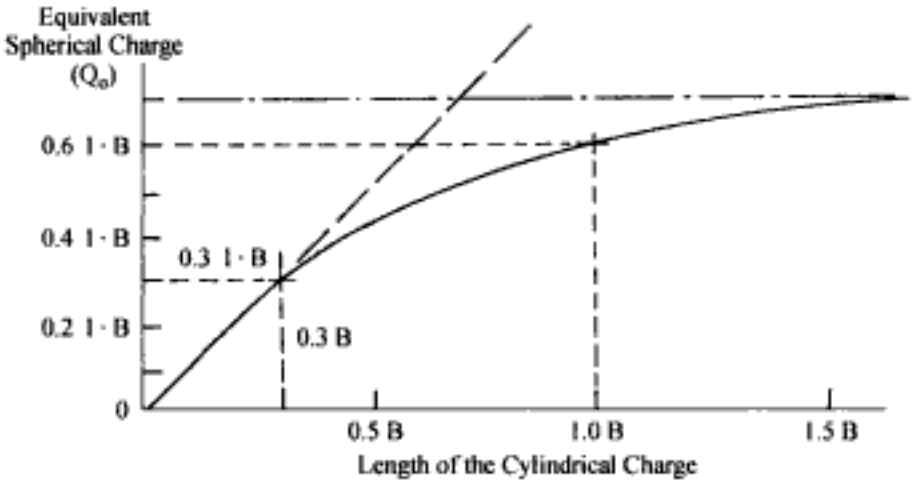

Figure 4.8. Toe breaking equivalence of spherical and cylindrical charges (Langefors & Kihlström, 1963).

has the same effect at the toe as a spherical charge placed directly at the toe elevation with a mass $0.3 \times l \times B$. For charges shorter than $0.3B$ this relationship holds as well, ie the elongated charge of a given weight has the same effect at the toe as a spherical charge of the same weight. For elongated charges with lengths greater than $0.3B$, the effect at the toe diminishes rapidly with increasing length. The same effect could be achieved by considering the elongated charge extending from the toe elevation downward. Thus an elongated charge extending from $0.3B$ below the toe to $0.3B$ above the toe elevation (for a total explosive weight of $0.6 \times l \times B$) would, according to the curve have the same breaking capacity as a spherical charge with a weight of $0.6 \times l \times B$ placed directly at the toe elevation.

In transfering this concept to the collar region one finds that

$$T_C \leq 0.6B \tag{4.23}$$

Comparing Equations (4.18) and (4.23) one finds that

$$K_{TC} \leq 0.6 \tag{4.24}$$

Substituting this into Equation (4.22) yields

Thus

$$K_T \geq 0.7 \tag{4.25}$$

To this point in the discussion there has been no specific mention of the bench height. If one continues to increase the scale (hole diameter) as shown in Figure 4.9, the center of charge progresses further and further down the hole. The limiting condition is when the center of charge reaches the toe elevation (Fig. 4.10). This occurs for a hole diameter which yields a burden just equal to the bench height. The fifth and last of the fundamental relationships is

$$H = K_H B \tag{4.26}$$

where K_H = constant relating bench height to the burden.

The value of K_H is

$$K_H \geq 1 \tag{4.27}$$

Figure 4.9. The effect of charge diameter on the charge center of gravity location.

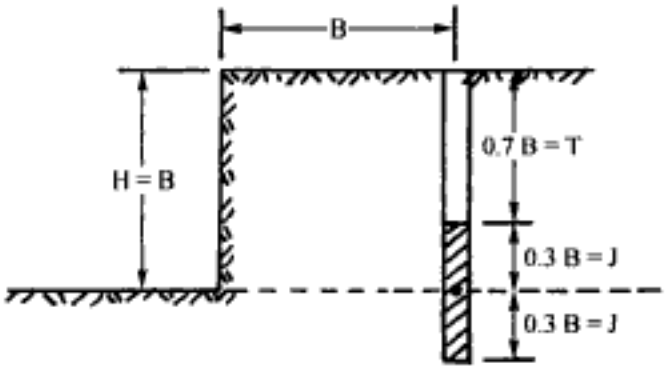

Figure 4.10. The limiting geometry for bench blasting.

For most open pit operations today K_H is between 1.5 and 2. Combining Equations (4.26), (4.27) and (4.11) one finds that

$$H \geq K_B D \tag{4.28}$$

Rearranging Equation (4.28) yields

$$D \leq \frac{H}{K_B} \tag{4.29}$$

which provides a rule of thumb for limiting the choice of hole diameter.

4.3 RATIOS FOR INITIAL DESIGN

In Section 4.2 the following five relationships were developed for preliminary blast design

Relationship 1: Spacing-Burden

$$S = K_S B$$

Relationship 2: Burden-Diameter

$$B = K_B D$$

Relationship 3: Subdrill-Burden

$$J = K_J B$$

Relationship 4: Stemming-Burden

$$T = K_T B$$

Relationship 5: Bench height-Burden

$$H = K_H B$$

In this section numerical values for the ratios K_S, K_B, K_J, K_T, and K_H will be presented for use during initial design (Ash, 1963).

Ratio K_S

As is discussed more fully in Chapter 5, the ratio of spacing and burden as drilled is based upon energy coverage of the bench. For a square pattern, the best energy coverage is achieved with $K_S = 1$ although there isn't too much difference when K_S is varied between $K_S = 1$ to $K_S = 1.5$. For a staggered drilling pattern, the best energy coverage is with $K_S = 1.15$. The efficiency of coverage is not substantially different for $K_S = 1.0$ to 1.5. A staggered pattern yields a much better uniformity of energy coverage than does a square one.

Ratio K_B

In Section 4.5 a detailed examination of this factor is presented. In brief, it has been found that

$K_B \cong 25$ when using *ANFO* ($\rho = 0.80$ gm/cm^3, $S_{ANFO} = 1$) in rock of medium density ($\rho_R = 2.65$ gm/cm^3). When using other explosives

ρ = density

S_{ANFO} = weight strength

in rock of this density one can use, as a first approximation,

$$K_B = 25\sqrt{\frac{\rho \times S_{ANFO}}{0.8 \times 1}} \tag{4.30}$$

If for example the explosive has a density of 1.2 gm/cm^3 and a weight strength relative to *ANFO* of 1.1 the appropriate K_B becomes

$$K_B = 25\sqrt{\frac{1.2}{0.8}\left(\frac{1.1}{1}\right)} = 32$$

Ratio K_J

The most common value of K_J is 0.3. In certain sedimentary deposits with a parting plane at toe elevation subdrilling may not be required. In very hard toe situations, the subdrilling may be increased over that indicated by using $K_J = 0.3$. However it is probably better to consider using a more energetic explosive. It must be remembered that the subdrill region generally forms the future crest/bench top for the bench below. Unwanted damage done at this stage may have a long and costly life. In addition excessive subdrill results in

1. A waste of drilling and blasting expenditures
2. An increase in ground vibrations
3. Undesirable shattering of the bench floor. This in turn creates drilling problems, abandoned blastholes and deviations for the bench below.
4. It accentuates vertical movement in the blast. This increases the chances for cutoffs (misfires) and overbreak.

Ratio K_T

The minimum recommended value for K_T for large hole production blasting is $K_T = 0.7$. Some specialists suggest the use of $K_T = 1.0$. Placing the charge too close to the collar can result in backbreak, flyrock and early release of the explosive gases with resulting poor fragmentation. On the other hand, increasing the length of stemming may reduce the energy concentration in the collar region to the point where large boulders result.

Ratio K_H

Currently most open pit operations have K_H values which are of the order of 1.6 or more. In some operations the burden is of the same order as the bench height ($K_H = 1$) which means that the blasting is similar to cratering with two free surfaces.

4.4 RATIO BASED BLAST DESIGN EXAMPLE

To illustrate the use of the geometrical relationships developed in Sections 4.2 and 4.3 assume that the initial design parameters are

- Rock = syenite porphyry ($SG = 2.6$),
- Explosive = *ANFO* ($\rho = 0.8$, $S_{ANFO} = 1$),
- Bench height (H) = 15 m,
- Hole diameter (D) = 381 mm (15 ins),
- Staggered drilling pattern, vertical holes,
- 4 rows of holes each containing 6 holes to make up 1 blast.

Using the design relationships, the following results are obtained

$K_B = 25$ (assumed)

$B = 25\ (0.381) = 9.5$ m

$S = 1.15B = 11$ m (staggered drilling pattern)

$T = 0.7B = 6.5$ m

$J = 0.3B = 3$ m

$L = H + J = 15\text{ m} + 3\text{ m} = 18$ m

The value of K_H is calculated to be

$$K_H = \frac{15}{9.5} = 1.6 \text{(acceptable)}$$

The layout for this corner blast would be as shown in Figure 4.11a. The burden (B) and hole spacing (S) dimensions (the pattern to be drilled) have been laid out with respect to the long face.

Figure 4.11b is a typical cross section through one of the holes. The volume (V_e) and weight (W_e) of explosive loaded into each hole is given by, respectively

$$V_e = \frac{\pi}{4} D^2 (L - T) = \frac{\pi}{4} (0.381)^2 (18 - 6.5) = 1.31 \text{ m}^3$$

$$W_e = V_e \rho = 1.31 \text{ m}^3 \times 800 \text{ kg/m}^3 = 1049 \text{ kg}$$

Since there are 24 holes in the round the total amount of explosive required (T_{EXP}) is

$$T_{EXP} = W_e \times n = 24 \times 1049 = 25{,}176 \text{ kg}$$

where n = number of holes.

The volume of rock which will be broken is

$$V_R = n \times B \times S \times H$$

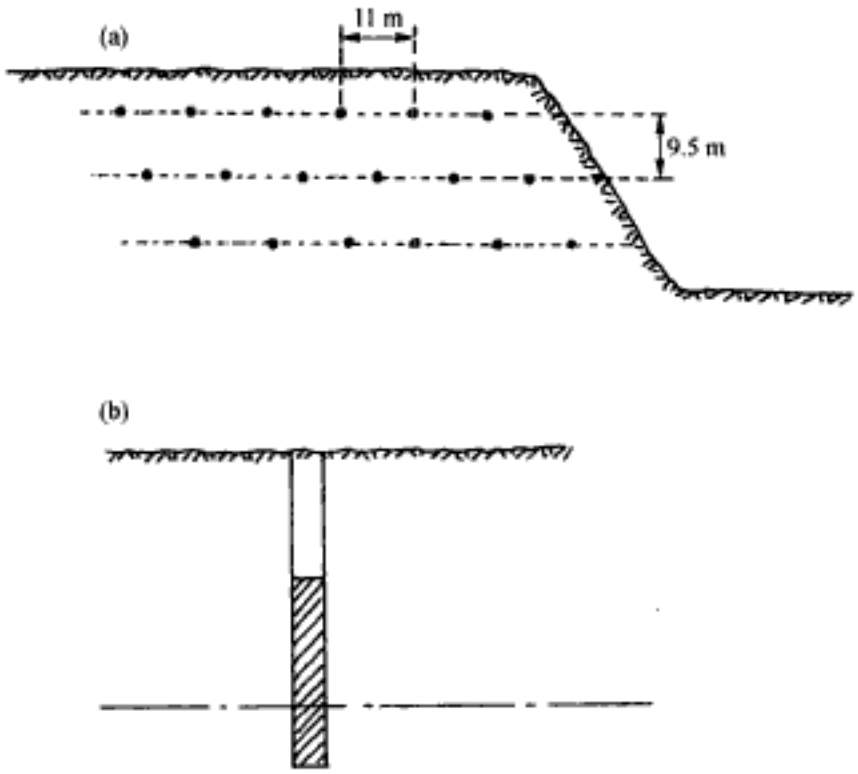

Figure 4.11. Layout for a corner blast.

Thus

$$V_R = 24\ (9.5)\ (11)\ (15) = 37{,}620\ \text{m}^3$$

Using a rock density of 2.6 t/m^3, a total of

$$T_R = \rho_R \times V_R = 97{,}812\ \text{tons}$$

would be broken. The resulting powder factor (*PF*) defined as the amount of explosive required to break one ton of rock is

$$PF_{ANFO} = \frac{T_{EXP}}{T_R} = \frac{25{,}176}{97{,}812} = 0.26\ \text{kg/ton}$$

The subscript *ANFO* has been added to the powder factor designation since it is explosive dependent.

To complete the design decisions have to be made regarding hole sequencing. This important topic is covered in Chapter 8 and the example will be continued at that time.

4.5 THE ASH DESIGN STANDARDS

4.5.1 *Introduction*

Before proceeding, it is well to have a reality check on these design equations. One of the classical papers in rock blasting 'The Mechanics of Rock Blasting' was written nearly 35

years ago and presented in four parts by Ash (1963). The present author highly recommends its reading even today by both students and practioners. The nomenclature and ratios K_B, K_H, K_J, K_T and K_S used in Sections 4.2 through 4.4 are the same as introduced by Ash in 1963 with the exception that the present author uses a bench height ratio K_H instead of the hole length ratio K_H* used by Ash. The former is more relevant when discussing open pit blasting with large holes versus quarry blasting which was the basis for much of the Ash field data. Thus the * will be attached to his K_H ratio to denote the difference in the calculation base from that used in the rest of the book.

In the introduction to Part II Ash (1963) states

'It is not enough just to understand what happens during blasting. Probably the most important thing to know is how blast effects can be controlled to suit the requirements of his operation. In this respect there are available five basic standards upon which to evaluate blasts, all of which are unitless (dimensionless) ratios. They can be applied to both underground and surface blasting with equal success. For simplicity, however, their use will be discussed as applied to surface (open-pit) blasting. The standards are defined as follows:

1. Burden Ratio (K_B) – the ratio of the burden distance in feet to the diameter of the explosive in inches, equal to 12 B/D.

2. Hole-Depth Ratio (K_H) – the ratio of the hole depth to the burden, both measured in feet, or H/B.*

3. Subdrilling Ratio (K_J) – the ratio of the subdrilling used to that of the burden, both expressed in feet, or J/B.

4. Stemming Ratio (K_T) – the ratio of the stemming, or collar distance to that of the burden, both expressed in feet, or T/B.

5. Spacing Ratio (K_S) – the ratio of the spacing dimension to that of the burden, both measured in feet, or S/B.'

4.5.2 *Field data*

In Part II of this paper Ash presented the design data reproduced in Tables 4.1 through 4.4. These data were collected from a wide range of operations and cover a correspondingly wide range of conditions:

- All types of surface blasting,
- 20 different rock types,
- Hole depths from 5 to 260 ft,
- Hole diameters from 1-5/8 ins to 10-5/8 ins,
- All grades of explosives.

All of the holes were vertical. The values of the ratios K_B, K_H*, K_J, and K_T were calculated from the data collected at the different operations, intervals were selected , and frequency distributions formed tabulating the number of operations in each interval. From these data the mean, the mode and the median values were calculated. These are given in Table 4.5.

For each of these ratios, Ash has provided some comments regarding their use. These are provided in his own words in the remaining subsections with only minor editing by the present author.

Table 4.1. The frequency distribution of the burden ratio K_B using data from all operations. After Ash (1963).

K_B Interval	Frequency
10-13	0
14-17	5
18-21	13
22-25	51
26-29	74
30-33	66
34-37	44
38-41	20
42-45	7
46-49	4
50-53	0
Total	284

Table 4.2. The frequency distribution of the hole depth ratio K_H^* using data from all operations. After Ash (1963)

K_H^* Interval	Frequency
0-0.9	0
1-1.9	43
2-2.9	70
3-3.9	56
4-4.9	45
5-5.9	22
6-6.9	22
7-7.9	11
8-8.9	4
9-9.9	2
10-10.9	8
11-11.9	0
12.12.9	1
Total	284

Table 4.3. The frequency distribution of the subdrill ratio K_J for all but coal strip operations. After Ash (1963).

K_J Interval	Frequency
0.0-0.0	15
0.1-0.19	18
0.2-0.29	27
0.3-0.39	26
0.4-0.49	25
0.5-0.59	2
0.6-0.69	6
0.7-0.79	2
0.8-0.89	0
Total	121

Table 4.4. The frequency distribution of the stemming ratio K_T for all but coal strip operations. After Ash (1963).

K_T Interval	Frequency
0.1-0.19	0
0.2-0.29	6
0.3-0.39	12
0.4-0.49	18
0.5-0.59	18
0.6-0.69	25
0.7-0.79	19
0.8-0.89	13
0.9-0.99	6
1.0-1.09	14
1.1-1.19	7
1.2-1.29	7
1.3-1.39	3
1.4-1.49	2
1.5-1.59	2
Total	152

Table 4.5. The range, mean, mode and median values for K_B, K_H*, K_J and K_T. After Ash (1963).

Ratio	Samples	Range	Mean	Mode	Median
K_B	284	14-49	30	38	29
K_H*	284	1.0-12.9	4.0	2.6	3.4
K_J	121	0-0.79	0.28	0.24	0.27
K_T	152	0.20-1.59	0.74	0.65	0.67

4.5.3 *Burden ratio (Ash, 1963)*

The most critical and important dimension in blasting is that of the burden. There are two requirements necessary to define it properly. To cover all conditions, the burden should be considered as the distance from a charge measured perpendicular to the nearest free face *and* in the direction in which displacement will most likely occur. Its actual value will depend on a combination of variables including the rock characteristics, the explosive used, etc. But when the rock is completely fragmented and displaced little or not at all, one can assume the critical value has been approached. Usually, an amount slightly less than the critical value is preferred by most blasters.

There are many formulae that provide approximate burden values but most require calculations that are bothersome or complex to the average man in the field. Many also require knowledge of various quantities of the rock and explosives, such as tensile strengths and detonation pressures, etc. As a rule, the necessary information is not readily available, nor is it understood.

A convenient guide that can be used for estimating the burden, however, is the K_B ratio. Experience shows that when $K_B = 30$, the blaster can usually expect satisfactory results for average field conditions (Table 4.5). To provide greater throw, the K_B value could be reduced below 30, and subsequently finer sizing is also expected to result.

Light density explosives, such as field-mixed *ANFO* mixtures, necessarily require the use of lower K_B ratios (20 to 25), while dense explosives, such as slurries and gelatins,

permit the use of K_B near 40. The final value selected should be the result of adjustments made to suit not only the rock and explosive types and densities but also the degree of fragmentation and displacement desired.

To estimate the desired K_B value one should know that densities for explosives are rarely greater than 1.6 or less than 0.8 g/cm^3. Also, for most rocks requiring blasting, the density in g/cm^3 rarely exceeds 3.2 nor is less than 2.2 with 2.7 far the most common value.

Thus, the blaster can, by first approximating the burden at a K_B of 30 make simple estimations toward 20 (or 40) to suit the rock and explosive characteristics, densities for the latter exerting the greater influence.

Thus

- For light explosives in dense rock use $K_B = 20$,
- For heavy explosives in light rock use $K_B = 40$,
- For light explosives in average rock use $K_B = 25$,
- For heavy explosives in average rock use $K_B = 35$.

Figure 4.12 illustrates the relationships between burdens and explosive diameters and can be used to approximate values for quick estimations. It should be noted, however, that the burden must be more carefully selected for small-diameter blastholes than for larger charges, a fact well confirmed by field experience.

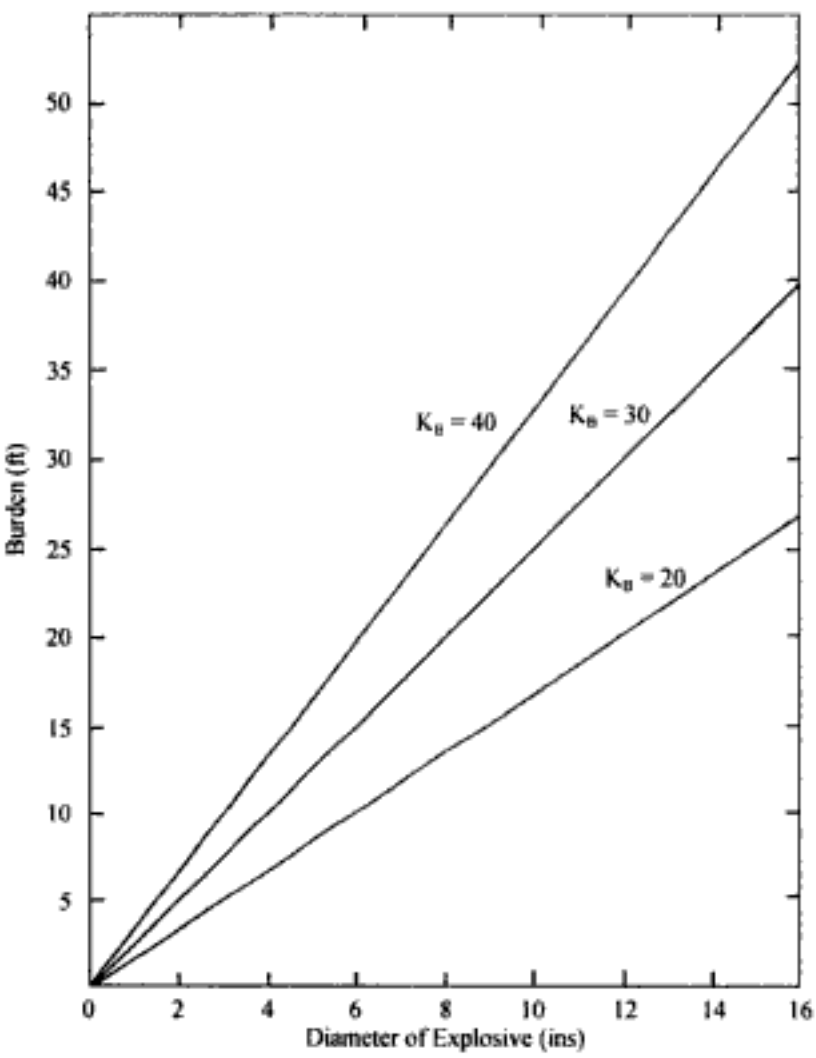

Figure 4.12. The relationship between burden and explosive diameter using the ash standard ratio (Ash, 1963).

4.5.4 *Hole depth ratio (Ash, 1963)*

As a rule, a blasthole should never be drilled to a depth less than the burden dimension if overbreak and cratering are to be avoided. In practice blastholes are generally drilled from 1-½ to 4 times the burden dimension. Blasting is most frequently done with a K_H^* value of 2.6 (Table 4.5).

4.5.5 *Subdrilling ratio (Ash, 1963)*

The primary reason for drilling blastholes below floor level (or grade) is to assure that a full face will be removed. Uneven floors caused by humps or toes generally create problems for later blasting, as well as for loading and haulage operations. For most conditions, the required subdrilling (J) should never be less than 0.2 the burden dimension, a K_J of at least 0.3 being preferred for quite massive ledges (Table 4.5).

The amount of necessary overdrilling logically depends upon the structural and density characteristics of the ledge, but also on the direction of the blastholes, in that inclined holes require less subdrilling, and horizontal holes no subdrilling whatsoever. Under certain conditions no subdrilling is required also for vertical holes, as would be the case for many coal strippings or rock quarries having a pronounced parting at the floor level. However for relatively massive rock drilling, at least 0.3 the burden below the floor will ensure that full ledge heights are obtained, provided, of course, that a proper K_H^* value is also used.

4.5.6 *Stemming ratio (Ash, 1963)*

Collar and stemming are sometimes used to express the same thing. However, stemming refers to the filling of blastholes in the collar region with materials such as drill cuttings to confine the explosive gases. But stemming and the amount of collar, the latter being the unloaded portion of a blasthole, perform other functions in addition to confining gases. Since an energy wave will travel much faster in solid rock than in the less dense unconsolidated stemming material, stressing will occur much earlier in the solid material than compaction of the stemming material could be accomplished. Thus the amount of collar that is left (T), whether or not stemming is used, determines the degree of stress balance in the region. The use of stemming material then assists in confining the gases by a delayed action that should be long enough in time duration to permit their performing the necessary work before rock movement and stemming ejection can occur. For stress balance in bench-blasting of massive material, the value of T should equal the B dimension.

Usually a K_T value of less than 1 in solid rock will cause some cratering, with back break and possible violence, particularly for collar priming of charges. However, if there are structural discontinuities in the collar regon, reflection and refraction of the energy waves reduce the effects in the direction of the charge length. Thus the K_T value can be reduced under such circumstances, the amount depending upon the degree of energy reduction at the density or structural interfaces. Field experience shows that a K_T value of 0.7 is a reasonable approximation for the control of air blast and stress balance in the collar region (Table 4.5).

4.5.7 *Spacing ratio (Ash, 1963)*

Commercial blasting usually requires the use of multiple blastholes, making it necessary for blasters to know whether or not there are any mutual effects between charges. If adjacent charges are initiated separately (in sequence), with a time-delay interval of sufficient length to permit each charge to complete its entire blasting action, there will be no interaction between their energy waves. However if the time interval for initiating adjacent charges is reduced, then complex effects will result.

The manner in which the zone of rock between holes is broken depends then not only on the particular initiation-timing system used but also on the spacing dimension. Ideal energy balancing between charges is usually accomplished when the spacing dimension is nearly equal to double that of the burden ($K_S = 2$) when charges are initiated simultaneously. For long-interval delays, the spacing should approximate the burden, or $K_S = 1$. For short-period delays, the K_S value will vary from 1 to 2 depending upon the interval used. However since structural planes of weakness such as jointing, etc., are not actually perpendicular to one another, the exact value for K_S normally will vary from 1.2 to 1.8, the preferred value of which must be tailored to local conditions. Most difficulties resulting from blasting can be attributed to the use of an unsuitable K_S relationship.

4.5.8 *Summary (Ash, 1963)*

Most blasting difficulties occur because of a lack in understanding of how rock is broken and the use of improper charge-placement and initiation-timing practices. The clues as to what could be wrong are often revealed by how a blast performs: whether or not uniform breakage results, toes are left, over-break and violence occur, and similar undesireable effects exist. Provided that the proper explosives are employed for the operating conditions, certain standards can be applied, to help in the evaluation of blasts. These standards can also assist in providing guidelines as to which direction adjustments should be made for correcting any difficulties. The standards are practical and simple to apply, being based on two fundamental, usually known quantities: explosive diameters and bench height. The standards are as follows:

K_B = 20 to 40 (30 average),
K^*_H = 1-½ to 4 (2.6 average),
K_J = 0.3 minimum,
K_T = 0.5 to 1 (0.7 average),
K_S = 1 to 2.

The standards will be found to be quite convenient and useful, after very little practice, not only for the initial design of blasts but also in providing guidelines upon which to correct formal blasting difficulties which invariably occur from time to time. However one must realize that the standards in themselves are not cure-alls, since blasting as such depends heavily on cost and safety considerations as well as on the explosive grades used, the materials characteristics, and the blasting techniques employed.

4.6 DETERMINATION OF K_B

The key dimensions required in the development of a blast design are based upon the burden which, in turn, is related to the borehole diameter through the burden factor K_B.

$$B = K_B D$$

The value for K_B

$$K_B = 25$$

has been found by the present author and others (Ash, 1963 for example) to work well for a wide range of hole diameters when using *ANFO* in rocks of medium density ($SG = 2.65$). Some guidance regarding the selection of K_B when using explosives in rocks of other densities is needed. The approach described in this section is proposed as a first approximation. The development of the basic equation for K_B will be first done using units of the metric system and then the equivalent formulae in the English system will simply be stated.

In addition to those parameters already introduced the following needed.

SG_E = specific gravity of the explosive
SG_R = specific gravity of the rock
PF_{EXP} = powder factor (kg/ton)
TF = tonnage factor (m^3/ton)

The basic geometry is shown in Figure 4.13 where one blasthole from the round has been isolated. The number of tons (T_R) broken is given by

$$T_R = K_S K_H B^3 \times SG_R \times \rho_{H_2O} \tag{4.31}$$

where

B = burden (m),
ρ_{H_2O} = density of water (mt/m^3)

Since in the metric system

$$\rho_{H_2O} = 1 \text{ mt/m}^3$$

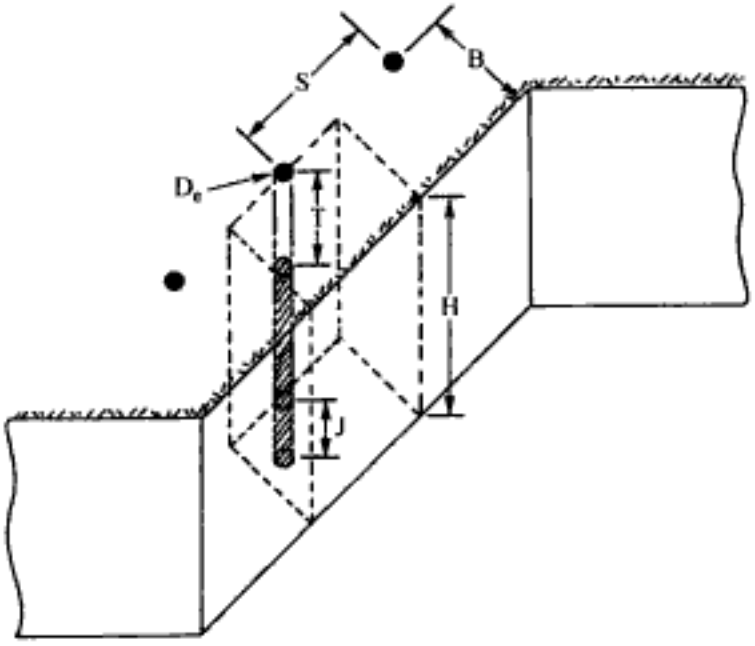

Figure 4.13. The rock volume associated with a blast hole.

this term will not be carried through the remaining equations. Knowing the powder factor required to provide the desired degree of fragmentation (PF_{EXP}), the amount of explosive required (E_{RQD}) is

$$E_{RQD} = T_R \times PF_{EXP} = K_S K_H B^3 \times SG_R \times PF_{EXP} \tag{4.32}$$

The total amount of explosive available (E_{AVL}) is

$$\begin{aligned} E_{AVL} &= \frac{\pi}{4}(D_e)^2 \left(BK_H + BK_J - BK_T\right) SG_E = \\ &= B\frac{\pi}{4}(D_e)^2 \left(K_H + K_J - K_T\right) SG_E \end{aligned} \tag{4.33}$$

where D_e = explosive diameter (m).

Setting the amount of explosive required to that available yields

$$SG_R K_S K_H B^3 PF_{EXP} = B\frac{\pi}{4}(D_e)^2 \left(K_H + K_J - K_T\right) SG_E \tag{4.34}$$

Solving Equation (4.34) for B one finds that

$$B = D_e \left[\left(\frac{\pi}{4} \right) \left(\frac{SG_E}{SG_R} \right) \left(\frac{1}{PF_{EXP}} \right) \left(\frac{K_H + K_J - K_T}{K_H \square K_S} \right) \right]^{1/2} \tag{4.35}$$

As can be seen by comparing Equation (4.35) to Equation (4.11), K_B is equal to

$$K_B = \left[\left(\frac{\pi}{4} \right) \left(\frac{SG_E}{SG_R} \right) \left(\frac{1}{PF_{EXP}} \right) \left(\frac{K_H + K_J - K_T}{K_H K_S} \right) \right]^{1/2} \tag{4.36}$$

The powder factor based on the actual explosive used (PF_{EXP}) will be replaced in Equation (4.36) by the equivalent *ANFO* powder factor (PF_{ANFO})

$$PF_{EXP} = \frac{PF_{ANFO}}{S_{ANFO}} \tag{4.37}$$

where S_{ANFO} = relative weight strength of the explosive *EXP* to *ANFO*.

Equation (4.36) then becomes

$$K_B = \left[\left(\frac{\pi}{4} \right) \left(\frac{SG_E}{SG_R} \right) \left(\frac{S_{ANFO}}{PF_{ANFO}} \right) \left(\frac{K_H + K_J - K_T}{K_H K_S} \right) \right]^{1/2} \tag{4.38}$$

This is quite a powerful formula as will be demonstrated through a series of examples.

Example 1. One of the major ways that the equation can be used is to study the effect of changes in the explosive on the blasting pattern while keeping other factors of the design

- Hole diameter,
- Bench height,
- Rock type,
- Spacing ratio K_S,
- Subdrill ratio K_J,
- Stemming ratio K_T,

the same. The bench height ratio K_H depends upon the burden which in turn depends upon K_B. Hence it will change. The approach is, therefore, to write Equation (4.38) twice using subscripts to denote Explosive 1 and Explosive 2.

Explosive 1:

$$K_{B1} = \left[\left(\frac{\pi}{4}\right)\left(\frac{SG_{E1}}{SG_R}\right)\left(\frac{S_{ANFO}}{PF_{ANFO}}\right)_1 \left(\frac{K_H + K_J - K_T}{K_H K_S}\right)_1 \right]^{1/2} \tag{4.39}$$

Explosive 2:

$$K_{B2} = \left[\left(\frac{\pi}{4}\right)\left(\frac{SG_{E2}}{SG_R}\right)\left(\frac{S_{ANFO}}{PF_{ANFO}}\right)_2 \left(\frac{K_H + K_J - K_T}{K_H K_S}\right)_2 \right]^{1/2} \tag{4.40}$$

Taking the ratio of Equations (4.40) and (4.39) one finds that

$$\frac{K_{B2}}{K_{B1}} = \left[\left(\frac{SG_{E2}}{SG_{E1}}\right)\left(\frac{PF_{ANFO}(1)}{PF_{ANFO}(2)}\right)\left(\frac{S_{ANFO}(2)}{S_{ANFO}(1)}\right) \frac{\left(\frac{K_H + K_J - K_T}{K_H K_S}\right)_2}{\left(\frac{K_H + K_J - K_T}{K_H K_S}\right)_1} \right]^{1/2} \tag{4.41}$$

If the *ANFO* equivalent powder factor is maintained constant (often the case), then Equation (4.41) reduces to

$$\frac{K_{B2}}{K_{B1}} = \sqrt{\frac{(SG_E \times S_{ANFO})_2}{(SG_E \times S_{ANFO})_1}} \times \sqrt{\left(\frac{K_H + K_J - K_T}{K_H K_S}\right)_2} \times \sqrt{\left(\frac{K_H K_S}{K_H + K_J - K_T}\right)_1} \tag{4.42}$$

If the variation of K_H with changing burden is neglected then

$$\left(\frac{K_H + K_J - K_T}{K_H K_S}\right)_2 = \left(\frac{K_H K_S}{K_H + K_J - K_T}\right)_1 \tag{4.43}$$

and the simplified expression becomes

$$\frac{K_{B2}}{K_{B1}} = \sqrt{\frac{(SG_E \times S_{ANFO})_2}{(SG_E \times S_{ANFO})_1}} \tag{4.44}$$

Thus, as a first approximation, the K_B ratio is equal to the square root of the bulk strength ratio for the explosives involved.

To refine the value of K_{B2}, an iteration process involving the three equations

$$B_2 = K_{B2}\ D_e \tag{4.45}$$

$$K_{H2} = \frac{H}{B_2} \tag{4.46}$$

$$K_{B2} = K_{B1}\sqrt{\frac{(SG_E \times S_{ANFO})_2}{(SG_E \times S_{ANFO})_1}}\sqrt{\frac{K_{H2} + K_J - K_T}{K_{H2}\ K_S}}\ \sqrt{\frac{K_{H1} K_S}{K_{H1} + K_J - K_T}} \tag{4.42}$$

in sequence is used. The initial value of K_{B2} is substituted into Equation (4.45) and solved for B_2. The value of K_{H2} is then found from Equation (4.46) which then is input into

Equation (4.42). The resulting value of K_{B2} is compared with the initial estimate. If they are the same, the process stops. If not than this new value of K_{B2} is input into Equation (4.45) and the process continues. It converges rapidly to a stable solution.

Example 2: This same procedure can be used to evaluate the effect of changing other variables. Rock density is one parameter of interest. Equation (4.38) is written assuming two materials having different densities (specific gravities).

Material Density 1:

$$K_{B1} = \left[\left(\frac{\pi}{4}\right)\left(\frac{SG_E}{SG_R}\right)_1\left(\frac{S_{ANFO}}{PF_{ANFO}}\right)_1\left(\frac{K_H + K_J - K_T}{K_H K_S}\right)_1\right]^{1/2} \tag{4.47}$$

Material Density 2:

$$K_{B2} = \left[\left(\frac{\pi}{4}\right)\left(\frac{SG_E}{SG_R}\right)_2\left(\frac{S_{ANFO}}{PF_{ANFO}}\right)_2\left(\frac{K_H + K_J - K_T}{K_H K_S}\right)_2\right]^{1/2} \tag{4.48}$$

Although not necessary it will be assumed that the following remain constant

- Hole diameter,
- Explosive,
- Bench height,
- Spacing ratio K_S,
- Subdrill ratio K_J,
- Stemming ratio K_T.

The bench height ratio K_H depends upon the burden which in turn depends upon K_B and hence it will change. Dividing Equation (4.48) by Equation (4.47) one finds that

$$\frac{K_{B2}}{K_{B1}} = \left[\left(\frac{SG_{R1}}{SG_{R2}}\right)\left(\frac{K_{H2} + K_J - K_T}{K_{H2} K_S}\right)\left(\frac{K_{H1} K_S}{K_{H1} + K_J - K_T}\right)\right]^{1/2} \tag{4.49}$$

If the variation of K_H with changing burden is neglected, then as a first approximation

$$\frac{K_{B2}}{K_{B1}} = \sqrt{\frac{SG_{R1}}{SG_{R2}}} \tag{4.50}$$

Once the initial value of K_{B2} is found, an iteration process involving the three equations

$$B_2 = K_{B2} D_e \tag{4.45}$$

$$K_{H2} = \frac{H}{B_2} \tag{4.46}$$

$$\frac{K_{B2}}{K_{B1}} = \sqrt{\frac{SG_{R1}}{SG_{R2}}}\sqrt{\frac{K_{H1} K_S}{K_{H1} + K_J - K_T}}\sqrt{\frac{K_{H2} + K_J - K_T}{K_{H2} K_S}} \tag{4.49}$$

is performed until a stable value for K_{B2} is obtained.

In the English system, Equation (4.38) becomes

$$K_B = (2000)^{1/2}\left[\left(\frac{\pi}{4}\right)\left(\frac{SG_E}{SG_R}\right)\left(\frac{S_{ANFO}}{PF_{ANFO}}\right)\left(\frac{K_H + K_J - K_T}{K_H K_S}\right)\right]^{1/2} \tag{4.51}$$

where PF_{ANFO} = *ANFO* equivalent powder factor (lbs/ton), 2000 = lbs/ton.

When using the iteration process it is important to maintain a consistent set of units. Thus if the burden is expressed in feet, then the hole diameter in Equation (4.45), for example, must also be in feet.

4.7 SIMULATION OF DIFFERENT DESIGN ALTERNATIVES

In Section 4.5 a theoretical basis for evaluating different design alternatives was presented. Here two design variations will be considered starting with the pattern in use at the mine today.

Hole diameter = 12¼ ins,
Bench height = 40 ft,
Burden = 25 ft,
Spacing = 29 ft,
Subdrill = 7 ft,
Stemming = 17 ft,
ANFO: $S_{ANFO} = 1.0$,
$SG_{ANFO} = 0.82$,
$Q = 912$ cal/gm,
Rock: $SG = 2.65$,
$PF_{ANFO} = 0.5$ lbs/ton.

One question might be 'What would the pattern be using 15″ diameter holes?' Using Equation (4.51) one would first determine the current value of K_B. The required input values are

$$K_H = 40/25 = 16$$
$$K_J = 7/25 = 0.3$$
$$K_T = 17/25 = 0.7$$
$$K_S = 29/25 = 1.15$$
$$SG_{expl} = 0.82$$
$$SG_{rock} = 2.65$$
$$S_{ANFO} = 1$$
$$PF_{ANFO} = 0.50$$

Substituting these values into Equation (4.51) one finds that

$$K_B = \left[2000\left(\frac{\pi}{4}\right)\left(\frac{0.82}{2.65}\right)\left(\frac{1}{0.50}\right)\left(\frac{1.6+0.3-0.7}{(1.6)(1.15)}\right)\right]^{1/2} = (634)^{1/2} = 25.2$$

This is what might have been expected using the guidelines of Ash (1963). For the 15 inch diameter holes, the first approximation for the burden would be

$$B = K_B\left(\frac{D_e}{12}\right) = 25.2\left(\frac{15}{12}\right) = 31.5 \text{ ft}$$

This however changes the value of K_H to

$$K_H = \frac{H}{B} = \frac{40}{31.5} = 1.27$$

Substituting this into Equation (4.51) keeping all other values constant one finds that

$$K_B = \left[972\left(\frac{1.27 + 0.3 - 0.7}{1.27(1.15)}\right)\right]^{1/2} = 24.1$$

Iterating until a stable value is found yields

$$K_B = 24.3$$

The resulting pattern with the 15″ diameter holes is

$$B = 30 \text{ ft}$$

$$S = 34.5 \text{ ft}$$

$$T = 21 \text{ ft}$$

$$J = 9 \text{ ft}$$

The powder factor

$$PF_{ANFO} = \frac{\left(\frac{\pi}{4}\right)\left(\frac{15}{12}\right)^2 (40 + 9 - 21)0.82 \times 2000}{30 \times 34.5 \times 40 \times 2.65} = 0.51 \text{ lbs/ton}$$

is slightly different from the expected value of 0.50 due to round off. As was pointed out earlier, this pattern would be expected to yield a more coarse fragmentation than with the 12¼″ holes. To maintain the same fragmentation, the powder factor would have to be increased. This can be easily included in the calculation.

Another possible question deals with 'what happens to the pattern if the explosive is changed?' Assume that the mine is considering replacing *ANFO* by a heavy *ANFO* with the following properties.

$SG = 1.10$

$Q = 815$ cal/gm

The weight strength of this product with respect to *ANFO* is

$$S_{ANFO} = \frac{815}{912} = 0.89$$

Using Equation (4.44) the value of K_{B2} is

$$K_{B2} = K_{B1}\sqrt{\frac{1.10 \times 0.89}{0.82 \times 1.00}} = 1.09\, K_{B1}$$

Since

$$K_{B1} = 25.2$$

then

$$K_{B2} = 27.5$$

The new burden would be

$$B_2 = 27.5\left(\frac{12.25}{12}\right) = 28.1 \text{ ft}$$

and K_{H2} becomes

$$K_{H2} = \frac{40}{28.1} = 1.42$$

This is now substituted into Equation (4.49) to arrive at a new approximation for K_{B2}.

$$K_{B2} = K_{B1}\sqrt{\frac{(SG \times S_{ANFO})_2}{(SG \times S_{ANFO})_1}} \times \sqrt{\left(\frac{K_H + K_J - K_T}{K_H K_S}\right)_2} \times \sqrt{\left(\frac{K_H K_S}{K_H + K_J - K_T}\right)_1}$$

Most of the terms are constant and it can in this case be simplified to

$$K_{B2} = (25.2)\sqrt{\frac{(1.10)(0.89)}{0.82(1.0)}}\sqrt{\frac{1.6(1.15)}{1.6+0.3-0.7}}\sqrt{\frac{K_{H2}+0.3-0.7}{K_{H2}(1.15)}}$$

$$K_{B2} = 34.1\sqrt{\frac{K_{H2}-0.4}{1.15\,K_{H2}}} \qquad (4.52)$$

Substitution of $K_{H2} = 1.42$ into Equation (4.52) yields

$$K_{B2} = 26.95$$

The new burden is

$$B_2 = 26.95\left(\frac{12.25}{12}\right) = 27.51 \text{ ft}$$

and the corresponding value of K_{H2} is

$$K_{H2} = \frac{H}{B_2} = \frac{40}{27.51} = 1.45$$

This is substituted into Equation (4.52) and the process continued until a stable value of K_{B2} results. In this case it is

$$B_2 = 27.0$$

The blast pattern would be

$B = 27.0\,(12.25/12) = 27.6$ ft

$S = 31.7$ ft

$J = 8.3$ ft

$T = 19.3$ ft

The powder factor becomes

$$PF_{actual} = \frac{\left(\frac{\pi}{4}\right)\left(\frac{12.25}{12}\right)^2 (40 + 8.3 - 19.3)(1.10)(2000)}{27.6 \times 31.7 \times 40 \times 2.65} = 0.563 \text{ lbs/ton}$$

In terms of the *ANFO* equivalent powder factor this becomes

$$PF_{ANFO} = PF_{actual} \times S_{ANFO} = 0.56 \times 0.89 = 0.50 \text{ lbs/ton}$$

which is as expected.

As indicated, this approach to the paper evaluation of different blast designs is quite general. The costs associated with the different designs can be easily added to translate the results into an expected fragmentation cost per ton.

4.8 ROCK STRUCTURE AND BLAST PATTERN DESIGN

Figure 4.14 shows the type of radial cracking which one might expect when blasting a single hole in a brittle, massive rock formation. There will be a relatively few long cracks (6-8) spaced uniformly around the hole. As one approaches the hole the cracks will be shorter and more numerous.

The maximum length (R_c) of the radial cracks for a given explosive and rock type can be shown to be directly dependent on the hole radius. Thus as the hole diameter is increased from 150 mm to 310 mm the length of the longest cracks would be expected to about double. This is consistent with the design relationship

$$B = K_B D$$

presented earlier since the burden should be related to the lengths of the cracks generated

$$B \alpha R_c \tag{4.53}$$

If the strength of the explosive used in a hole of given diameter is increased or decreased, the outer crack radius should change accordingly. This is reflected in the value of K_B chosen. Since in general, a larger diameter hole is less expensive to drill than one of smaller diameter (on a cost/volume basis) the natural conclusion would be to drill as large diameter holes as possible. Unfortunately fragmentation considerations would suggest just the opposite, ie the holes should be smaller to better distribute the explosive throughout the rock mass. To illustrate this some simple geometric reasons will be given.

Figure 4.15 shows two possible blast patterns using different size holes but the same explosive. The specific energy (powder factor) is the same for both. A simplified representation of the radial cracks after blasting is shown in Figure 4.16 for each pattern. As the hole diameter is increased and the pattern expands, the distance between adjacent crack tips becomes greater. For the case shown

$$L > L'$$

Thus even though the energy density is the same, the fragmentation is more coarse. Generally as the pattern is spread, the powder factor (energy factor) must be increased to maintain acceptable fragmentation. One way of doing that is to limit the pattern spread to some proportion of the theoretical value. As shown in Figure 4.17, there is now an overlap of the longest fractures. Another way of accomplishing this would be to increase the energy of the explosive being used.

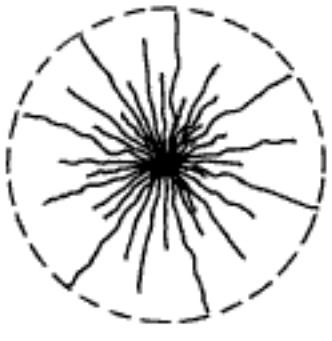

Figure 4.14. An idealized representation of the radial cracking surrounding a single hole.

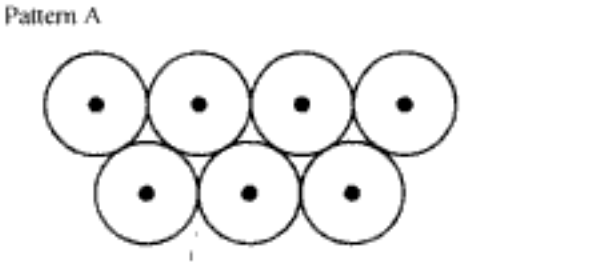

Figure 4.15. The extent of cracking for two patterns with different hole diameters.

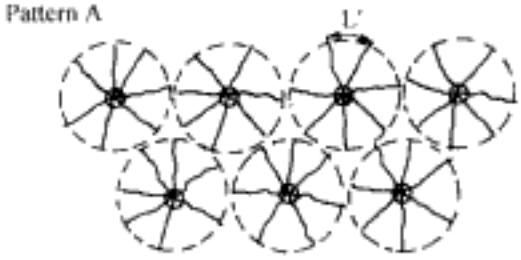

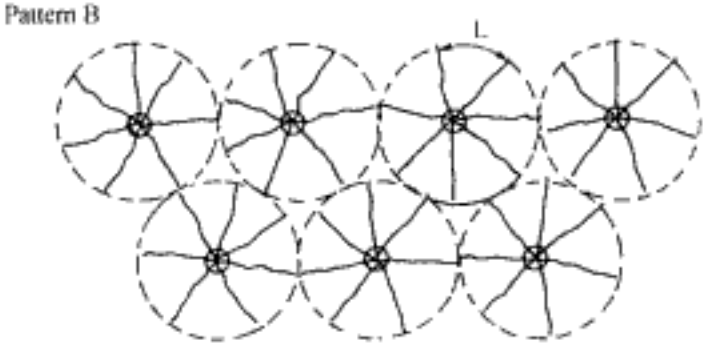

Figure 4.16. Maximum block dimensions for the hole patterns shown in Figure 4.15.

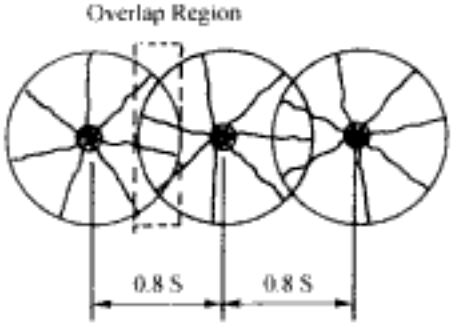

Figure 4.17. Fragmentation enhancement achieved by reducing the spacing.

Therefore, even in massive rocks, because of

– The point introduction of energy into the rock,
– Fracture geometry,

there are limiting hole diameters/burdens/spacings which yield acceptable fragmentation. It is well known that an actual rock mass generally contains many discontinuities of different types. The most common being

– Joints,
– Bedding planes/layering,
– Foliation,
– Faults.

If such structures (joints in particular) are now introduced, such as is shown in Figure 4.18, the story becomes even more complex. The radius of influence for any given hole is significantly reduced since

1. The radial cracks will not cross the gaps formed by the joints.
2. The high pressure gasses can be short-circuited by the less resistant joints compared with the fresh cracks. Therefore the primary fracturing effectiveness is reduced as well as that produced by a sustained heave of the fractured material.

Although these pre-existing cracks limit the formation of new cracks and provide avenues of escape for the explosive gases, mobilization of these is a major reason why the specific breakage energy in blasting is much lower than other processes which must attack the intact rock.

Figure 4.19 shows two potential drilling patterns in the jointed rock. The smaller diameter, closely spaced holes yield almost one hole per block and the fragmentation would be expected to be good. On the other hand, the larger holes on wide spacings could yield a large number of substantial blocks largely isolated from the effect of the explosive by the

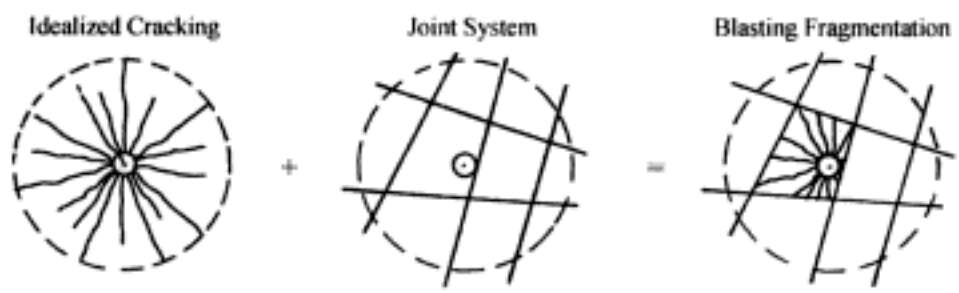

Figure 4.18. Effect of jointing on fragmentation.

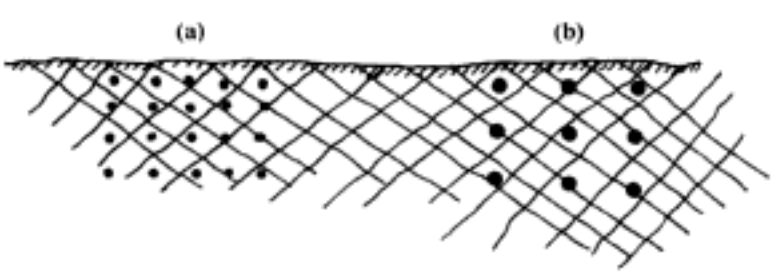

Figure 4.19. Two possible blast patterns superimposed on jointed rock.

joints. Pattern (a) would have higher associated drilling and blasting costs than Pattern (b). By assigning costs to the degree of fragmentation, an 'optimum' pattern can be determined.

The orientation of the major structures can have a significant effect on blasting results. There are three cases to be considered (Burkle, 1979).

- Shooting with the dip
- Shooting against the dip
- Shooting along the strike

In shooting with the dip (Fig. 4.20) one finds

(a) a tendency to get more back break
(b) less toe problems
(c) a smoother pit floor
(d) more movement away from the face and therefore a lower muckpile profile.

When shooting against the dip (Fig. 4.21) one finds

(a) less backbreak since the strata is dipping into the wall.
(b) the toe would be more difficult to pull.
(c) a rougher floor condition.
(d) the muckpile may be higher with less movement from the face.

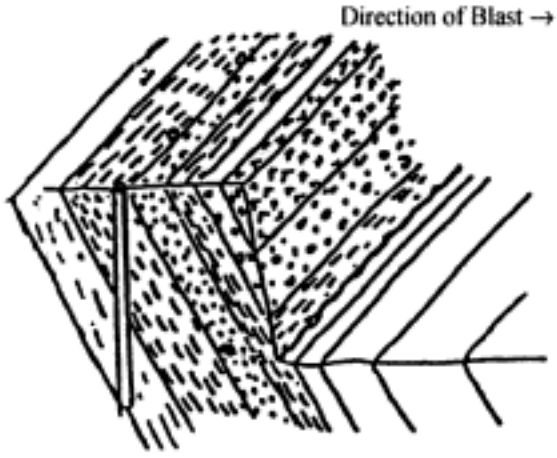

Figure 4.20. Diagrammatic representation of shooting in the dip direction (Burkle, 1979).

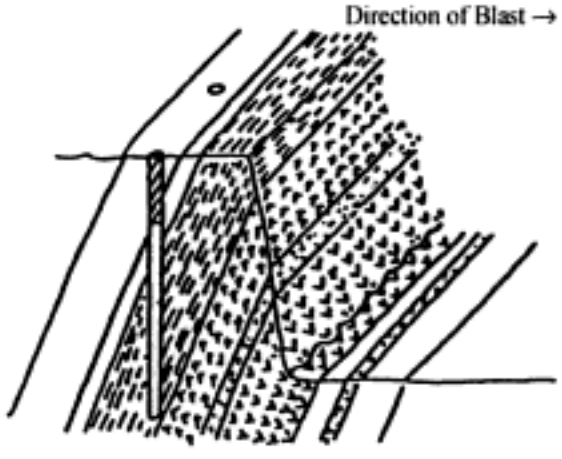

Figure 4.21. Diagrammatic representation of shooting against the dip (Burkle, 1979).

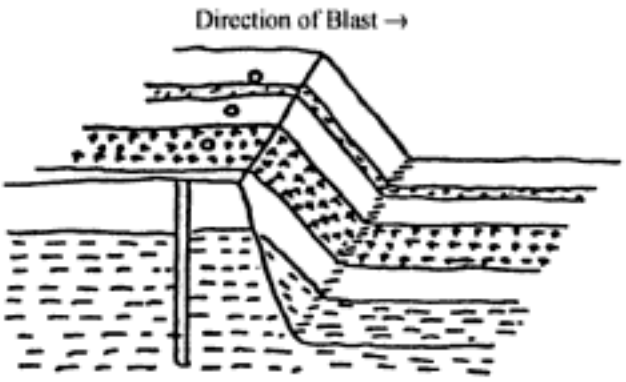

Figure 4.22. Diagrammatic representation of shooting along strike (Burkle, 1979).

Finally, when shooting along the strike (Fig. 4.22) one finds that the floor can be highly sawtoothed due to the different rock types intersecting the floor. For the same reasons the back break is irregular. These are some of the worst conditions for those involved in drilling and blasting. To overcome this, the working face may be reoriented to a more favorable conditions.

The formations should be examined to identify the strike and dip direction of the most prominent joints. In igneous and metamorphic rock formations, one should consider aligning the rows of holes parallel to the alignment of the dominant joint system. In sedimentary rocks, the drill holes should be placed in rows drilled parallel to the formation strike line.

4.9 MEASURE-WHILE-DRILLING SYSTEMS

Modern drilling machines may be equipped with systems which monitor amongst other variables

- Penetration rate
- Torque
- Pulldown pressure
- Rotary speed

as a function of hole advance. This practice has been given the name Measure-While-Drilling (MWD). From these data one can calculate quantities such as the specific energy (energy required to remove a unit volume of rock) which can be related to the difficulty of breaking rock. One such record for a rotary drill used in coal formation rocks (Peck et al., 1990) is shown in Figure 4.23. The strength differences in the various rock types can be easily seen. Based upon such results decisions can be made regarding, for example, the placement of higher energy explosives, stemming, etc.

One mining property where the MWD technique has been used with success is at Highland Valley Copper in British Columbia (Daly & Assmus, 1992). Due to poor fragmentation, high toe areas, excessive shovel wear and tear, etc an integrated program to improve drilling and blasting practices was initiated in the early 1980s. In this sub-section a brief overview of their program and the results achieved at the Valley Pit will be presented. In 1992 the time at which the paper (Daly & Assmus, 1992) upon which this section is based was written, the production from the pit was about 200,000 tons per day of ore and waste from benches 12.5 m in height.

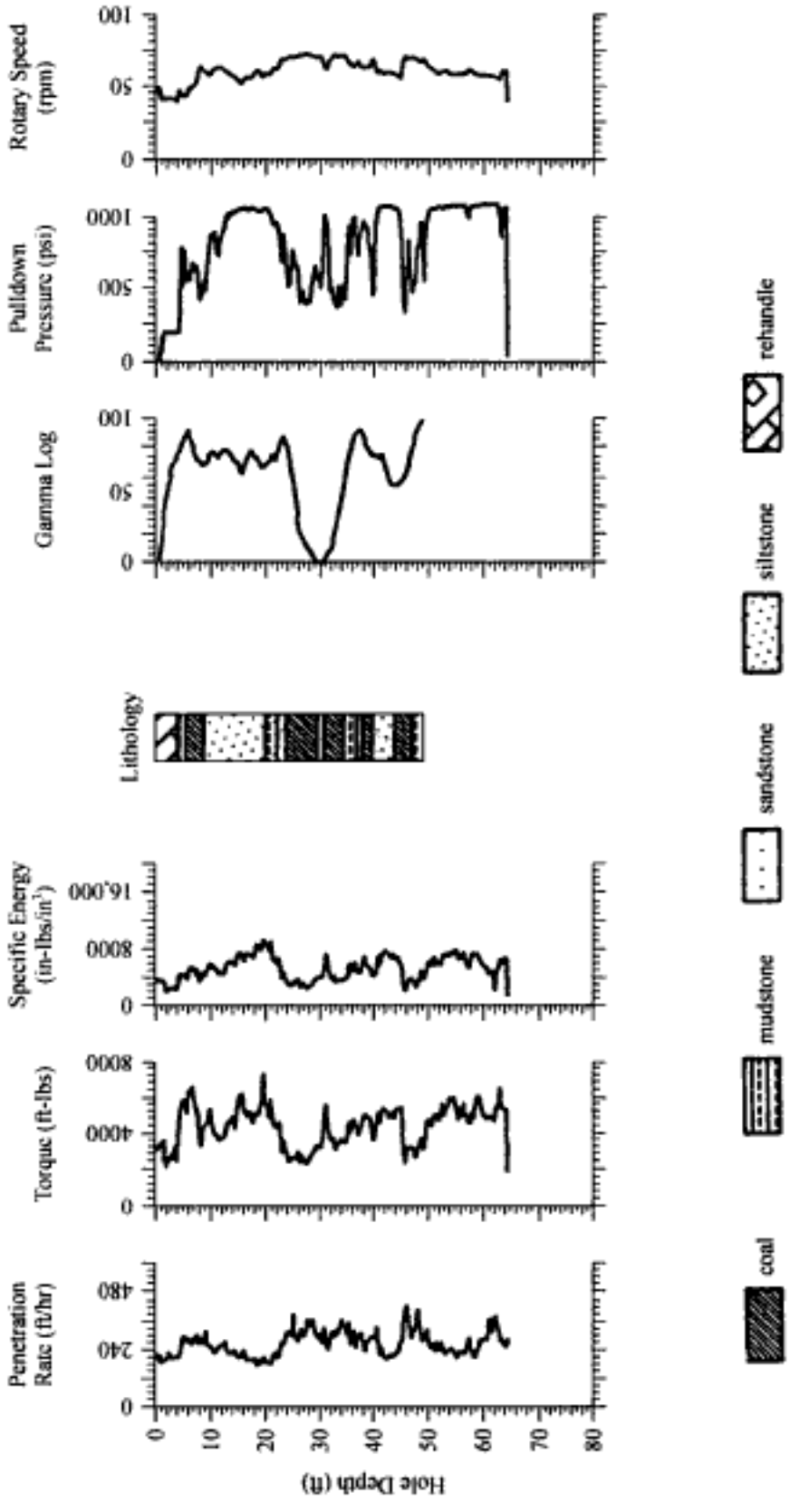

Figure 4.23. Typical monitoring record for a rotary drill operating in coal measure rocks (Peck et al. 1990).

The ore host rock is Bethsida quartz monzonite. The other rock types present are (a) quartz and quartz feldspar porphyry which occur in dikes ranging from 0.3 to 35 m thick and (b) lamprophyre dikes averaging 4.5 m thick. These dike materials are hard and unaltered. The quartz monzonite has experienced various degrees of hydrothermal alteration. The alteration zones commonly strike north-south and dip steeply to the east. Other more local structural trends are

- North-south fractures and faults dipping steeply to the west,
- East-west fractures dipping steeply to the south,
- Southeast striking fractures dipping moderately northeasterly or southwesterly.

This combination of structure and alteration type and intensity largely determines the rock blastability.

Rock strength is a traditional component of a blastability classification system. The field strength categories used by Highland Valley Copper are given below:

Category	Estimated rock mass compressive strength (psi)
R1	182-1825
R2	1825-7300
R3	7300-14,600
R4	14,600-29,000
R5	>29,000

There are other factors, however, which determine the overall blastability. The rock mass-blasting zone classification system which was developed divided the Bethsaida quartz monzonite into the three categories poor, fair and good. Rock with a blastability classification 'poor' means Bethsaida quartz monzonite with an R5 strength. It can either be fresh to weakly altered or intensely argillicaly altered but intensely silicified (approximately 39-59%). Joint spacing is commonly 1.5 to 6 m and joints tend to be master joints with 12 m or more (bench height) continuity and continuity along strike of 50 m or more. These master joints divide the rock mass into large blocks which, when blasted, result in very chunky muck. The classification 'good' means R2 or R3 rock strength material, usually moderate to intensely argillicly altered Bethsaida quartz monzonite cut by frequent fractures, shears and gouge-filled faults. The intense fracturing and the strong alteration renders the rock soft and friable and blastable into fine muck. The rock classified as 'fair' consists of moderate to moderate-intense argillicly altered Bethsaida quartz monzonite with an average R3 uniaxial compressive strength. It is commonly well-fractured and yields blocky muck approximately 0.3 m in diameter.

A combination of geotechnical mapping, penetration rate data, toe elevation contouring and observations on shovel and drill performance were used to determine the character and extent of the blast zones. The procedure used to develop the blast zones was as follows (Daly & Assmus, 1992):

1. The actively mined faces and the final walls of the bench are mapped recording all pertinant geotechnical information.
2. The alteration zones are projected along the predominant structural trends across the bench using a hydrothermal alteration model.
3. Experience gained from the overlying bench is utilized:
   a. Blasthole drilling penetration rate maps

b. Toe elevation contours (0.3 to 0.6 m intervals) to show the high relief areas.
c. Shovel and drill performance data as they drilled and mucked the bench. Hard zones are indicated by areas which required re-drilling due to poor fragmentation and tough-digging zones for the shovels indicated hard zones.

4. The penetration rate data and toe elevation data were then used to verify or modify the blast zone contacts as projected across the bench from the geotechnical mapping.

Once each bench is mapped and a blast zone outlined, a blast pattern size is determined for each zone. When the blast plan for each new bench is made up, a particular powder factor is assigned to each blast zone, according to the blasting results, digging performance and geotechnical characteristics of that zone on the last bench. Tough digging and very chunky muck mean that the powder factor must be increased, whereas fine muck and easy digging indicate the powder factor can be reduced. The extent of the blast zones with a particular powder factor may also change from bench to bench depending on the dip and plunge of the structural/alteration make-up of the zones.

After a pattern has been blasted, the broken rock is monitored to see if the digging is adequate and the fragmentation acceptable for both the shovel digging the muck and the crusher, if it is ore. At the Valley Pit the ore must be blasted more for the crushers than for the shovels. Poor digging is manifested by chunky and poorly broken muck, a lot of scraping of the face by the shovel to dislodge chunks, shaking of the boom cables and rocking on the tracks as the bucket breaks loose a hard chunk. This is very hard on the shovel.

The topography of the toe can be a good indication of the success of the blast. High toes of 1.5 m to 3 m were common in the poor zones in the early days until the blasting was refined. On the other hand, low toes and fine, floury muck indicate overblasting. When a bench has been mined out and mapped a new blast plan is outlined for the next bench.

Experience has shown that the geotechnical mapping and drill penetration times have the greatest impact on determining blastability zones. Figure 4.24 shows two main poor zones on the 1125 bench. The northern zone consists of very chunky, tough Bethsaida quartz monzonite bound together by a closely spaced network of quartz-bornite stringers and hardened by quartz-grain silicification. The southern zone consists of fresh to weakly altered Bethsaida on the west side and a quartz vein network on the east side resulting in tough digging. Both of these geological zones correlated well with 35 to 49 minute/hole penetration rate contours shown in Figure 4.25. Both zones were blasted with 7.3 m by 8.4 m patterns and a powder factor of 0.267 kg/t. The central 'fair' zone is a vertically persistent zone that exhibits closely spaced fracturing (commonly 0.3 m spacing or less) and moderate-intense argillic alteration. This zone strikes northerly and dips consistently easterly at about 60° and plunges to the north. Correlating quite well with the 20 minute penetration rate contours, it was blasted using a 7.8 m by 9.1 m pattern and a powder factor of 0.228 kg/t. Without the information provided by the mapping and penetration rate, normally one pattern would have been used for the entire bench. Based on the use of this information, the pattern spacing was widened due to this more friable zone, thus saving explosives and still achieving good fragmentation. The pattern sizes used for the 1125 bench (west wall) are:

Zone	Pattern size	Powder factor (kg/t)
Poor	7.3 m × 8.4 m	0.267
Fair	7.8 m × 9.1 m	0.228
Good	9.1 m × 10.4 m	0.174

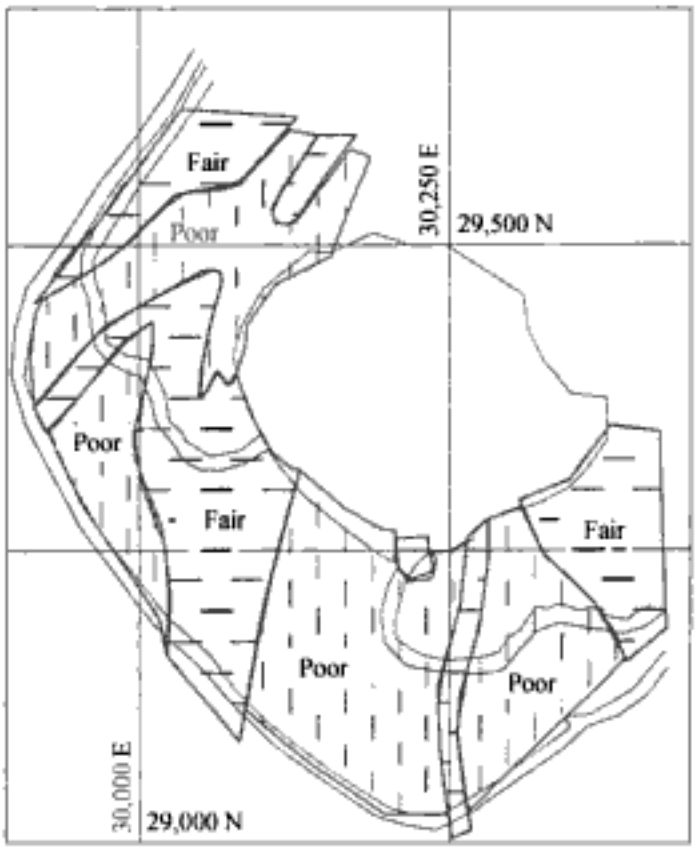

Figure 4.24. Dig-ability plan for the 1125 bench of the Valley pit (Daly & Assmus, 1992).

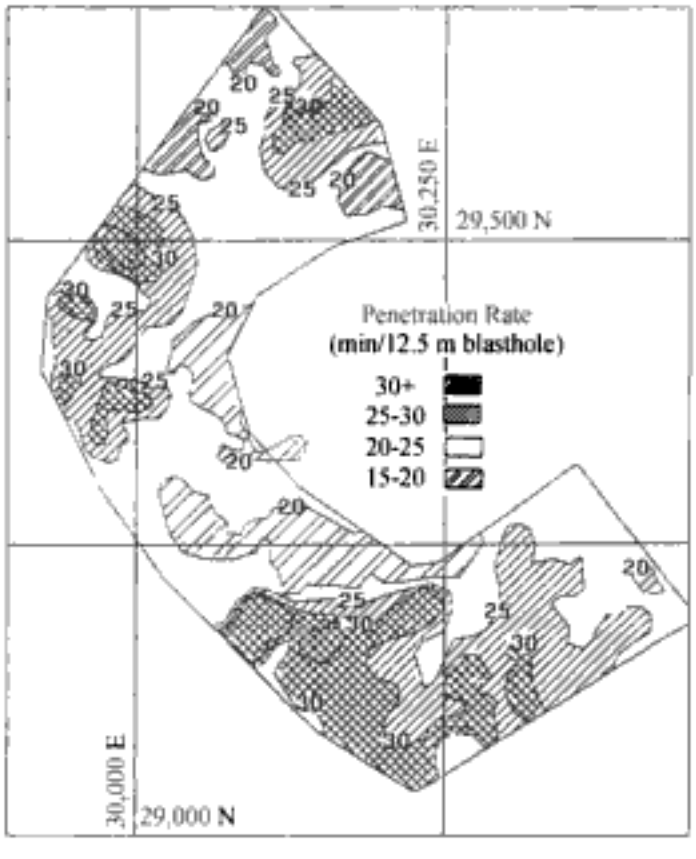

Figure 4.25. Blasthole drill penetration rate for the 1125 bench of the Valley pit (Daly & Assmus, 1992).

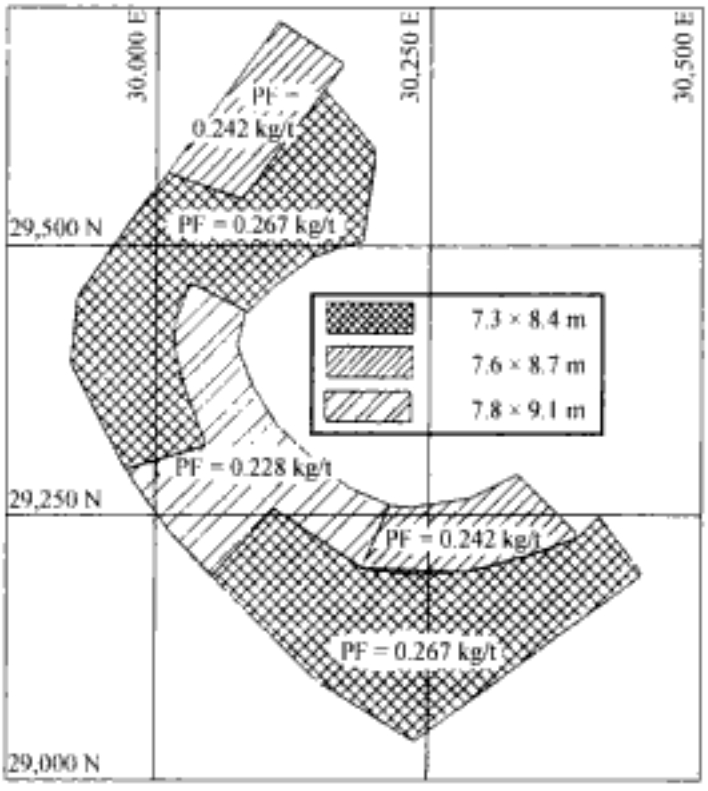

Figure 4.26. Pattern sizes for the 1125 bench of the Valley pit (Daly & Assmus, 1992).

These are shown in Figure 4.26.

In conclusion, by accurately determining the blastability zones, explosives, blasting accessories, blasthole drilling and shovel and truck operations can be optimized with a subsequent substantial cost savings. The benefits of better fragmentation to the truck-shovel operations are measured in increased productivity and decreased maintenance costs. From a maintenance point of view there is less shovel breakdown, less replacement of crowd transmissions, better dipper life and increased teeth and adaptor life. The trucks benefit from less impact on the box during loading of smaller sized chunks and truck operators appreciate the gentler loading resulting from the finer muck.

4.10 ROCK BLASTABILITY

An attempt to relate blastability to rock and rock mass properties has been reported by Lilly (1986). The blastability Index (*BI*) is defined as

$$BI = \frac{1}{2}[RMD + JPS + JPO + SGI + H] \tag{4.54}$$

where *RMD* = rock mass description, *JPS* = joint plane spacing, *JPO* = joint plane orientation, *SGI* = specific gravity influence, *H* = hardness.

The ratings for the different parameters are given in Table 4.6. The Moh's scale of hardness used to define *H* is given in Table 4.7. Historical data from the iron mines located in northwest Western Australia were used in constructing the *ANFO* powder factor – blastability index curve shown in Figure 4.27. These mines are typically large scale, rope shovel operations. *ANFO* is the primary explosive and large primary crushers are used. A *BI*

Table 4.6. Ratings for the blastability index parameters. After Lilly (1986).

Parameter	Rating
1. Rock mass description (*RMD*)	
1.1 Powdery/Friable	10
1.2 Blocky	20
1.3 Totally massive	50
2. Joint Plane Spacing (*JPS*)	
2.1 Close (< 0.1 m)	10
2.2 Intermediate (0.1 to 1 m)	20
2.3 Wide (> 1 m)	50
3. Joint Plane Orientation (*JPO*)	
3.1 Horizontal	10
3.2 Dip out of face	20
3.3 Strike normal to face	30
3.4 Dip into face	40
4. Specific Gravity Influence (*SGI*)	
SGI = 25 *SG* − 50, where *SG* is equal to the specific gravity of the rock	
5. Hardness (*H*)	
(Moh's hardness scale)	

Table 4.7. Moh's scale of hardness (Roberts, 1977).

Material	Moh's hardness
Talc	1
Rock salt, gympsum	2
Calcite	3
Fluorspar	4
Apatite	5
Feldspar	6
Quartz	7
Topaz	8
Corundrum	9
Diamond	10

value of 100 refers to a massive, extremely hard, iron-rich cap rock. It has a specific gravity of 4. Soft, friable shales have an index of around 20. The energy factor axis was added by Lilly (1986) to allow consideration of other explosives. The following two examples were used by Lilly (1986) to illustrate the application of the Blastability Index.

Example 1. A highly laminated, soft ferruginous shale which has horizontal to sub-horizontal bedding

$RMD = 15$
$JPS = 10$
$JPO = 10$
$SGI = 10$
$H = 1$
$TOTAL = 46$ and $BI = 23$.

From Figure 4.27, the powder factor is about 0.1 kg/tonne.

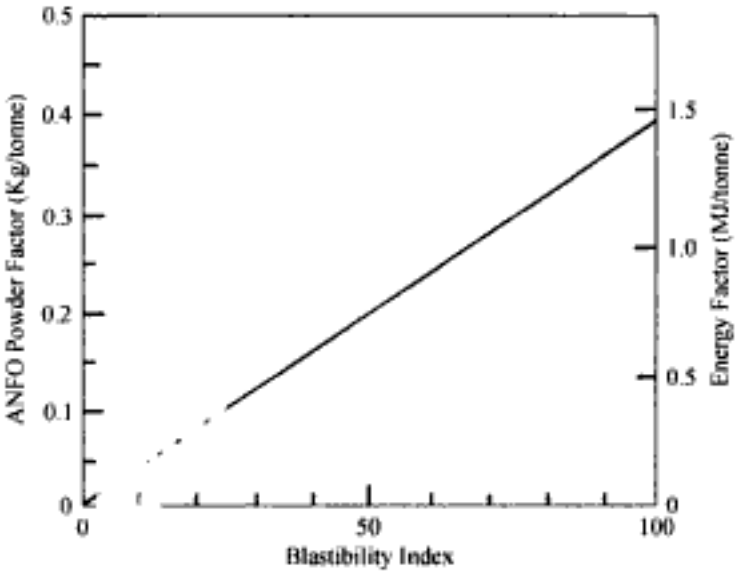

Figure 4.27. Explosive use as a function of the blastability index (Lilly, 1986).

Example 2. A well-jointed, blocky quartzite in which the bedding planes strike roughly normal to the bench face

$RMD = 20$
$JPS = 15$
$JPO = 30$
$SGI = 15$
$H = 8$
$TOTAL = 88$ and $BI = 44$

From Figure 4.27 powder factor is about 0.18 kg/tonne.

Although Figure 4.27 has been constructed for the stated (Australian) mining and rock mass conditions, one can, using the BI, easily construct a similar curve for other conditions using available field data. When using front-end loaders, for example, higher powder/energy factors will be required to achieve the appropriate fragmentation and muck pile shape than for a rope shovel operation.

4.11 FRAGMENTATION PREDICTION

4.11.1 *The basic model*

The engineering of fragmentation is going to be an important part of mining in the future. As loading machines become more automated and belt conveying is the rule rather than the exception, a size specification for the fragmented material will be required. This section presents some fundamental background information in that regard. Most of this information has been adapted from publications by Cunningham (1983, 1987).

A relationship between the mean fragment size and applied blast energy per unit volume of rock (powder factor) has been developed by Kuznetsov (1973) as a function of rock type. His equation is given below

$$\bar{X} = A\left(\frac{V_o}{Q_T}\right)^{0.8} Q_T^{1/6} \tag{4.55}$$

where $\overline{X}$ = mean fragment size, cm., A = rock factor = 7 for medium rocks, 10 for hard, highly fissured rocks, 13 for hard, weakly fissured rocks, V_o = rock volume (cubic meters) broken per blasthole = Burden × Spacing × Bench Height, Q_T = mass (kg) of TNT containing the energy equivalent of the explosive charge in each blasthole.

The relative weight strength of *TNT* compared to *ANFO* (*ANFO* = 100) is 115. Hence Equation (4.55) based upon *ANFO* instead of *TNT* can be written as

$$\overline{X} = A\left(\frac{V_o}{Q_e}\right)^{0.8} Q_e^{1/6}\left(\frac{S_{ANFO}}{115}\right)^{-19/30} \tag{4.56}$$

where Q_e = mass of explosive being used (kg), S_{ANFO} = relative weight strength of the explosive to *ANFO* (*ANFO* = 100).

Since

$$\frac{V_o}{Q_e} = \frac{1}{K} \tag{4.57}$$

where K = powder factor (specific charge) = kg/m^3.

Equation (4.56) can be rewritten as

$$\overline{X} = A(K)^{-0.8} Q_e^{1/6}\left(\frac{115}{S_{ANFO}}\right)^{19/30} \tag{4.58}$$

Equation (4.58) can now be used to calculate the mean fragmentation ($\overline{X}$) for a given powder factor. Solving Equation (4.58) for K

$$K = \left[\frac{A}{\overline{X}} Q_e^{1/6}\left(\frac{115}{S_{ANFO}}\right)^{19/30}\right]^{1.25} \tag{4.59}$$

one can calculate the powder factor required to yield the desired mean fragmentation. Cunningham (1983) indicates that in their experience the lower limit for A even in very weak rock types is

$$A = 8$$

and the upper limit is

$$A = 12$$

In an attempt to better quantify the selection of '*A*', the Blastability Index initially proposed by Lilly (1986) has been adapted for this application (Cunningham, 1987). The equation is given below.

$$A = 0.06 \times (RMD + JF + RDI + HF) \tag{4.60}$$

where the different factors are defined in Table 4.8.

Two examples illustrating this procedure have been given by Cunningham (1987)

Example 1: A massive fine grained lava

Here UCS is 400 MPa, Young's modulus is 80 GPa and the density is 2.9 t/m^3. There is little jointing closer than the anticipated drilling pattern. UCS determines the Hardness Factor.

$RMD = 50$,

$JF = 0$,

Table 4.8. Cunningham's 'A' Factor.

Symbol	Quantity	Rating
A	Rock factor	8 to 12
RMD	Rock Mass Description	
	– powdery/friable	10
	– vertically jointed	*JF*
	– massive	50
JF	*JPS* + *JPA*	
JPS	Vertical Joint Spacing	
	– < 0.1m	10
	– 0.1 to *MS*	20
	– *MS* to *DP*	50
MS	Oversize (m)	
DP	Drilling pattern size (m) assuming *DP* > *MS*	
JPA	Joint plane angle	
	– dip out of face	20
	– strike perpendicular to face	30
	– dip into face	40
RDI	Density influence	25 × *RD* – 50
RD	Density (t/m^3)	
HF	Hardness factor	
	– If *Y* < 50 GPa	*HF* = *Y*/3
	– If *Y* > 50 GPa	*HF* = *UCS*/5
Y	Youngs modulus (GPa)	
UCS	Unconfined compressive strength (MPa)	

$$RDI = 25 \times 2.9 - 50,$$
$$HF = 80:$$
$$ROCK\ FACTOR = 0.06 \times (50 + 22.5 + 80) = 9.15$$

Example 2: A friable, horizontally layered carboniferous shale
Here the average Young's Modulus is 18 GPa and the density is 2.3t/m^3. Y determines the Hardness Factor.

$$RMD = 10,$$
$$JF = 0,$$
$$RDI = 25 \times 2.3 - 50,$$
$$HF = 6:$$
$$ROCK\ FACTOR = 0.06 \times (10 + 7.5 + 6) = 1.41$$

It is of importance to know the *fragmentation distribution* as well as the mean fragment size. In that regard it has been found that the Rosin-Rammler formula

$$R = e^{-\left(\frac{X}{X_C}\right)^n} \tag{4.61}$$

where X = screen size, X_C = characteristic size, n = index of uniformity, R = proportion of material retained on the screen, gives a reasonable description of fragmentation in blasted rock. The characteristic size (X_C) is simply a scale factor. It is the size through which 63.2% of the particles pass. If the characteristic size (X_C) and the index of uniformity (n)

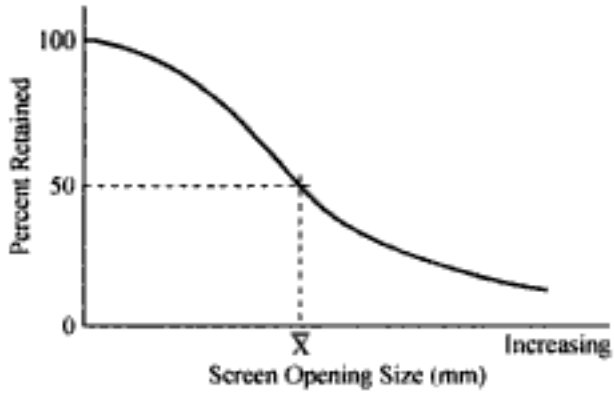

Figure 4.28. A typical fragmentation curve showing the percent retained as a function of screen opening.

are known then a typical fragmentation curve such as shown diagrammatically in Figure 4.28 can be plotted.

Equation (4.61) can be rearranged to yield the following expression for the characteristic size

$$X_C = \frac{X}{\left[\ln \frac{1}{R}\right]^{1/n}} \tag{4.62}$$

Since the Kuznetsov formula gives the screen size $\overline{X}$ for which 50% of the material would pass, substituting these values

$$X = \overline{X}$$

$$R = 0.5$$

into Equation (4.62) one finds that

$$X_C = \frac{\overline{X}}{(0.693)^{1/n}} \tag{4.63}$$

The expression for n developed by Cunningham (1987) from field tests is

$$n = \left(2.2 - 14\frac{B}{D^*}\right)\left[\frac{1+\frac{S}{B}}{2}\right]^{0.5}\left(1-\frac{W}{B}\right)\left(\frac{L}{H}\right) \tag{4.64}$$

where B = burden (m), S = spacing (m), D^* = hole diameter (mm), W = standard deviation of drilling accuracy (m), L = total charge length (m), H = bench height (m).

The burden (B) and spacing (S) values used in Equation (4.64) apply to the drilling layout and *not* the timing layout. When there are two different explosives in the hole (bottom charge and column charge) Equation (4.64) is modified to

$$n = \left(2.2 - 14\frac{B}{D^*}\right)\left[\frac{1+\frac{S}{B}}{2}\right]^{0.5}\left(1-\frac{W}{B}\right)\left[\frac{\text{abs}\,(BCL - CCL)}{L} + 0.1\right]^{0.1}\left(\frac{L}{H}\right) \tag{4.65}$$

where BCL = bottom charge length (m), CCL = column charge length (m), abs = the absolute value.

These equations apply for a square (in-line) drilling pattern. If a staggered drilling pattern is employed, n is increased by 10%.

The value of n determines the shape of the Rosin-Rammler curve. High values indicate uniform sizing. Low values on the other hand suggest a wide range of sizes including both oversize and fines. The effect of the different blasting parameters on 'n' are indicated below:

Parameter	'n' increases as the 'Parameter':
Burden/hole diameter	Decreases
Drilling accuracy	Increases
Charge length/bench height	Increases
Spacing/burden	Increases

It is normally desired to have uniform fragmentation so high values of n are preferred. Experience by Cunningham (1987) has suggested that:

1. The normal range of 'n' for blasting fragmentation in reasonably competent ground is from 0.75 to 1.5, with the average being around 1.0. More competent rocks have higher values.
2. Values of 'n' below 0.75 represent a situation of 'dust and boulders' which, if it occurs on a wide scale in practice, indicates that the rock conditions are not conducive to control of fragmentation through changes in blasting. Typically this arises when stripping overburden in weathered ground.
3. For values below 1 variations in the uniformity index (n) are more critical to oversize and fines. For $n = 1.5$ and higher, muckpile texture does not change much, and errors in judgement are less punitive.
4. The rock at a given site will tend to break into a particular shape. These shapes may be loosely termed 'cubes', 'plates' or 'shards'. The shape factor has an important influence on the results of sieving tests, as the mesh used is generally square, *and will retain the majority of fragments having any dimension greater than the mesh size.*

This combination of the Kuznetsov and Rosin-Rammler equations yields what has been called the Kuz-Ram Fragmentation Model. Caution should be exercised when applying this simple model. The following points should be remembered (Cunningham, 1983):

– Initiation and timing must be arranged so as to reasonably enhance fragmentation and avoid misfires or cut-offs.
– The explosive should yield an energy close to its calculated Relative Weight Strength.
– The jointing and homogeneity of the ground require careful assessment. Fragmentation is often built into the rock structure, especially when loose jointing is more closely spaced than the drilling pattern.

4.11.2 *Kuz-Ram model application*

There are many different blasting scenarios which can be evaluated using the Kuz-Ram Fragmentation Model. The two examples considered by Cunningham (1983) will be explained in some detail. The information common to both is

D = hole diameter = 50, 75, 115, 165, 200, 250 and 310 mm,
S/B = spacing-burden ratio = 1.30
J = stemming = 20 × hole diameter (m)
W = hole deviation = 0.45 m
A = rock constant = 10
ρ = density of *ANFO* = 900 kg/m^3
H = bench height = 12 m

Example 1. Constant mean fragmentation
In this first example, the patterns for each of the 7 drill hole diameters are to be determined under the constraint that the mean fragmentation for each should be maintained constant at $\overline{X}$ = 30 cm. This is the type of problem one has when the ore must pass through a small crusher. The fragmentation distribution and maximum boulder size are also to be calculated.

Step 1: The amount of explosive (Q_e) which will be contained in each hole above the level of the bench toe is calculated.

$$Q_e = \frac{\pi D^2}{4} L \rho \tag{4.66}$$

where D = hole diameter (m), L = loaded length above the bench toe (m) = $H - 20D$, H = bench height (m).

The values of L and Q_e are given in Table 4.9 for the different hole diameters. It should be noted that the effect of any subdrilling has not been included.

Step 2: The powder factor (K) required to obtain the mean fragment size $\overline{X}$ = 30 cm in rock with a constant A = 10 is calculated using

$$K = \left[\frac{A}{\overline{X}} Q_e^{1/6} \left(\frac{115}{S_{ANFO}} \right)^{19/30} \right]^{1.25}$$

For *ANFO*, S_{ANFO} = 100 and hence

$$K = \left[\left(\frac{10}{30} \right) Q_e^{1/6} \left(\frac{115}{100} \right)^{19/30} \right]^{1.25} \tag{4.67}$$

The resulting values have been added to Table 4.9.

Table 4.9. Calculated values of L, Q_e, and K as a function of hole diameter for Example 1.

D (m)	L (m)	Q_e (kg/hole)	K (kg/m^3)
50	11	19.4	0.525
75	10.5	41.8	0.616
115	9.7	90.7	0.723
165	8.7	167.4	0.822
200	8.0	226.2	0.875
250	7.0	309.6	0.934
310	5.8	394.0	0.983

Step 3: One uses the known values of K and Q_e to determine the volume of rock (V_o) which can be broken.

$$V_o = \frac{Q_e}{K} \tag{4.68}$$

Since the bench height (H = 12 m) and the spacing-burden ratio is maintained constant (S/B = 1.30), the values of B and S are found using Equations (4.69) and (4.70)

$$B \times S = \frac{V_o}{H} \tag{4.69}$$

$$B = \left(\frac{B \times S}{1.30}\right)^{1/2} \tag{4.70}$$

The values are given in Table 4.10.

Step 4: The values of n are calculated using Equation (4.64)

$$n = \left(2.2 - 14\frac{B}{D^*}\right)\left(\frac{1+\frac{S}{B}}{2}\right)^{0.5}\left(1-\frac{W}{B}\right)\left(\frac{L}{H}\right)$$

where D^* = borehole diameter in mm.

The results are given in Table 4.11

Table 4.10. Calculated values of V_o, B and S as a function of hole diameter for Example 1.

D (mm)	V_o (m³)	$B \times S$ (m²)	B (m)	S (m)
50	36.95	3.08	1.54	2.00
75	67.86	5.65	2.08	2.71
115	125.45	10.45	2.84	3.69
165	203.65	16.97	3.61	4.70
200	258.51	21.54	4.07	5.29
250	331.48	27.62	4.61	5.99
310	400.81	33.40	5.07	6.59

Table 4.11. Calculated values of n and X_c for Example 1.

D (mm)	n	X_c (cm)
50	1.230	40.4
75	1.332	39.5
115	1.352	39.3
165	1.288	39.9
200	1.217	40.5
250	1.096	41.9
310	0.931	44.5

Step 5: The characteristic size (X_C) is determined applying Equation (4.62)

$$X_C = \frac{X}{\left[\ln \frac{1}{R}\right]^{1/n}}$$

for the special case when

$$X = \overline{X} = 30 \text{ cm}$$

$$R = 0.50$$

Thus

$$X_C = \frac{30}{(\ln 2)^{1/n}} \tag{4.71}$$

The resulting values for X_C have been added to Table 4.11.

Step 6: One uses Equation (4.61)

$$R = e^{-\left(\frac{X}{X_C}\right)^n}$$

to calculate values of R (the fraction retained) for different sizes (X). In this case the sizes selected are 5 cm, 30 cm, 50 cm and 100 cm. Using the values of n and X_C for the 200 mm diameter hole one finds that

$$R = e^{-\left(\frac{X}{40.5}\right)^{1.227}}$$

Substituting the desired values for X yields

X (cm)	R
5	0.925
30	0.500
50	0.275
100	0.050

which means that 5% (R = 0.05) of the material would be retained on a screen with 100 cm openings. As expected 50% (R = 0.50) would be retained on a screen with 30 cm openings. The values for the other hole diameters are given in Table 4.12.

Table 4.12. Percent (expressed as a ratio) retained as a function of the hole diameter and screen size.

Hole diameter (mm)	Percent retained (R)			
	X = 5 cm	X = 30 cm	X = 50 cm	X = 100 cm
50	0.926	0.5	0.273	0.047
75	0.938	0.5	0.254	0.032
115	0.94	0.5	0.25	0.029
165	0.933	0.5	0.263	0.038
200	0.925	0.5	0.275	0.05
250	0.907	0.5	0.297	0.075
310	0.878	0.5	0.328	0.119

Step 7: One uses Equation (4.72) to calculate the maximum boulder size (BDR)

$$X = X_C \left(\ln \frac{1}{R} \right)^{1/n} \tag{4.72}$$

This is defined as the screen size through which 98% (the mean size + 2 standard deviations) of the material would pass. The maximum boulder size for the different hole diameters, corresponding to $R = 0.02$ are given in Table 4.13.

The results are plotted in Figure 4.29. As can be seen, as the blasthole diameter increases

(a) the specific charge required increases quite steeply

(b) the size of the maximum boulder only shows large increases above a hole diameter of 115 mm. This is because of the conflicting results of relative drilling accuracy and equality of distribution of explosives. The former improves and the latter deteriorates as hole size increases.

(c) although mean fragmentation remains constant, the proportions of both fines and coarse material increase.

Example 2. Constant powder factor
In this second example the powder factor (K) will be held constant at

$$K = 0.5 \text{ kg/m}^3$$

and the

– Maximum boulder size,
– Mean fragment size,
– Fragment size distribution,

will be calculated as the hole diameter is changed from 50 mm up to 310 mm.

As in the previous example the following will be assumed

ANFO ($\rho = 900 \text{ kg/m}^3$)

$S/B = 1.3$

Stemming = 20 times the hole diameter (m)

The amount of charge per hole (Q_e) and the charge length (L) are the same as in Example 1. The burden and spacing values are given in Table 4.14. The values of n are now calculated using Equation (4.64). These values have been added to Table 4.14. The mean fragment size ($\bar{X}$) is calculated using Equation (4.58)

Table 4.13. Maximum boulder size (cm) as a function of hole diameter.

D (mm)	Maximum boulder size (cm)
50	122
75	110
115	108
165	115
200	124
250	145
310	193

Table 4.14. Charge length, burden, spacing and n values for Example 2.

D (mm)	L (m)	B (m)	S (m)	n
50	11	1.58	2.05	1.235
75	10.5	2.31	3.01	1.336
115	9.7	3.41	4.43	1.343
165	8.7	4.63	6.02	1.268
200	8.0	5.39	7.00	1.194
250	7.0	6.30	8.19	1.073
310	5.8	7.11	9.24	0.912

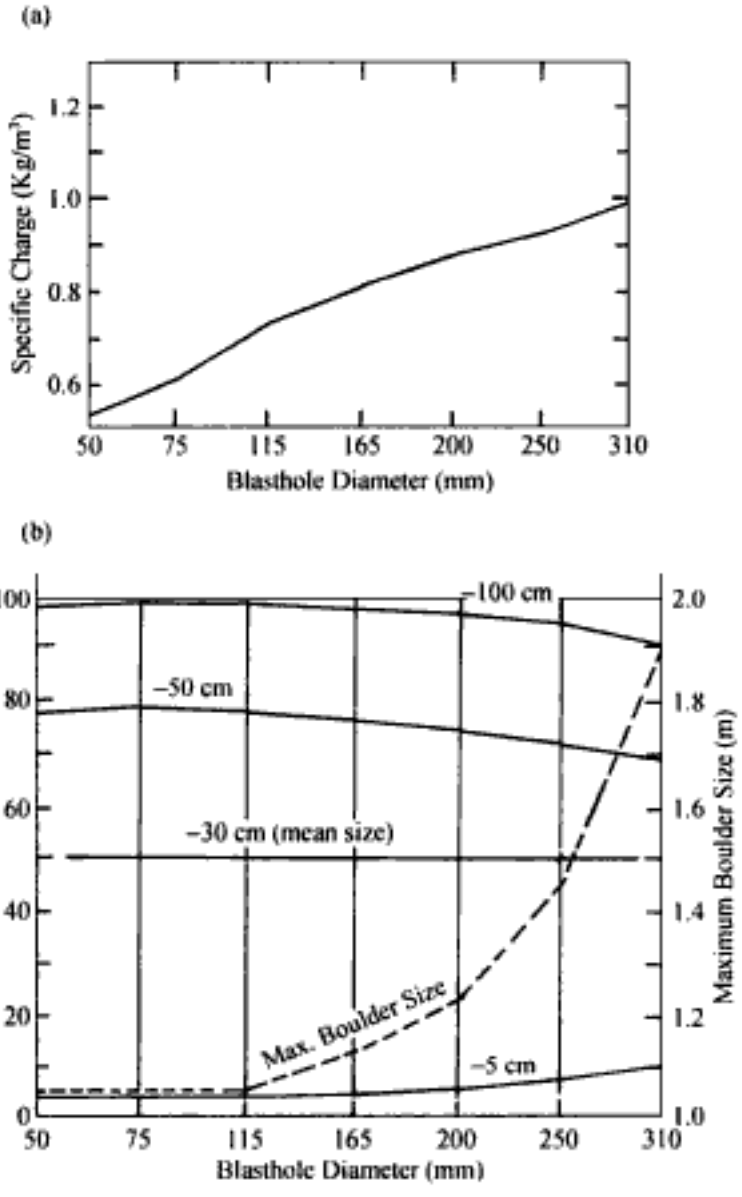

Figure 4.29. Specific charge, weight percent passing and maximum boulder size as a function of blasthole diameter. Cunningham (1983, 1987).

$$\overline{X} = A\,(K)^{-0.8} Q_e^{1/6} \left(\frac{115}{E}\right)^{19/30}$$

The calculated values are given in Table 4.15. The characteristic size X_C is obtained from

$$X_C = \frac{\overline{X}}{(\ln 2)^{1/n}}$$

These values have been added to Table 4.15. Finally, the maximum boulder size (screen size passing 98% of the material) as determined from

$$BDR = X_C \left(\ln \frac{1}{0.02}\right)^{1/n}$$

are added to Table 4.15. The percentages retained on screens having opening sizes of 100 cm and 5 cm have been calculated using

$$R = e^{-\left(\frac{x}{X_C}\right)^n}$$

are given in Table 4.16. The values have been plotted in Figure 4.30. It is seen that as blasthole diameter increases,

(a) mean fragment size increases by over 60%

(b) the coarse (+100 cm) fraction increases from 5% to 25%

(c) fines do not vary much but are minimal for the medium diameters. More fines are generated in small diameters owing to the proximity of holes and the greater effect of drilling inaccuracy. In large diameter holes they are caused by intensive crushing around the blasthole wall.

(d) the maximum boulder size increases from just over 1 m to almost 2.8 m.

In overburden the fragmentation is seldom a critical factor and blast design for larger blastholes might be based on a constant powder factor.

Table 4.15. Calculated values of $\overline{X}$, X_c, and *BDR* as a function of hole diameter.

D (m)	$\overline{X}$ (cm)	X_C (cm)	*BDR* (cm)
50	31.2	41.98	127
75	35.4	46.6	129
115	40.3	52.9	146
165	44.7	59.7	175
200	46.95	63.8	200
250	49.5	69.7	249
310	51.5	76.97	343

Table 4.16. The fraction retained by screens with openings of 100 cm and 5 cm as a function of hole diameter.

D (mm)	*R* (100)	*R* (5)
50	0.054	0.930
75	0.062	0.951
115	0.095	0.959
165	0.146	0.958
200	0.181	0.953
250	0.229	0.943
310	0.281	0.921

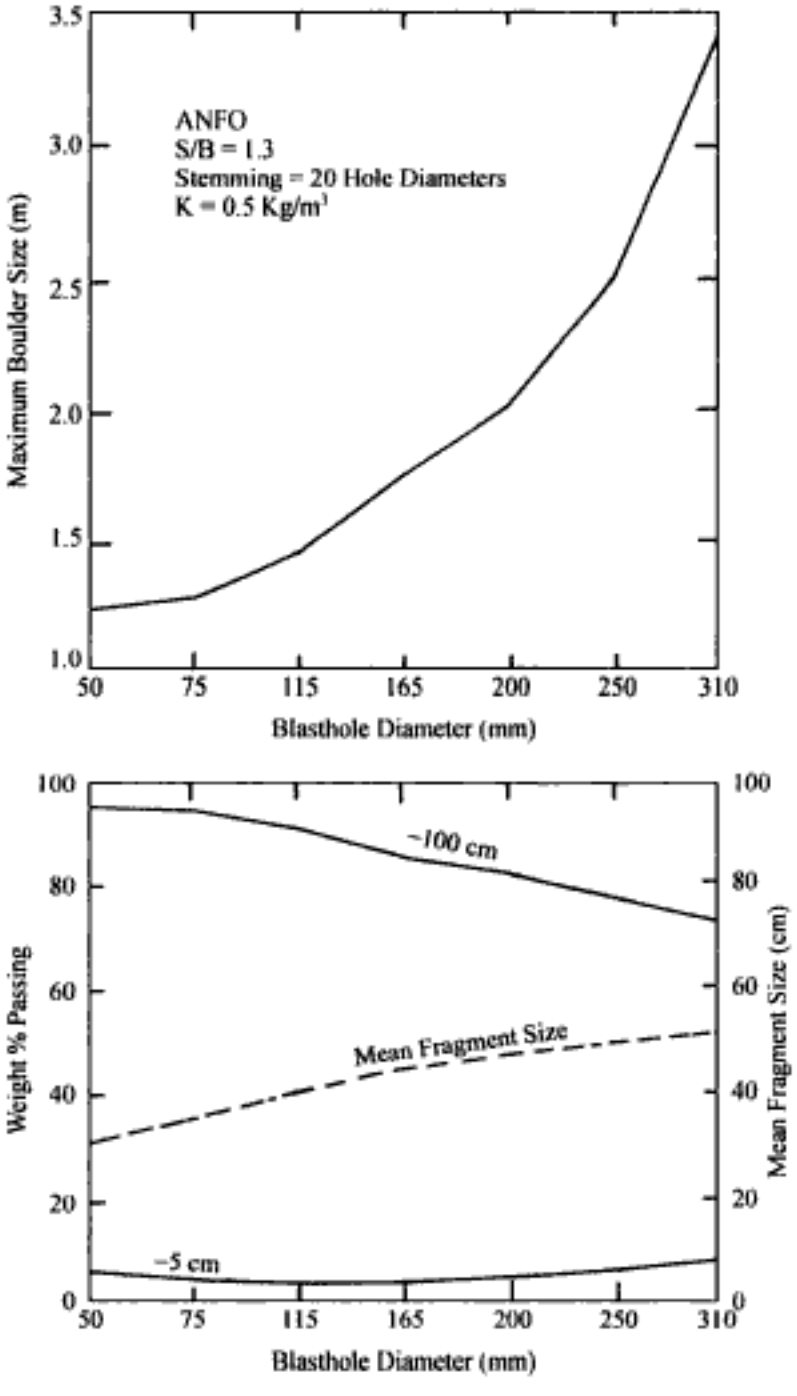

Figure 4.30. Weight percent passing, maximum boulder size, and mean fragment size as a function of blasthole diameter. Cunningham (1983, 1987).

REFERENCES AND BIBLIOGRAPHY

AECI Explosives and Chemicals Limited 1978a. Parameters in surface blasting. *Explosives Today*. 2(11), March.

AECI Explosives and Chemicals Limited 1978b. Blasthole drilling and initiation patterns in surface blasting. *Explosives Today*. 2(12), June.

AECI Explosives and Chemicals Limited 1983a. Secondary blasting. *Explosives Today*. 2(33), 3rd Quarter.

AECI Explosives and Chemicals Limited 1983b. Geology and fragmentation. *Explosives Today*. 2(34), 4th Quarter.

AECI Explosives and Chemicals Limited 1984. Drilling accuracy. *Explosives Today*. 2(36), 2nd Quarter.

AECI Explosives and Chemicals Limited 1986. The design of surface blasts. *Explosives Today*. 2(41), Mar.

AECI Explosives and Chemicals Limited 1987a. Stemming. *Explosives Today*. 2(46), June.

AECI Explosives and Chemicals Limited 1987b. The safe and efficient initiation of explosives. *Explosives Today*. 2(47), Sept.

AECI Explosives and Chemicals Limited 1987c. Toe vs Collar priming. *Explosives Today*. 2(48), December.

Andersen, O. 1952. *Blast Hole burden design-introducing a new formula*. Australian IMM. no 166-167: 115-130.

Anonymous 1954. Drilling and blasting: Drill rounds. *E&MJ*. 155(5): G20-G22.

Anonymous 1981. Open-pit and underground blasting techniques. Engineering fundamentals series. *Mining Engineering*. 33(8): 1215-1219. *Material extracted from Blasters' Handbook*, prepared by E.I. Du Pont De Nemours & Co, Inc, Explosives Products Division, Wilmington, DE.

Ash, R.L. 1961. Drill pattern & initiation-timing relationships of multiple hole blasting. Quarterly CSM, V 56, pp. 309-324.

Ash, R.L. 1963a. The mechanics of rock breakage (Part 1). *Pit and Quarry*. 56(2): 98-100.

Ash, R.L. 1963b. The mechanics of rock breakage (Part 2) – Standards for blasting design. *Pit and Quarry*. 56(3): 118-122.

Ash, R.L. 1963c. The mechanics of rock breakage (Part 3) – Characteristics of explosives. *Pit and Quarry*. 56(4): 126-131.

Ash, R.L. 1963d. The Mechanics of rock breakage (Part 4) – Material properties, powder factor, blasting cost. *Pit and Quarry*. 56(5): 109-118.

Ash, R.L. 1967. Field conditions and their relationships to blasting design. Proceedings of the 40th Annual Meeting of the Minnesota Section, *AIME and the 28th Annual Mining Symposium*, Jan 16-18, Duluth, Minn., pp. 189-196.

Ash, R.L. 1968. The design of blasting rounds. In Surface Mining (E.P. Pfleider, ed.). AIME, New York. pp. 373-397.

Ash, R.L., C.J. Konja & R.R. Rollins 1969. Enhancement effects from simultaneously fired explosive charges. Trans. Soc. Min. Engrs. (AIME). vol 244, Nov 4.

Ash, R.L. 1973. The Influence of Geological Discontinuities on Rock Blasting. PhD Thesis, Univ. of Minnesota, 289 pp.

Ash, R.L. 1974. Considerations for proper blasting design. *Proc. 2nd Annual Blasting Conference*. Kentucky Dept. of Mines, May.

Ash, R.L., T.D. Harris & N.S. Smith 1978. Should blasthole subdrilling be loaded with explosives? *Proceedings of the 4th Conference on Explosives and Blasting Technique. SEE*. pp. 93-101.

Ash, R.L. & C.J. Konya 1979. Improper spacing: a major problem with surface blasting. *Proceedings of the 5th Conference on Explosives and Blasting Technique. SEE*. pp. 180-184.

Ash, R.L. 1992. Section 6.2.2 Design of Blast Rounds. Surface Mining, 2nd Edition (B. Kennedy). SME. pp. 565-583.

Atlas Powder Company. *Surface Shot Design and Shot Calculations*. pp. 19.

Atlas Powder Company. 1981. *Workshop Manual 'Surface Blasting Course'*.

Atlas Powder Company.1987. *Explosives and Rock Blasting*. Maple Press. 662pp.

Bauer, A. 1972. Current drilling and blasting practices in open pit mines. *Mining Congress Journal*. 58(3): 20-27.

Bauer, A. 1978. Trends in drilling and blasting. *Proceedings of the 4th Conference on Explosives and Blasting Conference, SEE*, 291-325.

Bauer, A. 1978. Trends in drilling and blasting. *CIM Bulletin*. 71(797): 81-90.

Bauer, A. & M.D. Brennan 1979. Blast Designs to Improve Dragline Stripping Rates.Final Report-Phase I. Prepared for US Dept of Energy under contract USDOE DE-AC01-77QQ90147. DOE Report FE 9124-1, April.

Belland, J.M. 1966. Structure as a control in rock fragmentation. *CIM Bulletin*. 59(645): 323-327.

Bhandari, S. 1975. Improved fragmentation by reduced burden and more spacing on blasting. *Mining Magazine*. 132(3): 187-198.

Bhandari, S. 1983. Influence of joint directions in blasting. *Proceedings of the 9th Conference on Explosives and Blasting Technique. SEE*. pp. 359-369.

Borquez, G.V. 1981. Estimating drilling and blasting costs – an analysis and prediction model. *E&MJ*. 182(1): 83-89.

Brace, S.J. 1994. Small diameter explosives-choosing for underground blasting applications. *Proceedings of the 5th High-Tech Seminar on Blasting Technology, Instrumentation, and Explosives Applications, New Orleans, Louisiana* (July 9-14). Blasting Analysis International, Inc. pp. 681-711.

Bradbury, P.N. 1986. A common sense approach to cutting drill and blasting costs. *Proceedings of the 12th Conference on Explosives and Blasting Technique. SEE.* pp. 103-106.

Brooks, R.R., L.P. McTavish, S. Kaleta & R.D. Turner 1978. Production blasting practice at Hamersley Iron Pty, Limited. *Proceedings of the Rock Breaking Symposium.* Aus. I.M.M., Melbourne Branch, pp. 176-189.

Buchta, L. 1982. Open pit bench blasting-how to improve results. *World Mining.* 35(6): 64-71.

Bulow, B.M. & C.K. McKenzie 1990. Hole to Hole Explosive Interaction in production blasting at Mount Tom Price. FRAGBLAST '90. *Proceedings of the 3rd Int Symp. on Rock Fragmentation by Blasting. Brisbane August* 26-31. pp. 325-333.

Burkle, W.C. 1979. Geology and its effect on blasting. *Proceedings of the 5th Conference on Explosives and Blasting Technique. SEE.* pp. 105-120.

Burkle, W.C. 1986. Optimum drilling and blasting procedures. Preprint 86-3. Paper presented at the SME Annual Meeting in New Orleans, Louisiana, Mar 2-6. pp. 12.

Cheshire, M.A. 1963. The advantages of inclined holes at hard rock faces. *Quarry Managers Journal.* 47(5): 177-186.

Chiappetta, R.F., A. Bauer, P.J. Dailey & S.L. Burchell 1983. The use of high-speed motion picture photography in blast evaluation and design. *Proceedings of the 9th Conference, SEE.* pp. 258-309.

Chiappetta, R.F., S.L. Burchell, J.W. Reil & D.A. Andersson 1986. Effects of accurate MS delays on productivity, energy consumption at the primary crusher, oversize, ground vibrations and airblast. *Proceedings of the 12th Conference on Explosives and Blasting Technique. SEE.* pp. 213-240.

Chiappetta, R.F. & M.E. Mammele 1988. Analytical high-speed photography as a diagnostic tool in blast design. Preprint No. 88-71 Society of Mining Engineers. For presentation at the SME Annual Meeting, Phoenix, Az (Jan 25-28) 13pp.

Chiappetta, R.F. & B. Vandenberg 1990. High-speed motion picture photography analysis in 3D. FRAGBLAST'90. *Proceedings of the 3rd Int. Symp. on Rock Fragmentation ' v Blasting, Brisbane, Australia.* 26-30 August. Published by the Austral. Inst. of Min. and Metall. Victoria, Australia.

Chiappetta, F.R., & B. Vandenberg 1994. High-speed motion picture photography analysis in 3D – A new approach to analyzing full scale blasts. *Proceedings of the 5th High-Tech Seminar on Blasting Technology, Instrumentation, and Explosives Applications. New Orleans, Louisiana* (July 9-14). Blasting Analysis International, Inc. pp. 929-943.

Chiappetta, R.F. 1994. Presplitting techniques for conventional, air deck and dimension stone applications. *Proceedings of the 5th High-Tech Seminar on Blasting Technology, Instrumentation, and Explosives Applications. New Orleans, Louisiana* (July 9-14). Blasting Analysis International, Inc. pp. 339-407.

Chiappetta, R.F. 1994. Generating site specific blast designs with state-of-the-art blast monitoring instrumentation and PC based techniques. *Proceedings of the 5th High-Tech Seminar on Blasting Technology, Instrumentation, and Explosives Applications. New Orleans, Louisiana* (July 9-14). Blasting Analysis International, Inc. pp. 741-772.

Chiappetta, R.F., B. Vandenberg & J.R. Pressley 1994. Workshop #11. Portable, multi-channel and continuous velocity of detonation recorders. *Proceedings of the 5th High-Tech Seminar on Blasting Technology, Instrumentation, and Explosives Applications. New Orleans, Louisiana* (July 9-14). Blasting Analysis International, Inc. pp. 1205-1319.

Cunningham, C.V.B. 1983. The Kuz-Ram model for prediction of fragmentation from blasting. *Proceedings, First Int. Symp. on Rock Fragmentation by Blasting, Luleå, Sweden,* August 22-26, pp. 439-453.

Cunningham, C.V.B. 1987. Fragmentation estimations and the Kuz-Ram model – Four years on. *Proceedings, Second Int. Symp. on Rock Fragmentation by Blasting, Keystone, Colorado,* August 23-26, pp. 475-487.

Cunningham, C.V.B. 1988. Control over blasting parameters and its effect on quarry productivity. *Proceedings, Institute of Quarrying Conference, Durban, South Africa.* March 11. Daly, and Assmus, 1992. CIM Bulletin

Daly, S. & D. Assmus 1992. Blast optimization and stability enhancement through geotechnical mapping at Highland Valley Copper. CIM Bulletin, 85(962): pp. 78-84.

Davids, T. & B.J.J. Botha 1994. The application of mid-column air decks in full scale production blasts. *Proceedings of the 5th High-Tech Seminar on Blasting Technology, Instrumentation, and Explosives Applications. New Orleans, Louisiana* (July 9-14). Blasting Analysis International, Inc. pp. 437-457.

Dick, R.A. & J.J. Olson 1970. Choosing the proper borehole size for bench blasting. *Proceedings of the 43rd Annual Meeting of the Minnesota Section, AIME and the 31st Annual Mining Symposium, Univ of Minn., Duluth,* Jan. pp. 201-207.

Dick, R.A. & J.J. Olson 1972. Choosing the proper borehole size for bench blasting. *Mining Engineering,* 24(3): 41-45.

Dick, R.A., L.R. Fletcher & D.V. D'Andrea 1983. *Explosives and Blasting Procedures Manual.* USBM IC 8925. 105pp.

Dimock, R.R & G.D. Clayton 1977. Kennecott's delayed blasting technique cuts costs, improves pit stability. *Mining Engineering.* 29(4): 37-40.

E.I. DuPont de Nemours and Co. *DuPont Blasters' Handbook.* 1977 Edition. Wilmington, Del. 494 pp.

Duval Corporation 1974. Blasthole pattern layout methods.

Ellis, O.W. 1993. Optimizing energy distribution in shot design. *Stone Review.* 9(4): 15-17.

Floyd, J.L. 1987. The utilization of personal computers for blast design and analysis. *Proceedings of the 13th Conference on Explosives and Blasting Techniques. SEE.* pp. 172-183.

Fordyce, B.G. & W.B. Parker 1979. Rock-handling techniques at Sishen iron-ore mine. *JSAIMM.* 79 (15): 454-464.

Gadberry, A.R. 1981. Mine planning-Its effect on drilling and blasting. *Proceedings of the 7th Conference on Explosives and Blasting Technique. SEE.* pp. 108-112.

Gadberry, A.R. 1984. Reducing boulders (Part 1). *Explosives Engineering.* 2(3): 22-28.

Gadberry, A.R. 1984. Poor breakage: What does it really cost. *Explosives Engineering.* 2(4): 20-21.

Gadberry, A.R. 1985. Management's effect on drilling and blasting. *Proceedings of the 11th Conference on Explosives and Blasting Technique. SEE.* pp. 284-292.

Gibbs, J.M. 1965. Open-pit drilling and blasting at Craigmont Mines Limited. *CIM Bulletin.* 58(638): 628-631.

Gustafsson, R. 1973. *Swedish Blasting Technique.* SPI Publisher, Gothenburg, Sweden, 327pp.

Hagan, T.N. 1975. Initiation sequence: Vital element of open pit blast design. Design Methods in Rock Mechanics (C.Fairhurst & S.L. Crouch, eds) *Proceedings of the 16th US Symposium on Rock Mechanics, Minneapolis, Minn. ASCE,* 1977. pp. 345-355.

Hagan, T.N. 1977. The effects of blast geometry and initiation sequence on blasting results. Chapter 6. in *Australian Mineral Foundation's 'Drilling and Blasting Technology'* Course, Adelaide, May. 55pp.

Hagan, T.N. 1977. Effects of delay timing on blasting techniques. Chapter 7 in *Australian Mineral Foundation's 'Drilling and Blasting Technology'* Course, Adelaide, May. 37pp.

Hagan, T.N. 1977. Good delay timing-prerequisite of efficient bench blasts. *Proc. Australas. Inst. Min. Metall.,* (263): 47-54.

Hagan, T.N. & G. Harries. 1977. The effects of rock properties on blasting results. Chapter 4 in *Australian Mineral Foundation's 'Drilling and Blasting Technology'* Course, Adelaide, May. 31pp.

Hagan, T.N. 1979. Accurate delay timing and cutoffs. Chapter 10 in the *workshop proceedings for 'Influence of Rock Properties on Drilling and Blasting'* Adelaide, 25-29 June. Australian Mineral Foundation, Inc. pp. 256-273.

Hagan, T.N. 1979. The control of fines through improved blast design. *Proc Australas Inst Min Metall.* (271): 9-20.

Hagan, T.N. *Safety and Efficiency in Quarry Blasting Manual.* ICI Australia Operations Pty, Ltd Explosives Division. For course March 26-28 in Sydney.

Hagan, T.N. & G. Harries 1979. The effects of rock properties on the design and results of blasting. Chapter 2 of the *Australian Mineral Foundation's Workshop Course Manual 'Influence of Rock Properties on Drilling and Blasting'.* Adelaide.

Hagan, T.N. 1983. The influence of controllable blast parameters on fragmentation and mining costs. *Proceedings of the 1st Int. Symp. on Rock Fragmentation by Blasting,* Luleå. pp. 31-52.

Hagan, T.N. 1983. Field measurements of rock mass properties: an essential requirement for optimising blast designs. *Proc. Int. Symp. on Field Measurements in Geomechanics,* Zurich, Sept 5-8. pp. 105-113.

Hagan, T.N. & J.K. Mercer 1983. Safe and Efficient Blasting in Open Pit Mines. Manual written for the course given at Karratha, Australia 23-25 November. ICI Australia Operations Pty., Ltd. Explosives Division.

Haghighi, R.G. & C.J. Konya. 1985. The effect of bench movement with changing blasthole length. *Proceedings of the 11th Conference on Explosives and Blasting Technique (Mini-Symposium). SEE.* pp. 95-105.

Haghighi, R.G. & C.J. Konya 1986. Effect of geology on burden displacement. *Proceedings of the 12th Conference on Explosives and Blasting Technique (Mini-Symp). SEE.* pp. 92-102.

Harries, G. & B.L. Grieve 1978. Blasting of high density ores. *Proceedings of the Rock Breaking Symposium.* Aus. I.M.M., Melbourne Branch, pp. 171-176.

Heltzen, A.M. (ed.) 1974. Fjellsprengnongs teknikk. Teknologisk Forlag, Oslo. p177.

Hissem, W.D. 1986. Drilling and cost analysis using a personal computer and spreadsheet. *Proceedings of the 12th Conference on Explosives and Blasting Technique. SEE.* pp. 284-293.

Hoek, E. & J.W. Bray 1973. *Rock Slope Engineering*. Chapter 11. Blasting. Instn of Min Met., London. pp. 271-307.

Holmberg, R. 1975. Computer calculations of drilling patterns for surface and underground blasting. Design Methods in Rock Mechanics (C. Fairhurst & S. Crouch, eds) *16th Symposium on Rock Mechanics, Univ. of Minnesota, Minneapolis.*

Jones, M. 1985. *Secondary blasting*. Downline, Issue No 4. p4. Dec. ICI Explosives.

Just, G.D. 1979. Rock fragmentation by blasting. *CIM Bulletin*. 72(803): 143-148.

Just, G.D. 1979. Stemming of blastholes in mining excavations. *Proc Australas. Inst. Min. Metall.* (269): 7-15.

Kidman, V.T. 1981. The use of high speed photography to improve blasting. Proceedings, Workshop Course 153/81. '*Drilling and Blasting in Open Pits and Quarries*'. Australian Mineral Foundation. Brisbane 30 Mar-3 April pp. 56-112.

King, B.M., G.D. Just & C.K. McKenzie 1988. *Improved evaluation concepts in blast design*. Trans IMM (Sect A). 97 (Oct): A173-181.

Kirby, I. 1984. *Matching explosive to rock*. Downline. Issue No 2, Dec. pp. 4-5. ICI Explosives.

Kochanowsky, B.J. 1960. *Theory and practice of inclined drilling for surface mining*. Mineral Industries Bulletin, Penn State University, vol 30, n3, Dec.

Kochanowsky, B.J. 1962. Some factors influencing blasting efficiency. *Int Symp. on Mining Res.* (G.B. Clark, editor) Pergamon Press, New York, pp. 157-162.

Konya, C.J. & J.Davis 1978. The effects of stemming consist of retention in blastholes. *Proceedings of the 4th Conference on Explosives and Blasting Technique. SEE.* Annual Meeting, New Orleans. pp. 102-112.

Konya, K.J. 1988. Problems with malfunctioning blastholes. *Proceedings of the 14th Conference on Explosives and Blasting Technique. SEE.* pp. 334-348.

Kuznetsov, V.M. 1973. *The mean diameter of the fragments formed by blasting rock*. Soviet Mining Science, 9(2): 144-148.

Lake, D., S. Conway, A. Bartfay, J. Yorsz, R.F. Chiappetta & B. Vandenberg 1994. Blast diagnostics and instant diagnostics using the SVC500 Solid State, High-speed video system. *Proceedings of the 5th High-Tech Seminar on Blasting Technology, Instrumentation, and Explosives Applications. New Orleans, Louisiana* (July 9-14). Blasting Analysis International, Inc. pp. 915-927.

Langefors, U. 1962. Bench blasting with AN-explosives. *Proceedings, Int Symp. on Mining Research* (G.B. Clark, ed.). Pergamon Press, New York. pp. 249-271.

Langefors, U. & B. Kihlström 1978. *The Modern Technique of Rock Blasting*. John Wiley & Sons, Inc., New York. 405 pp.

Lilly, P.A. 1986. An empirical method of assessing rock mass blastability. *Proceedings, Large Open Pit Mining Conference* (J.R. Davidson, ed.), The Aus IMM, Parkville, Victoria. October pp. 89-92.

MacLachian, R.R. & M.J. Scoble 1986. Techniques for the evaluation of rock mass structure and strength in blast design. *Proceedings of the 12th Conference on Explosives and Blasting Technique (Mini-Symp). SEE.* pp. 132-144.

Mahoney, T.P. 1986. Drilling and blasting practices. *Proceedings of the 12th Conference on Explosives and Blasting Technique. SEE.* pp. 142-145.

Matthews, R.H. 1971. Blasting practices at the Goldsworthy Mine. *Proceedings of the Rock Breaking Seminar. Dept of Min. & Met. Eng., Univ of QLD*, Feb 24-25, pp. 137-149.

Maynard, B.C. 1990. A blast design model using the inherent fragmentation of a rock mass. *CIM Bulletin*, 83 (940): 71-77.

Mecir, R. & D. Valek 1963. Question of optimum timing in millisecond delay blasting of holes. *Int Symp of Mining Res.* vol 2. (G.B. Clark, editor), Univ of Missouri, Rolla. Pergamon Press. pp. 273-282.

Moore, D.J. 1975. Practical application of empirical blast design. *Proceedings First Conference on Explosives and Blasting Technique, SEE*, pp. 28-47.

Morrey, W.B., R. Shaw & G.G. Riley 1969. Review of blasting practice in open-pit mining: 1-Canadian practice;2-British practice. *Proc of the 9th Commonwealth Mining and Metallurgical Congress.* pp. 443-472.

Nielsen, K. 1985. Sensitivity analysis for optimum open pit blasting. *Proceedings of the 11th Conference on Explosives and Blasting Technique. SEE.* pp. 85-95.

Pearse, G.E. 1955. *Rock blasting: Some aspects on the theory and practice*. Mine & Quarry Engineering. 21(1): 25-30.

Peck, J., Hendricks, C & M. Scoble 1990. Blast optimization through performance monitoring of drills and shovels. *Proceedings, Mine Planning and Equipment Selection* (Singhal & Vavra, eds). A.A. Balkema, Rotterdam, pp. 159-166.

Pelley, M.H. 1978. A report on improvements in drilling and blasting practices at IOC's Carol Lake project. *CIM Bulletin.* 71(797): 73-80.

Phillips, T.H. 1988. Management of the drilling and blasting practices at the Mission Mine. Preprint Number 88-29. Paper presented at the SME Annual Meeting, Phoenix, AZ, Jan 25-28. pp. 4.

Porter, D.D. 1974. Use of rock fragmentation to evaluate explosives for blasting. *Mining Congress Journal.* 60(1): 41-43.

Preston, C.J. & N.J. Tienkamp 1984. New techniques in blast monitoring and optimization. *CIM Bulletin.* 77(867): 43-48.

Pugliese, J.M. 1972. Designing Blast Patterns Using Empirical Formulas – A comparison of calculated patterns with plans used in quarrying limestone and dolomite with geologic considerations. *USBM IC 8550.* 33pp.

Roberts, A. 1977. *Geotechnology:* An Introductory Text for Students and Engineers. Pergamon Press, Oxford.

Sen, G.C. & J. Mensah 1989. Fragmenting oversize boulders. *Proceedings of the 15th Conference on Explosives and Blasting Technique. SEE.* pp. 71-86.

Sickler, R. & P. Worsey 1987. The application of high tech automation in drilling and blasting. *Proceedings of the 13th Conference on Explosives and Blasting Techniques. SEE.* pp. 254-267.

Smith, N.S. 1976. Burden-Rock Stiffness and Its Effect on Fragmentation in Bench Blasting. PhD Thesis. Univ. of Missouri, Rolla.

Smith, N.S. & R.L. Ash 1977. How the blasthole burden, spacing and length affect rock breakage. *Proceedings of the 3rd Conference on Explosives and Blasting Tech. SEE.* pp. 138-148.

Spaeth, G.L. 1960. *Formula for proper blasthole spacing.* Eng. News Record. 164 (April): 53.

Snyder, T.J. 1988. Working with explosives suppliers to optimize pit productivity and costs. *Proceedings of the 14th Conference on Explosives and Blasting Technique. SEE.* pp. 99-110.

Sprott, D.L. & B.W. Martin 1990. *Blast performance analysis. International Mining.* 7 (April): 20-22.

Stagg, M.S., S.A. Rholl & R.E. Otterness 1989. The effect of explosive type and delay between rows on fragmentation. *Proceedings of the 15th Conference on Explosives and Blasting Technique. SEE.* pp. 353-366.

Tham, G.H.P. 1983. Differentiated blasting technique for optimum fragmentation at Aitik Copper Mine, Sweden: A case study. *Proceedings 1st Int. Symp. on Rock Fragmentation by Blasting, Luleå, Sweden.* pp. 495-504.

Thompson, S.D. & L. Adler 1984. Selecting a burden formula for surface mine blasting. *Proceedings of the 1984 Symposium on Surface Mining, Hydrology, Sedimentology an Reclamation. Univ of Kentucky, Lexington.* Dec 2-7, pp. 103-108.

Thomas, N.L. 1986. Blasting factors influencing the choice of blasthole size for quarrying. *Proceedings of the 12th Conference on Explosives and Blasting Technique. SEE.* pp. 5-19.

Tousley, G.H., Jr. 1976. The professional approach to drilling and blasting operations. Preprint No. 76-F-312. Soc. of Min. Engrs. of AIME. For presentation at the 1976 SME-AIME Fall Meeting & Exhibit (Denver, Colo) Sept 1-3.

Van Ormer, H.P., Jr. 1983. The changing economics of percussion blast hole drilling. *Proceedings of the 9th Conference on Explosives and Blasting Technique. SEE.* pp. 451-478.

Zaburunov, S.A. 1990. Blasting: Mind over materials. *E&MJ.* 191(4): 20-25.

CHAPTER 5

Drilling patterns and hole sequencing

5.1 BLAST ROUND TERMINOLOGY

Production blasting is most often conducted in the middle of a wall (face blast) or at the corner between two faces (corner blast). These are shown diagrammatically in Figure 5.1. The holes are drilled in rows. These rows may be in-line (Fig. 5.2a), which applies to square or rectangular hole patterns, or they may be staggered (Fig. 5.2b). The term 'square' means simply that the rows and columns of holes are at right angles to one another in plan and are therefore 'square' with each other. The actual pattern may be square or rectangular in shape.

The rows of holes may then be *shot*

– Hole-by-hole

or

– Row-by-row.

The 'as-shot' rows of holes may be different than the 'as-drilled' rows used when laying out the drilling pattern. The 'as-drilled' rows are normally defined as those with the row axis parallel to the long face of the bench.

The orientation of the shot rows with respect to the drilled face can be described by the letter '*V*'. The angle of the '*V*' is defined as that existing between the long bench face and the blasted face. Consider, for example, the face blast shown in Figure 5.3. This particular pattern which has the form of a chevron is used for taking a notch out of a long face. The characteristics of such a chevron are

– It causes the rock pile to be concentrated in a central position

– Because of impacts between rocks in the different rows additional fragmentation may result.

Here the bottom of the '*V*' opening consists of 2 holes and the pattern is termed a *closed* chevron. The corner blast shown in (Fig. 5.4) is an example of an *open* chevron.

The open chevron pattern yields flatter, more evenly spread rock piles than the closed chevron. Hence they are well suited to the use of front end loaders. Some other advantages of the open over the closed chevron are that they

– Minimize the possibility of tight toe problems

– Are easier to connect up since the paths can be easily seen.

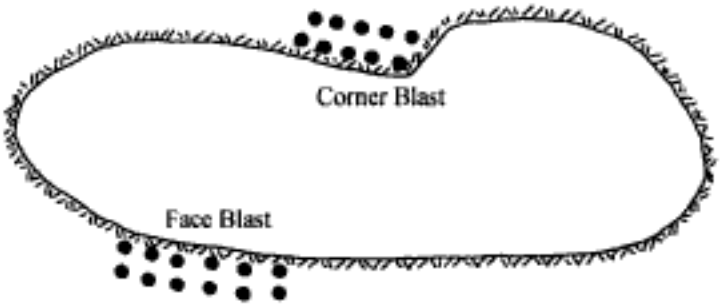

Figure 5.1. Bench representation showing a face and a corner blast.

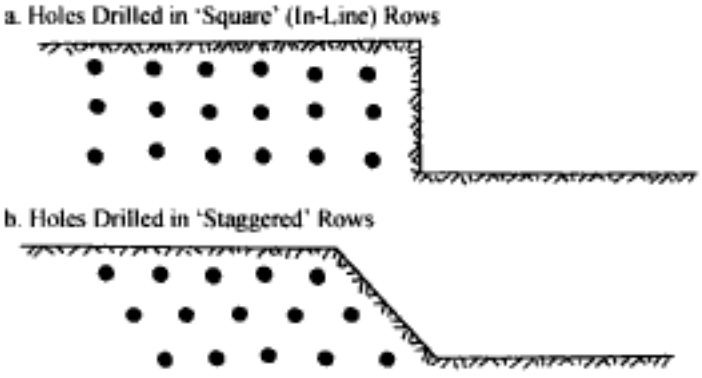

Figure 5.2. Definition of 'square' and 'staggered' patterns.

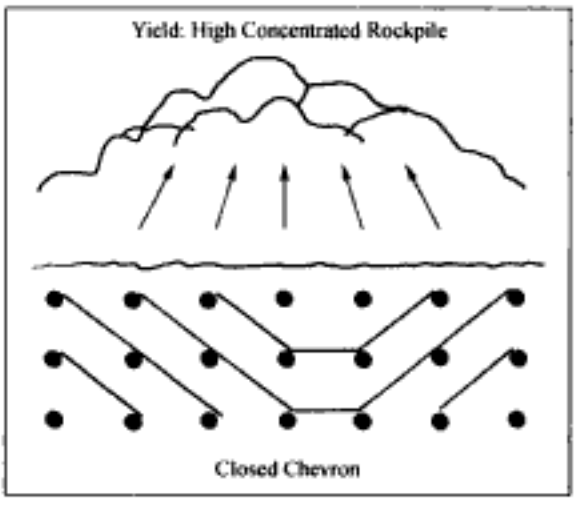

Figure 5.3. A closed chevron pattern (AECI, 1978b).

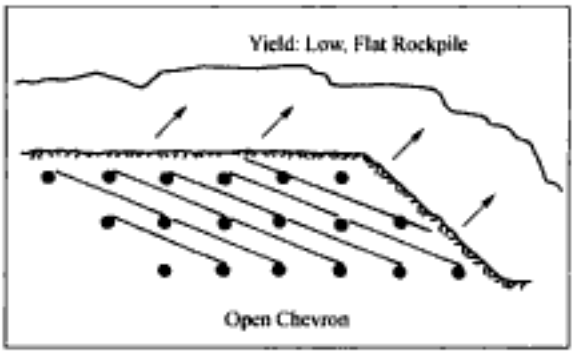

Figure 5.4. An open chevron pattern (AECI, 1978b).

By drawing the initiation lines at different angles through the hole pattern one can create different chevron patterns. The so-called 'flatness' of these patterns is denoted by the number 0, 1, 2, etc following the '*V*'.

Considering a single front row hole, the chevron which intersects the nearest hole in the next row, i.e. the hole immediately behind, defines the '*V*0' chevron. If the angle of the chevron is flattened so that it extends through the next nearest hole, this defines the '*V*1' chevron, and so on. These definitions as applied to a square drilling pattern are shown in Figure 5.5.

Figure 5.6 shows the same definitions as applied to the staggered drilling pattern. They appear flatter since the sideways distance is increased by half the spacing. The '*V*0' patterns are the same as 'in-line' firing. The *V*1 and *V*2 chevrons are those most commonly used.

As indicated, the 'as-drilled' burden (*B*) and spacing (*S*) dimensions are taken with respect to the long axis of the pattern. Figure 5.7 shows the drilled burden and spacing for a corner cut. If the square pattern is shot 'in-line' to the *Y* direction then the 'as-shot' burden and spacing are the same as the 'as-drilled'. If the square pattern is shot 'in-line' to the *X* direction then the 'as-shot' burden is equal to the 'as-drilled' spacing and the 'as-shot' spacing is equal to the 'as-drilled' burden. The 'as-shot' values are often preceded by the words 'ini-

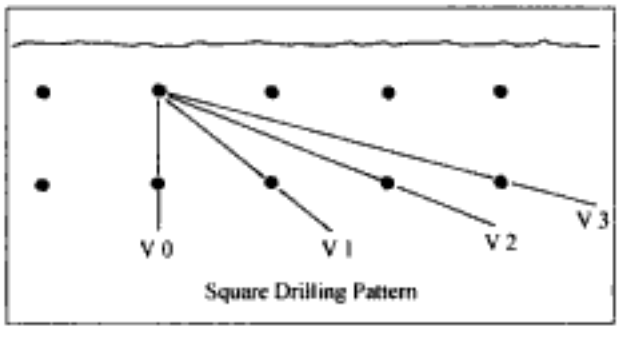

Figure 5.5. A square drilling pattern initiated in various ways (AECI, 1978b).

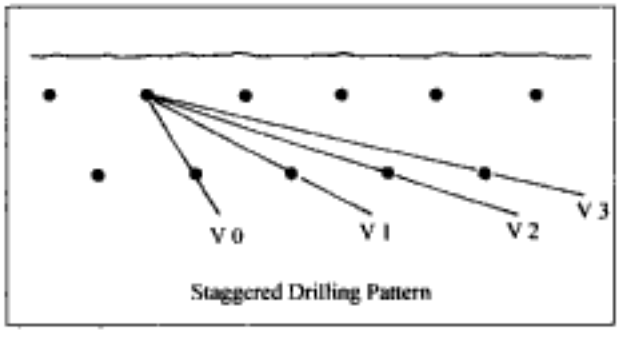

Figure 5.6 A staggered drilling pattern initiated in various ways (AECI, 1978b).

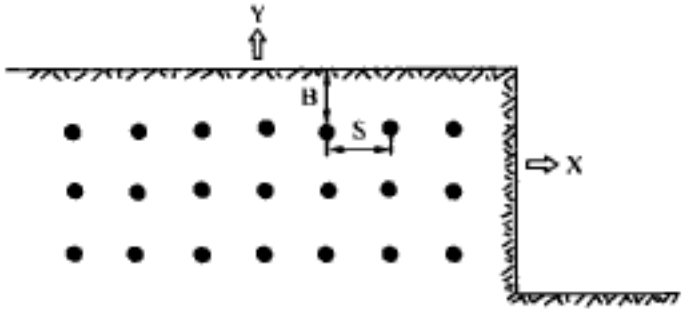

Figure 5.7. A corner cut drilled in a square pattern.

tiation' or 'effective' to distinguish them from the 'as-designed' or 'as-drilled'. If a *V*1 initiation pattern is used (Fig. 5.8), then the firing direction would be at 45° to the long face The effective (initiation) burden (B_e) is the distance between the chevrons. In this case it is

$$B_e = \frac{B}{\sqrt{2}} \tag{5.1}$$

The effective (initiation) spacing (S_e) is the distance between holes in the same chevron

$$S_e = B\sqrt{2} \tag{5.2}$$

Thus the effective spacing-burden ratio becomes

$$\frac{S_e}{B_e} = 2 \tag{5.3}$$

whereas for the drilled pattern it is

$$\frac{S}{B} = 1 \tag{5.4}$$

The actual burden (B_a) in front of the blasthole lies somewhere between the drilled (B) and initiation (B_e) values as shown in Figure 5.9. The initiation ratio (S_e/B_e) is useful for comparing the different patterns. Table 5.1 summarizes the Initiation Ratios (S_e/B_e) for the *V*1 and *V*2 chevrons at various *S*/*B* ratios.

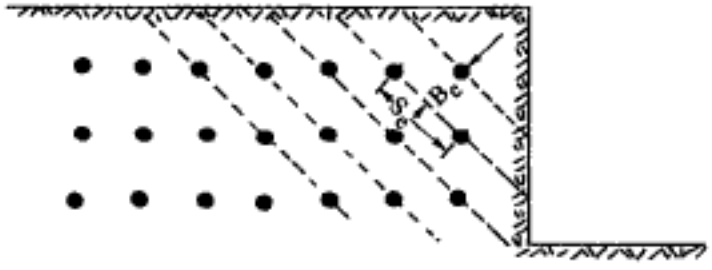

Figure 5.8. The corner cut shot as *V*1.

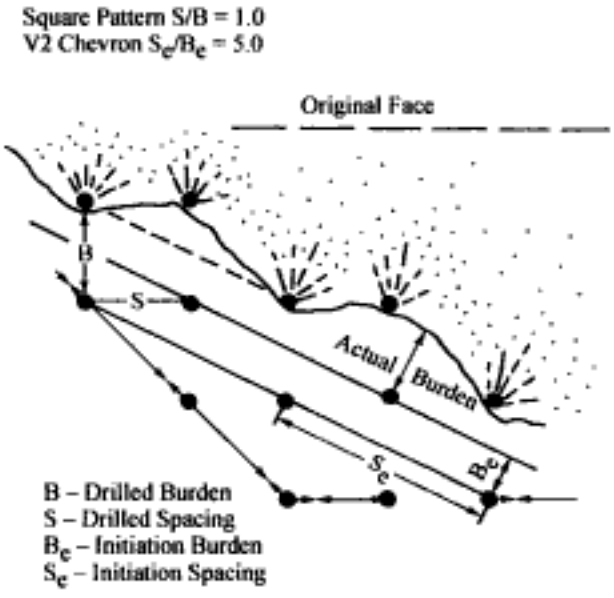

Figure 5.9. A diagrammatic representation of the actual burden on a hole (AECI, 1978b).

Table 5.1. Initiation (S_i/B_i) ratios obtained with *V*1 and *V*2 chevrons at various drilling (S/B) ratios. (AECI, 1978b).

Chevron type	Square drilling pattern			Staggered drilling pattern		
	$S/B = 1$	$S/B = 1.25$	$S/B = 1.5$	$S/B = 1$	$S/B = 1.25$	$S/B = 1.5$
*V*1	2.0	2.1	2.2	3.3	3.6	4
*V*2	5.0	5.8	6.7	7.3	8.6	10

5.2 ENERGY COVERAGE

In examining the best type of 'as-drilled' and 'as-initiated' patterns to be used, consideration must be given to effective energy coverage of the volume to be fragmented and then selection of the initiation geometry to make best use of the energy. The concept of cylindrical fragmented plugs of rock around each charge (in the absence of a free surface) is a useful tool in this regard. One considers the rock influenced by each blast hole to be bounded by a cylinder of influence radius R. Rock lying outside of this radius will also be affected but in a very minor way. Figure 5.10 is a view looking down on a bench for which the 'plugs' have been drawn. In this particular square design the influence radii just touch in both the burden and spacing directions. Thus

$$S = 2R \tag{5.5}$$

$$B = 2R \tag{5.6}$$

and hence

$$S = B$$

The plan area of bench assigned per hole by this layout is A_H

$$A_H = B \times S = B^2 \tag{5.7}$$

and the plan area (A_I) per hole which is influenced by the explosive is

$$A_I = \pi R^2 = \frac{\pi B^2}{4} \tag{5.8}$$

Thus the percent of the plan area assigned to the hole which is influenced by the charge (% I) is

$$\%I = 100\frac{A_I}{A_H} = 100\frac{\pi}{4} = 78.5\% \tag{5.9}$$

The staggered hole layout shown in Figure 5.11 is an alternative. The hole spacing (S), the burden (B) and the influence radius (R) have all remained the same. The only change is that the rows have been translated by a distance R from their positions in Figure 5.10. The area assigned (A_H), the area of influence (A_I) and the percent area influenced (%I) are the same as for the square layout. However, the fragmentation results are often better with the staggered pattern. The reason for this is that even though the *total* 'non-influenced' or 'un-touched' area is the same in both cases, for the staggered pattern the 'un-touched' area is broken down into two smaller areas rather than one larger area (compare Figs 5.10 and 5.11). For the square pattern, the distance (d_n) from the nearest hole to the center of the untouched region is

$$d_n = \frac{B}{2}\sqrt{2} = R\sqrt{2} = 1.41R \tag{5.10}$$

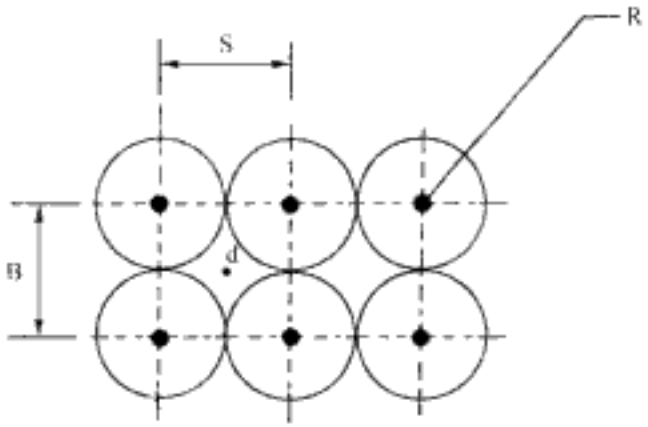

Figure 5.10. Square layout with the hole influence regions touching ($S/B = 1$).

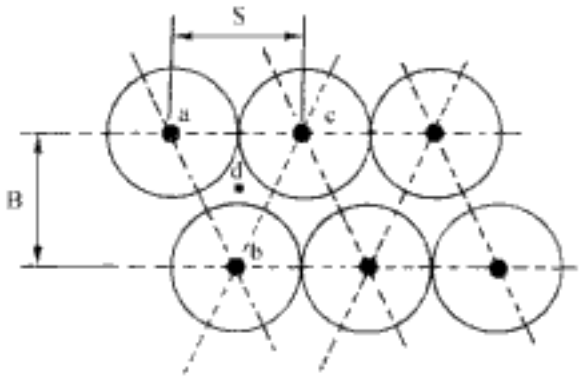

Figure 5.11. Staggered layout with the row influence regions touching ($S/B = 1$).

For the staggered pattern (Fig. 5.11), the figure abc constructed by connecting the nearest holes is an isoceles triangle. The sides *ac* and *bc* are of equal length. The point *d* which is equi-distant from each corner lies along the altitude line. The distance from the three corners is

$$d_n^* = 1.25R \tag{5.11}$$

In summary, even though the percent energy coverage has not changed with this staggered design, the un-touched area has been redistributed into two smaller pieces and the maximum distance from any charge has been reduced from $1.41R$ to $1.25R$. Thus the fragmentation is expected to be better.

In reviewing the layout in Figure 5.11 it is obvious that the easiest way of reducing the untouched area is to reduce the burden dimension while keeping the spacing constant. In Figure 5.12 the burden has been reduced until the radii of influence are just touching. The center-to-center spacing to all adjacent charges is now equal to $2R$. The triangle abc formed is an equilateral triangle with included angles of 60°. The length (L_A) of the altitude of such a triangle is

$$L_A = \sqrt{3}R \tag{5.12}$$

which is just equal to the burden (B') dimension

$$B' = \sqrt{3}R \tag{5.13}$$

Since the spacing is

$$S = 2R$$

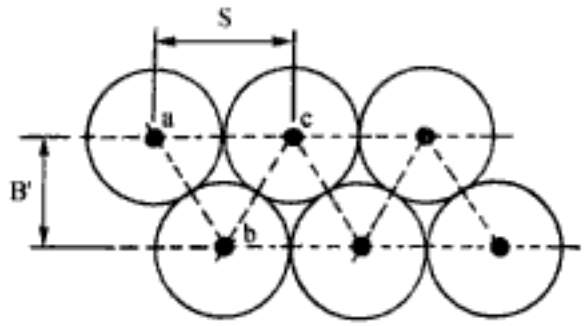

Figure 5.12. Staggered layout with the row influence regions touching ($S/B' = 1.155$).

the burden to spacing ratio is

$$\frac{B'}{S} = \frac{\sqrt{3}R}{2R} = 0.866 \tag{5.14}$$

The inverse of Equation (5.14), the spacing to burden ratio, which is normally quoted is

$$\frac{S}{B'} = \frac{2}{\sqrt{3}} = 1.155$$

The new bench area assigned to each hole with this layout is

$$A'_H = 2R(\sqrt{3}\,R) = 2\sqrt{3}\,R^2 \tag{5.16}$$

The area influenced by the explosive is

$$A'_I = \pi R^2 \tag{5.17}$$

and hence the percent coverage is

$$\%I = \frac{A'_I}{A'_H} = \frac{100\pi}{2\sqrt{3}} = 90.7\% \tag{5.18}$$

If the spacing

$$S = 2R$$

and burden

$$B' = \sqrt{3}R \tag{5.19}$$

are maintained but the rows translated with respect to one another to form a square layout, the result is as shown in Figure 5.13. In the burden direction there is an overlap of the influence circles and in the spacing direction, they just touch. The specific drilling (the number of drill holes per plan area) is the same for both Figures 5.12 and 5.13. Now the area per hole affected by explosive energy can be shown to equal

$$A'_I = \left(\frac{2\pi}{3} + \frac{\sqrt{3}}{2}\right) R^2 \tag{5.20}$$

while the assigned plan area to the hole is

$$A'_H = 2\sqrt{3}\,R^2 \tag{5.21}$$

Thus the efficiency of the energy coverage is

$$\%I = 100\frac{A'_I}{A'_H} = 85.5\% \tag{5.22}$$

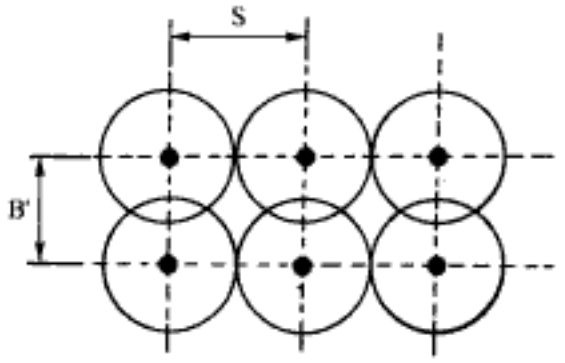

Figure 5.13. The square pattern ($S/B' = 1.155$) with contact in the row direction and overlap in the burden direction.

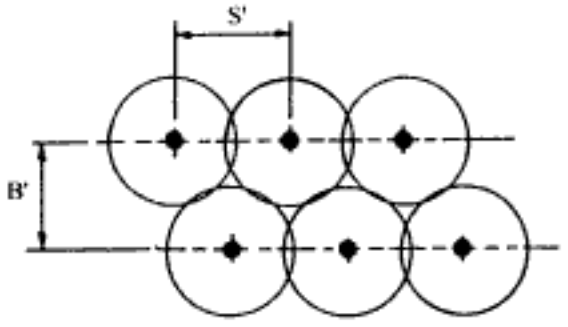

Figure 5.14. Staggered pattern ($S'/B' = 1.0$) with the spacing reduced to achieve total coverage.

which is substantially less than for the staggered pattern. The distance from the nearest charge to the center of the untouched region is, as before, also greater than with the staggered pattern.

Beginning with the staggered pattern shown in Figure 5.12 one would now like to reduce the untouched area to zero. The condition that there should be no untouched region means that the distance d_n from each triangle corner to the midpoint should be the radius of influence R

$$d_n = R \tag{5.23}$$

Working through the geometry it can be shown that the new hole spacing (S') should be

$$S' = \sqrt{3}R \tag{5.24}$$

This design is shown in Figure 5.14. There remains an untouched area because the burden has not as yet been adjusted. Maintaining the ideal staggered geometry in which

$$B'' = \frac{\sqrt{3}}{2} S' \tag{5.25}$$

one finds that

$$B'' = \frac{3}{2} R \tag{5.26}$$

Figure 5.15 is the result of reducing the burden from B' to B'' and the spacing from S to S'. As can be seen, the region untouched by the explosive charge has now vanished.

$$\%I = 100\%$$

The layout area for each hole is now

$$A''_H = B'' \times S' = \frac{3\sqrt{3}}{2} R^2 = 2.6\, R^2 \tag{5.27}$$

as opposed to

$$A_H = 4R^2 \tag{5.28}$$

in the original design shown in Figures 5.10 or 5.11. This means that the specific drilling has increased by a factor of 1.54 while increasing the energy coverage from 78.5% to 100%. An alternative to this is to try and increase the radius of influence R by changing to a more energetic explosive.

Table 5.2 presents the relative efficiencies for different burden to spacing patterns. The efficiencies given are relative to the pattern shown in Figure 5.15 which has an efficiency of 100%. When examining patterns and pattern modification one must keep firmly in mind (a) the changes which occur in the specific drilling and (b) the practicality of drilling the pattern as designed.

As can be seen from Table 5.2, the staggered pattern produces a more uniform distribution of the fracture circles and thus more even fragmentation in the rock pile for the same powder factor. Optimum coverage is obtained with equilateral triangles, however it varies rather little over the range from $S/B = 1$ to $S/B = 1.5$.

The benefits of these staggered patterns may be less evident in highly fractured ground where existing fracture planes limit the development of new radial cracks.

The observant reader should have noted that the design burden on the front row of holes as measured from hole to crest is ½ that of the succeeding rows. This seeming inconsistency is explained by the fact that the bench face is normally sloped such as shown in Figure 5.16. The front row of holes are laid out such that the toe burden is B. A typical bench face angle (70°) and bench height ($1.5B$) give a hole to crest distance of approximately $1/2\,B$. The upper part of the hole is charged less than the other holes in the round to account for this. Figure 5.17 shows the circles of influence superimposed on a two row blast.

When taking into account both drilling and blasting aspects the most desirable overall drilling/initiation pattern (AECI, 1978b) is

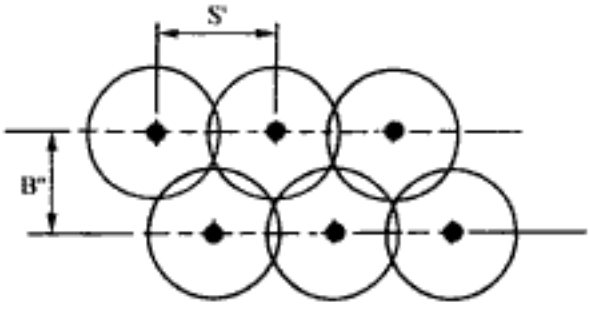

Figure 5.15. Staggered drilling pattern ($S'/B'' = 1.15$) with the burden reduced to achieve total coverage.

Table 5.2. Effect of drilling patterns and S/B ratios on the area covered by the fracture circles. Equilateral triangular layout = 100% (AECI, 1978b).

S/B ratio	Square pattern %	Staggered pattern %
1	77	98.5
1.15Δ	76	100
1.25	75	99.5
1.5	71	94.6
2.0	62	77

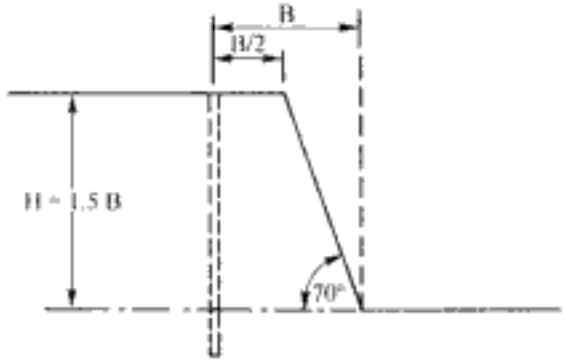

Figure 5.16. Section view through the bench.

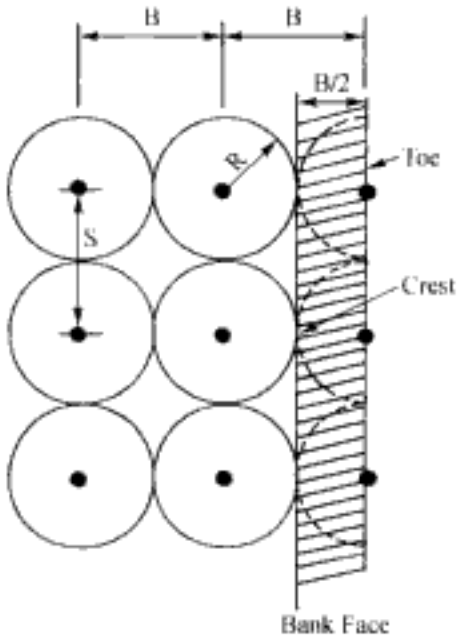

Figure 5.17. Location of the first row of holes with respect to the bank face.

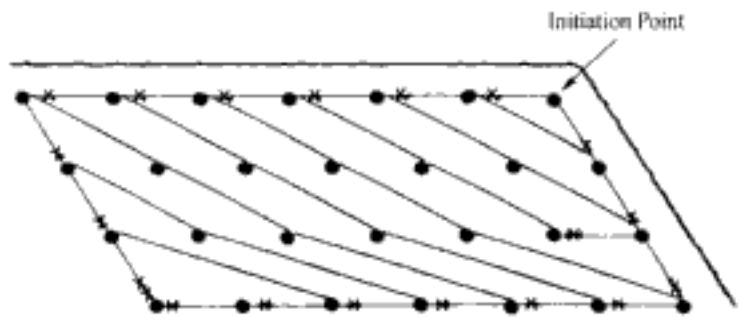

Figure 5.18. A favorable drilling pattern and initiation pattern (AECI, 1978b).

– A staggered drilling pattern with $S/B = 1.25$,
– $V1$ chevron initiation which gives $S_c/B_c = 3.6$.

This is shown in Figure 5.18.

5.3 THE INFLUENCE OF FACE SHAPE

A major conclusion from the previous section is that the *staggered pattern* ($B/S = 1.25$) is best from both ease of drilling and energy distribution viewpoints. The most appropriate burden-spacing relationship for both single and multiple row blasts must now be selected. This topic has two separate but related aspects.

1. Face shape
2. Time delay between holes

The influence of face shape on fragmentation can be practically demonstrated (Hagan, 1983a) by considering the blasting of boulders. If a hole is drilled to the center of such a boulder and a small charge inserted, the boulder can be broken. The required powder factor is of the order of 0.10 kg/m^3 (0.08 lbs/ton), which is much lower than that required in standard production blasting.

The theoretical explanation for this is that the spherical charge sends out a spherical strain wave which, upon meeting the spherical surface of the boulder, is totally reflected back toward the charge. The reflected waves cooperate with one another to encourage maximum crack creation and growth. Of major importance here is that (a) all points on the face are equidistant from the charge and (b) the face completely wraps itself around the charge.

Figure 5.19 shows the results of a series of model experiments conducted by Field and Ladegaard-Pedersen (1969a, b) who investigated the effect of face shape on fragmentation. Under the same charge-burden conditions, the convex surface shows a much higher (more intense) degree of fragmentation than the other surfaces. Since the concave surface dissipates the effect of the strain wave there is no break-out even though part of the surface is within 12 mm of the charge. For the saw-tooth surface part of the wave is reflected towards the cracks and part is reflected from effectively two angled sources. The large number of radial cracks are all about the same length.

The spherical charge and spherical rock geometry (Fig. 5.20a) is not a practical alternative in production blasting. Stepwise however one can arrive at some practical geometries. Figure 5.20b shows a short rock cylinder containing a spherical charge. The results would not be expected to be too different from that of the spherical rock mass. This is not a practical geometry either. However the half cylinder shown in Figure 5.21 starts approaching a practical design element. Such a series of elements could be stacked as in Figure 5.22 yielding a column design. The decking of charges (charges separated by inert sections) practiced at a number of operations is similar in principle. Even though the spherical charge shape is not practical per se, various investigators have shown that in crater blasting cylindrical charges with length to diameter (L/D) ratios ≤ 6 approximate such charges quite well.

Figure 5.23 shows a logical division of a typical cylindrical charge. At the collar and toe regions, the short cylinder configuration containing an equivalent spherical charge basically applies. In the region in between, the representation is a line charge shooting to a curved face. The strain wave reflections coming off this face encourage a high degree of fragmentation. The obvious problem is that of producing such a curved face in reality. As one normally draws the blast designs, the faces are flat and not curved. This is often true, as will be shown later, for S_e/B_e ratios of 2 or less. However for S_e/B_e ratios of the order of 3 to 4 such curved surfaces do result. Consider, for example, the staggered 3 row pattern shown in Figure 5.24.

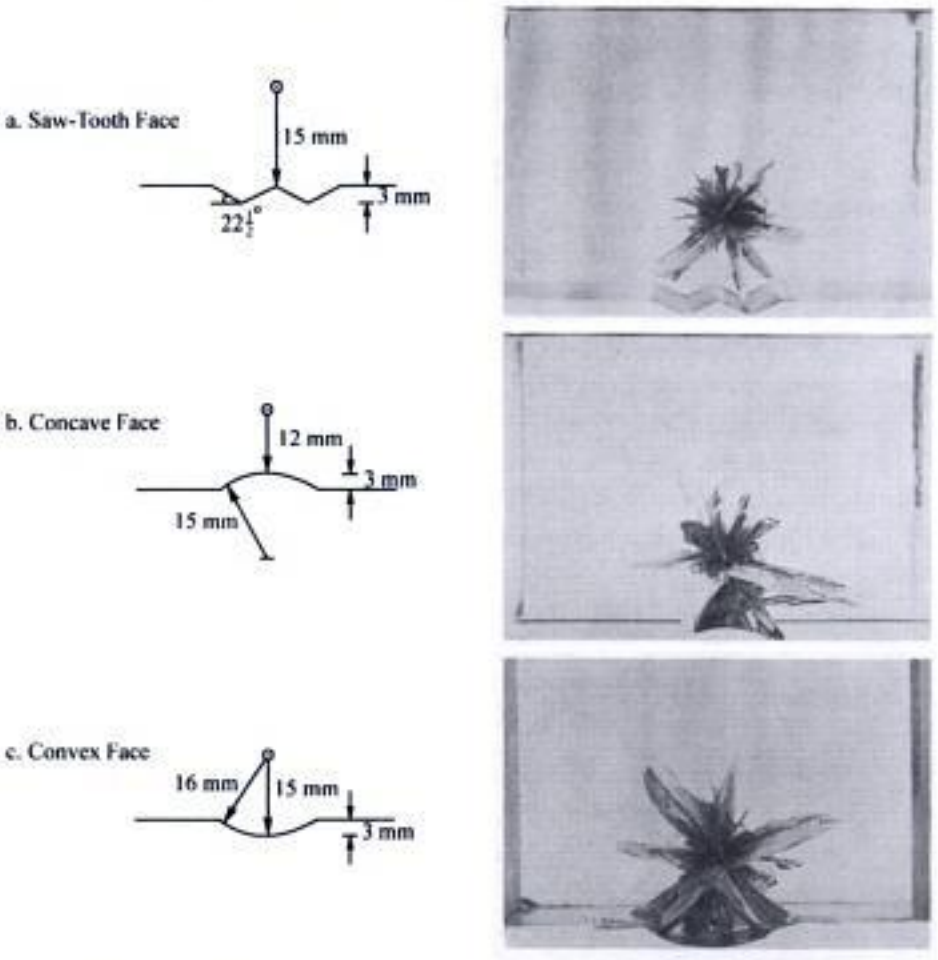

Figure 5.19. Effect of face shape on the fragmentation (Field & Ladegaard-Pedersen, 1971).

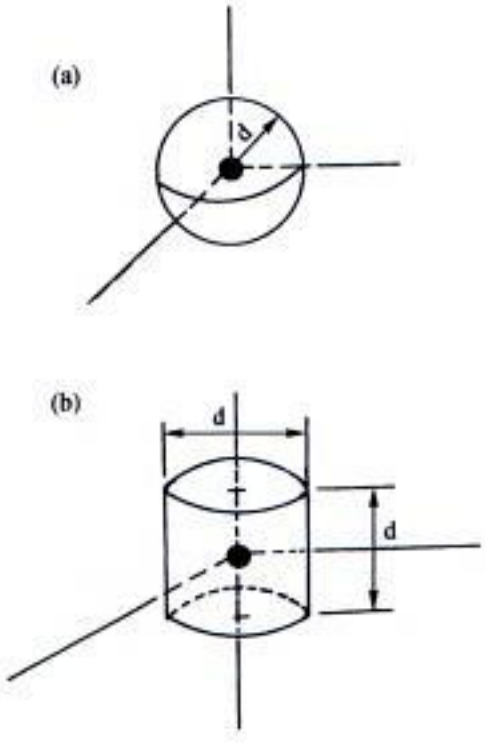

Figure 5.20. A spherical charge shooting to (a) spherical surface and (b) a full cylindrical surface (Hagan, 1983).

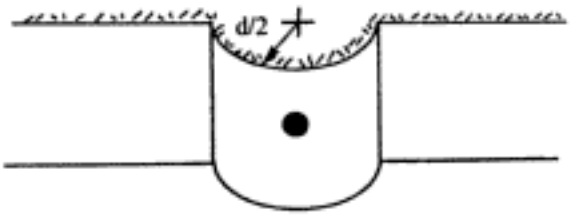

Figure 5.21. A half cylinder face geometry with a spherical charge.

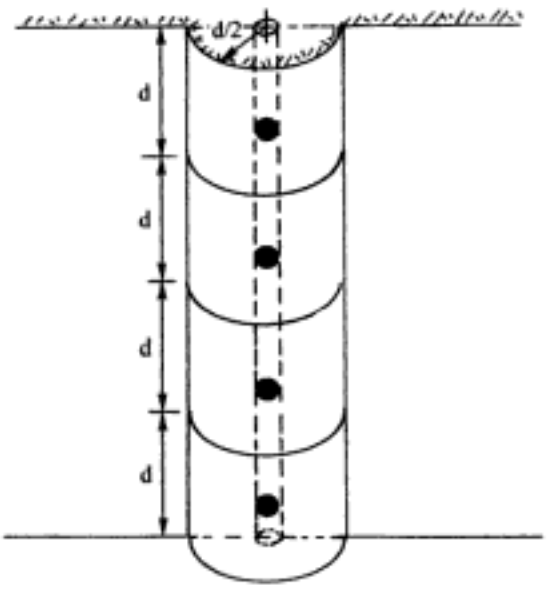

Figure 5.22. A column charge made up of stacked spherical charge units.

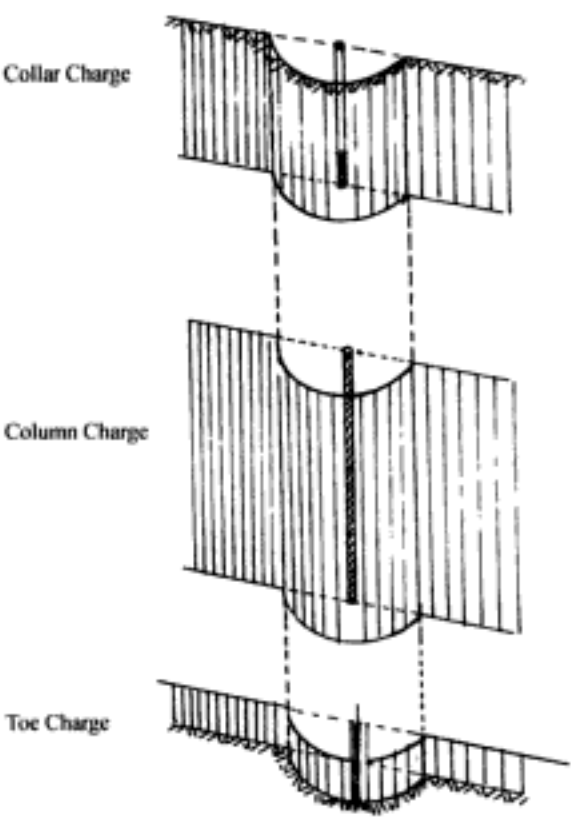

Figure 5.23 Exploded view showing the collar, the column, and the toe charges.

When the holes of such a staggered pattern are shot individually, the geometry prior to shooting hole 8 is as shown in Figure 5.25.

As can be seen, although the shape to be blasted is not cylindrical it is not too far from it. Rather than shooting each hole individually as was done here, the same exact effect can be achieved with a *V*1 firing pattern.

In summary, optimum fracturing is obtained by ensuring that each blasthole fires independently. This can be achieved in two ways

– Initiate each blasthole in sequence,

– Arrange that simultaneously initiated blastholes are far enough apart to prevent mutual interaction between their stress fields. This can for example be achieved by 'chevron' firing.

In practice (Hagan, 1977a,b,c) it is usually not considered expedient to initiate blastholes individually in sequence, although this technique finds application where blasting vibration considerations impose a restriction on the charge mass detonated per delay. Normally, the best solution is to resort to chevron firing, which is simply achieved and in most case gives excellent results.

The main parameter which determines whether or not stress interference takes place between 'simultaneously' initiated blastholes, is the S_e/B_e ratio at the time of firing. In homogenous rock where S_e/B_e is less than 2, the adverse cooperation of adjacent holes results in reduced fragmentation. Real benefits are obtained as S_e/B_e is increased above 2, reaching a maximum at about 8, but with little real improvement above 4.

A series of delay patterns is shown in Figure 5.26. The interested reader is encouraged to evaluate them regarding predicted fragmentation.

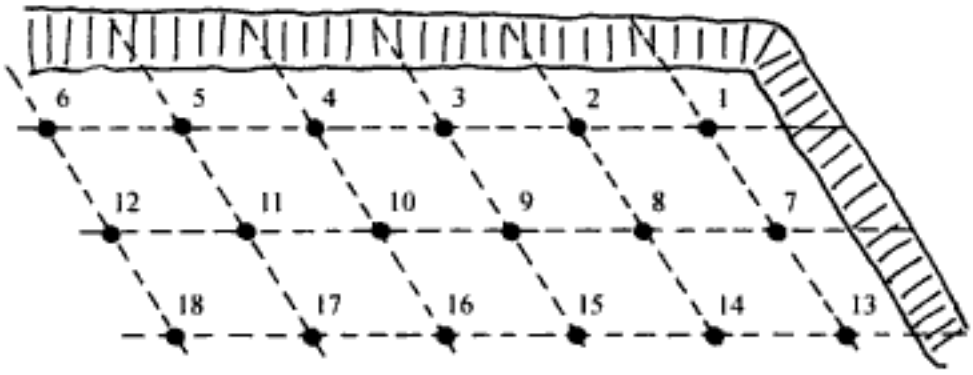

Figure 5.24. The geometry when shooting hole-by-hole.

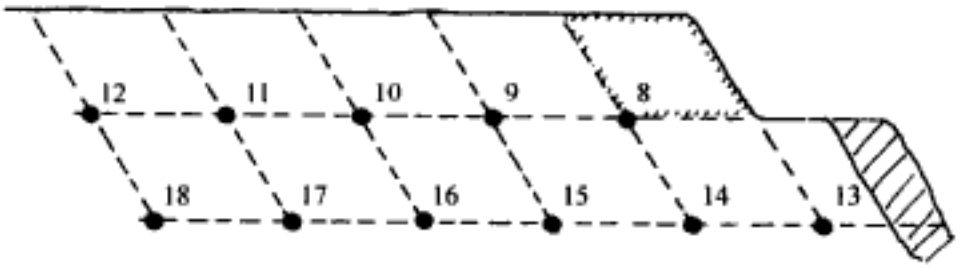

Figure 5.25. The face geometry prior to shooting hole 8.

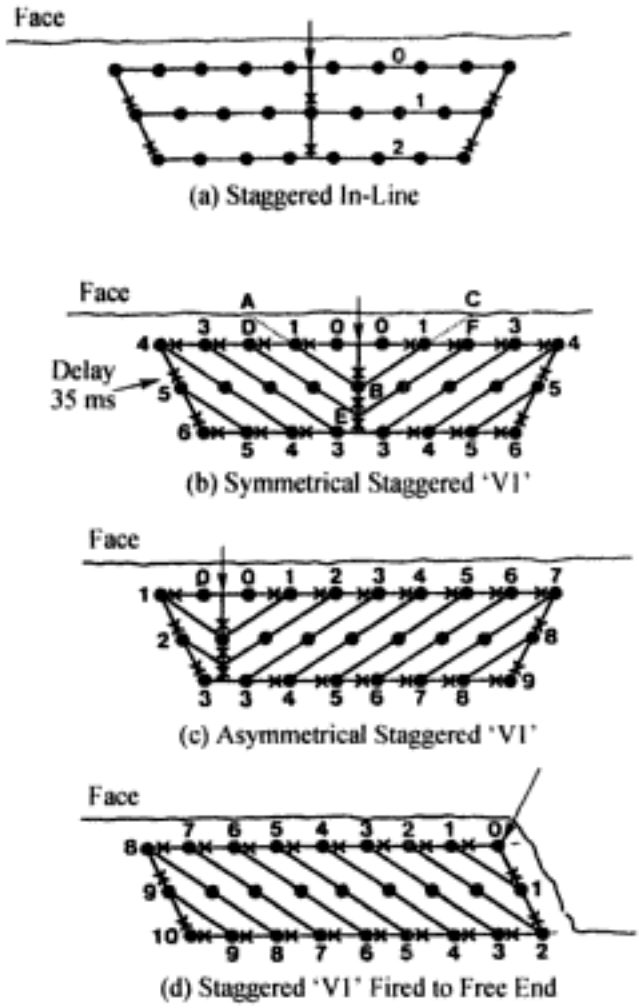

Figure 5.26. Some typical delay patterns (Hagan & Mercer, 1983).

5.4 ONE AND TWO ROW BLASTS

Some of the principles discussed will now be applied to one and two row blasts. The first example will assume instantaneous initiation of all holes (in-line firing towards the free face) while maintaining $S \times B$ constant. This means that the amount of rock broken by each hole remains constant. Four different burden-spacing relationships are shown in Figure 5.27. As can be seen a cratering (failure) angle of 140° has been superimposed. Even though the powder factor is the same in all cases the type of fragmentation will differ.

In the case of the wide spacing (Fig. 5.27b), the charges would produce craters basically independently of one another. For the closest spacing (Fig. 5.27c), the holes would simply split along the hole line thereby releasing the gases very early and producing large chunks.

The patterns lying in between these extremes, $S = B$ and $S = 1.15\,B$ reveal good energy coverage and are those which are used in practice today. Figures 5.28 and 5.29, respectively, show the results of model experiments for $S/B = 0.5$ and $S/B = 2.0$ while maintaining $S \times B$ constant. The results reveal what intuition would suggest.

The following rules (Hagan, 1977a) apply for a single line of holes.

1. An elongated pattern (where S > B) is generally most effective in massive, hardbreaking formations. A larger spacing tends to cause more twisting and tearing of the rock, less splitting along the line of the blastholes, and less overbreak.

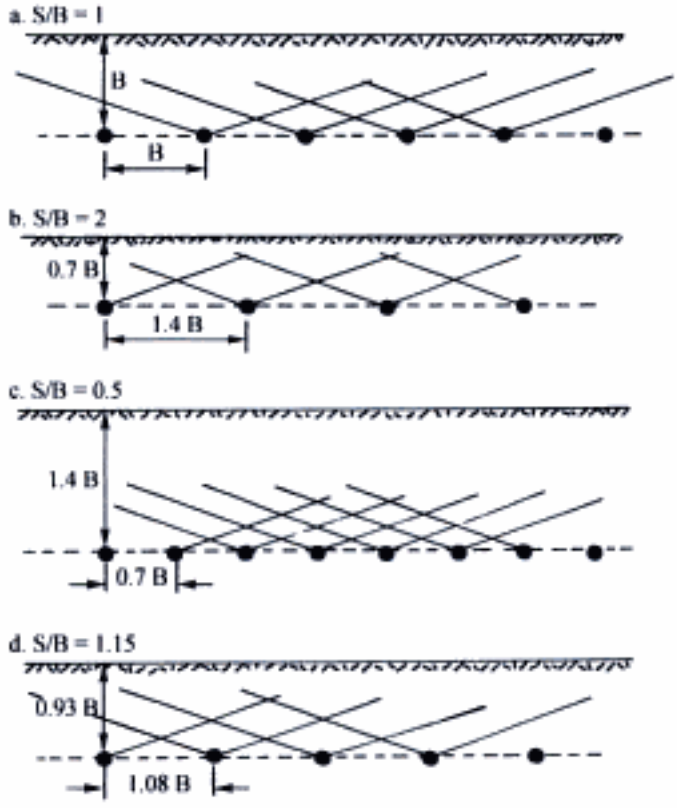

Figure 5.27. Fragmentation for different *S/B* ratios while retaining B × S constant.

Figure 5.28 Laboratory fragmentation for S/B = 0.5 (Langefors & Kihlström, 1963).

2. With greater spacings (and smaller burdens) there is less chance of cutoffs.

3. Spacings considerably greater than the burden can be used to advantage where structural planes such as joints run parallel to the face.

4. Spacings appreciably less than the burden tend to cause premature splitting between blastholes and early loosening of the stemming. Both of these effects encourage rapid release of gases to the atmosphere. Overbreak is usually considerable. This loss of gas energy detracts from overall breakage in the burden. Large slabs are often found in the muckpile.

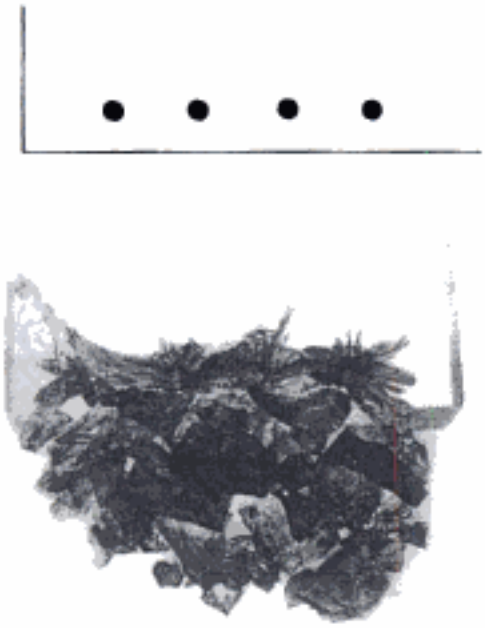

Figure 5.29. Laboratory fragmentation for S/B = 2 and S × B the same as in Figure 5.28 (Langefors & Kihlström, 1963).

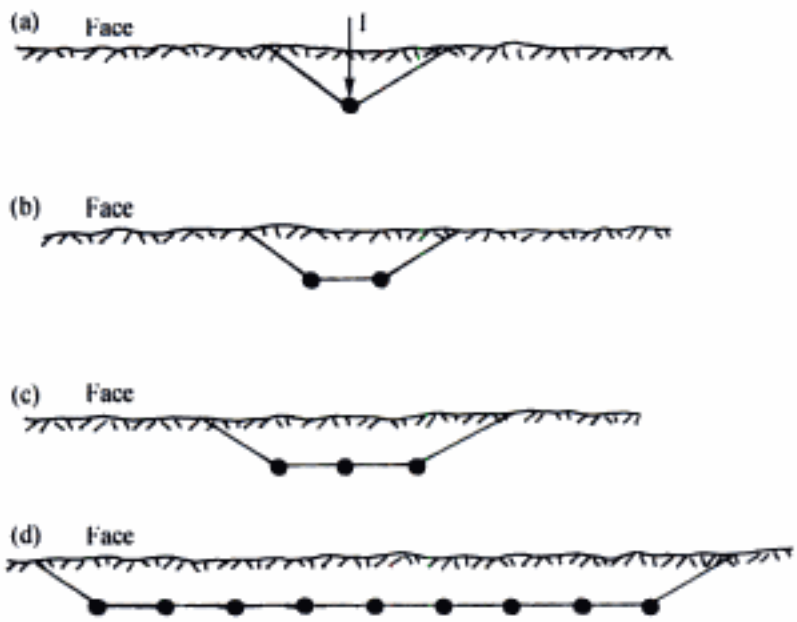

Figure 5.30. The effect of end conditions when shooting single rows (Hagan & Mercer, 1983).

The effect of the numbers of holes shot at one time can be seen in Figure 5.30. For the single charge configuration (Fig. 5.30a), a high degree of confinement is provided by the side rock. In tearing the burden from the adjacent stationary rock mass, side free surfaces having a total length P are created. This requires the expenditure of significant energy. The overall effect is fragmentation of the prism involved but also back break. When two holes are shot together, the amount of fixed perimeter/charge is reduced to $0.5P$/hole. They cooperate on breaking the included volume as opposed to the wall. Although positive with respect to backbreak, this cooperation can result in a poorer fragmentation and greater heave. When one moves to the 9 hole blast the fixed wall/hole is $P/9$. Thus with respect to edge effect and back break, the general principle is that it is better to shoot longer rather than shorter rows.

Consider now the use of delays between the holes. Figure 3.31 shows a row of holes with center initiation. Through the use of delays, the direction of the blast motion and hence

the burden are changed. Once the center hole has been removed, the succeeding holes have two surfaces to which to break. The shape of the volume associated with each hole now more closely resembles that of a half cylinder thereby yielding better fragmentation and less damage to the remaining wall rock. However, the delay time must be sufficient for the rock to move prior to the initiation of the next hole.

The next step is to consider two rows of holes drilled in a square pattern. Conceptually the rows will be considered to be shot instantaneously as shown in Figure 5.32. The front row can obviously break to the free surface as was described earlier. Because the rows are shot at the same time, the front row has not moved. The free surface for the second row is therefore the same as for row 1. Hence, the easiest (closest) surface to which the second row can break is upward (cratering). With this design, the backbreak from row 2 is expected to be high and the resulting muck pile would be very tight if any real breakage occurred. The corner holes in the second row, in particular, are highly constrained. In addition, very high ground vibrations would be expected. In reviewing this design, the first alternative would be to put in a single delay between the first and second rows as shown in Figure 5.33. The amount of delay chosen must be enough for the front row to move outward sufficiently for a recognizable free surface to be formed between the rows. Although an improvement, the corner holes are still highly constrained. If the rock lying between holes is not completely broken such as shown in Figure 5.34, then the face configuration for the second row of holes is poor from a fragmentation point of view since it is concave rather than convex.

Figure 5.31. A single row of holes with center initiation and delays between holes (Hagan & Mercer, 1983).

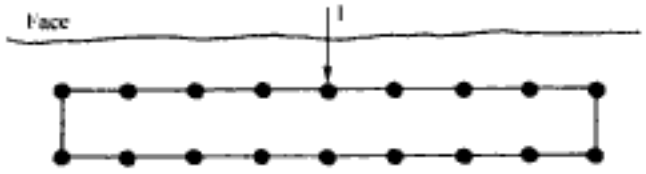

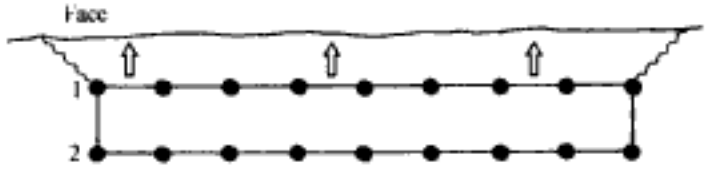

Figure 5.32. Double row shot instantaneously (Hagan & Mercer, 1983).

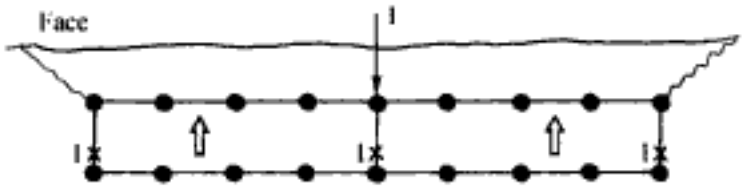

Figure 5.33. Double row with delays between the rows (Hagan & Mercer, 1983).

Figure 5.34. Corner holes shot on separate delays (Hagan & Mercer, 1983).

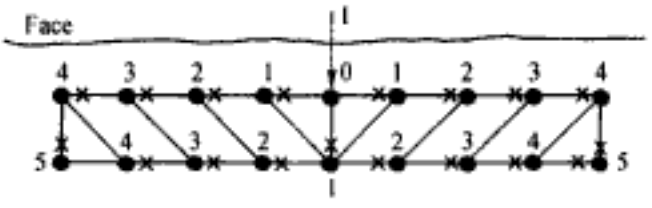

Figure 5.35. Delays used to provide a square '*V*' pattern (Hagan & Mercer, 1983).

An improved design for this two row blast (Mercer & Hagan, 1978) is shown in Figure 5.35 in which a series of delays is used. It is termed a square '*V*' pattern. As can be seen, with the exception of the holes shown on the 0 and 1 delay lines, the remainder of the round has been changed from being shot in-line to staggered.

5.5 SIZE AND SHAPE OF BLAST

As indicated earlier, since most blasts are fired either to a single vertical face or to a free end (Fig. 5.36), these are the only two which will be addressed here. The blast should be as *long* as practicable.

For multiple row blasts, the length (L) of the blast should be at least 1.5 times but preferably 3-4 times the width of the cut. Where the blast length is less than about 1.5 times its width, the stationary rock on *one* or *both* sides of the blast has a restraining or drag effect on forward rock movement (Hagan & Mercer, 1983).

Blasts should be as *large* as possible. The number of rows of blastholes is usually dictated by the working width of the bench/pit and the burden. With large blasts (Hagan, 1977a, 1983a):

1. Productivity is generally improved since the amount of unproductive move/travel time is reduced for all of the unit operations. The drills and shovels can spend a greater amount of time working at one place and the charging of the holes is more efficient. There is a reduced cyclicity of blasting and hence fewer delays involved in moving equipment back and forth.

2. Fragmentation generally improves with an increase in the number of rows. In massive or blocky strata, single-row blasts often give inadequate fragmentation. There are fewer blast boundaries created when fragmenting a block of ore with large blasts than with smaller blasts. The fragmentation at such boundaries tends to be poorer than within the heart of a blasted block due largely to

   (a) The operator's inability to drill an entirely regular blasthole pattern alongside the boundary.

   (b) The gases liberated in the blastholes rapidly escape through cracks alongside the boundary. These cracks are the result of the overbreak caused by the adjoining blast. The early loss of gas pressure means poorer fragmentation and muckpile looseness. Furthermore there is an increased chance for flyrock.

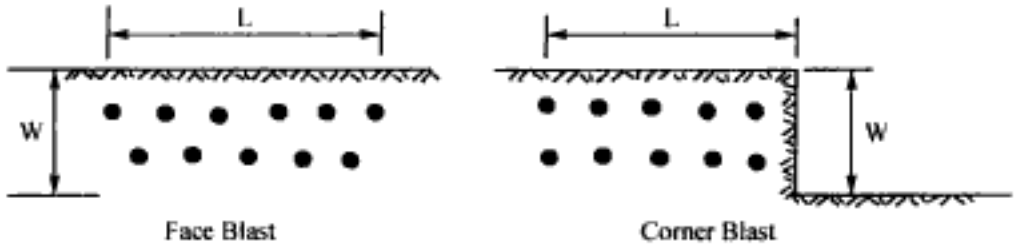

Figure 5.36. Dimensions for corner and face blasts.

Figure 5.37. Providing relief for the back rows.

3. The frequency of environmental disturbances is reduced and hence potential noise/dust complaints.

4. Large chunks of rock that often sit in the newly exposed face (but are effectively detached from the rock mass thereby preventing penetration of explosion-generated strain waves), are usually thrown out virtually intact in the subsequent blast. The percentage of such blocks in the muck pile decreases with an increase in the number of rows (Hagan, 1975).

There are some disadvantages with large blasts however (Hagan, 1977a, 1983a).

1. Overbreak of the back row and sides increases with the number of rows. This is because progressive relief of burden is achieved with greater difficulty towards the back of a deep blast. Where there are too many rows, back-row charges will not see an effective free face (Fig. 5.37).

2. The ground vibrations increase with the number of rows.

3. The displacement of the back rows may be poor resulting in 'tight' digging conditions.

4. Where blasts are well designed, the amount of 'diggable overbreak' is virtually independent of the number of rows in a blast. In highly fissured strata, for example, it may be possible to take advantage of the greater amount of diggable overbreak from single-row shots. If a 4-row blast would be replaced by 4 single-row blasts, the volume of diggable overbreak would increase by a factor as high as four.

5.6 SOME SEQUENCING PRINCIPLES

There are a number of principles which should be applied for achieving the best fragmentation when designing a blast. These principles which have been extracted from Hagan (1975, 1977a,b,c, 1979c, 1983a) are summarized below:

General principles

1. Charges should detonate in the sequence that maximizes the successive development of effective free faces.

2. Each charge should be given just sufficient time to effectively detach its quota of the burden from the rock mass before the next charge detonates.

3. When allocating delay numbers in the blast design phase, the designers should construct lines of breakage for each charge. By doing this

– Any instances of poor sequencing are exposed,

– Alternative superior delay allocations can be made.

4. The scatter between initiation periods even for the same delay number mean that holes go independently.

5. Initiation should commence at that point in a blast which gives the best possible progressive relief for the maximum number of blastholes.

(a) If there is a free end, initiation should begin at that end (Fig. 5.38a).

(b) If there is no free end, initiation should begin near, but not at, one end of the blast block (Fig. 5.38b).

(c) If a buffer of broken rock lies alongside one end of a blast block, initiation should begin near the end of the block remote from the buffer (Fig. 5.38c). The principal direction of rock movement will then be roughly parallel to the buffered face and the blast will be hardly aware of the buffer's presence.

6. When shooting in-line holes simultaneously, the spacing: burden ratio should be as large as possible to achieve the best fragmentation. However, where the *S/B* ratio is too large, each charge fragments and displaces a prismatic section of rock. The face midway between back-row blastholes may remain intact especially near floor level where the large spacing would appear as toe.

7. It is essential to have good control on the blast hole layouts. Large diameter holes should be within 1 foot of the designed location.

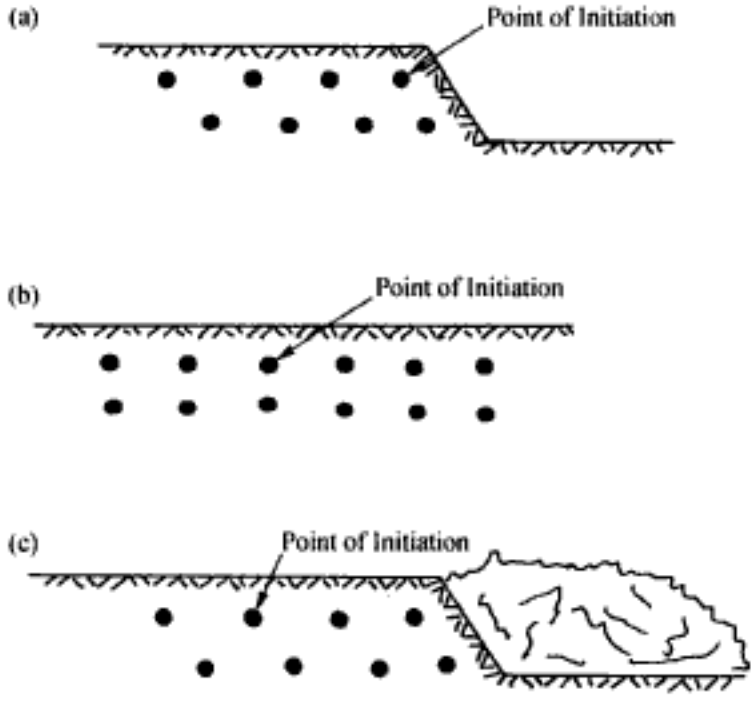

Figure 5.38. 'Best' initiation points under various conditions (Hagan, 1979c).

Single row blasts

1. Short delay intervals between holes give better fragmentation than instantaneous blasts.

2. The optimum delay interval increases with the burden dimension. The optimum inter-row delay is rarely less than 5 ms/m of burden.

3. If the inter-hole delay is considerably longer than the detachment period, blocks of rock within the progressively created faces have sufficient time to detach themselves from, but remain perched alongside, the rock mass to be blasted. By the time their corresponding blastholes fire, these blocks are often thrown out intact into the muckpile. Such blocks are usually larger than the mean fragment size in the muckpile. Their formation should be minimized by selecting an inter-hole delay that is not too long.

4. If the inter-hole delay is too short, then the additional free face is not created. The charges then act almost as though they have been initiated simultaneously.

Multiple row blasts

1. The initiation sequence should be such that each charge shoots to a free face that is extensive, preferably convex (with respect to the charge) and reasonably close.

2. A square pattern fired in a '*V*' provides better fragmentation than one shot in-line (i.e. row-by-row). The '*V*' shot is *effectively staggered* and has a S_e/B_e ratio of 2.0 rather than 1.0. This situation is shown in Figure 5.39b.

3. Fragmentation usually improves as the effective spacing: effective burden S_e/B_e ratio increases up to about 4.0.

This value is best achieved by:

– Drilling blastholes in a staggered pattern (an equivalent triangular or slightly more elongated grid)
– Using a *V*1 initiation sequence.

If the holes (Fig. 5.40a) in the *V*0 pattern are shot one at a time, then the effective burden (as defined as the perpendicular distance between hole rows is $0.57B$ and the spacing is $2B$. The S_e/B_e ratio is 3.51. The actual peak burden is $1.15B$.

If the holes are shot on the same delay (Fig. 5.40b) then $S_e/B_e = 1.15$ and the holes would cooperate with one another. For the staggered drilling pattern shot as *V*1 (Figure 5.41), the calculated burden is $0.57B$ and S is $2B$. However in this case even if shot on the same delay, the holes would function independently.

4. The blasting engineer should ask himself whether the inter-hole delay

(a) will create new effective faces in time for the subsequent rows
(b) can cause cut-offs when using surface delay systems

Easy forward movement limits the uplifting forces which are largely responsible for cut-offs. Fragmentation and muckpile looseness are greatly influenced by the availability of effective free faces.

5. As a rule, blasts are fired

– Along the long axis of a staggered pattern,
– Along the diagonal of a square pattern.

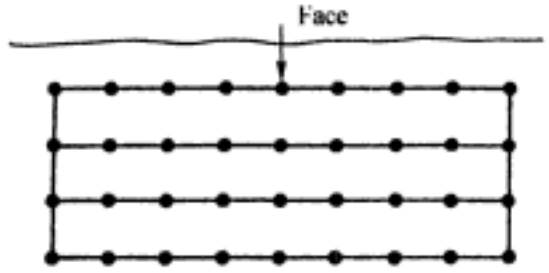

(a) Square Instantaneous

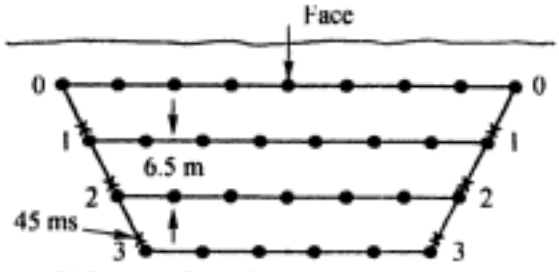

(b) Staggered In-Line

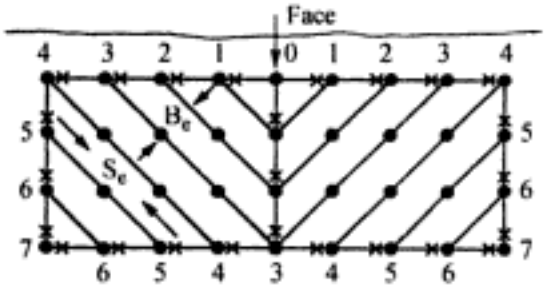

(c) Square 'V'

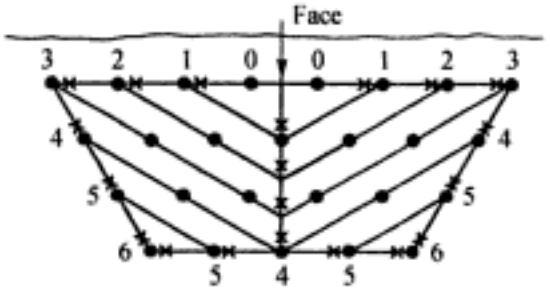

(d) Equilateral Triangular Staggered 'V1'

Figure 5.39. Delay patterns for multiple row blasts (Hagan & Mercer, 1983).

6. For a multi-row blast where it is considered necessary to detonate each hole on a separate delay, the delay time between holes in successive rows can be excessive leading to the possibility of 'cut-off' holes. To overcome this down-the-hole non-electric delays can be used.

7. To reduce projection into the pit, the front row of holes should be loaded according to the amount of back break experienced from the previous blast. It is usual to increase the stemming height by reducing the explosive column length in the front row of holes. This produces a much better muck pile profile with considerably less 'tail' to the blast.

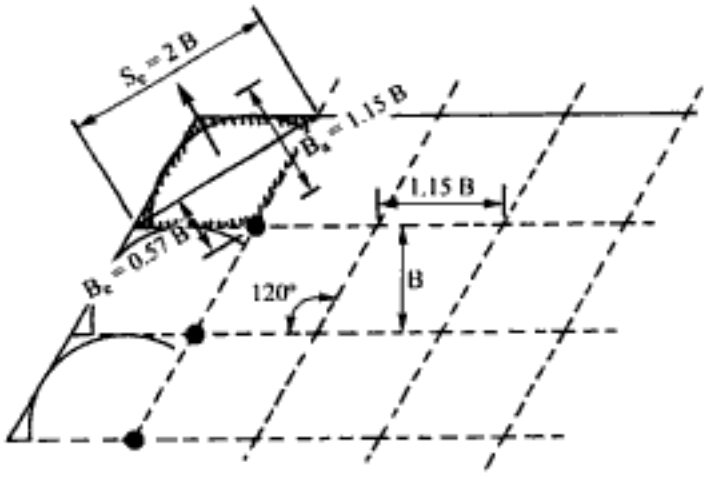

a. Individual delays, VO initiation sequence.

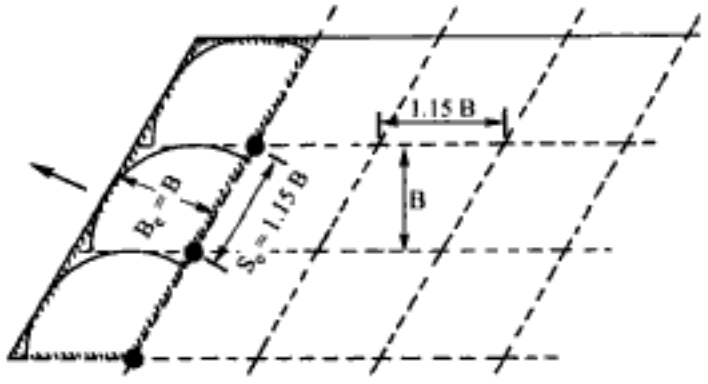

b. Same delay, VO initiation sequence.

Figure 5.40. Staggered pattern shot hole-by-hole using a *V*I initiation sequence.

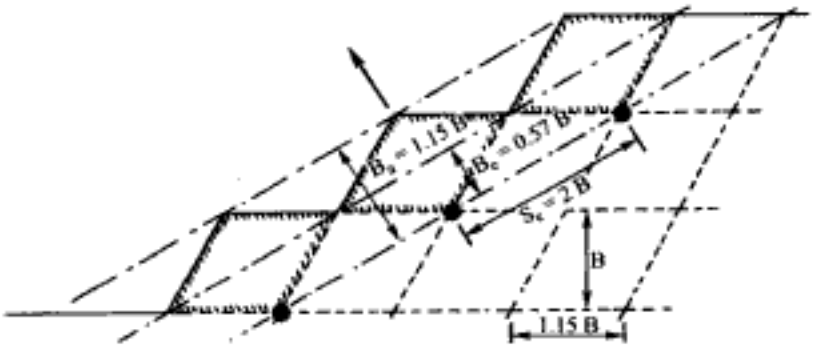

Figure 5.41. Staggered pattern shot row-by-row using a *V*I initiation sequence.

8. If the toe of the first row is not displaced sufficiently, charges in the second and subsequent rows will be *choked* increasingly as the blast proceeds and the likelihood of cut-offs increases.

9. Slope stability increases with the inter-row delay. The amount of ripping and disruption of final faces decreases with increases in the areas of effective faces associated with the use of longer delays.

10. If the number of rows is large, blastholes at or towards the rear may give quite unacceptable fragmentation. They may be incapable of displacing the rock forward. The charges can only crater to the horizontal face. The result is

– High muckpile,
– Toe problems,
– Tight digging,
– Likelihood of airblast, flyrock and overbreak (with associated clean-up operations and instability potential).

11. The optimum inter-row delay lies in the time range which allows good fragmentation and displacement of each burden without the presence of cutoffs.

REFERENCES AND BIBLIOGRAPHY

AECI Explosives and Chemicals Limited 1978a. Parameters in surface blasting. *Explosives Today*. Series 2, No 11, March.

AECI Explosives and Chemicals Limited 1978b. Blasthole drilling and initiation patterns in surface blasting. *Explosives Today*. Series 2, No 12, June.

AECI Explosives and Chemicals Limited 1986. The design of surface blasts. *Explosives Today*. Series 2, no 41, Mar.

Ash, R.L. 1961. Drill pattern & initiation-timing relationships of multiple hole blasting. *Quarterly CSM*, V 56, pp. 309-324.

Ash, R.L. 1963a. The mechanics of rock breakage (Part 1). *Pit and Quarry*. 56(2): 98-100.

Ash, R.L. 1963b. The mechanics of rock breakage (Part 2) – Standards for blasting design. *Pit and Quarry*. 56(3): 118-122.

Ash, R.L. 1963c. The mechanics of rock breakage (Part 3) – Characteristics of explosives. *Pit and Quarry*. 56(4): 126-131.

Ash, R.L. 1963d. The Mechanics of rock breakage (Part 4) – Material properties, powder factor, blasting cost. *Pit and Quarry*. 56(5): 109-118.

Ash, R.L. 1967. Field conditions and their relationships to blasting design. *Proceedings of the 40th Annual Meeting of the Minnesota Section, AIME and the 28th Annual Mining Symposium*, Jan 16-18, Duluth, Minn., pp. 189-196.

Ash, R.L. 1968. The design of blasting rounds. In *Surface Mining* (E.P. Pfleider, ed.). AIME, New York. pp. 373-397.

Ash, R.L. 1974. Considerations for proper blasting design. *Proc. 2nd Annual Blasting Conference. Kentucky Dept. of Mines*, May.

Ash, R.L. & C.J. Konya 1979. Improper spacing: a major problem with surface blasting. *Proceedings of the 5th Conference on Explosives and Blasting Technique. SEE.* pp. 180-184.

Ash, R.L. 1992. Section 6.2.2 *Design of Blast Rounds. Surface Mining*, 2nd Edition (B. Kennedy, editor). SME. pp. 565-583.

Atlas Powder Company. *Surface Shot Design and Shot Calculations*. 19pp.

Atlas Powder Company. 1981. *Workshop Manual 'Surface Blasting Course'*.

Atlas Powder Company.1987. *Explosives and Rock Blasting*. Maple Press. 662pp.

Bauer, A. & M.D. Brennan 1979. *Blast Designs to Improve Dragline Stripping Rates.Final Report-Phase I*. Prepared for US Dept of Energy under contract USDOE DE-AC01-77QQ90147. DOE Report FE 9124-1, April.

Bhandari, S. 1975. Improved fragmentation by reduced burden and more spacing on blasting. *Mining Magazine*. 132(3): 187-198.

Bulow, B.M. & C.K. McKenzie 1990. Hole to Hole Explosive Interaction in production blasting at Mount Tom Price. FRAGBLAST '90. *Proceedings of the 3rd Int Symp. on Rock Fragmentation by Blasting. Brisbane* August 26-31. pp 325-333.

Chiappetta, R.F., S.L. Burchell, J.W. Reil & D.A. Andersson 1986. Effects of accurate MS delays on productivity, energy consumption at the primary crusher, oversize, ground vibrations and airblast. *Proceedings of the 12th Conference on Explosives and Blasting Technique. SEE.* pp. 213-240.

Dick, R.A., L.R. Fletcher & D.V. D'Andrea 1983. *Explosives and Blasting Procedures Manual. USBM IC* 8925. 105pp.

E.I. DuPont de Nemours and Co. DuPont *Blasters' Handbook*. 1977 Edition. Wilmington, Del. 494 pp.

Ellis, O.W. 1993. Optimizing energy distribution in shot design. *Stone Review*. 9(4): 15-17.

Field, J.E.& A. Ladegaard-Pedersen 1969a. Controlled fracture growth in rock blasting. Report DL 1969:8 Swedish Detonic Research Foundation.

Field, J.E.& A. Ladegaard-Pedersen 1969b. The importance of the reflected shock wave in rock blasting. Report No. DL 1969:7 Swedish Detonic Research Foundation.

Field, J.E.& A. Ladegaard-Pedersen 1971. The importance of the reflected shock wave in rock blasting. Int. J. Rock Mech. Min Sci. 8(3): 213-226.

Gustafsson, R. 1973. *Swedish Blasting Technique*. SPI Publisher, Gothenburg, Sweden, 327pp.

Hagan, T.N. 1975. Initiation sequence: Vital element of open pit blast design. Design Methods in Rock Mechanics (C.Fairhurst & S.L. Crouch, eds*) Proceedings of the 16th US Symposium on Rock Mechanics, Minneapolis, Minn. ASCE*, 1977. pp. 345-355.

Hagan, T.N. 1977a. The effects of blast geometry and initiation sequence on blasting results. Chapter 6. in *Australian Mineral Foundation's 'Drilling and Blasting Technology' Course, Adelaide*, May. 55pp.

Hagan, T.N. 1977b. Effects of delay timing on blasting techniques. Chapter 7 in Australian Mineral Foundation's 'Drilling and Blasting Technology' Course, Adelaide, May. 37pp.

Hagan, T.N. 1977c. Good delay timing-prerequisite of efficient bench blasts. Proc. *Australas. Inst. Min. Metall.*, (263):47-54.

Hagan, T.N. 1979a. Accurate delay timing and cutoffs. Chapter 10 in *the workshop proceedings for 'Influence of Rock Properties on Drilling and Blasting' Adelaide*, 25-29 June. Australian Mineral Foundation, Inc. pp. 256-273.

Hagan, T.N. 1979b. The control of fines through improved blast design. Proc *Australas Inst Min Metall.* (271): 9-20.

Hagan, T.N. 1979c. Designing primary blasts for increased slope stability. *Proceedings, Fourth Congress Int. Soc. of Rock Mechanics, Montreaux, Switzerland*, Sept 2-8. Vol 1. pp. 657-664.

Hagan, T.N. 1980. *Safety and Efficiency in Quarry Blasting Manual*. ICI Australia Operations Pty, Ltd Explosives Division. March 26-28 in Sydney.

Hagan, T.N. 1983a. The influence of controllable blast parameters on fragmentation and mining costs. *Proceedings of the 1st Int. Symp. on Rock Fragmentation by Blasting*, Luleå, Sweden. pp. 31-52.

Hagan, T.N. 1983b. Field measurements of rock mass properties: an essential requirement for optimising blast designs. *Proc. Int. Symp. on Field Measurements in Geomechanics*, Zurich, Sept 5-8. pp. 105-113.

Hagan, T.N. & G. Harries 1977. The effects of rock properties on blasting results. Chapter 4 *in Australian Mineral Foundation's 'Drilling and Blasting Technology' Course, Adelaide*, May. 31pp.

Hagan, T.N. & G. Harries 1979. The effects of rock properties on the design and results of blasting. Chapter 2 of the *Australian Mineral Foundation's Workshop Course Manual 'Influence of Rock Properties on Drilling and Blasting'*. Adelaide.

Hagan, T.N. & J.K. Mercer 1983. Safe and Efficient Blasting in Open Pit Mines. *Manual written for the course given at Karratha*, Australia 23-25 November. ICI Australia Operations Pty., Ltd. Explosives Division.

Hoek, E. & J.W. Bray 1973. *Rock Slope Engineering*. Chapter 11. *Blasting*. Instn of Min Met., London. pp. 271-307.

Holmberg, R. 1975. Computer calculations of drilling patterns for surface and underground blasting. Design Methods in Rock Mechanics (C. Fairhurst & S. Crouch, eds) *16th Symposium on Rock Mechanics, , Minneapolis. Minn. ASCE*. 1977. pp. 357-364.

Langefors, U. & B. Kihlstrom 1978. *The Modern Technique of Rock Blasting*. John Wiley & Sons, Inc., New York. 403pp.

Mercer, J.K. & T.N. Hagan 1978. Progress towards optimum blasting – a key to increased productivity and profitability. *Proceedings, 11th Commonwealth Mining and Metallurgy Congress*. Hong Kong, May. pp. 683-690.

Moore, D.J. 1975. Practical application of empirical blast design. *Proceedings First Conference on Explosives and Blasting Technique. SEE.* pp. 28-47.

Pugliese, J.M. 1972. Designing Blast Patterns Using Empirical Formulas – A comparison of calculated patterns with plans used in quarrying limestone and dolomite with geologic considerations. *USBM IC 8550*. 33pp.

Stagg, M.S., S.A. Rholl & R.E. Otterness. 1989. The effect of explosive type and delay between rows on fragmentation. *Proceedings of the 15th Conference on Explosives and Blasting Technique. SEE.* pp. 353-366.

CHAPTER 6

Sinking cut design

6.1 INTRODUCTION

To develop new bench levels in an open pit mine, a sinking (ramp) cut is used (Fig. 6.1). It is different from the usual production blasting done in the mine in that the free surface to which the breakage occurs is horizontal. The blastholes are oriented perpendicular rather than parallel to the free surface and rock movement is against gravity. Thus special blast design procedures are required.

It will be assumed that production drillholes of the same large diameter will be used for the entire cut. At the shallow end the cut depth is only a few multiples of the hole diameter and the blasting resembles cratering. At the deep-end, the sinking cut resembles a full benching operation. From a strictly practical viewpoint, a certain minimum drilling geometry (hole depth, pattern) is required. If 9 7/8″ diameter holes are being drilled, for example, it is not practical to drill them on 1 m centers to a depth of 1 m as might be theoretically required at the entry to the ramp. It is also not practical to vary the pattern and depth from hole to hole. Thus the cut is designed in a sequence of segments. Within each segment the hole depth and pattern is maintained constant. A certain amount of subdrilling will be required to ensure that the eventual ramp satisfies the desired grade. The initiation sequence must be such as to allow sufficient rock movement before the next holes detonate. Finally, careful blasting techniques should be used when the ramp is to form part of the final pit wall.

The overall sinking cut design requires specification of:

1. Drilling depth
2. Burden/spacing
3. Hole loading
4. Initiation sequence.

The approach described in this section is broadly based upon a paper by Chung (1982). It has been expanded somewhat by the author to assist in concept understanding. The blasting nomenclature has been changed to make it consistent with that used throughout this book.

The discussion will be broken down into three parts according to geometry.

1. Bench blasting
2. Crater blasting
3. Transition zone

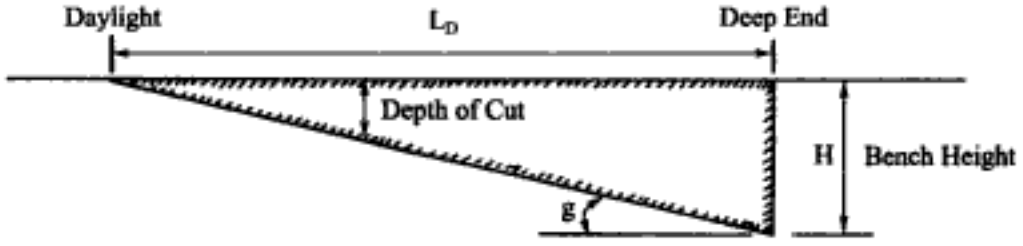

Figure 6.1. Diagrammatic representation of a sinking cut.

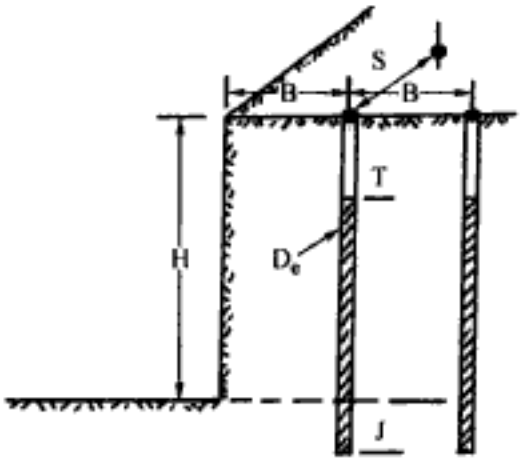

Figure 6.2. The blast pattern at the full cut end.

6.2 BENCH BLASTING ZONE

At the full depth (bench blasting) end of the cut, the situation is as shown in Figure 6.2. As was seen from the basic design formulas (Chapter 4) there are a series of relations relating burden (B), spacing (S), subdrilling (J) and stemming (T) for a given rock type, hole diameter (D_e) and explosive. For consistency these same terms will be used

$$B = K_B D \tag{6.1}$$

$$S = K_S \mathrm{B} \tag{6.2}$$

$$J = K_J B \tag{6.3}$$

$$T = K_T B \tag{6.4}$$

A series of blasting tests will be assumed to provide K_B, K_J and K_T. Using Equation (6.3) the burden-subdrill relationship becomes

$$B = \frac{J}{K_J} = mJ \tag{6.5}$$

where m = proportionality constant = $1/K_J$

Given the amount of subdrill (J), the corresponding burden (B) can be calculated.

Expressing the ramp grade as a ratio (G) the distance L_D from the beginning of the ramp to the full benching zone is given by

$$L_D = \frac{H}{G} \tag{6.6}$$

6.3 THE SHALLOW ZONE

The shallow-zone (Fig. 6.3) is defined as that region of the cut controlled by either (a) the minimum pattern dimension or (b) the minimum drill (cut) depth. The hole depth and charge size is constant throughout this region. An enlarged view of the holes at the deep end of the shallow zone is shown in Figure 6.4. Several design simplifications will be used.

1. The top of the charge is placed at the desired grade level. Cratering is assumed complete to the top of the charge. Hence the cut depth (H') is equal to the stemming length.

2. The relationship between the cut depth (H'), the charge length (J'), and the charge diameter (D_e) is given by

$$(H' + \frac{J'}{2}) = 19(\frac{D_e}{2}) \tag{6.7}$$

The use of the prime notation simply means that they apply to the shallow end.

3. In this region, packaged rather than bulk explosives will probably be used in the holes. The length J', that of a single cartridge, can be expressed as a function of the hole diameter

$$J' = K_e D_e \tag{6.8}$$

where K_e = length to diameter ratio of a single explosive charge. It depends upon the explosive and the packaging.

For the hole diameters under consideration (≥ 8 ins.), K_e is of the order of 2 to 3. The average value of 2.4 will be assumed to apply. Thus

$$J' = 2.4D_e \tag{6.9}$$

4. The burden (B') is related to the amount of subdrill by

$$B' = mJ' \tag{6.10}$$

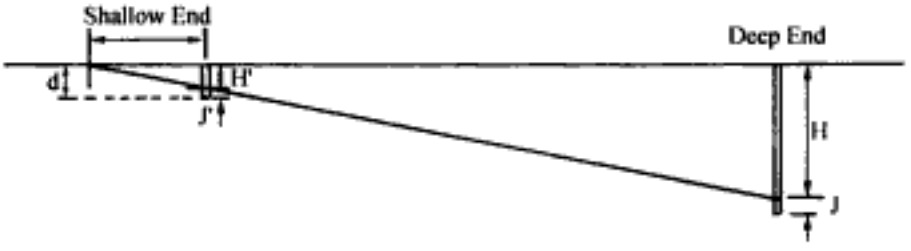

Figure 6.3. Delineation of the shallow end.

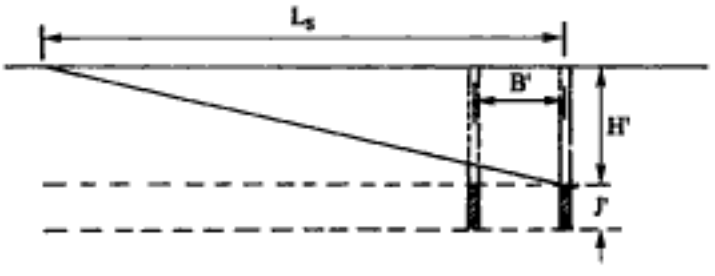

Figure 6.4. Enlarged view of the shallow end blasting region.

Combining Equations (6.7) and (6.9) one finds that the depth H' of the cut in the shallow region is

$$H' = 8.3D_e \tag{6.11}$$

The length of the shallow region is given by

$$L_S = \frac{H'}{G} \tag{6.12}$$

6.4 THE TRANSITION REGION

The length (L_T) of the transition region

$$L_T = L_D - L_S \tag{6.13}$$

has now been defined as has the depth of cut and the subdrill depths

	Shallow end	Deep end
Cut depth	H'	H
Subdrill depth	J'	J

at both ends of this zone. The subdrill depth for this zone, as shown in Figure 6.5, is assumed to increase linearly from the shallow to the deep end. This is shown by the dashed line in Figure 6.5 which intercepts the surface at a distance X away from the daylighting point.

Using similar triangles it can be shown that

$$(H' + J')/(L_S + X) = (H + J)/(L_D + X) = (H_t + J_t)/(L_t + X) = K \tag{6.14}$$

Equation (6.14) can now be solved for distance X

$$X = [(H' + J')\,L_D - (H + J)\,L_S]/[(H + J) - (H' + J')] \tag{6.15}$$

The amount of subdrilling (J_t) at any point (L_t) in the transition zone can be determined using

$$J_t = K\,(L_t + X) - H_t \tag{6.16}$$

$$H_t = L_t \times G \tag{6.17}$$

The burden for the holes in the transition zone is given by

$$B_t = mJ_t \tag{6.18}$$

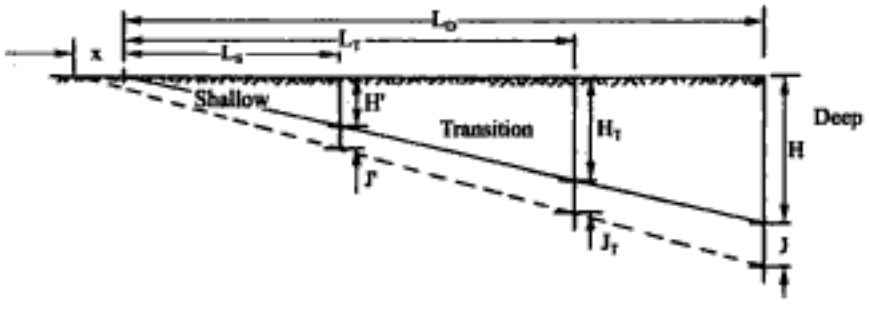

Figure 6.5. The transition zone.

These equations can now be used to calculate the patterns for different cut depths or the cut depths for given patterns given the results from a reference blast.

6.5 SINKING CUT EXAMPLE

The example given by Chung (1982) will be used to illustrate the process. The details of the normal production blasting in the ramp area are

Hole diameter (D_e) = 0.25 m (9 7/8")
Explosive = *ANFO*
Explosive density = 850 kg/m^3
Burden (B) = 7 m
Spacing (S) = 7 m
Bench height (H) = 12 m
Subdrill (J) = 1.8 m
Stemming (T) = 4.5 m
Length of charge = 9.3 m
Amount of explosive = 391 kg

The fragmentation was deemed to be satisfactory. Using this information, the problem is to design a 30 m wide sinking cut driven at a grade of 8% (G = 0.08) from the surface to a depth of 12 m.

Step 1. The characteristics of the deep zone are calculated/summarized.

H = 12 m

L_D = 12/0.08 = 150 m

D_e = 0.25 m

$B = S$ = 7 m

J = 1.8 m

$L_D = B/D_e$ = 7 m/0.25 = 28

$K_j = J/B$ = 1.8/7 = 0.26

$K_T = T/B$ = 4.5/7 = 0.64

$m = B/J$ = 7/1.8 = 3.89

Step 2. The characteristics of the shallow zone are calculated/summarized.
The packaged *ANFO* has a length to diameter ratio of 2.4. Cartridges 8" in diameter are used.

$J' = 2.4\ D_e = 2.4\ (0.25) = 0.6$ m

$H' = 8.3\ D_e = 8.3\ (0.25) = 2.08$ m

L_S = 2.08/0.08 = 26 m

$B' \cong J' \times m = 0.6\ (3.89) = 2.3$ m

Step 3. The characteristics of the transition zone are calculated/summarized

$$L_T = 150 - 26 = 124 \text{ m}$$

$$X = \frac{(2.08 + 0.6)\,150 - (12 + 1.8)\,26}{(12 + 1.8) - (2.08 + 0.6)} = 3.88 \text{ m}$$

$$K = \frac{12 + 1.8}{150 + 3.88} = 0.09$$

Step 4. The values for any point in the transition zone can now be calculated. The distance $L_t = 50$ m will be selected as an example.

$$L_t = 50 \text{ m}$$

$$H_t = 50 \times 0.08 = 4 \text{ m}$$

$$J_t = 0.09\,(50 + 3.88) - 4 = 0.85 \text{ m}$$

$$B_t = 3.89 \times 0.85 = 3.31 \text{ m}$$

This process can be repeated for any desired position within the transition zone.

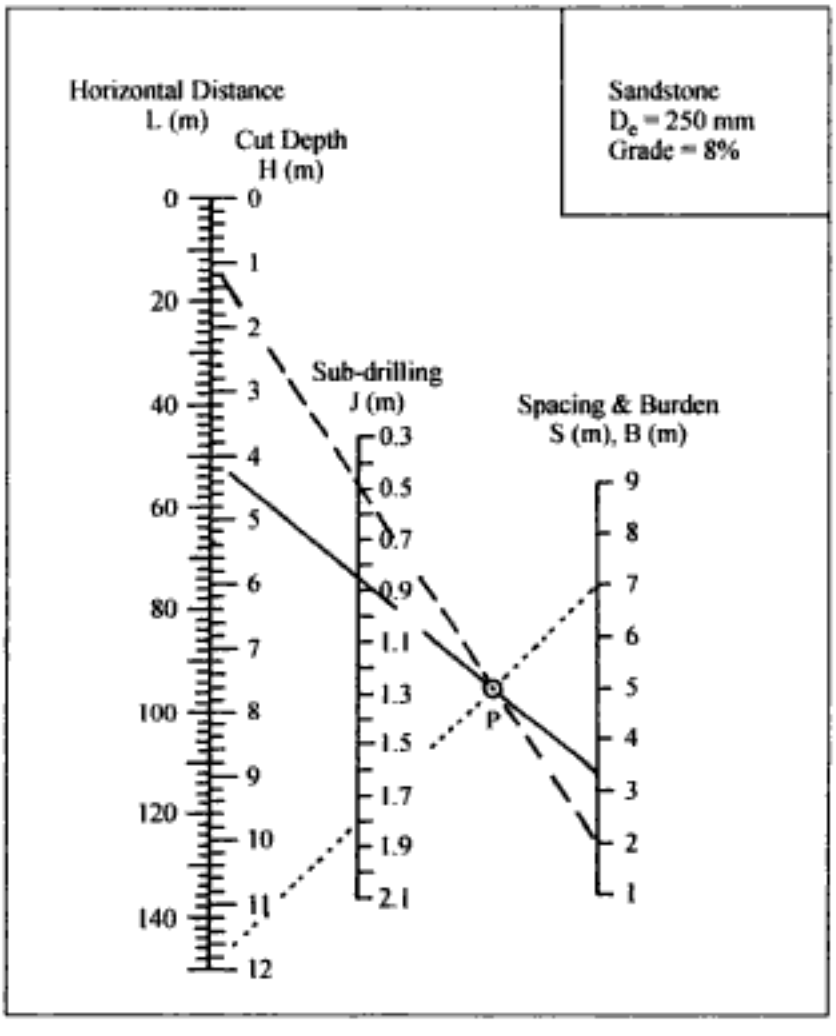

Figure 6.6. Sinking cut design nomograph (Chung, 1982).

Step 5. A design nomograph is prepared to simplify the design process.

Figure 6.6 shows the nomograph prepared by Chung for the present example. It consists of four scales

- Horizontal distance *L*,
- Depth of cut *H*,
- Subdrilling *J*,
- Burden and spacing.

To demonstrate its use draw the line passing through the point representing a horizontal distance of 50 m and the alignment point P. The line intersects the other 3 scales to give

$$H = 4 \text{ m}$$

$$J = 0.85 \text{ m}$$

$$B = 3.3 \text{ m}$$

Step 6. The nomograph is used for design.

The cut is divided into 2 parts, Part I extends from 0 to 80 m and Part II extends from 80 m to 150 m. The required ramp width is 30 m. Although there are many other combinations which could be used, integer dimensions will be used as much as possible for burden and spacing. At the deep end the nominal burden and spacing is 7 m. At the shallow end they are 2 m. Hence the actual design involves the transition from the 7 m pattern to the 2 m pattern.

The first step in the layout is to determine the horizontal distance regimes in which the pattern is constant. Some judgement is required in this regard. Lines corresponding to burdens of 6.5, 5.5, 4.5, 3.5 and 2.5 m are drawn through the alignment point. The corresponding horizontal distances are given in the Table 6.1.

These lines are then superimposed on the plan map of Figure 6.7 and the nominal burden × spacing values added. The detailed layout for the region of 0 to 81 m is shown in Figure 6.8.

Table 6.1. Hole burden as a function of the horizontal distance along the cut.

Burden (m)	Horizontal distance (m)
6.5	136
5.5	110
4.5	81
3.5	53
2.5	28

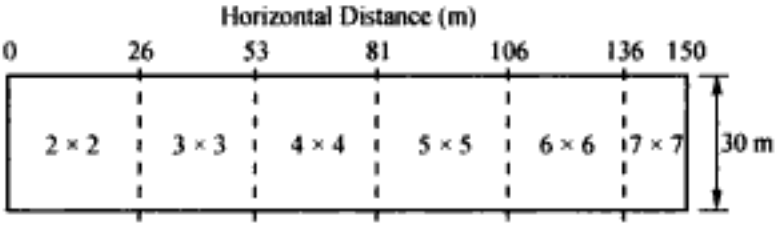

Figure 6.7. Plan view of the sinking cut showing the different pattern regions.

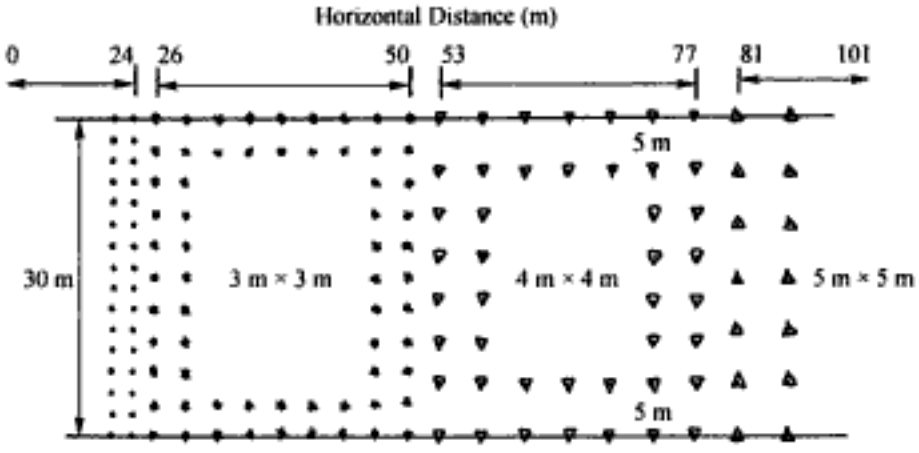

Figure 6.8. Detailed layout for the shallow end.

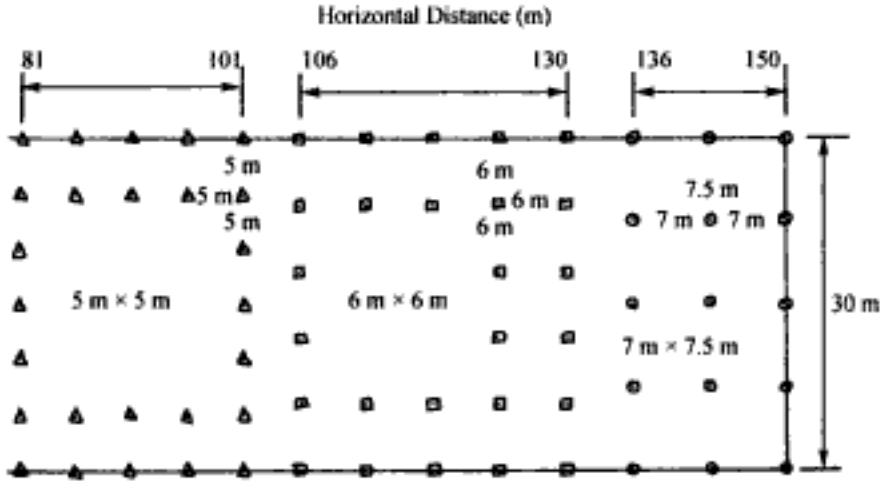

Figure 6.9. Detailed layout for the transition zone.

Table 6.2. Hole depth applying for the different patterns.

Pattern	Hole depth (m)
7 × 7	13.8 m
6 × 6	12.4 m
5 × 5	10.2 m
4 × 4	7.8 m
3 × 3	5.3 m
2 × 2	3.1 m

The detailed layout of Part II now begins from the deep end. The spacing is increased to 7.5 m to conform to the 30 m width but the burden remains at 7 m. The results are shown in Figure 6.9.

Step 7. Determine the drilling depth for each pattern.

These depths are selected in the same way as the deepest hole (Cut + Subdrill) using the nomograph. The results are summarized in Table 6.2 and in Figure 6.10.

Step 8. The amount of explosive to be placed in each hole is now determined.

At the deep end (7 m × 7 m pattern) the length of stemming (T) in the hole is equal to 0.64 B. Since this hole is bulk loaded with *ANFO* the amount of powder is

$$W = \frac{\pi}{4} D_e^2 (H + J - T)\, 850 = \frac{\pi}{4} (0.25)^2 (12 + 1.8 - 4.5)\, 850 = 388 \text{ kg}$$

The length of the explosive column is 9.3 m.

In the shallow zone (2 m × 2 m pattern) a single cartridge (0.203 m) 8 ins. in diameter and 0.490 m (19 ins.) in length is used in each hole. The amount of explosive is

$$W = \frac{\pi}{4} d^2 L\, (850) = \frac{\pi}{4} (0.203)^2 (0.490)\, (850) = 13.5 \text{ kg}$$

The explosive length converted to the full hole diameter (0.250 m) is 0.32 m. These values are in good agreement with the values given by Chung (1982) in Table 6.3.

Step 9. Design the initiation sequence.

The complete cut may be blasted in one shot or in sections. The advantage of one shot is that pit disturbance is minimized. However, a large number of delay intervals are required to avoid a high explosive charge/delay and the resulting ground vibrations. The possibility of cutoffs is also increased.

Figure 6.11 shows the sequence recommended by Chung for the blast between 50 m to 150 m.

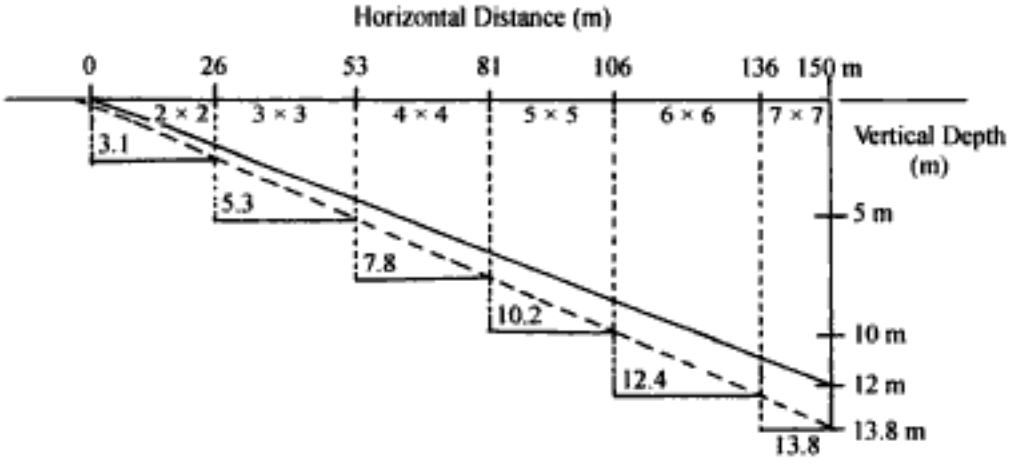

Figure 6.10. Cross-section showing the drilling depths in the different regions.

Table 6.3. Charge length and weight for the different patterns.

Burden & spacing (m)	Charge length (m)	Charge weight (kg)
7	9.3	391
6	5.0	210
5	1.8	76
4	0.7	29
3	0.4	17
2	0.3	13

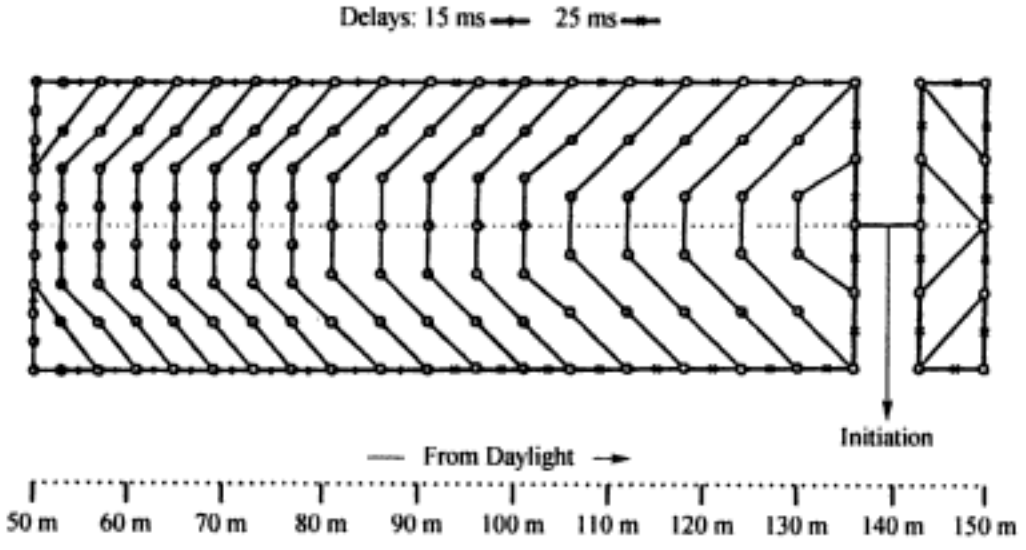

Figure 6.11. Delay sequence without wall control blasting (Chung, 1982).

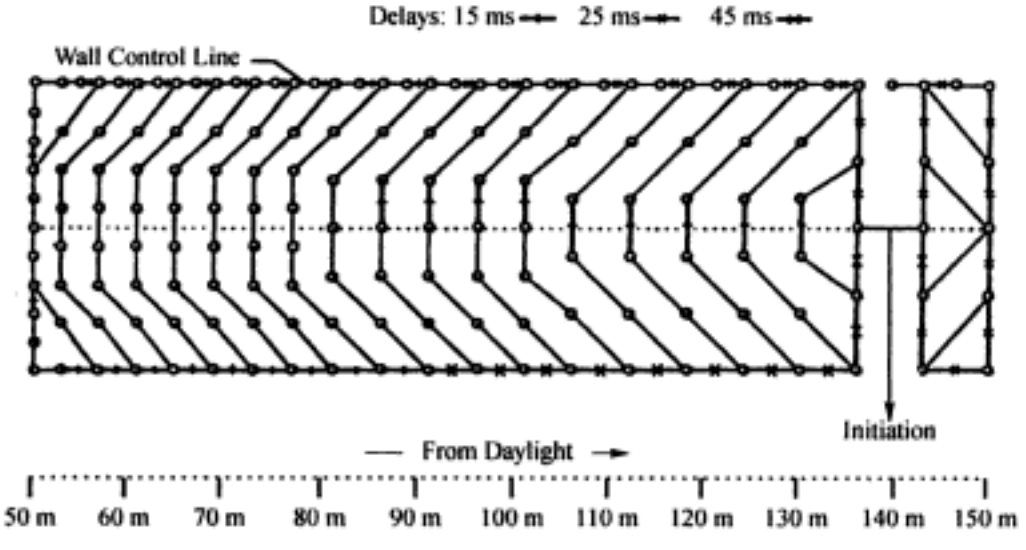

Figure 6.12. Delay sequence with wall control blasting (Chung, 1982).

Note that the initiation begins at the deep end with the instantaneous firing of the two middle holes. This helps to ease the breaking at grade for holes up the ramp and to reduce cutoffs caused by flying rocks coming from the shallow holes.

When a conventional surface delay system is used, Chung suggests the following delay intervals between firing lines.

25 msec delays – deep end,

15 msec delays – shallow end.

Figure 6.12 shows a tie-in method for a sinking cut in which one side will become part of the permanent pit wall. The holes along the wall control line are

– Drilled to final grade,
– No more than 1/3 of the normal loading should be used in these holes.

To further reduce blast vibration in the wall, a 15-msec delay is introduced in each firing line. A combination of surface and in-hole delays may also be used.

REFERENCES AND BIBLIOGRAPHY

Armbrust, J.C. 1988. Morenci Mine – Blasting and Dewatering of the 4050 Drop Cut. Preprint No. 88-146. Presented at the SME Annual Meeting, Phoenix, Arizona, Jan 25-28. 3pp.

Barlow, V.S. 1958. *How the Bingham Pit Makes a Dropcut*. EMJ 159(6): 92-93.

Chung, S.H. 1982. Computerized sinking cut design in open-pit mining. CIM Special Volume 30. *Rock Breaking and Mechanical Excavation* (P. Baumgartner, ed.), Vancouver, BC, May 13-14, pp. 87-90.

E.I. DuPont de Nemours and Co. DuPont *Blasters' Handbook*. 1977 Edition. Wilmington, Del. 494 pp.

Hagan, T.N. & J.K. Mercer 1983. Safe and Efficient Blasting in Open Pit Mining. *Workshop Proceedings. ICI Australia. Karratha*, 23.25 Nov.

CHAPTER 7

Bulk blasting agents

7.1 INTRODUCTION

This section will deal very briefly with the most common blasting agents/explosives used in open pit mining. The emphasis is on bulk loading of blastholes using a mix-pump truck rather than on packaged products since this practice is dominant by far in surface mining applications. A blasting agent is defined (Dick, 1968, 1972) as a chemical mixture which

- Contains no ingredient that is in itself an explosive,
- Cannot be initiated by a No. 8 detonator in the unconfined state (in the open air).

These two favorable conditions have a major impact on shipment, storage and handling procedures. A bulk explosive, on the other hand, does contain an ingredient that is, in itself, an explosive and/or can be initiated by a No. 8 detonator. In this Chapter the terms bulk explosive and bulk blasting agent will, for simplicity, be used interchangeably. The reader must keep in mind that the two are not at all the same. As will be seen, ammonium nitrate (*AN*) is a major component of most blasting agents. The reliable detonation of blasting agents requires, in general, initiation by a high explosive primer in good contact with the charge. The characteristics *WR* = water resistance, *MD* = recommended minimum diameter (mm), *LD* = loaded density (g/cm^3) of the most common types of bulk explosives are summarized in Table 7.1.

The main factors which influence the selection of an explosive, in addition to price, are (Hagan & Mercer, 1983):

1. Water resistance,
2. Strength,
3. Density,
4. Sensitivity,
5. Velocity of detonation,
6. Fumes,
7. Storage and handling qualities,
8. Physical characteristics,
9. Inflammability.

Each of these factors will be briefly described using material extracted from Hagan & Mercer (1983). The water resistance of blasting agents and high explosives varies considerably. In general, all deteriorate progressively in wet conditions. The amount of deterio-

Table 7.1. Common types of bulk explosives (AECI, 1983).

Explosive type	WR	MD	LD	Characteristics
ANFO	Nil	50	0.8	Porous prilled AN with 6% absorbed fuel oil
AL*ANFO*	Nil	150	0.85-0.95	AN with up to 15% atomized aluminum powder
Gelled Blasting Agents/Slurries	Excellent	125	0.85-1.45	AN solution incorporating fuel, sensitizing and gelling agents
Emulsified Blasting Agents/Emulsions	Excellent	100	0.9-1.36	Similar to a slurry but with water resistance provided by emulsifying the AN solution with fuel oil instead of using gelling agents
Heavy *ANFO*	Varies	150-250	1.0-1.36	Emulsion matrix incorporating AN prills to form an energetic, high-density, low cost explosive

ration increases with the severity and period of exposure. The effectiveness of explosives is reduced when penetrated by water and, on prolonged exposure, eventually reaches a point at which the detonation wave is not able to propagate through the explosive column. Whatever the explosive type used, the period of exposure to blasthole water should be kept to a minimum. This means that the blast should be fired as soon as possible after charging.

Strength refers to the energy generated by the detonation of an explosive. Stronger explosives develop greater energy and are capable of doing more work. As indicated in Chapter 3 there are two strength values of importance; weight strength (energy/kg, for example) and bulk strength (energy/volume). The total amount of energy placed in a borehole depends upon the explosives weight strength and its density. An explosive with a high weight strength and high density is often used at the bottom of the hole where the work to be done is the greatest. An explosive with a lower density can be used as an upper column charge where less energy is normally required. If the density of the explosive is greater than 1.0 g/cm^3 it will sink in water. If it is less, it will float.

Sensitivity is a measure of the ease with which an explosive can be detonated by heat, friction, impact or shock. An explosive with high sensitivity is easily initiated and the detonation wave travels from one end of the charge column to the other without any tendency to fade or die out. Explosives having low sensitivities are more difficult to initiate and the detonation wave, once developed, is less capable of travelling the entire length of the explosive column.

Velocity of detonation (*VOD*) is the speed with which a detonation wave propagates through a column of explosive. As a general rule, the higher the *VOD*, the greater the brisance or shattering effect. Where better breakage in tough massive rocks is required, one generally would prefer a higher velocity explosive. In rock which is relatively weak or which exhibits a close network of natural cracks and planes of weakness, one would select one with a lower *VOD* yielding less shock energy but greater heave.

Toxic fumes produced by the detonation of charges in open pit blasts do not normally present any hazard since they are rapidly dispersed into the open air. On very calm days in the bottom of deep pits, however, operators should avoid exposure to post detonation fumes. Rusty-orange colored fumes, for example, indicate the presence of nitrogen dioxide.

Most explosives are perishable in the sense that their characteristics change (deteriorate) with time. Both climate and magazine conditions are important factors affecting shelf life.

The physical characteristics of the various types of blasting agents and high explosives differ markedly. *ANFO*-type blasting agents are loose, free-flowing granular compositions. Watergel blasting agents have a rubbery, gel-like consistency. Emulsion blasting agents have a consistency between that of hair cream and a firm putty.

Inflammability is a measure of the ease with which an explosive or blasting agent can be ignited. *ANFO*-type blasting agents ignite readily and burn well. Because of their water content, watergels and emulsions will not support combustion unless an outside source or flame is applied continuously.

7.2 ANFO

Ammonium nitrate (AN) when mixed with fuel oil (FO) in the weight ratio of 94/ 6 makes up the most common blasting agent used in open pit mining today. The basic reaction is

$$3NH_4NO_3 + CH_2 \Rightarrow CO_2 + 3N_2 + 7H_2O + 912 \text{ kcal/kg} \quad (7.1)$$

As is discussed in some detail in Chapter 11, the published values for the amount of energy released when *ANFO* detonates (which in this case is given as 912 kcal/kg) can vary rather widely. The primary reason for this is that different authors and manufacturers assume different formulations for fuel oil each of which has an associated heat of formation. In the commonly written reaction (7.1), the symbol CH_2 is used to represent the fuel oil. In practice the actual organic compound is much more complicated than this and the ratio between the number of hydrogen and carbon atoms, for example, may be only approximately 2. The heat of formation for the constituent CH_2 is not found in a standard reference such as the Handbook of Chemistry and Physics. Instead one finds values for organic compounds made up of multiples of CH_2 such as C_6H_{12}, C_7H_{14}, etc. For each of these there are different arrangements of the atoms yielding different heats of formation. To add to the confusion, explosion products other than those given in reaction (7.1) may be included. Thus the so-called 'standard' *ANFO* is far from standard.

As shown in Figure 7.1, the maximum strength is obtained when about 5.5% fuel oil by weight is added. When too little fuel oil is added, the energy drops rapidly and various nitrous oxides (NO_x) are formed. When too much fuel oil is added the energy also decreases. In this case the deadly gas carbon monoxide (CO) is formed.

Consistent, efficient blasting with *ANFO* is only achieved by placing charges with a known, uniform density and mix in every blasthole. Although various forms of AN are available and could be used, the specially manufactured porous prills are preferred. The quality of porous prill ammonium nitrate is defined (AECI, 1990) by:

- Density control
- Prill porosity
- Prill hardness
- Prill thermal stability
- Effectiveness and inertness of the anti-caking agent used

The density of crystalline AN is about 1.73 gm/cm^3 and that for fuel oil about 0.75 gm/cm^3. Assuming an oxygen-balanced ratio of 94.5/5.5 then the overall density for such a

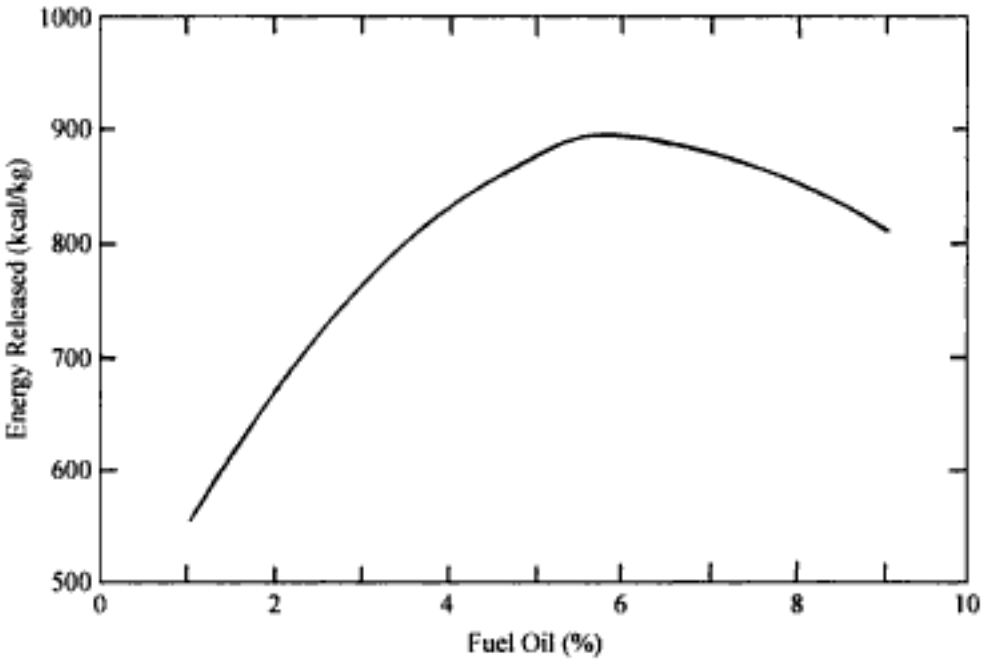

Figure 7.1. Relative *ANFO* energy as a function of the percent fuel oil used (Hagan, 1980).

mixture would be 1.675 gm/cm^3. However, as indicated, the AN is not in crystalline form but rather as porous prills. For good blasting grade prills, the prill size-distribution is between 6 and 20 mesh (US Standard Screen). This corresponds to particle sizes lying in the range of 0.84 to 3.36mm (0.033 to 0.132 inches). Normal *ANFO* is about 50% by volume air and thus the density in the loose-poured form is about

$$1.675/2 = 0.84 \text{ gm/cm}^3$$

The air volume is distributed about 70% between the prills and 30% as internal pore space. Thus the free void space between the prills accounts for about 35% of the overall volume. The density of *ANFO* as placed in the hole can vary from about 0.8 gm/cm^3 to nearly 1.0 gm/cm^3 depending upon the method of emplacement (how much the free void space is reduced in the process). *ANFO* is relatively incompressible so that the density at the bottom of long column charges will not be much higher than that at the top. The 'dead press' density (that for which *ANFO* will not detonate even under the action of a powerful primer) is about 1.25 gm/cm^3.

Although distillates other than fuel oil are available, fuel oil has the following advantages:

- Relatively inexpensive,
- Mixes readily with AN to produce a uniform mix,
- Readily available at all mine sites.

Solid fuels such as carbon are not as effective as liquid fuels in *ANFO*. As a result they have only been used as a partial rather than a total replacement for fuel oil.

As can be seen in Figure 7.2, blasthole diameter has a significant effect on the velocity of detonation. The *VOD* is less for smaller diameters than for larger diameters due to the proportionally larger resistance to detonation propagation provided by the rough hole perimeter. This *VOD* -diameter dependence carries over to the borehole pressure and the shock energy-heave energy partitioning. The total energy yield is not affected, however.

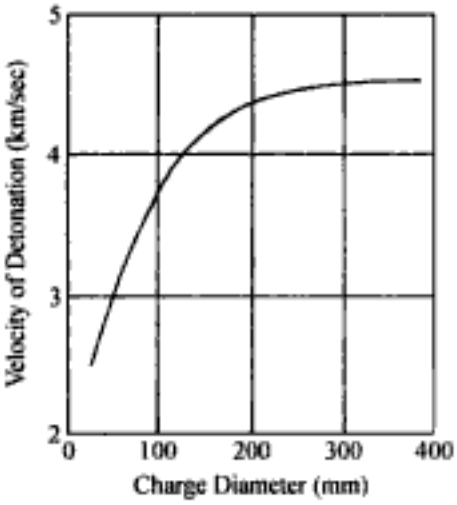

Figure 7.2. Effect of charge diameter on the velocity of detonation for *ANFO*. Clark (1981), Anonymous (1976).

Table 7.2. Polythene liner sizes for different blasthole diameters (Hagan & Mercer, 1983).

Blasthole diameter (mm)	Nominal diameter of liner (mm)	Nominal size of layflat (mm)
127	140	220
143	156	245
152	166	260
175	191	300
187	204	320
200	216	340
229	248	390
251	274	430
270	293	460
311	337	530

Initiation sensitivity decreases with increasing blasthole diameter. For diameters greater than about 150 mm (6″), cast primers weighing at least 400 g (1 lb) are recommended. Charges of bulk *ANFO* are only detonator sensitive when confined in small diameter blastholes (diameters less than about 3″).

A major advantage with ANFO is its low cost per unit of energy delivered. A major disadvantage and limitation is its lack of water resistance. Ammonium nitrate dissolves easily in water even with the added fuel oil. ANFO containing more than about 10% water will fail to detonate. 'Damp' holes should be pumped dry, charged and shot as quickly as possible. Even in 'wet' conditions good blasting results can be obtained with ANFO but only if the ANFO is kept dry. Some water or sludge always remains at the bottom of de-watered blastholes. This will destroy the ANFO in that part of the hole faced with the most difficult breaking unless a plastic borehole liner is used. Table 7.2 gives some typical dimensions of these liners (Hagan & Mercer, 1983). The insertion of these liners into holes making water can be a slow and tedious process. It also has two inherent risks (AECI, 1982)

1. The *ANFO* column may be 'pinched-out' by water pressure around the tubing. This will decrease the breaking effect of the *ANFO* and may even result in detonation failure in these holes.

2. The lay-flat tubing may be torn by projections in the side of the blasthole allowing water to destroy the *ANFO*.

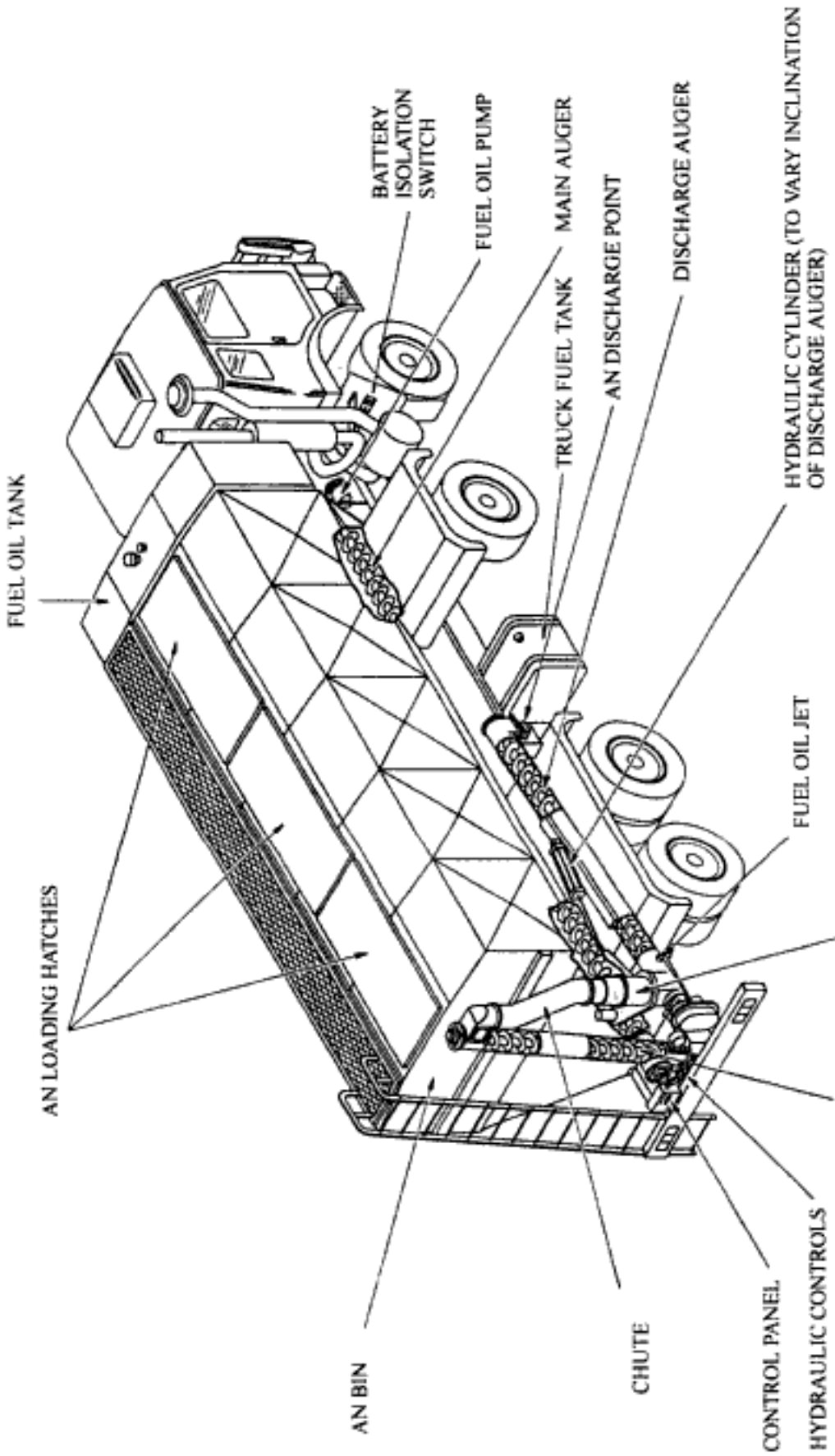

Figure 7.3. A typical truck for bulk loading *ANFO* (Hagan & Mercer, 1983).

At the blast site, a bulk *ANFO* truck (Fig. 7.3) mixes the AN and FO in the oxygen balanced ratio. The resulting *ANFO* is either blown using a pneumatic delivery system or augered into the blastholes. In the pneumatic system the discharge hose is typically 10 m long. Where the truck is driven between two rows of large diameter blastholes four, and sometimes six, blastholes can be charged from each position of the vehicle. With the auger system, normally two or three holes can be charged from one truck position. *ANFO* discharge rates are usually in the range of 180-500 kg/minute. A weighted measuring tape is often used to check the buildup of the explosive charge in the hole. A wide range of truck capacities (3-15 tons) is available.The time required to refill the truck depends largely upon the method for loading the AN feeder.

When using dry blasting agents the following precautions should be taken (Dick, 1972)

1. They should not be used in the presence of excessive water unless external protection in the form of a rigid cartridge or a plastic borehole liner is supplied.
2. Close control must be exercised in ingredient mixing to maximize energy release and minimize toxic fume generation. A colored dye may be added to the fuel to provide a visual check on mixing.
3. The charge diameter must exceed the critical diameter, preferably with a good safety margin.
4. Adequate priming is essential. When in doubt, overpriming is recommended since heavy priming will partially overcome many unfavorable field conditions. In marginal situations the addition of boosters up the borehole will assist propagation.
5. When using electric blasting caps, approved equipment should be used for pneumatic loading and precautions against static electricity should be taken. The use of nonconductive protective plastic tubing increases static electricity hazards by insulating the charge from the ground.
6. The possible hazard of *ANFO*'s reactivity with rock, particularly rock with a high sulfide content should be investigated.
7. Even an oxygen-balanced mixture can produce noxious fumes if insufficient detonation occurs because of water deterioration, separation of ingredients, poor confinement, insufficient compaction, inadequate charge diameter, or inadequate initiation. These conditions also cause poor powder performance. The use of plastic borehole liners can increase fume production.
8. The low air-gap sensitivity of dry blasting agents makes them susceptible to misfires caused by charge separation.
9. Holes loaded with dry blasting agents should not be allowed to stand for excessive periods after loading because of their susceptibility to water deterioration and segregation of liquid fuels.

7.3 ALUMINIZED ANFO

The addition of paint grade aluminum as a fuel increases the total energy output of the explosive or blasting agent to which it is added. The equation describing the detonation of ammonium nitrate and aluminum is given in Equation (7.2)

$$3NH_4NO_3 + 2Al \rightarrow 6H_2O + Al_2O_3 + 3N_2 + 1620 \text{ kcal/kg} \qquad (7.2)$$

In this case the NH_4NO_3/Al weight ratio is 81.6/18.4. Simply comparing the energies given in reactions (7.1) and (7.2) would suggest that the weight strength when using aluminum as the fuel instead of fuel oil is greater by a factor of

$$1620/912 = 1.78$$

Although true, this is somewhat misleading since some of the heat is bound to the solid product Al_2O_3 and is not available for use in the pressurization of the explosion gasses. In practice aluminum is never the only fuel used. One way of increasing the strength of *ANFO* is through the addition of aluminum powder (Crosby & Pinco, 1991, 1992). This combination, is usually referred to in the literature as AL*ANFO*. Figure 7.4 illustrates the percentages of fuel oil required in *ANFO* at various levels of added aluminum in order to maintain maximum energy output. Fuel grade aluminum must conform to certain specifications regarding size, purity density and flow characteristics. The particle size of the aluminum is generally in the mesh range –18 to +150. Particles larger than 20 mesh tend to react sluggishly whereas particles finer then 150 mesh present a dust explosion hazard. Figure 7.5 shows the relative weight and bulk strengths (*ANFO* at a density of 0.85 g/cm^3 = 100) with increasing aluminum content in *ANFO*. As indicated by Hagan & Mercer (1983), increments in available energy start to decrease as the Al content increases beyond 10% and the increments for each percent increase in Al past 15% are relatively small. Hence, the most common compositions contain between 5% and 15% aluminum by weight. The increased energy per unit weight means that more work can be performed with the same volume of explosive. In certain rock types, this means that through the addition of aluminum better fragmentation can be achieved for the same pattern or that the hole pattern can be spread. Such aluminized blasting agents are often used as the toe load in bench blasting. Water resistance is not changed, however, from that of ordinary *ANFO* and the sensitivity is also the same. Figure 7.6 shows a typical bulk *ANFO* truck capable of delivering aluminized *ANFO*.

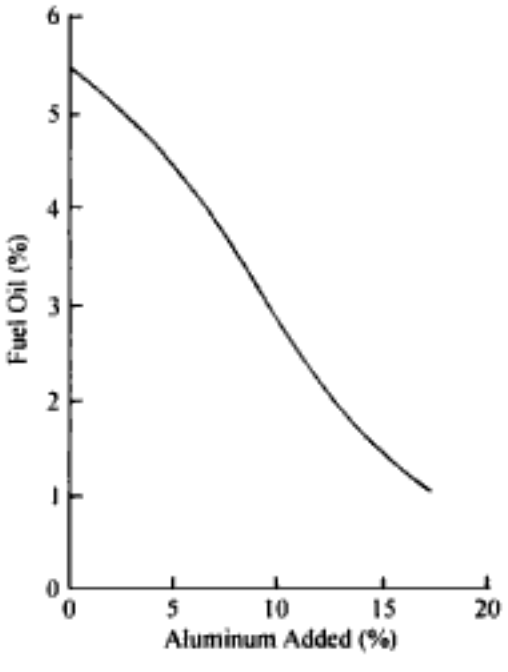

Figure 7.4. Percent fuel oil (by weight) required to obtain maximum energy output in *ANFO* at various levels of aluminum addition. (Crosby & Pinco, 1991b)

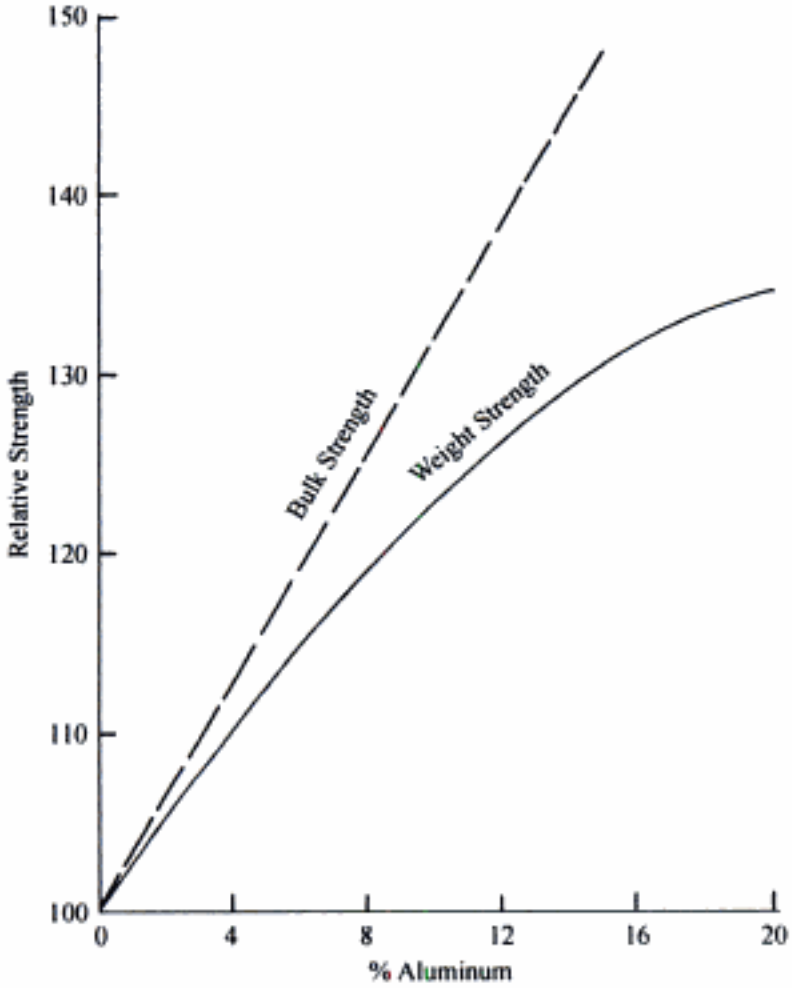

Figure 7.5. Relative weight strength and bulk strength as a function of the percent aluminum added to *ANFO* (Hagan & Mercer, 1983).

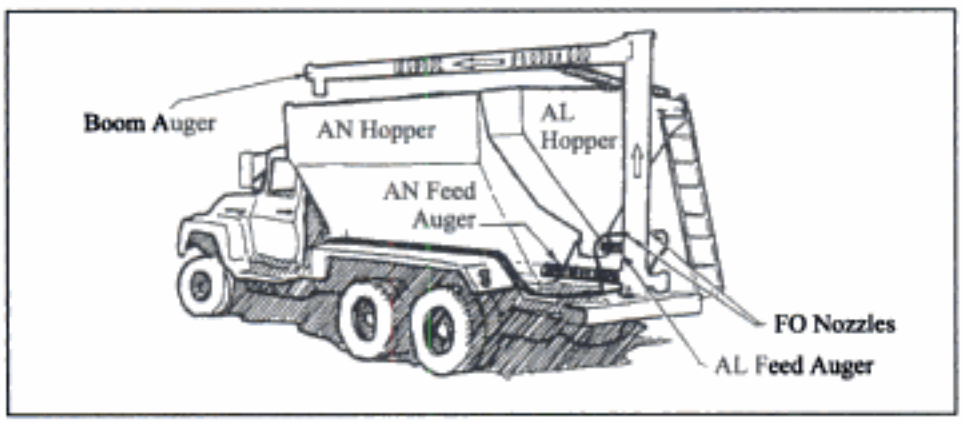

Figure 7.6. Truck for loading aluminized *ANFO*. (Crosby & Pinco, 1991b)

7.4 LIGHT ANFO

There are some situations where bulk blasting agents which have strengths less than bulk *ANFO* are desired. One such situation is the minimization of back break/blast damage from pit perimeter holes. From Chapter 3 it will be recalled that an expression for the detonation pressure (P_{DET}) is

$$P_{DET} = 0.25\ \rho\ (VOD)^2 \tag{7.3}$$

where P_{DET} = detonation pressure (MPa), ρ = explosive density (kg/m^3), *VOD* = detonation velocity (km/sec).

The explosion pressure (that which would be applied to the hole wall) can, without much error, be taken as one half of this value. One technique for reducing the applied wall pressure is to leave a gap between the outer wall of the explosive charge and the hole wall. As the explosion gases expand to come into contact with the borehole wall, the presure drops. Assuming adiabatic expansion, one can write

$$P_h = P_e \left(\frac{D_e}{D_h} \right)^{2\gamma} \tag{7.4}$$

where P_h = the effective pressure at the hole wall, P_e = explosion pressure for *ANFO*, D_e = diameter of the explosive, D_h = diameter of the hole, γ = the equivalent adiabatic expansion factor for the pressure range, $P_e \rightarrow P_h$.

In practice the explosion pressure is also reduced due to the smaller diameter charge and a smaller degree of confinement than that for the fully charged blast hole. This technique, which is called 'decoupling', is discussed in detail in Chapters 10 and 17. In practice, a plastic pipe is inserted in the hole and it is filled with bulk *ANFO*. Although effective, it is cumbersome since it involves the handling and filling of these pipes with explosive. Some other means for accomplishing these reduced wall pressures which involve the use of fully charged holes is desireable.

To reduce the pressure applied to the wall by the explosive gasses (and thereby the amount of damage) one can, according to Equation (7.3), reduce the density, the *VOD*, or both. In this regard, Hagan & Mercer (1983) have described the use of bulk loaded *ANFO*/polystyrene compositions. Reliable detonations have been consistently achieved in large diameter blastholes containing as much as 90% polystyrene by volume. Both the density and the energy concentration decrease directly with the percentage of the polystyrene. Due to the lower shock energy and gas volumes produced the amount of damage is limited. The polystyrene is added to the *ANFO* just before the charging operations begin. To minimize segregation of the *ANFO* and polystyrene due to the density differences, the polystyrene particles should be about the same diameter as the prills and spherical. A small amount of water (1.5% by weight maximum) added to the polystyrene-*ANFO* mixture has been found to add 'tackiness' and assist in mixing.

Wilson & Moxon (1988) conducted both laboratory and field tests in which low density materials such as polystyrene, bagasse (the stalks remaining after extracting the sugar from sugar cane), sawdust, perlite, etc were mixed together with *ANFO* and detonated. In the field tests a bowl truck such as shown in Figure 7.7 was used for mixing and delivery to the hole. Their results, given in Table 7.3 for a 50/50 volume mixture (*ANFO*/additive) and in Figure 7.8 for bagasse, sawdust and polystyrene as a function of % volume additive, indicate that the *VOD* of *ANFO* can be significantly reduced by the addition of a low density additive. Since the greatest effect on P_{DET} is obtained if both the *VOD* and the density are significantly lowered, the most attractive systems for large scale use (of those tested) are

- *ANFO*/bagasse,
- *ANFO*/sawdust,
- *ANFO*/polystyrene,
- *ANFO*/peanut skin.

The additives used in the experiments are believed to lower the detonation pressure of *ANFO* by acting as a low grade fuel which reacts or burns more slowly in the presence of ammonium nitrate than does fuel oil. The mixtures are also very poorly oxygen-balanced which further reduces the *VOD*.

The conclusions of their study were:

– Sawdust, polystyrene and bagasse will all form stable homogeneous mixtures with *ANFO* in a tumble mixer. A viscous oil (400cs) such as Prorex 25 is required to aid mixing in the polystyrene/AN system.

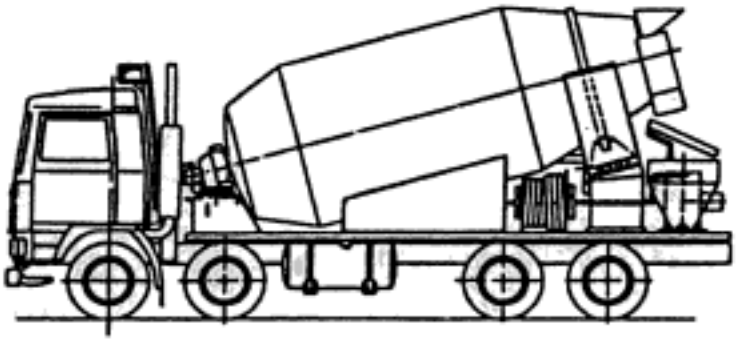

Figure 7.7. Truck mounted agitator bowl dispensing unit. Close, 1986.

Table 7.3. The explosive properties of the low density explosive mixtures studied. All results are for 50/50 by volume mixtures (Wilson & Moxon, 1988).

Mixture	Diameter (mm)	Density (kg/m^3)	*VOD* (km/sec)	P_{DET} (MPa)
ANFO	100	820	2.44	1220
	158	820	3.28	2210
	190	820	3.51	2530
	258	820	3.70	2800
	Infinite	820	4.50	4150
ANFO/Bagasse	190	380	2.70	690
	258	380	3.13	930
	Infinite	380	3.60	1230
ANFO/sawdust	100	500	2.21	610
	190	500	2.59	840
	258	500	2.90	1050
	Infinite	500	3.30	1360
ANFO/Polystyrene	100	410	–	–
	150	410	2.00	410
	190	410	1.90	370
	258	410	2.21	500
	Infinite	410	2.40	590
ANFO/Perlite	190	540	2.40	780
ANFO/Vermiculite	190	580	2.51	910
ANFO/Wheat	190	720	1.90	650
ANFO/Peanut Skin	190	460	2.21	560
ANFO/Coal Refuse				
–50/50	190	730	–	–
–75/25	190	710	2.30	940

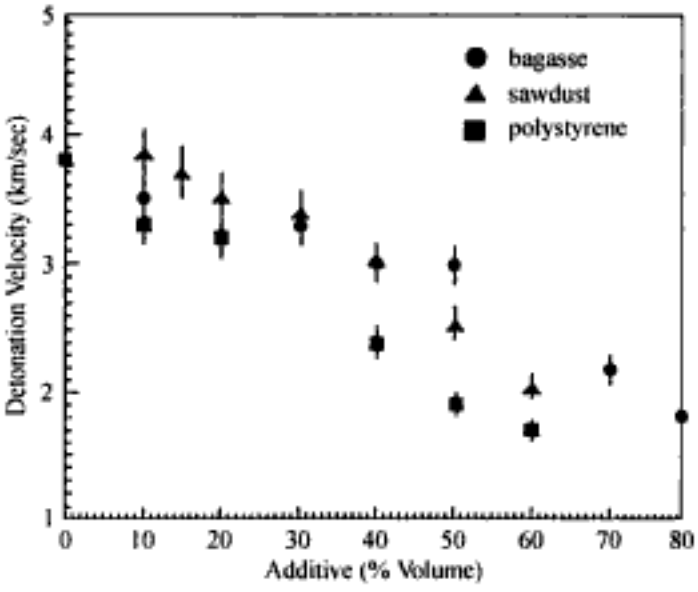

Figure 7.8. The effect of additive concentration on the *VOD* and detonation pressure of Basasse, polystyrene and sawdust systems. Wilson & Moxon, 1988.

– Sawdust and bagasse can be easily mixed with *ANFO* in a bowl truck to produce a homogeneous mixture, Polystyrene/AN/Prorex 25 mixtures should also be able to be formed in this manner.

– Sawdust/*ANFO*, polystyrene/AN/Prorex 25 and bagasse/*ANFO* mixtures all have lower detonation pressures than *ANFO*. The magnitude of the detonation pressure of the mixture can be controlled by the proportions of additive used in its preparation making it possible to more closely match the explosive to the material in which it is being used.

– Sawdust/*ANFO*, polystyrene/AN/Prorex 25 and bagasse/*ANFO* mixtures do not segregate when loaded into a borehole.

The field trials indicated that low density explosives can lead to significant cost savings without compromising fragmentation or production.

7.5 WATERGELS/SLURRIES

ANFO was first introduced to the mining community in 1955. Due to its low cost, relatively high weight strength and good handling properties, it met with nearly immediate acceptance and success. It had certain drawbacks, however

– No water resistance,
– Low density,
– Low energy range,

which meant that it was not suited for all applications. In 1958, Melvin A. Cook, then at the University of Utah, published his now classic book The Science of High Explosives (Cook, 1958). In it, he reported the development of water-compatible bulk explosives (slurry explosives) and their use for underwater blasting at the Knob Lake operation of the Iron Ore Company of Canada. His original slurries consisted of AN-TNT-H_2O.

Prior to discussing slurries in detail, it is considered worthwhile to examine some of the basic reactions involved. The reaction describing the detonation of a dry mixture consisting of only AN and TNT is:

$$21NH_4NO_3 + 2C_6H_2CH_3(NO_2)_3 \rightarrow 47H_2O + 14CO_2 + 24N_2 + 1010 \text{ kcal/kg} \quad (7.5)$$

The heat of explosion (Q) for this mixture with a weight ratio of 78.7/21.3 is 1010 kcal/kg. Appropriate values for other ratios of this dry mix as published by Cook (1958) are:

AN/TNT: 50/50
- density = 1.0 gm/cm^3
- Q = 870 kcal/kg
- explosion pressure = 32 kbars

AN/TNT: 76.5/23.5
- density = 1.0 gm/cm^3
- Q = 975 kcal/kg
- explosion pressure = 31 kbars

Since water is one of the products of the explosion (as indicated in Equation 7.5) it was perhaps logical to consider the effect of adding water to the reactants (left) side of the equation. The result would be a water-based AN-TNT explosive. By accomplishing this, Cook (1958) obtained much higher densities and explosion pressures but somewhat lower heats of explosion as compared to the AN/TNT mixtures without water. Two examples by Cook (1958) are given below:

AN/TNT/H_2O: 40/40/20
- density = 1.41 gm/cm^3
- Q = 710 kcal/kg
- explosion pressure = 50 kbars

AN/TNT/H_2O: 65/20/15
- density = 1.40 gm/cm^3
- Q = 760 kcal/kg
- explosion pressure = 59 kbars

These values should be compared to that for *ANFO* as published by Cook (1974) and Sudweeks (1985):

$$3NH_4NO_3 + CH_2 \rightarrow CO_2 + 7H_2O + 3N_2 + 885 \text{ kcal/kg} \quad (7.6)$$

The value of Q given in Equation (7.6)

$$Q = 885 \text{ kcal/kg}$$

is different from that presented in Equation (7.1)

$$Q = 912 \text{ kcal/kg}$$

This provides just one concrete example of the variety of values found in the literature for the amount of energy released when standard *ANFO* (94/6) detonates. Although Q is relatively independent of density, the explosion pressure is density dependent. For a density of

$$\rho = 0.8 \text{ g/cm}^3$$

which is typical for bulk-poured *ANFO*, the explosion pressure is approximately (Cook, 1974)

$$P_e = 19.4 \text{ kbars}$$

Hence, these early slurries had densities and explosion pressures which were higher than *ANFO* but heats of explosion which were lower. Due to the density and weight strength combination, the bulk strengths of these slurries were higher than for *ANFO*. In overcoming the drawbacks associated with *ANFO* as presented in the introduction to this section, these slurries offered exciting application possibilities to, not the least, hard rock blasting under wet conditions. Based upon this invention, a new explosives company was formed. Originally called the Intermountain Research and Engineering Company the name was later changed to Ireco Chemicals.

These early slurries were not formed by a simple mixing of AN, TNT (or some other fuel) and water, stirring, and then pouring the resulting mixture into the hole. Rather it involved (Sudweeks, 1985)

- Pre-dissolving the ammonium nitrate in a small amount of water
- Thickening the solution with a guar gum or starch
- Adding fuel components as soluble or finely divided insoluble materials (solid 1)
- Adding dry oxidizers to reduce the overall water content (solid 2)
- (Optionally) cross-linking the gum thickeners to produce a gelled product

The presence of the solids (solid 1 and solid 2) as well as the ammonium nitrate crystals that precipitated upon cooling of the formulation lead to the general designation of 'slurries' for these composite blasting agents/explosives. Due to the water used to dissolve the salts and suspend the insolubles and the 'gell-like' nature of the resulting product, they have also been given the name 'water gels'. Although some reserve the term 'water gel' for products which have been cross-linked to a semi-solid, jelly-like consistency and the term 'slurry' for more fluid products (Dick, 1972), they are often used interchangeably. Such will be the case in this section. Slurries, which, as indicated, entered the blasting scene in the late 1950s, can be either blasting agents or explosives depending on the ingredients used and the degree of cap-sensitivity.

Although it seems that water is an unlikely constituent for an explosive, a certain amount is necessary to provide the required consistency and texture of a watergel. If more water than that required for suitable consistency is used, the weight strength is decreased. On the other hand, if too little water is used, the liquid phase is insufficient and the resulting high viscosity hinders pumping. The water content also serves to reduce hazard sensitivity associated with fire, friction and impact. The water content ranges from 5 to 40 percent by weight with the average being 15 percent (Dick, 1972).

Because the commonly used oxidizers, ammonium nitrate and sodium nitrate are soluble, the water resistance of a water gel depends on its physical state. Although starches were used to thicken some of the earlier slurries, guar gum (polysacchride) is commonly used today. The thickened slurry is gelled with a cross-linking agent to set up an impenetrable barrier which prevents leaching of the soluble salts by water permeating through the borehole. Modern gelling and cross-linking technology makes it possible to produce these slurries in any desired consistency, from a free flowing liquid to a cohesive gell.

Slurries can be divided into three categories (Dick, 1972):

1. Those containing high-explosive fuel sensitizers,
2. Those containing metallic fuel-sensitizers,
3. Those containing none of these high-energy-type ingredients.

Whereas the first generation of slurries had to be sensitized with molecular explosive additives such as TNT or with smokeless powder to make them detonable, later refinements

in formulation and manufacturing techniques have allowed sensitization with organic salts like amine nitrates and perchlorates or very finely divided paint-grade aluminum. Today, most formulations are sensitized using only mechanically or chemically generated small air or gas bubbles (Sudweeks, 1985).

The presence of air bubbles or void space is necessary for efficient detonation as well as for appropriate determination of sensitivity level, detonation velocity, and the critical diameter (the smallest diameter in which detonation will propagate). Two types of ingredients, aerating agents and gas formers, can be used. Physical agitation will also aerate a slurry. In using gas formers, care must be taken that the system remains stable.

One of the mechanisms by which it is believed that sensitization by air bubbles occurs is that of hot-spot formation as illustrated in Figure 7.9. When the very high pressure shock wave from the initiator cap or booster passes into the slurry charge, it compresses the air bubbles. This compression occurs so rapidly that the volume change is essentially adiabatic and the gas in the bubble heats up to a very high temperature. As this heat is dissipated to the surrounding material, explosive decomposition occurs. This process is fast enough so that the release of energy contributes to the propagation of the shock wave through the entire column of explosive (Sudweeks, 1985).

Slurry ingredients can be selected as desired to vary the energy, sensitivity, oxygen balance, rheology, and the stability of the final product. It is possible to adjust the fume and detonation characteristics and the physical properties to meet specific requirements of varying applications. Tables 7.4 and 7.5 list some of ingredients used in a slurry formulation. Table 7.6 presents representative formulations for two slurries. In Table 7.7 the detonation parameters for five typical slurries are given. The energy and gas volume values have been calculated (Sudweeks, 1985) assuming the formation of the highest energy products. The relative weight and bulk strengths are determined with respect to *ANFO* (Q = 885 kcal/kg, density = 0.82 g/cm^3) on the basis of the theoretical energy. By varying the type and the quantity of fuel (and especially the aluminum powder), water gels can be tailored to exhibit a wide range of weight and bulk strengths (Fig. 7.10). Variations in density affect the weight strength and the *VOD* as shown in Figure 7.11. The *VOD* increases

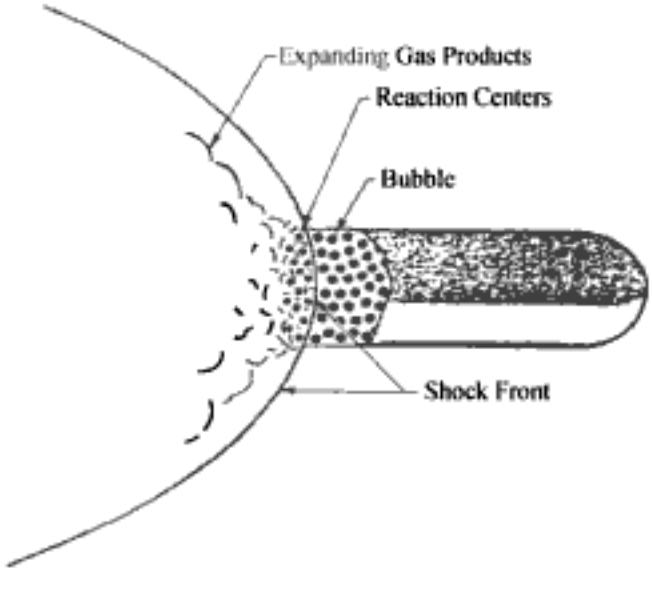

Figure 7.9. Diagrammatic representation of the sensitization mechanism in watergels. Sudweeks, 1985.

Table 7.4. Slurry ingredients (Sudweeks, 1985).

1. Oxidizers
   - ammonium nitrate
   - sodium nitrate
   - calcium nitrate
   - sodium perchlorate
2. Soluble fuels
   - ethylene glycol
   - methyl alcohol
   - sugar
   - alkylamines
3. Insoluble fuels
   - particulate aluminum
   - coal dust
   - charcoal
   - sulfur powder
   - fuel oil
4. Thickeners
   - guar gum
   - starch
   - synthetic water-soluble polymers

Table 7.5. Some ingredients claimed to have been used in slurries (Robinson, 1969 and Dick, 1972).

1. Fuel-sensitizers

Explosive	*Non-Explosive*
TNT	Aluminum
PETN	Sugar
RDX	Urea
Pentolite	Ferrosilicon
Composition B	Ferrophosphorous
Guanideine nitrate	Wood pulp
	Dinitrotoluene
	Hexamine
	Ethylene glycol
Smokeless powder	Fuel oil
Nitrostarch	Parafin
Alkylamine nitrates	Coal
	Carbon
Nitromannite	Sulfur
	Gilsonite
	Lignosulphonates
	Plant fibers and meals
	Glycerin

2. Oxidizers
   - Ammonium nitrate
   - Sodium nitrate
   - Nitric acid
3. Cross-linking agents
   - Boron compounds
   - Potassium dichromate
   - Antimony compounds
   - Bismuth compounds
   - Periodates
   - Litharge

Table 7.5. Continued.

4. Gelling agents
Guar gum (polysaccharide)
Starch
Acrylamide polymers
5. Gas formers
Peroxides
Acetone and creosote
Sodium and potassium nitrate
Sodium bicarbonate
6. Aerating agents
Fibrous pulps and meals
Vermiculite
Resin microballoons
Perlite
Glass microballoons
Cork

Table 7.6. Representative slurry formulations expressed in weight percent (Sudweeks, 1985).

Ingredient	Slurry 1	Slurry 2
Ammonium nitrate	53.1	57.4
Sodium nitrate	–	14.4
Water	15.8	14.4
Thickeners	0.4	0.5
Ethylene glycol	–	0.4
Fuel oil	5.0	–
Sulfur	–	2.0
Gilsonite (asphalt)	–	3.6
Aluminum	–	7.0
Dry prills	24.8	–
Trace ingredients	0.9	0.3
	100.0	100.0

Table 7.7. Typical slurry properties (Sudweeks, 1985).

Property	Slurry				
	1	2	3	4	5
density[a] (gm/cm^3)	1.10	1.12	1.15	1.17	1.21
energy (cal/gm)	680	764	830	940	1145
wt strength[b]	0.83	0.91	1.00	1.12	1.34
gas vol (mol/kg)	45	44	42	40	37
VOD[c] (m/s)	4000 for all mixes				
VOD (ft/sec)	13120 for all mixes				

a: average borehole density
b: *ANFO* = 1 at density 0.82 gm/cm^3
c: 6-in. diameter at 5°C.

with density up to a certain critical density beyond which the *VOD* falls rapidly. The weight strength is approximately constant up to this critical density (Sudweeks, 1985).

Like *ANFO*, slurries can be used in several forms. They can be (a) delivered as separate products and mixed at the site, (b) delivered premixed for bulk loading, (c) packaged

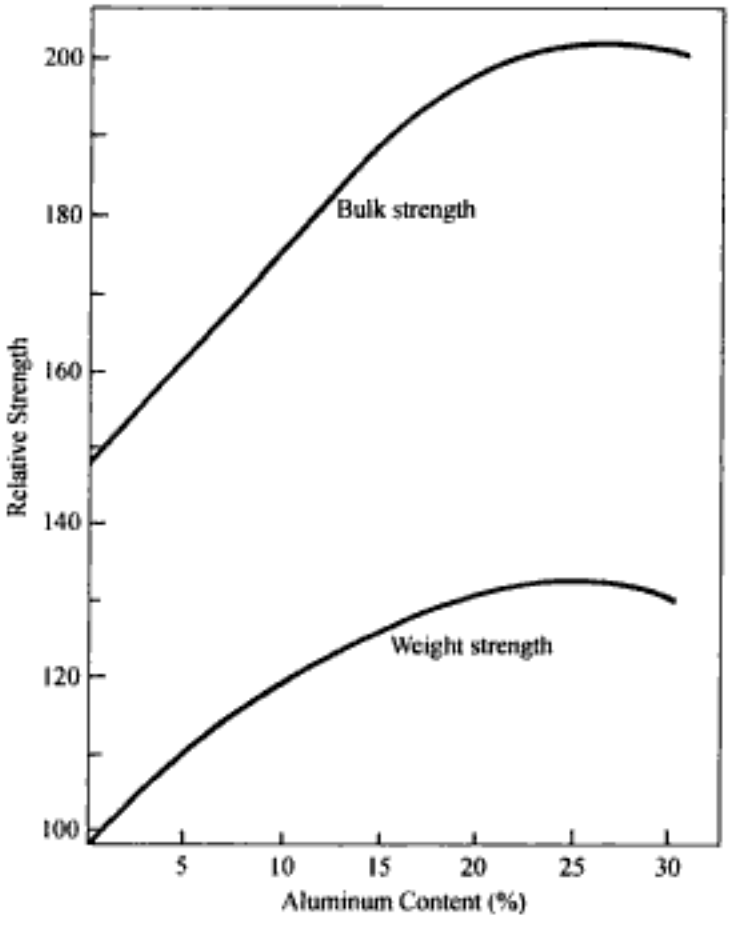

Figure 7.10. Variation of strength of a typical watergel blasting agent with aluminum content (Hagan & Mercer, 1983).

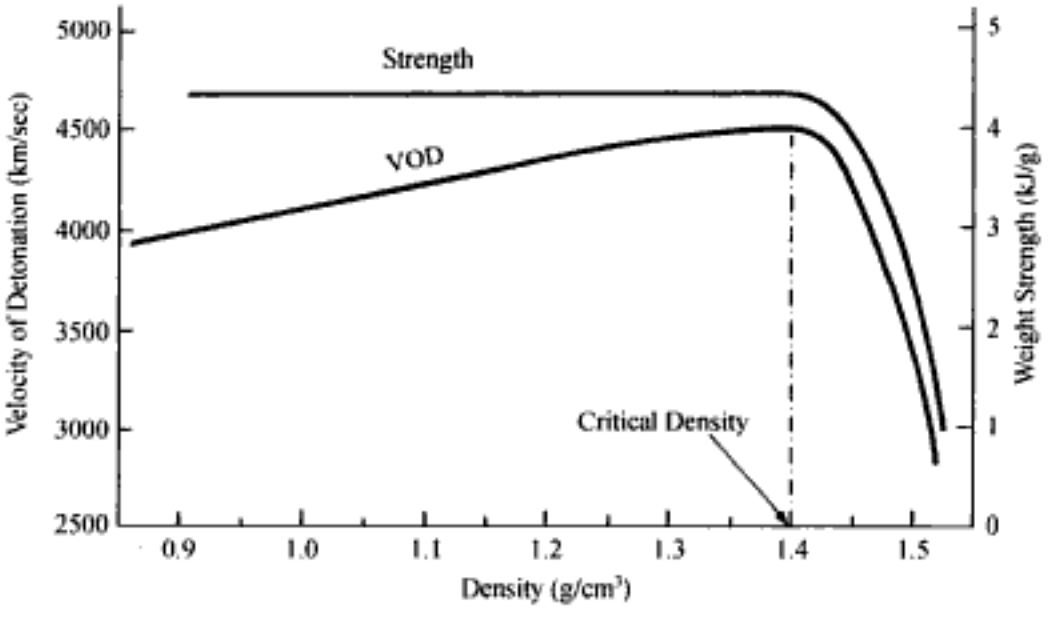

Figure 7.11. Variation of *VOD* and weight strength of a typical watergel blasting agent with density (Hagan & Mercer, 1983).

in polyethylene for hand loading, or (d) cartridged. In bulk loading, trucks bring either separate ingredients or the mixed product directly to the borehole. A mobile plant for mixing and pumping water gel explosives is shown in Figure 7.12. As indicated, watergels begin as high temperature, saturated aqueous (water-based) solutions of AN (sometimes with sodium nitrate). At the central distribution facility, these solutions are loaded into the insulated 'oxidizer solution tank'. Mix trucks are equipped to carry (Hagan & Mercer, 1983):

1. A hot oxidizer solution thickened by gums
2. Dry porous prilled AN (optional)
3. Dry powdered fuels and/or a liquid fuel
4. A cross-linking solution, and
5. A gassing solution

The use of the high temperature solution results in higher fluidities and lower pumping pressures. At the hole, fuels, sensitizers and sometimes more AN prills are added. The fuels used in watergels include aluminum powder and fuel oil. These ingredients are metered by pumps and augers into the truck's mixing chamber from where the composition flows into a surge funnel and is then pumped through the charging hose into the blasthole. By varying the type and quantity of the fuel (especially aluminum powder), water gels can be tailored to exhibit a wide range of weight and bulk strengths. As it is pumped bubbles of air and/or gas are added by aeration or by injecting a very small amount of a gassing solution. Addition of the bubbles is very important for density control of the watergel. If the density is too high, the bottoms of deep column charges can 'dead press' due to the collapse of the bubbles. Under such conditions, even the most powerful primers will not initiate the column. If, on the other hand, the density is too low, the watergel will float in water filled blastholes. The liquid phase is thickened with gums and then gelled with cross-linking agents. Thickening and cross-linking commence as soon as the watergel is mixed so that it is highly viscous by the time it leaves the loading hose. The cross-linking agents are used to

– Keep the solids in suspension,
– Provide a satisfactory degree of cohesiveness,
– Maximize water resistance.

Final thickening to a highly waterproof gel takes place within a few minutes of entering the blasthole. When completely gelled, watergels have a rubbery, porridge-like consistency.

The mix-pump trucks used for delivering watergels directly to the hole are highly versatile. Varying compositions of explosives, for example a high-strength bottom charge followed without interruption by a lower strength column charge, can be pumped into the borehole. Trucks of 2.5 to 12 ton capacity are equipped to discharge two or more compositions at rates up to 350 kg/minute. The ingredients are metered by pumps and augers into the trucks mixing funnel. From here they are pumped through a long, flexible rubber hose (38 mm ID, 50 m long) to the hole.

Some points (Dick, 1972) which should be kept in mind regarding slurries are:

1. Close control over ingredient mixing is important.
2. Adequate charge diameter and adequate priming are essential. The placement of boosters up the borehole may be beneficial.
3. Cap sensitive slurries do not require primers.

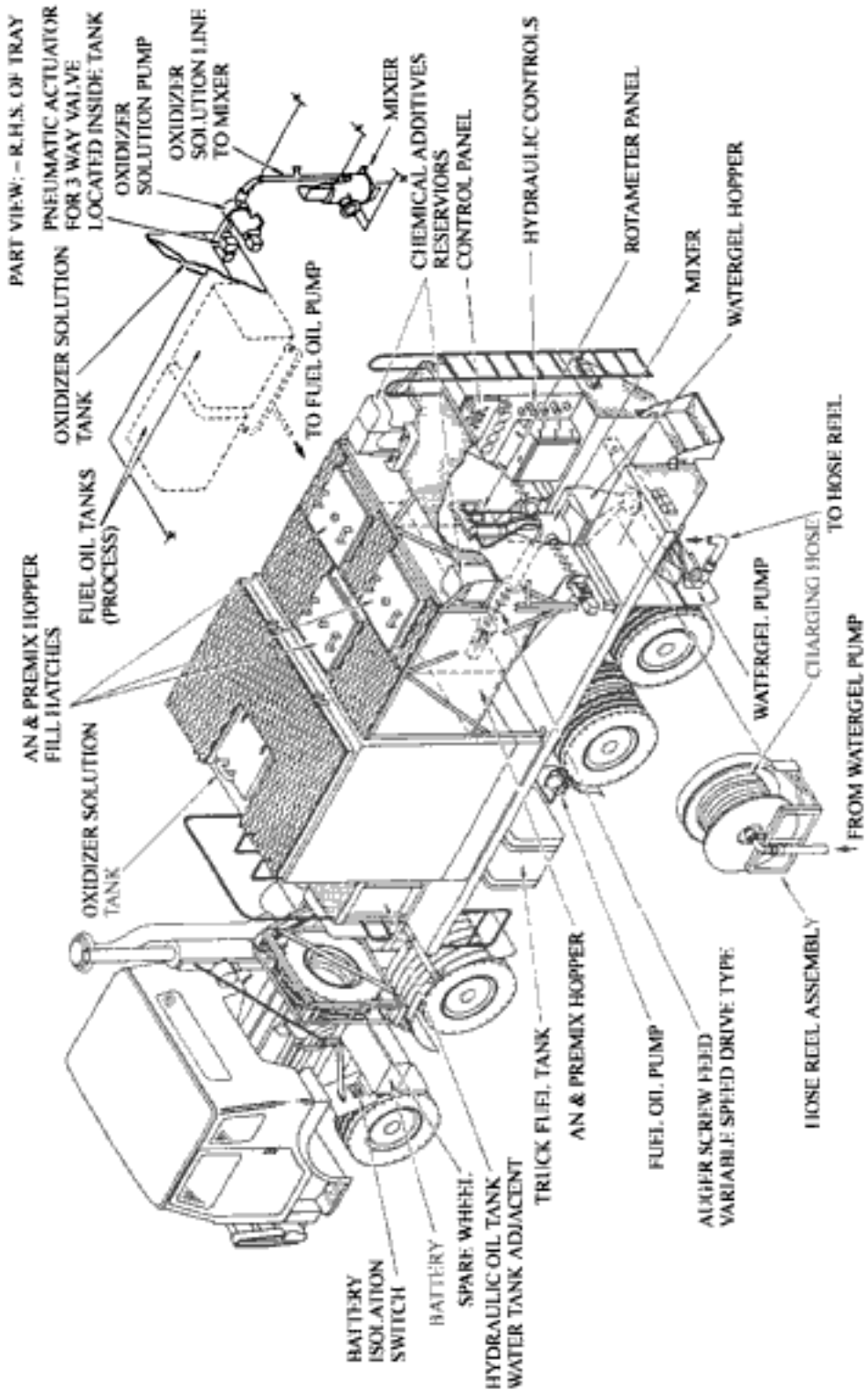

Figure 7.12. A typical pump truck for the loading of watergel explosives (Hagan & Mercer, 1983).

4. Loading equipment should be designed to avoid metal-to-metal contact even when pumping or mixing the most insensitive slurries.

5. Acid or other reactive ingredients in slurries may cause dangerous reactions in some rocks.

6. Noxious fumes may result from insufficient detonation, even in oxygen-balanced mixtures.

7. A low air-gap sensitivity makes some cartridged slurries susceptible to misfires caused by separation of charges.

8. The sensitivity of some slurries is seriously impaired by low temperatures.

9. Some aerated slurries reportedly have an increased sensitivity at high altitudes.

7.6 EMULSIONS

An *emulsion* is defined as an intimate mixture of two liquids that do not dissolve in each other. Expressed in more technical terms, an emulsion is described as a two-phase system in which an inner or dispersed phase is distributed in an outer or continuous phase. Some examples of emulsions found in everyday life (Hopler, 1991) are:

Oil-in-water	*Water-in-oil*
Asphalt driveway sealer	Margarine
Floor polish	Cold cream
Latex paints	Hydraulic fluids
Mayonnaise	Printing inks
Ice cream	Butter
Milk	Shoe polish
Cutting oils	

The materials in both columns consist of very small droplets of one material enclosed in a continuous matrix of another material. Close study of the items in the two lists reveals that those materials in the left column dissolve in water, whereas those in the right are completely insoluble in water. For the 'water-in-oil' emulsions, a thin film of oil surrounds each microscopic droplet of water or solution, thus protecting the water or solution from external water.

Interest in explosive emulsions began in the early 1960s (Sudweeks, 1985). In this application, the oxidizer salt solution (normally ammonium nitrate (*AN*) plus sodium nitrates and/or calcium nitrates in water) is suspended in the oil phase.

Over the years, although oxidizers and fuels have maintained a fairly constant chemistry, the physical form of these chemicals has changed drastically (Anonymous, 1985). There has been a progressive reduction in particle size from solids, to salt solutions plus solids, to the micro-droplets of an emulsion explosive. The importance of particle size lies in the increase in the rate and efficiency of reactions as the proximity of one unit of oxidizer to one unit of fuel becomes more intimate. Table 7.8 summarizes these statements in chronological order.

This progression through the years as described by Anonymous (1985), is both interesting and informative and is included in abbreviated form here. In modern dynamites, the nitrate salts are usually blends of grains and prills. The liquid sensitizer, which also functions as a fuel, coats the grains and penetrates into the pores of the prills. An intimate

proximity exists only at the liquid-solid and solid-solid contacts. The proximity of the oxidizer and fuel decreases rapidly away from those boundaries. While dynamites provide a high level of sensitivity and performance, they represent relatively crude mixtures and low-efficiency reactions. *ANFO* represents a very simple form of oxidizer/fuel combination. The porous ammonium nitrate prill absorbs the liquid hydrocarbon fuel and no other chemical sensitizer is required. The relationship is still that of a surface-coated particle. The intimacy decreases away from the contact boundary to produce an improved but less than ideal reaction efficiency. Slurry explosives were the first to utilize nitrate salts in water solution form. This improved the accessibility of the oxidizer to the fuel, particularly when liquid sensitizer-fuels were used. The use of thickeners and gelling agents to stabilize the fluid phase prevented segregation of solid ingredients and provided water resistance. Since much of the oxidizer is still in solid form, the slurry formulations are considered as a compromise. In the emulsion explosives both the oxidizer and the fuels are liquids. Rather than being dry prills, the emulsion oxidizer is a highly concentrated solution of ammonium nitrate and/or other salts. By the use of emulsifiers and precise processing methods, the 'particle size' of droplets of this solution has been reduced to microscopic proportions. Surrounding each microscopic droplet is a film of oil. The result is still a 'mixture' of fuel and oxidizer similar to black powder, dynamite and *ANFO* but the particle size comes as close as possible to mimicking the intimacy of combination found in molecular explosives such as NG or TNT. Typical emulsion oxidizer droplets (or cells) surrounded by a near molecular thickness of oil, have a diameter of from about 2 to 10 microns. The proximity of units of each has begun to approach molecular proportions. The characteristic sizes of the oxidizers in the different explosives are shown in Table 7.9. As can be seen, the velocity of detonation which is a good indicator of reaction efficiency is very dependent on the particle size.

Table 7.8. Physical form and category of the major components in explosives (Anonymous, 1985).

Explosive	Oxidizer	Fuel	Sensitizer
Dynamite	SOLID	SOLID	LIQUID
	nitrate salts	meals	nitroglycerine
		absorbents	voids/bubbles/friction
ANFO	SOLID	LIQUID	
	nitrate salts	diesel oil	voids/friction
Slurry	SOLID/LIQUID	SOLID/LIQUID	SOLID/LIQUID
	salt solutions	aluminum	TNT, fine aluminum
	nitrate salts	carbonaceous	bubbles
Emulsion	LIQUID	LIQUID	
	salt solution	oils, waxes	bubbles

Table 7.9. Characteristic sizes of oxidizers (Anonymous, 1985).

Explosive	Size (mm)	Form	*VOD* (km/sec)
ANFO	2.000	All solid	3.2
Dynamite	0.200	All solid	4.0
Slurry	0.200	Solid/liquid	3.3
Emulsion	0.001	Liquid	5.0-6.0

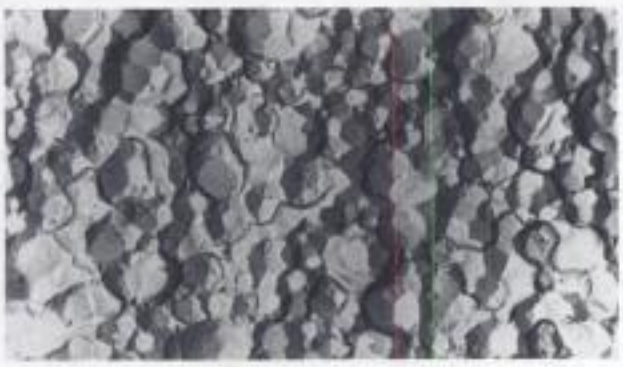

Figure 7.13. Structure of a typical emulsion explosive as viewed using an electron microscope. Magnification = 10,000x (Anonymous, 1985).

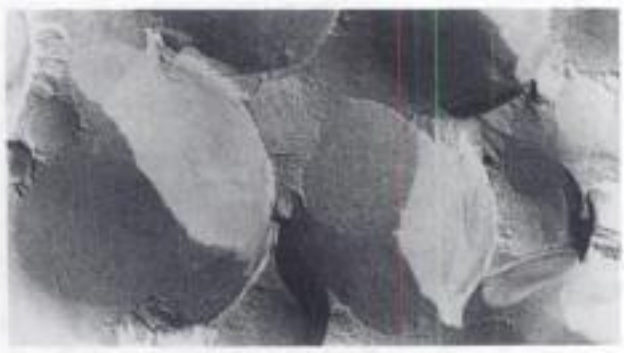

Figure 7.14. Structure of a typical emulsion explosive as viewed using an electron microscope. Magnification = 50,000x (Anonymous, 1985).

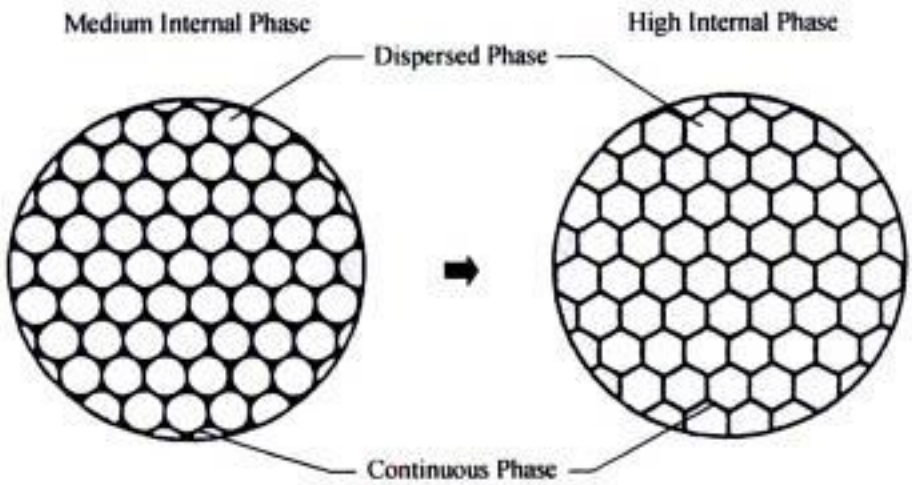

Figure 7.15. Cross sections through a concentrated emulsion (Sudweeks, 1985).

The structure of a typical emulsion explosive is exemplified in the Figures 7.13 and 7.14. In Figure 7.13, an electron microscope view at 10,000 × magnification, shows that the solution droplets are packed together so tightly that the conventional representation of them as spheres is not true. Like balloons forced into a box each droplet assumes a polyhedral shape. Figure 7.14, an electron microscopic view at 50,000 × magnification, shows each polyhedral droplet coated with only a film of continuous fuel phase in the order of millionths of a millimeter thick. Figure 7.15 shows stylized drawings of cross sections of emulsions with medium and high (tight packing) internal phase ratios for comparison. From this it is easy to see how a relatively high viscosity can be obtained just by the nature of the system without the need of added thickeners. The inherent viscosity of these emulsion systems ranges from a low of 10,000 to 20,000 cP up to 1,000,000 cP or more depending on the type of fuel phase

used. Because of oxygen balance constraints, a large amount of oxidizer salt solution is needed to react with a relatively small amount of oil fuel. On a volumetric basis, this requires approximately a 90/10 ratio of aqueous phase to fuel phase (Sudweeks, 1985).

The main sensitization of emulsion slurries is provided by the intimacy between fuel and oxidizer achieved when the oxidizer solution is dispersed into very small droplets.

Even with the greatly increased fuel/oxidizer intimacy, emulsions need to be additionally sensitized by the presence of small air bubbles, just as aqueous slurry explosives do. Without the cross-linked gel network of aqueous slurries, however, emulsions do not hold air bubbles as well. Therefore sensitization and density control are usually provided by adding very small glass microballoons. These hollow glass spheres range in diameter from 30 to about 150 microns, with an average diameter of 60-70 microns. Although small, these bubbles are still significantly larger than the dispersed droplets of an emulsion explosive. This is shown diagrammatically in Figure 7.16 with emulsion on the left and a microballoon on the right (Sudweeks, 1985).

Emulsion explosives can be tailored to exhibit a wide range of characteristics. Two general examples of emulsion formulations are shown in Table 7.10. Various types of oils and/or waxes (Table 7.11) can be used in the fuel phase to adjust the fluidity of the product from that of a pourable or pumpable consistency to that of a firm, but moldable solid.

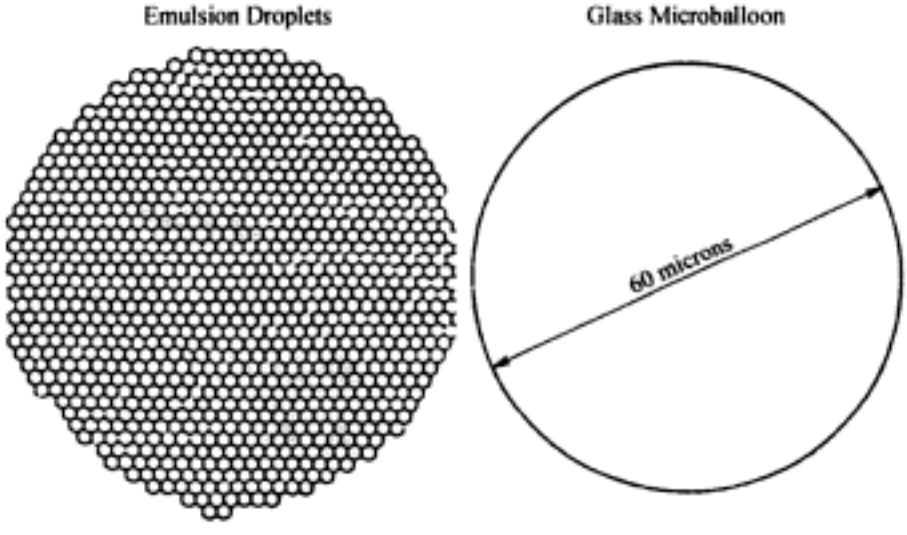

Figure 7.16. Size comparison of emulsion droplets and a single glass microballoon (Sudweeks, 1985).

Table 7.10. General emulsion formulations – percent by weight (Sudweeks, 1985).

Ingredient	Emulsion 1	Emulsion 2
Ammonium nitrate	78.0	70.7
Sodium nitrate	–	10.7
Water	13.5	7.3
Emulsifier	1.5	0.8
Oil and wax	5.5	3.1
Aluminum	–	5.0
Microballoons	1.5	2.4
Total	100.0	100.0
Oxygen balance	–7.4	0.7

Table 7.11. Product consistencies with common oils and waxes (Anonymous, 1985).

Fuel	Consistency	Uses
1. Fuel oil	thin, pumpable when cold	cold repumpable; small to intermediate diameter holes; *HANFO*
2. Parafin oil	thin, pumpable when hot	large diameter bulk; slumpable; intermediate to large diameter packages
3. Parafin oil and parafin wax	thick, soft, sticky	small diameter plastic cartridges; secondary blasting packs
4. Crude waxes	sticky, putty-like	small to intermediate diameter paper cartridges-tampable and stable
5. Flexible wax (micro-crystalline)	non-sticky putty	small diameter paper cartridges-tampable

Table 7.12 Typical emulsion properties (Sudweeks, 1985).

Property	Emulsion				
	1	2	3	4	5
density[a] (gm/cm^3)	1.25	1.25	1.25	1.25	1.25
energy (cal/gm)	722	784	846	969	1170
wt strength[b]	0.86	0.93	1.00	1.13	1.35
gas vol. (mol/kg)	42.8	41.7	40.6	38.4	34.8
VOD[c] (m/s)	5200 for all mixes				
VOD (ft/sec)	17,060 for all mixes				

a: average borehole density
b: *ANFO* =1 at density 0.82 gm/cm^3
c: 6-in. diameter unconfined at 5°C.

In comparison with aqueous-based slurries, the increased intimacy between fuel and oxidizer in emulsions is believed responsible for their enhanced detonation properties listed in Table 7.12. Emulsion detonation velocities tend to be in the 5000 to 6000 m/sec range with detonation pressures from 100 to 120 kbar. The densities with microballoons (1.1 to 1.4 g/cm^3) also tends to be higher than the gassed densities of aqueous slurries so that the bulk strengths are higher. The aluminum content can also be varied to produce an energy series just as was done with the slurries (Sudweeks, 1985).

As opposed to water gels, this mixing of emulsions does not take place in a mix-pump truck but rather at a central manufacturing plant located in the vicinity of the mine. There are two approaches being used to produce stable emulsions.

1. The chemical approach is based upon the use of emulsifiers for forming and stabilizing the emulsion. Mixing is done with a relatively low shear (energy) mixer.
2. The mechanical approach uses a high shear (energy) mixer with less use of emulsifying agents.

The advantages of high shear mixers are that both capital and ingredient costs tend to be less. On the other hand, it has been generally observed that chemical stabilization is superior to mechanical stabilization and lower energy mixing is of inherently higher safety.

Heated sources of aqueous phase, oil phase and emulsifiers – stabilizers are required for all products. The mix temperature is of the order of 80°C. In the manufacture of pack-

Hidden page

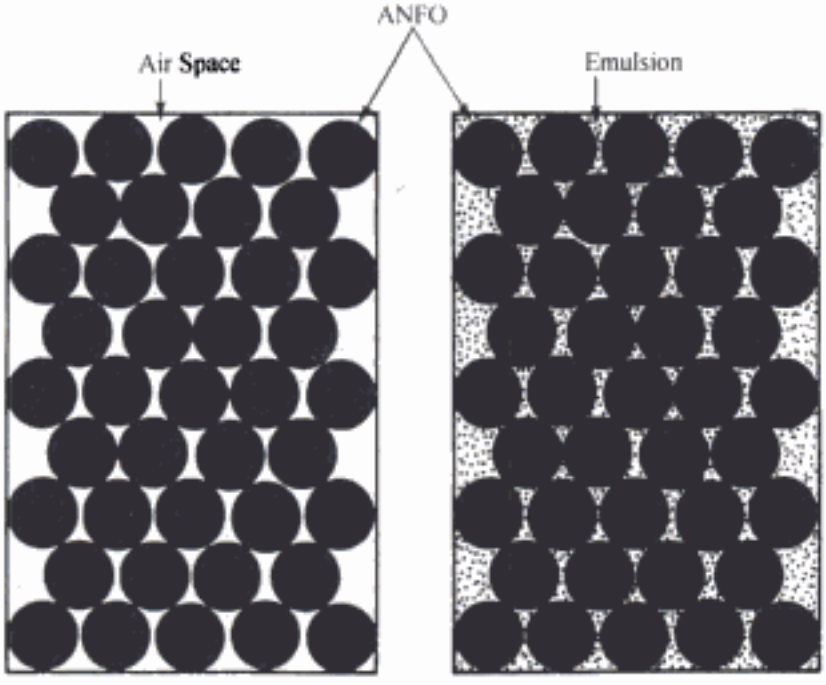

Figure 7.17. With heavy ANFO the air spaces between the prills are filled with emulsion (Atlas Powder Company 1987).

dense and more water resistant than *ANFO* with relatively little added cost. The principle behind Heavy *ANFO* (H*ANFO*) is to fill the volume between the prills with emulsion. The basic idea is shown diagrammatically in Figure 7.17. The water resistance and/or the density of the mix can be tailored by changing the emulsion level.

The production of H*ANFO* involves two separate technologies.

1. Production of the matrix emulsion
2. Mixing and loading of the final product.

The production of the matrix emulsion was the subject of the previous section. In this section the focus will be on the mixing/loading of the final product and the properties of the resulting H*ANFO*. There are two variations of the basic H*ANFO* truck.

Alternative 1. A concrete mixer such as shown in Figure 7.8 is used. The H*ANFO* is batch mixed and chute loaded into the hole. This has the advantage of delivering a uniform product at a very high rate. The disadvantage is being able to load only a single product at a time.

Alternative 2. A truck-mounted H*ANFO* plant (see Fig. 7.18) consisting of an AN bin, an emulsion bin, an aluminum bin, and a fuel oil tank. This one truck can thereby load 1. A completely waterproof product, or 2. *ANFO*, or 3. All the variations in between.

The second alternative will be considered here. The preparation of H*ANFO* is relatively simple. The emulsion matrix may be prepared at a fixed plant, and transported by tank truck for on-site storage in the tanker, or by pump transfer to fixed tanks. Since it is non-explosive this greatly reduces transportation and storage limitations. The *ANFO* is delivered to the site by a standard bulk *ANFO* mix truck. An emulsion matrix tank is added to a standard *ANFO* truck plus a pump and piping to inject the matrix into the delivery auger. This mixing of the *ANFO* and matrix takes place after combining the AN with the

fuel oil. The matrix pumping rate determines the ratio of the blend in a constant speed auger. It has been found that even a relatively short length of auger provides good mixing. The product is then dropped into the hole. When it is being augered into the hole, H*ANFO* looks very much like wet *ANFO*. At low matrix levels, the prills are coated but remain free flowing. Even at fairly high matrix levels, the coating is fairly thin. Since the average prill is 2 mm to 3 mm in diameter, even at 25% to 30% matrix, the coating is only about 0.1 mm thick. Depending upon the AN prill type and the matrix density, all spaces between prills will be filled in the 35% to 40% matrix range. Since some emulsion is absorbed into the pores of the prills, a somewhat higher matrix level than this is required to actually fill all the spaces. With an increase in the emulsion level the prills are forced apart. Above about 55%, the volume of the matrix phase is greater than that of the AN prills. Hence instead of *HANFO* one is now using an *ANFO* 'doped' emulsion. With high emulsion ratios one must consider whether the air volume in the prills provides sufficient sensitization. Often additional sensitivity must be added. The matrix level, as seen in Table 7.13, has a profound effect on density, relative bulk strength (RBS), sensitivity as measured by the critical diameter), cohesiveness and water resistance. (Evans & Taylor, 1987)

The proper selection (Van Ormmeren, 1992) of the blend ratio depends on several factors, including

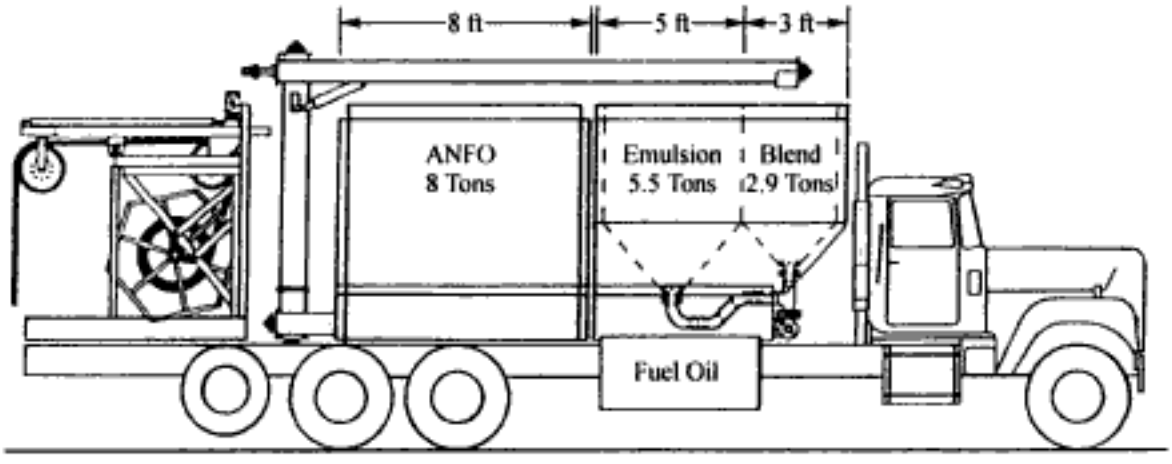

Figure 7.18. An example of a emulsion delivery vehicle. Hopler, 1992.

Table 7.13. The effect of matrix level on the physical properties of heavy *ANFO* (Evans & Taylor, 1987). The emulsion is considered to have a relative weight strength (RWS) of 80 and a density of 1.40 g/cm^3.

% Matrix by Weight	Density (g/cm^3)	RBS	Critical Diameter (mm)	Cohesiveness	Water Resistance
0	0.84	100	75	None	None
10	0.93	107	100	None	None
20	1.04	118	125	Free Flowing	Slight
30	1.15	128	125	Somewhat	Fair
40	1.28	140	150	Cohesive	Good
45	1.35	145	175	Cohesive	Very Good
50	1.40	149	200	Very Cohesive	Excellent

1. Borehole environment (wet vs dry),
2. Borehole diameter,
3. Pumped vs augered product,
4. Need for 'gas energy' versus 'shock energy' (brisance),
5. Prill quality.

Table 7.14 presents some basic guidelines which should be followed. If conditions are wet and some degree of water resistance is needed, then a higher percent emulsion should be used in the blend. Blends having an emulsion content under 30% have little or no water resistance. A 50% emulsion blend has good water resistance. A higher percent blend has excellent water resistance.

Other factors which affect the water resistance are depth of water, distance which the product travels through water when augered from the collar of the hole, and sleep time.

As shown in Table 7.15 the *VOD* of blends (as measured in the borehole) is dependent on hole diameter, emulsion/*ANFO* ratio and the type of emulsion product used (sensitized with microballoons versus unsensitized). The theoretical or calculated energies for various blends are shown in Table 7.16. As can be seen, the energy remains relatively constant for

Table 7.14. Guidelines for the % blend In H*ANFO* (Van Ommeren, 1992).

Blend (% Emulsion)	Guidelines
25% or less	Use only in dry holes with diameters of 5" or greater
50%	Use an auger system for loading Holes less than 9" should be dewatered before 50% blend is augered into the holes In 9" holes, 50% blend may be augered from the hole without dewatering. Care should be taken to adjust the rate of loading to permit full settlement of the blend to prevent entrapment of water pockets Holes larger than 9" can be readily loaded through water from the top of holes at rates of 250 to 500 pounds per minute Do not pump blends with less than 60% emulsion.
60-70%	Use in more severe conditions of high heads of water or sleeping times which exceed three days Use a pumping system with a reel and hose to permit pumping from the bottom of the hole up
70% or more	Blends with a minimum of 70% emulsion are recommended for holes 3" to 4" in diameter

Table 7.15. The Velocity of Detonation as a Function of the Mix Ratio and Hole Diameter for Heavy *ANFO* (Van Ommeren, 1992).

Ratio	Unsensitized Emulsion/*ANFO*			Sensitized Emulsion/*ANFO*			
(Emulsion: *ANFO*)	6-3/4"	7-7/8"	9"	3-1/2"	6-3/4"	7-7/8"	9"
25/75	15900	–	16800	–	–	–	17000
30/70	15600	–	16500	–	16200	–	16900
35/65	15300	–	–	–	–	–	17700
40/60	14700	15600	17200	–	–	16500	18000
45755	12900	–	–	–	17500	–	19000
50/50	11400	–	14000	–	17500	–	18800
60/40	NR	NR	NR	–	–	–	–
75/25	NR	NR	NR	17100	–	–	–

NR = not recommended

Table 7.16. Energy of bulk emulsion/*ANFO* blends (Van Ormmeren, 1992).

	Emulsion/*ANFO* Weight Ratio					
	25/75	30/70	40/60	50/50	60/40	75/25
Sensitized Emulsion						
density (gm/cm^3)	1.15	1.21	1.25	1.30	1.28	1.26
ABS (cal/gm)	1016	1035	1030	1040	985	925
RBS (*ANFO* = 100)	138	140	140	141	134	125
Unsensitized Emulsion						
density (gm/cm^3)	1.16	1.22	1.30	1.36	–	–
ABS (cal/gm)	1030	1075	1080	1095	–	–
RBS (*ANFO* = 100)	140	145	146	148	–	–

Table 7.17. Recommended primer size (Van Ormmeren, 1992).

Borehole Diameter (ins)	Primer
2-1/2 to 3-1/2	2" to 2-1/2" dynamite* primer, 1 lb cast booster
4" to 5"	3" dynamite primer, 2 lb cast booster
5" to 6",	4" dynamite primer, 3 lb cast primer
6-1/4" and larger	5" dynamite primer, 3 to 5 lb cast booster combination primer

* Only specially formulated ammonia gelatin dynamites should be used as primers.

blends between 25 to 50%. For blends higher than 50% emulsion, there is some reduction in the calculated energies. Blends using greater than 50% unsensitized emulsion are not recommended due to lack of sensitivity of the end product (Van Ormmeren, 1992).

Although initiation/priming of bulk explosives is one of the topics discussed in some detail in Chapter 8, some of the guiding principles as extracted from Van Ormmeren (1992) will be included here. The initiation of emulsion/ANFO blends (or ANFO) is accomplished by applying the detonation pressure developed by primer detonation onto the surface of the explosive product. If the diameter of the primer is the same as that of the blasting agent, then the pressure wave of the primer is applied uniformly to the entire surface of the blasting agent. If the primer diameter is small in relation to the explosive column charge, then the area of pressure transfer is greatly reduced. In addition, the primer must be of sufficient length to quickly insure development of its steady state velocity. In boreholes 7" in diameter and above it is not economic to use a primer of hole diameter dimension. It is reasonable, however, to use a 'combination' primer. In practice, this means using a one to four pound cast primer in combination with a bag of high velocity explosive (such as straight emulsion) which surrounds the primer and matches the hole diameter. The objective is for the detonation front to reach full detonation velocity and pressure (> 100 kilobars) in a very short distance when initiated by a small primer. The recommended primer sizes (Van Ormmeren, 1992) as a function of borehole diameter are given in Table 7.17.

Larger primers should be used under severe conditions such as wet holes sleeping for more than one shift, or long drops through water when augering blends into larger holes.

Like most explosives, the performance of blends can be adversely affected by detonating cord. According to Van Ormmeren (1992), the factors which influence the performance are types of blend, hole diameter, and detonating cord strength. Although the best guideline is to eliminate the use of detonating cord, if this is not possible, then the lowest strength detonating cord which is compatible with the initiating/primer system should be used. In no event should the detonating cord strength exceed those given in Table 7.18.

Table 7.18. Recommended maximum strength detonating cord (Van Ommeren, 1992).

Hole diameter (ins)	Maximum strength cord
Under 7-7/8	Do not use
7-7/8 to 9	25 grain
10-5/8 and greater	40 grain

This ability to combine *ANFO* and emulsion in proportions ranging from 100:0 to 0:100 at the hole offers the blasting engineer the opportunity to vary energy, sensitivity, water resistance, density, etc nearly at will to suit the conditions at hand. The challenge now is how to best utilize this powerful tool.

REFERENCES AND BIBLIOGRAPHY

AECI Explosives and Chemicals Limited 1981. The strength of explosives. *Explosives Today*. Series 2, No 23, March.

AECI Explosives and Chemicals Limited 1982. The use of *ANFO* in surface blasting. *Explosives Today*. Series 2, No 30, December.

AECI Explosives and Chemicals Limited 1983. Bulk explosive systems. *Explosives Today*. Series 2, No 32 (revised), 2rd Quarter, Oct.

AECI Explosives and Chemicals Limited 1984. Introduction to explosives. *Explosives Today*. Series 2, No 35, 1st Quarter.

AECI Explosives and Chemicals Limited 1987. The safe and efficient initiation of explosives. Part 1 – Principles. Series 2, No 47. September.

AECI Explosives and Chemicals Limited 1990. *ANFO* quality. *Explosives Today*. Series 3, No 9, Sept.

AECI Explosives and Chemicals Limited 1988. The historical development of commercial explosives. *Explosives Today*. Series 3, no 1, Sept.

Anonymous 1975. *Programming Your Blast With Gulf Explosives*. Gulf Oil Chemical Company. 47pp.

Anonymous. Explosive selection criteria. *Explosives Engineering*. Excerpted from USBM IC 8925. pp. 19-21.

Anonymous 1976. Puzzled about primers for large-diameter ANFO charges? Here's some help to end the mystery. *Coal Age*. 81(8): 102-107.

Anonymous 1985a. Recommended methods for the disposal of unwanted explosives. *Downline. Issue* No. 4 Dec. ICI Explosives. pp. 8-9.

Anonymous 1985b. Emulsion explosives. *Downline*. Issue No. 4 Dec. ICI Explosives. pp. 6-7.

Anonymous 1986. Emulsion explosives (Part 2). *Downline. Issue* No. 5 Sept. ICI Explosives. pp. 6-8.

Anonymous 1987. *Modern explosives – emulsions and dense ANFO*. World Mining Equipment. 12 (March/April): 34-35.

Anonymous 1990a. Blasting technology advances. *International Mining*. 7 (April): 13-19.

Anonymous 1990b. Innovations enhance the power of explosives. *Coal*. 95(7): 51-55.

Anonymous 1990c. Innovations enhance the power of explosives. *Coal*. 95(7): 51-55.

Atlas Powder Company. 1987. *Explosives and Rock Blasting*. Maple Press. 662pp.

Atlas Powder Company. *Slurries*. 6pp.

Atlas Powder Company. *Nitroglycerin Explosives*. 3pp.

Bacca, D.A. 1994. Borehole dewatering techniques and systems. *Proceedings of the 5th High-Tech Seminar on Blasting Technology, Instrumentation, and Explosives Applications. New Orleans, Louisiana* (July 9-14). Blasting Analysis International, Inc. pp. 83-93.

Bauer, A. 1978. Trends in drilling and blasting. *Proceedings of the 4th Conference on Explosives and Blasting Technique. SEE*. pp. 291-325.

Bauer, A. G. Glynn, R. Heater & P. Katsabanis 1984. A laboratory comparative study of slurries, emulsion and heavy AN/FO explosives. *Proceedings 10th Conference on Explosives and Blasting Technique. See*. pp. 299-321.

Bauer, A.W., A. Bauer, K.K. Feng & R.R. Vandebeek 1987. Evaluation of propagation sensitivity of commercial explosives in large diameter holes. *Proceedings of the 13th Conference on Explosives and Blasting Technique* (3rd Mini-Symp.). *SEE*. pp. 1-13.

Borg, D.G. 1994. Emulsion explosives technology. *Proceedings of the 5th High-Tech Seminar on Blasting Technology, Instrumentation, and Explosives Applications*. New Orleans, Louisiana (July 9-14). Blasting Analysis International, Inc. pp. 1-18.

Brufia, J.C. 1985. POWERAN emulsion/*ANFO* explosives systems. *Proceedings of the 11th Conference on Explosives and Blasting Technique. SEE*. pp. 293-305.

Bunn, C.F. 1975. Explosives and blasting agents. *Proceedings of the 1st Conference on Explosives and Blasting Technique. SEE*. pp. 7-16.

Chironis, N.P. 1991. Innovations in surface mine blasting. *Coal*. 96(7): 37-42.

Clark, G.B. 1981. Basic properties of ammonium nitrate fuel oil explosives (ANFO). *Quarterly, Colorado School of Mines*. vol 76 no 1, January.

Close, J. 1986. The development and application of Duponts emulsion explosives systems in the Bowen Basin. *Proceedings, Large Open Pit Mining Conference, AusIMM/IE*. Oct. pp. 99-107.

Contestabile, E. & R.R. Vandebeek 1987. Relating explosives sensitivity laboratory results to field tests. *Proceedings of the 13th Conference on Explosives and Blasting Techniques. SEE*. pp. 241-253.

Cook, M.A. 1958. The Science of High Explosives. *American Chemical Society Monograph Series*, No. 139, Reinhold, New York, 440pp.

Cook, M.A. 1961. AN slurry blasting agents. *Colo School of Mines Quarterly*, vol 56, no 1, 199pp.

Cook, M.A. 1968. Explosives: a survey of technical advances. *I&EC*. vol 60, July, pp. 44-55. (American Chemical Society).

Cook, M.A. 1970. Slurry blasting forges ahead. *Mining Magazine*. 123(1).

Cook, M.H. 1974. The Science of Industrial Explosives. Ireco Chemicals. *Graphic Service and Supply*, Inc, 449pp.

Crosby, W.A. & M.E. Pinco 1989. When to use aluminum in bulk explosives. *Journal of Explosives Engineers*. 9(2): 30-34.

Crosby, W.A. & M.E. Pinco 1989. Review of the use of aluminum in bulk explosives for the mining industry. *Explosives Engineering* 7(3): 34, 36-37.

Crosby, W.A. & M.E. Pinco 1992. More power to the pop: When to use aluminum in bulk explosives. *E&MJ*. 193(5): ww. 28-31.

Dannenberg, J. 1973. Blasthole dewatering cuts costs. *Rock Products*. 76(12): 66-68.

Dannenberg, J. 1982. Open pit explosives: Full use of explosives' energy helps beat the cost of inflation. *E&MJ*. 183(7): 62-69.

Day, J.T., M.L. Thomas & L.L. Udy 1987. The importance of explosive energy on mining costs. *Proceedings of the 13th Conference on Explosives and Blasting Techniques. SEE*. pp. 131-143.

Dick, R.A. 1968. Factors in selecting and applying commercial explosives and blasting agents. USBM IC 8405. 30pp.

Dick, R.A. 1972. The Impact of Blasting Agents and Slurries on Explosives Technology. USBM IC 8560. 44pp.

Dick, R.A., L.R. Fletcher & D.V. D'Andrea 1983. Explosives and Blasting Procedures Manual. USBM IC 8925. 105pp.

Dick, R.A., D.V. D'Andrea & L.R. Fletcher 1993. Back to basics: Properties of explosives. *Explosives Engineering*. 10(6): 28-45.

Dow Chemical Corp. 1974. *MS-80 Metallized Blasting Agents Deliver High Energy Efficiently*.

Drury, F.C. & D.J. Westmaas 1978. Considerations affecting the selection and use of modern chemical explosives. *Proceedings of the 4th Conference on Explosives and Blasting Technique. SEE*. pp. 128-153.

Drury, F.C. 1980. Ammonium nitrate blasting agents from manufacture to field use. *Proceedings of the 6th Conference on Explosives and Blasting Technique. SEE*. pp. 415-429.

E.I. DuPont de Nemours and Co. DuPont *Blasters' Handbook*. 1977 Edition. Wilmington, Del. 494 pp.

Elith, N. 1986. *Measuring the properties*. Downline. pp. 8-9. Issue No. 5, Sept. ICI Explosives.

Evans, W.B. & D.P. Taylor 1987. Blended *ANFO*-based explosives. CIM Bulletin. 80(905): 60-64.

Finger, M., Helm, F., Lee, E., Boat, R., Cheung, H., Walton, J., Hayes, B. & L. Penn 1976. Characterization of commercial, composite explosives. *Proceedings of the 6th Int. Symp. on Detonation* (August 24-27). Report ACR-221 of the Office of Naval Research, Dept of the Navy, Arlington, VA.

Gehrig, N.E. 1982. The future of slurry explosives. *Proceedings of the 8th Conference on Explosives and Blasting Technique. SEE*. pp. 217-228.

Givens, R.W., D.L. McDorman & G.S. Williams 1990. The effect of prill specifications on *ANFO*-emulsion blends. *Explosives Engineering.* 8(2): 34-42.

Grant, C.H. & V.N. Cox 1963. A comparison of metallized explosives. Trans. Society of Mining Engineers. 226: 299-306.

Grant, C.H. 1964. Successful aluminum slurry blasts pavedway for Dow's 'explosives algebra'. *E&MJ.* 165(3): 98-102.

Grouhel, P.H.J. and R.D. Hunsaker 1995. An introduction of a revolutionary low density bulk explosive for surface blasting operations. Proceedings, EXPLO '95. Brisbane 4-7 Sept. pp. 67-71.

Gulf Blasting Materials 1967. *The new look of blasting with Ammonium nitrate-fuel oil mixtures.*

Gulf Blasting Materials *Gulf Blasting Guide.*

Gulf Explosives 1975. *Programming Your Blast With Gulf Explosives.*

Hagan, T.N. & J.K.Mercer 1983. Workshop *Proceedings, Safe and Efficient Blasting in Open Pits. ICI Australia Operations Pty limited.* Karratha, 23-25 November.

Harries, G. & D.P. Gribble 1993. The development of a low shock energy explosive – ANRUB. *Proceedings, Rock Fragmentation by Blasting* (Rossmanith, ed.). A.A. Balkema, pp. 379-386.

Heltzen, A.M. & K. Kure 1980. Blasting with *ANFO*/polystyrene mixtures. *Proceedings of the 6th Conference on Explosives and Blasting Technique. SEE.* pp. 105-116.

Heltzen, A.M. 1986. *ANFO* and polystryrene beads. *International Mining.* 3(May): 51.

Hopler, R.B. *The historical development of commercial detonators, and a review of the methods used to compare their ability to initiate high explosives.* Ireco Inc. 30pp.

Hopler, R.B. 1991. *History and development of packaged explosives, progressing from Nobel's inventions to the recent introduction of emulsions.* 40pp. Ireco Incorporated. *Proceedings of the 3rd High-Tech Seminar on Blasting Technology, Instrumentation and Explosives Applications.* San Diego, California. Blasting Analysis International, Inc. June 2-7.

Hopler, R.B. 1992. *History of the development and use of bulk loaded explosives from black powder to emulsions.* Ireco Inc. 23pp.

Hopler, R.B. 1993. Custom-designed explosives for surface and underground coal mining. *Mining Engineering.* 45(10): 1248-1252.

Hopler, R.B. 1994. The high explosives industry in the United States: The first 20 years – 1865-1885. *Proceedings of the 5th High-Tech Seminar on Blasting Technology Instrumentation and Explosives Applications. New Orleans, Louisiana* (July 9-14). Blasting Analysis International, Inc. pp. 411-434.

Hunsaker, R.D. 1984. Repumpable emulsion slurries. *Proceedings of the 10th Conference on Explosives and Blasting Technique. SEE.* pp. 390-394.

ICI Australia. Blasting in Quarries and Open Pits. 34pp.

Institute of Makers of Explosives Rules for Storing, Transporting & Shipping Explosives. *Safety Library Publication* No. 5.

Institute of Makers of Explosives Recommended Industry Standards. *Safety Library Publication* No. 6.

Institute of Makers of Explosives 1964. *Safety in the Handling and Use of Explosives. Pamphlet* No. 17, 69pp.

Institute of Makers of Explosives How to Destroy Explosives. *Pamphlet* No. 21.

Ireco Explosives Technical Data *Pump Trucks.*

Ireco Incorporated *Blaster's Record Book.*

Ireco Incorporated *Explosivees Engineers' Guide.*

Ireco Incorporated *Prevention of Accidents in the Use of Explosive Materials.*

Ireco Incorporated *Repump System.*

Ireco Incorporated *Iremex/ANFO System.*

Ireco Incorporated *ANFO and Iremex Heavy ANFO Trucks.*

Joyce, D.K. & T.C. Matts 1990. Explosives and explosives loading equipment selection. *Mine Planning and Equipment Selection* (Singhal & Vavra, eds) Balkema, Rotterdam. pp. 471-474.

Konya, C.J., R.R. Britton & J.S. Gozon 1985. Explosive selection – A new approach. *Proceedings of the 11th Conference on Explosives and Blasting Technique. SEE.* pp. 340-347.

Liu, Q., A. Bauer & R. Heater 1988. The channel effect for AN/FO, slurries and emulsions. *Proceedings of the 14th Conference on Explosives and Blasting Technique (4th Mini-Symp.) SEE.* pp. 33-48.

Lydon, D.M., T.B. Harrington & W.B. Sudweeks 1989. Repumpable emulsion/*ANFO* blends: the best of both worlds. *Proceedings of the 15th Conference on Explosives and Blasting Technique. SEE.* 287pp.

Manon, J.J. 1978. Explosives: their classification and characteristics. *E/MJ Operating Handbook of Mineral Surface Mining and Exploration* (Richard Hope, ed.). E/MJ Mining Informational Services, McGraw-Hill, NY. pp. 152-156.

Manon, J.J. 1978. How to select an explosive or blasting agent for a specific job. *E/MJ Operating Handbook of Mineral Surface Mining and Exploration* (Richard Hope, ed.). E/MJ Mining Informational Services, McGraw-Hill, NY. pp. 172-183.

Mason, C.N. & W.C. Montgomery 1978. Aluminum additives impart energy and sensitivity to many explosives. *E/MJ Operating Handbook of Mineral Surface Mining and Exploration* (Richard Hope, ed.). E/MJ Mining Informational Services, McGraw-Hill, NY. pp. 184-186.

Mohanty, B. 1981. Energy, strength and performance, and their implications in rating commercial explosives. *Proceedings of the 7th Conference on Explosives and Blasting Technique. SEE.* pp. 293-306.

Moxon, N.T. & J. Wilson 1989. The development of a low shock energy ammonium nitrate based explosives. *Proceedings of the 15th Conference on Explosives and Blasting Technique. SEE.* pp. 297-314.

Nielsen, K. and A.M. Heltzen. 1987. Recent Norwegian experience with polystyrene diluted *ANFO* (Isanol). *Proc. Second Int. Symp. on Rock Fragmentation by Blasting. Soc.of Exp. Mech. Bethel, Conn.* pp. 231-238.

Osten, L. 1985. Improved fragmentation and safety with proper borehole loading techniques. *Proceedings of the 11th Conference on Explosives and Blasting Technique. SEE.* pp. 306-319.

Paddock, R.C. 1987. A primer on explosives costs. *Coal Mining*, March. 24(3): 42-44.

Paine, G.G., G. Harries & C.V.B. Cunningham 1987. ICI's computer model SABREX-Field calibration and applications. *Proc. 13th Conf. on Explosives and Blasting Technique. SEE.* pp. 199-213.

Persson, A. 1975. *ANFO* blasting agent: initiation, detonation, toxic gases. Report TM1-1975 of the Swedish Detonic Research Foundation. In Swedish.

Persson, P-A. 1973. How an explosive can seem expensive and yet shave blasting costs. *E&MJ.* 174(6): 110-113.

Pilshaw S.R. 1987. Dewatering blastholes cuts explosives costs. *Coal Mining.* 24(Nov.): 43-45.

Rainbird, M.W. 1995. Tailoring explosives to the ground type, application and operating environment. *Proceedings, EXPLO'95. Brisbane*, 4-7 Sept. pp. 47-50.

Robinson, R.V. 1969. Water gel explosives – Three generations. *CIM Bulletin.* 62(692): 1317-1325.

Rollins, R.R. 1984. Detonation measurements of blasting agents. *Proceedings of the 10th Conference on Explosives and Blasting Technique. SEE.* pp. 322-330.

Rollins, R.R. & R.W. Givens 1989. Emulsion performance evaluation. *Proceedings of the 15th Conference on Explosives and Blasting Technique (5th Mini-Symp). SEE.* pp. 83-90.

Sadwin, L.D. & W.I. Duvall 1965. A comparison of explosives by cratering and other methods. Trans. Soc. of *Mining Engineers.* 232 (June): 110-115.

Scott, A. & A. Cameron 1988. The field evaluation of explosives performance. *Proc. Explosives in Mining Workshop, AusIMM, Melbourne*, Nov. pp. 51-58.

Sudweeks, W.B. 1985. Physical and chemical properties of industrial slurry explosives. *I&EC* (Industrial Eng. Chem.) Product Research & Development. 124 (3): 432-436.

Swanson Engineering, Inc. Blasthole Dewatering.

Thornley, G.M. & A.G. Funk 1981. Aluminized blasting agents. *Proceedings of the 7th Conference on Explosives and Blasting Technique. SEE.* pp. 271-292.

Tread Corporation. *From Rail Car to Blast Hole.*

Tremblay, D., M. Lemieux & R. Mason 1989. Iron Ore Company of Canada (IOC) blast optimization with emulsion explosives. *Proceedings of the 15th Conference on Explosives and Blasting Technique. SEE.* pp. 339-352.

Van Ommeren, C. 1989. A consumer's guide to bulk emulsions and emulsion/*ANFO* blends. *Proceedings of the 15th Conference on Explosives and Blasting Technique. SEE.* pp. 271-286.

Viking Explosives and Supply, Inc. Blasthole Dewatering System.

Wade, C.G. 1978. Emulsions – viva la difference. 1978. *Proceedings 4th Conference on Explosives and Blasting Technique. SEE.* pp. 222-233.

Watts, R.T. 1988. Bulk loading for you? *Explosives Engineering.* 6(2): 22-23.

Watts, R.T. 1992. Calibration of bulk trucks. *Explosives Engineering.* 10(1): 6-7.

Wilson, J.M. and N.T. Moxon 1988. The development of a low shock energy ammonium nitrate based explosive. *Proceedings. Explosives in Mining Workshop, AusIMM, Melbourne*, Nov. pp. 27-31.

Wingfield, B.G. 1991. Bulk explosives loading and delivery systems including economics. *Proceedings, Third High-Tech Seminar on Blasting Technology, Instrumentation and Explosives Applications*, San Diego, California. June 2-7. Blasting Analysis International.

Yancik, J.J. 1969. *Monsanto Blasting Products-ANFO Manual: Its explosive properties and field performance characteristics*. 37pp.

Yancik, J.J. & A.A. Arias 1969. Technique for selection of optimum explosive system: Essential element to achieving optimum blasting. *Presented at the 11th Convention of Mining Engineers, Lima, Peru*. Dec. 28pp.

CHAPTER 8

Initiation systems

8.1 INTRODUCTION

In the previous chapters, the principles involved in the layout of blast rounds have been discussed. In this chapter the focus is on some of the aspects of putting the design into practice. It is assumed that the holes have been laid out and drilled in the designed pattern and the objective is now to communicate to the holes

(a) The sequence in which the holes (or portions of the hole) should fire.
(b) The time delay between holes.
(c) The energy required to begin the detonation process.

The communications system may be likened to a network of roads carrying both timing information and energy. There are a series of major thoroughfares called *trunklines* which communicate between holes as well as a number of smaller branch roads called *downlines* which communicate the information down the individual holes. Each section of the network has a certain speed limit determined by detonation velocity, burning velocity, the speed of light, etc. A series of traffic lights, called *delays*, which also control the arrival times may be inserted along both the trunklines and downlines. The different communications systems will be discussed here. There are also a number of devices used in the hole for

(a) changing one form of energy to another and
(b) amplifying the energy signals received.

An example of the first is the electric cap in which electrical energy is used to trigger a release of chemical energy. An example of the second are primers which when triggered by a small amount of energy, emit a large amount. The concept of 'sensitivity' is very important in the design of initiating systems. For example a certain explosive may be 'cap-sensitive' which means that the energy-density provided by the cap is sufficient to initiate the explosive. Another explosive may not be cap-sensitive. In this case an energy-amplifier is needed between the cap and the explosive.

To illustrate the concept of energy transformation and amplication, a simple example will be presented. Consider first the electric signal used to energize a blasting cap. The resistance of the fusehead is 1 ohm and the applied current is 2 amps. The electric power involved is

$$P = I^2 R = (2)^2\,(1) = 4 \text{ watts} \tag{8.1}$$

This is applied over a time period (T) of about 1 msec (1×10^{-3} second). Hence the electrical input energy is

$$\text{Electrical energy} = P \times T \tag{8.2}$$
$$\text{Electrical energy} = 4 \times 10^{-3} \text{ watt-sec} = 1.11 \times 10^{-9} \text{ kwh}$$

In terms of the units normally used when discussing explosives this is approximately

$$\text{Electrical energy} \cong 0.95 \times 10^{-6} \text{ kcal}$$

This application of energy causes the PETN contained in the cap (0.45 gms for a No. 8 cap) to detonate. The energy released is 1462 kcal/kg or

$$\text{Cap energy} = (1462)\,(0.00045) = 0.658 \text{ kcal}$$

The energy amplification factor (EA_1) in this process is

$$EA_1 = 0.658/(0.95 \times 10^{-6}) \cong 690{,}000$$

The cap is inserted into a 1 lb (454 gm) primer which releases 1100 kcal/kg. The total amount of primer energy released is

$$\text{Primer energy} = 499 \text{ kcal}$$

and the amplification factor

$$EA_2 = \frac{499}{0.658} = 758$$

The primer is located at the bottom of an *ANFO* ($\rho = 0.8$ gm/cm^3) column, 381 mm (15″) in diameter and 9 m (30 ft) in length. The total amount of energy released (912 kcal/kg) is

$$\text{Explosive energy} = 7.5 \times 10^5 \text{ kcal}$$

The amplification factor in this case is

$$EA_3 = (7.5 \times 10^5)/499 = 1500$$

The overall energy amplification factor when going from the electrical signal to the explosive column is

$$EA \text{ (overall)} = (EA_1)(EA_2)(EA_3) = (7.5 \times 10^5) / (0.95 \times 10^{-6}) = 7.9 \times 10^{11}$$

Thus the electrical energy has been amplified almost a trillion times.

8.2 INITIATION AND PROPAGATION OF THE DETONATION FRONT

Because of the very short times separating the series of events involved in the detonation of a typical explosive column, one might view the initiation and propagation of a stable detonation front as occurring instantaneously. For some applications this simplification can be made without significant error. The next level of complexity would be to include the time of passage of the detonation front through the column but to assume that a constant *VOD* applies already from the time of initiation. This approximation is commonly introduced in considering various layouts. There are times however when a more detailed examination and deeper understanding of the process is of benefit. In this short section, a simplified description of the complex processes involved in going from initiation by a cap

to propagation of a stable detonation front in an explosive column will be presented. An explosion, as defined by Drury & Westmaas (1978), is a supersonic thermo-chemical process whereby mixtures of gases, liquids and solids react to form shock, heat and expanding gas. To initiate the reaction, a source of ignition having the proper temperature and pressure conditions must be present. The phenomenon responsible for the mechanical initiation of an explosion in a wide range of explosives is the formation within the explosive of 'hot spots'. This concept, which was briefly introduced in the previous chapter, will be expanded upon here. A 'hot spot', as the name implies, is a point in an explosive where the temperature far exceeds the temperature in the surrounding area. The presence of this thermal anomaly, initiates the reaction between the fuel and the oxidixer at that point. As more and more of these hot spots become involved, the overall reaction front changes both in shape and velocity of propagation. Eventually a stable detonation front forms which propagates through the column at a constant velocity (*VOD*) and amplitude (detonation pressure) independent of the initiation procedure.

The original 'hot spot' is the cap. The hot temperature generated in the near vicinity of the cap initiates the chemical reaction in the adjacent primer material. In addition a shock wave is generated which travels outward from this point. When this shock wave encounters a gas or air filled void in the near vicinity, the gas is compressed adiabatically and very rapidly to a high temperature. The material in the vicinity of this void is now introduced into the reaction process. Each of these new hot spots acts as a generator which seeks out new voids in their immediate vicinities. The 3D spreading process takes place at a speed equal to the *VOD* of the material involved. In the primer the *VOD* is very high being of the order of 7500 m/sec or even higher. On reaching the primer boundaries, the process continues with each current hot spot generating waves which seek out new voids to be compressed in the surrounding bulk explosive/blasting agent. Normally the rate of travel (*VOD*) in the the blasting agent is less than that in the primer. Since, the primer is generally smaller in diameter than that of the hole it takes some time for this process of hot spot propagation to reach the wall of the hole. Here the generating wavelets are reflected back into the explosive column. Eventually a stable detonation front is developed in the column. The time necessary for this to occur is called the run-up time and the distance from the point of initiation at which it occurs is called the run-up distance.

As indicated, the presence of voids in the explosive mixture which will become future hot spots is essential to successful detonation of a column of explosives. In *ANFO* the hot spots are created by the void spaces existing between and within prills. In watergels and emulsions, bubbles or micro-balloons are artificially introduced to serve this function. The explosive is said to be 'sensitized' through their introduction. If there are no voids present or the void volume is very small, then there will be no detonation. The presence of voids is reflected in the density of the explosive. For a loose mix of *ANFO* prills the void space is high and the resulting density is of the order of 0.8 gm/cm^3. As the prills are broken and compacted, the density increases. There is a critical density for which detonation will not proceed. In the case of *ANFO* it is of the order of 1.25 gm/cm^3. Drury & Westmaas (1978) indicate that the reason wet *ANFO* does not detonate is that the water has filled the voids which eliminates the potential for hot spot formation. In the same way, if not properly 'sensitized' with bubbles, watergels/emulsions will not detonate. At the bottom of long explosive columns, the air bubbles may collapse due to the weight of the charge. The result is that the effective density is greater than the critical density and detonation will not propagate. In such a case the explosive is said to be 'dead-pressed'.

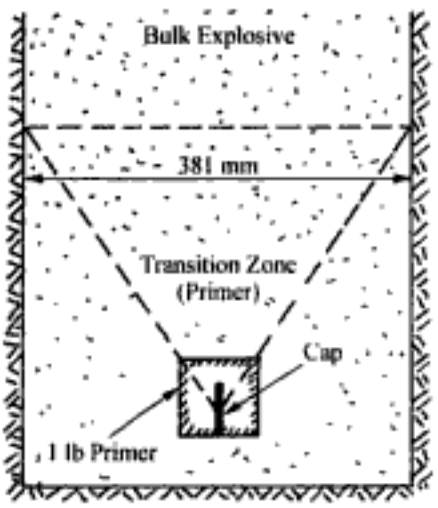

Figure 8.1. Diagrammatic representation of the cap and primer in the borehole.

Obviously for the initiation process to work properly the primer must be sensitive to the cap and the explosive column must be sensitive to the primer. Furthermore the rate at which a stable detonation front is built up depends upon the relative geometries, detonation pressures and detonation velocities of the components involved. Figure 8.1 shows the relative size of the cap and a 1 lb primer in the 15″ diameter blasthole. Since the primer is so much smaller than the hole diameter, it can be imagined that it takes some time for a stable front of hot spots to be developed from the original hot spot created by the cap. These ideas will be further explored as the chapter proceeds.

8.3 PRIMERS AND BOOSTERS

There is unfortunately no consistency in the literature regarding usage of the two terms 'Primer' and 'Booster'. In this text the term 'primer' refers to the explosive charge that initiates the powder column. Caps/detonating cord are always attached to or inserted into the primer. A primer *is* a 'booster' in the sense that it takes input energy from the cap or detonating cord and boosts or amplifies it to the point where it will effectively detonate the explosive column. The initiator plus the primer will be referred to as the priming unit (Fig. 8.2).

The primer must have sufficient energy to (a) initiate the detonation reaction in the main charge and (b) sustain it until the primed explosive produces enough energy to support the detonation reaction by itself (Dupont Blasters Handbook, 1977).

Most operators prefer special cast primers. These are available in a wide range of sizes and weight (Table 8.1) and are manufactured with one or more axial holes. The most common sizes used in open pit mining are ¾ lb or 1 lb. Primers generally have a detonation velocity of the order of 7.5 km/sec, a density of 1.6 g/cm^3, a detonating pressure of 200 kbars and a weight strength relative to *ANFO* of 1.18.

As will be discussed later, there are a number of initiating systems available. The one which will be used to illustrate priming principles here will be based on the use of detonating cord. The detonating cord is fastened (tied) to the primer which is then lowered into the blast-hole to the position where initiation is to occur. The hole is then filled to the designed level with explosive. If it is desired to initiate the column at several points along

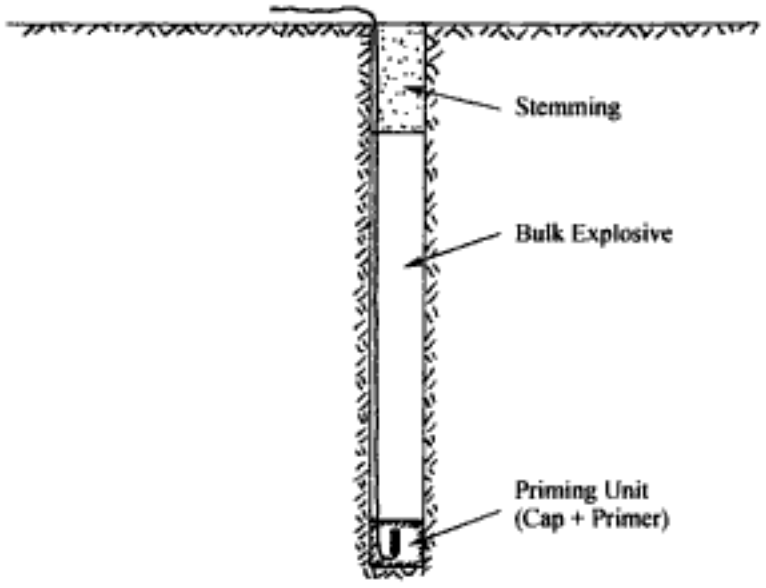

Figure 8.2. Cross-section through a borehole showing the priming unit.

Table 8.1. Typical dimensions of cast primers.

Size (lbs)	Diameter (ins)	Length (ins)
1/3	1 5/8	3 1/4
1/2	1 5/8	4 1/2
3/4	2	4 1/4
1	2 1/4	4 9/16
2.5	3	8
4	4	8

the column at nearly the same time (multiple-point priming), then as each priming point is reached during the charging operation a primer is slid into the hole along the detonating cord. The cord serves to guide them into position and provides positive contact and initiation.

'Boosters' are blasting agents/explosives of higher bulk strength than the main primary column charge which, when inserted at various points along the column increase the energy density (and hence the breaking ability) at those points (Fig. 8.3). The booster *does not* increase the *total* energy output of the primary explosive (i.e., *ANFO*). However, because of its generally higher detonation velocity and pressure than the main explosive, it may 'overdrive' (increase the *VOD*) of the adjacent explosive. The detonation pressure (P_{DET}) and hence the borehole pressure (P_e) are temporarily increased since

$$P_{DET} = 0.25\ \rho\ (VOD)^2 \tag{8.3}$$

and

$$P_e = 0.5\ P_{DET} \tag{8.4}$$

where P_{DET} = detonation pressure (MPa), ρ = density (kg/m^3), *VOD* = detonation velocity (km/sec), P_e = explosion pressure (MPa).

Thus the shock energy would be increased at the expense of the heave energy. Boosting may be of interest at a region where a hard band crosses the borehole or at hard to pull toes. Boosters also help to maintain detonation propagation in relatively insensitive bulk explosives.

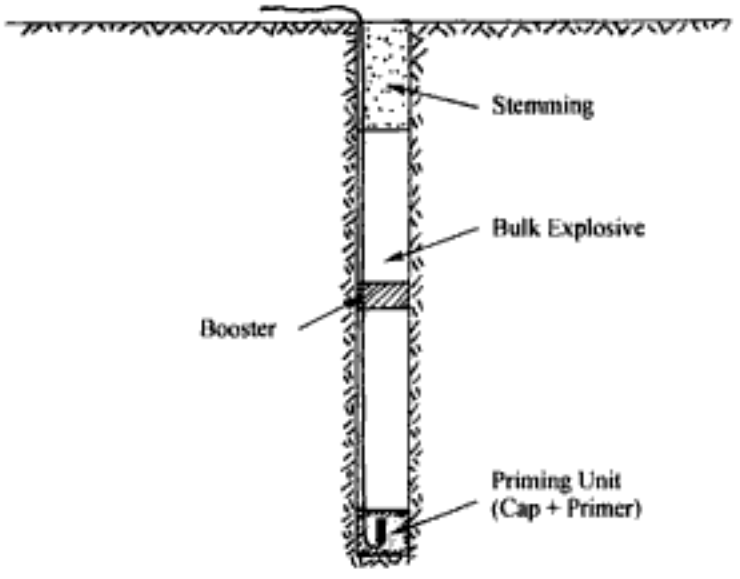

Figure 8.3. The addition of a booster to the explosive column.

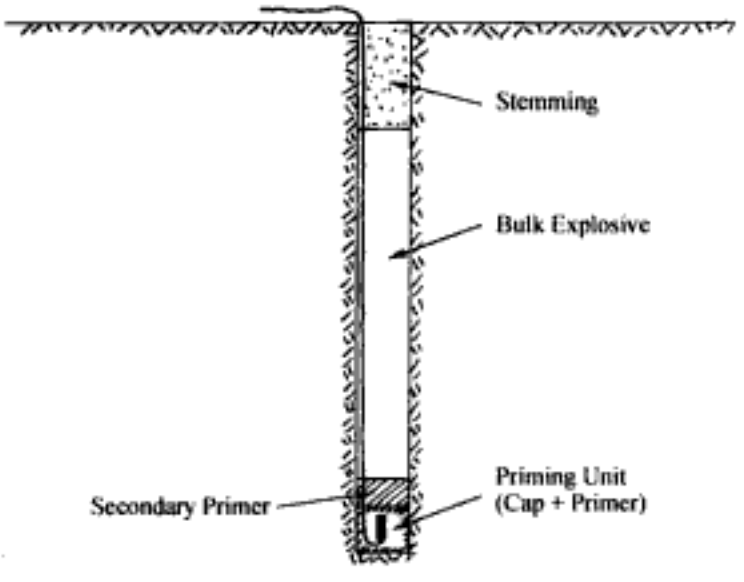

Figure 8.4. The addition of a secondary booster.

The relative cost of primers on a weight (or even energy) basis is much higher than other explosives.

Explosive	Relative cost/unit mass
ANFO	1
Primer	15
Packaged watergel/emulsion	6-8

Therefore it is sometimes of interest to consider the use of a system such as shown in Figure 8.4. Here a bag of high *VOD* watergel/emulsion/slurry is placed between a smaller primer and the primary bulk explosive. It serves as a *secondary* primer. This is sometimes referred to as 'booster priming' or 'combination priming'. This secondary primer which fills the borehole diameter greatly reduces the run-up distance at a fraction of the cost of using equivalent large diameter cost primers.

Some very useful rules which apply to all types of priming units have been provided in the Dupont Blasters' Handbook (1977).

1. The detonator or detonator cord should be fastened so that it cannot be pulled out of or off the primer cartridge or container.
2. The detonator or detonating cord should be placed in the safest and most effective position in the primer cartridge. The primer should protect the detonator or detonating cord.
3. The wires of electric blasting caps or detonating cord must not be subjected to damaging pulls, strains or abrasion.
4. A primer with adequate water resistance should be selected.
5. A system should be developed that allows the entire primer assembly to be loaded safely, easily and in the desired position in the charge.
6. The primer should never be tamped or abused.
7. It is economically sound to use the type, the size, and the number of primers known to insure reliable and efficient priming with a margin of confidence.
8. The detonator should always be directed toward the main charge.
9. The diameter of the primer should approach that of the borehole.
10. The detonation pressure of the primer should always exceed that of the explosive being primed.

The following recommendations are provided in the Dupont Blasters' Handbook (1977) regarding multiple-point priming.

A. Multiple-point priming is *recommended.*

1. In water-filled holes where the sensitivity of the main charge may be affected by water seepage into the product. This is especially true if the holes are not to be shot immediately.
2. Where packaged *ANFO* products having poor cartridge-to-cartridge sensitivity are used. One primer for every two cartridges is recommended.
3. Where blocky or seamy ground may cause cutoffs. This is especially true in deep holes.
4. In ragged (caving) holes where column separation is suspected or probable.
5. Where vibration levels must be controlled by using different delays in decks in each blasthole.

B. Multiple-point priming should be considered when using relatively insensitive explosives.

1. To insure that the explosive detonates along the entire length of the borehole.
2. To minimize cutoffs because of ground movement.
3. To initiate the hole at a faster linear rate.
4. To minimize any disruption of the products by the detonating cord.

8.4 THE END INITIATION OF EXPLOSIVE COLUMNS

The diameter and length of the primer are important when initiating explosive columns. In returning to some of the ideas introduced in Section 8.2, consider the point-initiated bulk explosive loaded into the borehole as shown in Figure 8.5. Upon detonation, the detonation front spreads initially outward as a spherical surface eventually meeting the hole wall.

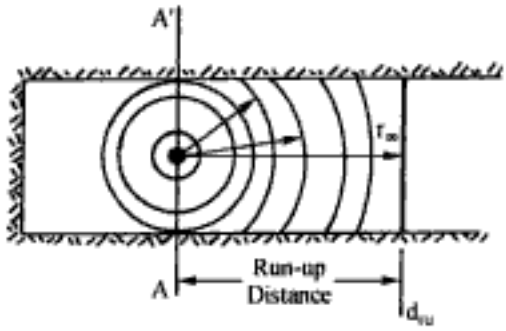

Figure 8.5. Diagrammatic representation of run-up.

As the distance from the point becomes large (r_∞) the detonation wave front becomes essentially planar and under ideal conditions this steady state detonation velocity is maintained through the explosive column. The distance required to reach steady state velocity is called the *run-up distance* (d_{ru}). This distance depends on the strength and geometry of the primer and that of the bulk explosive. At the time of initiation, the velocity of detonation at the primer position is that characteristic of the primer but zero everywhere else along that line. At d_{ru}, the velocity of detonation is characteristic for the explosive of that diameter and confinement. Experiments (Junk, 1972b) have shown that the steady-state *VOD*'s are independent of the type, weight and shape of the primer. Between the point 0 and point d_{ru} the average detonation velocity increases. After d_{ru} it is constant. Thus there is a zone of transient velocity and one of steady state velocity. As indicated the length of the run-up zone varies. Figure 8.6 shows the situation for *ANFO* confined in a tube 76 mm in diameter. The primer-hole diameter ratio varies from 1/3 up to 1. As can be seen the run-up distance is long for the small diameter primer. When the primer has a diameter greater than about half that of the hole, the initial *VOD* is greater than that which can be maintained in the column. In such cases, there is a 'run-down' distance similar to the run-up distance discussed earlier. For *ANFO* in large diameter holes the run-up distance is of the order of 4 to 6 d. The bulk explosive is said to be 'underdriven' by the primer in Case D (Fig. 8.6). In Case A it is said to be 'overdriven'.

As shown in Figure 8.7 the detonation pressure produced by the primer is also important. In this case the primer has the same diameter as that of the explosive column and primers of different detonation pressures have been used. Since the detonation pressure for *ANFO* is of the order of 4000 MPa, the conclusion is that the primer should always have a detonation pressure greater than that of the explosive filling the column in order to minimize the run-up distance. Figure 8.8 shows a series of *VOD* versus distance curves for *ANFO* placed in a 10-5/8″ diameter blasthole and detonated using primers of different geometrical and detonation characteristics. For the 1-lb cast primer (diameter about 2″) the run-up distance is about 3.5 times the hole diameter with a starting *VOD* about 60% that of terminal. For the 5-lb cast booster, the starting *VOD* is about 85% of terminal with about the same run-up. As the size and strength of the primer is increased the run-up decreases until it is eventually overdriven. Obviously there are cost consequences to these performance improvements which must be carefully considered when selecting the priming technique.

The position along the hole at which the priming occurs also changes the explosive performance. In bench blasting, the preferred position of initiation is near the toe. The reason for this is that as the detonation progresses towards the collar the expanding gases are confined entirely by the rock mass until the detonation wave blows out the stemming. The time

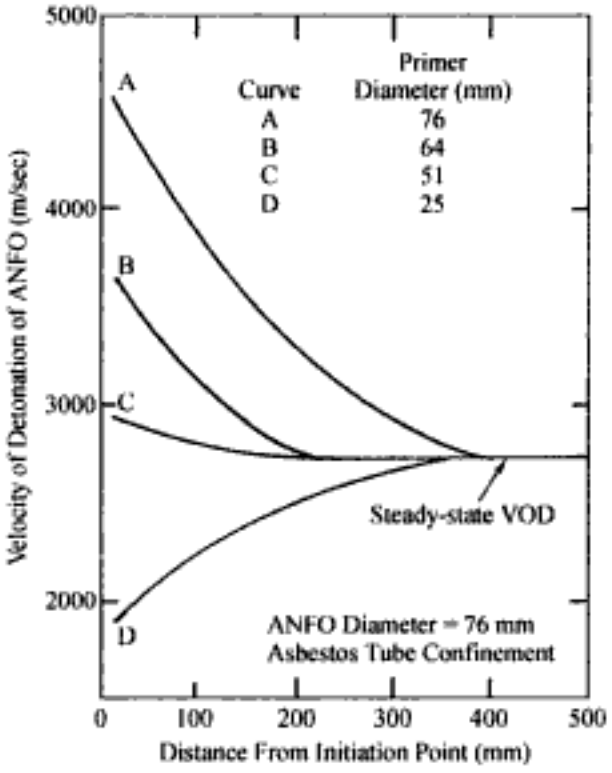

Figure 8.6. Velocity of detonation as a function of distance from the initiator and primer diameter (Junk, 1972a and Hagan, 1979.).

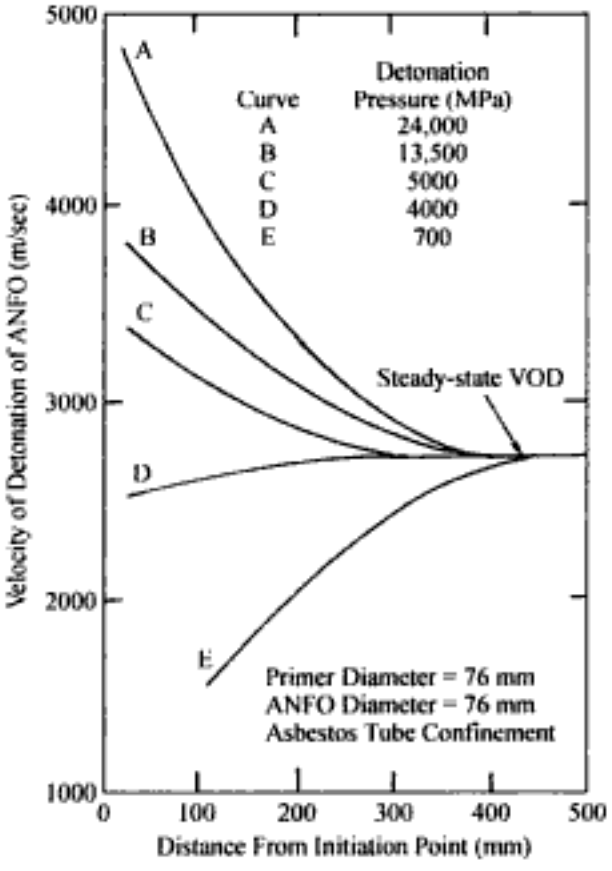

Figure 8.7. Effect of primer detonation pressure on initial velocity of *ANFO*. Junk, 1972a.

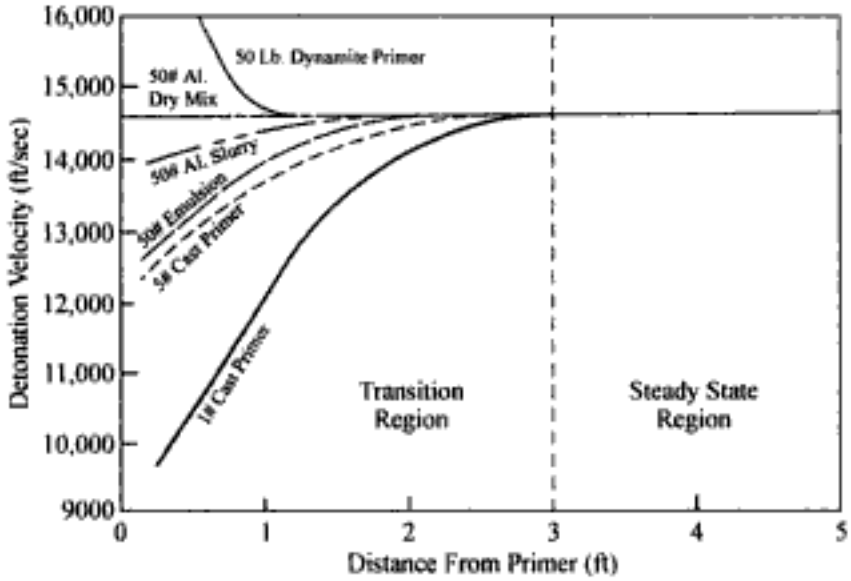

Figure 8.8. Effect of the primer characteristics on the run-up distance for *ANFO* in a 10-5/8" blasthole. Gulf Explosives, 1975.

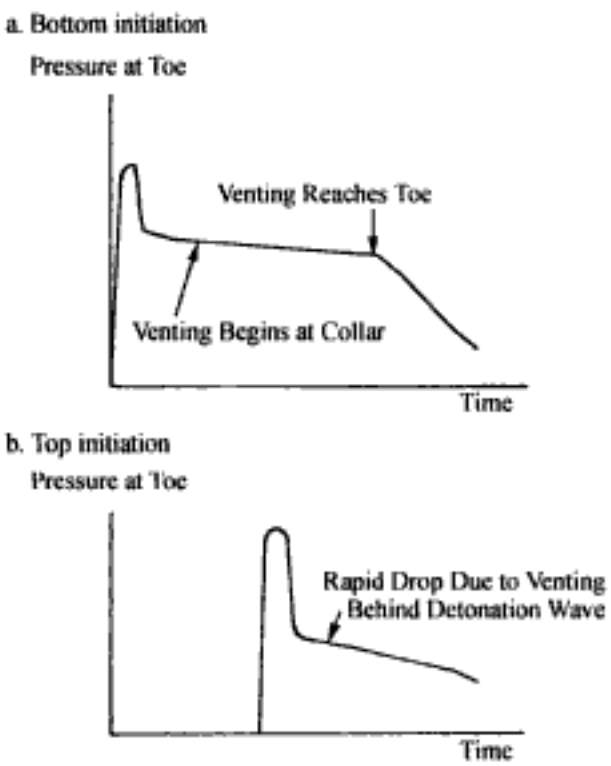

Figure 8.9. Toe pressure variation with collar and toe initiation. AECI, 1987.

interval between commencement of detonation and when gas pressure starts to fall at the collar as the stemming begins to eject, is typically 3 to 4 milliseconds depending on the detonation velocity and column length. With hole bottom initiation (Fig. 8.9a), the subsequent pressure drop takes longer to reach the toe than with top initiation (Fig. 8.9b). In addition, the impulse of the shock wave is towards the collar which tends to lift the burden.

Hence vibrations are reduced and swell increased. With bottom initiation the energy is not only confined longer than with top initiation but it works more effectively (AECI, 1987b).

8.5 THE SIDE INITIATION OF EXPLOSIVES

One can now extend the general initiation process described previously to examining the effect of detonating cord running through a column of explosive. Figure 8.10a shows the typical case when the detonating cord runs along the side of the hole. For hole sizes typically used in open pit mining, the cord size is so small (a typical diameter for down line is of the order of 0.25 in.) in comparison that it appears as a line initiator. However, if the detonation pressure is sufficiently high (Fig. 8.10b) side initiation of the column can occur. The proximity of the cord to the hole wall enhances the effect of the detonation. If the detonation pressure is high but not sufficiently high to initiate the explosive, dead-pressing of the explosive in the near vicinity of the cord can result (Fig. 8.10c). As the hole diameter becomes larger, the significance of this affected area compared to the total cross-sectional area becomes small. The inverse is obviously true. In any case, the energy which is contained and paid for both in terms of the hole and the explosive is lost. As indicated, the 'dead-press' density for *ANFO* is of the order of 1.25 g/cm^3.

The situation resulting when the detonating cord is positioned in the center of the column such as shown in Figure 8.11a. It should be noted that this would only be accomplished with a great deal of trouble in bulk blasting. However, if the cord detonates but is not sufficiently strong to initiate the surrounding bulk explosive, then there can be a 'dead-pressed' zone in the center of the charge (Fig. 8.11b). In small diameter holes, this may be sufficient to prevent the detonation of the hole or produce only a partial detonation.

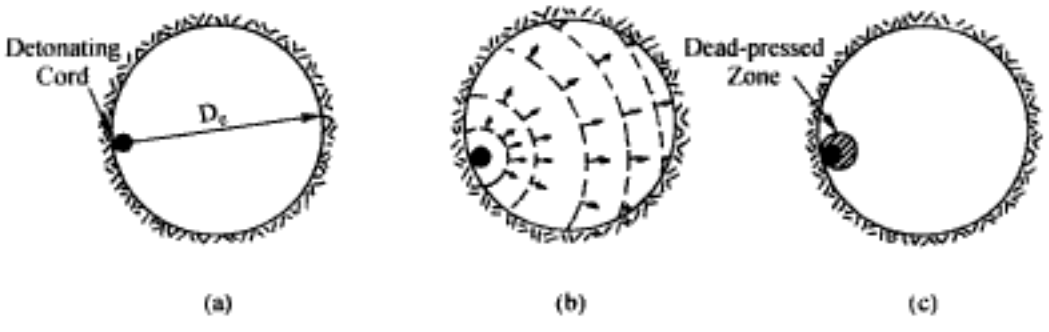

Figure 8.10. Dead-pressed zone due to detonating cord located along the borehole wall.

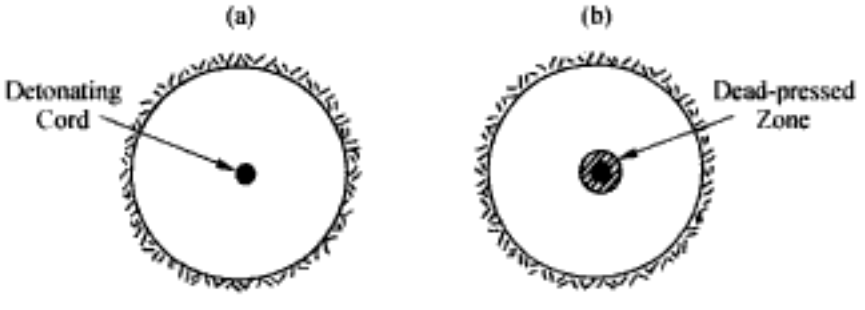

Figure 8.11. Dead-pressed zone from center-positioned detonating cord.

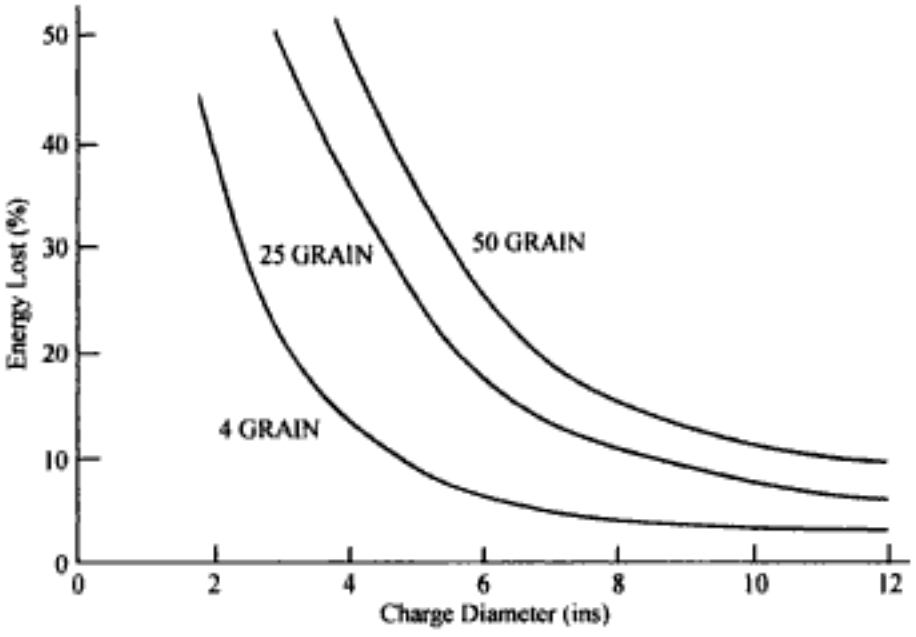

Figure 8.12. The explosive energy lost due to the effect of the detonating cord. Drury & Westmaas, 1978.

In summary, the effect of the detonating cord (assuming that detonation is not produced) is to decrease the energy of the remaining explosive column. The extent of the energy loss is shown as a function of the hole diameter and detonating cord strength for *ANFO* in Figure 8.12. In general, the extent of the energy loss depends upon

- The explosive,
- The energy of the downline,
- The hole diameter,
- The strength of the confining rock,
- The time delay between the downline firing and the returning detonation front from the explosive column.

There are also systems based upon the use of very low strength detonating cords which produce little or no damage to low sensitivity explosives. They require, however, a detonator/primer/secondary primer/to initiate the explosive column.

Today, there are several non-electric systems based upon 'cords' which do not detonate but instead carry a flame to a detonator. In passing through the explosive column, they do not damage it. An example of this is Nonel. Initiating systems based upon the use of electric wires carrying current to the detonator also do not damage the explosive column. These are discussed later in this chapter.

There are some situations in which it is *desired* to side initiate columns of explosive. In 'tracing' (Hagan, 1980 and Hagan & Mercer, 1983), a line of detonating cord of high enough strength to initiate the column is strung along the side of the hole and the hole filled with explosive. Because the maximum distance for the detonation front to travel while building up velocity is the hole diameter D_e (Fig. 8.10a) and the diameter of the line primer is much smaller than the hole, the mean *VOD*, $\overline{V}_S$, is much lower than the steady state *VOD*, $\overline{V}_e$, achieved in end initiated charges. This is true even when the side initiation is caused by very high strength detonating cord. Since the detonation pressure and hence the explosion pressure is proportional to the square of the *VOD*, there is a major difference in

the final borehole pressures. Thus although the total energy released from end initiated and continuously side initiated explosives is the same, the energy partitioning is quite different. For side initiation, the amount of shock energy is significantly reduced. More importantly however, the initial borehole pressure is very similar to the final equilibrium pressure which is somewhat lower than with end initiation. This means that the pressure is maintained at a higher level for greater displacements of the burden. Thus the change from end initiation to side initiation produces a reduction in shock energy and an increase in heave energy. End initiation is most effective in hard, brittle massive rocks whereas side initiation is most effective in rocks which are soft, weak and/or exhibit a large number of natural cracks and planes of weakness. Since heave energy is primarily responsible for mass movement, side-initiated charges perform well where maximum displacement of the burden is required. The advantages of side initiation have also been used in the gentle blasting of perimeter holes.

8.6 INITIATING DEVICES

There are a number of techniques which can be used for introducing energy into a column of explosives and thereby initiate detonation. In this section the primary ones will be briefly described.

8.6.1 *Cap and fuse*

Black power (gun powder) is a very old technique for generating a rapid release of energy. Invented by the Chinese in the 4th century it eventually found it's way to Europe through the activities of the Barbarians in the early part of the 12th Century. Black powder consists of a mixture of

- Carbon,
- Sulfur,
- Potassium nitrate (salt peter),

in the following ratio:

$$8C + 3S + 10KNO_3 \rightarrow 3K_2SO_4 + 2K_2CO_3 + 6CO_2 + 5N_2$$

Unconfined, black powder burns or deflagrates. When inserted in the confines of a borehole, however, the hot gaseous products produce pressures high enough to fracture rock. Black powder is still used today in some applications. It is considered to be a very low energy blasting agent rather than an explosive. The gaseous proportion is 100% of the total energy released. There is no shock component.

Safety fuse consists of a core of black powder (gunpowder) wrapped in textiles with layers of water-proofing materials like bitumen. It is enclosed in a tough outer jacket. These coverings are designed to protect the black powder core from the penetration of water and fuel oil. Fuse is lit by a match or a special lighter. It sputters as the flame front travels along the fuse. The burning rate of safety fuse is approximately 100 seconds/meter.

At the end of the fuse is a plain detonator (cap) containing a small amount of a heat sensitive primary explosive such as mercury fulgamate. The cap consists of a small aluminum cylinder approximately 6mm in diameter, closed at one end, and loaded with a double-layered charge which is pressed into the base (Fig. 8.13). The upper primary ex-

Hidden page

$$\Delta t_1 = 43 \times 10^{-6} \text{ sec} = 43 \text{ μsec.}$$

If delay times longer than those naturally provided by the cord are desired, separate delay elements are added to the circuit. The detonating relay connector (DRC) shown in Figure 8.14 is one such design. As can be seen, the connector is designed and constructed for easy hookup. The detonating cord trunkline is cut and each of the free ends is looped through one end of the connector. The design shown in the figure actually consists of two delay elements (of the same number) one on either side of the central section containing the hole for the downline. A simplified drawing of the concept is shown in Figure 8.15. As can be seen the high explosive (*HE*) ends are pointed toward one another. Thus if the detonation in the trunkline comes from the right hand side of the figure delay element 1 will function. At the end of the delay period, *HE*1 will explode, setting off the downline running through the central hole and knotted. *HE*2 will also explode setting off the next section of detonating cord without delay. If however the detonation in the trunk line occurs from the left then delay element 2 is in function. This system is a security measure should

Table 8.3. Strength of common detonating cord.

Nominal PETN core load (grams/ft)	(g/m)	Approximate external diameter (ins)
15	3	0.14
18	4	0.165
25	5	0.170
30	6	0.175
40	8	0.190
50	10	0.20-0.30*
100	20	0.25
200	40	0.30
400	80	0.40

*Depends upon breaking load

(a) Top View

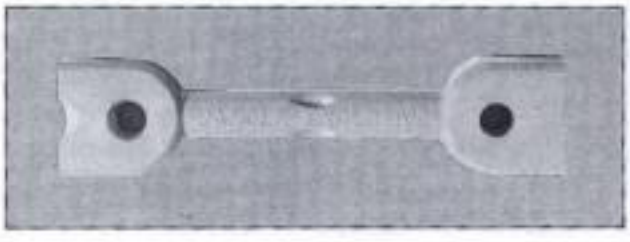

(b) Side View

Detonating Relay Connector

Figure 8.14. Detonating relay connector. ICI, Firing With Detonating Cord.

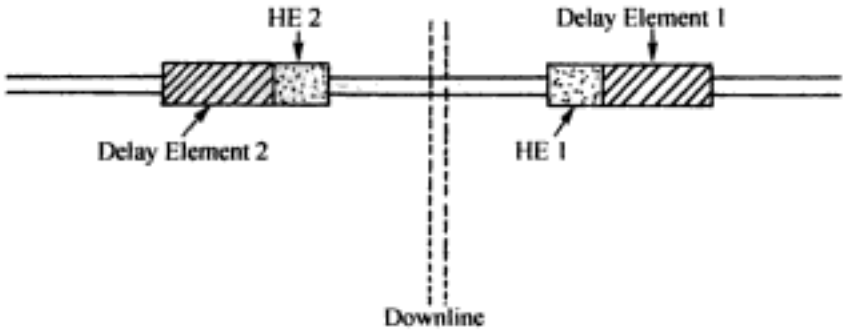

Figure 8.15. Diagrammatic representation of the detonating relay connector.

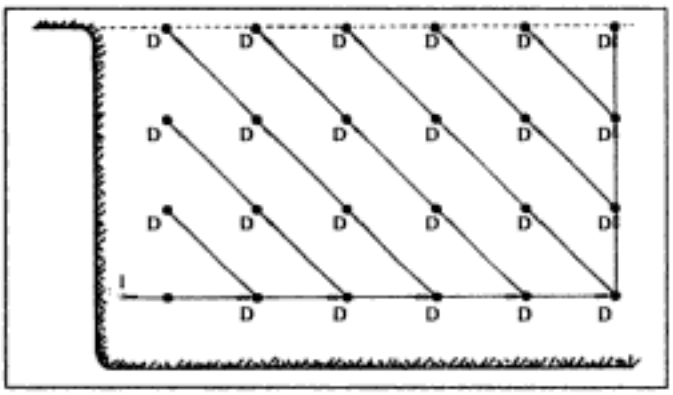

Figure 8.16. Delay location (D) for a corner shot. ICI, Firing With Detonating Cord.

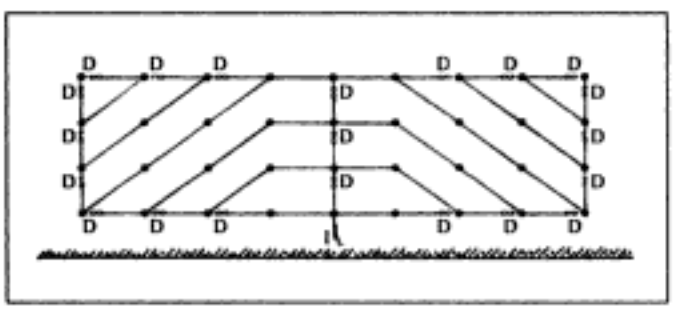

Figure 8.17. Delay location (D) for a face shot. ICI, Firing With Detonating Cord.

a portion of the trunkline be cut-off for any reason. There is also no 'right-or-wrong' direction when connecting them up.

Figures 8.16 and 8.17 show two common delay patterns used in surface mining. The delay element (*D*) is inserted as *close* as possible to the hole firing next and as far away as possible from that firing first. One may use single trunk line arrangements such as shown in Figure 8.16 or closed loop trunklines (Fig. 8.17). If in the former, the trunk line should be disturbed either prior to or during blasting, the detonation will proceed only as far as the break and then stop. In large complicated blasts the closed loop design is generally used. In this case, firing information has two paths by which to reach the individual holes.

Table 8.4 gives the nominal delay times for detonating relay connectors. Although relays with firing times of 25 ms, 35 ms and 45 ms fulfill the majority of delay blasting requirements, in some situations in which ground conditions and/or blasthole patterns are such that cutoffs due to premature ground movement are likely to occur, relays with short delay times (e.g. 15 ms) may help to avoid misfires. Where cutoffs cannot easily occur, there are advantages in increasing the delay time up to 45 ms or even 60 ms.

Table 8.4. Nominal delay times for surface detonating cord connectors (ms).

15
25
35
45
60

Detonating relay connectors are a convenient and safe means of firing a short delay blast with detonating cord. Their advantages are:

– Unaffected by stray currents or static electricity,

– Simply tied into the trunkline system wherever necessary to achieve the desired sequence of firing,

– The number of holes which can be fired in a single blast is virtually unlimited.

Although used primarily as surface delays, it is even possible to connect such delays in downlines.

There are several different design options when using detonating cord downlines. Three will be discussed here:

Case 1. The detonating cord used has enough energy to initiate primers but not the bulk loaded explosives making up the column. Normally the core load of the downline is of the order of 10 g/m. In this situation as the detonation in the cord reaches the position of the primer it detonates. Use of packaged explosives of the same type as those bulk loaded is a special case of this procedure.

Case 2. The detonating cord used has enough energy to initiate the explosives used in the explosive column.

Case 3. The detonating cord used does not have enough energy to detonate either the column explosive or the primer. A cap with or without a delay element is used between the downline and the primer.

In Case 1, the points of initiation are at the primer locations. The primer uppermost in the hole would detonate first followed by the others. Down hole delays may be inserted into the downlines (Fig. 8.18a). Normally however the delay between primers would simply be that provided by the detonating cord itself. The following steps have been recommended for use by ICI (ICI, Firing With Detonating Cord) when priming and charging non-detonator sensitive bulk *ANFO* and water gels.

Step 1. Check that the blasthole is unobstructed to full depth.

Step 2. Make a simple knot in the detonating cord 1.0 to 1.5 m from the end. Thread on the primer and make a further knot to hold the primer securely between the two knots. Now tie the end of the detonating cord to a piece of rock small enough to pass freely down the blasthole yet heavy enough to act as a good sinker (Fig. 8.18b).

Step 3. Lower the sinker and primer into the blasthole. When the sinker is on the bottom and while maintaining tension on the downline cut the detonating cord from the reel 1.0 to 1.5 m from the collar. The tension will keep the downline straight and should hold the bottom primer above the sinker, clear of any fine cuttings or sludge.

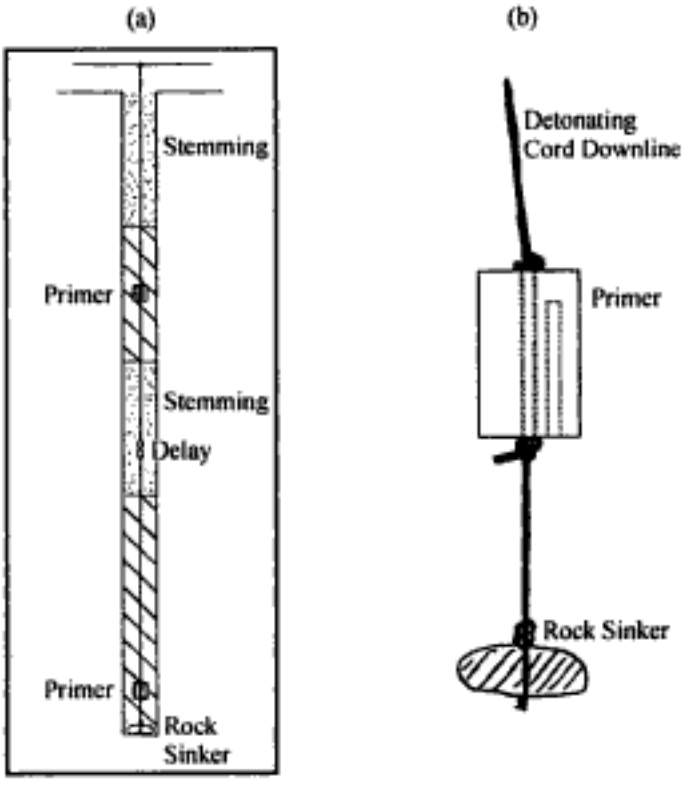

Figure 8.18. Attachment of primers to detonating cord. ICI, Firing With Detonating Cord.

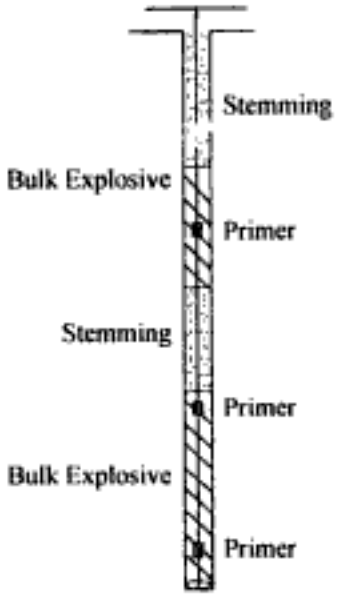

Figure 8.19. Primer location for decked charges. ICI, Firing With Detonating Cord.

Step 4. Anchor the downline at the collar by placing it under a rock or tying it to a stake. Pour or pump in the *ANFO*, watergel, emulsion, etc. Slide additional primers down the detonating cord as needed during charging. These may be to prime the tops and bottoms of decks of explosive or to effect multipoint priming of a full column of explosive. Charging is interrupted as necessary to insert stemming between decks. Maintaining the tension on the detonating cord will avoid snagging by loading hoses, permit primers to slip into position quickly and ensure that the bottom primer is embedded in explosive uncontaminated by dirt or sludge (Fig. 8.19).

When using a packaged or cartridged non-detonator sensitive packaged explosive, the same procedure as just described is used except that a primer should be slid down the detonating cord after every 2 cartridges. The first primer is sent down on top of the first cartridge into the hole (Fig. 8.20).

In Case 2, the detonating cord has sufficient energy to initiate the explosive without the use of a true primer. The following steps have been given by ICI (ICI, Firing With Detonating Cord) for use in the priming and charging of cartridged, detonator sensitive explosives.

Step 1. Check that the blasthole is unobstructed to full depth with a mirror and measuring tape or a plumb line gauge.

Step 2. Attach the detonating cord to the bottom 'primer' cartridge so that the cord cannot be readily pulled out. Figure 8.21 shows one method for large diameter explosives.

Step 3. Insert a rod or spindle through the axial hole in the reel of detonating cord. The spindle may be held in one hand while the primer cartridge is lowered into the blasthole with the other. It is preferable, however, to mount the spindle in a cradle at the side of the blasthole so that both hands can be used to lower the primer cartridge to the bottom of the blasthole.

Step 4. Ensure that the primer cartridge is at the bottom of the blasthole. In a dry hole, raising the cartridge about 0.5 m from the bottom and allowing it to fall freely will produce an audible 'thunk'. Waterfilled holes should be checked with the measuring tape.

Step 5. Cut the detonating cord from the reel approximately 1.0 m from the collar of the blasthole. Wrap or tie the tail end of the detonating cord to a rock or piece of wood to hold it to one side and prevent it from falling into the hole. This tail will

(a) compensate for any slumping of the first cartridge into the cuttings or sludge at the hole bottom and

(b) be used to make a connection to the surface trunkline.

Step 6. Move the reel of detonating cord away from the blasthole just primed or move it on to the next one. A reel should never be left connected to the downline. In the event

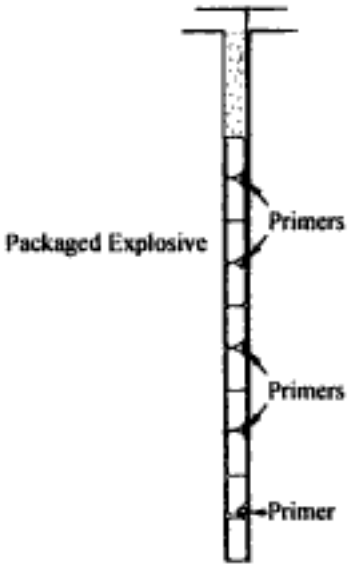

Figure 8.20. Primer location when using packaged explosives. ICI, Firing With Detonating Cord.

Hidden page

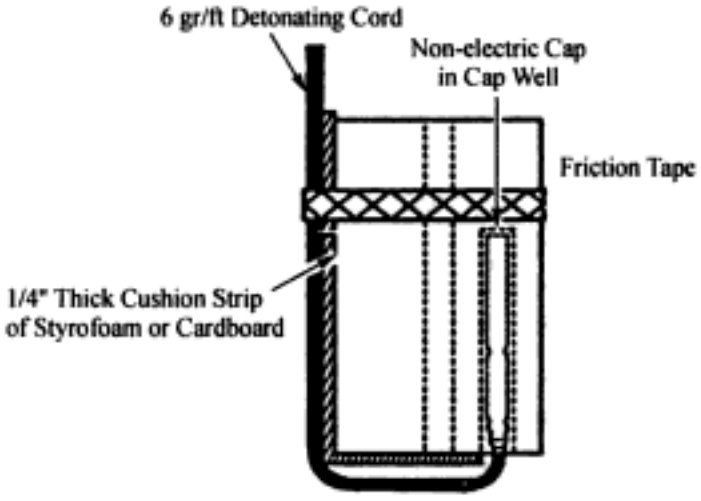

Figure 8.23. Attachment of cord and cap to the primer. DuPont Blasters Handbook, 1977.

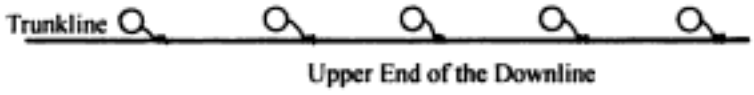

Figure 8.24. Trunkline-downline arrangement.

Figure 8.23 shows one technique for attaching a primer to a low energy (6 grains/ft or 1.3 g/m) detonating cord terminated in a delay cap. As can be seen the cord is run *beside* the cast primer and the cap is pushed into the well. A 1/4" thick cushioned strip of styrofoam or card board is used to absorb the shock of the detonating cord. The cord is taped to the primer using friction tape. The low energy cord will not initiate the primer but it could cause it to crack if run through the center hole. In this case, initiation of the explosive column occurs at the primer position. As indicated, delay caps may be used. To achieve multiple priming of the hole, separate lines must be run from the surface.

The detonating cord downlines must now be attached to the surface trunkline system. There are several ways in which this may be done. Figure 8.24 shows diagrammatically the detonating cord trunk line running past the line of holes. The simplest method of connecting the two lines is through the use of a knot or a wrap. It is very important that the connection be tight and made at approximately right angles as shown in Figure 8.25. Figure 8.25d shows a method which can be used for extending trunk lines.

8.6.3 *Non-electric systems*

Although the detonating cord-based ignition system is non-electric as well, the 'non-electric' as used in this book refers to the Nonel and Nonel-type systems. The Nonel system developed by Nitro Nobel in Sweden is based upon the use of a tough sealed plastic tube (OD = 3 mm, ID = 1.2 mm) the inside of which is coated with a reactive substance. A shock wave and spark are transmitted to the tube using either a special blasting machine or a detonator. The shockwave whirls up a dust cloud of the reactive material which is initiated by the spark. This dust explosion travels along the tube at a speed of about 2000 m/sec. The entire reaction takes place *within the tube* which remains intact throughout the process. Because of this

– The tube by itself is not classified as an explosive

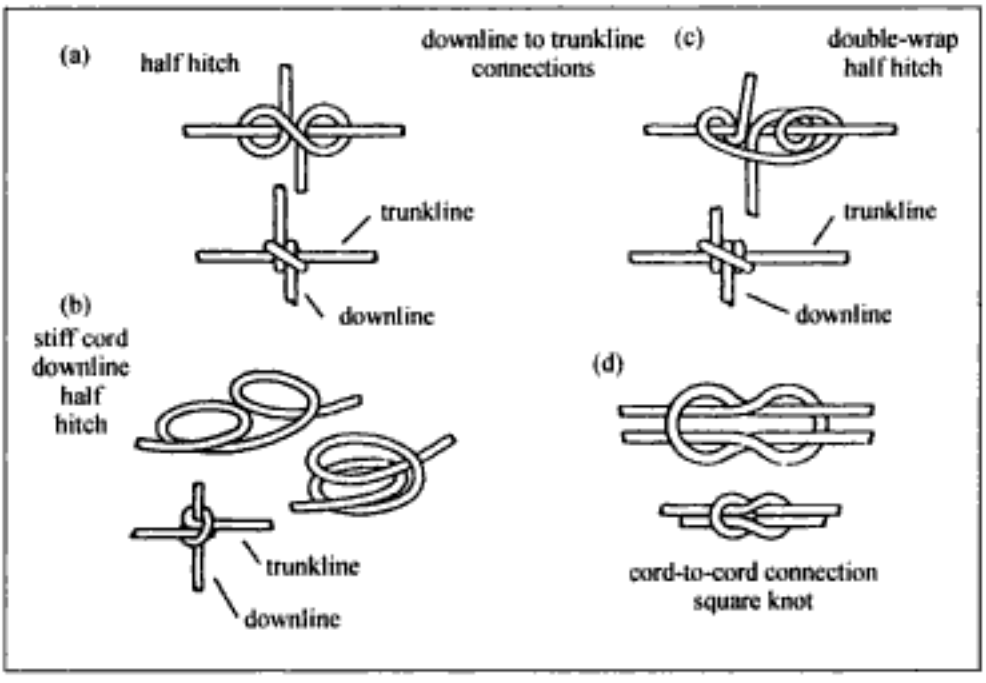

Figure 8.25. Attachment of the downlines to the trunkline. Dick et al., 1993.

– It does not affect anything around it. When used as a downline, it does not affect the surrounding explosive

– The reaction is quite silent. This has environmental advantages over detonating cord, for example.

The difference between the detonation front in Nonel tube and detonating cord is rather dramatically illustrated in Figure 8.26. To avoid moisture entering into the tube and thereby destroying the 'dust-type' of explosion, the tubes are cut to length and sealed at the factory. One end is simply sealed, the other is equipped with a delay detonator (Fig. 8.27). The detonators with their attached tubes (Fig. 8.28) are then packed in aluminum foil bags. The range of the available detonators is shown in Table 8.5.

A series of special connectors have been developed to join together a number of tubes. A connecting block is shown dismantled in Figure 8.29. It consists of a transmitter cap (strength of about 1/7 that of a normal high strength detonator) and a plastic block into which the ends of four Nonel tubes may be inserted. The block is designed to ensure that all ends are in intimate contact with the cap. As seen in Figure 8.30 when the shock wave signal of the Nonel tube (1) reaches the connector (2) the transmitter (donor) cap will be actuated. The transmitter cap in turn initiates all of the connected Nonel tubes (receptors). In this way the initiating impulse passes (3) to one or more detonators and also the next connector (4), where the procedure is repeated. Figure 8.31 shows a fully utilized connector. They symbols shown in Figure 8.32 will be used when describing some typical bench rounds.

Figures 8.33 and 8.34 show two arrangements for hooking up a small bench round. In Figure 8.33 one connector has been used per hole and in Figure 8.34 the connectors have been fully utilized for maximum economy. The zig-zag connection shown in Figures 8.33 and 8.34 *should not* be used in wide bench rounds since, in this case, the *inherent delay* in the Nonel surface lines becomes important. Recommendations for the first period delay to

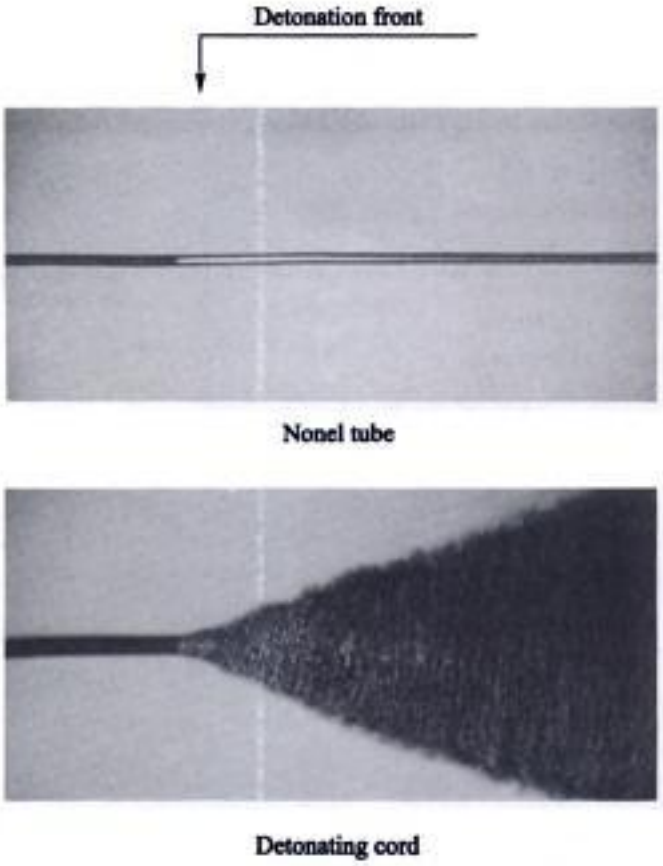

Figure 8.26. Comparison of the disturbance associated with Nonel and detonating cord. Nitro Nobel, Questions and Answers About Nonel.

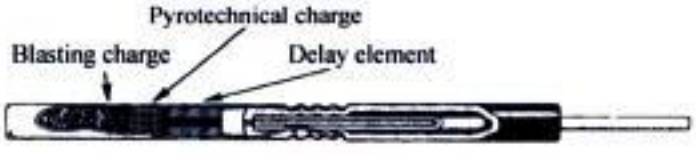

Figure 8.27. Blasting cap used with the Nonel system. Nitro Nobel, Questions and Answers About Nonel.

Table 8.5. Period range for Nonel detonators (Nitro Nobel, Nonel users guide).

Period number	Number of periods	Delay (ms)	Interval (ms)
3 → 20	18	75-500	25
24, 28, 32, 36, 40, 44	6	600-1100	100
50, 56, 62, 68, 74, 80	6	1250-2000	150

be used based upon the maximum length of the coupled surface tubing are given in Table 8.6. In wide rounds it is suggested that all the rows of holes be connected in the same way. Two possibilities are shown in Figures 8.35 and 8.36. Priming units are made up in the same way as has already been discussed with respect to detonating cord blasting. Although normally not a problem it should be noted that the breaking/stretching loads of Nonel tube are significantly less than those of detonating cord, for example. Special tubes with respect to strength, wear resistance and temperature are however, available.

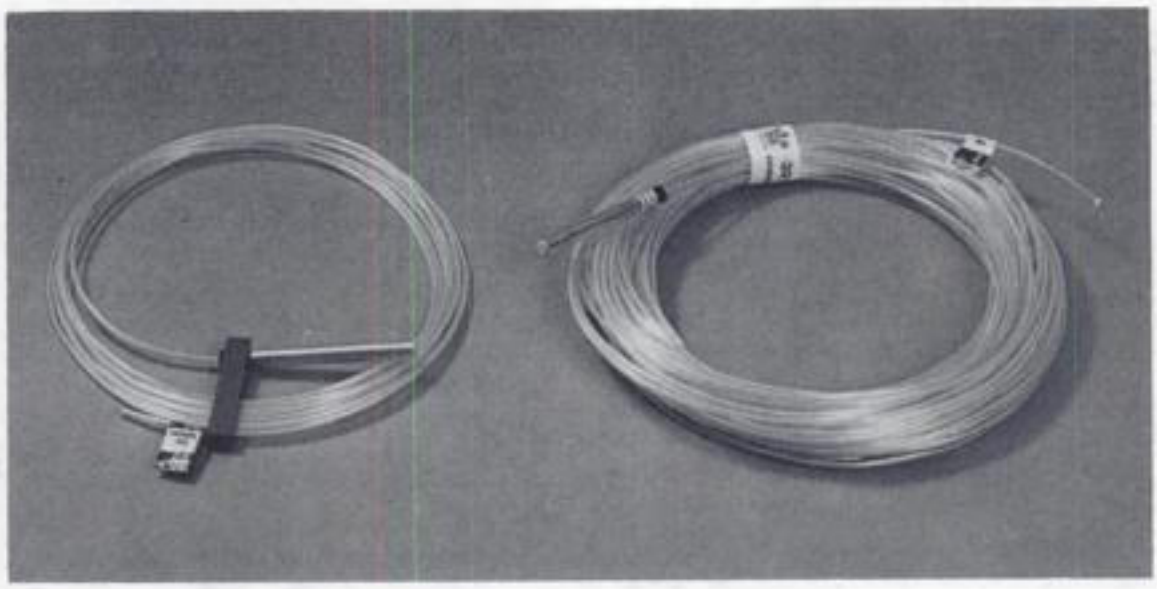

Figure 8.28. Nonel tubes. Nitro Nobel, Nonel Users Guide.

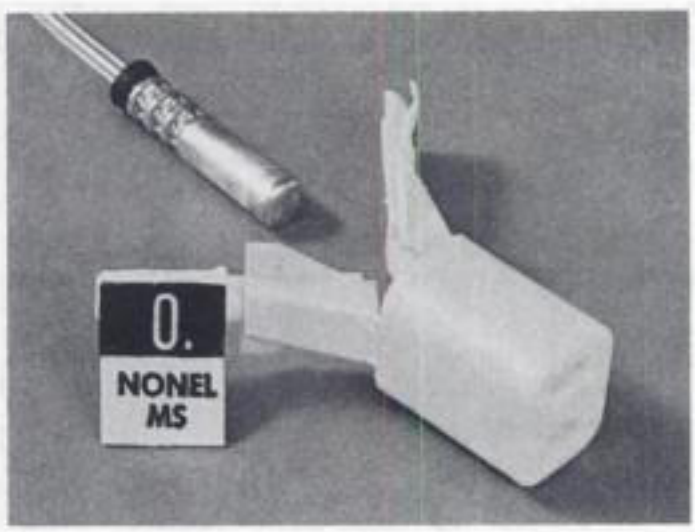

Figure 8.29. A Nonel connector block. Nitro Nobel, Nonel Users Guide.

8.6.4 *Electric initiation systems*

Many mines today employ initiation systems based upon the use of electric delay detonators. Figure 8.37 is a cut-away view showing the construction of one such detonator. The cap is designed so that electricity flows through a circuit comprised of the leg wires and a bridge wire. The bridge is a short, hair-like, high resistance alloy wire similar to the filament in an electric light bulb. Like the filament in the bulb, the bridge heats quickly on the application of sufficient electric current.

The power generated

$$P = I^2R$$

is released as heat. The heat is sufficient to initiate the heat sensitive ignition charge (mercury fulminate, lead azide, etc.) which detonates the base charge (generally PETN) of the cap. The amount of base charge contained within the cap determines its strength. Cap designations such as No. 6, No. 8, etc. are used. The time between the application of the

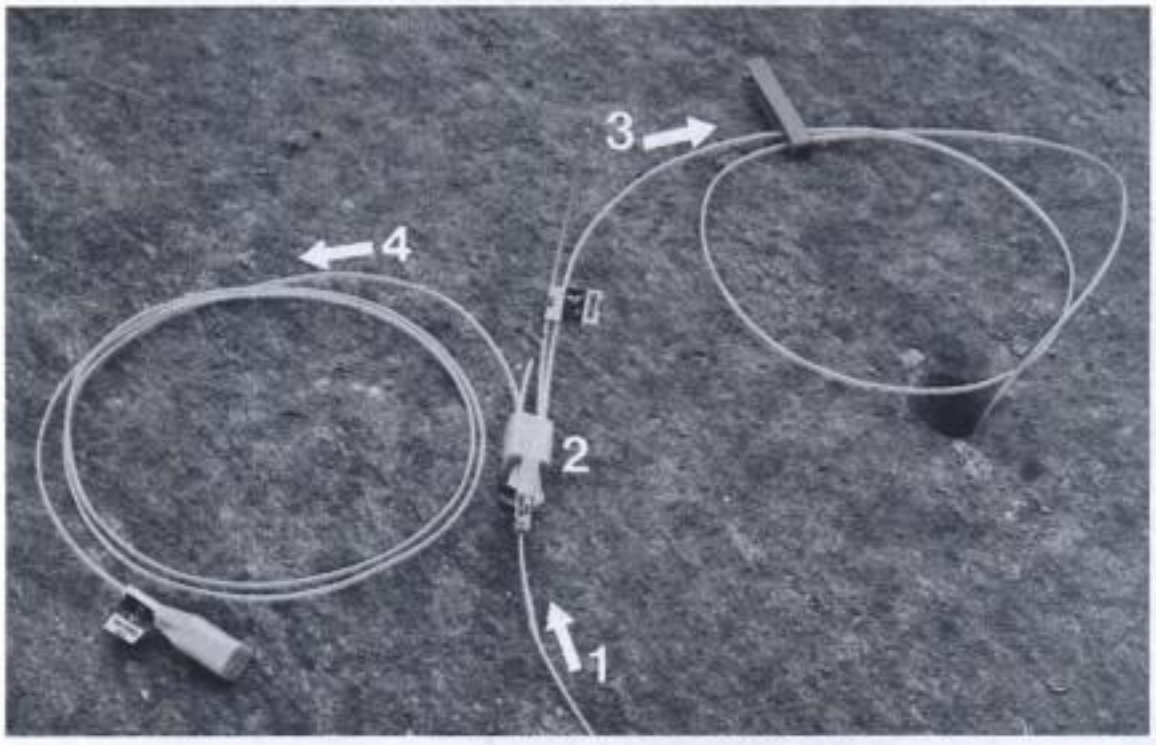

Figure 8.30. Typical connector arrangement. Nitro Nobel, Nonel Users Guide.

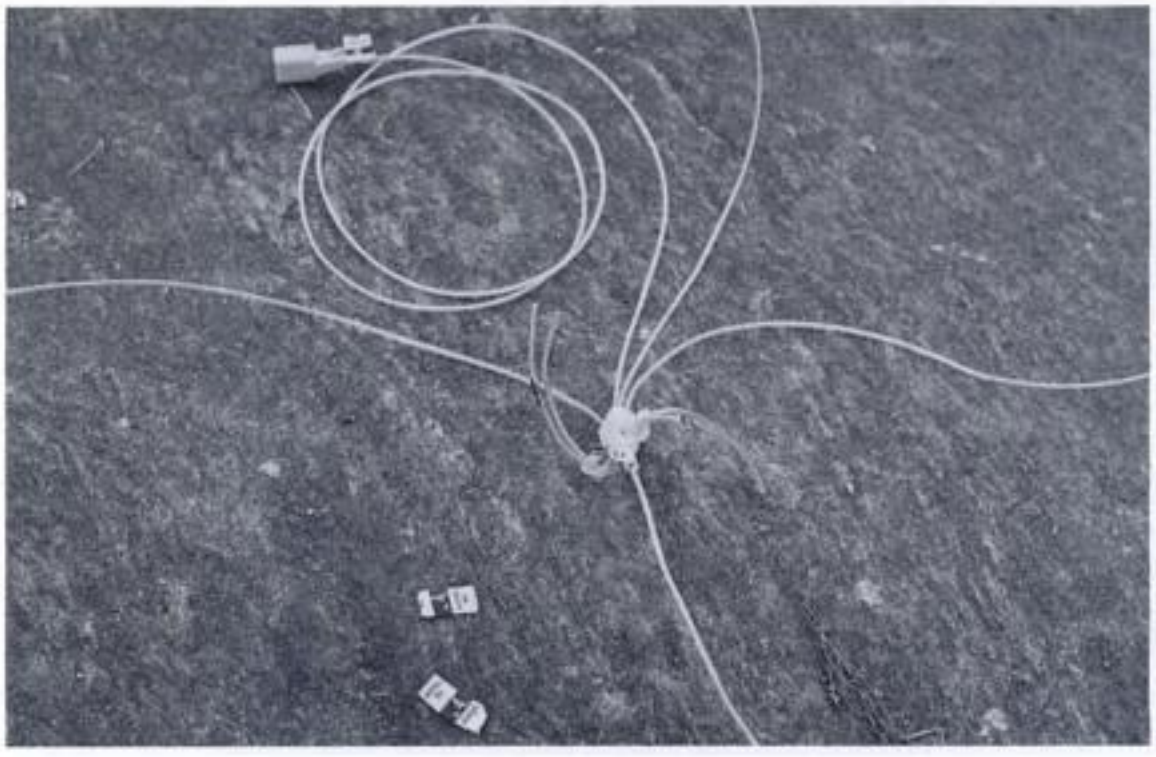

Figure 8.31. A fully utilized block. Nitro Nobel, Nonel Users Guide.

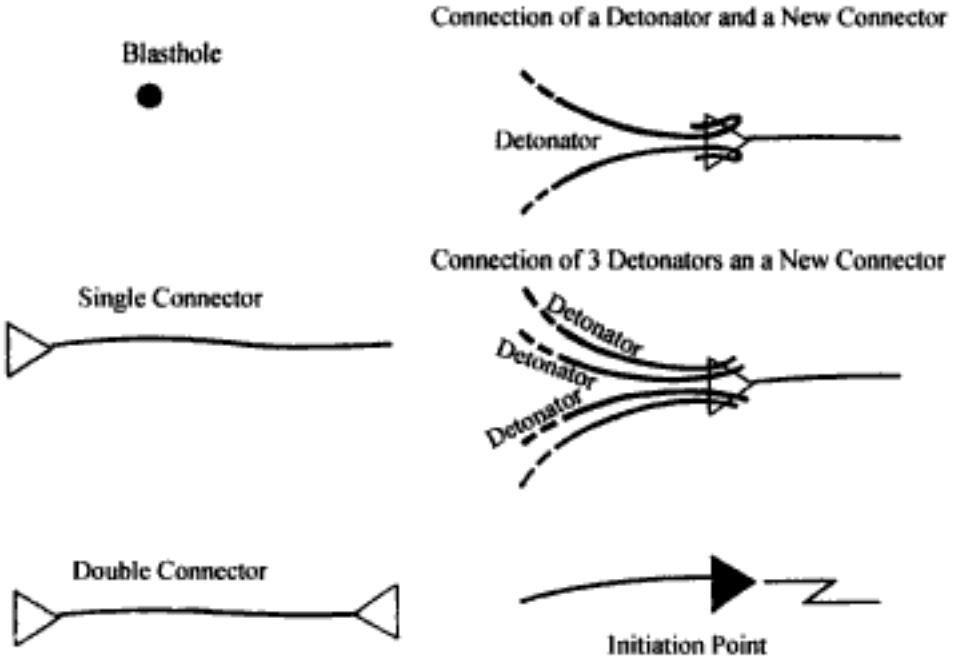

Figure 8.32. Symbols used in the Nonel designs in Figures 8.31 and 8.32. Nitro Nobel, Nonel Users Guide.

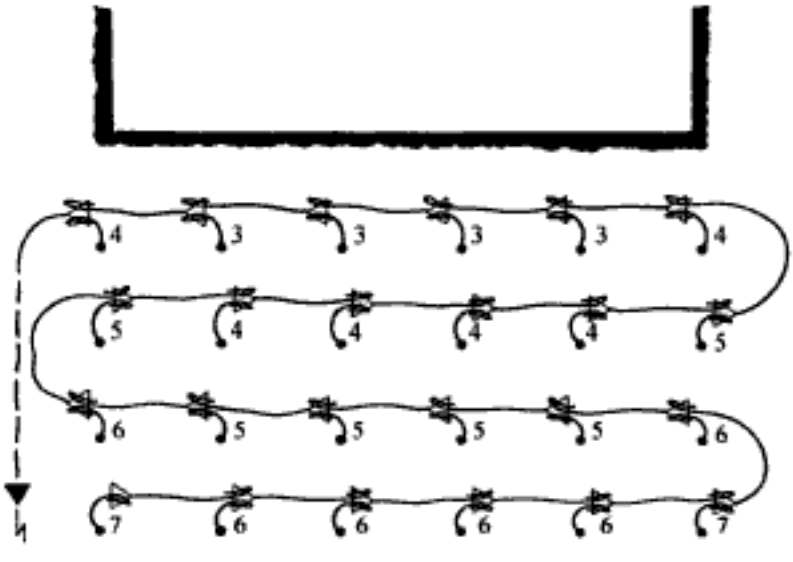

Figure 8.33. A zig-zag connection pattern with one connector per hole. Nitro Nobel, Nonel Users Guide.

current and initiation for a given cap is termed the 'lag-time'. As shown in Figure 8.38 the amount of time required to heat the bridge wire depends upon the applied current. With higher current levels, the time is reduced. There is a certain critical level of current below which there is little or no temperature increase. If the applied current is just above the critical level an appreciable amount of time may be required before the critical temperature is reached and the cap initiates. In such cases, large variations in initiation times may result with caps of the same delay. Excessive currents on the other hand may cause arcing and thereby failures of delay caps. Some recommendations regarding minimum firing currents are given in Table 8.7.

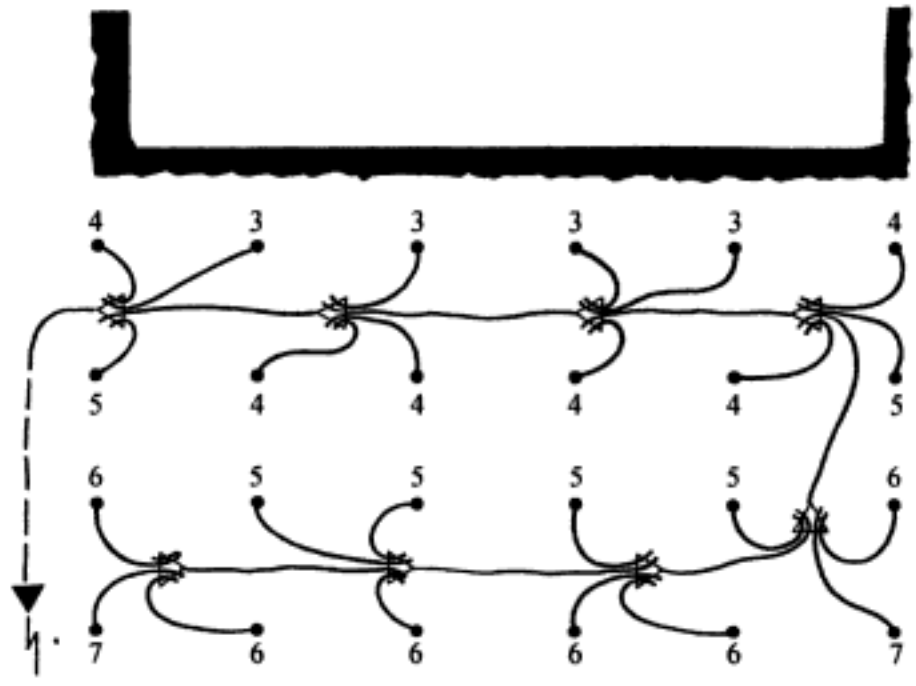

Figure 8.34. A zig-zag connection pattern with fully utilized connectors. Nitro Nobel, Nonel Users Guide.

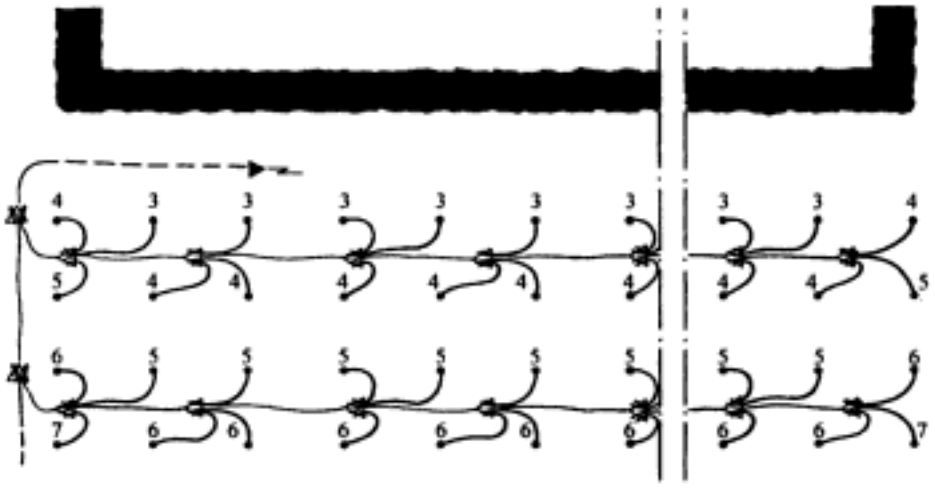

Figure 8.35. Nonel design for wide benches with end connection. Nitro Nobel, Nonel Users Guide.

Table 8.6. Recommended first period in the round (Nitro Nobel, Nonel users guide).

Maximum coupled length of NONEL tubing on the surface, metres	Milliseconds required for the entire surface initiation	Recommended first period in round
Up to 150	Max 75	3
150-200	75-100	4
200-250	100-125	5
250-300	125-150	6
etc.	etc.	etc

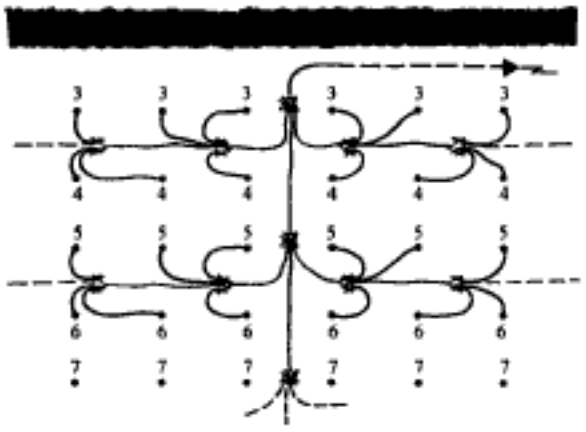

Figure 8.36. Nonel design for wide benches with center connection. Nitro Nobel, Nonel Users Guide.

a. Construction of an Electric Fusehead

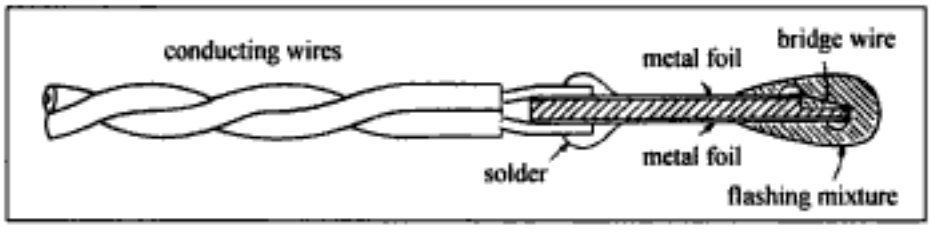

b. Instantaneous Electric Detonator

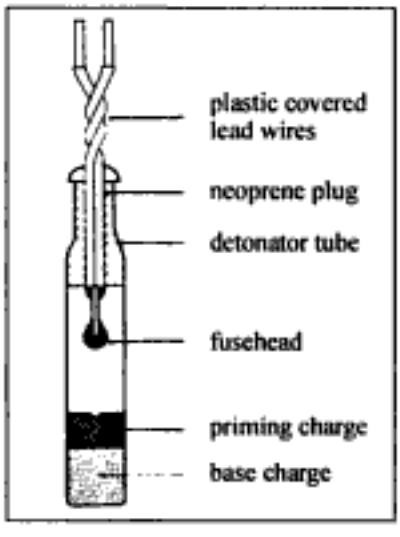

c. Delay Detonator

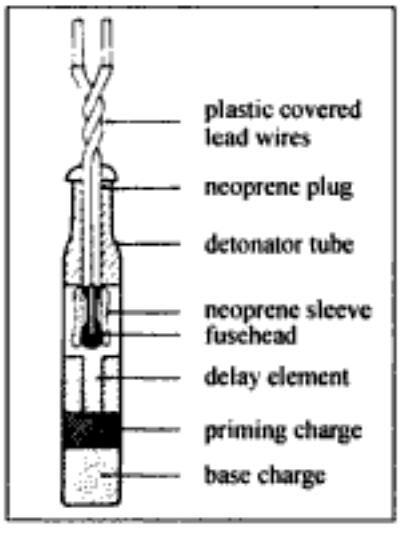

Figure 8.37. An electric blasting cap. ICI, Firing Electrically.

Since the electric current travels with the speed of light in the lead wires, no time delay is introduced in the system by varying lead lengths. Without special delays in the system, all of the holes would be initiated at the same time. Delays are created in the caps by inserting various lengths of compounds between the resistive element and the ignition charge which burn at a given rate. The heat generated by the resistive element causes the delay portion to begin burning. When the burn front reaches the ignition charge, detonation begins. There are two series of delays

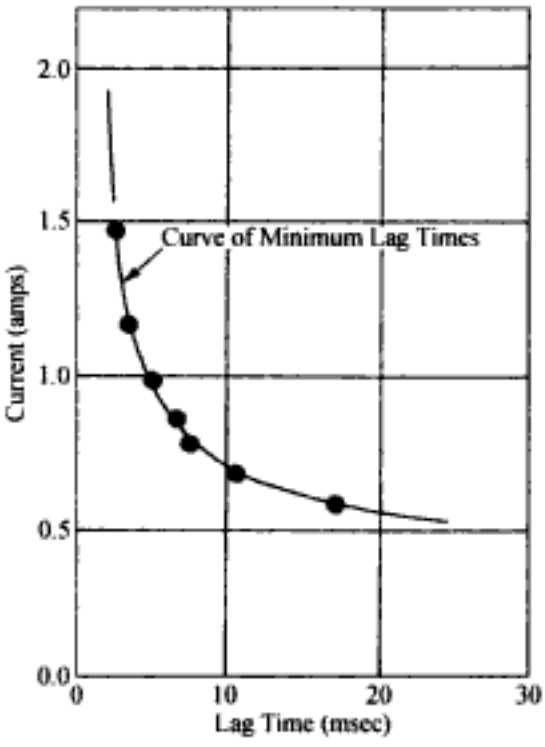

Figure 8.38. Current versus lag time plot for an electric blasting cap. ICI, Handbook of Blasting Tables.

Table 8.7. Recommended minimum firing currents. Austin Powder Company.

Type Circuit	Recommended firing current	
	DC	AC
Single Cap	0.5 amp	0.5 amp
Single Series	1.5 amp	2.0 amp
Parallel Series	1.5 amp/series	2.0 amp/series
Parallel	1.0 amp/cap (min)	1.0 amp/cap (min.)
	10.0 amps/cap (max)	10.0 amps/cap (max)

– Millisecond delay series,
– Half second delay series.

The relationship between delay number and the delay time varies among manufacturers. As a general rule the delay between delay numbers in the millisecond series, is 25 ms. In the half second series the interval is 500 ms. Tables 8.8 and 8.9 present typical delay numbers and intervals for the two series.

The use of the term 'nominal' has been used in the tables to describe the delay times since the true delay is very dependent upon the quality control exercised in the manufacturing process. Small variations in the characteristics of the delay material can lead to a spread in actual delay times around the nominal value. Table 8.10 shows the results of a testing series conducted by Winzer et al. (1979) on caps from four manufacturers. The caps from manufacturers 1, 2 and 3 were from their ms delay series. The caps from manufacturer 4 were non-electric (detonating cord type) ms delays. To arrive at a statistically representative data base, 30 initiators of each delay period were tested. The rated times, the measured mean times ($\bar{X}$) plus the standard deviation (S) have been given. As can be seen there is considerable deviation from the nominal times (T) given by the manufac-

Table 8.8. Millisecond delay series, Austin Powder Company.

Delay No	Nominal delay time (ms)	Delay No	Nominal delay time (ms)
1	25	16	400
2	50	17	425
3	75	18	450
4	100	19	475
5	125	20	500
6	150	21	550
7	175	22	600
8	200	23	650
9	225	24	700
10	250	25	750
11	275	26	800
12	300	27	850
13	325	28	900
14	350	29	950
15	375	30	1000

Table 8.9. Half second delay series, Austin Powder Company.

Delay No	Nominal delay time (ms)
0	0
1	500
2	1000
3	1500
4	2000
5	2500
6	3000
7	3500
8	4000
9	4500
10	5000
11	5500
12	6000

turer. Furthermore, the scatter around the mean firing time increases with an increase in the delay period. Over the past few years, the spread has been considerably reduced. Bajpayee & Mainiero (1990) performed a similar series of tests on the electric detonators from two manufacturers. Twenty detonators of each delay period were tested. The results are presented in Table 8.11. As can be seen, the standard deviation is independent of the period and of the order of 4 ms. Bajpayee & Mainerol (1990) also calculated values of the 'Winzer Index' (Winzer et al., 1979) which is a measure of the likelihood of detonators in two successive periods overlapping. This index is defined as

$$W = \frac{TH - TL}{(SH^2 + SL^2)^{1/2}} \tag{8.3}$$

where W = Winzer index, TH = average delay time for a group of detonators of a given delay period (secs), TL = average delay time for a group of detonators of the next lower period (secs), SH = standard deviation of the group corresponding to TH (secs), SL = standard deviation of the group corresponding to TL (secs).

Table 8.10. Firing times for millisecond delay caps (Winzer et al., 1979).

	Manufacturer A			Manufacturer B			Manufacturer C			Manufacturer D		
Period	T (ms)	$\bar{X}$	S	T (ms)	$\bar{X}$	S	T (ms)	$\bar{X}$	S	T (ms)	$\bar{X}$	S
0	5	5	NA	12	12	NA	1	1	NA	–	–	–
1	25	27.9	4.4	25	28.6	4.0	8	5.7	1.4	25	38.8	1.8
2	50	51.1	6.2	50	50.8	5.9	25	25.3	4.4	50	59.5	9.4
3	75	86.2	4.2	75	62.7	4.9	50	48.6	5.3	75	81.9	1.4
4	100	111.7	5.6	100	98.5	7.1	75	73.0	11.8	100	110.3	3.2
5	125	140.4	7.8	130	138.7	4.5	100	100.1	5.1	125	135.8	2.9
6	150	173.4	6.0	170	178.5	9.4	125	135.8	6.2	150	168.5	5.7
7	175	185.1	5.9	205	202.5	6.1	150	154.5	5.7	175	168.9	7.8
8	200	183.4	9.6	240	253.9	19.6	175	186.3	7.5	200	234.3	5.8
9	250	279.2	9.6	280	326.9	22.3	200	217.4	7.5	250	255.1	3.9
10	300	307.0	11.7	320	324.3	18.0	250	272.0	12.5	300	486.5	23.8
11	350	362.4	34.4	360	382.9	55.9	300	318.5	12.5	350	356.0	4.7
12	400	428.1	19.8	400	401.5	34.2	350	382.1	20.1	400	403.5	6.4
13	450	440.8	18.9	450	496.8	21.2	400	441.6	17.1	450	466.7	12.1
14	500	523.7	24.0	500	506.9	25.5	450	452.1	17.9	500	506.6	7.6
15	600	649.0	51.8	550	697.8	50.1	500	556.4	22.3			
16	700	735.3	46.3	600	797.8	48.0	550	569.7	17.9			
17	800	913.0	56.1	700	1144.6	73.6	650	708.5	29.5			
18	900	992.3	65.1	900	1050.8	101.4	750	813.2	36.2			
19	1000	1166.0	60.7	1200	1366.1	112.1	875	911.1	36.6			

Table 8.11. Firing accuracy of detonators. Bajpayee & Mainiers, 1990.

1. Manufacturer 1

Period	T (ms)	$\bar{X}$	S	slowest (ms)	fastest (ms)	100 S/$\bar{X}$ (%)	Winzer Index
1	25	24.69	3.22	29.00	18.50	13.04	2.47
2	50	43.41	6.86	57.90	31.85	15.80	2.99
3	75	70.45	5.88	78.35	56.10	8.35	2.69
4	100	95.26	7.12	115.60	85.40	7.47	3.12
5	125	120.26	3.68	126.60	112.00	3.06	4.82
6	150	146.33	3.97	153.60	140.20	2.71	5.53
7	175	172.37	2.54	176.20	166.60	1.47	5.83
8	200	195.23	2.99	203.40	190.00	1.53	6.22
9	225	219.85	2.59	224.80	216.20	1.18	6.08
10	250	246.38	3.51	254.40	239.80	1.42	4.36
11	275	272.33	4.81	284.00	265.20	1.77	3.37
12	300	294.51	4.49	305.40	287.80	1.52	5.84
13	325	327.67	3.48	333.00	319.80	1.06	3.20
14	350	343.83	3.65	350.00	338.50	1.06	4.04
15	375	370.53	5.51	384.50	359.00	1.49	4.95
16	400	403.05	3.59	409.50	396.00	0.89	5.96
17	425	435.88	4.18	442.00	426.50	0.96	3.49
18	450	453.23	2.69	457.00	448.50	0.59	4.20
19	475	481.53	6.18	505.50	473.50	1.28	3.82
20	500	523.20	9.00	537.00	503.50	1.72	

Table 8.11. Continued.

2. Manufacturer 2

Period	T (ms)	$\overline{X}$	S	slowest (ms)	fastest (ms)	100 S/$\overline{X}$ (%)	Winzer Index
1	25	26.95	0.87	28.65	25.55	3.23	17.19
2	50	50.66	1.07	52.50	49.05	2.11	9.49
3	75	69.72	1.70	72.95	66.20	2.44	9.54
4	100	92.26	1.64	95.40	88.40	1.78	9.44
5	125	119.69	2.40	124.40	115.90	2.01	9.34
6	150	157.88	3.31	165.30	151.20	2.10	2.80
7	175	176.18	5.63	188.80	164.20	3.20	3.18
8	200	194.87	1.67	199.00	192.40	0.86	9.58
9	225	220.51	2.09	224.40	217.60	0.95	9.08
10	250	247.49	2.11	253.40	244.00	0.85	6.32
11	275	273.53	3.54	279.00	268.00	1.29	5.05
12	300	299.23	3.56	308.80	292.80	1.22	8.40
13	325	342.37	3.60	351.50	336.00	1.05	2.31
14	350	358.06	5.77	370.60	349.80	1.61	4.24
15	375	385.80	3.09	391.00	380.00	0.80	7.55
16	400	441.83	3.64	428.50	416.50	0.86	4.12
17	425	444.43	4.11	452.50	437.50	0.92	2.24
18	450	457.18	3.93	464.50	450.00	0.86	5.69
19	475	488.35	3.82	496.00	483.00	0.78	5.77
20	500	515.90	2.86	520.50	511.50	0.55	

A Winzer value less than 3 indicates significant probability of overlap between adjacent delay periods. As can be seen from Table 8.11, with only a few exceptions, the W values are considerably greater than 3. This suggests that, in general, the probability is low for order reversal when using detonators of adjacent number.

The type of cap and the delay number is marked on the base of the cap. For example an H followed by a 5 means No. 5 Half Second Delay (Fig. 8.39). The resistance of the cap depends upon the length and type of the legwire as well as the type of the cap. Some typical values are given in Tables 8.12 and 8.13. The resistance of fuseheads without lead wires is between 0.9 and 1.6 ohms. There are three different types of wires used to complete the blasting circuit (this is synonymous with the trunklines and downlines of the detonating cord circuit). These are

- Leg wires,
- Connecting wires,
- Blasting cables/firing line/leadwire.

Table 8.14 presents nominal resistance values for copper wire. The wire used in connecting up the round varies with the application

- 25 AWG is used for light duty
- 23 AWG (twin twisted) is used for extending lead wires down the blasthole
- 21 AWG (twin duplex) is used for rugged and abrasive duty

The blasting cables selected vary with the

- Type of duty,
- Distance from the power source,

Hidden page

Table 8.14. Nominal resistance of copper wire.

Gauge No	ohms/1000 ft
4	0.25
6	0.40
8	0.63
10	1.0
12	1.6
14	2.5
16	4.0
18	6.4
20	10
21	16
23	18
25	26

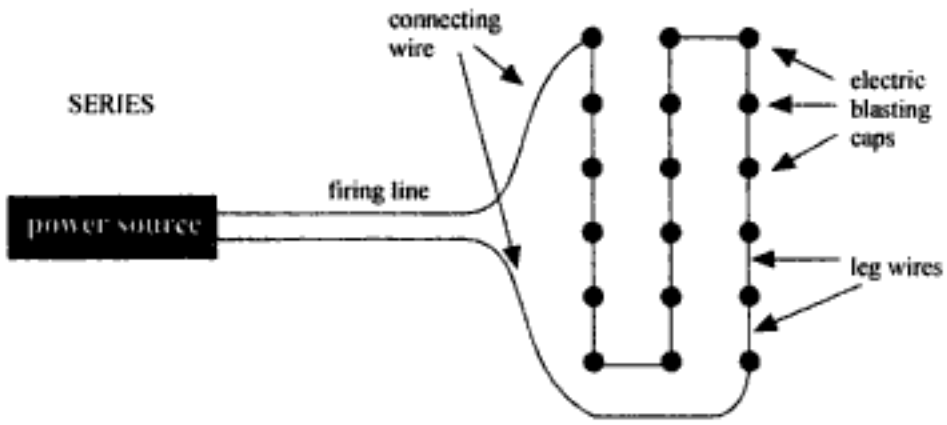

Figure 8.40. A series connection. Dick et al., 1993.

The straight parallel circuit (Figure 8.41b) has also been given for comparison. The selection depends upon the type of power source, the number of delays to be shot, etc. The underlying principle however in all cases is to provide the required current to the caps. The power sources used consist of

- Twist type blasting machines
- Rack bar type blasting machines
- Condenser discharge blasting machines
- Power line sources

The detailed circuit calculations may be found in any good Blasters' Handbook (Dupont, CIL). Very efficient and reliable condenser discharge blasting machines have become available in the last few years. They have their own power pack integrated into the machine. It develops sufficient amperage so that complicated parallel circuits are seldom necessary. Using simple parallel-series circuits any number of series can be fired at any one time. If many holes are involved it is advisable to include a balanced number of holes per series.

Figure 8.42 shows the three step process for making a primer unit using an electric blasting cap and a cast primer. The primer itself contains a cap sensitive region near the cap well. Figure 8.43 shows the preferred method of primer assembly using cap sensitive

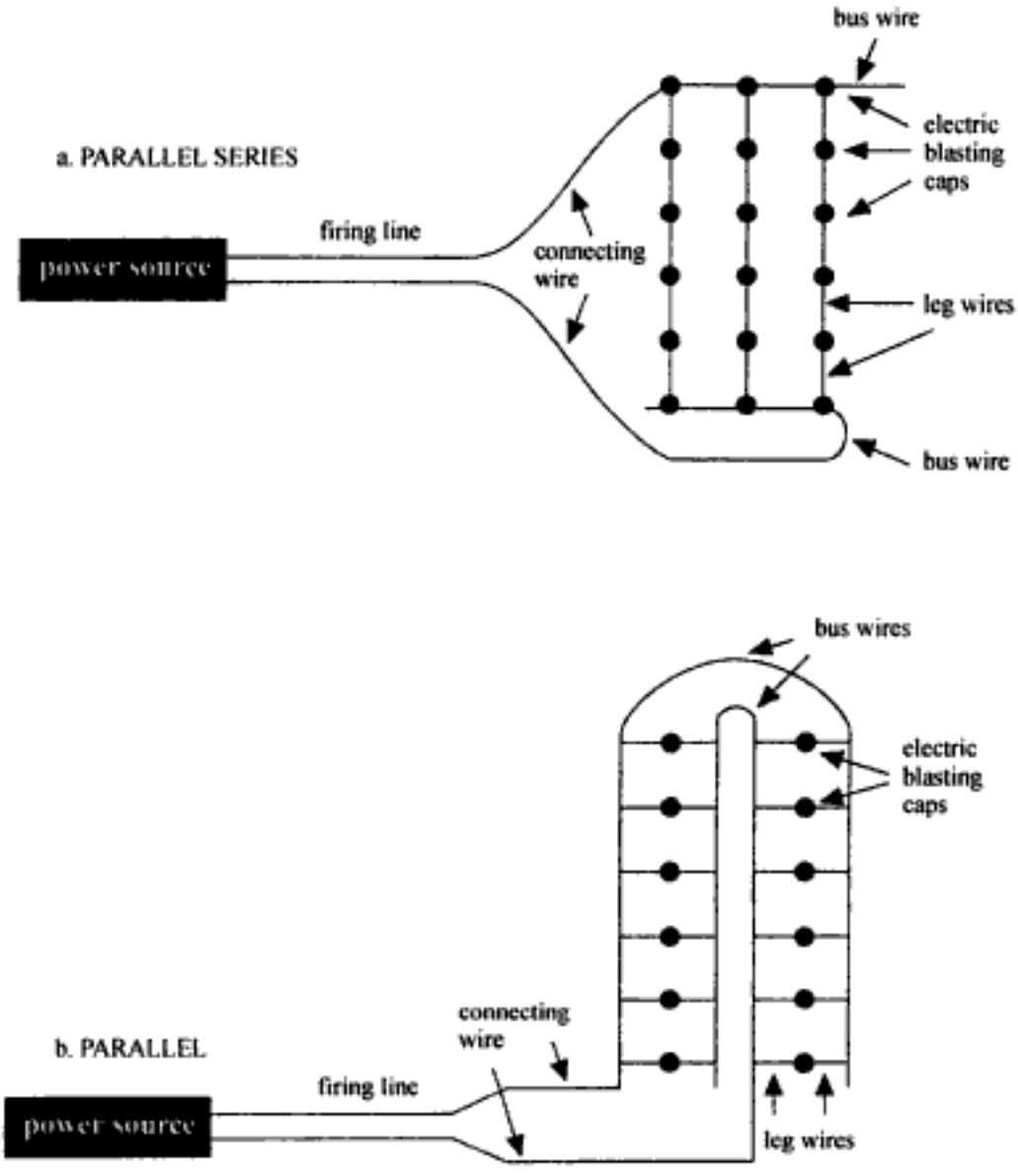

Figure 8.41. Parallel and parallel-series connections. Dick et al., 1993.

cartridges over four inches in diameter. The procedure is as follows (Dupont Blasters' Handbook, 1977):

1. Punch a hole in the side approximately 10 inches from the lower end of the cartridge.
2. Insert the cap as far as it can be pushed by the finger into the cartridge. The cap should be near the center of the cartridge and pointing in the direction of the main charge.
3. 'Throw' two half hitches around the cartridges one above and one below the cap, the support the charge weight during loading and to hole the cap in position.

This type of arrangement would be used for priming bulk loaded *ANFO*, Aluminized-*ANFO*, watergels and emulsions. During charging and stemming the lead wires should be held under light tension along one side of the blasthole to avoid abrading the insulation. There are a number of advantages (Dupont Blasters' Handbook, 1977) when using electric detonators.

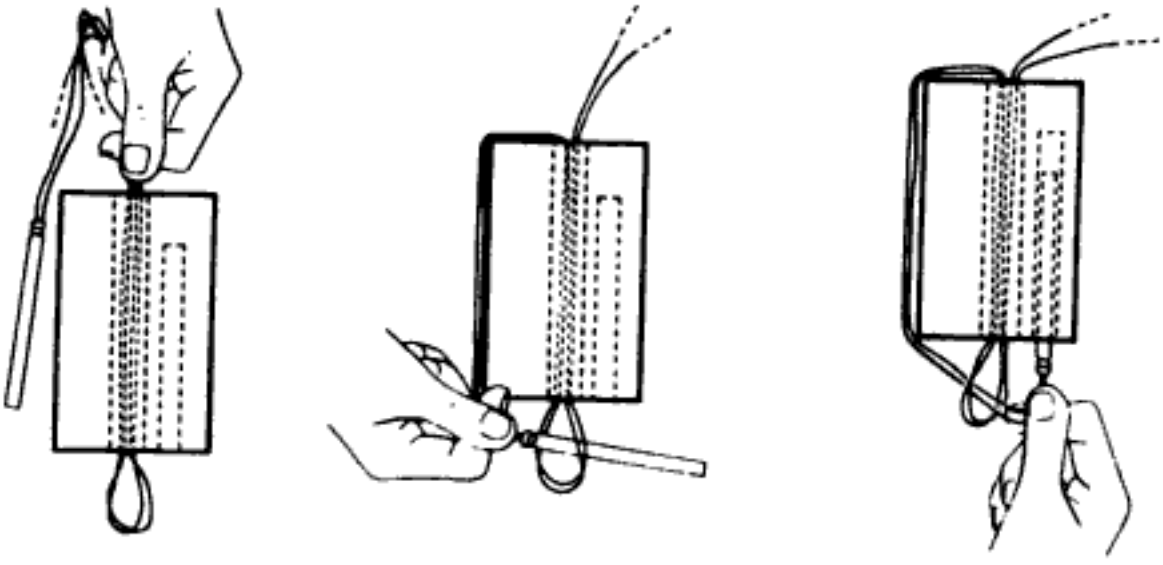

Figure 8.42. Attaching an electric blasting cap to a cast primer. DuPont Blasters Handbook, 1977.

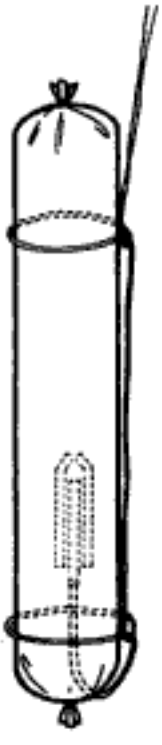

Figure 8.43. Attaching an electric blasting cap to a cartridge. DuPont Blasters Handbook, 1977.

1. Since electricity travels at the speed of light, all holes are ignited simultaneously. Once the electric current has been introduced it is virtually impossible to have a cutoff from flyrock or a shift in formation causing legwire breakage. The caps are initiated before such damage can occur.

2. It gives a greater degree of control over the firing time and the point of detonation than is possible with the other methods. With an electric detonator the explosive column can be initiated at the bottom of the borehole thereby prolonging gas confinement for more efficient utilization of the explosive force and better blasting action on the burden.

3. The blasting circuits may be checked right up to the time of firing.

4. No damage is done to the explosive column via the lead wires (as, for example, by detonating cord).
5. There is no noise associated with the initiation lines.
6. Through the use of sequential blasting machines, a wide range of delays are available. Delays are introduced in the electrical circuits only by those associated with the caps themselves and through external means such as the blasting machine.

The major disadvantage (Dupont Blasters' Handbook, 1977 and AECI, 1986a, b and 1989) deals with safety concerns regarding sources of extraneous electricity

1. Stray current,
2. Static electricity,
3. Electrical storms,
4. Radio frequency (*RF*) energy,
5. Blasting near high voltage power lines.

that may find their way into an electric blasting circuit.

'Stray current' applies generally to electrical currents which flow through the earth or from electrically operated equipment to earth. Sources of stray current are usually nearby machinery, and powerlines. It finds its way into a blasting circuit the same way that firing current leaks out, i.e. through

– Splices not insulated from earth,
– Bare spots in legwire, connecting wire or firing line.

Thus legwire shunts should be left intact just as long as possible and no electrically powered equipment should be operated closer than 15m (50 ft) from the blasting circuit. Static electricity can come from a variety of sources. A main one in blasting operations is the build up of static electricity with the passage of *ANFO* mixtures through an insulated, non conducting loading hose in a pneumatic loading system. Caps have special static protection to handle this problem. Extremely large amounts of electrical energy are released by a lightning stroke. The powerful electric fields that are characteristic of thunderstorms represent a hazard to any material capable of being detonated. No positive protection against detonation by lightning has been developed, and hence no activity with explosives should be conducted during the approach or progress of an electrical storm. From a practical standpoint the possibility of a premature explosion due to RF energy is extremely remote. There are published tables which indicate safe distance to both mobile and fixed radio/TV transmitters.

When blasting near high voltage power lines, one must consider both hurting the power line and vice versa. There are four factors that must be evaluated regarding the effect of the power line on the blasting circuit. These are

1. Capacitive coupling,
2. Inductive coupling,
3. Stray current,
4. Lead/circuit wires throw over the power line by the blast.

The techniques for checking/avoiding these problems are found in blasting manuals, e.g. Dupont Blasters Handbook (1977). If normal safety precautions are taken and intelligence injected in the loading procedure, danger to all personnel can be minimized.

8.6.5 *Electronic blasting caps*

Introduction

Over the years, the manufacturers of pyrotechnic delays have invested in manufacturing, process, and chemical improvements in order to achieve the highest level of precision and accuracy possible. Significant improvements have been realized, however, even the most precise pyrotechnic delay compositions in a detonator are subject to variability of different kinds (Watson, 1997):

1. Detonator delay compositions can shift over time due to the chemistry of fuel and oxidizers in the mix.
2. Delays may shift either up or down depending on the chemistry.
3. Temperature at time of use or storage may affect delay performance.
4. Humidity and storage conditions may affect performance.
5. Potential lot to lot variability of delay periods.

This variability is often described by the so-called coefficient of variation (CV) which expresses the standard deviation as a percentage of the mean. It is defined as

$$CV(\%) = 100\frac{S}{\bar{X}} \tag{8.5}$$

where CV = coefficient of variation (%), $\bar{X}$ = mean, S = standard deviation.

In general 'cap scatter' with chemical delay compositions may have CV values ranging from less than 1 percent up to 2 or 3 percent. Even though this variability may be insignificant for some blast designs, it may be quite limiting to others. As indicated by Watson (1997), it is only through the use of electronic delay technology that detonator timing precision can be eliminated as a blast performance variable.

Worsley & Tyler (1983) in their paper entitled

'The Development Concept of the Integrated Circuit Electric Detonator'

presented at the 9th Conference on Explosives and Blasting Technique sponsored by the Society of Explosives Engineers in 1983 were the first to describe how electronic delay detonators might be applied in mining applications. Since that time, a great deal of development work has been carried out by a number of companies and the resulting detonators/systems are just now slowly being introduced into the marketplace. At the time of this writing (1998), the unit cost of the detonators is still several times that of pyrotechnic delays. When the possibility of electronic delay detonators first arose, it was anticipated that, by analogy with the renowned economies of scale associated with other electronic systems such as inexpensive quartz watches, they would eventually carry low price tags. However, after some years of actual development, the magnitude of the problem has now been fully realized and as Cunningham & Jones (1995) have pointed out the initial analogy to the quartz watch was highly misleading since:

1. When a wrist watch malfunctions, it doesn't blow one's arm off. Furthermore, if it just stops, one does not have to contend with a ton of primed, but inaccessible, high explosive.
2. A watch is not thrown into a blasthole and subjected to significant static and dynamic stresses, let alone the often extreme voltages of electro-magnetic pulse.
3. A watch has a self-contained battery – it does not have to be powered through hundreds of meters of cable laid across rough terrain.

4. A watch is passive – it just displays time. It does not have to pass numerous messages back and forward before unleashing sufficient energy to finely fragment thousands of tons of rock.

They conclude that 'with the wiring, connections and rigorous quality requirements, the cost of any electronic initiation system will not be lower than competing pyrotechnic systems, no matter what the volumes. Since pyrotechnic blasting systems are unemcumbered by these considerations and have the edge in terms of cost, robustness and simplicity of use, it is important to identify what uniquely justifies the development and implementation of electronic delay detonators'.

Quite simply, the potential user must evaluate the benefits such as:

1. Increased timing precision
2. Essentially unlimited number of intervals
3. Safety against unintended initiation
4. Programming of delay times after placement in the hole
5. The possibility for pure computer transfer of the firing plans from a central or portable computer to the firing machine and further to the blasting caps.

to be gained from the use of such detonators against the associated costs.

Prior to presenting some details regarding electronic detonators and their associated systems it is well to explore in more detail the possible reasons for considering their use. Heilig & McKenzie (1988) performed an extensive study of cap scatter using pyrotechnic delays. The first task was to determine the sample size required to obtain a reliable estimate of the mean and the standard deviation for the firing times from a single batch. Figure 8.44 shows the variation in sample mean as the sample size increases from 1 to 100. By testing a relatively small number of detonators (< 30, it is possible to obtain a result which with 95% probability differs by less than 1% from the true mean. Figure 8.45 shows the normal distribution in delay times that one might expect if one were to test a large number of caps having the same delay number (500 ms in this case) from the same manufactured batch. The distribution is normal and its shape can be specified by the mean and the standard deviation. As indicated earlier, the standard deviation is frequently expressed as a percentage of the mean through the use of the coefficient of variability.

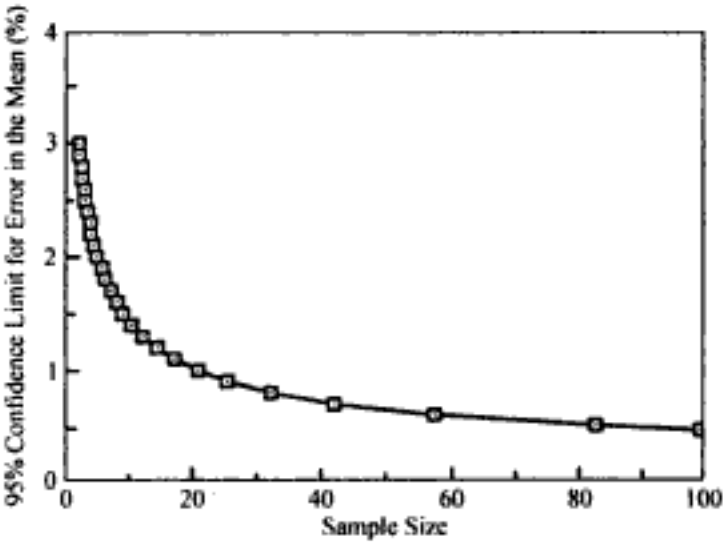

Figure 8.44. Percentage error in determining the error in the mean for increasing sample size (95% confidence level). Heilig & McKenzie (1988).

Hidden page

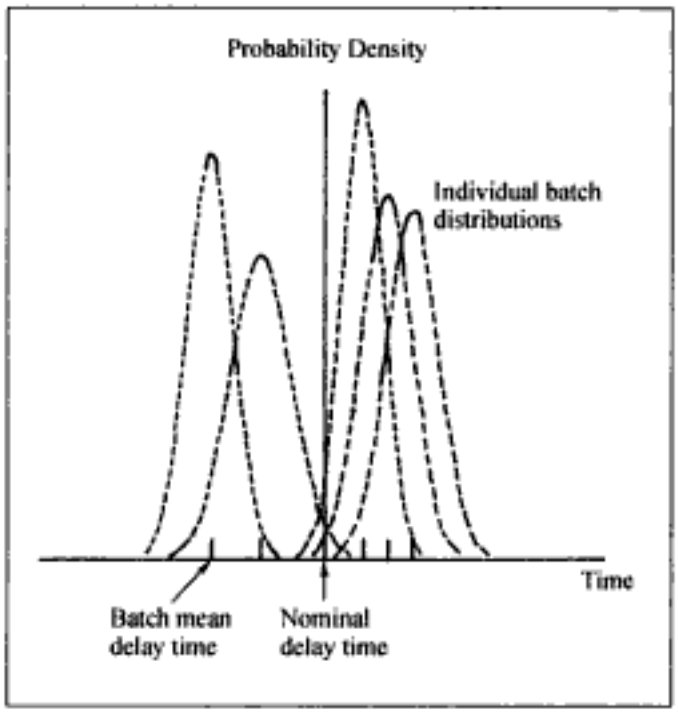

Figure 8.46. Delay scatter within batches and between batches. Heilig & McKenzie (1988).

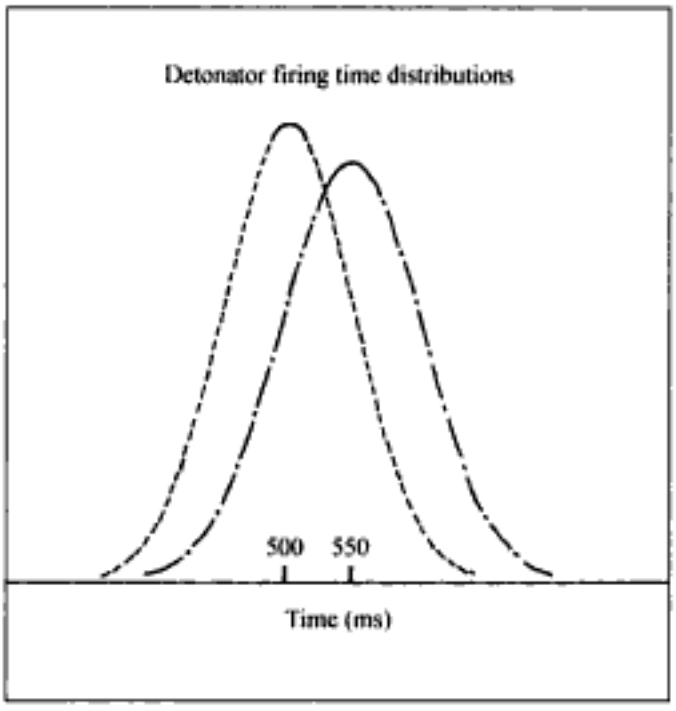

Figure 8.47. Time distributions for two adjacent period delay caps. Heilig & McKenzie (1988).

However as pointed out by Larsson et al. (1988) the total number of available intervals with pyrotechnic caps (Table 8.15) is limited today. Hence, one may face the problem of having to limit blast size. This problem does not exist for electronic detonators due to the very low scatter in observed delay times. Thus one application for which the use of precision delays should be considered is for large blasts where firing order must be maintained.

In smoothwall blasting, the holes in the smoothwall row should be initiated at as nearly the same time as possible to achieve the best results (Svärd, 1993). Even when care is

taken to assure that all caps come from the same batch and thereby minimize the scatter for a given delay, much better results have been observed when conventional delays have been replaced by electronic delays.

As has been discussed earlier, there is a sequence of different events associated with blasting a single hole in a bench. These are shown diagrammatically (Atlas Powder Company, 1986) in Figure 8.48. A certain amount of time is associated with the initiation and the completion of each event. With the new precision opportunities offered through the use of

Table 8.15. Available conventional pyrotechnic delays (Larsson et al., 1988).

Series	Period number	Number of delay periods	Interval (ms)	Delay time (ms)
MS	1-20	20	25	25-500
	24, 28, 32, 36			
	40, 44 and 48	7	100	600-1200
	56, 64, 72 and 80	4	200	1400-2000
LP	1-12	12	500	500-6000

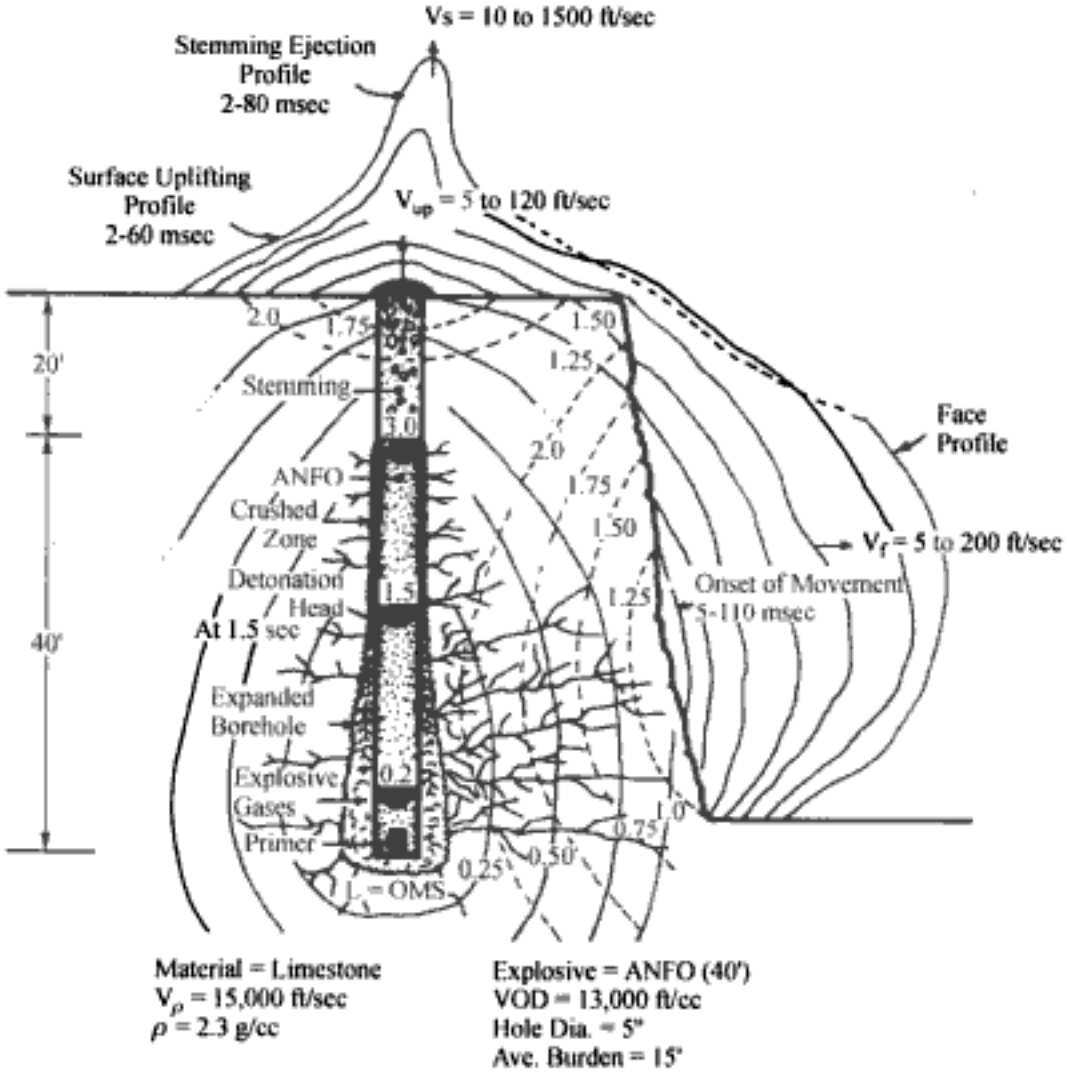

Figure 8.48. A summary of the events and their timing during a blast. Atlas Powder Company, 1987.

electronic detonating delays the engineer can now consider how groups of holes or even portions of single holes should be initiated to encourage or discourage different types of interactions. Through such timing controls one should be able to accomplish certain very specific objectives such as increased fragmentation, increased throw, decreased ground vibration, etc. This is the opportunity area which is lightly explored at present and offers the possibility for major blasting improvement. Even given a significantly higher cost per detonation unit, it takes only a relatively small improvement to justify the additional costs. With the widespread availability of this new tool on the horizon, it is up to blast designers to show how the higher unit detonator costs can be translated into overall production savings.

Electrical energy source (Nitro Nobel AB)

Outwardly, the Nitro Nobel AB electronic detonator (Larsson et al. 1988, Svärd 1992, 1993) looks like a conventional electric one. It has the same dimensions and is equipped with two lead wires. The detonators are marked with Period Numbers between 1 and 250. On the inside, as shown diagrammatically in Figure 8.49, it is quite different. In principle, the detonator consists of an electronic delay unit in combination with an instantaneous detonator. An integrated circuit, a so-called 'chip' (4), constitutes the heart of the detonator, which also contains a capacitor (5) for energy storage, and separate safety circuits (6) on the input side (towards the lead wires) in order to protect against various forms of electric overload. The chip itself also has internal safety circuits on the inputs. The fuse head (3) for the initiation of the primary charge (2) is specially developed to provide a short initiation time with a minimum of scatter.

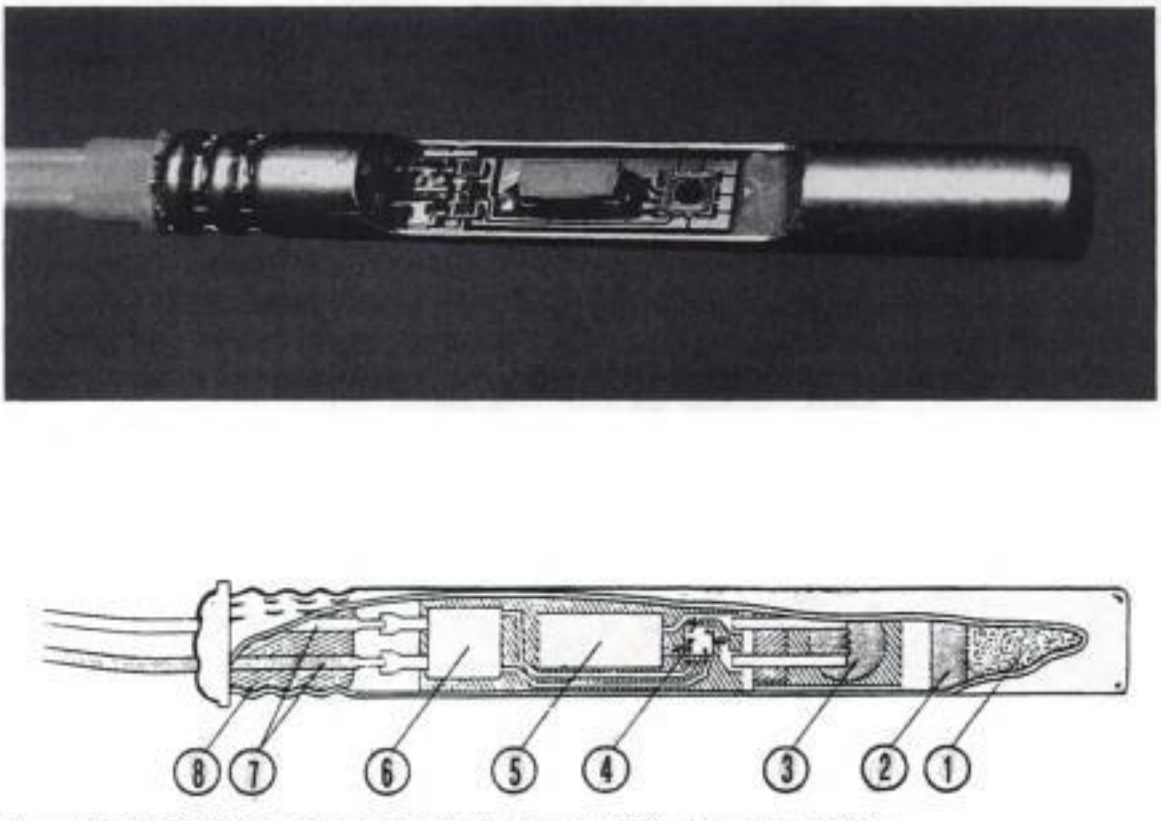

Figure 8.49. The Nitro Nobel electronic detonator. Persson, 1992, Anonymous, 1993a.

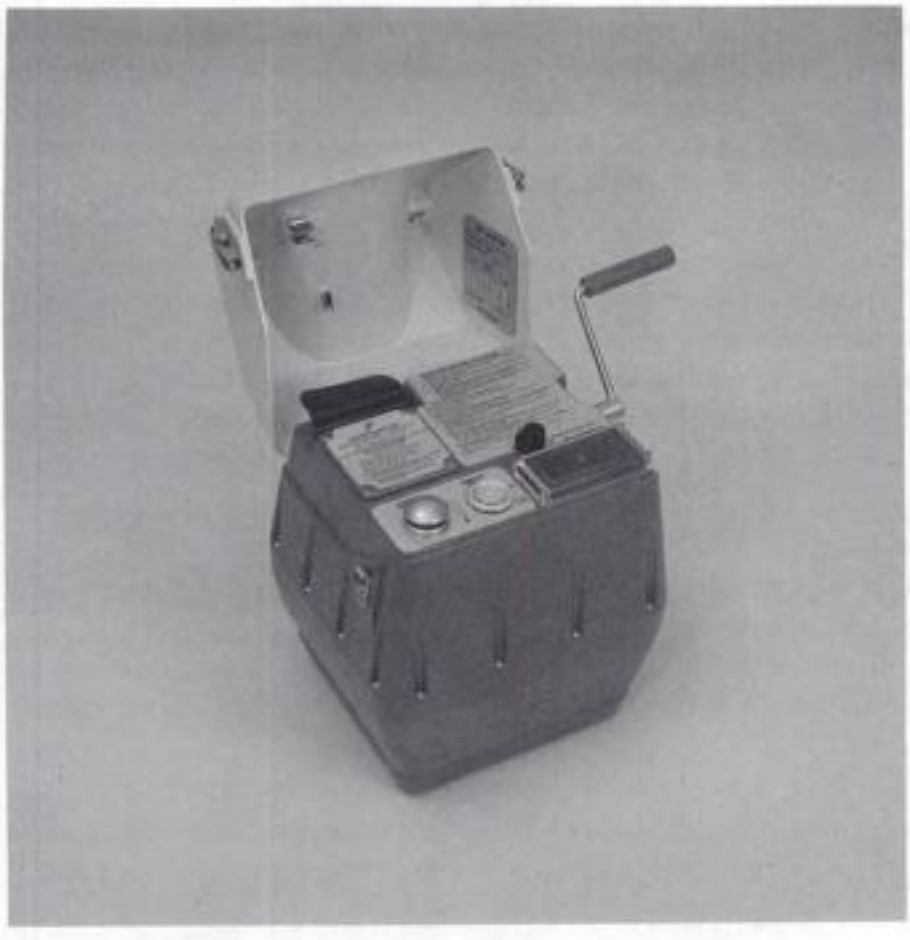

Figure 8.50. Electronic detonator blasting machine. Holmberg, 1998.

The Period Numbers indicate the order in which the detonations will occur rather than the delay time. Each detonator has its own time reference but the final delay time is determined in cooperation with the blasting machine just before initiation.

Typical characteristics for the electronic detonator include:

– Initially has no initiation energy of its own
– Cannot be brought to detonate without a unique activation code
– Receives its initiation energy and activation code from the blasting machine
– Is equipped with over-voltage protection. Small excess loads are dissipated via internal safety circuits. Higher voltages (> 1000 V) are limited by means of a spark-gap. Large excess loads will burn a fuse in the detonator which incapacitates it, without making it detonate.

– An initiation system which operates at low voltages (< 50 V) which is a great advantage considering the risk of current leakage.

The blasting machine (Fig. 8.50) which constitutes the central unit of the initiation system supplies the detonators with energy and determines the delay time to be allocated to each Period Number. Since it is micro-computer controlled, it's mode of operation can be altered with various control programs, while it can be uniformly designed from a hardware point of view. The controls for the initiation of the round are designed as conven-

tionally as possible. In the usual way there is a charging button and a firing button. A panel with lamps indicates what is happening and gives the go-ahead signal when the round is ready to be fired. If any errors are detected they are indicated on the panel and the blasting machine resets the system. The time information is stored in a special time memory in the unit. Time allocation to the detonators is carried out by uniquely coded signals to eliminate any possibility of error. The detonators do not react to any other code than the one from the blasting machine and the risk for unintentional initiation because of spurious signals from other energy sources is thus eliminated. The blasting machine automatically performs an operation status control. This is done automatically by the machine. The ready signal for firing is given only after approved result of this check.

To fully utilize the advantages of the electronic detonator, the 'advanced' system is characterized by:

– Shortest time between two adjacent period numbers (= the interval time) is 1 ms.
– Longest delay is 6.25 secs.
– A detonator with a lower period number cannot be given a longer delay time than a detonator with a higher period number.
– Detonators with different period numbers cannot be closer to each other (measured in milliseconds) than the difference in the numbers. For example the interval between No. 10 and No. 20 must be at least 10 ms.
– Maximum number of detonators connected to each blasting machine is about 500.

Many different number combinations can be used to achieve the desired delay times for a particular round. In practice this means that the user, for most rounds, only needs a sufficient number of different period numbers in stock and not certain fixed numbers as today.

The preparatory work for a blasting operation includes the determination of delay times for each blasthole in the round and the charging of the holes with detonators with suitably chosen period numbers. The blasting machines memory is then programmed with the necessary time information adapted to the period numbers chosen. This can be carried out with a computer or via a special programming unit connected to the blasting machine.

The round is connected (Fig. 8.51) in parallel with arbitrary polarity. The detonators are connected via a terminal block to a two-wire bus cable using special pliers. The bus cable is connected to the blasting machine via a terminal box and a firing cable.

The mode of operation during blasting, and the interaction between the blasting machine and the detonators are shown in a simplified way in Figure 8.52. The handling includes

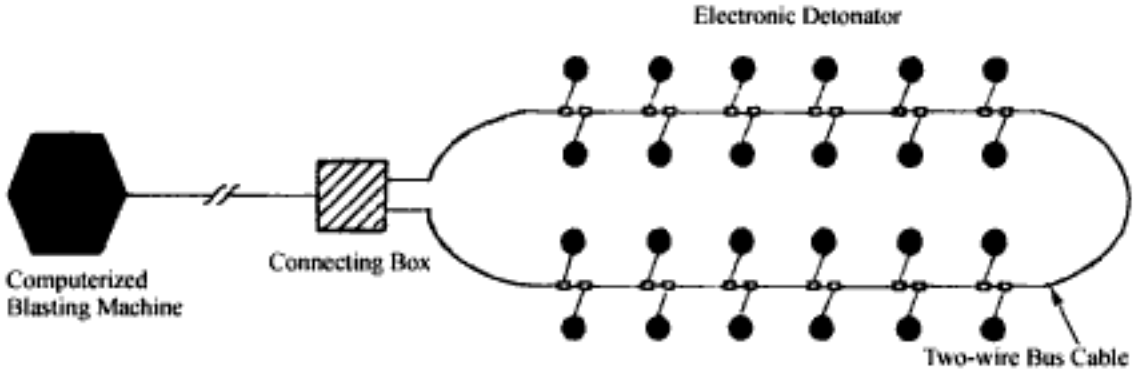

Figure 8.51. Electronic detonator circuit. Larsson et al., 1988.

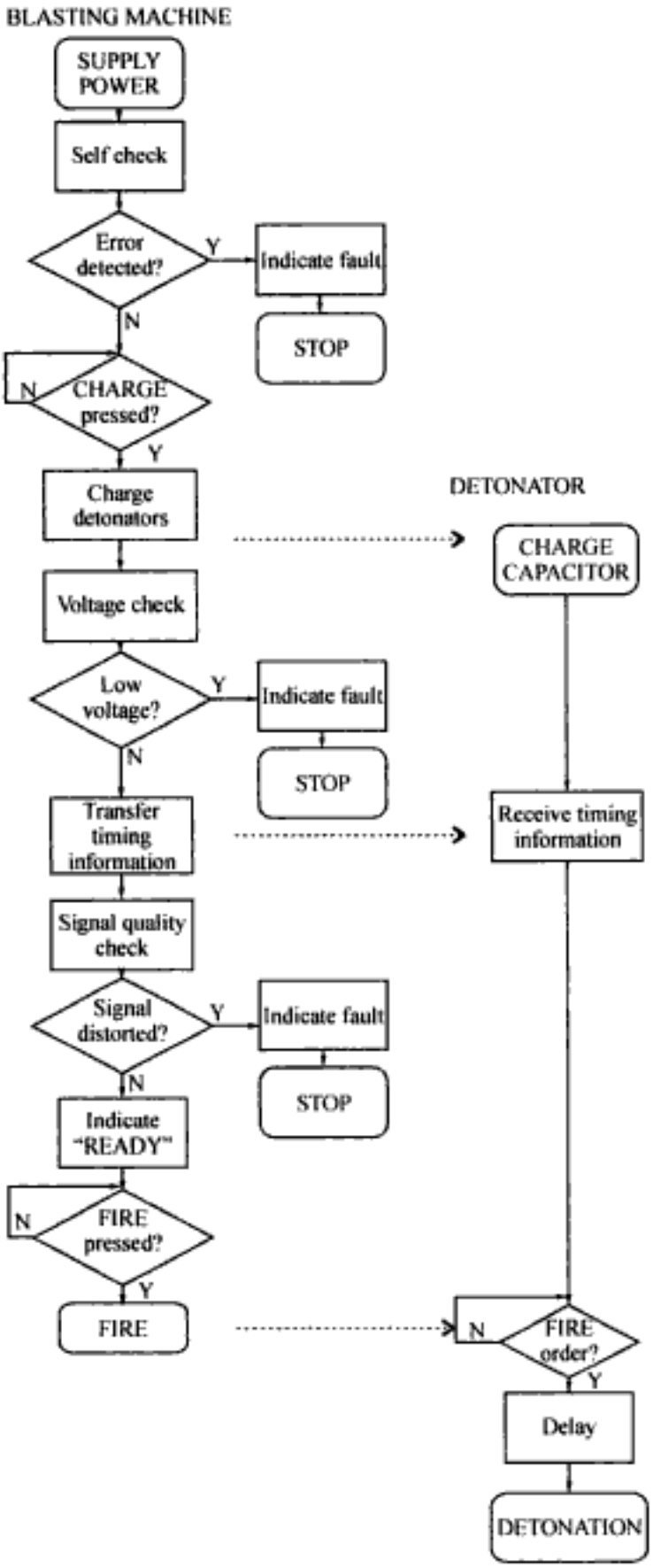

Figure 8.52. Simplified function diagram. Larsson et al., 1988.

two manual operations and the exact time for the blast is determined by the operator. Apart from that, everything is carried out automatically. The operation can be interupted, however, at any time until the firing signal has been sent to the detonators. After that, the detonators are released from the signalling system and will detonate with high time-accuracy.

Electrical energy source (ICI)

The material included in this section has been largely extracted from Cunningham, 1994a, b and Cunningham & Jones, 1995. ICI's EXEX 1000 system shown diagrammatically in Figure 8.53, which was commissioned for production blasting in November 1993, has been used for a number of full-scale production blasts in open cast coal, ring blasting and quarrying. The system is built around a fully programmable electronic delay detonator with tube dimensions only slightly greater than normal. The characteristics of the detonator are:

– Every detonator is programmed remotely in the hole, just prior to blasting
– Any detonator in the hook-up can be allocated any delay from zero to 15 seconds in 1 ms steps.
– They are extremely robust, both physically and electronically, and have various safe-guards against accidental firing.

The detonator downline consists of a strong six core cable, fed from a downline connector block (DCon). The DCon is connected by means of a crimping tool to the harness line, a five-core ribbon cable from the blast programmer. Up to 250 detonators can be fired on each harness, of which four can be driven by one programmer. The programmers can be linked together to expand the number of delays available for a blast.

Circuit breaks and leakage must be detected as early as possible during deployment of the detonators. Test equipment which is incapable of prematurely firing any detonator, even if the safety interlocks in the system fail, has been developed, and is used to check the integrity of detonator units as loading proceeds.

The blast programmer which addresses each of the detonators individually through harnesses serves three functions:

– Testing for circuit integrity and detonator condition,
– Programming of the delays, either directly using the keypad, or by means of a PC computer,
– Activating the blast by charging the capacitors and sending the firing signal.

Color coded keys serve to prevent the programmer from being used for firing purposes during the testing and programming cycle, and passwords are used to prevent the unauthorized use of the equipment.

The blast commander is the graphics-driven timing software. Normally run on a notebook computer it is down-loaded to the blast programmer once all is approved. It is key to the effective exploitation of the electronic detonators. Essentially, the blasting engineer defines the blast layout and then allocates delays to the holes. The pattern is checked by simulating the blast and timing contours can be generated to examine movement trends. Following a blast, the printout provides a record of the positions of all holes and delays used.

The advantages of the system are:

1. Because delays are not programmed until the blast was hooked up, the men on the job do not need to concern themselves with details of sequence in a physically arduous situation, but only with the routing of the harness.

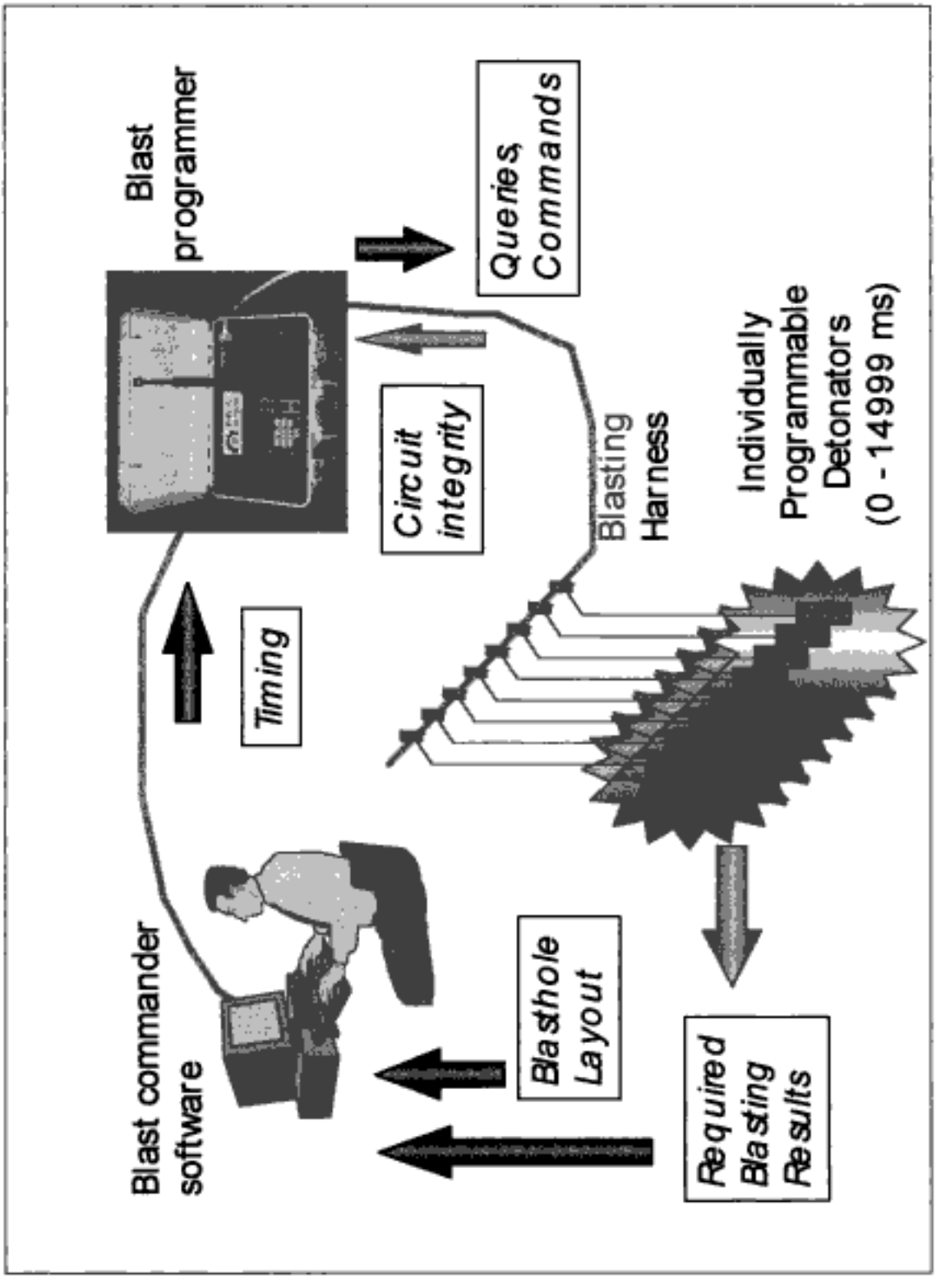

Figure 8.53. The EXEX 1000 blast initiation system. Cunningham, 1994.

2. The decision on timing can be taken with a holistic view of the blasthole layout, knowing that all the holes shown are, in fact, in place.

3. There is no need to be concerned with premature cut-offs since all detonators are initiated prior to the first one firing.

At the time of publication, an improved system, the EXEX 2000, has just been introduced.

Shock Tube Energy Source

The material included in this section has been largely extracted from Watson, 1997. The DIGIDET ™ electronic detonator developed by The Ensign-Bickford Company and shown diagrammatically in Figure 8.54 utilizes a standard shock tube lead as the 'input' signal. The tube is sealed in an internal isolation cup molded from semi-conductive plastic to protect the unit from static discharges or other spurious electrical energy. The shock tube signal is transformed into an electrical pulse through the use of three principal components: a small explosive charge (booster) coupled to a highly efficient piezo-ceramic element (generator) and an electrical energy storage cell (capacitor). This energy generation and storage mechanism is described in United States Patent 5, 173, 569. Several other patents related to this device are pending.

Upon receipt of a (thermal) signal from some energetic transmission line such as a shock tube, the small explosive charge in the booster detonator fires. This activates the piezo-ceramic device, which in turn causes current to flow through the steering diode to charge the storage capacitor. A voltage regulator provides a substantially constant voltage source to the oscillator to control the frequency of the oscillator. Upon initial application of the input voltage, a 'power-on reset' circuit preloads the counter. Once the voltage on the storage capacitor has increased beyond a threshold setting, the counter begins decrementing upon each input pulse from the oscillator. As the counter digitally decrements past zero, the output to the firing switch is activated and all remaining energy in the storage capacitor is dumped to the igniter. The end result is an electronic delay detonator that can be initiated by nonelectric means.

Figure 8.55 shows a block diagram of the electronic delay circuit. The internal electronics are rendered immune from radio frequency and other electric field energy sources by the metallic cap shell. The shell completely surrounds the electronic elements, creating a Faraday cage that requires the field strength to be zero at all points in the shell. This effect has been confirmed through extensive testing, including testing to MIL-STD 461-D which has demonstrated the unit's non-susceptibility to initiation from extremely high electric field density environments.

Laboratory and field testing indicates that the system (both surface and in-hole units) maintains a +/– one millisecond range when used in a typical blast design pattern. Figure 8.56 indicates the level of variability over a sample of delay ranges. Table 8.16 shows firing times from an actual blast.

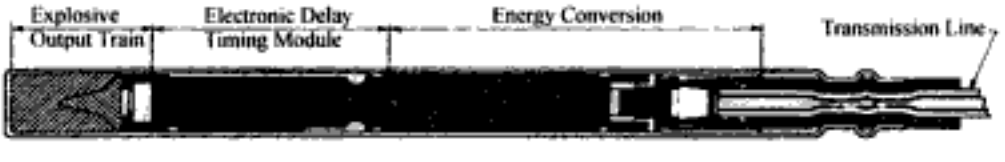

Figure 8.54. Cross-section of the Digidet electronic detonator. Watson, 1997.

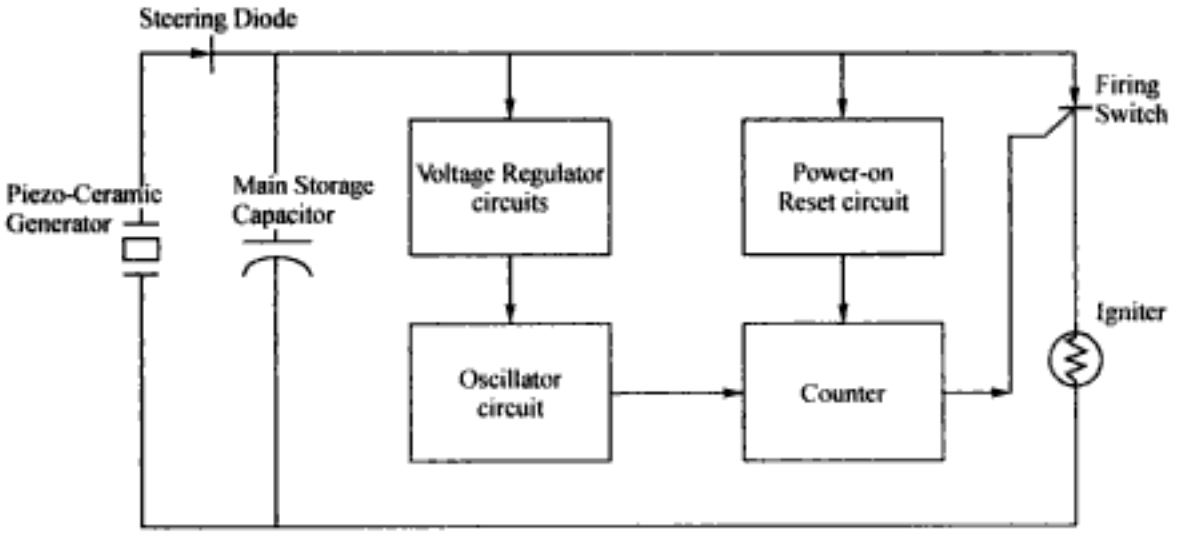

Figure 8.55. Block diagram of the Digidet detonator circuit. Watson, 1997.

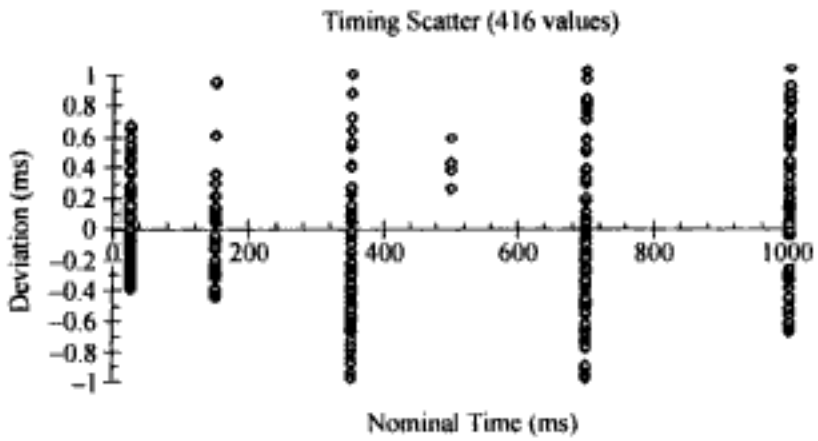

Figure 8.56. Deviation of Digidet detonator timing over various delay ranges. Watson, 1997.

Table 8.16. Actual firing times from a blast when using DIGIDET ™ detonators (Watson, 1997).

Firing time (ms) Planned	Actual	Variation
500	500.125	0.125
535	535.125	0.125
570	571	1.0
605	605.875	0.875
640	641	1.0
675	675.5	0.5
710	709.875	–0.125
560	560.625	0.625
595	595.375	0.375
630	629.75	–0.250
665	665.5	0.500
700	700.75	0.750
735	734.875	–0.125
770	770	0.0

Table 8.17. Preliminary product specifications for the DIGIDET ™ (Watson, 1997).

Physical dimensions	Standard 2.5″, 2.7″, 3.5″ x 0.296″ OD aluminum shell with variable length shock tube lead.
Delay principle	Factory programmed
Range of delay times	3ms to 10,000ms
Storage and operating temperature range	-65°F to 150°F
Impact sensitivity	same as Primadet detonator
Shock sensitivity	same as Primadet detonator
Vibration resistance	Passes MIL-STD 810C Method 514.2; MIL-STD 331 Test 119
RFI resistance	MIL-STD 461-D RS103 (200 V/m from 14 kHtz to 18 GHtz)
ESD through shock tube	30,000 volts at 100pF

No electronic testing or blasting circuit protocol, other than the hookup and inspection procedures currently used for standard blast initiation are required. There are no blasting machines, programming interfaces, data input, or electrical connections of any type. Training is limited to that needed for conventional nonelectric initiation systems. Unlike other electronic systems, these detonators can be used in combination with existing shock tube or detonating cord products as required.

The shock tube's lead length must be considered when hooking up the system. The detonator timing is programmed at the time of manufacture and is precisely matched to the length of the tube. The unit's delay time is calculated from the end of the shock tube. For example, a twenty foot (20′) 1000 ms detonator would have a different programmed time delay than a sixty foot (60′) 1000 ms delay. Both units, though, would shoot precisely at 1000 ms when fired from the end of the shock tube. The actual firing time would change if the point of initiation is varied from the end of the shock tube. Since shock tube detonates at approximately 1980 meters/second (6500 ft/sec), a 1000 ms delay would decrease incrementally in time by 1 ms for every 6.5 ft change in the initiation point from the end of the tube. Given adequate length of tubing, this feature would provide a limited amount of 'tunability' or flexibility for delay times.

Safety, reliability, and 'User-Friendly Precision' were the three primary design specifications. The other product specifications are given in Table 8.17. The first DIGIDET ™ detonators were shot by The Ensign-Bickford Company in late 1995 and testing has continued through 1996 and 1997. A second generation design of this technology is planned for field use in 1998.

8.6.6 *The non-primary-explosive detonator (NPED)*

The material included in this section has been largely extracted from Anonymous (1992), and Holmberg (1994, 1997). Today, most detonators with pyrotechnic delays are constructed as shown in Figure 8.57a. The electric detonator is equipped with a bridge wire which, when electrically heated, sets a fuse head on fire. This, in turn, ignites the delay charge. When the delay charge has been consumed, a small charge of primary explosive placed between the pyrotechnic delay and the secondary explosive base charge is ignited. The primary explosive transforms the relatively slow chemical combustion of the delay element into a detonation of the secondary explosive.

Primary explosives generally consist of single molecules which (a) allows them to decompose very quickly when initiated and (b) gives them the ability, when ignited, to tran-

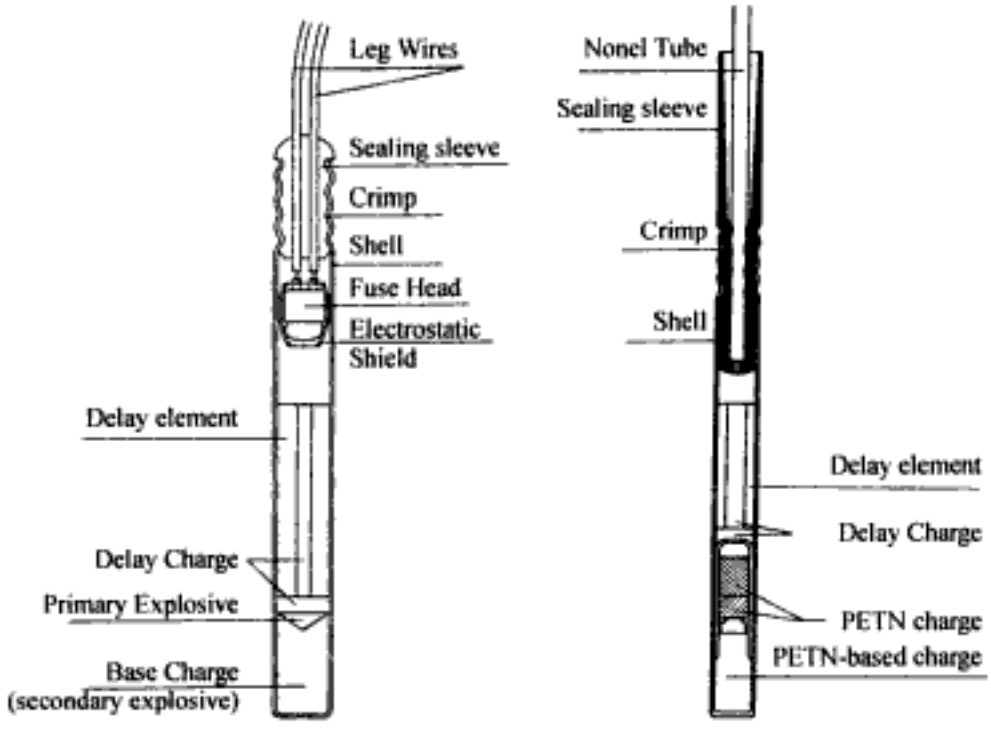

a. Conventional Electric Blasting Cap

b. NPED Blasting Cap

Figure 8.57. Comparison of a conventional electric blasting cap with the NPED blasting cap. Anonymous, 1992.

sit from burning to detonation over distances as small as a fraction of a millimeter even under atmospheric conditions. A few milligrams is enough to achieve detonation. These properties make primary explosives very suitable for use in the initiation process. On the other hand, their extreme sensitivity to heat, friction and impact make them risky to handle. Some common examples of primary explosives are mercury fulminate ($HgC_2N_2O_2$), lead styphnate ($PbC_6H_3N_3O_9$), lead azide (PbN_6), and silver azide (AgN_3).

Secondary explosives are much less sensitive to initiation than are primary explosives and can often burn under atmospheric pressure conditions without any transit from deflagration to detonation. Two examples of secondary explosives are PETN ($C_5H_8(NO_3)_4$) and hexogen/RDX ($C_3H_6N_3(NO_2)_3$).

The basic concept for the new detonator shown diagrammatically in Figure 8.57b is the replacement of the primary explosive (as used in the conventional cap) with a secondary explosive which, in this case, is PETN. The idea comes from China and is described in US Patent 4,727,808. The new cap which has been developed by Nitro Nobel AB is compatible with most of the usual lead systems such as Nonel.

The exterior of the new detonator appears exactly the same as a traditional cap. The interior, however, has been extensively modified. As can be seen, the sensitive primary explosive, lead azide, has been replaced by an initiation element consisting of a steel shell, a sealing cup, PETN charges and a delay charge. Through carefully designed density and quality variations in the PETN, the combustion front accelerates as it moves along the initiation element. By the time the front reaches the base charge, the initial deflagration process has changed to full detonation. This phenomena is called DDT (Deflagration to Detonation Transition).

An interesting description (Anonymous, 1992a) of the differences between the conventional and the NPED concepts is:

'A conventional blasting cap can be likened to a gasoline engine where a spark plug (primary explosive) is used to ignite the fuel/air mixture. The NPED blasting cap can be likened to a diesel engine where the fuel/air mixture requires only high compression to be ignited. This compression is achieved in the initiation element'.

This cap has significant safety and environmental advantages over more conventional caps containing lead azide. The new non-primary explosive detonator is much less sensitive to different external stimuli than the conventional one which means that a higher degree of safety is introduced in all operations

- Manufacturing,
- Transportation,
- Storage,
- Use.

Another benefit with the new detonator is that due to the elimination of the lead azide, the amount of lead discharged from each cap into the environment is reduced by about 50%. In the future even the lead-containing delay element constituents will be replaced by with ones without lead.

8.6.7 *Magnadet Detonators*

As described in Section 8.6.3, when electric detonators are used to initiate an explosive charge, the cap is generally first inserted into a primer and then the cap plus primer are inserted into the hole. The ends of the leg wires are kept twisted together (shorted) until just prior to blasting at which time they are connected into the blasting circuit. Because of electrical continuity of the circuit (circuit wires, legwires, cap bridge wire) it can be checked both during hook-up and prior to firing.The bridge wire used to ignite the match in the cap is of small diameter and high resistance. When current is applied to the circuit, the wire heats up. This ignites the match which causes the delay substance in the cap to begin to burn, etc. With this type of circuit arrangement there is always the chance, albeit very small, that extraneous electricity in the form of:

1. Stray electricity,
2. Static electricity,
3. Radio frequency energy,
4. Lightning,

may be accidently introduced into the circuit and set-off part or all of the blast.

As introduced by Atlas Powder Company in the early 1980s, the basic idea behind the Magnadet detonator was to electrically isolate the cap legwires from the circuit wires and thereby largely eliminate this danger. In this section, the description of the Magnadet detonator as extracted from the paper by Kremer (1991) will be presented.

The transfer of electrical energy from the blasting circuit to the detonator legwires occurs through a mini-transformer attached during manufacture at the ends of the legwires. The detonator legwires are wrapped three times around an iron toroid (the mini-transformer) in such a way that they always remain completely shunted and isolated. The toroid itself is housed in a plastic connector (Fig. 8.58).

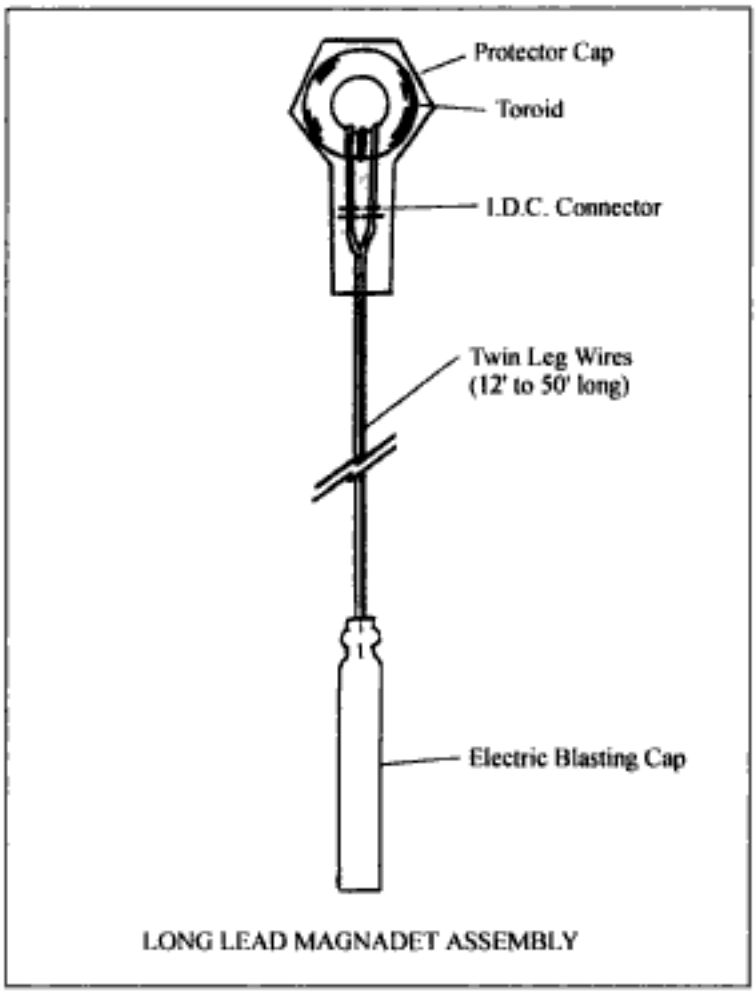

Figure 8.58. The long lead Magnadet assembly.

The detonator consists of a standard, highly accurate delay detonator with a heavy, low resistance bridgewire/match assembly shielded against low firing currents.

The detonators are connected into the primary blasting circuit by simply passing a single #18 AWG copper wire through each of the toroids (Fig. 8.59). This single pass results in the creation of a 3:1 turn transformer. An AC current (rather than a direct current) is induced into the detonator legwires from the primary blasting circuit. The primary circuit, in turn, is wired into a blasting machine or onto the terminal board of a sequential blasting machine. To successfully fire Magnadets, the blasting machine must be specially designed to generate a high frequency (10 to 30 kHz) alternating current.

Because the detonator legwires are electrically isolated from the primary blasting circuit, the possibility of premature ignition from extraneous electricity has been greatly reduced. The nature of the protection will now be briefly discussed. Due to the transformer coupling between the legwires and the primary blasting circuit, the chance of premature ignition from stray DC current entering the primary blasting circuit has been eliminated. Typical AC power which is found around mining operations (50 or 60 Hz) will not affect Magnadets since they can only be activated by AC currents in the high frequency (10 to 30 kHz) band. Stray currents will not enter the detonator legwires themselves since they are always shunted and insulated.

With regard to static electricity, the heavy, low resistance bridgewire plus the high voltage static discharge protection built into the match ignition system provides a great

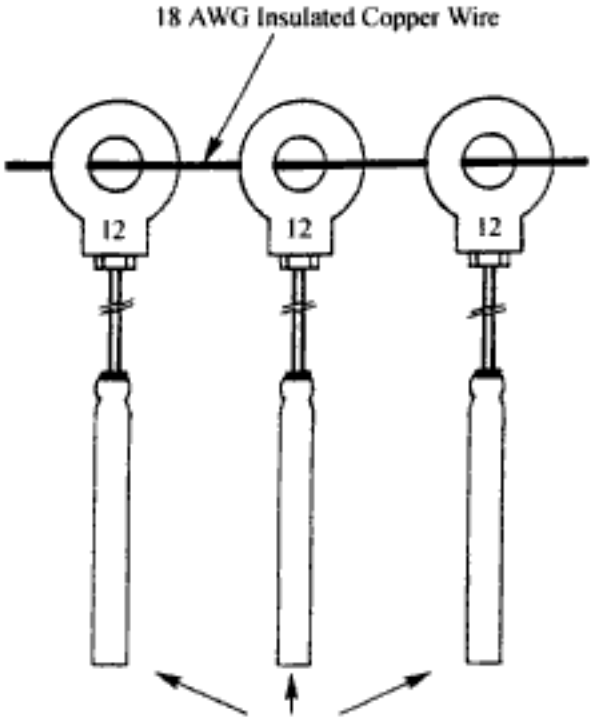

Figure 8.59. Magnadet hook-up.

degree of protection. The detonators themselves can withstand a static discharge down a non-isolated legwire of at least 1.0 Joule at 10 Kv and still not fire. Static energy discharged into the primary blasting circuit presents even less of a hazard.

Radio frequency (*RF*) energy presents a very minimal hazard for conventional electric detonators. This hazard is even less for Magnadets. Although the potential for RF energy to be induced into the primary blasting circuit loop does exist, for this energy to be even a theoretical hazard it must be transmitted at 25 MHz or below. The induced current, if any, would be reduced by 1/3 due to the 3:1 transformer winding. To fire the detonator's ignition system, the resultant current would still have to be high enough to overcome the low resistance bridgewire.

Of all conventional electric detonators, the transformer coupling offers the highest degree of protection against the dangers of lightning. However, as with any ignition system, electric or non-electric, all personnel must be evacuated from the blast area during the approach of a lightning storm.

Although, as originally conceived, the system had many benefits, it also had some drawbacks which limited its application. First, the detonators were manufactured with maximum leg wire lengths of 50 ft. Secondly, the number of available interval numbers restricted their use to smaller shots. Thirdly, although the primary blasting circuit could be checked for continuity, the detonator legwire portion could not. Finally, only straight delay period sequences could be fired since no sequential timing machine was available.

These have now been overcome with the introduction of the Mini-Magnadet. It is a standard Magnadet detonator with 5 cm (2 inch) long legwires attached to the toroid (Fig. 8.60). As shown in Figure 8.61, a sliding delay primer can be made by simply placing the detonator into the appropriate well of any standard cast booster and positioning the toroid over the 'through tunnel' using a plastic 'nail'. One leg of the 18 AWG copper wire downline is then passed through the primer tunnel and the primer is lowered into the

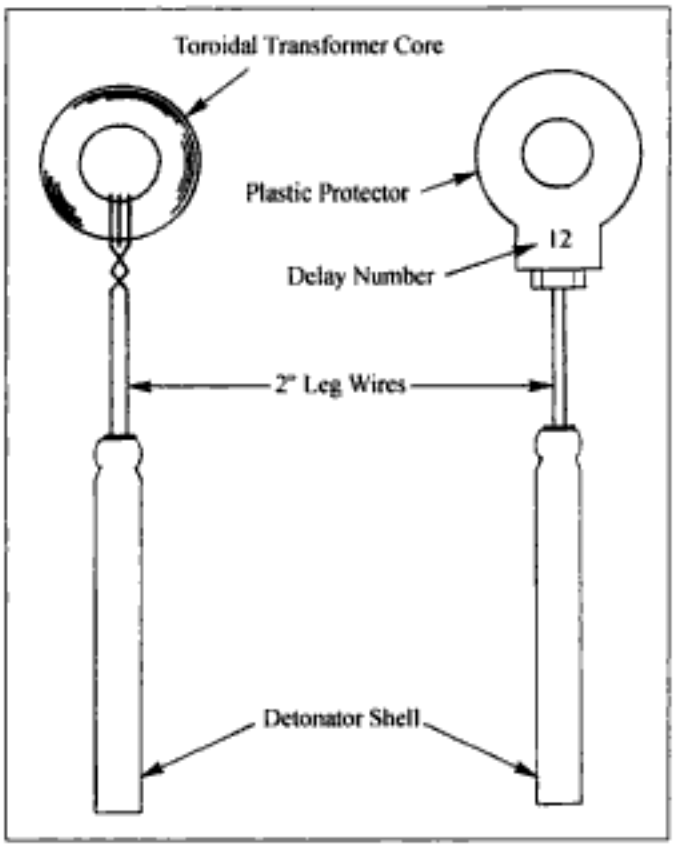

Figure 8.60. The mini-Magnadet assembly.

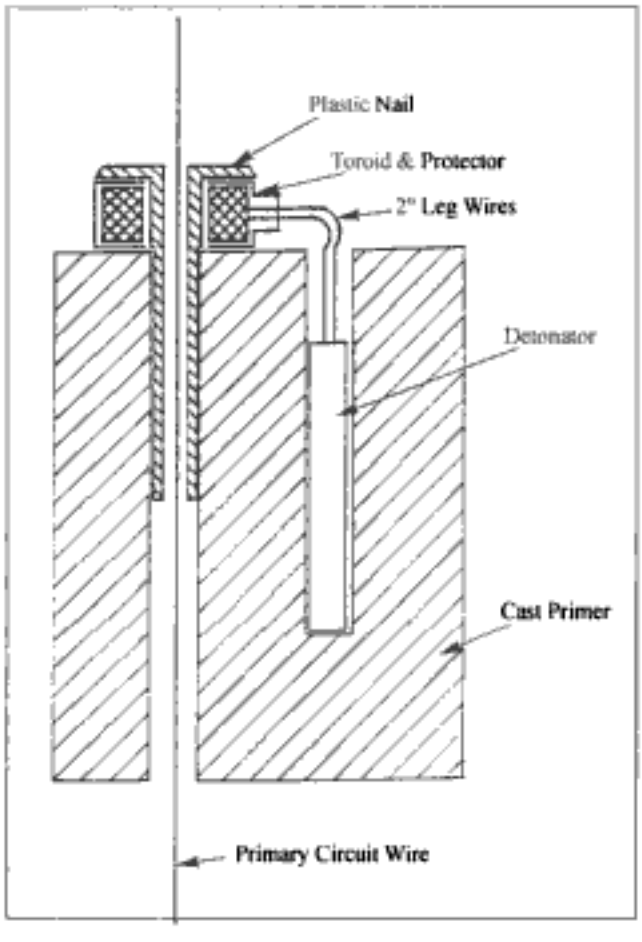

Figure 8.61. The primer assembly using the mini-Magnadet.

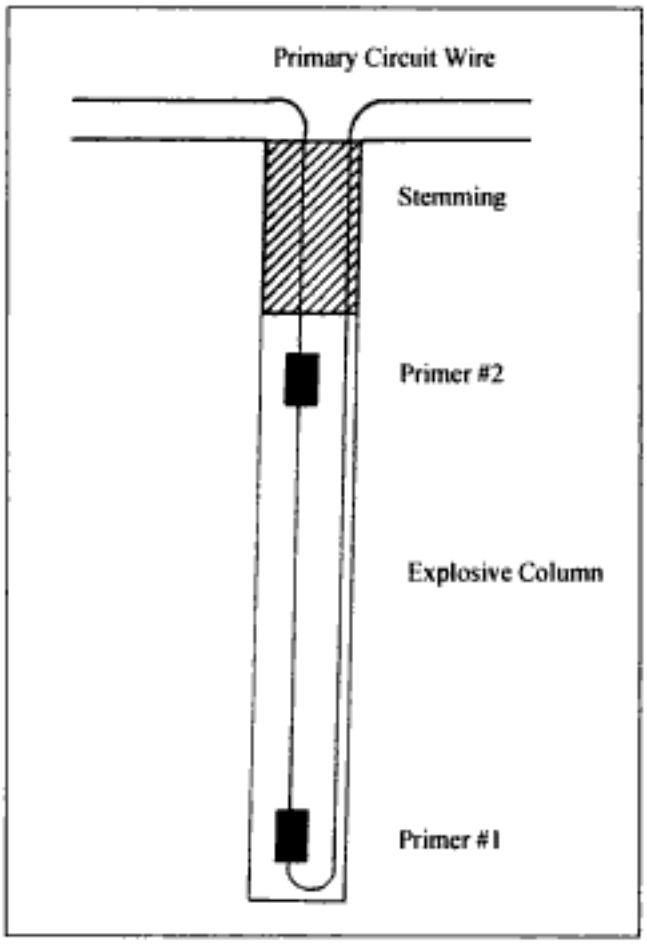

Figure 8.62. Magnadet circuit within a blasthole.

hole. The weight of the primer will carry the primer and the circuit wire to the hole bottom (see Figure 8.62). Any subsequent primers needed to load the blasthole are made up in the same manner and simply slide down one of the primary circuit wires. The primary circuit wiring now becomes the downline and can be checked for continuity with any standard blasting galvanometer. It is now possible to load any depth blasthole with as many primers as desired with only one circuit wire running down and back up the hole (Fig. 8.62). All holes are then wired into series by connecting all the primary circuit downlines using a standard wire splice (Fig. 8.63). The primary circuit is then wired into the Magnadet blasting machine which generates a high frequency, alternating current.

With the introduction of the Mini-Magnadet and sequential blasting machine the explosive user can now fire large bench blasts sequentially. The total system is very easy and quick to load, and downlines can be checked for continuity. The system is also highly resistant to premature ignition from extraneous electricity hazards.

8.7 BLAST SEQUENCING

8.7.1 *Introduction*

Delayed detonation of holes within a shot is desirable for three reasons (Gulf Explosives, 1975):

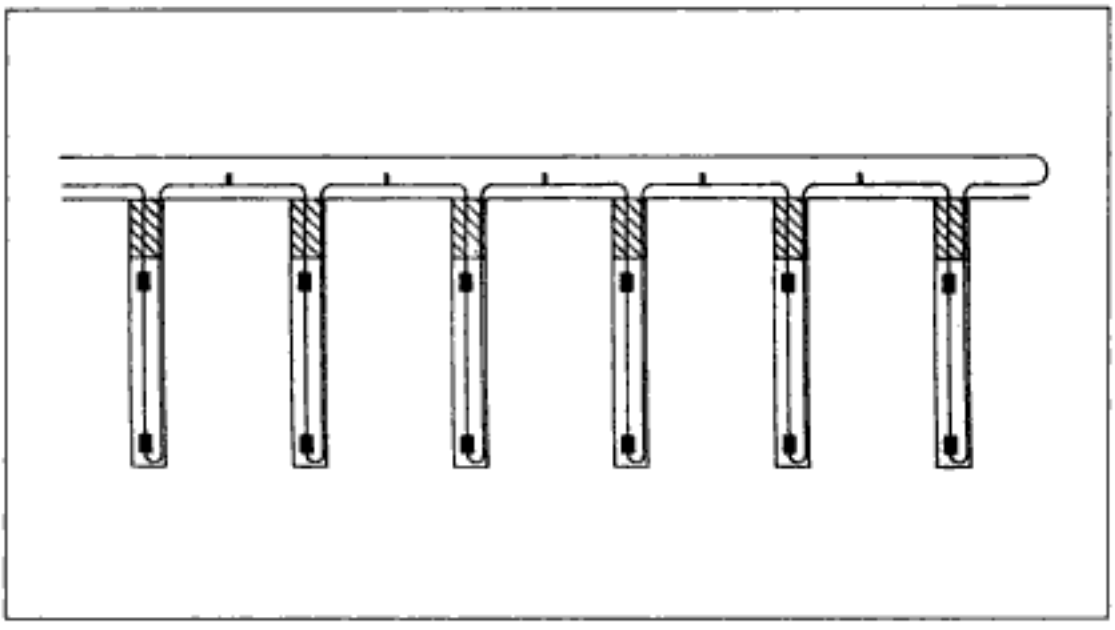

Figure 8.63. Magnadet surface connection.

1. Increased fragmentation,
2. Controlled displacement of broken muck,
3. Decreased vibration from blasting.

The delays can be inserted into the system through (a) the trunkline, (b) the downlines, or (c) through a combination of (a) and (b). There are three major trunkline systems available

- Electric,
- Detonating cord,
- Nonel,

the characteristics of which have been discussed in Section 8.6. Each of these has an associated transmission velocity.

System	Transmission	Velocity
Electric	speed of light	410,000 km/sec.
Detonating Cord	*VOD*	7000 m/sec.
Nonel	*VOD*	2000 m/sec.

Each of these systems could fire a sequence of holes without introducing additional delays by using instantaneous (zero delay) caps at the hole collar. Delays, if desired, could be introduced into the downline portion of the circuit. On the other hand, surface delays of various kinds may be introduced into these surface systems. For all three systems, caps terminating the trunkline system at the hole collars may have built-in delays. Delays at other points in the system may also be introduced. The techniques used are:

Electric	–	Sequential blaster (electronic delays of cap series)
Detonating cord	–	Delay caps (detonating connectors)
Nonel	–	Delay caps (detonating connectors)

The different delay numbers (times) have already been discussed. The use of surface delays introduced either automatically (due to the finite transmission velocities) or on purpose must be carefully evaluated. Rock movement (flyrock, heave, venting) may produce disruptions in the circuits. The result is *cutoffs* and *misfired* holes.

One way of minimizing this danger is through the use of down hole delays. There are three types of downline systems

- Electric,
- Detonating cord,
- Nonel.

For the electric and Nonel downline systems the delay is associated with the delay cap being used. Initiation would occur at the location of the primer. The energy associated with the downline itself is insufficient for initiating the explosive column. The detonating cord downline is associated with three types of delays. If the detonating cord has sufficient strength, the column of explosive may be side initiated. Initiation would begin at the top of the column with the detonation proceeding downward. If the cord is of insufficient strength to initiate the column of explosive but able to initiate primers, then the initiation would occur at the primer locations beginning with the first one met by the cord. If the cord is of insufficient strength to initiate the primers, then the cord terminates in a cap. A delay element may be included in this cap which is inserted in a primer and the initiation point would be there. For the strong (high energy) detonating cord system the downhole delay would be very small. For the weak (low energy) detonating cord system, the cap delay would be similar to the other down hole systems.

There are a number of trunkline-downline combinations which can be formed (Table 8.18) and therefore the different possibilities for creating delays are multiplied.

It is sometimes desirable to have hole bottom initiation and to then carry this initiation signal to other parts of the column other than simply via the column itself. One example is when decked charges are used (Fig. 8.64). In this case an electric cap plus primer is placed at the desired location in the hole. A line of high strength detonating cord then carries the signal up the column to primers located in the decks.

In summary, there are a great number of ways in which hole sequencing may be accomplished.

8.7.2 *Timing considerations*

In previous chapters a general introduction to the blast fragmentation process has been presented. A certain amount of time is required for the different events to occur. Because of the importance of timing to successful blasting, a simple example illustrating the principles has been included. It will be assumed that

Table 8.18. Combinations of trunkline and downline.

Trunkline	Downline electric	detonating cord	Nonel
Electric	X	X	X
Detonating cord		X	X
Nonel		X	X

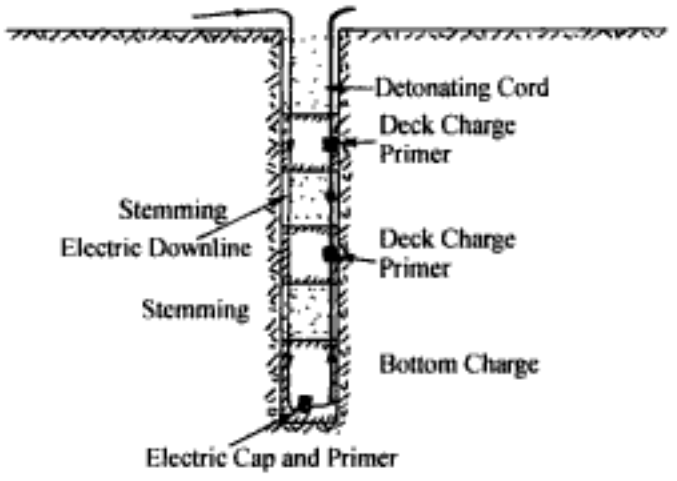

Figure 8.64. Electric blasting cap initiator with detonating cord up-line.

– Rock type is granite
– Wave velocity (c) = 3000 m/sec.
– Vertical bench face
– Hole diameter D = 0.229 m (9″)
– Bench height = 12 m
– Burden (B) = 25D = 6 m
– Subdrill = 0.3B = 2 m
– Stemming = 0.7B = 4 m
– Hole spacing = 1.15B = 6.9 m
– Explosive = *ANFO*
– Explosive detonation velocity = 4000 m/sec.
– Detonating cord downline
– Detonating cord detonation velocity = 7000 m/sec.
– Primer located at the bench toe elevation
– No downhole delay
– Crack propagation velocity = 0.38c = 1140 m/sec
– Gas streaming velocity = 1000 m/sec.

The basic geometry is shown in Figure 8.65.

Summarized below are the time requirements for the various events.

1. Time for the initiation instructions to go from the surface (collar of the borehole) to the primer

$$t_{init} = \frac{12\ \text{m}}{7000\ \text{m/ sec}} = 1.71\ \text{msec}$$

2. Time for the subdrill column to detonate

$$t_{e1} = \frac{2\ \text{m}}{4000\ \text{m/ sec}} = 0.5\ \text{msec}$$

3. Time for the above grade column to detonate

$$t_{e2} = \frac{8\ \text{m}}{4000\ \text{m/ sec}} = 2.0\ \text{msec}$$

4. Time for the shock wave to travel to the bench toe

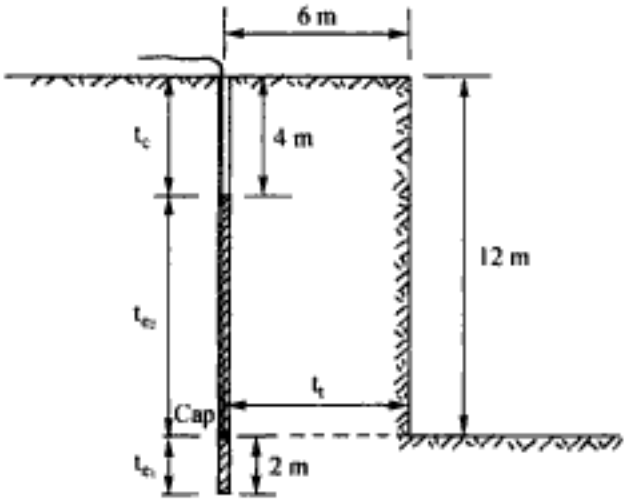

Figure 8.65. Diagrammatic representation of the different times involved in a blast.

$$t_t = \frac{6\text{ m}}{3000\text{ m/ sec}} = 2.0\text{ msec}$$

5. Time for the shock wave to travel from the top of the explosives column to the hole collar

$$t_c = \frac{4\text{ m}}{3000\text{ m/ sec}} = 1.3\text{ msec}$$

6. Time for the radial cracks to travel outward from the explosive column to the (vertical) free surface.

$$t_{rc}(\text{shortest path}) = \frac{6\text{ m}}{1140\text{ m/ sec}} = 5.3\text{ msec}$$

$$t_{rc}(138° \text{ angle}) = \frac{16.7\text{ m}}{1140\text{ m/ sec}} = 14.6\text{ msec}$$

7. Time for the explosive gases to reach the vertical free surface

$$t_{eg}(\text{shortest path}) = \frac{6\text{ m}}{1000\text{ m/ sec}} = 6\text{ msec}$$

$$t_{eg}(138° \text{ angle}) = \frac{16.7\text{ m}}{1000\text{ m/ sec}} = 16.7\text{ msec}$$

8. Time after detonation begins for spalling to begin at the hole collar

$$t_{spalling} = t_{e2} + t_c = 3.3\text{ msec}$$

9. Time after detonation begins to form a crater at the hole collar (assuming radial cracking from the top of the charge)

$$t_{cr}(\text{shortest path}) = 2.0 + \frac{4\text{ m}}{1140\text{ m/ sec}} = 5.5\text{ msec}$$

$$t_{cr}(138° \text{ angle}) = 2.0 + \frac{11.2\text{ m}}{1140\text{ m/ sec}} = 11.8\text{ msec}$$

10. Time after detonation for the gases to reach the vertical surface

$$t_{vs}(\text{shortest path}) = 2.0 + \frac{4\ \text{m}}{1000\ \text{m/ sec}} = 6\ \text{msec}$$

$$t_{vs}(138° \text{ angle}) = 2.0 + \frac{11.2\ \text{m}}{1000\ \text{m/ sec}} = 13.2\ \text{msec}$$

11. Assuming that the burden moves at 15 m/sec, the time required for it to move 100 mm (4 ins)

$$t_{100} = \frac{0.10\ \text{m}}{15\ \text{m/ sec}} = 6.7\ \text{msec}$$

The 100 mm crack is considered sufficient to prevent the shock wave from the next hole from being disturbed. This deformation is also sufficient to disrupt the surface cord lines.

12. The maximum surface time delay (detonating cord + delay) and yet avoid a cut off between holes in the same row is

$$t_{max} = t_{init} + t_{vs} + t_{100} = 1.7 + 13.2 + 6.7 = 21.6\ \text{msec}$$

Since the hole spacing is 6.9 m, this amounts to a time delay per meter of

$$t_{holes} = \frac{21.6\ \text{msec}}{6.9\ \text{m}} = 3.13\ \text{ms/ m}$$

This is in agreement with the rule-of-thumb for surface delay initiation which states that *'Surface initiation delay time should not exceed 1 ms/foot of spacing between the holes.'*

13. The minimum desired surface time delay between rows of holes.

$$t_{Delay} = t_{eg} + t_{100} = 16.7 + 6.7 = 23.4\ \text{msec}$$

Expressed in terms of meters of burden this becomes

$$t_{rows} = \frac{23.4\ \text{msec}}{6\ \text{m}} = 3.9\ \text{msec/ m}$$

The rule-of-thumb from Langefors & Kihlström (1963) is that for best fragmentation the delay time between rows is given by

$$\tau = K_{DT}B \tag{8.8}$$

where K_{DT} = constant = 3 to 5 ms/m, B = burden (m), τ = delay time (msec).

Gulf Explosives (1975) has suggested that for

– 230 to 380 mm diameter blastholes

and

– surface delay systems the optimum delay time usually varies from

1. 8 ms/meter of effective burden for
   - Long stemming columns,
   - Low powder factors ~ 0.25 kg/m^3,
   - Soft, highly fissured strata of low density to
2. 4 ms/meter for
   - Short collars,
   - High powder factors ~ 0.60 kg/m^3,

– Dense, hard, massive rocks.

If sufficient time (delay) is not provided between holes there will be no place for the muck to move. This will result in:

– Hard, high bottom,
– Excessive toe on the next shot,
– A great deal of ragged cratering and attendant flyrock in the upper region of the borehole.

The long delay times between holes pose problems only when using surface delays. One way of overcoming this is through a combination of long period downhole delays and short period surface delays.

The bottom-hole delay placed in each hole is selected so that the desired number of holes are energized before the first hole detonates. The surface delays are selected to provide the desired rock breakage. Assume for example that the 4 holes shown in Figure 8.66 are to be blasted with a 25 msec delay period between the holes. There is to be no chance of surface cutoff. To accomplish this all holes are to be energized before the first hole detonates. The bottom hole – surface hole delay system (assuming no cap timing deviation) is shown. The time difference between when Cap 1 and Cap 4 are initiated is

$$\text{Time diff} = t_{12} + t_{23} + t_{34} + 3\,(\text{Surface Delay}) = 3\text{ ms} + 3\,(25\text{ ms}) = 78\text{ ms}$$

The minimum bottom hole delay should be 78 msec. To account for cap scatter, a 100 msec bottom hole delay has been selected. The placing of this delay at the bottom of each hole is easy for those doing the charging since it is the same delay number in each hole. The surface delays are then added during the final tie-up. To allow as much flexibility in the surface tie up as possible, the initial bottom hole delay should be large.

Through the years, the amount of time delay desired to provide the best fragmentation has changed. Today, the constant K_{DT} in the Langefors Formula (8.1) has been increased to 3 to 5 ms/ft of burden. This is an increase by about a factor of 3 from that originally proposed. The longer total delay times are achieved through a combination of surface delays and in-hole delays.

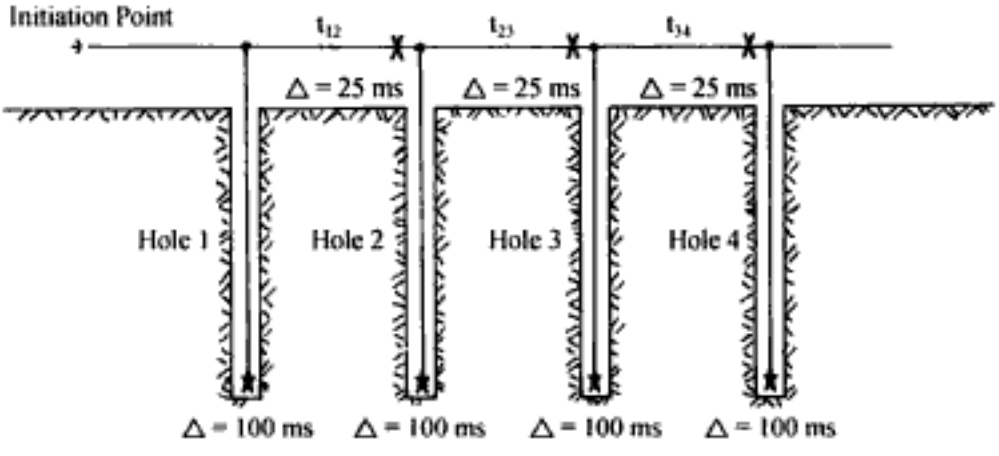

Figure 8.66. Combination of in-hole and surface delays.

8.8 INITIATION EXAMPLE

There are a large number of factors to be considered when deciding upon the sequencing of holes:

- Type of fragmentation desired,
- Surface or in-hole delays,
- Firing direction,
- Shape of muck pile/loading equipment,
- Number of delays available,
- Type of trunkline system,
- Environmental constraints (ground vibration/air blast, etc.).

In some cases a maximum delay time is specified to avoid cutoffs between holes. In other cases the minimum amount of time between holes or rows of holes to achieve the best fragmentation may control. Environmental constraints may determine the maximum number of holes which can be shot on the same delay.

In Chapter 5 a blast design example was begun in which a round (Fig. 8.67) involving four rows of holes was to be shot. Each row contains 6 holes. Here the example will be continued to arrive at an initiation scheme. It will be assumed that

- There are no environmental restrictions on the number of holes to be shot/delay,
- Detonating cord trunk lines with surface delays will be used,
- The firing direction will be as determined using a *V*1 design,
- To avoid cutoffs a maximum surface delay of 3.3 ms/m (1 ms/ft) can be used,
- To minimize a misfired round, there should be 2 detonating cord routes to each hole,
- A minimum number of delays are to be used.

The detonating cord hookup is shown in Figure 8.68. Detonating cord of strength 5 g/m is selected. As can be seen, the effective burden (B_e) is less than the drilled burden (B)

$$B_e = \frac{B}{\sqrt{2}} = \frac{9.5}{\sqrt{2}} = 6.7 \text{ m}$$

The effective spacing on the other hand increases to

$$S_e = S\sqrt{2} = 9.5\sqrt{2} = 13.4 \text{ m}$$

Using the effective burden dimension of B_e = 6.7 m one finds that the maximum recommended surface delay between rows is

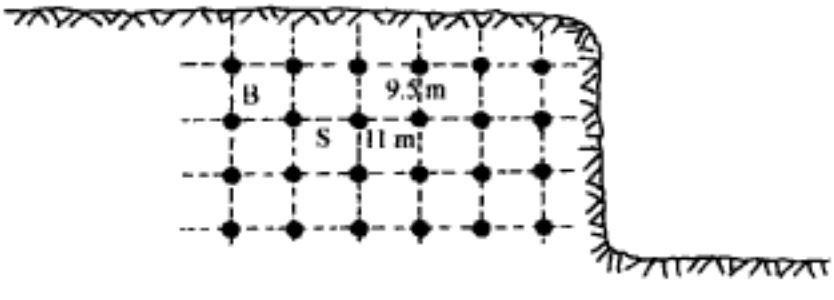

Figure 8.67. Bench round drilled in a square pattern.

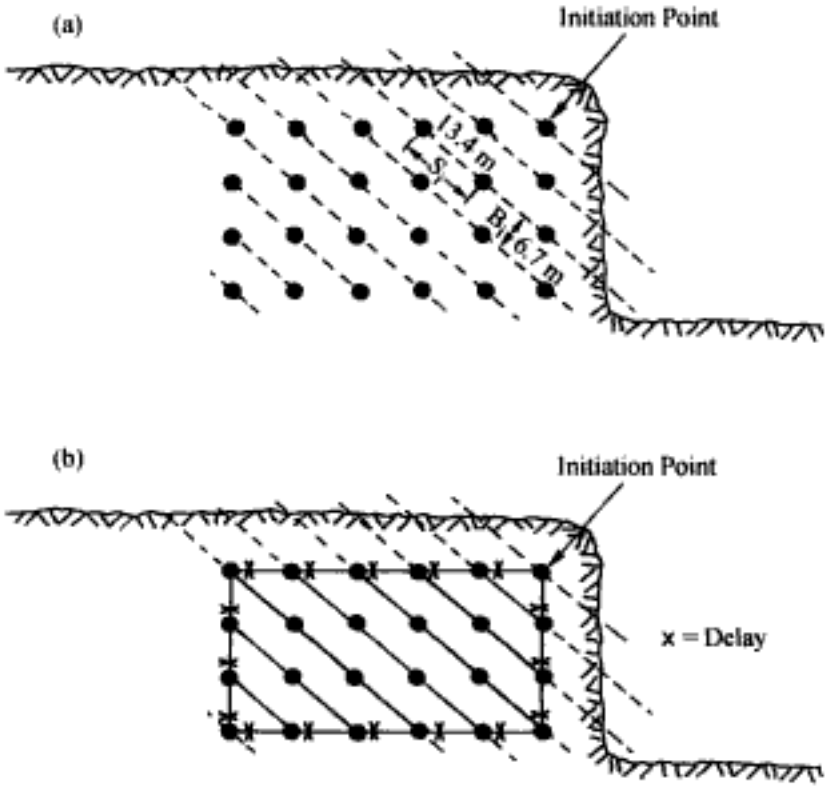

Figure 8.68. Bench round shot in a *V*1 pattern.

$$\text{Delay} = 6.7 \text{ m} \times 3.3 \text{ ms/m} = 22 \text{ ms}$$

A standard Period 1 millisecond delay from some suppliers is

$$D_1 = 30 \text{ ms}$$

For others it would be

$$D_1 = 25\text{ms}$$

Both are somewhat greater than desired although the 25 ms delay could probably be successfully used. To provide at least some movement of the row in front prior to the next row firing requires a time delay of between 3 to 5 ms/m of burden. Thus the minimum time delay between rows from a fragmentation viewpoint is of the order of magnitude of

$$T_{min} = 20 \text{ to } 33 \text{ ms}$$

In theory, only one delay number (25 ms) would be required for the round. However with so many holes involved, the last holes to fire could be quite heavily choked (due to the decreasing free forward movement with row number) using such a delay. If today's delay recommendations of 3 to 5 ms/ft of burden are used instead one finds that the desired time delay is

$$T(\text{desirable}) = 65 \text{ to } 110 \text{ ms}$$

between rows. This cannot be accomplished with surface delays alone. The reader is encouraged to make a design using a combination of available surface and in-hole delays.

Each hole has a primacord downline which will be tied into the trunkline. Tied to the bottom of the downline is a cast 1 lb (454 gm) primer. The downline has a strength of

10 g/m. This is strong enough to initiate the primer but weak enough so that the explosive column is not initiated by the cord itself. The cast primer is located at the toe elevation (see Fig. 8.69).

One important concern is the safety of neighboring structures. There are several procedures which can be used to determine whether the size of the charge shot per delay (W) and the distance from the blast (D) are compatible with the structures. These are discussed in detail in Chapter 9.

However, one of the techniques, based upon the use of scaled distance (D_s).

$$D_s = \left(\frac{R}{W}\right)^{1/2} \tag{8.9}$$

where W = maximum amount of explosive (lbs) shot within an 8 ms time interval, R = distance of the shot to the structure (ft), D_S = scaled distance (ft/lb$^{1/2}$), will be briefly presented in order to complete the example. The limits on D_S are dependent upon the distance D as shown in Table 8.19.

If the actual scaled distance exceeds the allowable scaled distance then no damage would be expected. In the case of this example an important structure is located 6000 ft from the blast. The question is whether the blast as designed (four holes/delay) can be shot without damaging the structure. The amount of explosive shot per delay is

$$W = 4 \times 1049 \text{ kg} = 4196 \text{ kg} = 9230 \text{ lbs}$$

Since the distance is 6000 ft, the actual scaled distance D_S is

$$D_S = 6000/9230^{1/2} = 62.41$$

This is greater than the allowable

$$D_S \text{ allowable} = 60$$

for this distance and hence the blast should be safe from a ground vibration viewpoint.

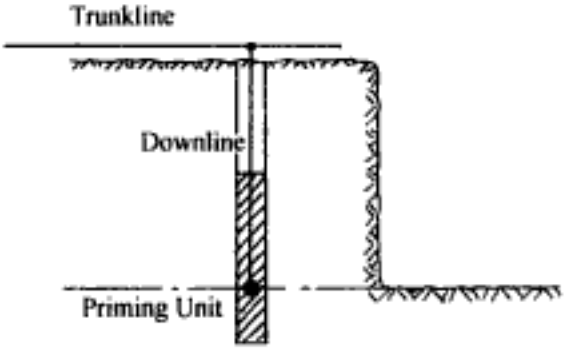

Figure 8.69. Cross-section showing the charging and initiating design.

Table 8.19. Allowable scaled-distance versus distance from the shot.

Distance D_v (ft)	Allowable scaled distance
0-300	50
300-5000	55
> 5000	60

REFERENCES

AECI Explosives and Chemicals Limited. 1979a. Electric blasting. *Explosives Today*. Series 2, no 16, June.

AECI Explosives and Chemicals Limited. 1979b. Electric blasting: series circuits. *Explosives Today*. Series 2, no 17, Sept.

AECI Explosives and Chemicals Limited. 1979c. Electric blasting: parallel circuits. *Explosives Today*. Series 2, no 18, December.

AECI Explosives and Chemicals Limited. 1980a. Electric blasting: series-in-parallel circuits (Part 1). *Explosives Today*. Series 2, no 19, March.

AECI Explosives and Chemicals Limited. 1980b. Electric blasting: series-in-parallel circuits (Part 2*). Explosives Today*. Series 2, no 20, June.

AECI Explosives and Chemicals Limited. 1982. The Use of Cordex 10. *Explosives Today*. Series 2. No. 29. September.

AECI Explosives and Chemicals Limited. 1984. Introduction to Explosives. *Explosives Today*. Series 2, no 35, 1st Quarter.

AECI Explosives and Chemicals Limited. 1985. Nonel in surface blasting. *Explosives Today*. Series 2, No 38, June.

AECI Explosives and Chemicals Limited. 1986a. Safety in electric detonators (Part 1). *Explosives Today*. Series 2, no 42, June.

AECI Explosives and Chemicals Limited. 1986b. Safety with electric detonators (Part 2). *Explosives Today*. Series 2, no 43, Sept.

AECI Explosives and Chemicals Limited. 1987a. The safe and efficient initiation of explosives (Part 1-Principles). *Explosives Today*. Series 2, No 47, September.

AECI Explosives and Chemicals Limited. 1987b. The safe and efficient initiation of explosives (Part 2-Intrmediate and large diameter holes). *Explosives Today*. Series 2, No 48, December.

AECI Explosives and Chemicals Limited. 1988. Safety in surface blasting. *Explosives Today*. Series 2, no 50, June.

AECI Explosives and Chemicals Limited. 1989. Static electricity. *Explosives Today*. Series 3, no 4, June.

Andrews, A.B. 1981. Design criteria for sequential blasting. *Proceedings of the 7th Conference on Explosives and Blasting Technique. SEE.* pp. 173-192.

Anonymous 1976. Puzzled about primers for large-diameter *ANFO* charges? Here's some help to end the mystery. *Coal Age*. 81(8): 102-107.

Anonymous 1984. CB radios: A blasting hazard? *Downline. Issue* No. 1, Summer. pp. 4-5. ICI Explosives.

Anonymous 1992. Non-electric blast initiation: How to select the right system. *E&MJ*. 193(5): 16FF-16GG.

Anonymous 1993. *The electronic detonator*. Nitro Nobel Magazine. July. 19 pp.

Anonymous 1992. *The NPED blasting cap – What is it*? Sprängnytt (Nitro Nobel). No. 1. March. p. 18. In Swedish.

Anonymous 1993. *The electronic blasting cap – An advanced tool for the competent blaster*. Spräng Nytt (Nitro Nobel), Nr 1, March, p. 8. In Swedish.

Atlas Powder Company. *Initiation Systems Products*.11 pp.

Atlas Powder Company, 1987. *Explosives and Rock Blasting*. Maple Press. 662 pp.

Atlas Powder Company. *Electrical Hook-Ups: Surface Blasting*. 11 pp.

Atlas Powder Company. 1981. *Workshop Manual 'Surface Blasting Course'*.

Atlas Powder Company. *Electric blasting circuits-calculations*. 14 pp.

Atlas Powder Company. *Sequential blasting*. 57 pp.

Atlas Powder Company. *Atlas SF Electric Blasting Caps*.

Austin Powder Company. *Austin Delay Connectors*.

Austin Powder Company. *Rock-Star Electric Detonators*. Product Information Bulletin RS891.

Bajpayee, T.S., Mainero, R.J. & J.E. Hay 1985. *Overlap probability for short period-delay detonators used in underground coal mining*. USBM RI 8888.

Bajpayee, T.S. & R.J. Mainero 1990. Firing accuracy of electric detonators. *Proceedings 16th Annual Conference on Explosives and Blasting Technique. SEE.* pp. 89-102.

Ball, M.J. & R. Watt. 1982. Field experience with new methods of shotfiring. *Proceedings of the 8th Conference on Explosives and Blasting Technique. SEE.* pp. 169-175.

Bhushan, V., C.J. Konya & S. Lukovic 1986. Effect of detonating cord downline on explosive energy release. *Proceedings of the 12th Conference on Explosives and Blasting Technique (Mini-Symp). SEE.* pp. 41-55.

Hidden page

Ensign-Bickford Company 1981. Nonel Primadet: H.D. Nonel Primadet System, Technical Bulletin.
Ensign-Bickford Company 1984. *Primacord Handbook*. 59 pp.
Ensign-Bickford Company 1990. *MS Connector* series-Primadet.Technical Bulletin.
Ensign-Bickford Company 1991. *Product and Blast Design Guide*.
Feasler, J. M. 1977. New developments in surface blast initiation systems- Nonel noiseless trunkline delays and Nonel lead-in. *Proceedings of the 3rd Conf on Explosives and Blasting Tech. SEE.* pp. 183-187.
Florin, H. 1988. A new type of nonelectric detonator. *Proceedings of the 14th Conference on Explosives and Blasting Technique. SEE.* pp. 389-396.
Gray, E. 1976. Controlled sequential blasting. *Proc of the 2nd Conf on Explosives and Blasting Technique. SEE.* pp. 341-354
Gregg, W.B., Jr. 1994. ACCUBLAST detonator-a new era of precision in all-electronic detonators. *Proceedings of the 5th High-Tech Seminar on Blasting Technology, Instrumentation and Explosives Applications. New Orleans, Louisiana* (July 9-14). Blasting Analysis International, Inc. pp. 33-65.
Gulf Explosives. 1975. Programming Your Blast With Gulf Explosives. 23 pp.
Hagan, T.N. 1974. Optimum priming systems for ammonium nitrate – fuel oil type explosives. *Proceedings, Southern and Central Queensland Conference of the AusIMM. Parkville, Victoria, Australia.* July. pp. 283-297.
Hagan, T.N. 1975. Initiation sequence: Vital element of open pit blast design. Design Methods in Rock Mechanics (C.Fairhurst & S.L. Crouch, eds) *Proceedings of the 16th US Symposium on Rock Mechanics, Minneapolis, Minn.ASCE*, 1977. pp. 345-355.
Hagan, T.N. 1977a. Optimum initiation, priming and boostering systems. Chapter 3 in *Australian Mineral Foundation's 'Drilling and Blasting Technology' Course, Adelaide*, May. 44 pp.
Hagan, T.N. 1977b. Effects of delay timing on blasting techniques. Chapter 7 in *Australian Mineral Foundation's 'Drilling and Blasting Technology' Course, Adelaide*, May. 37 pp.
Hagan, T.N. 1977c. Good delay timing-prerequisite of efficient bench blasts. *Proc. Australas. Inst. Min. Metall.*, (263): 47-54.
Hagan, T.N. 1979. Accurate delay timing and cutoffs. Chapter 10 in the *workshop proceedings for 'Influence of Rock Properties on Drilling and Blasting' Adelaide*, 25-29 June. Australian Mineral Foundation, Inc. pp. 256-273.
Hagan, T.N. *Safety and Efficiency in Quarry Blasting Manual*. ICI Australia Operations Pty, Ltd Explosives Division. For course March 26-28 in Sydney.
Hagan, T.N. & J.K. Mercer 1983. Safe and Efficient Blasting in Open Pit Mines. Manual written for the course given at Karratha, Australia 23-25 November. ICI Australia Operations Pty, Ltd. Explosives Division.
Hanger, C.A. 1994. Non-electric sequential blasting for open pit mining application. *Explosives Engineering*. 12(1): 9, 10, 16-20.
Heilig, J.H & C.K. McKenzie 1988. Delay variability – the measurement, analysis and implication on rock blasting. *Proceedings, Explosives in Mining Workshop. AusIMM, Melbourne, Victoria,* Nov. pp. 33-38.
Hercules Incorporated 1969. *Explosives Technical Data*. Safety Fuse.
Hercules Incorporated 1972. *Hercules Explosives Engineer's Guide*.
Hercules Incorporated *Cap facts: Planning the series firing circuit.*
Hercules Incorporated *Cap facts: Using the blasting galvanometer.*
Hercules Incorporated *Cap facts: Recommended firing circuits.*
Hercules Incorporated *Cap facts: How an electric delay cap functions.*
Hercules Incorporated Cap Facts- Planning the Firing Circuit. Bulletin ECF-109.
Hercules Incorporated 1982. Hercudet Nonelectric Delay Blasting System. Sales Brochure 200-295A.
Holmberg, R. 1992. Nitro Nobel's new non-primary explosive detonator. *Proceedings, First International Concrete Blasting Conference* (E.K. Lauritzen & J. Schneider, eds), Copenhagen. Danish Federation of Explosive Engineering. pp. 51-56.
Holmberg, R. 1994. Rock blasting in a simple and modern way. Sprängnytt (Nitro Nobel). No. 3, October, pp. 10-13. In Swedish.
Holmberg, R. 1997. Environmental aspects regarding the use of initiating systems and explosives. *Proceedings from the Blasting Committee's Discussion Meeting. Stockholm,* March 11. pp. 163-169. In Swedish.
Holmberg, R. 1998. Private communication.
Hopler, R.B. 1975. The Hercudet system of initiation. *Proceedings of the 1st Conference on Explosives and Blasting Technique. SEE.* pp. 121-129.

Hidden page

Svärd, J. 1992a. The possibilities with accurate delay times – results of some field tests using electronic blasting caps. *Proceedings, 4th High-Tech Seminar: Blasting Technology, Instrumentation and Explosives Applications.* Blasting Analysis International, Inc. Nashville, Tenn. June 20-25.

Svärd, J. 1992b. The possibilities with accurate delay times – the results of some field tests conducted with electronic detonators. Lecture presented at *the Nitro Nobel Blasting Conference Göteborg-Kiel,* January 15-16. In Swedish.

Svärd, J. 1992c. The possibilities with accurate delay times – the results of some field tests conducted with electronic detonators. *Proceedings of the 4th High-Tech Seminar on Blasting Technology, Instrumentation and Explosives Applications.* Blasting Analysis International, Inc. Nashville, Tennessee. June 20-25.

Svärd, J. 1993. Possibilities with accurate delay time. *Proceedings of 4th Int. Symo. on Rock Fragmentation by Blasting – FRAGBLAST-4.* H.-P. Rossmanith, editor. Vienna, Austria 5-8 july. A.A. Balkema, Rotterdam. pp. 71-78.

Tansey, D.O. 1979. The DuPont sequential blasting system. *CIM Bulletin.* 72 (July): 80-115.

Tansey, D.O. 1980. A delay sequencing blasting system. *Proceedings of the 6th Conference on Explosives and Blasting Technique. SEE.* pp. 345-375.

Teller, A.E. 1972. Axial priming improves AN/FO blasting. *Rock Products.* 75(4): 76-78, 105-107.

Treleaven, T. 1991. Practical applications and blast designs with nonelectric initiation systems. *Proceedings, Third High-Tech Seminar on Blasting Technology, Instrumentation and Explosives Applications.* Blasting Analysis International, Inc. *San Diego,* Calif. June 2-7.

Treleaven, T. 1994. Non electric shock tube initiation systems, delay pattern applications & hook-ups. *Proceedings of the 5th High-Tech Seminar on Blasting Technology, Instrumentation and Explosives Applications. New Orleans, Louisiana* (July 9-14). Blasting Analysis International, Inc. pp. 997-1128.

Watson, J.T. 1997. A New Generation of Shock Tube Detonators. *Proceedings, Seventh High-Tech Seminar on State-of-the-Art, Blasting Technology, Instrumentation and Explosives Applications.* Blasting Analysis International, Inc. *Orlando, Florida,* July 28-August 1, 1997.

Winzer, S.R. 1978. The firing times of ms delay blasting caps and their effect on blasting performance. *Report to the NSF. Martin Marietta laboratories,* June.

Winzer, S.R., Furth, W & A. Ritter 1979. Initiator firing times and their relationship to blasting performance. *Proceedings, 20th US Symposium on Rock Mechanics. Austin, Texas.* June 4-6. pp. 461-470.

Worsey, P.N. & L.J. Tyler 1983. The development concept of the integrated electronic detonator. *Proceedings of the 9th Conference on Explosives and Blasting Technique. SEE.* pp. 489-496.

CHAPTER 9

Environmental effects

9.1 GROUND MOTION

9.1.1 *Introduction*

Blasts, if not properly designed, may result in ground motions of sufficient intensity to damage

- Mine plant and structures,
- Neighboring structures outside of the mine permit area.

Over the years a number of design guidelines have emerged relating ground motion to structural damage. Comprehensive regulations in this regard have been developed by the US Office of Surface Mining Reclamation and Enforcement (OSMRE). These are presented in this section together with explanatory material as to how one might best comply with the regulations. In preparing this section the author has drawn heavily upon the *Blasting Guidance Manual* (Rosenthal & Morlock, 1987) put out by the OSMRE.

The regulations are based upon the peak particle velocity (PPV) produced during blasting. In certain cases, peak particle acceleration (PPA) and peak particle displacement (PPD) are of overriding importance. Computer manufacturers commonly restrict the PPA and owners of large generators place limits on the displacement (AECI, 1982). A conversion nomogram for this purpose is given in Figure 9.1. Knowing the predominant frequency of vibration and one of the three quantities:

- Acceleration (a),
- Velocity (v),
- Displacement (d)

one can easily obtain the other two.

Table 9.1 lists a series of blasting factors and their influence on ground vibration control. Of these, the three primary variables affecting ground motion at any particular site are:

- Distance from the blast to the position of interest
- Explosive charge weight per delay period
- Frequency of vibration

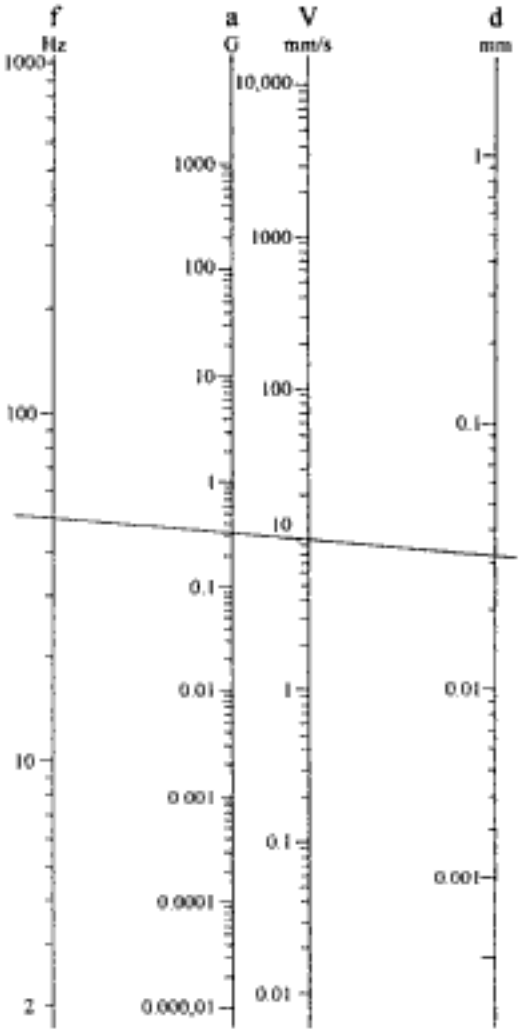

Figure 9.1. Nomogram showing relationship between frequency, peak particle acceleration velocity and amplitude (AECI, 1982).

Table 9.1. Factors which influence ground motion (Rosenthal & Morlock, 1987).

Variables within the control of mine operators	Influence on ground motion		
	Significant	Moderately significant	Insignificant
1. Charge weight per delay	X		
2. Delay interval	X		
3. Burden and spacing		X	
4. Stemming (amount)			X
5. Stemming (type)			X
6. Charge length and diameter			X
7. Angle of borehole			X
8. Direction of initiation		X	
9. Charge weight per blast			X
10. Charge depth			X
11. Bare vs. Covered primacord			X
12. Charge confinement	X		
Variables not in the control of mine operators			
1. General surface terrain			X
2. Type and depth of overburden	X		
3. Wind and weather conditions			X

The regulations and the design/monitoring procedures needed for complying with the regulations go together and they will be discussed that way in this section. The four procedures are

1. Maximum peak-particle velocity limit
2. Scaled distance equation
3. Modified scaled distance equation
4. Blasting level chart

Each will be described separately.

All of the procedures are based upon limiting the peak particle velocity at the structure of importance. However, the amount of site evaluation and monitoring time and expense involved in meeting the criteria vary considerably between the four. The possibilities for both long and short term savings in the overall blasting programs also vary considerably.

9.1.2 *Maximum peak particle velocity limit*

Using this procedure the maximum ground vibration shall not exceed the limits given in Table 9.2 at the location of any dwelling, public building, school, church, or community or institutional building outside the permit area. In addition, all structures in the vicinity of the blasting area, such as water towers, pipelines and other utilities, tunnels, dams, impoundments, and underground mines shall be protected from damage by establishment of maximum allowable limit on the ground vibration. The particle velocity shall be recorded in three mutually perpendicular directions (Fig. 9.2). The planes of motion are normally considered to be (AECI, 1982).

1. Longitudinal (sometimes called radial). The horizontal motion in a direct line towards the blast is measured.
2. Transverse (tangential). The horizontal motion at 90° to the radial direction is measured.
3. Vertical. The vertical motion is measured.

Table 9.2. Peak particle velocity limits as a function of distance from the blasting site (Rosenthal & Morlock, 1987).

Distance (D) from the blasting site (feet)	Maximum allowable peak particle velocity (V_{max}) for ground vibration (in/sec)
0 to 300	1.25
301 to 5000	1.00
5001 and beyond	0.75

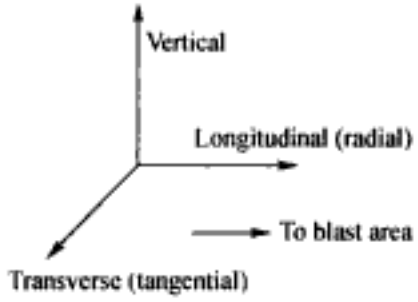

Figure 9.2. Definition of the vertical, longitudinal and transverse vibration directions (AECI, 1982).

The maximum allowable peak particle velocity applies to *each* of the three measurements. Note that it is *not necessary* to develop a vector sum resultant velocity.

A seismograph record shall be provided for each blast. The monitoring equipment required is relatively simple since only peaks need to be recorded. No frequency content is required. If the peak particle velocities are below those given in Table 9.2, then the blast should be in compliance with the regulations. To be able to *design* such a blast one needs some procedures and guidelines. These are provided under the following two procedures; 'Scaled-Distance' and 'Modified Scaled Distance'.

9.1.3 *Scaled-distance equation*

The scaled-distance equation

$$W = \left(\frac{D}{D_S}\right)^2 \tag{9.1}$$

where W = the maximum weight of explosives (lbs), D = distance (feet) from the blasting site to the nearest protected structure, D_S = the scaled-distance factor, may be used to determine the allowable charge-weight of explosives to be detonated in any 8-millisecond period without seismic monitoring. The scaled-distance factors which are to be applied without seismic monitoring are given in Table 9.3. These values are intended for general use and as a result must be conservative. In many cases they are *very* conservative.

To illustrate this assume that a sensitive structure is located at a distance of 1000 ft from a forthcoming blast. Using Table 9.3 the permitted scaled-distance factor is 55. Thus the total amount of explosive which can be shot within an 8 msec period is

$$W = \left(\frac{D}{D_S}\right)^2 = \left(\frac{1000}{55}\right)^2 = 330 \text{ lbs}$$

Actual measurements made at the site suggest that the velocity attenuation formula (see Section 9.1.4) is

$$V = 160\,(D_S)^{-1.6} \tag{9.2}$$

For the distance of 1000 ft, the permitted particle velocity (Table 9.2) is 1.0 in sec. Substituting this into Equation (9.2) one finds that the site specific scaled distance factor is

$$D_S \cong 24 \tag{9.3}$$

Thus the amount of explosive which could be shot per delay and still satisfy the velocity limits is

$$W = \left(\frac{1000}{24}\right)^2 = 1736 \text{ lbs}$$

Table 9.3. Scaled-distance factors to be applied without seismic monitoring (Rosenthal & Morlock, 1987).

Distance (D) from the blasting site (Ft)	Scaled-distance factor
0 to 300	50
301 to 5000	55
5001 and beyond	65

Table 9.4. Maximum amount of explosive/delay as a function of distance from the blast and the seismic-distance factor.

Actual distance from blast (ft)	Maximum amount of explosive (lbs) per 9 msec or greater delay		
	$D_s = 50$ (0-300′)	$D_s = 55$ (301′-5000′)	$D_s = 65$ (> 5001′)
50	1.0		
75	2.3		
100	4.0		
150	9.0		
200	16.0		
250	25.0		
300	36.0		
350		40	
400		53	
500		83	
600		119	
700		162	
800		212	
900		268	
1000		331	
2000		1322	
3000		2975	
4000		5290	
5000		8265	
6000			8521
10,000			23,700

The difference between 330 and 1736 lbs/delay obviously has a major impact upon blast design.

The advantage of choosing the scaled-distance equation approach for blast design is that it is simple. No measurements need to be made. One simply substitutes the appropriate values into the scaled distance formula. The disadvantages are that the design tends to be very conservative and since no monitoring is done nothing is learned in a quantitative way to improve further blasts. Table 9.4 presents the maximum amount of explosive (lbs) which can be shot per 9 msec or greater delay as a function of distance and scaled distance.

9.1.4 *Modified scaled-distance equation*

Many years of experience have shown that the peak particle velocity is related to the scaled distance by the relationship

$$V = H\,(D_S)^{-\beta} \tag{9.4}$$

where V = peak particle velocity (in. /sec), H = particle velocity (in/sec) for $D_S = 1.0$, D_S = scaled distance (ft/lb$^{1/2}$), β = constant.

This is sometimes called an attenuation equation since the value of exponent β is positive. The values of H and β are highly site specific. H can range from as low as 20 up to 1000 or more. The exponent β will generally lie in the range of 1.1 to 2.4. The attenuation formula which describes (approximately) the values used in the regulations (Table 9.5) is

$$V = 4273\ D_S^{-2.08}$$

The high value of H (H = 4273) makes it very conservative particularly at close range (small values of D_S).

The regulations allow the mine operator to develop and use a site specific form of the scaled distance equation. For the operator this means obtaining values of H and β for the site in question. The regulations state that the modified factors selected shall be such that the particle velocity will not (at the 95-percent confidence level) exceed the maximum allowable peak particle velocity given in Table 9.2. To be able to demonstrate this to the regulatory authorities, a set of data

1. Peak particle velocity (V_{max}),
2. Distance (D) from the measuring site to the blast (ft),
3. Maximum amount (lbs) of explosive (W) per shot within an 8 msec delay,

must be collected from a series of blasts. The data should

– Be collected over as wide a range of scaled distances as possible,
– Be spread evenly over this range.

These data *must* be collected at as low a scaled-distance as it is hoped will be authorized and preferably lower than this. Each of these components (V_{max}, D and W) must be determined with care. The three ground motion components are to be separately measured and that yielding the peak particle velocity is used in the calculation. For each blast D and W are represented by a single number, the scaled distance, D_S. Hence from each blast one obtains a data pair (V, D_S).

Since there is a high confidence level (95%) imposed, the results must be collected from a relatively large series of blasts. The OSMRE indicates that 30 pairs is acceptable if the data are good.

Figure 9.3 shows the type of record that would be obtained. As can be seen

V = 7.5 mm/sec
W = 15 kg

Table 9.5. Peak particle velocity and seismic-distance factor comparison (Rosenthal & Morlock, 1987).

V (in/sec)	D_s
1.25	50
1.0	55
0.75	65

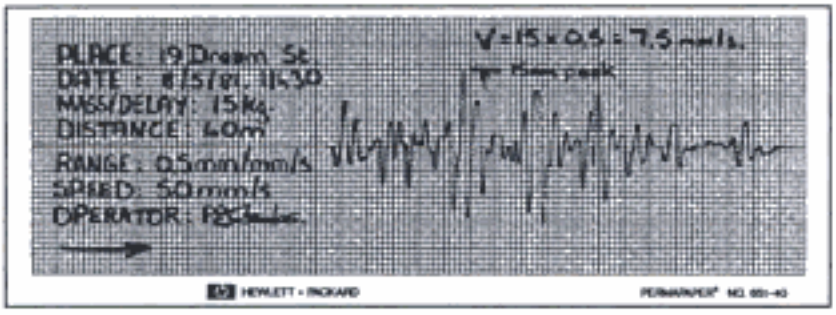

Figure 9.3. Typical chart recorder output from a blast (AECI, 1982).

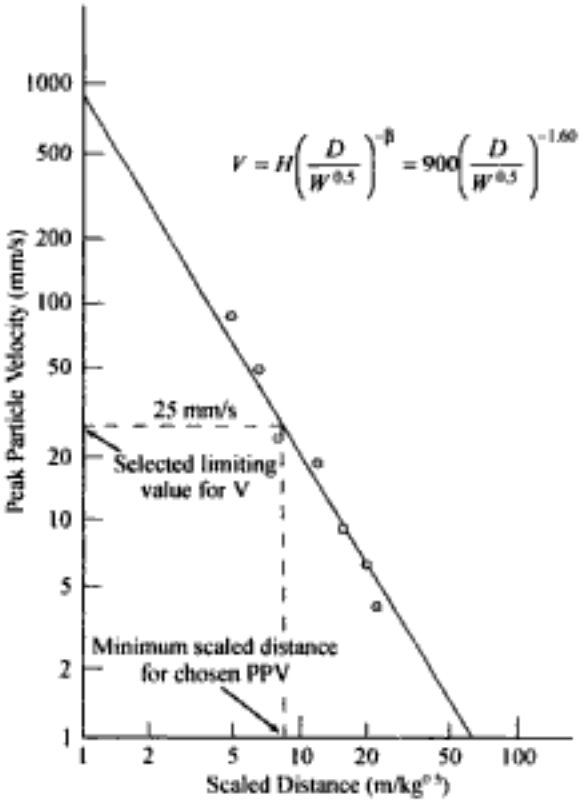

Figure 9.4. Example of log-log plot of peak particle velocity against scaled distance (AECI, 1982).

$$D = 40 \text{ m}$$

The data pair used in the calculation (AECI, 1982) is then

$$D_S = \frac{40}{15^{1/2}} = 10.33$$

$$V = 7.5 \text{ mm/sec}$$

If one takes logarithms of both sides of Equation (9.4), one obtains

$$\log V = \log H - \beta \log D_S \tag{9.5}$$

Substituting

$$y = \log V$$
$$x = \log D_S$$
$$a = \log H$$
$$b = -\beta$$

into Equation (9.5) one finds that it is of the form

$$y = a + bx \tag{9.6}$$

This means that the V and D_S data should plot as a straight line on log-log graph paper. The slope of the line is equal to $-\beta$ and H is the velocity intercept at $D_S = 1$. Seven pairs of data have been plotted in Figure 9.4. A curve is passed through the points using least squares regression analysis. The 'best fit' values of H and β are obtained as well as an indication of the 'goodness of fit' in the form of a coefficient of determination (r^2). The

value of r^2 should not be less than 0.7. The standard deviation used in establishing the confidence level is not likely to be under about 0.2. It should not be greater than about 0.5.

For a given data set, the design curve is moved with respect to the data so that the 95% confidence level is achieved. If the standard deviation becomes too large, the H variable of the attenuation formula increases to the point that the 95% confidence level will only be attainable at large scaled distances – those approaching the allowable non-site specific scaled distances. Once the curve has been developed, the line representing the maximum allowed particle velocity is drawn, in this case it is 1.0 in/sec and the scaled distance read ($D/W^{1/2}$). One can also use the attenuation equation directly

$$V = 900\left(\frac{D}{W^{1/2}}\right)^{-1.60} \tag{9.7}$$

to find the same result. This equation can now be used without the need for monitoring each blast. It should however be checked periodically to make sure that nothing has changed at the site or in the blasting procedures being followed. The advantage of choosing this option is that a blasting criterion fitting the site is developed. In the process of developing the equation, a considerable amount of information regarding the site and the blasting practices are obtained. Initial expense is incurred for the monitoring, however further round by round monitoring, although desirable, is not required.

9.1.5 *Blasting-level chart*

In the fourth option the blasting-level chart shown in Figure 9.5 may be used to determine the maximum allowable ground vibration if the predominant frequency is known. As can be seen, for frequencies greater than 30 Hz the maximum allowable particle velocity jumps to 2 in/sec. This is based upon the fact that structures (buildings) have low natural fre-

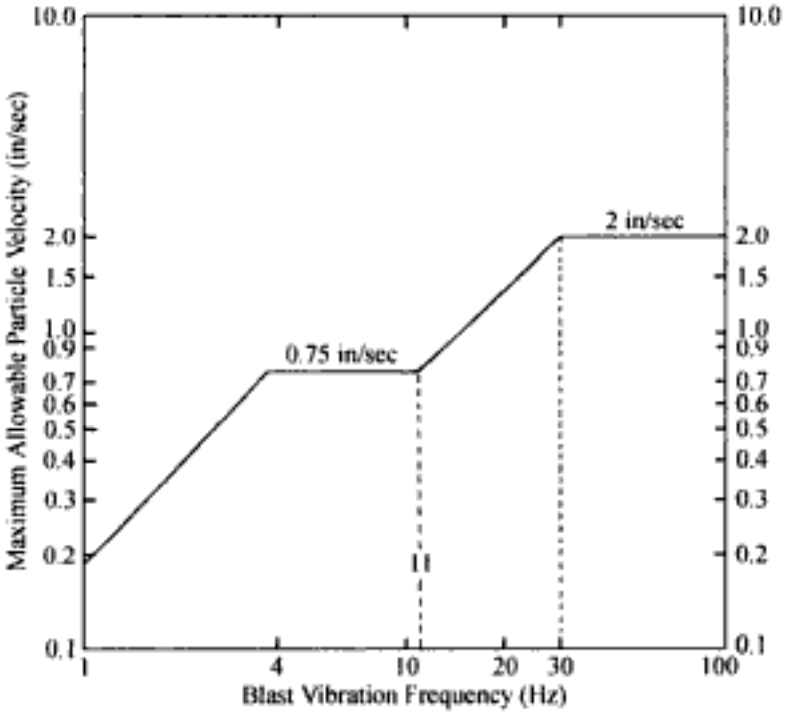

Figure 9.5. OSMRE peak particle velocity versus vibration frequency limits (Rosenthal & Morlock, 1987).

quencies of vibration and are most vulnerable to low frequency (less than 10 Hz) ground waves. They are relatively insensitive to frequencies in excess of 40 hertz (AECI, 1982).

In practice one must first conduct a series of test blasts at the site such as described in option 3. However, in addition to simply finding the peak particle velocity one must also collect frequency data. Instruments are available for doing this (Fig. 9.6 shows one such

Figure 9.6. Typical blast monitoring system (Matheson, 1996).

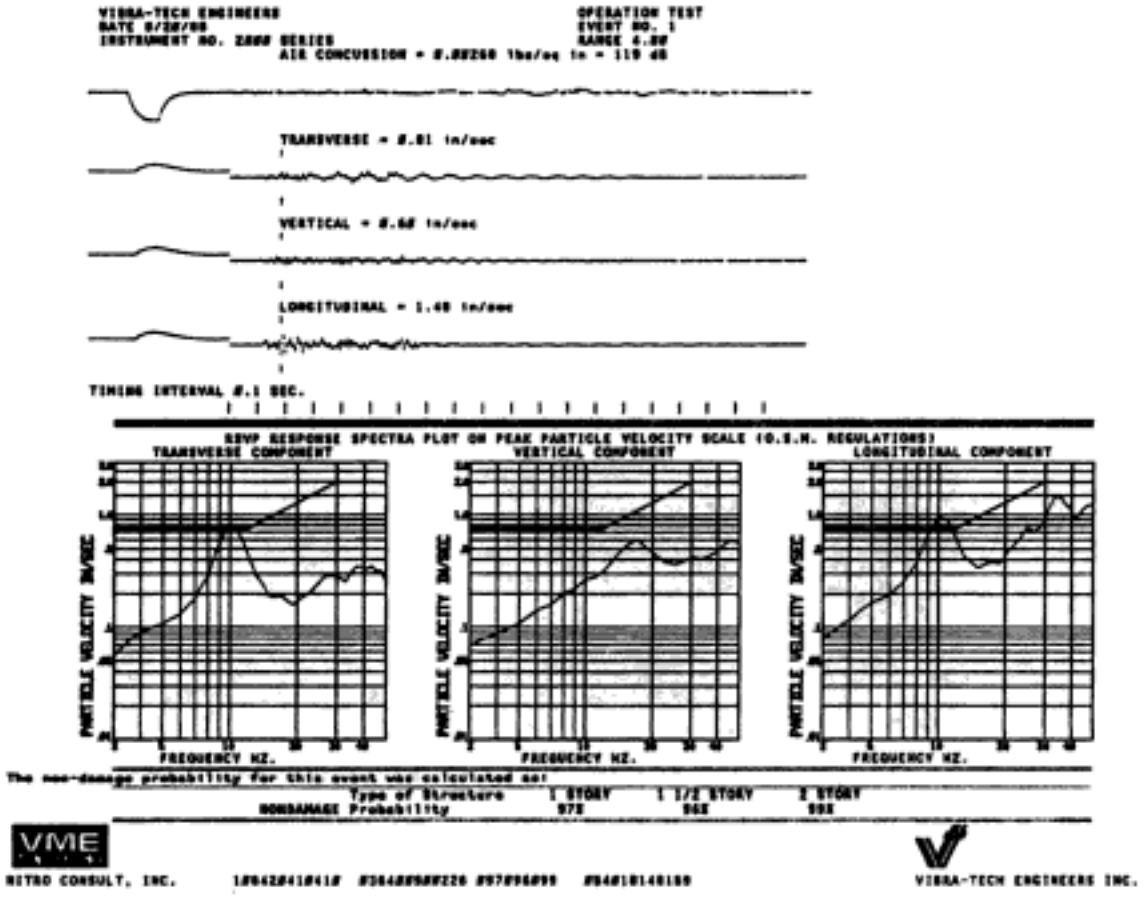

Figure 9.7. Example of the records produced from a monitored blast (Rosenthal & Morlock, 1987).

instrument). The type of output from the instrument is shown in Figure 9.7. The output is of the same format as specified in the regulations and the allowable curve is superimposed. Curves like this would be generated for different scaled distances. The highest value of D_S still in compliance could be used for design. To be able to use this approach, seismographic records including both particle velocity *and* vibration frequency levels must be provided for each blast. The method used for determining the predominant frequency must be approved by the regulatory authority.

There are a number of advantages with this option. When blasting close to structures the predominant frequencies tend to be higher, hence a higher charge weight per delay would be allowed than with the other options. A maximum amount of information is collected from each blast. Hence the possibilities for improving blasting would be high (knowing what was right or wrong with the blast). These type of records provide maximum protection when discussing possible complaints from the neighbors. The disadvantages are that they require relatively expensive instrumentation, trained users and the monitoring of each blast.

9.1.6 *Ground motion effects contained within the mine site*

As indicated, the regulations are based upon particle velocities which are well within damage limits. When dealing with the mine's own structures, a different type of 'damage cri-

terion' may be imposed than for structures belonging to others. Bauer & Brennan (1979) have compiled peak particle velocity-scaled distance data from a large number of open pit and strip mine blasts. A representative sample of 1500 recordings from different mines is shown in Figure 9.8. On these, an upper limit line has been superimposed. The OSMRE values using Table 9.5 have been superimposed as well. This provides some idea of the built-in conservatism contained in the regulations. Table 9.6 indicates peak particle velocity thresholds at which certain types of damage start to occur. These limits which have been superimposed on the upper limit plot of Figure 9.9 provide a useful set of guidelines for making a quick evaluation of potential damage to *mine* structures. If hairline cracking, for example, is deemed not to be a problem, then a certain scaled distance value might be selected for blast design which is significantly lower than those given in the regulations. From Figure 9.9 the scaled distance under poor conditions for which hairline cracks in plaster may be expected to occur is about 13. Depending upon the distance, the corresponding OSMRE value to be selected ranges from 50 to 65. Assuming that the blast is 500 ft from a certain mine structure (the managers house, for example) use of $D_S = 13$ would suggest that

$$W = \left(\frac{500}{13}\right)^2 = 1479 \text{ lbs}$$

could be shot per delay. Using the scale factor of 55 which is the OSMRE value appropriate for this distance one would obtain

$$W = \left(\frac{500}{55}\right)^2 = 83 \text{ lbs}$$

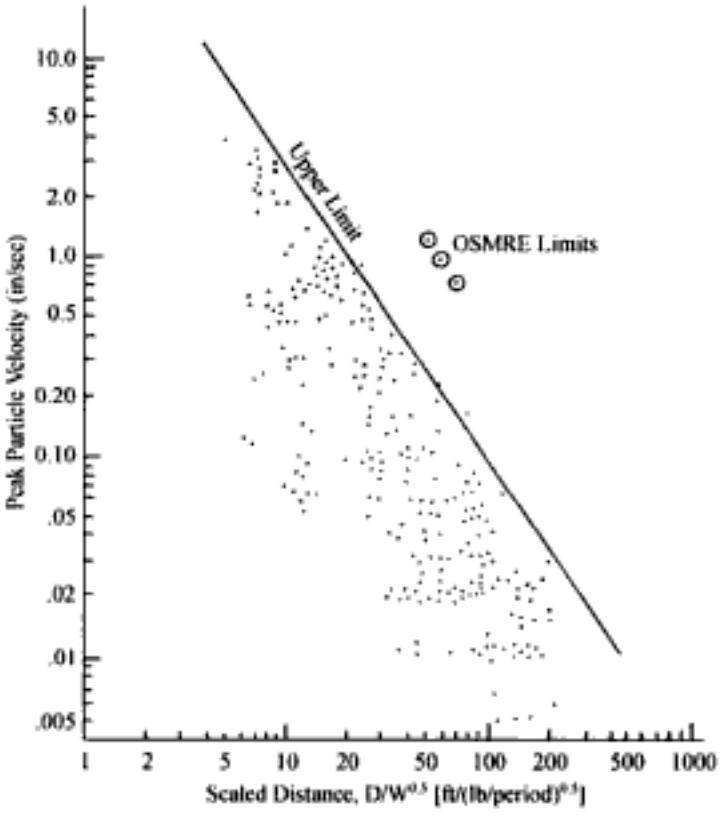

Figure 9.8. Compilation of peak particle velocity versus scaled-distance for a large number of surface mines (Bauer & Brennan, 1979).

Table 9.6. Type of damage related to the peak particle velocity in the ground waves from blasts (Bauer & Brennan, 1979).

Type of structure	Type of damage	Peak particle velocity threshold at which damage starts (in/sec)
Rigidly mounted mercury switches	Trip Out	0.1-0.5 (Has strong frequency dependence)
Houses	Plaster Cracking	2
Concrete block as in a new house	Cracks in Blocks	8
Cased drill holes, retaining walls on loose ground	Horizontal offset	15
Mechanical equipment-pumps, compressors	Shafts misaligned	40 (Beyond 10 in/sec major damage starts, such as possible cracking of cement block)
Prefabricated metal building on concrete pads	Cracked pads, building twisted and distorted	60

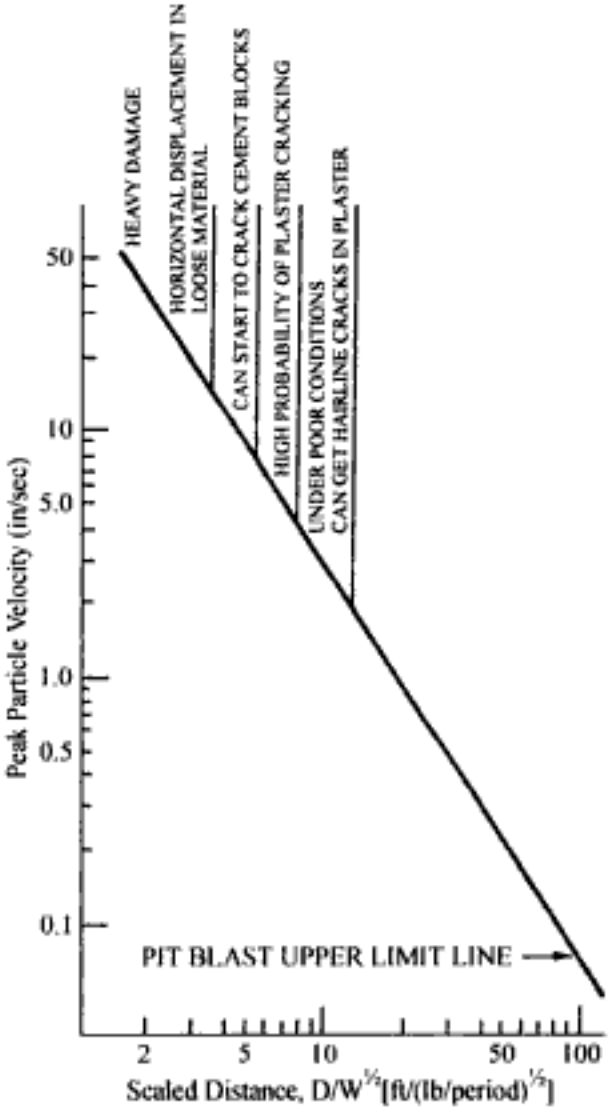

Figure 9.9. Damage limits superimposed on the peak particle velocity-scaled distance curve (Bauer & Brennan, 1979).

Hidden page

Hidden page

where P = pressure (kPa), W = mass of explosives (kg), D = distance from the explosive (m).

The airblast overpressure for *confined* blasthole may be estimated using

$$P = 3.3\left(\frac{D}{W^{1/3}}\right)^{-1.2} \tag{9.12}$$

Table 9.9 presents some air overpressure values which when inserted into Equations (9.11) and (9.12) could be used for evaluating the proper scaled distance. The USBM recommended safe limit is 3.5 kPa. To avoid disturbance to people the pressure should be less than 0.05 kPa ($P < 0.05$ kPa). Table 9.10 summarizes the factors which influence airblast.

The following are steps which can be taken to minimize airblast (AECI, 1981)

1. Ensure proper confinement of the explosive charges by:

   – The use of an adequate length of collar stemming, preferably of coarse angular material. Experience has shown that a minimum length of 30 hole diameters is needed to control airblast.
   – Not underburdening the front row of holes.
   – Not overburdening holes, thus preventing blown-out shots.
   – Ensuring proper timing to avoid blown-out shots caused by holes firing out of sequence.
   – Providing 300 mm of sand/soil cover over detonating cord surface lines. Experiments have shown that this reduces the acoustic energy transmitted to the atmosphere by 26 dB.
   – The use of pop-holes in place of lay-on charges where secondary blasting unavoidable.
   – The elimination of detonating cord in secondary blasting.

2. Where possible, change to mechanical breaking (drop balls, pneumatic breakers etc.) in lieu of secondary blasting.
3. Limit the maximum explosives charge per delay.
4. Use noiseless trunklines in those situations calling for a non-electric surface delay system.

Table 9.8 Charge mass versus distance for unconfined charges (AECI, 1981).

Charge mass (kg)	Distance (m) $D = 320\ W^{1/3}$	$D = 600\ W^{1/3}$
25	936	1754
50	1179	2210
75	1349	2530
100	1485	2785
150	1700	3188
200	1871	3509
300	2142	4017
400	2358	4421
500	2540	4762
1000	3200	6000
2000	4032	7560
5000	5472	10,260

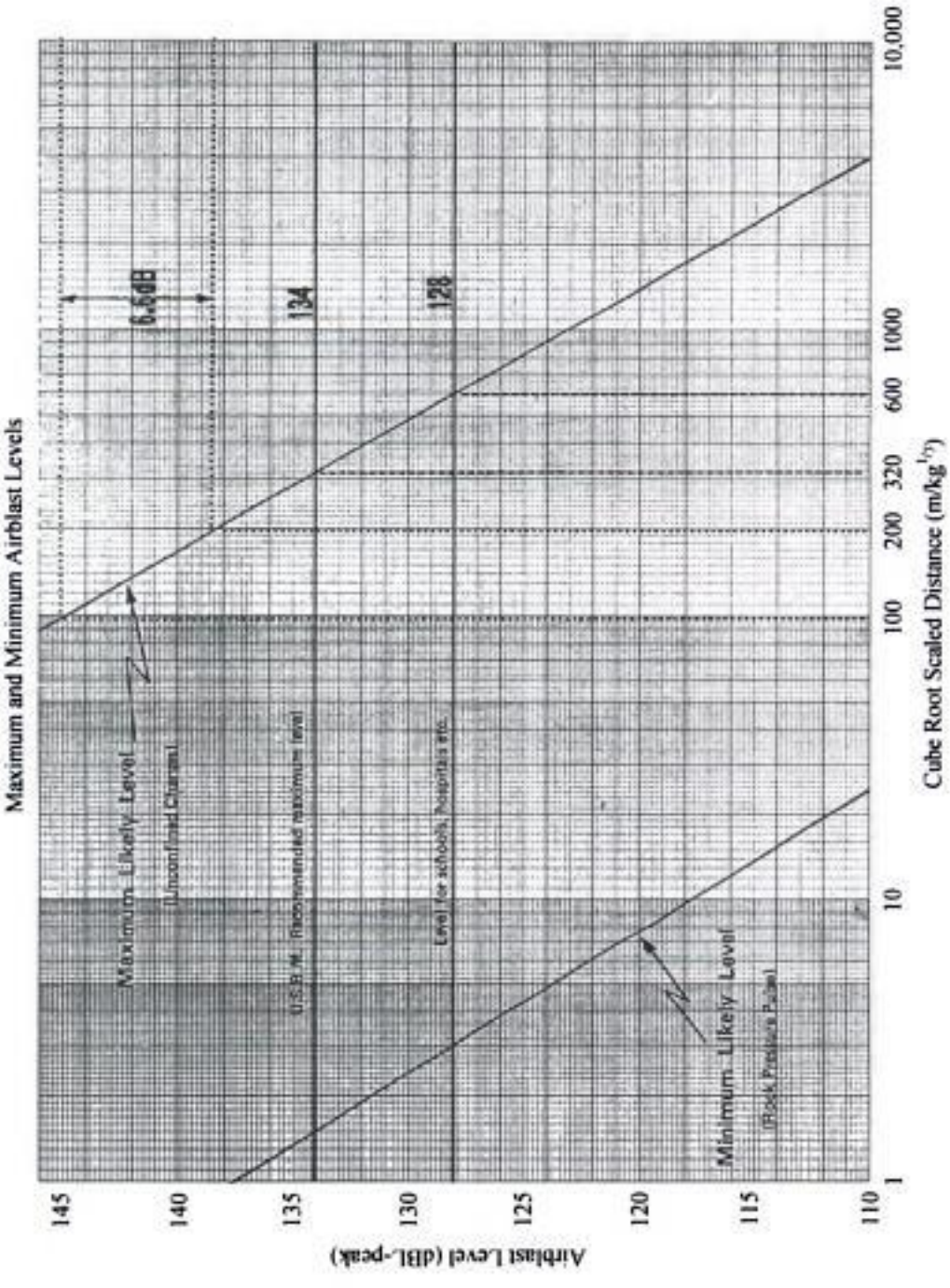

Figure 9.10. Airblast design nomograph (AECI, 1981).

Table 9.9. Effect of air overpressure on structures (Nicholls et al., 1971).

Effect	Air overpressure (kPa)
Dishes and loose window rattle	0.2
Poorly fitted window panes may break	5
All windows fail	14
USBM recommended safe limit	3.5

Table 9.10. Factors which influence airblast (Rosenthal & Morlock, 1987).

Variables within the control of mine operators	Influence on overpressure		
	Signicant	Moderately significant	Insignificant
1. Charge weight per delay	x		
2. Delay interval	x		
3. Burden and spacing	x		
4. Stemming (amount)	x		
5. Stemming (type)	x		
6. Charge length and diameter			x
7. Angle of borehole			x
8. Direction of initiation	x		
9. Charge weight per blast			x
10. Charge depth	x		
11. Bare or covered detonating cord	x		
12. Charge confinement	x		
Variables not in control of mine operators			
1. General surface terrain		x	
2. Type and depth of overburden	x		
3. Wind and weather conditions	x		

5. Where possible, direct the blast away from residential areas. It has been shown that a 5 to 10 dB difference in airblast levels can be expected between the front and the back of the blast.

6. Avoid blasting when wind is blowing towards a critical area. Strong wind is the most important weather factor influencing airblast propagation and can increase the airblast level by over 20 dB.

7. Avoid blasting in the early morning and late afternoon if a temperature inversion in the atmosphere is present. Such conditions cause air waves to be refracted back to earth and focussing effects can increase the airblast level by 10 dB.

8. Minimize frequency of blasting.

9. Time the blasting to coincide with periods of high ambient noise.

9.3 FLYROCK

Flyrock can be a very dangerous side effect of bench blasting. The borehole with its built-in rock bottom and its stemming plug, resembles a highly charged pressure vessel. As designed the explosive gases are to expend their energy in a more or less controlled fashion by generating and propagating cracks in the surrounding rock. Only in the last stages of gas expansion is the burden released and the remaining pressure used to heave the rock.

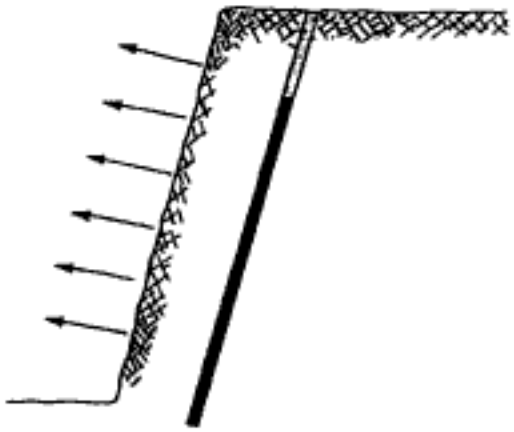

Figure 9.11. Idealized front from a rock blasting situation.

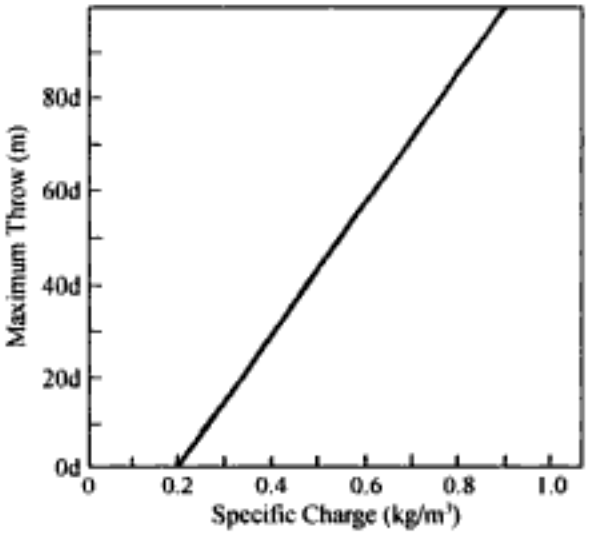

Figure 9.12. Maximum throw as a function of specific charge (Lundborg, 1981).

Figure 9.11 shows the idealized situation in which the stemming remains intact, the burden is uniform, and only a small part of the total explosive energy goes into heave and throw. Some very limited field studies reported by Lundborg (1973, 1974, 1981) and Lundborg et al. (1975) suggest that for granite the maximum throw (L) as a function of the hole diameter (d) and specific charge is as shown in Figure 9.12. When the specific charge (q) is

$$q \leq 0.2 \text{ kg/m}^3$$

there is no throw. For other values of q the maximum throw is expressed by

$$L = 143\, d(q - 0.2) \tag{9.13}$$

where d = hole diameter (ins), q = specific charge (kg/m^3), L = maximum throw (m).

A typical specific charge in bench blasting is 0.6 kg/m^3. In this case the maximum throw expression becomes

$$L = 57\, d$$

For a 10 inch hole diameter the maximum expected throw would be

$$L = 570 \text{ m}$$

There are a number of different situations in which the actual conditions depart markedly from the ideal. Figure 9.13 shows two such conditions.

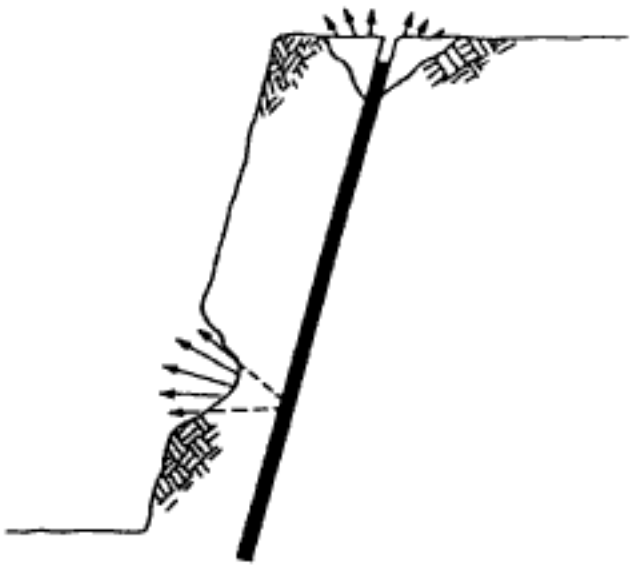

Figure 9.13. Two situations leading to increased flyrock (Lundborg et al., 1975).

– The explosive extends too high in the hole so that cratering to the upper surface occurs.

– An irregular face brings the explosive column too close to the free face resulting in cratering.

The lack of confinement offered by both of these situations provides a weak link for the gas to exploit. The rock plug involved is pushed out in an early stage of the gas expansion process and the expansion energy is expended in propelling a relatively small volume of rock at high velocity. Hence the throw distance can be very great.

Figure 9.14 illustrates the case where the toe distance through poor drill alignment, design, etc., is much greater than desired. The burden is not broken free by the blast and the explosive gases vent out through the fractured rock near the collar. Figure 9.15 shows the situation in multiple row blasting where the time delay between rows to too short to allow adequate relief before the next row detonates. The effective burden on the latter rows is much larger than that which can be reasonably displaced by the gas pressure. As a result the stemming is ejected and/or the collar region craters.

In all of these situations it is the cratering type of failure (Fig. 9.16) which is the most dangerous from a flyrock viewpoint. If the weakest link in the system is the column of stemming and not the collar rock, this can be ejected much like a projectile from a cannon barrel. Lundborg (1973) has made a series of computer simulations in which he examined maximum throw and boulder size as a function of hole diameter. He found that for granite with a specific gravity of 2.6, the relationships for the maximum throw (L) involving rocks of diameter ϕ are

$$L_{max} = 260\, d^{2/3} \tag{9.14}$$

$$\phi = 0.1\, d^{2/3} \tag{9.15}$$

where, d = hole diameter (ins), ϕ = boulder diameter (m).

Thus for a 10 inch diameter borehole the boulder size would be

$$\phi = 0.1\ (10)\ 2/3 = 0.47 \text{ m}$$

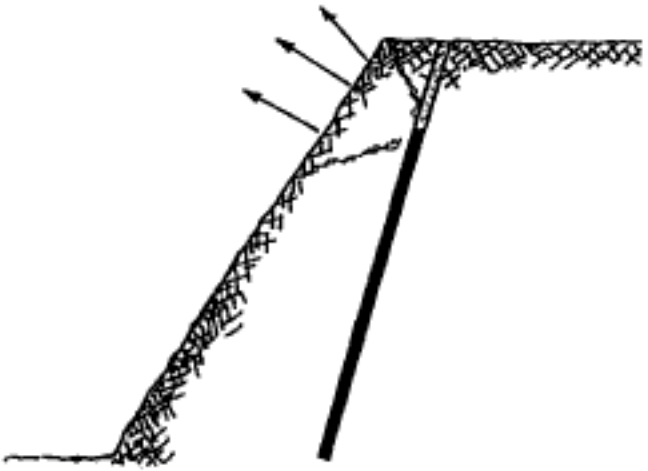

Figure 9.14. Flyrock from the crest region.

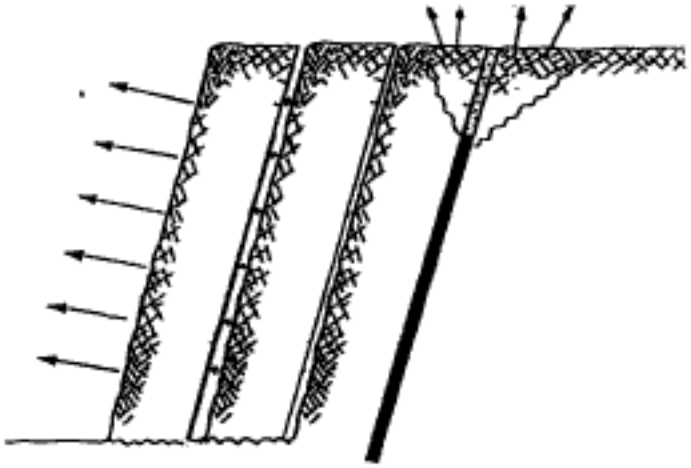

Figure 9.15. Inadequate relief provided by preceding rows.

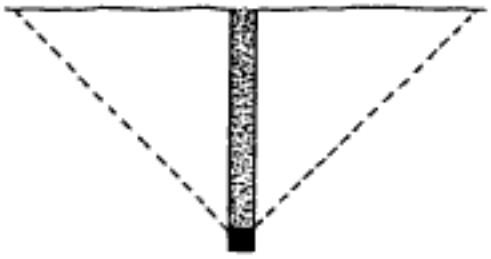

Figure 9.16. Diagrammatic representation of cratering (Lundborg et al., Holmberg, 1975).

and the corresponding maximum throw is

$$L_{max}\,(\text{m}) = 260\,(10)^{2/3} = 1208\ \text{m} \tag{9.16}$$

The results for a range of hole sizes (Fig. 9.17) suggest that very large areas must be evacuated in order to avoid accidents. Cratering gives much more throw than simple benching. Therefore efforts such as proper stemming, timing, etc., must be made to avoid these cratering effects. The OSMRE regulations (Rosenthal & Morlock, 1987) on flyrock state that

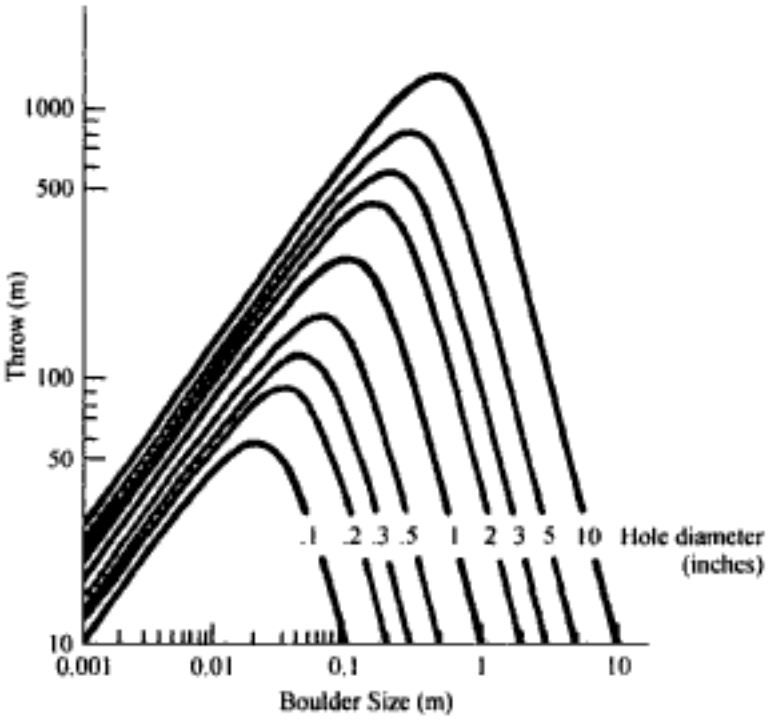

Figure 9.17. The maximum throw versus boulder size relationship for various hole diameters (Lundborg, 1973).

'Flyrock travelling in the air or along the ground shall not be cast from the blasting site-

1. *More than one-half the distance to the nearest dwelling or other occupied structure,*
2. *Beyond the area of access control for the given blast.*
3. *Beyond the permit boundary.'*

The problem obviously becomes that of estimating the maximum throw distance. The equations of Lundborg et al. (1975) provide one approach although the basis for them is weak and the range of hole diameters limited.

REFERENCES AND BIBLIOGRAPHY

AECI Explosives and Chemicals Limited 1981. Airblast. *Explosives Today*. Series 2, No 24, June.

AECI Explosives and Chemicals Limited 1982. The effects, measurement and control of ground vibrations. *Explosives Today*. Series 2, No 27, March.

AECI Explosives and Chemicals Limited 1984. Drilling accuracy. *Explosives Today*. Series 2, No 36, 2nd Quarter.

AECI Explosives and Chemicals Limited 1987. Stemming. *Explosives Today*. Series 2, No 46, June.

Anderson, D.A. 1989. The 8 millisecond 'criterion': have we delayed too long in questioning it? *Proceedings of the 15th Conference on Explosives and Blasting Technique. SEE.* pp. 381-396.

Anonymous 1985. Good neighbors. *Downline.* Issue 3, May: 10-11.

Anonymous Proposed Revisions to the Permanent Program Regulations Implementing Section 501(b) of the Surface Mining Control and Reclamation Act of 1977. *Downline*, Ensign-Bickford Company.

Arthur, J.D. 1979. Blasting safety requirements under the new surface mining law. *Mining Engineering*. 31(11): 1568-1569.

Atlas Powder Company *Blasting Vibration and Air Blast.* 13pp.

Atlas Powder Company 1981. *Workshop Manual 'Surface Blasting Course'.*

Atlas Powder Company 1987. *Explosives and Rock Blasting.* Maple Press. 662pp.

Attewell, P.B. & I.W. Farmer 1964. Ground vibrations from blasting- Their generation, form and detection. *Quarry Managers Journal*. 48(5): 191-198.

Attewell, P.B. & D. Haslam 1965. Prediction of ground vibration parameters from major quarry blasts. *Mining and Mineral Eng*. 1(16): 621-626.

Bauer, A. & J.W.Sanders 1968. Good blasting techniques and public relations. *Mining Congress Journal*. 54(11): 81-85.

Bauer, A & M.D. Brennan 1979. Blast Designs to Improve Dragline Stripping Rates. *Final Report-Phase I. Prepared fro the US Dept of Energy under contract USD.O.E. DE-AC01-77QQ90147*. DOE Report FE 9124-1, April.

Blair, D.P. 1990. Some problems associated with standard charge weight vibration scaling laws, FRAGBLAST '90, *Proceedings of the 3rd Int. Symp. on Rock Frag. by Blasting. Brisbane, Australia.*

Burgher, K.E. 1988. Determination of air blast overpressure levels. 1988. *Proceedings of the 14th Conference on Explosives and Blasting Technique. SEE.* pp. 123-135.

Chironis, N.P. 1980. How to get more blast, less bang. *Coal Age*. 85(6): 73-79.

Chironis, N.P. 1983. Back yard blasting on the quiet. *Coal Age*. 88(6): 62-68.

D'Andrea, D.V. & J. Bennett 1984. Safeguarding of blast-affected areas. *Explosives Engineering*. 2(1): 14-19, 28-30.

Devine, F.J., R.H. Beck. A.V.C. Meyer & W.I. Duvall 1965. Vibration levels transmitted across a presplit fracture. *USBM RI 6695*. 29p.

Devine, J.F., R.H. Beck, A.V.C. Meyer & W.I. Duvall 1966. Effect of charge weight on vibration levels from quarry blasting. *USBM RI 6774*. 37pp.

Dick, R.A., L.R. Fletcher & D.V. D'Andrea 1983. Explosives and Blasting Procedures Manual. *USBM IC* 8925. 105pp.

Dix, C.H. The mechanism of generation of long waves from explosives. *Geophysics*. 20: 87-103.

Dowding, C.H. 1985. *Blast Vibration and Control*. Prentice Hall, Englewood Cliffs, NJ.

Duvall, W.I. & D. Fogelson 1962. Review of criteria for estimating damage to residences from blasting vibrations. *USBM RI 5968*. 19pp.

Duvall, W.I., C.F. Johnson, A. Meyer & J. Devine 1963. Vibrations from instantaneous and milli-second delayed quarry blasts. *USBM RI 6151*. 34pp.

Duvall, W.I., T.C. Atchison & D.E Fogelson 1966. Empirical approach to problems in blasting research. Failure and Breakage of Rock (C. Fairhurst, ed.). *Proceedings of the 8th US Symp. on Rock Mechanics, Univ. of Minn*. Sept 15-17. AIME (SME), NY.

Eriksson, B. & A. Ladegaard-Pederson 1971. Flyrock during blasting (Part 1). *SveDeFo Report DS* 1971: 32. In Swedish.

Fletcher, L.R. & D.V. D'Andrea Control of flyrock in blasting. *Proceedings of the 12th Conference on Explosives and Blasting Technique. SEE.* pp.. 167-177.

Flinchum, R. 1992. Reduction of airblast and prevention of flyrock. *Proceedings, Fourth High-Tech Seminar: Blasting Technology, Instrumentation and Explosives Applications.* Blasting Analysis International, Inc. *Nashville, Tennessee.* June 20-25.

Foster, G.A. 1975. Air blast– the major cause of complaints from blasting? Its monitoring and possible control. *Proceedings of the 1st Conference on Explosives and Blasting Technique. SEE.* pp. 90-99.

Froedge, D.T. 1994. New technology in vibration measurements, analysis & data management. *Proceedings of the 5th High-Tech Seminar on Blasting Technology, Instrumentation and Explosives Applications. New Orleans, Louisiana* (July 9-14). Blasting Analysis International, Inc. pp. 901-913.

Gurin, A.A., V.N. Nazarenko, P.S. Malyi, A.A. Gul & V.I.. Grammakov 1975. Effect of the design of a column charge on the energy of the detonation products forming the air blast wave. *Soviet Mining Science*. 11: 561-566.

Habberjam, G.M. & J.R. Whetton 1952. On the relationship between seismic amplitude and charge of explosives fired in routine blasting operations. *Geophysics*. 17(1): 116-128.

Hagan, T.N. & B.J. Kennedy 1977. A practical approach to the reduction of blasting nuisances from surface operations. *Australian Mining* 69(11): 36.

Harries, G. 1980. Rock properties and their effect on blasting vibrations. Australian Mineral Foundation Blasting Workshop. Bowral July 5, 1980. pp. 113-133.

Hinzen, K.G., R. Ludeling, F. Heinemeyer, P. Roh & U. Steiner 1987. A new approach to predict and reduce blast vibration by modelling of seismograms and using a new electronic initiation system. *Proceedings of the 13th Conference on Explosives and Blasting Techniques*. pp. 144-161.

Holmberg, R. & P-A. Persson 1978. Ground vibrations in the near vicinity of blasts at Boliden AB's Aitik Mine. Swedish Detonic Research Foundation Report DS 1978: 1. 26pp. In Swedish

Holmberg, R. 1978. Flyrock and noise during blasting. Swedish Detonic Research Foundation Report DS 1978: 15. 38pp. In Swedish.

Instantel. DS-500 Analyzer sample diskette operating instructions.

Jansen, K., B. Kniivila, T. Lerick & A.B. Andrews 1984. Refinements in blasting practices at Minntac Mine. *Proceedings of the 10th Conference on Explosives and Blasting Technique. SEE.* pp. 245-263.

Jansen, K., B. Kniivila, T. Lerick & A.B. Andrews 1984. Improvements in blasting practice at Minntac Mine. *Proceedings of the 57th Annual Meeting of the Minnesota Section AIME and 45th Annual Mining Symposium. Duluth, Minnesota*, Jan 18-19. 19pp.

Konya, C.J. & J. Davis 1978. The effects of stemming consist of retention in blastholes. *Proceedings of the 4th Conference on Explosives and Blasting Technique. SEE.* pp. 102-112.

Konya, C.J., F. Otuonye & D. Skidmore 1982. Airblast reduction from effective blasthole stemming. *Proceedings of the 8th Conference on Explosives and Blasting Technique. SEE.* pp. 145-156.

Konya, C.J. & E.J. Walker 1988. Blasthole timing controls vibration, airblast and flyrock. *Coal Mining*. 25(Jan.): 38-40.

Kopp, J.W. 1987. Initiation timing influence on ground vibration and airblast. USBM IC 9135. *Proceedings, Surface Mine Blasting Technology Transfer Seminar,* April 15. pp. 51-59.

Kovach, R.L., F. Lehner & R. Miller 1963. Experimental ground amplitudes from small surface explosions. *Geophysics*. 28: 793-798.

Kringel, J.R. 1960. Control of airblast effect resulting from blasting operations. *Mining Congress Journal*, 28(4): 45-51.

Leet, L.D. 1960. *Vibrations From Blasting Rock*. Harvard University Press.

Leet, L.D. 1960. Vibrations from construction blasting. *Explosives Engineer*. Part 1: Jan-Feb. pp. 13-19, 30. Part 2: Mar-April, pp. 47-53.

Linehan, P. & J.F. Wiss 1982. Vibration and air blast noise from surface coal mine blasting. *Mining Engineering*. 34(4): 391-395.

Lundborg, N., Persson, A., Ladegaard-Pedersen, A. & R. Holmberg 1975. Keeping the lid on flyrock in open-pit blasting. *E/MJ*. 176(5): 95-100.

Lundborg, N. 1973. The calculation of maximum throw during blasting. *SveDeFo Report DS* 1973: 4. In Swedish.

Lundberg, N. 1974. The hazard of flyrock in rock blasting. *SveDeFo Report DS* 1974: 12. 19pp.

Lundborg, N. 1978. A method for calculating the probability of rock impact at large distances from the blast. *SveDeFo Report* DS 1978: 11. In Swedish.

Lundborg, N. 1979. The probability of flyrock damage. *SveDeFo Report DS* 1979: 10.

Lundborg, N. 1981. The probability of flyrock. *SveDeFo Report DS* 1981: 5. 39pp.

Lundborg, N., R. Holmberg & P-A Persson 1978. The dependence of ground vibrations on distance and charge size. Byggforskningen Rapport R11: 1978. 90pp. In Swedish.

Matheson, C. 1996. Vibra-Tech. Private Communication.

McKenzie, C.K., G.P. Stacey & M.T. Gladwin 1982. Ultrasonic characteristics of a rock mass. Int J. Rock Mech Min Sci & Geomech. Abstr. 19: 25-30.

Mine Safety and Health Administration 1983. Surface Coal Mining and Reclamation Operations; Initial and Permanent Regulatory Programs; Use of Explosives. Department of Labor. March 8. Federal Register.

Mine Safety and Health Administration 1991. Safety standards for explosives at metal and non-metal mines; final rule. 30 CFR Parts 56 and 57. Department of Labor. January 18. Federal Register.

Mojtabai, N. & J.J.K. Daemen 1987. Predicting low-amplitude long-distance ground vibrations induced by blasting. *Proceedings of the 13th Conference on Explosives and Blasting Technique (3rd Mini-Symp.). SEE.* pp. 106-117.

Morlock, C.R. & J.J.K. Daemen 1983. Keeping airblasts under control. *Proceedings of the 9th Conference on Explosives and Blasting Technique. SEE.* pp. 63-82.

Nicholls, H.R., C.F. Johnson & W.I. Duvall 1971. Blasting Vibrations and their Effects on Structures. USBM Bulletin 656. 105pp.

Ladegaard-Pedersen, A. & A. Persson 1973. Flyrock During Blasting (Part 2)-Experimental Investigations. *SveDeFo Report DS* 1973: 13. In Swedish. 35pp.

Ladegaard-Pedersen, A. & R.Holmberg 1973. The effect of charge geometry on flyrock caused by crater creation during bench blasting. *SveDeFo Report DS* 1973: 28. In Swedish. 28pp.

Petro, A.J. & D.A. Anderson 1986. Blast vibration problems: where do we go from here? *Journal of Mines, Metals & Fuels*. 34(11): 502-505.

Redpath, B. 1976. A review of airblast-induced window breakage. *Proceedings of the 2nd Conference on Explosives and Blasting Tech. SEE.* pp. 200-207.

Rosenthal, M.F. & G.L. Morlock 1987. *Blasting Guidance Manual. Office of Surface Mining Reclamation and Enforcement*. US Department of the Interior. March. 201 pp.

Roth, J., Britton, K.C., Campbell, R.W. & W.R. Ketler 1978. *Evaluation of Surface Mining Blasting* Procedures. Report (BuMines OFR 18-80) prepared by Management Science Associates for the US Bureau of Mines. June 6. 143 pp.

Roth, J. 1979. A *model for the determination of flyrock range as a function of shot conditions*. Report (OFR 77-81) prepared by Management Science Associates for the US Bureau of Mines. April 16.

Schneider, L. 1996. Back to basics: Flyrock (Part 1 – Safety and Causes). *Explosives Engineering*. 13(9): 18-20.

Schneider, L. 1997. Back to basics: Flyrock (Part 2 – Prevention). *Explosives Engineering*. 14(1): 32-36.

Shukla, K. 1978. Blasting-concern for neighbors and operators. *Proceedings of the 4th Conference on Explosives and Blasting Technique. SEE.* pp. 247-257.

Simmance, J.L.H. *Blast vibration monitoring and prediction.* pp. 14-17.

Simmance, J.L.H. 1989. Blast vibration monitoring &control-An overview. Lecture at Colorado School of Mines, Golden. April.

Siskind, D.E., M.S. Stagg, J.W. Kopp & C.H. Dowding 1980. Structure response and damage produced by ground vibration from surface mine blasting. *USBM RI 8507*. 74pp.

Siskind, D.E., Stachura, V.J., Stagg, M.S. & J.W. Kopp 1980. Structure response and damage by airblast from surface mining. *USBM RI 8485*.

Siskind, D.E. 1980. Damage to residential structures from surface mine blasting. Preprint No. 80-362. Paper presented at the SME-AIME Fall Meeting and Exhibit Minneapolis, Minn October 22-24. 17pp.

Siskind, D.E, and J.W. Kopp 1987. Blasting effects on Appalachian Water Wells. USBM IC 9135. *Proceedings, Surface Mine Blasting Technology Transfer Seminar,* April 15. pp. 96-102.

Stagg, M.S. & D.E. Siskind 1987. Effects of blast vibration on costruction material cracking in residential structures. USBM IC 9135. *Proceedings, Surface Mine Blasting Technology Transfer Seminar,* April 15. pp. 32-45.

Stachura, V.J., Siskind, D.E. & A.J. Engler 1981. Airblast instrumentation and measurement techniques for surface mine blasting. *USBM RI 8508*.

Blaster's Handbook, 6th edition. 1968. Canadian Industries Limited, Explosives Division, Montreal, Quebec, Canada.

Siskind, D.E. & M.S. Stagg 1987. Blasting vibration measurements near structures USBM IC 9135. *Proceedings, Surface Mine Blasting Technology Transfer Seminar,* April 15. pp. 46-50.

Vibra-Tech Engineers, Inc. Extracts from Office of Surface Mining Reclamation and Enforcement Blasting Guidance Manual.

Walker, S., P.A. Young & P.M. Davey 1982. Development of response spectra techniques for prediction of structural damage from open-pit blasting vibrations. *Trans. Instn. Min. Metall* (Sect A Min Industry). 91 (April): A55-A62.

Wells, J. 1997. Securing the blast area – How far is enough? *Explosives Engineering*. 14(1): 38-40.

Wheeler, R.M. 1994. Analyzing and interpreting blast vibration data using new windows-based software (Part 1). *Proceedings of the 5th High-Tech Seminar on Blasting Technology, Instrumentation and Explosives Applications. New Orleans, Louisiana* (July 9-14). Blasting Analysis International, Inc. pp. 1129-1162.

Wheeler, R.M. 1994. Evaluating delay effects on ground vibrations with simulated vibration waveforms (Part II). *Proceedings of the 5th High-Tech Seminar on Blasting Technology, Instrumentation and Explosives Applications. New Orleans, Louisiana* (July 9-14). Blasting Analysis International, Inc. pp. 1163-1203.

Worsley, P.N. 1986. Understanding vibrations from multihole blasts using short delay periods. *Explosives Engineering*. 3(6): 25-28.

CHAPTER 10

Perimeter blasting

10.1 INTRODUCTION

One of the characteristics of an explosive detonating in a borehole is that the shock wave portion of the energy is transmitted away from the hole wall in a very non-discriminating fashion. Specifically this means that the shock energy travels outward away from the hole into the surrounding rock mass independent of direction. For standard production applications this is generally of no consequence and, in fact, may be desirable since the objective is to produce a certain fragmentation of the host rock as inexpensively as possible. Breakage behind the hole is sometimes regarded as 'free muck'. This non-discrimination characteristic does, however, become a problem when blasting in the vicinity of the pit perimeter. What is considered 'free muck' in the context of production blasting now becomes 'back-break' which can have very expensive consequences.

Ideally one would like to be able to achieve the situation shown in Figure 10.1 where, after production blasting, the extent of the blast damage (BD) found running along the bench contour is little or non existent. On the production side (shown to the right in the Figures) of the blastholes (denoted as Region I) it is desired to have a very high degree of fragmentation to minimize the costs of loading, hauling and crushing. On the pit wall side of these holes (Region II), the objective is to produce zero or very minimum rock disturbance. In this way the designed optimum bench geometry (bench face angle, bench width, etc.) can be achieved.

In reality there is a blast damage transition (BDT) zone between these zones of maximum destruction and zero or minimum disturbance (Fig. 10.2). In practice, the actual position of the final wall often does not lie at the position of zero disturbance but rather somewhere within the transition zone. The width of the transition zone depends largely on the care taken in perimeter blasting. As the blast damage transition zone increases in size, the resulting slope angles become flatter with the overall result being higher stripping ratios/ore losses.

Figure 10.3 shows the final pit limits based upon three different perimeter blasting scenarios. With careful perimeter blasting (Case A), the final slope is made up of a series of double benches (30 m high) with a design face angle of 70° separated by catch benches 10 m wide. The overall slope angle is

$$\theta = 58°$$

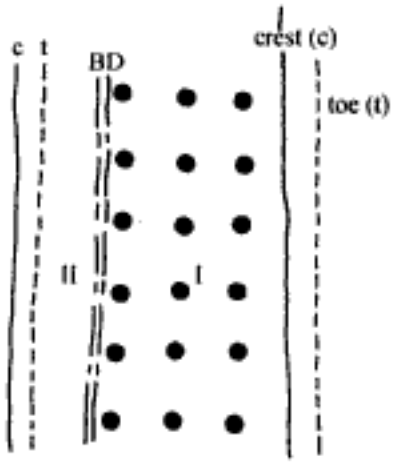

Figure 10.1. Plan view showing ideal blast damage zone (BD).

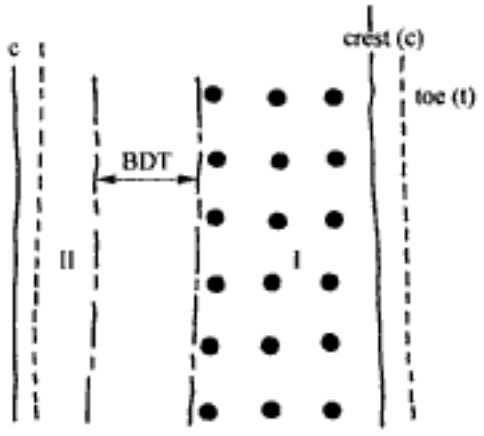

Figure 10.2. Plan view showing actual blast damage zone (BDT).

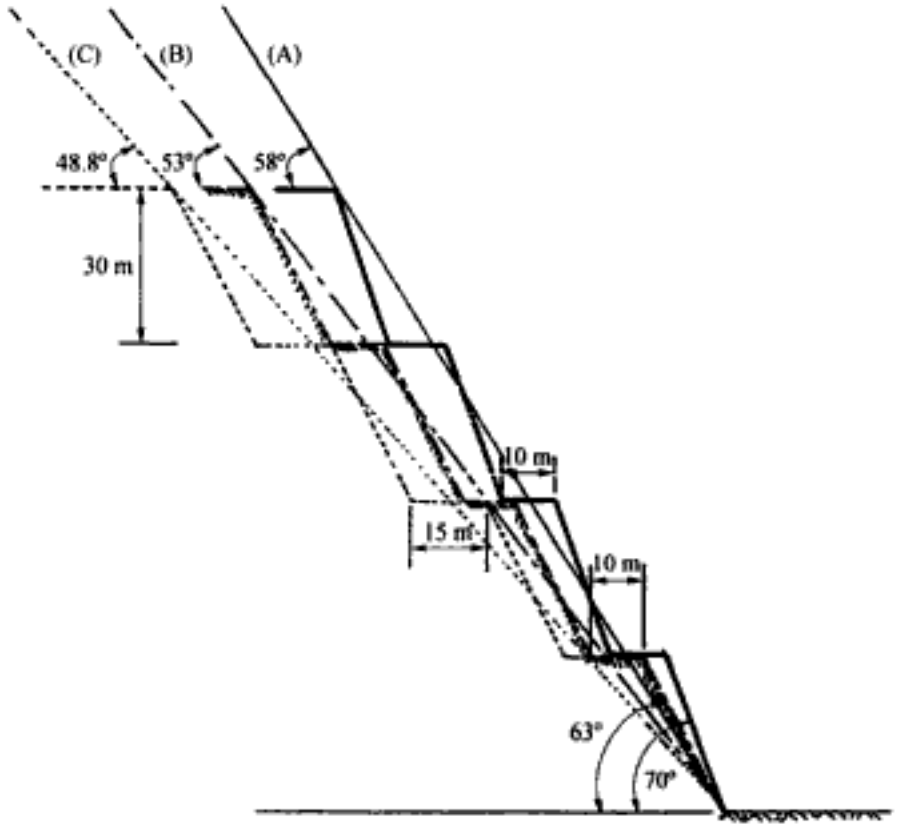

Figure 10.3. Effect of varying degrees of blast damage on overall slope angle.

If due to poor perimeter blasting, the face angle is 63° instead (Case B), then the slope angle drops as is shown to

$$\theta = 53°$$

The unplanned waste included between these two slopes must now be removed.

Catch benches are included in the slope design to contain rock which ravels off of the slopes. For poor blasting conditions wider benches will be required for two reasons.

1. There will be more material needing to be trapped.
2. The design width will have to be larger than the required width since the crest of the catch bench may ravel.

Assume for example that the required width is 15 m instead of 10 m. The overall slope angle (Case C) then becomes

$$\theta = 48.5°$$

This slope has also been superimposed on Figure 10.3. As can be seen, the as-planned and as-built pit outlines are quite different. The material included between the two must be removed. The associated rock removal costs must be compared to those associated with the as-planned design incorporating special drilling and blasting procedures. In addition to the obvious costs associated with extra stripping one must also consider the costs related to

- Safety,
- Extra cleanup,
- Scaling,
- Reinforcement.

Large amounts of loose bench face rock may result in hazardous working conditions both for personnel and machines. Remedial measures such as

- Scaling large areas
- Use of wire mesh, bolts or other types of artificial support

are expensive and difficult to implement.

In the blasting process, rock damage is produced in three ways.

- Creation of new cracks around the borehole by high detonation pressures.
- Creation and extension of cracks remote from the blasthole by explosion generated strain/shock waves.
- Extension of cracks around the borehole by the static strain field created by the gas pressure.

When considering ways of reducing unwanted cracking behind the holes, these three effects will have to be addressed. There are four different possibilities presented from explosive theory.

1. The length of the longest radial cracks emanating from the hole, as discussed in Chapter 4 depends upon the borehole pressure. If this pressure is reduced, the length of the cracks would similarly be reduced.

2. The length of the cracks has also been shown to be proportional to the radius of the blasthole. With a reduction in borehole diameter, the damage zone behind the hole would be reduced.

3. The formation of new cracks right around the borehole depends upon high detonation pressures. A reduction in detonation pressure would reduce cracking.

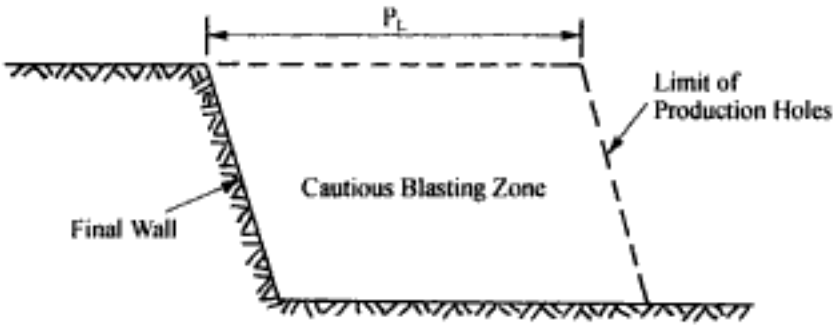

Figure 10.4. Transition zone between the production zone and perimeter.

4. The presence of pre-existing cracks at high angles to those being created/extended by the blast, causes the running cracks to be terminated. Thus the creation of such a crack line prior to blasting is a way of limiting damage. The amplitude of the shock wave generated by the explosion can be markedly attenuated by the creation of a crack (pre-split or line-drilled) line in back of the blast. If the crack is wide enough, no shock energy will pass.

Knowing how cracks are formed and extended during the blasting process is key to the development of techniques for preventing/minimizing their growth. In perimeter control blasting, the first step is to keep the powerful energy released by the production holes sufficiently far away (P_L) from the final limits to avoid damage (Fig. 10.4). The second step is to design the blast rounds within the cautious blasting zone so that the rock is broken but the final wall protected. The types of techniques/procedures one would consider include

- Use of less powerful explosives
- Decreasing hole diameters
- Reduction in burden and spacing
- Use of small diameter charges in the larger holes (de-coupled charges)
- Decking of explosives
- Creation (pre-splitting) of artificial cracks to limit extent of the radial cracking and shock wave transmission
- Special delay procedures (instantaneous shooting).

This chapter will begin with a brief discussion of the use of decoupling and decking to alter the form of the energy output from an explosive. This will be followed by a discussion of four techniques

- Line drilling
- Pre-split blasting
- Smoothwall blasting
- Trim blasting

used to prevent/minimize unwanted damage. The chapter concludes with a detailed presentation of several design procedures which can be used to assist in the design of perimeter blasts.

10.2 TAILORING THE ENERGY OF EXPLOSIVES

The concept of decoupled charges is an important one in the prevention of unwanted blast damage. It is therefore covered in some detail in a chapter of its own, Chapter 17. In this section a brief overview is presented.

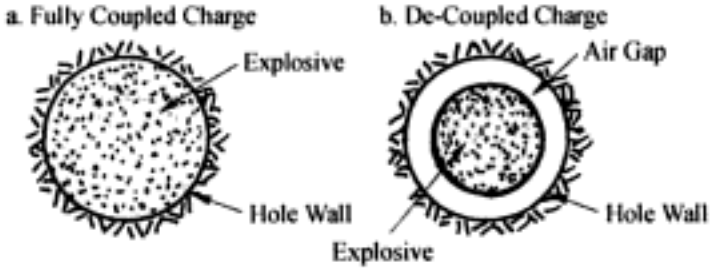

Figure 10.5. Wall protection using de-coupled charges.

Explosive and borehole are said to be *fully coupled* if the explosive completely fills the cross-sectional area (Fig. 10.5a). An example of this is the normal bulk loading of blastholes with ANFO. A *de-coupled* charge is one in which an annulus (Figure 10.5b) exists between the wall of the charge and the wall of the hole. The annulus between the charge and the borehole in this case is assumed filled with air. The coupling ratio (CR) is defined as

$$CR = \frac{D_e}{D_h} \tag{10.1}$$

where D_e = diameter of explosive, D_h = diameter of the hole.

An example in bench blasting would be the installation of 127 mm (5") diameter plastic (PVC) tubes in 251 mm (9 1/7) or 311 mm (12 1/4") blastholes and then filling the tubes with explosive.

In these cases the coupling ratios would become, respectively

(a) 251 mm holes

$$CR = \frac{127}{251} = 0.51$$

(b) 311 mm holes

$$CR = \frac{127}{311} = 0.41$$

The reason for de-coupling the charge is to reduce the amplitude of the shock wave generated in the rock mass and the magnitude of the gas pressure applied to the wall of the hole wall. The basic expression (10.2) for the adiabatic expansion of the gas from a detonating cylindrical charge in a bore hole is

$$P_e V_e^{\gamma} = P_h V_h^{\gamma} \tag{10.2}$$

where P_e = gas pressure at the diameter of the charge, V_e = charge volume/unit length of borehole, P_h = gas pressure at the wall of the borehole, V_h = hole volume/unit length of borehole, γ = ratio of the specific heats over the pressure range from P_e to P_h.

Since the hole and charge volumes per unit length of borehole are expressed by, respectively

$$V_e = \frac{\pi D_e^2}{4} \tag{10.3a}$$

and

$$V_h = \frac{\pi D_h^2}{4} \tag{10.3b}$$

Table 10.1. Dependence of the borehole wall pressure on the coupling ratio.

Charge diameter (mm)	*CR*	Borehole wall pressure (MPa)
100	1	2500
90	0.9	1900
80	0.8	1400
70	0.7	1000
60	0.6	660
50	0.5	410
40	0.4	230
30	0.3	110
20	0.2	40

then

$$\frac{P_h}{P_e} = \left(\frac{P_e}{P_h}\right)^{\gamma} = \left(\frac{D_e}{D_h}\right)^{2\gamma} = (CR)^{2\gamma} \tag{10.4}$$

As indicated earlier the outward pressure P_e at the wall of an explosive is given approximately by

$$P_e = 0.125\rho(VOD)^2 \tag{10.5}$$

where ρ = density (kg/m^3), VOD = detonation velocity (km/sec), P_e = pressure (MPa).

The pressure at the wall of the borehole is then

$$P_h = P_e(CR)^{2\gamma} \tag{10.6}$$

Table 10.1 shows the calculation of borehole wall pressure for a dynamite explosive

$\rho = 1390$ kg/m^3

$VOD = 3800$ m/s (50 mm diameter)

of various diameters in a 100 mm diameter hole. It has been assumed for the sake of the example that the VOD is independent of charge diameter and confinement and that

$\gamma = 2.0$

over the entire expansion range although as is discussed in Chapters 3, 11 and 17 this is a gross simplification. Using the rule that the wall pressure should be less than the dynamic compressive strength (DCS) of the rock, for granite with a DCS of 300 MPa one would choose a *CR* of between 0.4 and 0.5.

It should be noted that when using explosives of low detonation velocity (for example ANFO), the shock wave generated in the air in the annulus can have a higher velocity than the *VOD* and thereby precede the detonation front travelling in the explosive. This high pressure can increase the density of the ANFO in the column to above 1.25 gm/cm^3 thereby dead-pressing it. Hence the detonation will stop. As a result more energetic (higher *VOD*) explosives are often used.

Spherical charges may be treated in the same way. Equation (10.2) remains the same but expressions (10.3a) and (10.3b) become respectively

$$V_e = \frac{\pi D_e^3}{6} \tag{10.7a}$$

and

$$V_h = \frac{\pi D_h^3}{6} \tag{10.7b}$$

The expression for the pressure ratio becomes

$$\frac{P_h}{P_e} = \left(\frac{P_e}{P_h}\right)^{\gamma} = \left(\frac{D_e}{D_h}\right)^{3\gamma} = (CR)^{3\gamma} \tag{10.8}$$

A recent field study (Jinnerot & Nilsson, 1998) in which very detailed peak particle velocity (PPV) measurements were made at various distances from fully coupled and de-coupled charges suggests that free gas expansion to the wall of the borehole as classically assumed is not correct. The measured PPV values were significantly higher that would be predicted using hole wall pressures based on the use of Equation (10.6) and γ values appropriate for the expansion range. A best fit of the experimental result suggested that

$$\gamma \cong 1$$

rather that 1.7, for example. One explanation can be found by examining the behavior of the air gap directly after charge detonation. In the development of Equations (10.6) and (10.8) it is assumed that the air gap is fully deformable and the pressure contained in the cylindrical form of the charge simply changes shape to fill the new container. In going so, the pressure drops to the values determined by γ for the gas over the appropriate pressure range. If, on the other hand, one would consider the air gap to be rigid instead of fully deformable, then the problem can be likened to the application of a radial pressure (the explosion pressure) on the inside wall of a cylindrical hole of radius r_e in a rock mass of infinite extent. The air gap, at least momentarily, becomes an extension of the surrounding rock. From elasticity theory, the radial pressure at any radius r from the center of the cylindrical hole can be expressed as

$$\sigma_r = P_e\left(\frac{r_e}{r}\right)^2 \tag{10.9}$$

For the special case where $r = r_h$, Equation (10.9) can be rewritten in equivalent form as

$$P_h = P_e\left(\frac{D_e}{D_h}\right)^2 \tag{10.10}$$

Comparing Equations (10.10) and (10.6) one can see that if the air behaves in a rigid manner directly after the explosion, then the pressure that would be applied to the hole wall is that given by Equation (10.6) with $\gamma = 1$. The conclusion is that the γ value traditionally used in de-coupling equations actually refers to the behaviour of the annulus between the explosive charge and the hole wall and not to the explosive gas. That this is true, is evidenced by the change in behaviour of decoupled charges in water-filled holes and when the de-coupled charge lies along the side of a blasthole as opposed to being centralized. It is quite common to find γ values in the published literature (Atchison et al. (1964) and Chiappetta (1982), Calder & Bauer (1983)) dealing with de-coupling of the order of

$$\gamma \approx 1.2$$

Hidden page

10.3 SPECIAL DAMAGE CONTROL TECHNIQUES

10.3.1 *Introduction*

In the introduction to this chapter the concept of a blast damage transition zone (BDT) was presented with respect to the production holes. As the pit expands outward, the BDT follows along automatically unless some special measures are taken such as line drilling or pre-splitting. These are two of the techniques which will be discussed in this section. To facilitate this discussion on damage control techniques, consider the BDT shown diagrammatically in Figure 10.7 for a fully-charged 9-7/8″ diameter hole. It is convenient to subdivide the BDT into three zones based upon the level of damage. The extent of each zone is characterized by a radius from the center of the production charge. The zones, their extent (as expressed in terms of the hole diameter D) and the corresponding PPV values resulting when using ANFO in medium strength rock are assumed to be as follows:

Damage zone	Extent	PPV (m/sec)
Crushed (R_c)	4 → 6 D	20
Fractured (R_f)	12 → 15 D	5
Influenced (R_i)	50 → 60 D	1.5

These zones have been drawn on Figure 10.8 for a blast containing 2 rows of production blast holes (9-7/8″ diameter). As seen, it is a square pattern with 5 holes in each row, a burden of 20′ and spacing of 20′. In this example it has been assumed for simplicity that

$$R_c = 5\ \text{D} = 4\ \text{ft}$$

$$R_f = 12\ \text{D} = 10\ \text{ft}$$

$$R_i = 55\ \text{D} = 45\ \text{ft}$$

After blasting, the situation is shown in Figure 10.9. In the BDT zone there exists a crushed and a fractured zone surrounding each production hole. Although the crushed zone as well as a small portion of the fractured zone may have been loaded out along with the rock from production rows 1 and 2, here the rock will be assumed to still be in place. The zone lying between the fracture zone and the boundary of the BDT consists of an inner portion which has been influenced by both rows of blastholes (to a distance of about 25′) and an outer portion (20′ in extent) influenced by just one row of production holes.

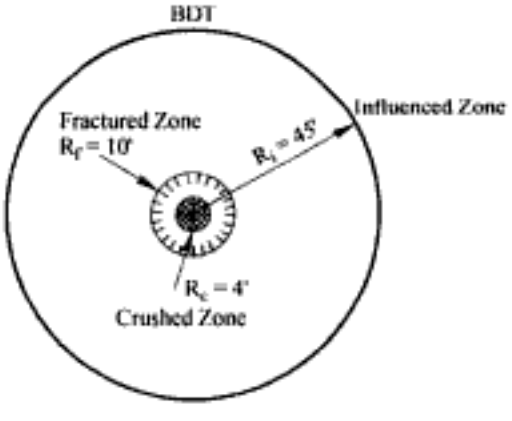

Figure 10.7. Diagrammatic representation of the BDT surrounding a fully charged hole.

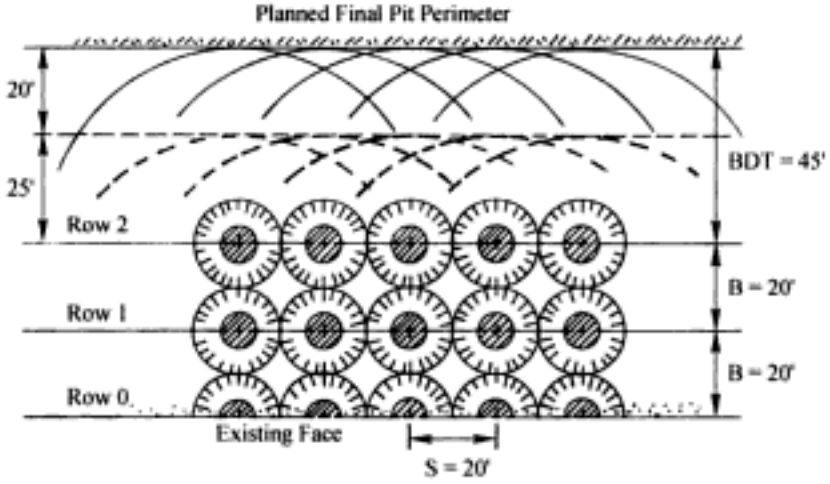

Figure 10.8. The BDT for two row production blast.

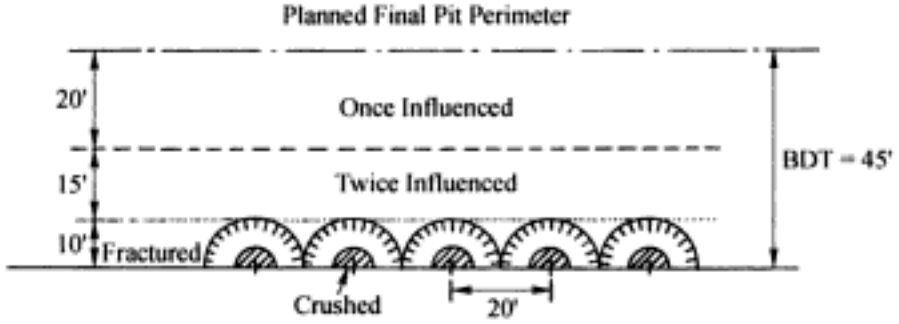

Figure 10.9. The BDT after blasting the two production rows.

Thus depending upon where one selects the position of the final pit limit within the BDT, one has an existing degree of pre-damage even if no further damage is induced during the remaining excavation. In the examples that follow the final pit limit will be selected at the BDT limit.

10.3.2 *Line Drilling*

Line drilling, as the name implies, involves the drilling of closely spaced holes along the limit of the excavation. This is shown with respect to the example case in Figure 10.10. The object is to create an artificial plane of weakness which serves to limit the extent of the fracture and influence zones from both the production holes and any buffer (helper) holes placed between the final production row and the perimeter. Generally, these line-drilled holes are not charged with explosive but, if charged, it is with detonating cord or a highly decoupled charge. The purpose for lightly charging the holes is to destroy the integrity of the rock web. As can be appreciated, close drilling control is essential for the method to succeed. The holes must be drilled so that they all lie in one plane corresponding with the dip of the final pit wall. Some recommendations for hole spacing as provided in the CANMET Pit Slope Manual-Chapter 7: Perimeter Blasting (1977) are included in Table 10.2. To get hole spacing one multiplies the values in the table by the hole diameter expressed in the same units. When line drilling 6″ diameter holes in copper ore, the hole spacing (c-c) should be 12″.

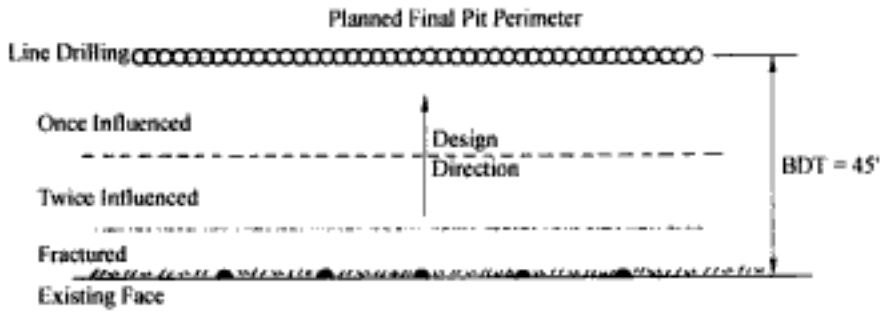

Figure 10.10. Line drilling positioned along the planned final perimeter.

Table 10.2. Factors for determining hole spacing (CANMET, 1977).

Rock type	Factor
Taconite	2.0
Copper ore	2.5
Asbestos ore	4.0

In the example there is 45 ft wide zone between hole row 2 and the perimeter. To excavate this rock one might consider using another row of production holes at normal burden and spacing and then one or two rows of smaller diameter buffer holes. As indicated by CANMET (1977) for line drilling to be most effective

– It must be used in conjunction with a buffer row
– The main excavation charges should be 1 to 3 rows from the pit limit.

Of the four methods discussed in this section, line drilling produces the best final surface – a smooth, clean face with no backbreak or crest fracture. However because of its high drilling cost, the method has not been commonly used in open pit work.

10.3.3 *Pre-split blasting*

As indicated, line drilling is the most effective method for creating a smooth and undamaged final rock wall. However the drilling costs are such that the technique can only be considered under very special circumstances today. The pre-splitting technique also involves the careful drilling of relatively closely spaced parallel holes along the final perimeter (Figure 10.11). Now however the holes are lightly charged and shot instantaneously. The objective is to generate a line of cracks connecting the holes. In this way, it is intended to achieve nearly the same effects

– Terminate the growth of the radial cracks
– Act as a barrier to the shock wave
– Provide an escape route for the explosive gases.

as with line drilling but at a significantly lower cost. Obviously to be of any use the pre-split line must be created prior to the blasting of any holes lying closer than 1-BDT distance away.

The explanations for exactly how the cracks between holes (Figure 10.12) are formed have varied over the years. As has been discussed earlier, when an explosive is detonated, a shock wave moves away from the borehole. This wave has two components. The radial

component is compressive and pushes the rock radially outward as it travels along. The tangential component is tensile and it tends to stretch the rock as it moves away from the hole. The outward velocity of the cracks generated by the tangential component is slower than that of the wave itself. If the adjacent holes are detonated at *precisely* the same time, then the surrounding regions will be influenced by the waves from both holes. The radial (compressive) wave component from hole 1 (Figure 10.13) will tend to close cracks trying to grow in the direction normal to the borehole line away from hole 2. The tangential (tensile) wave component from hole 1 will encourage the growth of cracks from hole 2 along the borehole line. The wave from hole 2 has the same effect on the cracks radiating from hole 1. The highly cracked zone between the holes becomes the path of least resistance for the gas pressure to escape and also encourages crack growth in this direction. The holes must be relatively close together for this interaction to occur. Since the holes are located far away from a free surface the reflected (tensile) radial component has little effect.

For true pre-split blasting, all of the holes must be initiated at the 'same time' and the charge should extend along the full length of the hole. There is sometimes confusion regarding what is meant by the requirement that the holes are shot at the 'same time'. To

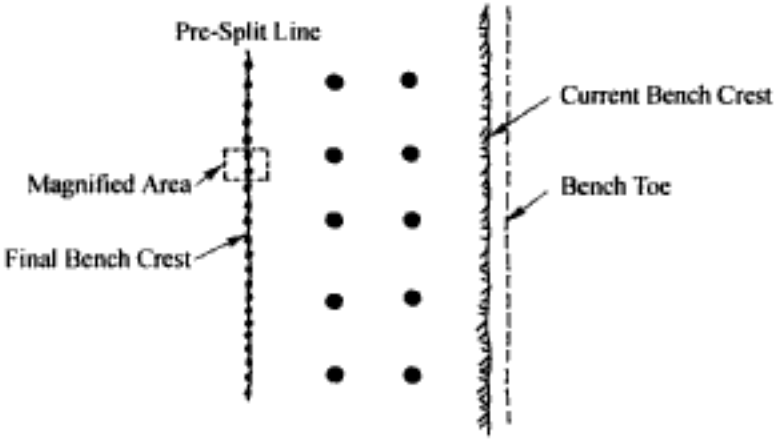

Figure 10.11. A pre-split line positioned along the planned final perimeter.

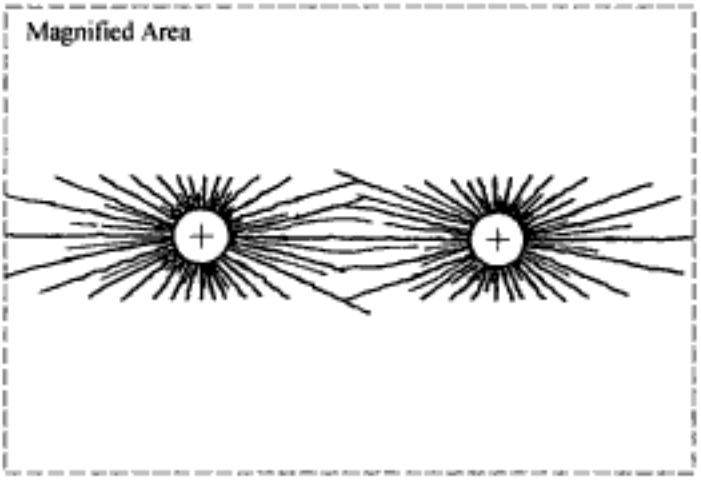

Figure 10.12. Idealized pre-split fracture pattern (AECI, 1978b).

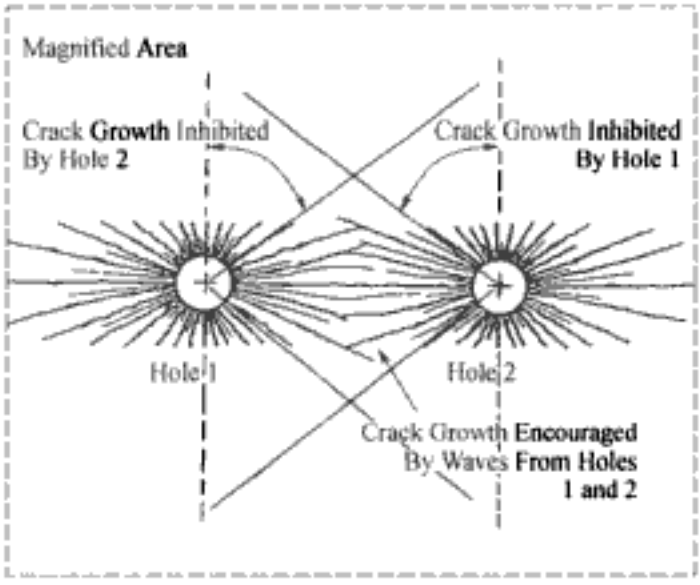

Figure 10.13. Crack growth inhibited zones (AECI, 1978b).

demonstrate this, consider the following example. In an open pit mine assume that pre-split holes 150 mm (6") in diameter have been selected and a spacing-hole diameter ratio of 10:1 is appropriate. Thus the center-center hole spacing would be 1.5 m (5 ft). Assuming that the longitudinal wave velocity in the rock is 3000 m/sec (10,000 ft/second) the time required for the wave to travel the 1.5 m between holes is

$$t = \frac{1.5}{3000} = 0.5 \text{ msec}$$

Thus for the waves from Holes 1 and 2 to interact in the region between the holes, the delay time would have to be less than 0.5 msec. Because of the spread in delay times even when using high precision caps, such precision is highly unlikely. To achieve near 'simultaneous' initiation of such pre-split holes today one often uses detonating cord down lines and side initiation. Electronic caps which are in the process of being introduced possibly could satisfy this requirement.

Because this close timing requirement is seldom realized in practice, this classical explanation of presplitting may not, in fact, be correct. The holes most probably do not detonate within the time window needed to have *active stress wave* interaction with the *growing* cracks. Favorably oriented cracks (those extending along the hole line) initiated by adjacent holes will be extended by the tensile component of the wave from the adjacent hole. The part of the theoretical process that would not be realized is the retardation of radial cracks in adjacent holes extending in directions normal to the hole line. However with the creation of a crack path between two adjacent holes the gases would preferentially flow in this direction as opposed to opening cracks oriented in other directions. The wedging due to the gas would extend the cracks. Since the gas pressure in the hole acts over a considerably longer time than does the wave, the timing of adjacent holes may not at all be as critical as suggested by classical theory. The most desirable situation would be for the holes to be shot close enough together in time so that the adjacent ones are still pressurized by gas (Figure 10.14). Their cooperation now provides a force oriented normal to the hole line. This completes the split and the gases are released.

The gas pressure should be high enough to encourage the growth of tensile cracks but low enough to prevent compressive failure (crushing) around the hole. The CANMET Pit Slope Manual (1977) suggests the following design relationship

$$\frac{S}{D} \leq \frac{P_W + T}{T} \tag{10.11}$$

where P_W = pressure at the borehole wall (MPa), T = rock tensile strength (MPa), D = hole diameter (m), S = spacing (m).

A first approximation for the value of the dynamic tensile strength is taken from Table 10.3.

As an example consider pre-split blasting in a rock with the following dynamic strength values

– Compressive strength = 40,000 psi (280 MPa)
– Tensile strength = 2500 psi (17 MPa)

The pre-split is to be done using a continuous column of 1-1/4 (32 mm) cartridges of an explosive with an explosion pressure of 450,000 psi. The hole diameter is 4". It is assumed that the effective dynamic expansion factor which applies for the air gap between the explosive and the hole wall is 1.2. The question is what hole spacing should be used. The explosive pressure applied to the wall is

$$P_W = 27{,}450 \text{ psi } (190 \text{ MPa})$$

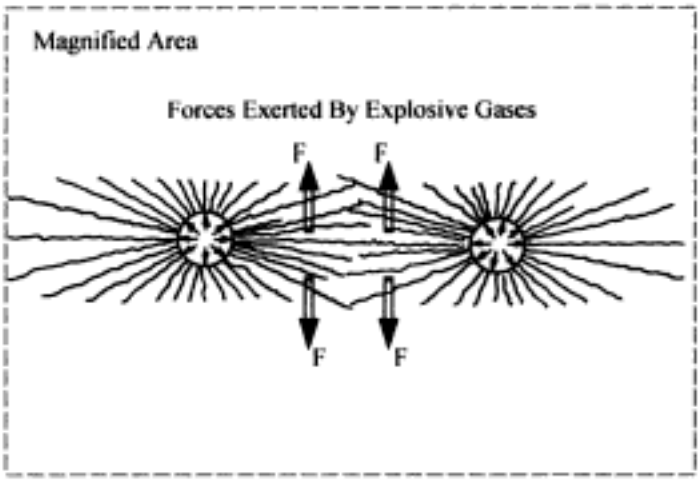

Figure 10.14. Crack extension by gas pressure. (AECI, 1978b).

Table 10.3. Dynamic tensile strength of rock (CANMET, 1977).

Rock type	Dynamic Tensile Strength (psi)	(Mpa)
Taconite	2500-6000	17-41
Copper ore	4000	27
Asbestos ore	700	5
Limestone	1000-2000	7-14

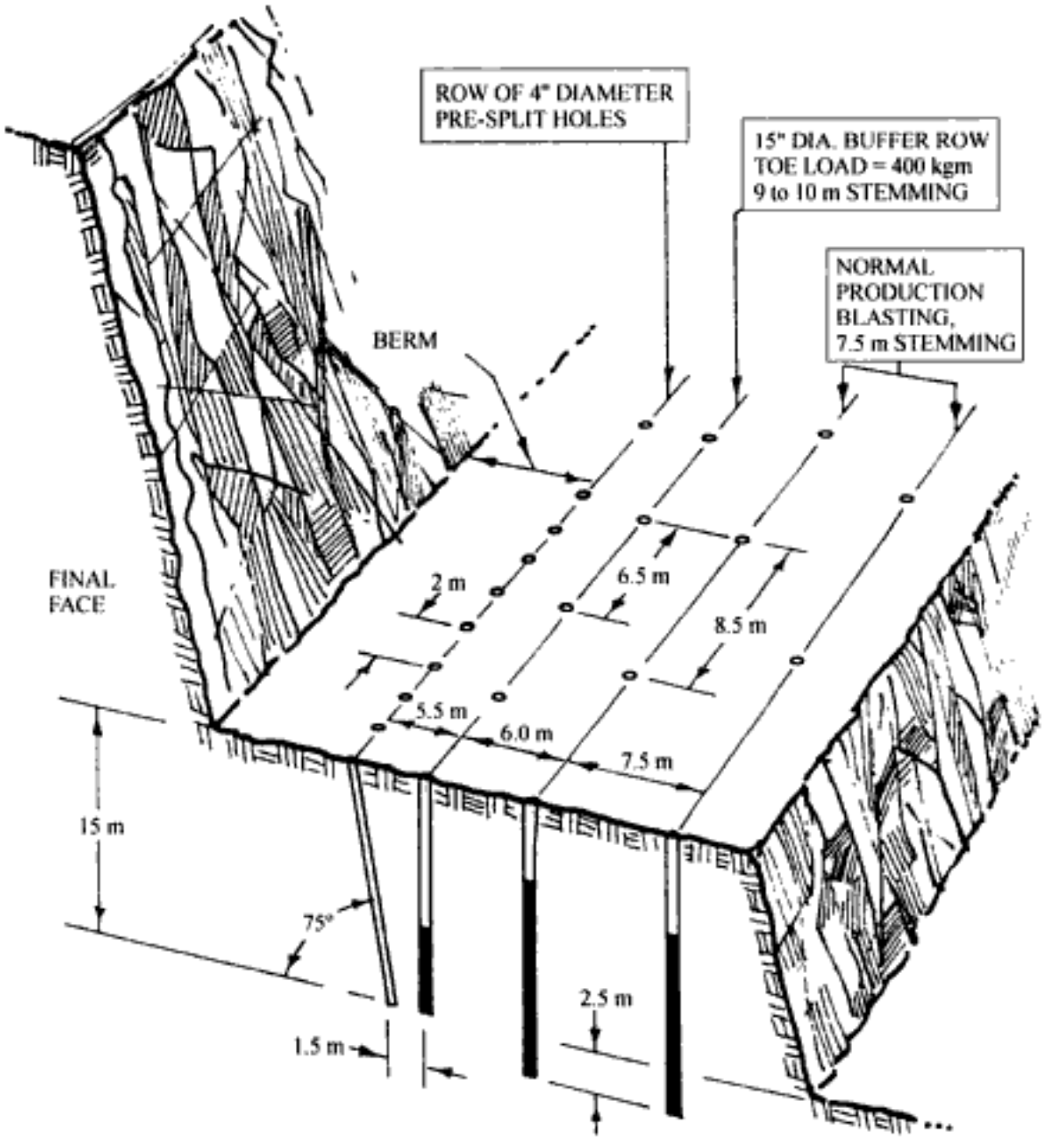

Figure 10.15. Production design with pre-splitting (Bauer,1982).

which is below the dynamic compressive strength of the rock. Using Equation (10.11) one finds that the spacing S is

$$S = 47.8 \text{ ins} = 4.0 \text{ ft } (1.2 \text{ m})$$

If the rock were highly jointed, its dynamic compressive strength would be lower, perhaps in the 20,000 psi (140 MPa) range. To avoid backbreak, a lower borehole pressure and hence closer spacing would be used.

Figure 10.15 shows a pre-split blast design (Bauer, 1982) where a row of 102 mm diameter pre-split holes have been used together with 381 mm diameter production/buffer holes. The pre-split line may be *fired* prior to the drilling of the production holes or just prior (100 to 150 msec) to firing the production holes. Table 10.4 provides recommenda-

Table 10.4. Recommended charge loads and blast geometries for pre-split blasting (Hagan & Mercer, 1983).

Blasthole diameter (mm)	Charge load (kg/m)	Suggested cartridge diameter (mm)	Blasthole spacing (m)
75	0.45	22*	0.75
90	0.65	25*	0.90
100	0.80	29*	1.00
115	1.10	32*	1.10
125	1.30	38*	1.20
150	1.85	45	1.45
200	3.30	55*	1.85
230	4.50	65*	2.00
250	5.30	80	2.15
270	6.10	80	2.25
310	7.80	80*	2.40

* Continuous column charge.

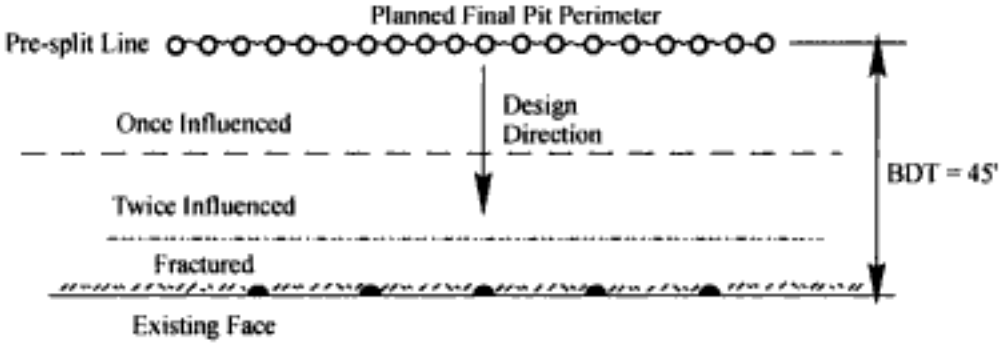

Figure 10.16. A pre-split line included in the example design.

tions for the charge density and spacing in presplitting. It should be remembered that structures such as bedding planes, joints and schistosity as well as the insitu stress state affect the pre-splitting results.

Just because a pre-split line has been created does not mean that care does not have to be taken regarding the design of the blasting pattern used between the final production row and the BDT. Quite the contrary is true. The crack line between the holes is often quite narrow and can be closed by the waves generated by highly charged holes in the near vicinity. Although damped, the waves may still have enough remaining energy to induce cracking beyond the pre-split line.

Figure 10.16 shows a pre-split line added to the example introduced earlier in the section. An additional production row of holes may be shot with the result that the pre-split line limits the zone of influence to a distance of 25 ft. The remaining rock is blasted using smaller diameter holes with closer spacing and smaller charges. The final row of holes is placed so that their associated fracture zone just extends to the pre-split line.

10.3.4 *Smoothwall Blasting*

In smoothwall blasting, as opposed to line drilling and pre-splitting, the final pit perimeter lies in the zone of influence from the final row of production holes. This is shown dia-

grammatically in Figure 10.17. Since the final row of holes lies in the influenced zone, some minor crest fracturing or backbreak may result but the amount of damage is much less than would be produced by the main production blast if no control blasting was used. There are five general rules (Hagan & Mercer, 1983) followed in the design of the smoothwall row

– The burden, spacing and charge concentration of the smoothwall line of holes are selected so that the extent of the associated influence region does not exceed that of the production holes. The hole size for the smoothwall and buffer row holes may be the same as in the production round with the required reduction in influence zone dimension occurring through pattern adjustments and decoupling or smaller diameter holes may be used with or without decoupling.

– The hole spacing is less than the burden. Often the relationship

$$\frac{S}{B} = 0.8 \tag{10.12}$$

is used (Figure 10.18)

– The holes in the smoothwall row are shot on the same delay with detonating cord downlines to assure as simultaneous detonation as possible.

– The delay time between the helper row (that adjacent to the smoothwall row) and the smoothwall row should be chosen so that the smoothwall holes can shoot to a free face.

– All of the smoothwall and buffer row holes are shot together with the main production round.

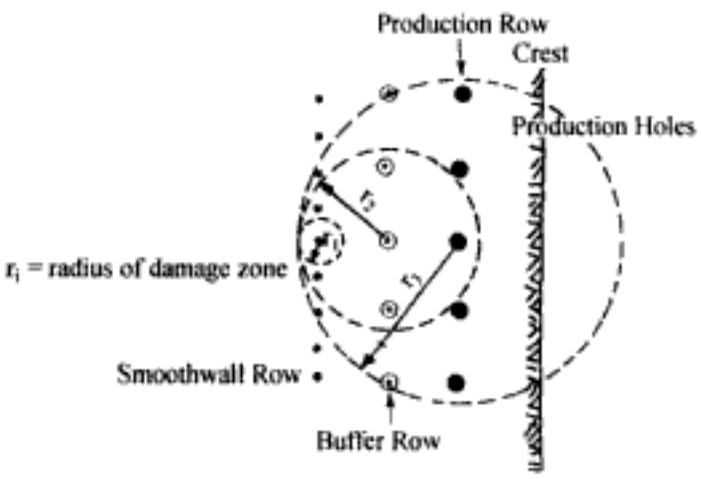

Figure 10.17. Periphery protection using smoothwall blasting (Holmberg and Persson, 1978).

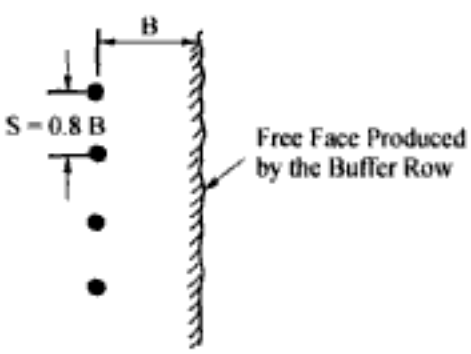

Figure 10.18. Smoothwall blasting geometry.

The first rule is required to simply satisfy the gentle blasting criteria that succeeding holes should not extend the damage beyond what has already been done. Rules 2, 3 and 4 are based upon the rock breaking effect which is to be created by the smoothwall holes. With simultaneous detonation, as discussed under Section 10.3.2, the radial cracks created will extend preferentially along the hole line. The gases stream into this line of least resistance as opposed to extending the other cracks (those both towards and away from the free face). Because the spacing is relatively small, this connection occurs rather quickly. The sustained gas pressure from the line of holes heaves the burden forward with relatively little twisting and distortion. As a result, smooth wall blasting can produce a relatively coarse fragmentation. If the delay timing between the helper and the smoothwall rows is too short, the gas pressure will remain longer in the smoothwall line with the possibility that cracks will be extended beyond the influence limit. The explosive is chosen such that high detonation pressures (and hence rock fracturing) are avoided. Once the smoothwall row has been designed, then one continues with the design inward toward the production row. This procedure is described in some detail in Section 10.4. Rule 5 leads to considerably less complicated blasting than the other three techniques. Today, it is much more common to use smooth wall blasting rather than pre-splitting, for example, in open pit mining operations because of

- Less drilling
- Less complicated blasting

Figure 10.19 shows an example of a bench blast design involving smoothwalling (Bauer, 1982). As can be seen in Figure 10.20, the design direction is from the expected boundary of influence from the production holes and works toward the face. The outer smoothwall row is placed so that the limit of its influence zone corresponds with that from the production holes.

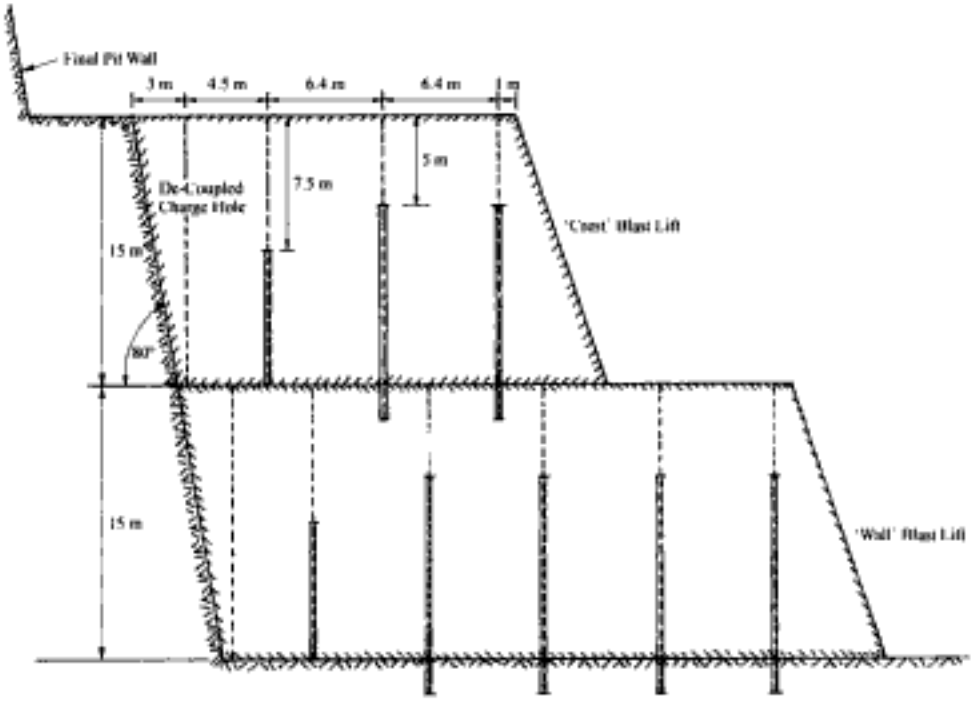

Figure 10.19a. Section view of the smoothwall design (Bauer,1982).

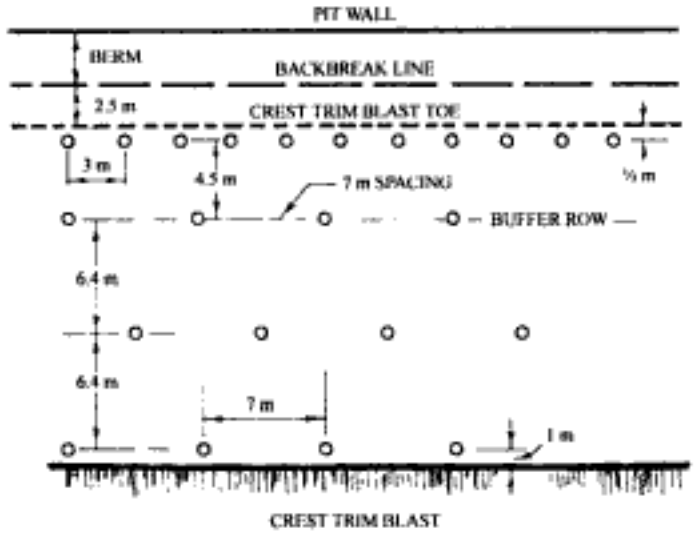

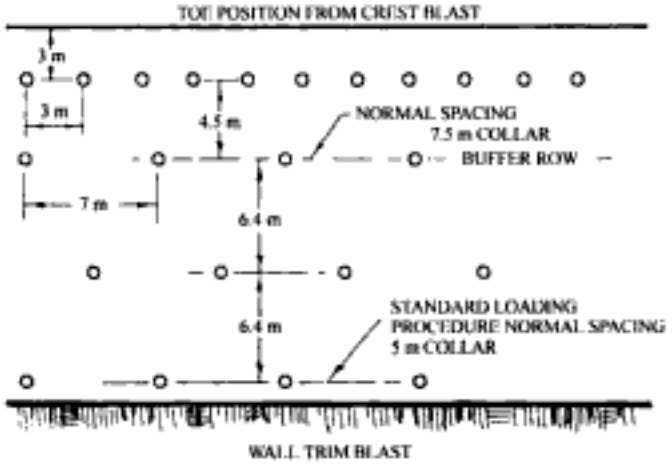

Figure 10.19b. Plan view of an actual smoothwall design (Bauer,1982).

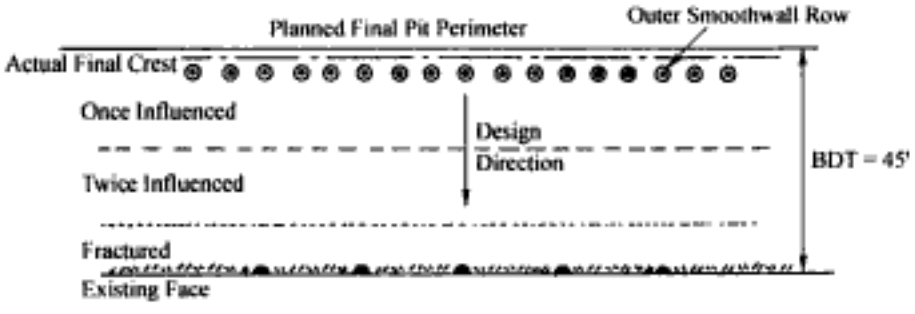

Figure 10.20. Smooth wall row superimposed on the example design.

10.3.5 *Trim blasting*

Trim blasting, as the name implies, involves trimming away some of the fractured and influenced rock from the pit perimeter after the production blast has been shot and cleaned up. The trimming may be accomplished using one or several rows of blast holes depend-

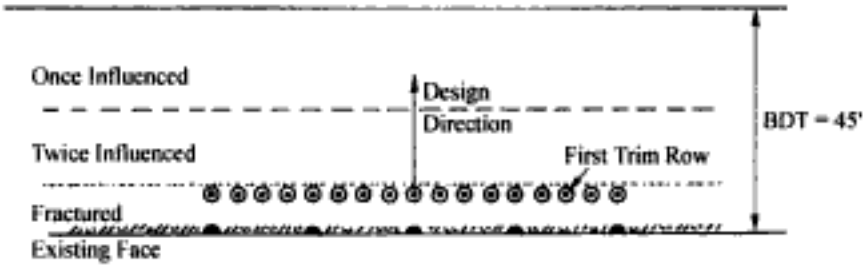

Figure 10.21. First trim row superimposed on the example design.

Table 10.5. Recommended charge loads and blast geometries for trim blasting (Hagan & Mercer, 1983).

Blasthole diameter (mm)	Charge load (kg/m)	Suggested cartridge diameter (mm)	Blasthole spacing (m)	Burden (m)
75	0.50	22*	1.15	1.55
90	0.70	25*	1.35	1.80
100	0.85	29*	1.50	2.00
115	1.05	32*	1.70	2.20
125	1.20	38*	1.80	2.40
150	1.70	55	2.20	2.80
200	2.75	55*	2.80	3.70
230	3.30	55*	3.30	4.20
250	3.75	80	3.60	4.60
270	4.15	80	3.90	5.00
310	4.80	90*	4.40	5.60

* Continuous column charge

ing on where in the BDT zone it is desired that the final crest should fall. The design process differs from the smoothwall technique in that the layout begins at the actual pit perimeter and works outward toward the desired final pit limit rather than vice versa. This is shown diagrammatically in Figure 10.21 with respect to the design example. Some rules for selecting the burden, spacing and charge concentration as a function of hole diameter are presented in Table 10.5. As in all other types of perimeter control, accurate drilling is important. To achieve the best results, the holes should be drilled at the final pit slope angle. The boreholes are drilled in a line along the planned excavation limits, loaded lightly, and blasted to remove the undesired material. As noted earlier, a reduced explosive load can be obtained in various ways. The use of low density, bulk-loaded explosives in larger diameter holes such as described in Chapter 7 is one way of improving the economics of the method.

10.4 PERIMETER CONTROL DESIGN APPROACHES

10.4.1 *Introduction*

As was discussed in Chapter 9, studies over the years have shown that blast damage to surface and underground structures due to blasting can be related to particle velocity. Although this has now changed, for many years the limiting particle velocity below which

no damage was expected to occur was 2 in/sec. The design techniques discussed in this section take the same approach regarding the damage to the rock mass. Techniques are presented for calculating the particle velocity at any given point surrounding a charge. Comparison to a particle velocity based damage criteria will then yield the extent of damage. Obviously the process also works in reverse. One can specify the maximum extent of damage and then calculate the limit charge.

10.4.2 *The Swedish approach*

The first step in the process of evaluating the extent of rock damage is to calculate the particle velocity. Figure 10.22 is a diagrammatic representation of a bench with the (R, Z) coordinate system oriented as shown. The overall charge length L is divided into a series of smaller pieces each having a length Δz (Fig. 10.23). Since the charge has a weight per unit length of q, the length Δz represents a weight

$$W = q\Delta z \tag{10.13}$$

where q = linear charge concentration (kg/m), Δz = incremental charge length (m).

The general equation for the particle velocity as a function of the charge weight (W) and the distance (R) from the center of a spherical charge (see Chapter 12) may be expressed as

$$V = K\frac{W^{\alpha}}{R^{\beta}} \tag{10.14}$$

where K, α, β = constants for a given site and explosive, R = radial distance from the observation point (r_o, z_o) to the center (r, z) of the incremental charge.

$$R = [(r - r_o)^2 + (z - z_o)^2]^{1/2} \tag{10.15}$$

This applies to a concentrated charge the length (Δz) of which is small compared to the distance R. In differential form Equation 10.14 becomes

$$dV = \frac{K\,(q\,dz)^{\alpha}}{R^{\beta}} \tag{10.16}$$

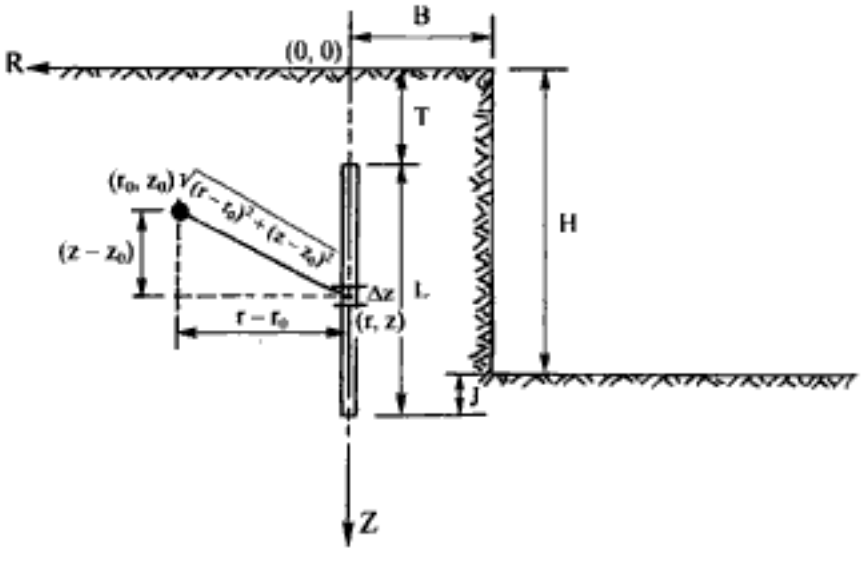

Figure 10.22. Nomenclature used for Swedish design (Holmberg & Persson, 1978).

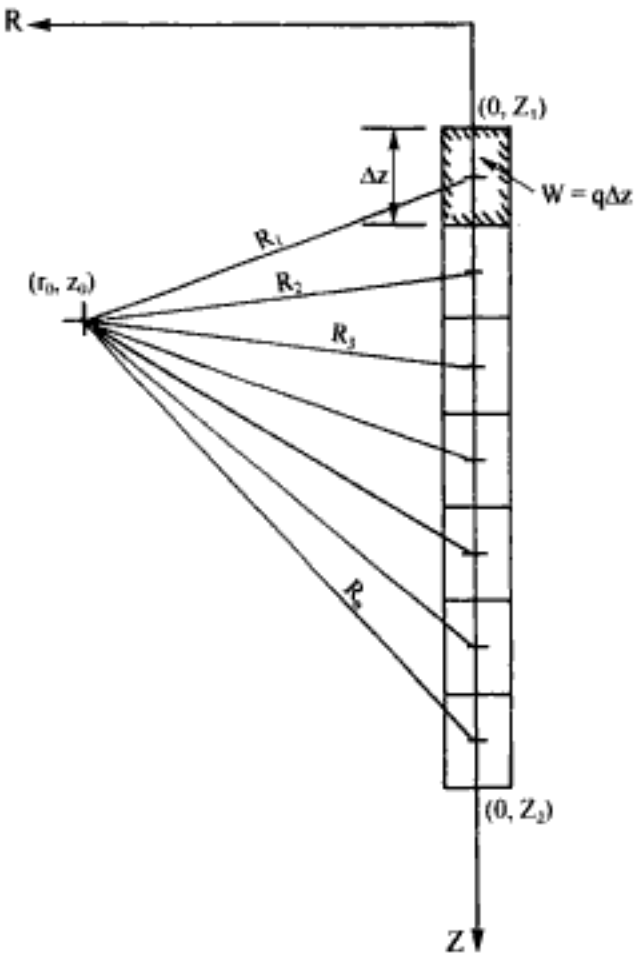

Figure 10.23. Division of the charge into incremental charges.

Substituting Equation (10.15) into Equation (10.16) one finds that

$$dV = K\frac{(q\,dz)^{\alpha}}{\left[(r-r_o)^2 + (z-z_o)^2\right]^{\beta/2}} = \\ = K\left(\frac{q\,dz}{\left((r-r_o)^2 + (z-z_o)^2\right)^{\beta/2\alpha}}\right)^{\alpha} \tag{10.17}$$

To find the total effect at the observation position (r_o, z_o), one must sum up the individual effects over the entire charge length. This can be done in two different ways. The first is to calculate the contributions arriving at the point of interest from each of the increments. These contributions do not arrive at the same time and hence this would need to be taken into account. Furthermore since they arrive from different directions one would need to resolve the total incremental contribution into directional components and then sum. Two simplifications would be to

– Neglect the differences in the times of arrival of the different incremental charges at the point of interest,

– Use the peak amplitude coming from each increment without regard to the arrival direction.

In this way one would calculate the maximum possible amplitude at the point. This is the approach taken by Holmberg & Persson (1978). By doing this the total contribution of the incremental charges can be obtained by simply integrating Equation (10.17) over the charge length. As can be seen from Figure 10.22, the top of the charge is at

$$z_1 = T \text{ (bottom of the stemming)}$$

and the bottom is at

$$z_2 = H + J \text{ (bottom of the subdrill)}$$

Integrating Equation (10.17) yields

$$V = K \left[q \int_{T}^{H+J} \frac{\mathrm{d}z}{\left[(r - r_o)^2 + (z - z_o)^2\right]^{\beta/2\alpha}} \right]^{\alpha} \tag{10.18}$$

This can be evaluated numerically for any given set of α and β values. A special case of Equation (10.14) is

$$V = K \left(\frac{R}{W^{1/2}} \right)^{-\beta} \tag{10.19}$$

the use of which was discussed in Chapter 9 with regard to ground motion. In comparing Equations (10.14) and (10.19) it is seen that they are identical for the special case when

$$\alpha = \frac{\beta}{2} \tag{10.20}$$

Equation (10.18) then becomes

$$V = K \left[q \int_{T}^{H+J} \frac{\mathrm{d}z}{\left[(r - r_o)^2 + (z - z_o)^2\right]} \right]^{\alpha} \tag{10.21}$$

which can be evaluated directly to yield

$$V = K \left\{ \frac{q}{r - r_o} \left[\tan^{-1}\left(\frac{H + J - z_o}{r - r_o} \right) - \tan^{-1}\left(\frac{T - z_o}{r - r_o} \right) \right] \right\}^{\alpha} \tag{10.22a}$$

The angles corresponding to the arctan function are expressed in radians. It will be assumed that the charge is located along the z axis, thus $r = 0$. Equation (10.22a) becomes

$$V = K \left\{ \frac{q}{r_o} \left[\tan^{-1}\left(\frac{H + J - z_o}{r_o} \right) - \tan^{-1}\left(\frac{T - z_o}{r_o} \right) \right] \right\}^{\alpha} \tag{10.22b}$$

For hard bedrock (granite, for example), Holmberg & Persson (1978) suggest that

$$K = 0.7$$

$$\alpha = 0.7$$

$$\beta = 1.5$$

can be used as standard values. These values were substituted into Equation (10.18) and the equation integrated numerically to produce the curves shown in Figure 10.24. The

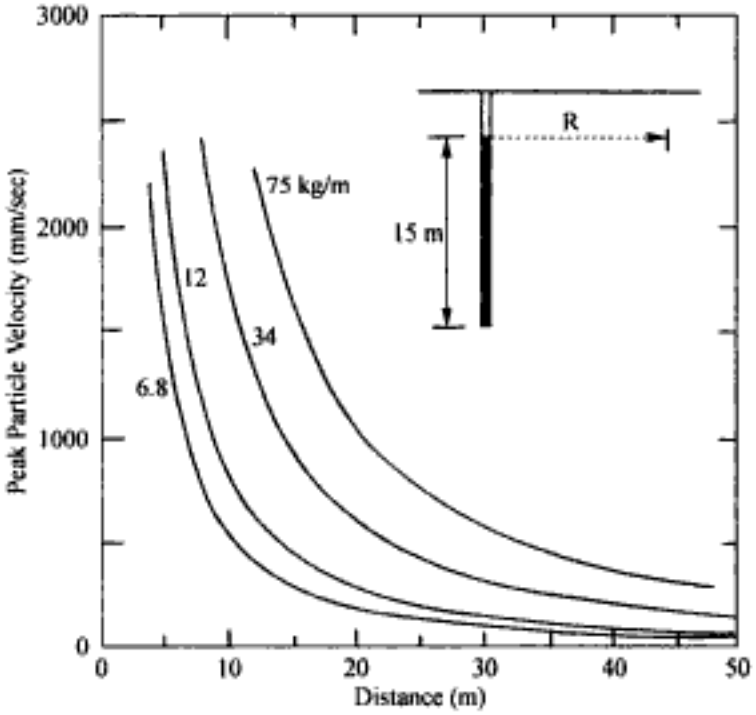

Figure 10.24. Peak particle velocity versus distance and linear charge concentration (Holmberg & Persson, 1978).

velocities are those expected along the horizontal line drawn through the top of the 15 m long charge (Fig. 10.25). These are not the maximum velocities generated by the explosion. They would be expected to occur along the line corresponding to the mid-height of the charge

$$Z = T + L/2$$

since in this approach the entire charge length has been assumed to detonate instantaneously and no resolution of the particle velocities in the different directions has been done.

The four curves in Figure 10.24 correspond approximately to the following hole diameters (D) when filled with ANFO at 0.80-0.82 g/cm^3.

D (m)	q (kg/m)
0.102	6.8
0.140	12
0.230	34
0.350	75

Figure 10.26 shows a cross section through the bench with the iso-velocity (equal-velocity) lines superimposed. This is for the case when q = 34 kg/m and L = 15 m.

The next step in the process is to determine the magnitude of the particle velocity which produces significant rock 'damage'. Studies have been made over many years in relating particle velocity to damage of structures. The damage has been found to be related to the building construction, the nature of the underlying material and the particle velocity. The safe-limits for a few case are given in Table 10.6. The problem is to determine the 'safe-limits' for rock in-situ. From extensometer measurements in nearby unloaded drillholes and core drilling before and after blasting Holmberg and Persson (1978) found that the safe-limit for *hard bedrock* was in the range of 0.7 to 1.0 m/sec. The 'damage' consisted

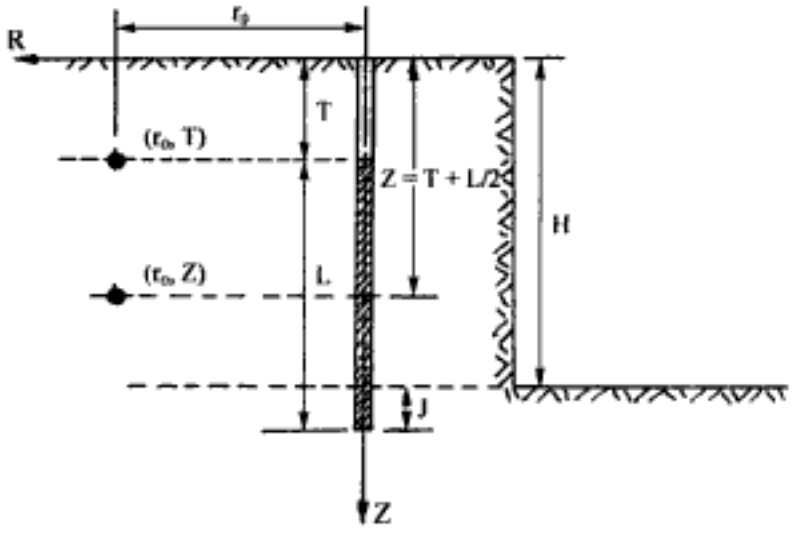

Figure 10.25. Geometry used in developing the curves in Figure 10.24.

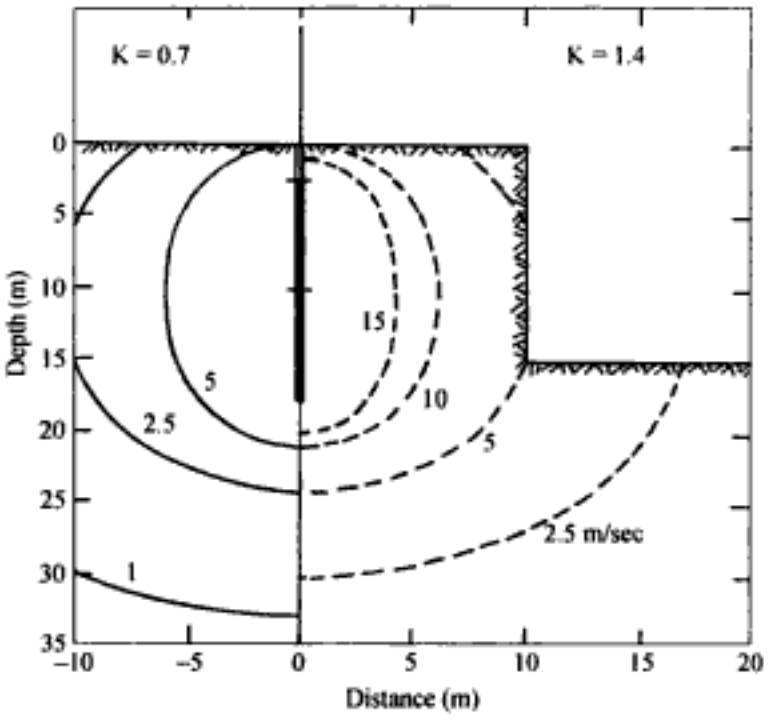

Figure 10.26. Iso-velocity contours (Persson, 1990).

of the expansion of existing joints and the formation of minute new cracks. These 'damage' threshold limits have been superimposed on Figure 10.27. For simplicity here it will be assumed that the level is 1 m/sec (Fig. 10.28).

To demonstrate one simple application of the curves for blast design near the final pit perimeter, consider the following example:

Explosive = ANFO (0.82 g/cm^3)
Production holes (D) = 350 mm
'Buffer' holes = 230 mm

Table 10.6. Safe-limits, below which no damage should be expected (Hagan & Mercer (1983).

Category of structure	Particle Velocity in/sec	mm/sec
Historical buildings, monuments and buildings of special significance.	0.08	2
Houses and low rise residential buildings.	0.4	10
Commercial and industrial buildings or structures of reinforced concrete or steel.	1	25

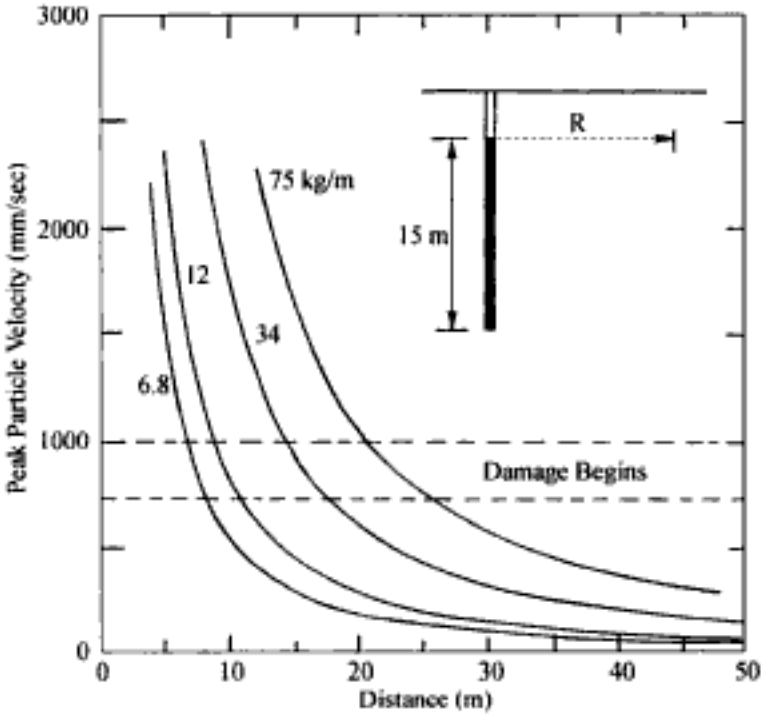

Figure 10.27. Peak particle velocity versus distance curves with the damage zone superimposed.

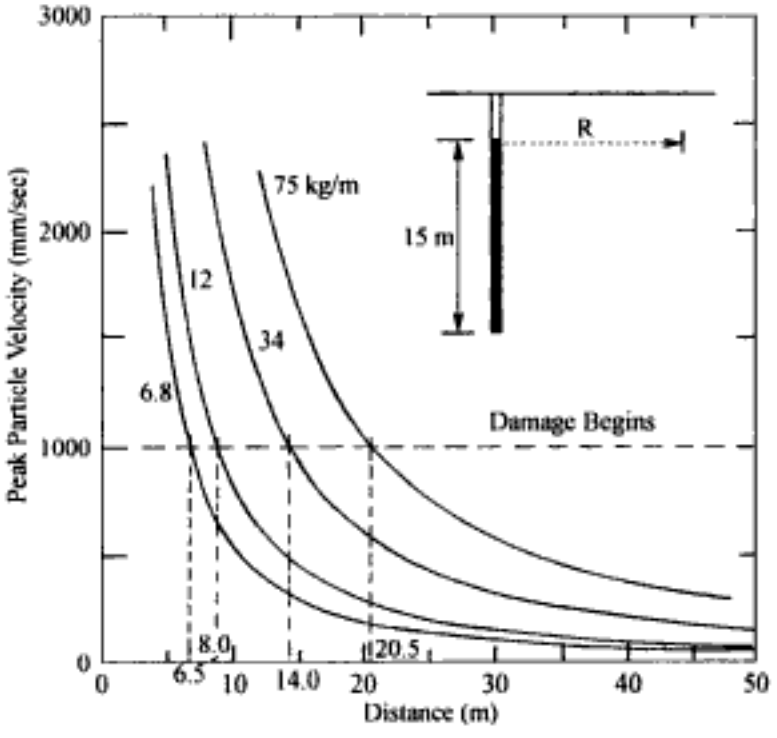

Figure 10.28. Peak particle velocity versus distance curves used in the sample problem.

'Trim' holes = 102 mm
Bench height = 15 m
Layout Parameters:
$K_B = 25$
$K_T = 0.7$
$K_J = 0.3$
$K_S = 1.0$ (Square Pattern)

A vertical bench face will be assumed to simplify the discussion.

In *Step 1*, the production, buffer and trim patterns are calculated.

1. *Production Pattern*
   $B = 25\ (0.350) \cong 9$ m
   $S = 9$ m
   $T = 6$ m
   $J = 3$ m
   $q = 75$ kg/m
2. *Buffer Pattern*
   $B = 25\ (0.230) \cong 6$ m
   $S = 6$ m
   $T = 4$ m
   $J = 2$ m
   $q = 34$ kg/m
3. *Trim Pattern*
   $B = 25\ (0.102) = 2.5$ m
   $S = 2.5$ m
   $T = 2$ m
   $J = 1$ m
   $q = 6.8$ kg/m

In *Step 2*, the present and final pit contours are drawn on the section (Fig. 10.29) for each bench. To cut the rock to the desired limits, the trim holes have been placed on the final

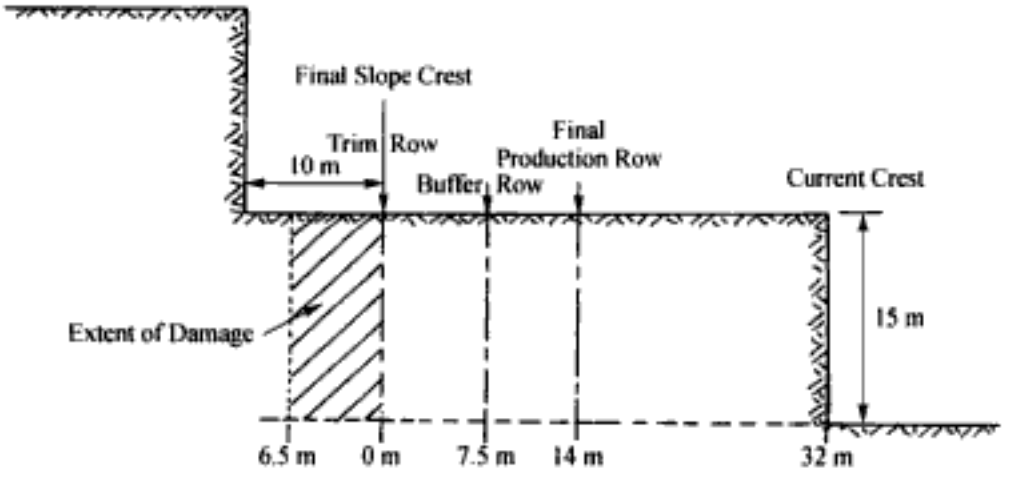

Figure 10.29. An initial design.

contour line. The expected 'damage limit' beyond this line (1m/sec) is shown on Figure 10.29. It extends 6.5 m into the final pit wall. The closest approach of the 'buffer' and production holes should be such that they do not cause damage beyond this line (further than 6.5 m into the final wall). From Figure 10.28 one can see that the respective limiting radii are

Buffer holes: $R = 14$ m
Production holes: $R = 20.5$ m.

Their closest approach positions to the final outline are shown in Figure 10.29.

Buffer = 14.0 – 6.5 = 7.5 m
Production = 20.5 – 6.5 = 14 m

In *Step 3*, the first attempt at a blasting pattern is drawn (Fig. 10.30). As can be seen, there would be 2 production holes (P_1, P_2) followed by 1 line of buffer holes (B_1) followed by 2 rows of trim holes (T_1, T_2).

However, this design has been based upon a constant powder factor (K_B = constant) being maintained throughout. As the burden on the holes is reduced they fall within the zone influenced (damaged) by the previous holes. A first approximation to the maximum extent of this 'major' damage zone will be the burden. This has been plotted on Figure 10.31 for the final production hole P_2 together with the proposed position of buffer hole B_1 with its expected major damage zone B_1'. As can be seen, B_1 lies well within the damage zone of the final production hole. There are three adjustments to the pattern which could be considered to take advantage of this.

1. The explosive in hole B_1 could be significantly reduced while maintaining the same burden and spacing.
2. The burden/spacing could be increased while maintaining the same charge.
3. The amount of explosive could be reduced somewhat while increasing the burden and spacing.

Option 2 cannot be considered since the hole would be moved closer to the final pit limit. The damage zone would then extend further into the wall. Option 1 is not of real interest since it is desirable, if possible, to eliminate the highest cost items, the holes. Thus it is Option 3 which is chosen.

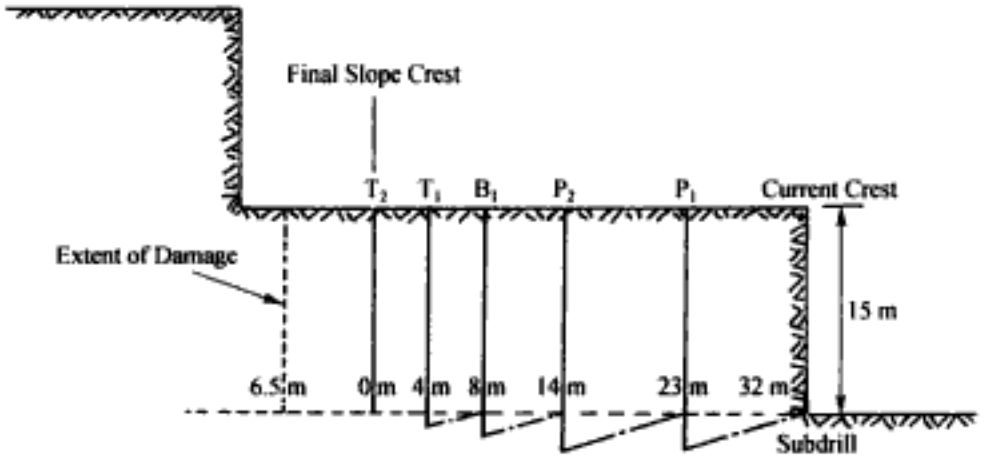

Figure 10.30. The sub-drilling added.

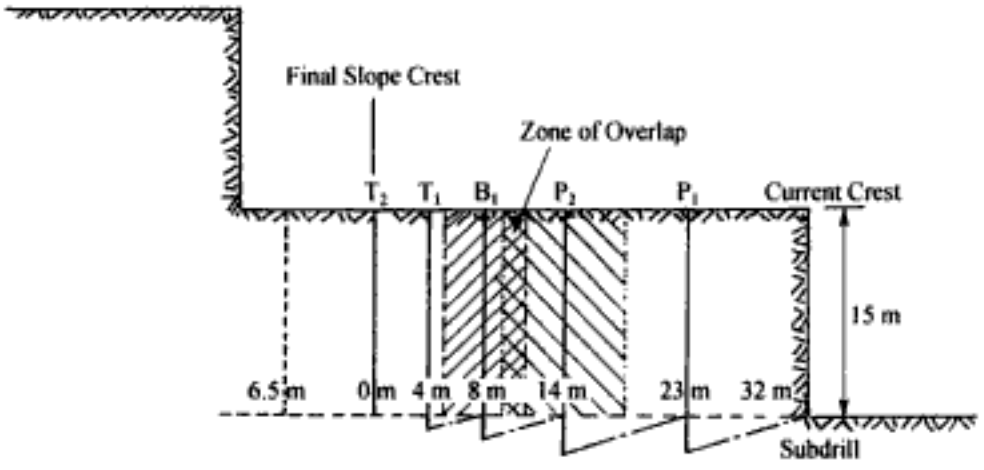

Figure 10.31. Overlap of damage zones from the production and buffer rows.

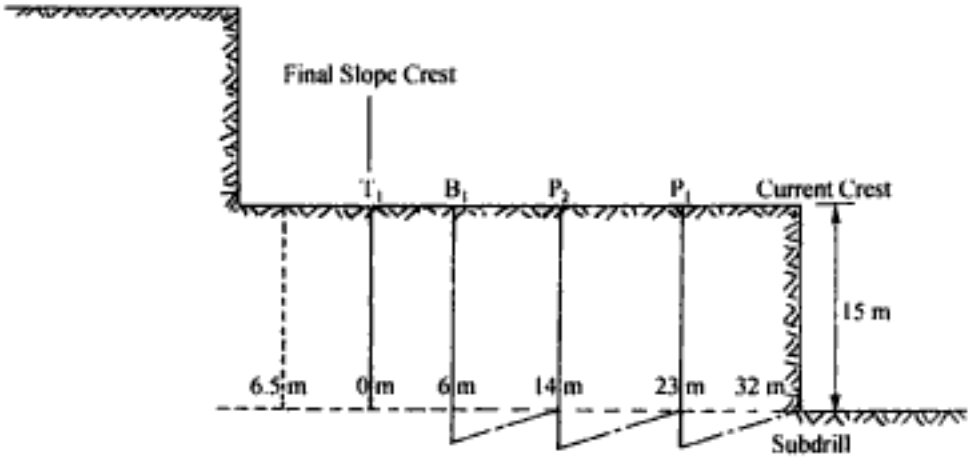

Figure 10.32. Modified blast design.

The best basis for a design change would be to know how much the rock was damaged by the previous blasting. The new value of K_B would be used to calculate values for B and S. Today such information is lacking and one resorts to a guided cut-and-try approach. From a practical viewpoint one would like to change the pattern so that there would be only one row of buffer holes and one row of trim holes.

Assume that the appropriate adjusted value is $K_B = 35$ for a loading density of 34 kg/m. This means that the powder factor is about cut in half.

$$B = 35\ (0.230) = 8\ \text{m}$$
$$S = 8\ \text{m}$$

The new row of buffer holes is shown in Figure 10.32. It now lies 6 m from the desired pit limit. The damage zone from Figure 10.28 is 14 m and it extends outside of that produced by the production blasting. To protect the remaining rock the charge/m must be reduced. The required value of r_o

$$r_o = 6\ \text{m} + 6.5\ \text{m} = 12.5\ \text{m}$$

Using Figure 10.28, a maximum charge concentration of about 26 kg/m is found which now affects the choice of the burden. A burden of 7 m, a spacing of 9 m and a charge density of 30 kg/m is about in balance. Thus the pattern would be staggered with respect to the production blast (such as is shown in Figure 10.33) to give a better distribution of the explosive. The portion remaining to be blasted has a width of 7 m. As can be seen, this falls zone falls completely within the damage zone produced by the buffer holes and a portion was affected by the production row as well. Therefore two rows of trim holes, the first row with a 4 m burden and the second with a 3 m burden would be used. The spacing would be at 4.5 m to conform to the regular pattern (Fig. 10.34).

Obviously there is considerable flexibility in the design. The damage produced by overlapping fragmentation patterns combined with the natural jointing and the digging ability of the loader may require only a single row of trim holes. The basic principle of maintaining a damage zone within that produced by the trim holes remains. The techniques for creating the reduced charge/various charge concentrations were discussed in Section 10.2.

Damage to the crest of the bench below due to the subdrilling is important to consider. As the burden is reduced the amount of subdrill due to the geometry effect is reduced naturally. For the trim holes no subdrill should be used. The burden should be reduced and all of the previous rock removed (no buffer rock) so that the gasses can push the rock without extending cracks into the desired final wall. The subdrilling from both the last row of the production holes and the buffer row should be kept away from the crest of the underlying bench. The trial design based upon use of the principles is shown in Figure 10.35.

As indicated, the curves given in Figure 10.28 are for the special case

$$V\,(\text{m/sec}) = 0.70\left(\frac{W^{0.7}}{R^{1.5}}\right) \tag{10.23}$$

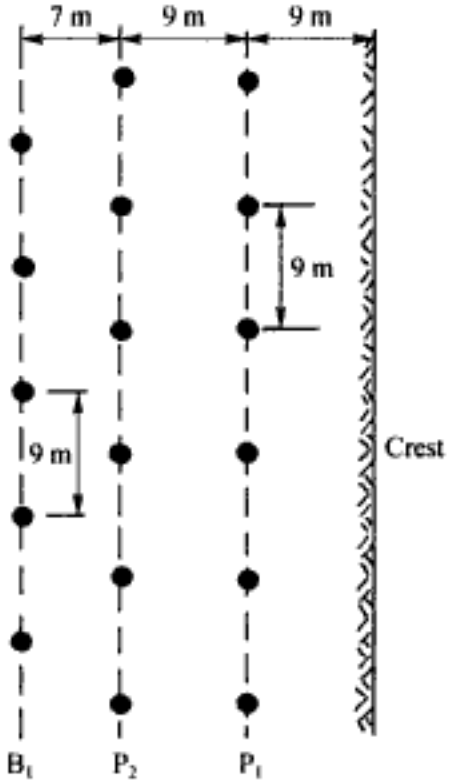

Figure 10.33. Plan view of the production and buffer rows.

Hidden page

$$V\,(\text{m/sec}) = 0.81\left(\frac{R}{W^{1/2}}\right)^{-1.51} \tag{10.24a}$$

where R = distance (m), W = charge weight (kg), or

$$V\,(\text{in/sec}) = 31.9\left(\frac{R}{W^{1/2}}\right)^{-1.51} \tag{10.24b}$$

where R = distance (ft), W = charge weight (lbs).

As can be seen, Equation (10.24a) is somewhat different from that used by Holmberg & Persson (1978) in the development of their curves. In comparing it to Equation 10.23 it is seen that now

$$K = 0.81$$

$$\beta = 1.51$$

$$\alpha = \beta/2 = 0.755$$

For this special case ($\alpha = \beta/2$), the particle velocity can be calculated using Equation (10.19b)

$$V = K\left\{\frac{q}{r_o}\left[\tan^{-1}\left(\frac{H+J-z_o}{r_o}\right) - \tan^{-1}\left(\frac{T-z_o}{r_o}\right)\right]\right\}^{\alpha}$$

To demonstrate the calculation, a rather typical bench geometry will be used (Fig. 10.36). Let

$$F = \left\{\tan^{-1}\left(\frac{H+J-z_o}{r_o}\right) - \tan^{-1}\left(\frac{T-z_o}{r_o}\right)\right\} \tag{10.25}$$

Substituting the values for H, J and T from Figure 10.36 into Equation (10.25) yields

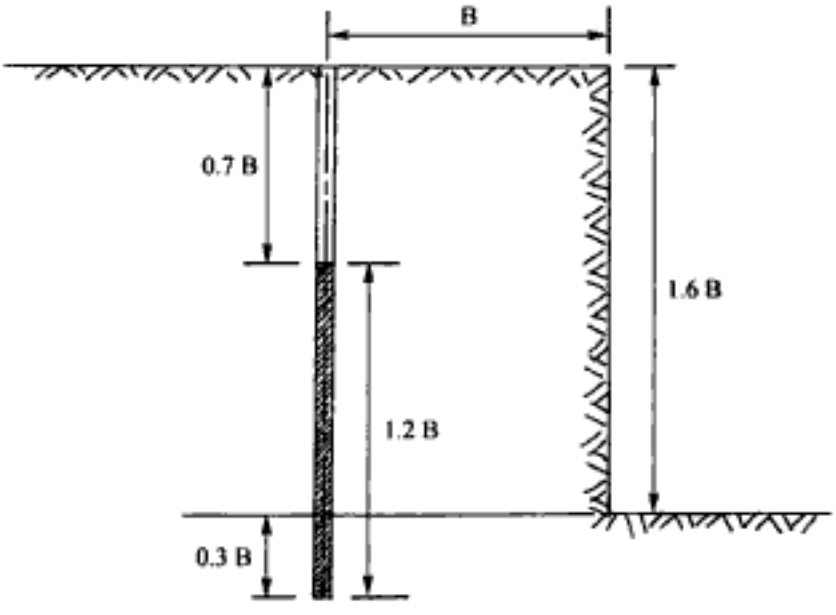

Figure 10.36. Bench geometry used in the development of iso-velocity lines.

$$F = \left\{ \tan^{-1}\left(\frac{1.6B + 0.3B - z_o}{r_o} \right) - \tan^{-1}\left(\frac{0.7B - z_o}{r_o} \right) \right\} \tag{10.26}$$

When the values for z_o and r_o are expressed in terms of burden B, the factor F (Equation 10.26) can be tabulated for easy general application. For the case when

$$r_o = 0.5B$$

$$z_o = 0.0B$$

then

$$F = \tan^{-1}\left(\frac{1.6B + 0.3B - 0.0B}{0.5B} \right) - \tan^{-1}\left(\frac{0.7B - 0.0B}{0.5B} \right)$$

$$= \tan^{-1}\left(\frac{1.9B}{0.5B} \right) - \tan^{-1}\left(\frac{0.7B}{0.5B} \right) = 75.26° - 54.46° = 20.8°$$

The value of F must be expressed in *radians* rather than degrees hence

$$F = 20.8°\left(\frac{\pi}{180} \right) = 0.363 \text{ radians}$$

Thus for the point

$$(0.5B, 0.0B)$$

the value for F is

$$F = 0.363 \text{ radians}$$

Geometrically the angles involved are shown as in Figure 10.37. The matrix of (r_o, z_o) points used for this example are shown in Figure 10.38 and the corresponding F values for these locations are given in Table 10.7.

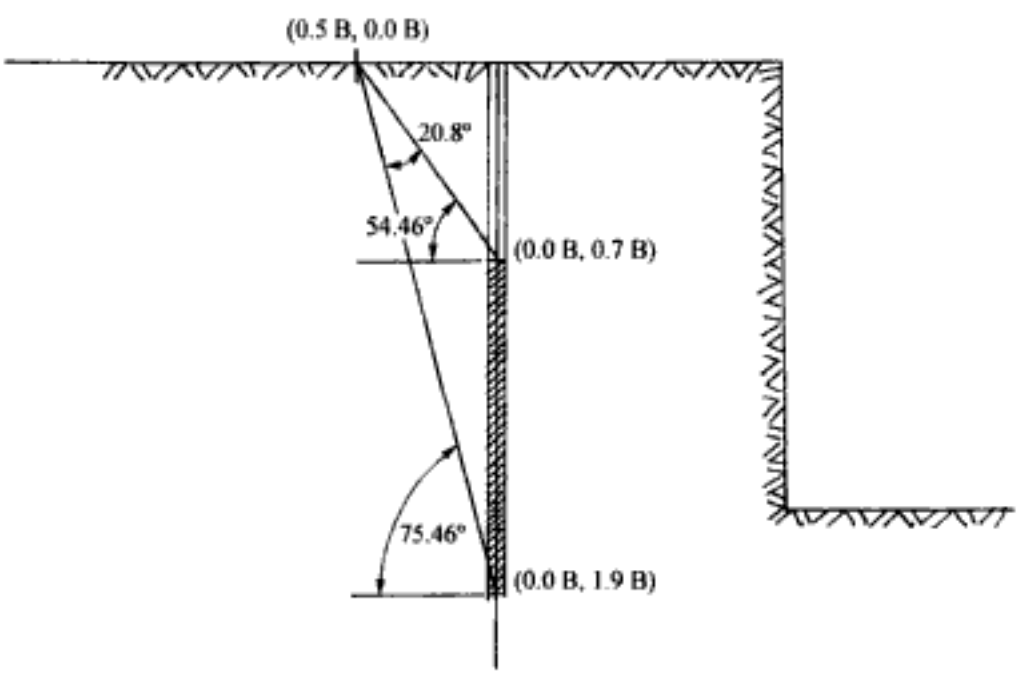

Figure 10.37. Drawing for the sample calculation.

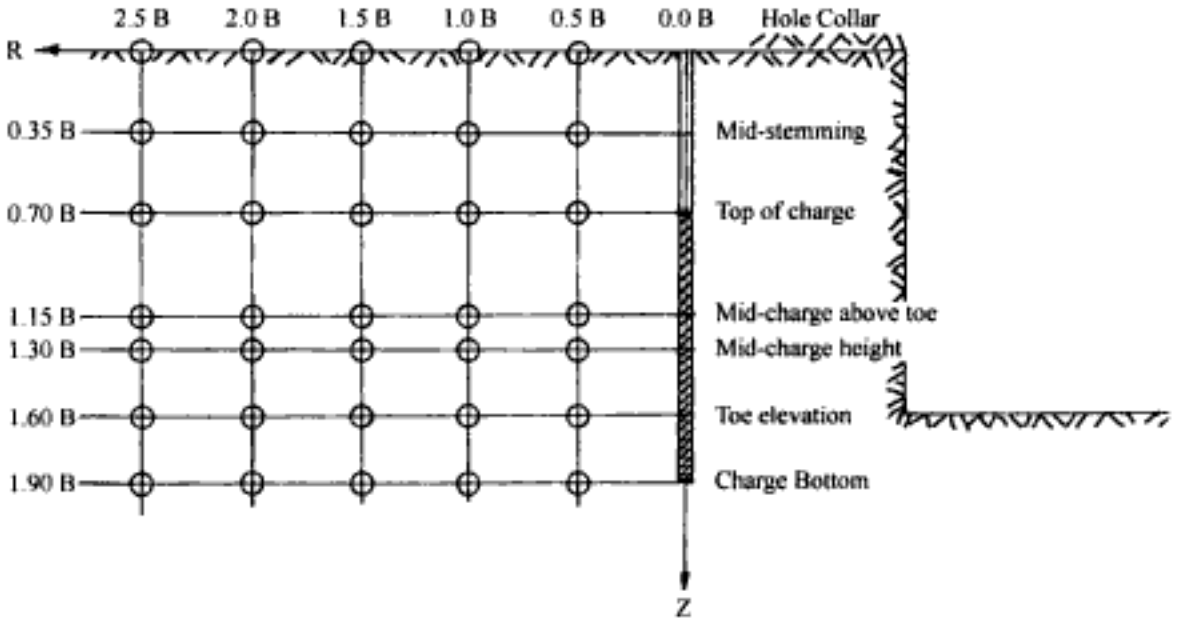

Figure 10.38. Matrix of calculation points.

Table 10.7. Values of the factor F (Expressed in Radians) for the Sample Bench Geometry.

z_o	r_o 0.5B	1.0B	1.5B	2.0B	2.5B
0	0.363	0.476	0.466	0.42	0.377
0.35B	0.648	0.661	0.573	0.486	0.416
0.70B	1.176	0.876	0.675	0.540	0.448
1.15B	1.716	1.066	0.755	0.580	0.470
1.30B	1.752	1.081	0.761	0.583	0.471
1.6B	1.604	1.024	0.74	0.572	0.465
1.9B	1.176	0.876	0.675	0.540	0.448

To continue the example it will be assumed that the hole diameter is 270 mm (10-5/8″) and ANFO is the explosive (ρ = 800 kg/m^3). Using the Ash formulas (K_B = 25), the burden is

$$B = 25\,(0.270) \cong 7\text{ m}$$

and the charge density q is

$$q\,(\text{kg/m}) = \frac{\pi}{4}(0.270)^2(800) = 45.8\,\text{kg/m}$$

The velocity at point (0.5B, 0.0B) is

$$V = 0.81\left[\frac{45.8}{0.5(7)} \times 0.363\right]^{0.755} = 2.63\,\text{m/sec}$$

In a corresponding way, the velocities corresponding to the other points in the matrix can be calculated. The results are given in Table 10.8. These can now be plotted such as shown in Figure 10.39 and the iso velocity contours added. At the free surface (z_o = 0),

Table 10.8. Particle velocities (mm/sec) at the different matrix locations.

z_o	r_o 0.5B	1.0B	1.5B	2.0B	2.5B
0	2630	1910	1384	1030	802
0.35B	4068	2447	1618	1150	864
0.70B	6380	3027	1830	1245	913
1.15B	8486	3510	1992	1314	947
1.30B	8621	3548	2004	1319	949
1.60B	8065	3405	1962	1300	939
1.90B	6380	3027	1830	1245	913

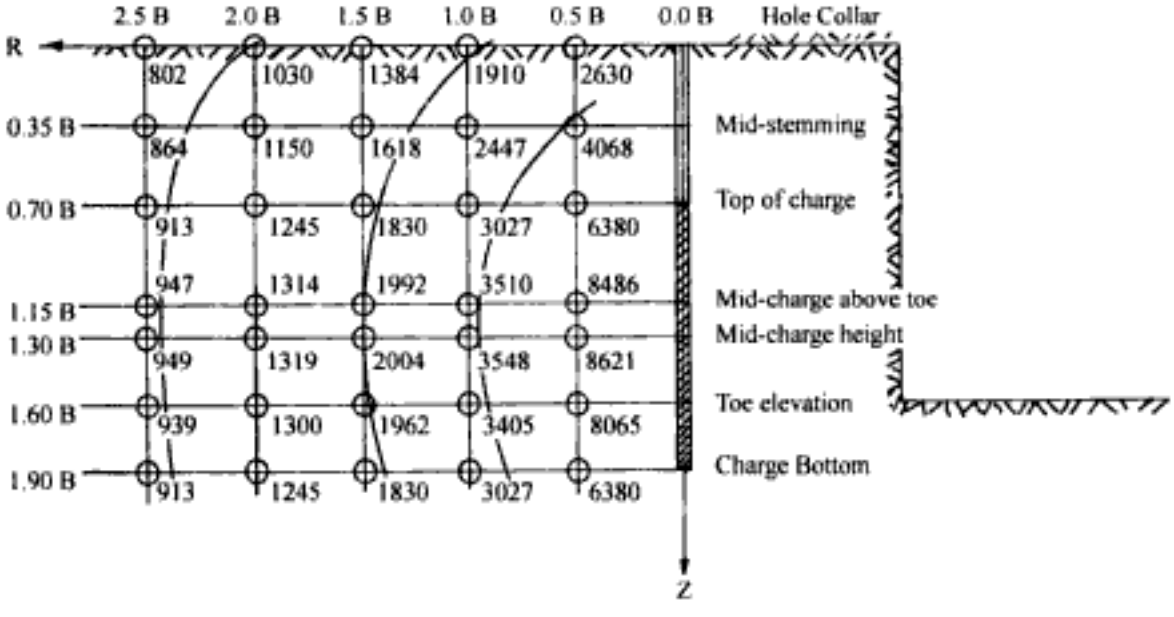

Figure 10.39. Contour plot of the particle velocities.

the damaging particle velocity will be expected to be less than deeper in the rock mass where the rock is confined. If one uses a limiting criterion of 1000 mm/sec then damage to a distance of 2 B behind the blast would be observed. In this case it would be

$$\text{Damage Zone} = 2 \times 7 \text{ m} = 14 \text{ m}$$

Figure 10.40 is a plot of the particle velocity at the elevation of the top of the charge and at the charge mid-height as a function of the distance (R) from the charge. This should be compared to Figure 10.27 of Holmberg & Persson (1978). Their curve is for $z_o = T$ which is located directly at the top of the charge.

This type of simulation has been performed for a number of different charge configurations, and the distance of $2B$ to $2.5B$ for the extent of damage (using the 1000 mm/sec criterion) seems to be relatively constant. Thus as a rough rule of thumb, the production blasts should be stopped at $3B$ from the final profile. Inside this zone, careful blasting should be planned.

Since the Holmberg-Persson approach is so widely used today, it is considered worthwhile, prior to continuing, to provide some additional background regarding its develop-

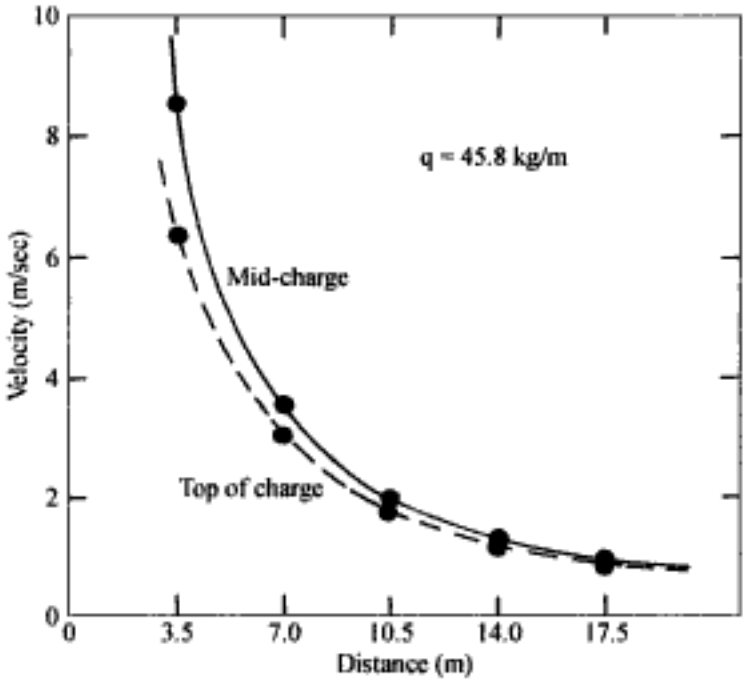

Figure 10.40. Variation of the peak particle velocity with distance for mid-charge and top-of-charge elevations.

ment. As indicated earlier, the basic equation relating the peak particle velocity to the charge weight (W) and the distance (R) from the measurement point to the charge is

$$V = K\frac{W^{\alpha}}{R^{\beta}}$$

where α, β, K = site specific constants, W = charge weight (kg), R = distance (m), V = peak particle velocity (mm/sec).

As a first approximation for application, Holmberg-Persson have suggested the use of

$K = 700$

$\alpha = 0.7$

$\beta = 1.5$

The basis for this selection of values is the extensive suite of field measurements conducted by the USBM over the years and reported in Bulletin 656 *Blasting Vibrations and Their Effects on Structures* by Nicholls et al. (1971). In their study a total of 171 blasts were recorded at 26 sites. The blast size ranged from 70 to 180,550 lbs explosive and the charge per delay ranged from 25 to 19,625 lbs. The rock types included

- Limestone
- Dolomite
- Diorite
- Diabase
- Basalt
- Sericite
- Schist
- Trap Rock
- Granite

– Gneiss
– Sandstone.

The hole diameters ranged from 3″ to 9″, the bench heights from low to 215 ft, charge lengths from 10 ft to 200 ft, and measuring distances from some 10's of feet up to several thousand feet. The explosives used were those normally used at the quarries. Thus explosive type varied both within and among quarries and could not be controlled. The blasts included both millisecond delayed and instantaneous. The method of initiation varied. For the different blasts and sites the Bureau measured the peak particle velocity using velocity gages. Normally three gages were mounted at each measuring point and oriented to register the radial, vertical and transverse particle velocities. For each of the blasts the Bureau plotted the peak particle velocity versus distance but eventually decided to use a scaled distance. The reasoning behind this is described below (Nicholls et al. 1971).

'The method of scaling distance by the square root of the charge weight per delay as determined empirically is a satisfactory procedure for removing the effect of charge weight on the amplitude of peak particle velocity. Other investigators have suggested that cube root scaling be used, because it can be supported by dimensional analysis. Cube root scaling can be derived from dimensional analysis if a spherical charge is assumed or if a cylindrical charge is assumed whose height changes in a specified manner with a change in radius. Taking the case of a sphere, a change in radius results in a volume increase proportional to the change in radius cubed. Weight is usually substituted for volume. The relationships result in cube root scaling. Blasting, as generally conducted, does not provide a scaled experiment. Charges are usually cylindrical. The height of the face or depth of lift are usually fixed. Therefore, the charge length is constant. Charge size is varied by changing hole diameter or the number of holes. The fixed length of the charge presents problems in dimensional analysis and prevents a complete solution. However, a change in radius, while holding the length constant results in a volume increase proportional to the radius squared. This indicates that the scaling should be done by the square root of the volume or weight as customarily used. It is the geometry involved, cylindrical charges, and the manner in which charge size is changed, by changing the diameter or number of holes which results in square root scaling being more applicable than cube root scaling to most blasting operations. The Bureau data, if analyzed using cube root scaling, does not show a reduction in the spread of the data which would occur if cube root scaling were more appropriate. In summary, the empirical results and a consideration of the geometry including the procedure used to change charge size, and dimensional analysis indicate that data of the type from most blasting should be scaled by the square root of the charge weight per delay.'

In the appendices to Bulletin 656 the Bureau has included

– Drawings of the field test geometry,
– Shot and loading data,
– The field results including scaled distance and peak particle velocity in the radial, vertical and transverse directions for each test site and each blast.

Hence it is possible for the interested reader to reanalyze the data as desired. It is important to note that in these tests

– The peak particle velocity is the maximum value regardless of where it occurred during the recording.

– The shot-to-gage distance was determined by measuring the distance from each gage to the center of the blasthole having the maximum charge weight per delay.

– The scaled distance is the distance from the blast-to-gage divided by the square root of the maximum charge weight per delay. For instantaneous blasts the total charge weight was used.

Lundberg et al. (1978) used the USBM data base in developing the constants used in their propagation equation. They read 1363 values of the peak vertical particle velocity together with the associated charge weights and distances into a computer program and calculated the best fit line. A plot of the results together with the superimposed line is shown in Figure 10.41. The resulting equation is

$$V = 730\left(\frac{R}{W^{0.43}}\right)^{-1.54} \tag{10.27}$$

and the values for K, α, and β become

$$K = 730$$

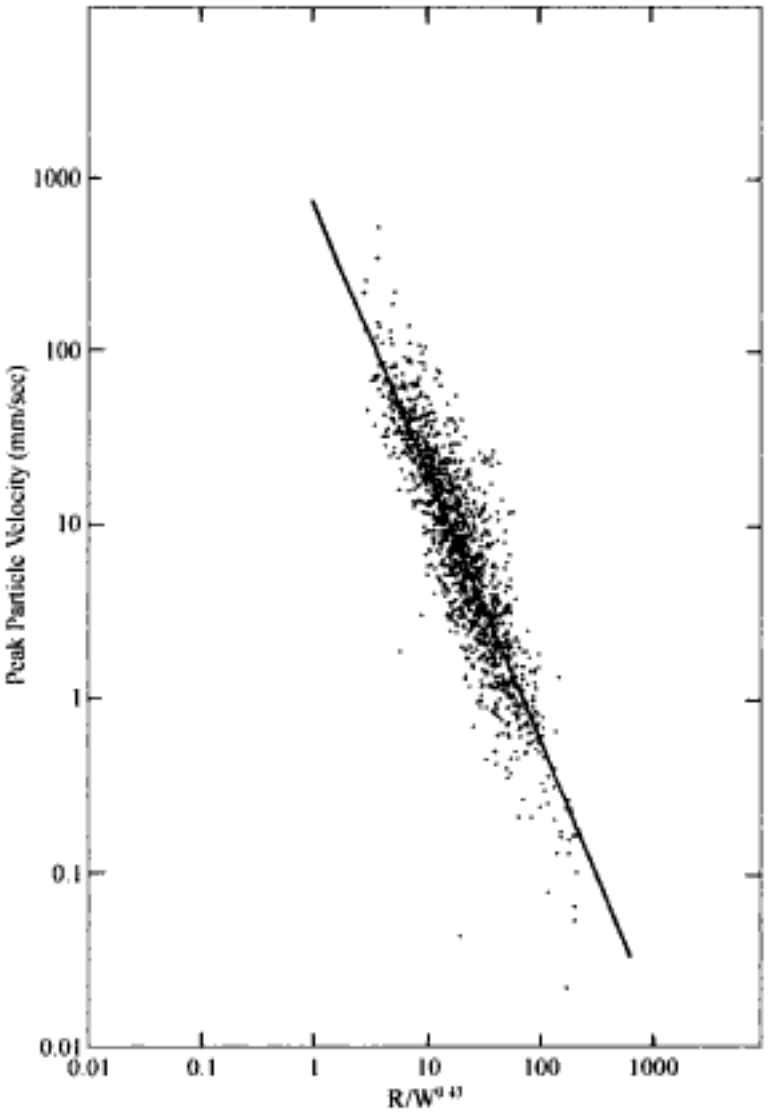

Figure 10.41. The vertical peak particle velocity as a function of $R/W^{0.43}$ based on the USBM data (Lundborg et al., 1978).

$\alpha = 1.54$

$\beta = 0.66$

The value of V calculated in this way is expressed in mm/sec. From this equation as developed from the USBM data it is natural to simplify the constants to

$K = 700$

$\alpha = 1.5$

$\beta = 0.7$

as used in the Holmberg-Persson approach. It is not square-root scaling but rather $W^{0.43}$. Lundborg et al. (1978) also fit the experimental data using square-root scaling. In this case the equation becomes

$$V = 323\left(\frac{R}{W^{0.50}}\right)^{-1.45} \tag{10.28}$$

The corresponding values for K, α and β become

$K = 323$

$\alpha = 1.45$

$\beta = 0.725$

As was noted earlier, a major simplification occurs in the evaluation of the Holmberg-Persson equations if

$\alpha = 2\beta$

Such is the case here. However as can be seen here, one must be careful when making such simplifications since the value of K is markedly affected. In any case, the commonly cited values for K, α and β are derived from a large data set of vertical particle velocity measurements. Individual curves (and the corresponding values of K, α and β) for a given site, rock type and blasting design can vary markedly from the 'best-fit' curve derived in this way. The reader is advised to go back and refer to the conditions under which the total data set was developed and possibly even go back to the original USBM data.

To use the design curves one must know the values of PPV corresponding to various levels of damage in the rock mass. Field experiments were conducted at the Aitik mine in Northern Sweden to obtain such values (Holmberg & Krauland (1977), Holmberg & Persson (1978), Persson et al. (1977), Holmberg (1983), Holmberg (1997)). These tests and the results obtained will now be briefly reviewed. The rock mass in which the tests were conducted is represented by biotite gneiss and sericite schist. It has a wave velocity of approximately 4000 m/sec. The main mineralization of economic interest is disseminated chalcopyrite. Gold and silver (0.3 and 4 g/ton respectively) are extracted from the copper concentrate. Figure 10.42 is a plan view showing the portion of the bench (Production Blast 213) which served as the site for the first test. In this blast a total of 96-251 mm (9-7/8″) diameter production holes were shot according to the delay sequence shown. There were 14 different delays used with the time interval between each group of delayed holes being 100 ms. The specification for the drilling and charging plan is as follows:

bench height = 13-14 m
hole depth = 16 m
spacing = 10 m

Hidden page

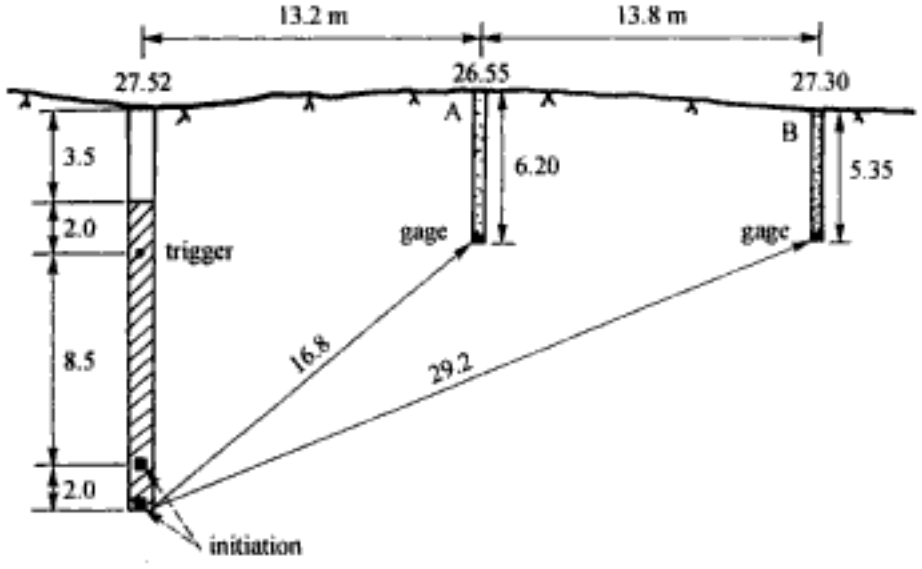

Figure 10.43. Section showing the position of the nearest production hole and the gage holes (Holmberg & Krauland, 1977).

the vertical peak particle velocity was the largest of the three components. The peak velocities and accelerations as measured were:

Quantity	Hole A	Hole B
Distance (m)	13.2	27.0
Acceleration (g)	1020	37
Velocity (mm/sec)	1520	693

The dashed lines labelled as 1, 2 and 3 in Figure 10.42 represent core holes diamond drilled before the production blast. The respective collars are denoted by the circles. Hole 1 (105 m long) and Hole 2 (90 m long) were drilled sub-horizontally through the round and approximately 50 m into undisturbed rock. The collars of Holes 1 and 2 were separated by about 50 m along the bench front and were 1 m up from the bench floor. These holes were oriented at right angles to the dominant joint systems. Both holes were surveyed using an Eastman Whipstock camera. Hole 3 was drilled from the upper surface and about 30 m behind the last production row at a dip of 50°. This angle was chosen so that the hole would cut the foliation direction at about right angles and yield information regarding damage at the same level as the production hole bottom. Due to hole caving problems it could not be surveyed. After the blast, three holes (4, 5 and 6) were diamond drilled parallel to and within 1 m of the respective holes 1, 2 and 3 drilled prior to blasting. They were then surveyed. All of the holes except Hole 5 were drilled so that a core 32 mm in diameter was obtained. For Hole 5 the core diameter was 42 mm. All cores were logged with respect to rock type and crack frequency. The logs revealed that there were two different rock types traversed

- pegmatite
- gneiss in all transition forms

After logging of the diamond drilled holes, an analysis was performed to determine how far behind the last production row newly created cracks were found to exist. Because of

- the large natural variation in the number of cracks over a shorter distance
- the effect of core hole deviation on core fracturing
- the presence of two different rock types

it was decided to evaluate the change in crack frequency before and after blasting based on logging intervals of 5 m. The number (N1) of core segments having lengths less than 0.1 m, the number (N2) with lengths greater than 0.1 m, and the total number of core pieces were tabulated as shown in Table 10.9 for the cores from Holes 1 and 4.

The cores from Holes 3 and 6 before and after blasting unfortunately showed so large variations that it was impossible to determine if any change in crack frequency occurred during blasting. Holes 2 and 5 could not be used since they were drilled with different hole diameters. An attempt was made to vary the standard length based upon the core diameter but that was not successful. Therefore the damage evaluation was done based upon the results of Holes 1 and 4. Figure 10.44 is a diagrammatic representation of the expected result. The bottom end of Hole 1 drilled prior to the production blast provides the 'undisturbed' baseline to which the core from Hole 4 is compared. In examining the results in Table 10.9, it is seen that the fracturing is higher in Hole 4 up through the interval 15-20 m. For succeeding intervals, the fracture frequency is basically the same. If one assumes that no new fracturing has occurred deeper than 20 m along Hole 4, than due to the fact that Holes 1 and 4 were drilled at 45° to the bench face this means that the new fracturing terminated at a distance of

$$\text{damage zone} = \frac{20}{\sqrt{2}} = 14 \text{ m}$$

Holmberg & Krauland (1977) using a semi-statistical approach indicate that

Table 10.9. The results of the RQD determinations for holes 1 and 4. After Holmberg and Krauland (1977).

Hole No.	Interval (m)	No. of pieces N1	N2	Average N	RQD length (m)	
1	0.0 → 5.0	11	15	26	0.19	0.84
4		34	13	47	0.11	0.47
1	5.0 → 10.0	17	19	36	0.14	0.82
4		45	15	60	0.08	0.57
1	10.0 → 15.0	25	20	45	0.11	0.73
4		39	18	57	0.09	0.56
1	15.0 → 20.0	30	16	46	0.11	0.68
4		63	7	70	0.07	0.29
1	20.0 → 25.0	49	10	59	0.08	0.35
4		38	14	52	0.10	0.54
1	25.0 → 30.0	38	12	50	0.10	0.57
4		27	18	45	0.11	0.65
1	30.0 → 35.0	22	16	38	0.13	0.68
4		26	17	43	0.12	0.64
1	35.0 → 40.0	28	17	45	0.11	0.65
4		30	16	46	0.11	0.61
1	40.0 → 45.0	9	14	23	0.22	0.82
4		15	17	32	0.16	0.76
1	45.0 → 50.0	12	17	29	0.17	0.82
4		17	17	34	0.15	0.74

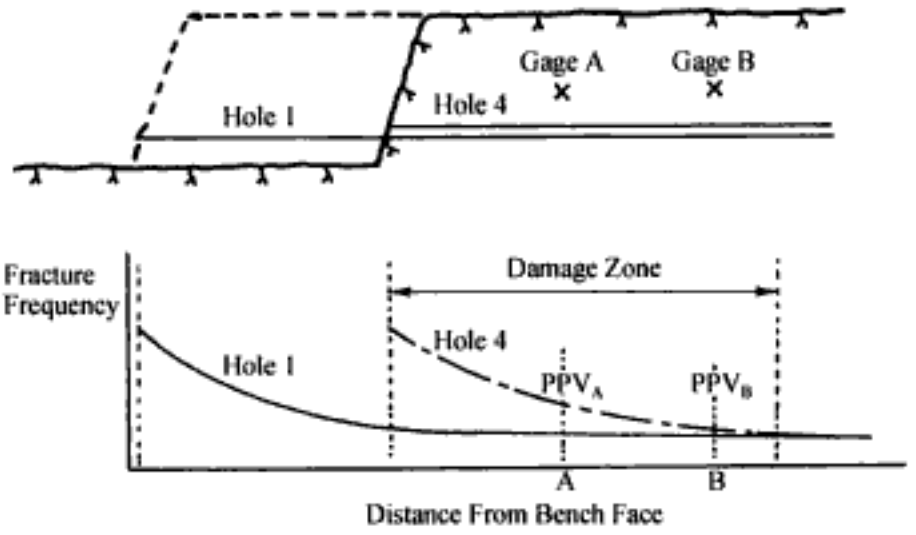

Figure 10.44. A theoretical taken section along the direction of Hole 1 showing the expected fracture frequency prior to the blasting (Hole 1) and after blasting (Hole 4) (Holmberg & Krauland, 1977).

'With a probability of 90%, the zone of new fracturing terminates within an interval of 18.6 to 44.9 m from the blast along the hole length. Since the diamond hole is drilled at 45° to the bench face, this means that with 90% probability new fracturing terminates within the interval 13.2 to 31.9 m behind the last row of holes. At a distance of 22.6 m behind the round there is a 50% probability that new fracturing has occurred. There is a 5% probability that the new fractures extend further back than 31.9 m.'

This interpretation of the extent of new 'fracturing' is, as will be shown shortly, extremely important when applying the design curves to field applications. Holmberg & Persson (1978) constructed the peak particle velocity versus distance curve for the test situation shown in Figure 10.45 assuming

$q = 75$ kg/m
$K = 700$
$\alpha = 1.5$
$\beta = 0.7$

The measured peak vertical particle velocities and distances

Distance-R (m)	PPV (mm/sec)
13.2	1520
27.0	693

have been superimposed together with a measurement made during an earlier test. As can be seen the results are well described by the curve.

In conjunction with a perimeter blasting round a second set of PPV versus distance measurements were made. The test geometry is shown in Figure 10.46. In this case the hole diameter was 171 mm (6-3/4 ins) and the explosive used was Reolit 10 which is somewhat weaker than Reolit A6. The properties are

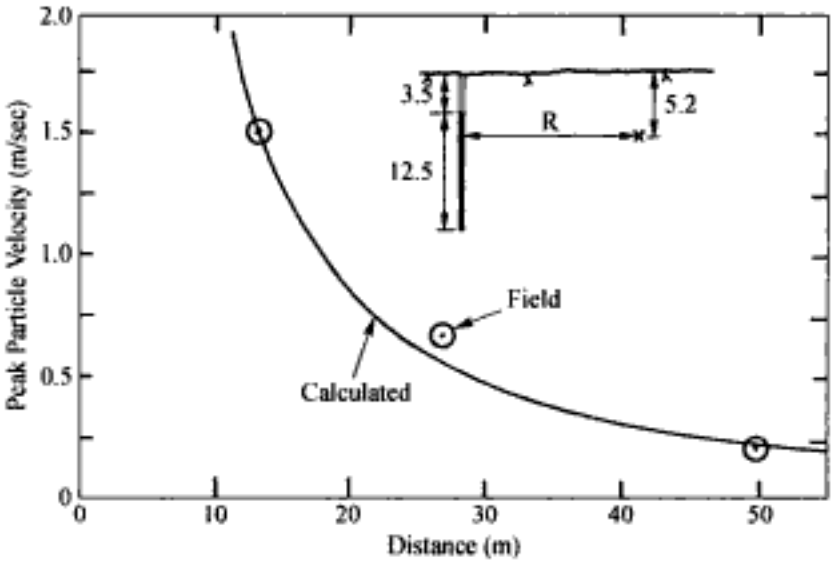

Figure 10.45. The calculated and the experimental values of peak particle velocity versus distance for the 250 mm charge (Holmberg & Persson, 1978).

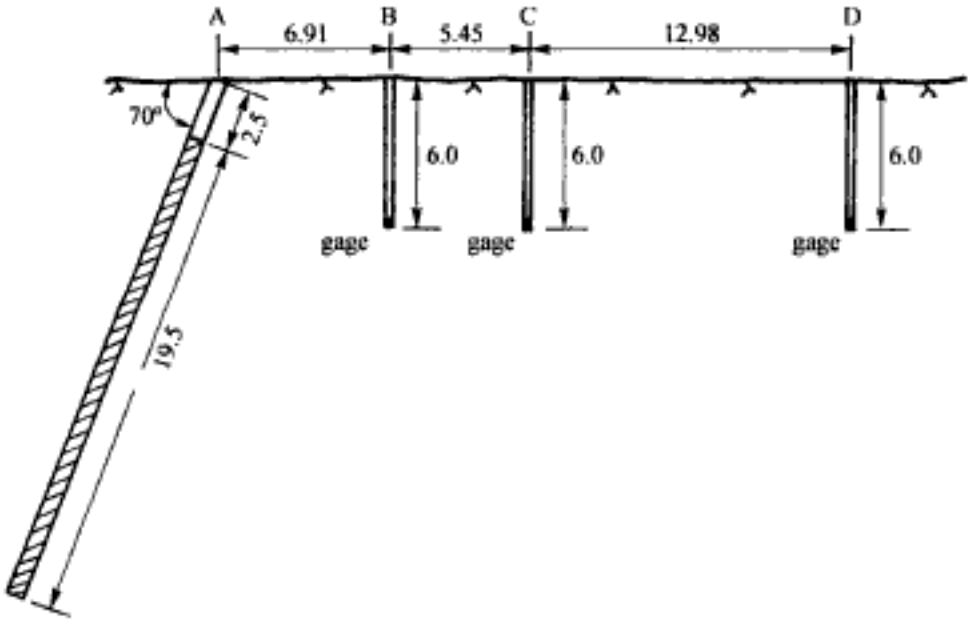

Figure 10.46. The test geometry for the blast using the 170 mm diameter hole (Holmberg & Persson, 1978).

type = aluminized TNT-based watergel
q = 34 kg/m
detonation velocity = 5000 m/sec (ideal)
density = 1.5 g/cm^3
weight strength = 57% (wrt blasting gelatin)

Only measurements of the vertical component were made in the three holes using accelerometers. The following dimensions apply:

Hole pair	Collar distance (m) (horizontal)	Gage-explosive distance (m) (at 90° to charge axis)
A-B	6.91	8.5
A-C	12.35	13.9
A-D	25.33	26.9

The maximum measured accelerations and derived vertical peak particle velocities at the different gage locations are

Quantity	Hole B	Hole C	Hole D
Distance (m)	8.5	13.9	26.9
Acceleration (g)	1031	303	29
PPV (mm/sec)	1442	562	283

The calculated and the experimental values for the PPV as a function of the distance have been plotted in Figure 10.47. Again as can be seen the agreement is good. No diamond drilling was done before and after blasting as in the previous test.

In Figure 10.48 the damage zone of 22.5 m as suggested by Holmberg & Persson (1978) has been added to the PPV versus distance curve for the 251 mm diameter fully charged hole. The intersection on the PPV axis occurs at about 700 mm/sec. If one would have used the 14 m distance instead (as suggested by the direct observations) as opposed to the statistical approach, then one would establish a damage criteria of about 1.4 m/sec. Assuming that the 14 m damage zone is representative one can see from Figure 10.42 that the inclined holes 3 and 6 actually lie, for the most part, in the zone of undisturbed rock. Hence the observation of no obvious difference in fracturing before and after blasting is logical. From the Aitik test conducted with the 251 mm diameter holes Holmberg & Krauland (1977) conclude that 'possibly with the exception of the near vicinity (within about 2 m) of the charge the increase in the number of

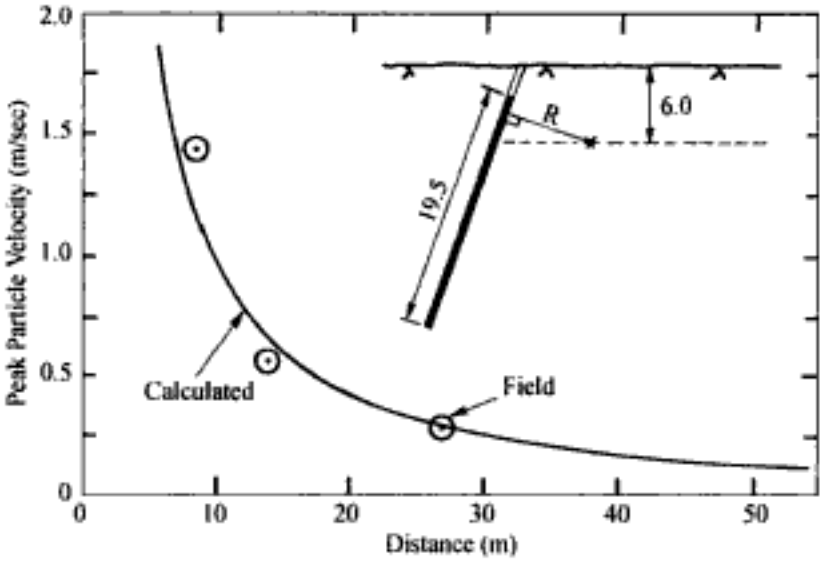

Figure 10.47. The calculated and the experimental values of peak particle velocity versus distance for the 170 mm charge (Holmberg & Persson, 1978).

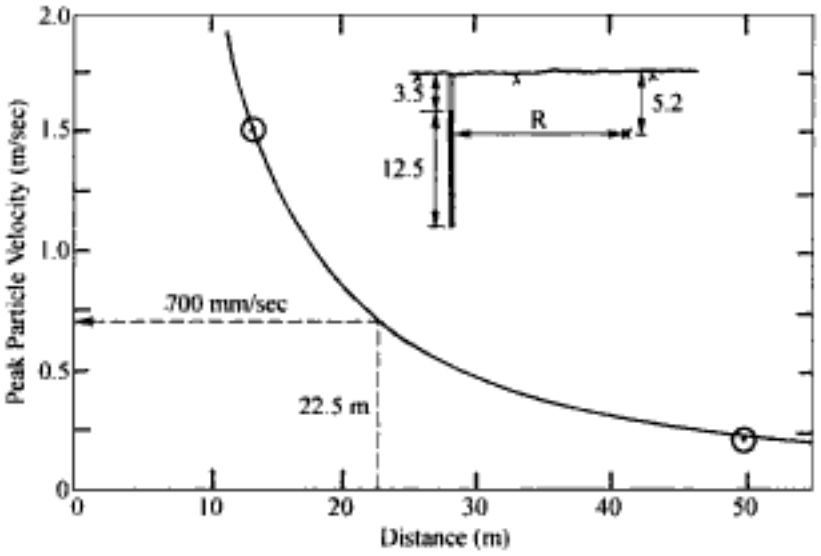

Figure 10.48. The experimental zone of disturbance superimposed on the theoretical curve for the 250 mm diameter hole.

cracks as a result of blasting is relatively little. The number of cracks increases by a factor of two from 4 to 8 cracks per meter up to 8 to 16 cracks per meter.' In conclusion, it should be recalled that this critical limit, whether 700 m/sec or 1400 mm/sec, corresponds to that point where an increase in cracking begins to occur in the rock mass. The actual limits to be imposed will depend upon both the application and the design.

Instead of standard procedure of calculating the velocity at a particular point (r_o, z_o) and then comparing this value with the critical velocity to see whether the point lies inside or outside of the damage zone, one can manipulate Equation (10.22b)

$$V = K\left\{\frac{q}{r_o}\left[\tan^{-1}\left(\frac{H+J-z_o}{r_o}\right)-\tan^{-1}\left(\frac{T-z_o}{r_o}\right)\right]\right\}^{\alpha}$$

so that the distance r_c corresponding to the critical particle velocity (V_c) can be determined directly. The procedure has been demonstrated by Ouchterlony et al. (1993) in analyzing the data from the Äspö site. In terms of the quantities shown in Figure 10.49 the charge length (L) may be expressed as

$$L = H + J - T \tag{10.29}$$

which can be rearranged to yield

$$H + J = L + T \tag{10.30}$$

Assuming that the elevation of the observation point (z_o) is located at the charge midheight then

$$z_o = T + L/2 \tag{10.31}$$

Using Equations (10.30) and (10.31), Equation (10.22b) may be written as

$$V = K\left\{\frac{q}{r_o}\left[\tan^{-1}\left(\frac{L}{2r_o}\right)-\tan^{-1}\left(\frac{-L}{2r_o}\right)\right]\right\}^{\alpha} \tag{10.32}$$

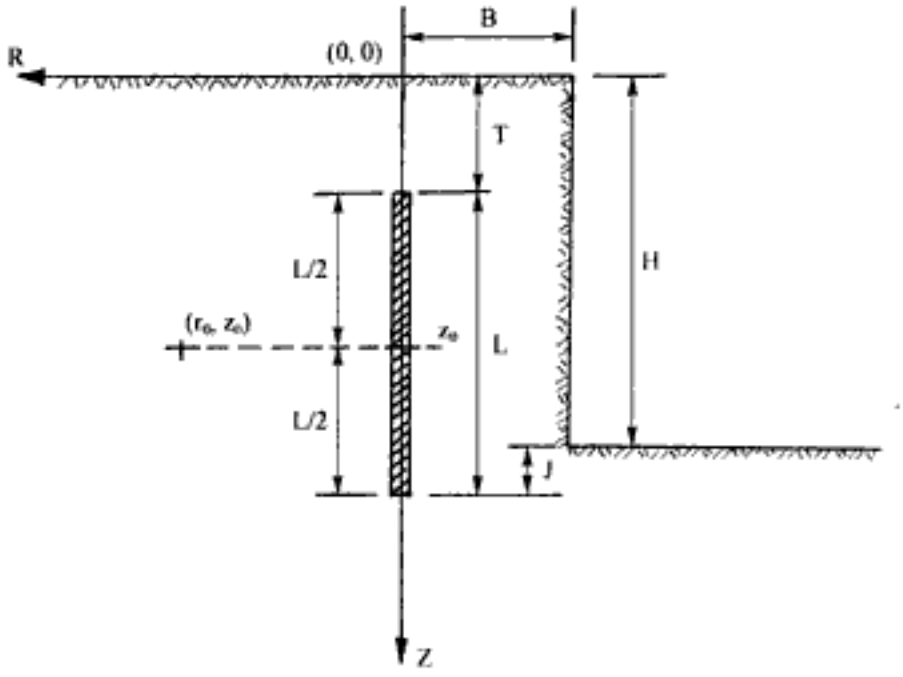

Figure 10.49. The geometry used in the analysis of (Ouchterlony et al., 1993).

Since

$$\tan^{-1}\left(\frac{-L}{2r_o}\right) = -\tan^{-1}\left(\frac{L}{2r_o}\right)$$

Equation (10.32) may be written as

$$V = K\{\frac{2q}{r_o}[\tan^{-1}(\frac{L}{2r_o})]\}^{\alpha} \tag{10.33}$$

But since

$$q = \frac{W}{L}$$

Equation (10.33) becomes

$$V = K\{\frac{2W}{Lr_o}[\tan^{-1}(\frac{L}{2r_o})]\}^{\alpha} \tag{10.34}$$

or

$$V = K\{\frac{W}{r_o^{\,2}(\frac{L}{2r_o})}[\tan^{-1}(\frac{L}{2r_o})]\}^{\alpha} \tag{10.35}$$

Equation (10.35) may be rewritten as

$$V = K(\frac{W}{r_o^{\,2}})^{\alpha}\{\frac{\tan^{-1}(\frac{L}{2r_o})}{\frac{L}{2r_o}}\}^{\alpha} \tag{10.36}$$

Letting

$$f = \frac{\tan^{-1}\left(\frac{L}{2r_o}\right)}{\frac{L}{2r_o}} \tag{10.37}$$

Equation (10.36) becomes

$$V = K\left(\frac{W}{r_o^2}\right)^{\alpha} f^{\alpha} = \frac{K}{r_o^{2\alpha}}(fW)^{\alpha} = K\left[\frac{r_o}{\sqrt{Wf}}\right]^{-\beta} \tag{10.38}$$

Rearranging Equation (10.38) one finds that

$$\frac{V}{K} = \left(\frac{r_o}{\sqrt{Wf}}\right)^{-\beta} = \left(\frac{\sqrt{Wf}}{r_o}\right)^{\beta} \tag{10.39}$$

or

$$\frac{\sqrt{Wf}}{r_o} = \left(\frac{V}{K}\right)^{1/\beta} \tag{10.40}$$

Equation (10.40) can be rewritten as

$$\sqrt{f} = \frac{r_o}{\sqrt{W}}\left(\frac{V}{K}\right)^{1/\beta} \tag{10.41}$$

Dividing the numerator and the denominator of the right hand side of Equation (10.41) by the charge length L one arrives at the equation developed by Ouchterlony et al. (1993).

$$\sqrt{f} = \left(\frac{r_o}{L}\right)\left(\frac{L}{\sqrt{W}}\right)\left(\frac{V}{K}\right)^{1/\beta} \tag{10.42}$$

Remembering that

$$f = \frac{\tan^{-1}\left(\frac{L}{2r_o}\right)}{\frac{L}{2r_o}}$$

then Equation (10.42) may be written as

$$\sqrt{\frac{\tan^{-1}\left(\frac{L}{2r_o}\right)}{\frac{L}{2r_o}}} = \left(\frac{r_o}{L}\right)\left(\frac{L}{\sqrt{W}}\right)\left(\frac{V}{K}\right)^{1/\beta} \tag{10.43}$$

It is seen that the desired quantity r_o appears on both sides of the equation. Although there are other ways of determining r_o, the graphical technique used by Ouchterlony et al. (1993) will be demonstrated here.

To do this let

$$Y = \left(\frac{r_o}{L}\right)\left(\frac{L}{\sqrt{W}}\right)\left(\frac{V}{K}\right)^{1/\beta} \tag{10.44}$$

and

$$Y = \sqrt{f} = \sqrt{\frac{\tan^{-1}\left(\frac{L}{2r_o}\right)}{\frac{L}{2r_o}}} \tag{10.45}$$

The velocity is set equal to the critical velocity V_c and all of the other quantities with the exception of r_o are known. The two curves for Y are then plotted as a function of r_o/L. The intersection point is where

$$\frac{r_o}{L} = \frac{r_c}{L}$$

Knowing the ratio r_c/L one can determine the desired value of r_c by multiplying by the length L.

The process will be illustrated by way of a numerical example taken from the study by Ouchterlony et al. (1993). A charge of Gurit 17 from Nitro Nobel AB was used in a 48 mm diameter hole. The appropriate explosive properties are:

Explosive = Gurit 17
Diameter = 17 mm
Density = 1000 kg/m^3
Length = 4.5 m
Weight strength of Gurit 17 with respect to Dynamex = 0.77

The charges were used in a gray granite/granodiorite with a grain size of 2-4 mm. Measurements of the peak particle velocity were made at various distances from the charge center. The results are plotted in Figure 10.50. Assuming that $\beta = 2\alpha$, the appropriate propagation equation has the form

$$V = K\left(\frac{R}{\sqrt{W}}\right)^{-\beta}$$

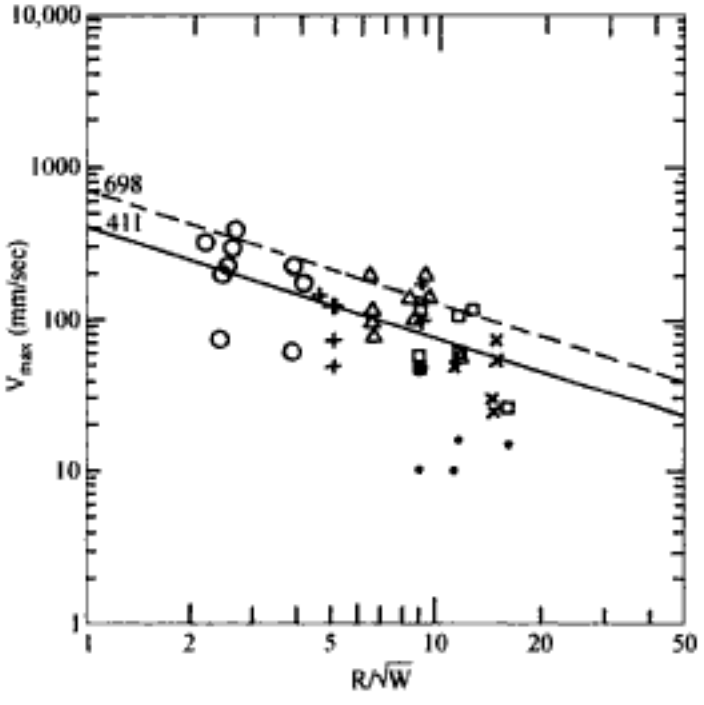

Figure 10.50. Site scaling law for the test rounds (Ouchterlony et al., 1993).

Using a linear regression approach the authors obtained the expression

$$V = 411\,(\frac{R}{\sqrt{W}})^{-0.74}$$

which describes the average line through the points. To be on the conservative side the intercept value was chosen to be 698 corresponding to the value of the normal intercept (411) plus one standard deviation. The charge weight W is given by

$$W = 4.5\,(0.017)^2(\frac{\pi}{4})\,(1000) = 1.0214 \text{ kg}$$

which when converted to the equivalent weight of Dynamex becomes

$$W_{Dyn} = 0.77\,(1.0214) = 0.79 \text{ kg}$$

In this example, the critical velocity has been assumed to be

$$V_c = 800 \text{ mm/sec}$$

Using these values Equation (10.44) can be written as

$$Y = (\frac{4.5}{\sqrt{W}})\,(\frac{800}{698})^{1/0.74}\,(\frac{r_o}{L}) = \frac{5.41}{\sqrt{W}}(\frac{r_o}{L}) \tag{10.46}$$

Similarly Equation (10.45) becomes

$$Y = \sqrt{\frac{\tan^{-1}(\frac{L}{2r_o})}{\frac{L}{2r_o}}} = \sqrt{\frac{\tan^{-1}\frac{0.5}{r_o/L}}{\frac{0.5}{r_o/L}}} \tag{10.47}$$

For the ratio $r_o/L = 0.2$ one finds that

$$\tan^{-1}(\frac{0.5}{r_o/L}) = \tan^{-1}(\frac{0.5}{0.2}) = \tan^{-1}(2.5)$$

This corresponds to

$$\theta = 68.20° = 1.190 \text{ radians}$$

The value for Y using Equation (10.46) becomes

$$Y = \frac{5.41}{\sqrt{0.79}}\,(0.2) = 1.22$$

Using Equation (10.47) the value for Y is

$$Y = \sqrt{\frac{1.190}{2.5}} = 0.69$$

If the ratio r_o/L had been the common solution for these two equations, then the Y values would have been identical. Since they are not identical another ratio must be tried. Values for the Y values appropriate for the two curves are now calculated for other r_o/L ratios in the same way. The results are shown in Figure 10.51. The two curves intersect at about

$$\frac{r_o}{L} = 0.075$$

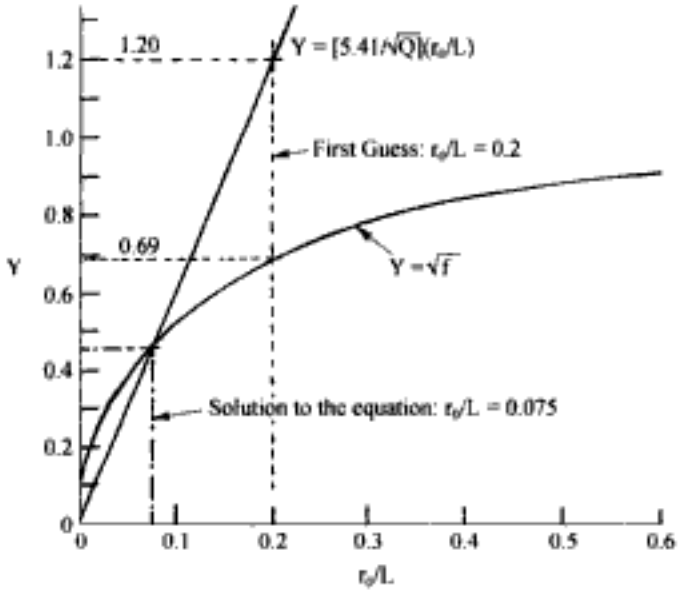

Figure 10.51. The graphical solution to the damage zone equation (Ouchterlony et al., 1993).

The value of r_c is therefore

$$r_c = 0.075\ (4.5\ \text{m}) = 0.34\ \text{m}$$

As was indicated earlier this procedure is used to determine the extent of the damage zone given the value of the critical velocity. Since the Ouchterlony et al. (1993) approach is based upon the Holmberg-Persson equation which assumes infinite detonation velocity and wave velocity and takes no account of the arrival directions of the elemental waves it is subject to the same limitations. Whereas Holmberg-Persson expressed the velocity in terms of the distance and eventually superimposed the critical velocity to obtain the distance, here the distance is determined directly.

10.4.3 *The Inspiration approach*

In 1986, Savely (1986) described a procedure for designing blasts near the final pit wall. In principle it is rather similar to the Swedish approach. The important distinction is that the explosive column is treated as a single spherical charge rather than as a distributed charge and thus the calculated velocities would be different with the two approaches. However as long as one is consistent in relating *observed* damage at a given site to the calculated velocities (using whatever method), a design procedure results. The steps followed by Savely (1986) in this practical application to the Inspiration Mine will be outlined below.

Step 1. Particle velocity-scaled distance curve

The first step to the prediction of blast damage is the development of an equation relating particle velocity to the weight (W) of explosive being used and the distance (R) from the center of the charge to the point of interest. Such a relationship is given below

$$V = K\left(\frac{R}{W^{1/2}}\right)^{-\beta} \tag{10.48}$$

where V = particle velocity (in/sec), R = distance (ft), W = amount of explosive (lbs), K, β = constants.

Initially there were no site specific data available for K and β. As a result, the upper and lower limiting curves presented by Oriard (1972, 1982) were applied (Fig. 10.52). The equations are

Lower limit

$$V = 25\left(\frac{R}{W^{1/2}}\right)^{-1.6} \tag{10.49}$$

Upper limit

$$V = 225\left(\frac{R}{W^{1/2}}\right)^{-1.6} \tag{10.50}$$

Table 10.10 is an attempt to relate observed blast damage with a limiting peak particle velocity. Blast damage observations were made at the mine when shooting a single blasthole/ delay in porphyry. The following applied.

Hole diameter = 230 mm (9 ins) or 270 mm (10 5/8 in)
Explosive = ANFO
Spacing = 7.5 m (25 ft)
Burden = 4.5 m to 6 m (15 to 20 ft)
Explosive/hole = 400 kg (900 lbs)
Surface delays = 17 ms or 25 ms.

At distances up to 40 to 50 ft behind the hole, blast damage in the form of

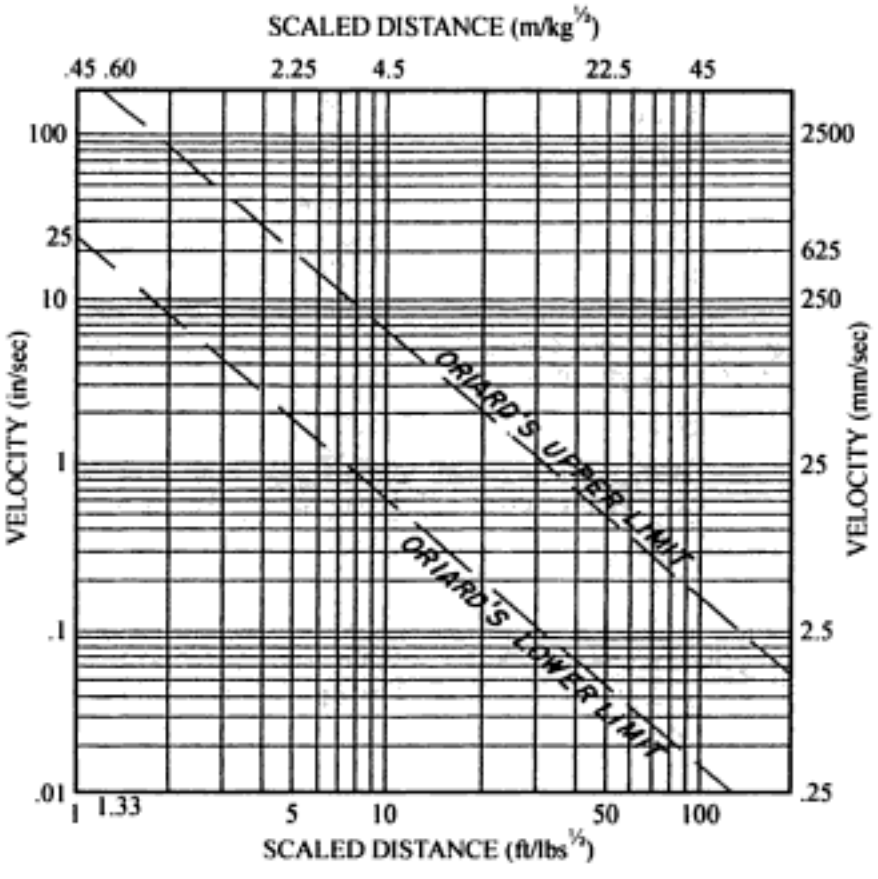

Figure 10.52. Velocity versus scaled distance nomograph used by Inspiration (Savely, 1986).

Table 10.10. Criteria for observable blast damage (Savely, 1986).

Observation	Conclusion	Limiting peak particle velocity mm/sec.	(in./sec)
Occasional falling of loose rocks from bench faces	No damage.	125	5
Partially loosened rock falls from faces that would have remained in place if not blasted	Possible damage, but probably acceptable	400	15
Portions of bench face fall, loosened rock falls, some fracturing in bench level.	Minor blast damage.	635	25
Backbreak extends into toe, crest of future benches heavily fractured, noticeable increase in fracture intensity on bench and in face, loose rock blocks in face, cratering near bench toe, heaved ground offset on structure.	Blast damage.	> 635	> 25

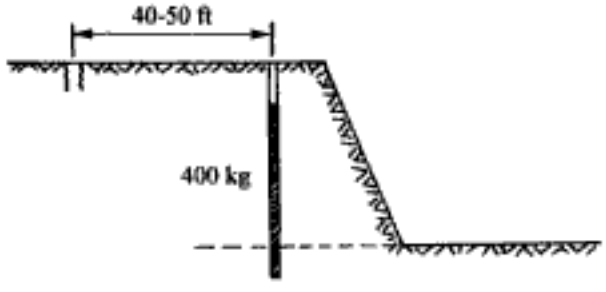

Figure 10.53. Geometry resulting in measured crest damage.

– Displacement along rock structure,
– Ground heave,
– New fractures,

was observed. This is shown diagrammatically in Figure 10.53. Using the values

R_d = damage limit = 40 ft
W = explosive weight/delay = 900 lbs

the scaled distance becomes

$$D_S = \left(\frac{40}{900^{1/2}}\right) = 1.333$$

Lacking velocity measurements, it was assumed that this corresponds to 25 in/sec. A velocity-scaled distance curve was then constructed going through this point with a slope similar to the others (Fig. 10.54). The equation of the resulting curve is

$$V = 40\left(\frac{R}{W^{1/2}}\right)^{-1.6} = \text{in/sec} \qquad (10.51a)$$

or

$$V = 1000\left(\frac{R}{W^{1/2}}\right)^{-1.6} = \text{mm/sec} \qquad (10.51b)$$

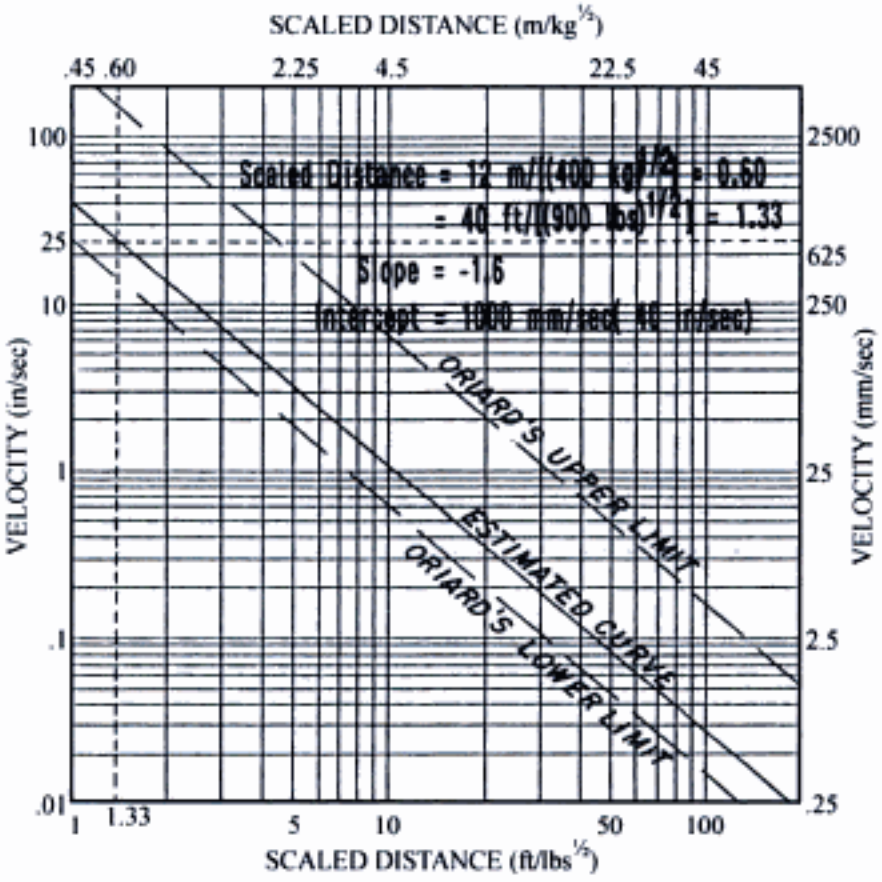

Figure 10.54. Velocity versus scaled distance relationship with the estimated curve superimposed (Savely, 1986).

Step 2. Design curves giving charge weight/delay as a function of distance from the charge were plotted for the different limiting velocities using either or both equations. The results are shown in Figure 10.55. In this case a peak particle velocity less than 381 mm/sec (15 in/sec) has been selected for use at the final pit wall. The distance R substituted into the equation is that from the centerline of the borehole in question to the planned bench crest. This is consistent with the way that the multiplying constant (40) in Equation (10.51a) was determined.

Step 3. A trial blast (shown in Figure 10.56) was designed. It was based largely on experience with regard to what is required to break the ground while staying within the limits of Equation (10.51).

The trim row was designed first. A total charge of 225 lbs of ANFO situated in 3 decks was chosen per hole. The holes had a spacing of 4.5 m (15 ft) or 1/2 that of the production holes. The horizontal distance from the hole to the future crest was 35 ft, hence the expected peak particle velocity is

$$V = 40\left(\frac{R}{W^{1/2}}\right)^{-1.6} = 40\left(\frac{35}{225^{1/2}}\right)^{-1.6} = 10.3 \text{ in/sec}$$

The distance between decks is 10 ft or about 12 hole diameters and the charges are roughly in proportion to the ease of breaking. These holes were drilled with the production rig and are 10 5/8 in (270 mm) in diameter and no subgrade drilling was done. The buffer holes

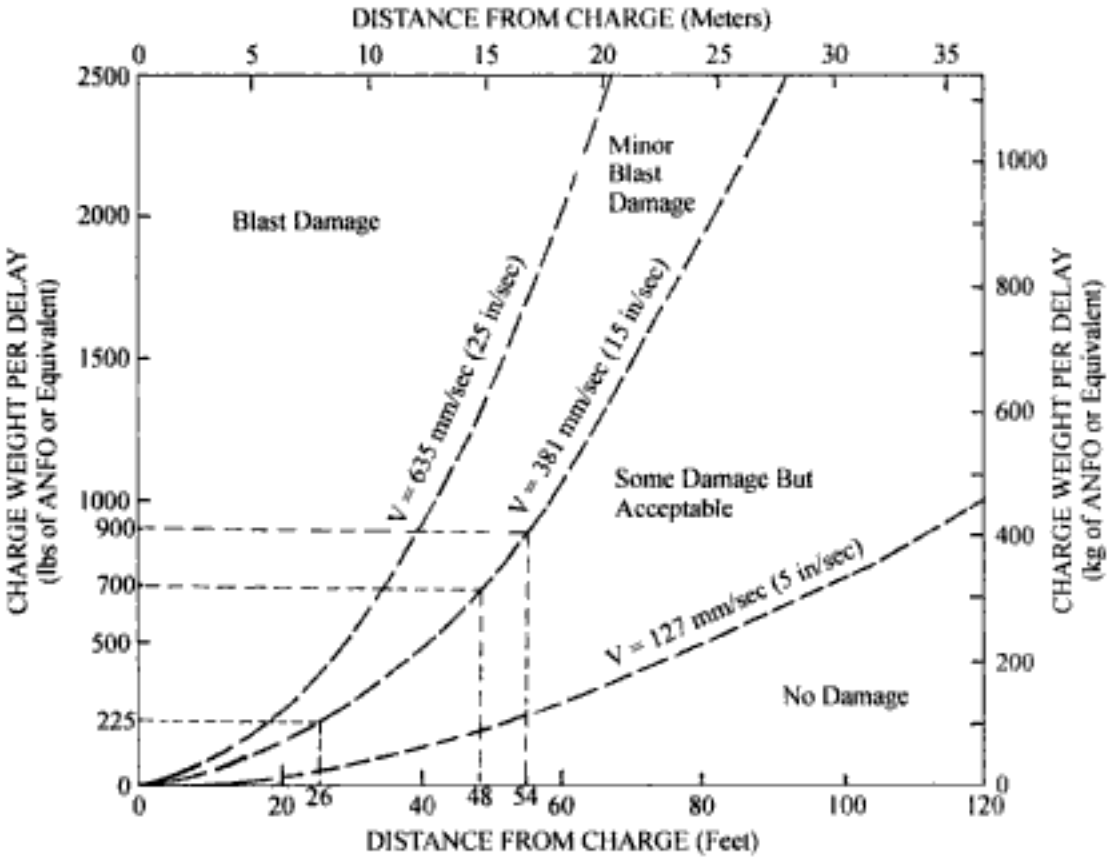

Figure 10.55. Charge weight per delay versus distance from charge for the different limits (Savely, 1986).

were laid out at a distance of 25 ft from the trim holes on the same spacing (30 ft) as that of the production holes. No subgrade drilling was done and the charge was increased to 700 lbs. Using the collar to crest distance of 60 ft, the expected peak particle velocity is

$$V = 40\left(\frac{60}{700^{1/2}}\right)^{-1.6} = 10.8 \text{ in/sec}$$

Finally the first row of production holes was located a distance of 30 ft. from the buffer holes. They have the following characteristics

Stemming = 32 ft
Subdrill = 10 ft
Charge length = 28 ft
Hole length = 28 ft
ANFO ($\rho = 0.84$ g/cm^3)
Total charge = 900 lbs

The expected crest peak particle velocity (PPV) is

$$V = 40\left(\frac{90}{900^{1/2}}\right)^{-1.6} = 7 \text{ in/sec}$$

As can be seen, the expected bench face angle was 68° and the expected overbreak at the toe of the trim holes was 10 ft. Limit of dig flags were set out for the shovel on the blasted crest with these dimensions in mind. The observations made during and after blasting were:

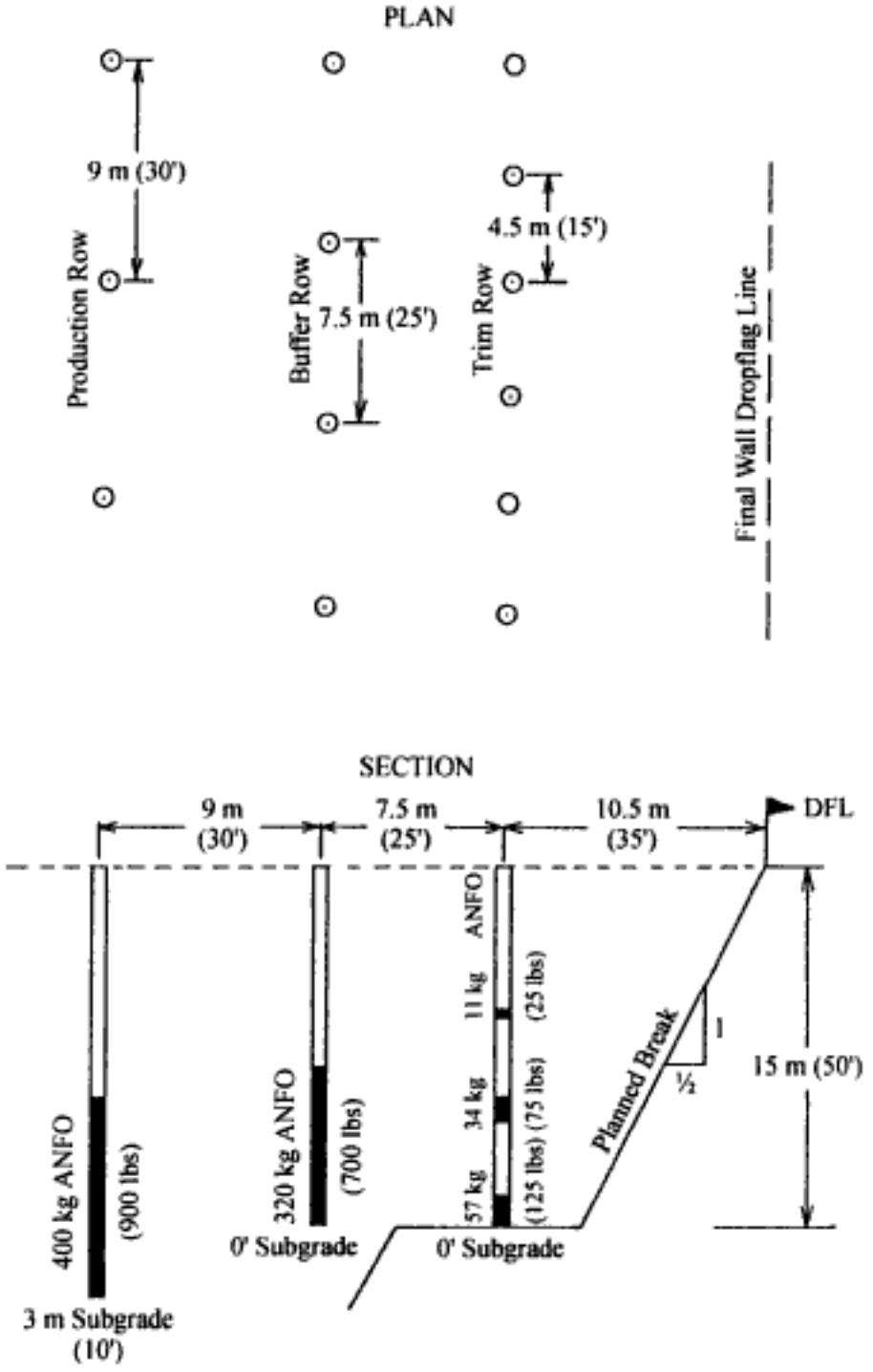

Figure 10.56. First design for achieving the desired slope angle (Savely, 1986).

- The presence of a hard to dig toe,
- Time consuming to charge the trim holes,
- Reduced back break.

Step 4. A modified design was prepared to address the observed problems. By this time the monitoring of a number of actual production blasts had been completed (Table 10.11). A typical set of records for one site is shown in Figure 10.57.

Table 10.11. Results from a series of test blasts in quartz monzonite porphyry.

Number	Blast num.	Scaled distance ($D/W^{0.5}$)	Maximum net velocity (in/sec)	Maximum transverse velocity (in/sec)	Maximum vertical velocity (in/sec)	Maximum longitudinal velocity (in/sec)
1	6401	5.03	8.41	2.9	6.8	4
2	6406	5.93	3.53	1	2.1	2.65
3	6408	8.52	1.43	0.5	0.6	1.2
4	6410	3.1	5.3	1.2	4.2	3
5	6415	2.69	5.95	1.8	4.3	3.7
6	6417	3.47	11.31	3.78	8.7	6.2
7	6418	3	5.88	2.5	4.7	2.5
8	6420	2.77	9.79	2.5	5.5	7.7
9	6425	3.52	4.89	1.7	2.7	3.7
10	6426	4.08	6.5	2.4	3.8	4.7
11	6518	5.3	1.87	1	1.38	0.9
12	6527	6.41	0.96	0.35	0.64	0.62
13	6528	13.3	0.69	0.4	0.39	0.4
14	6530	10.58	0.96	0.2	0.5	0.8
15	6537	8.05	1.82	0.76	0.7	1.5
16	6547	10.12	0.73	0.16	0.48	0.52
17	6549	14.98	0.62	0.2	0.3	0.51
18	6566	10.06	0.51	0.21	0.36	0.29
19	6607	8.08	1.69	1	1.1	0.8
20	6618	11.7	0.45	0.11	0.24	0.36
21	6628	10.2	0.79	0.38	0.52	0.45
22	6647	7.75	1.41	0.39	0.74	1.13
23	6661	9.5	0.37	0.14	0.21	0.27
24	6662	9.57	0.66	0.18	0.4	0.49
25	6672	7.3	1.74	0.68	1.6	0.01
26	6678	9.16	1.14	0.54	0.75	0.66
27	6679	13	3.48	0.68	1.31	3.15
28	6688	6.4	1.62	0.89	1.14	0.73
29	6691	7	4.38	2.23	3.39	1.64
30	6692	3.5	3.16	1.43	1.18	2.56
31	6735	12.7	1	0.32	0.77	0.56
32	6754	10.5	1.54	0.71	0.64	1.21
33	6773	55.8	0.01	0.01	0	0
34	6774	16.6	0.44	0.14	0.21	0.36
35	6653	15.31	1.28	0.68	0.88	0.64
36	6786	10	0.74	0.37	0.41	0.49
37	6792	10.1	1.06	0.55	0.77	0.47
38	6803	10.8	0.82	0.26	0.74	0.23
39	6815	20.8	0.36	0.07	0.16	0.31
40	6817	9.8	1.34	0.27	0.57	1.18
41	6822	4.5	0.05	0.03	0.04	0.01
42	6825	13.3	0.88	0.58	0.52	0.41
43	6833	15.6	2.67	1.21	1.78	1.58
44	6837	12.9	1.15	0.67	0.62	0.7
45	6843	10.3	0.8	0.3	0.54	0.51
46	6864	8.4	0.91	0.2	0.59	0.67

a. Blast Sketch

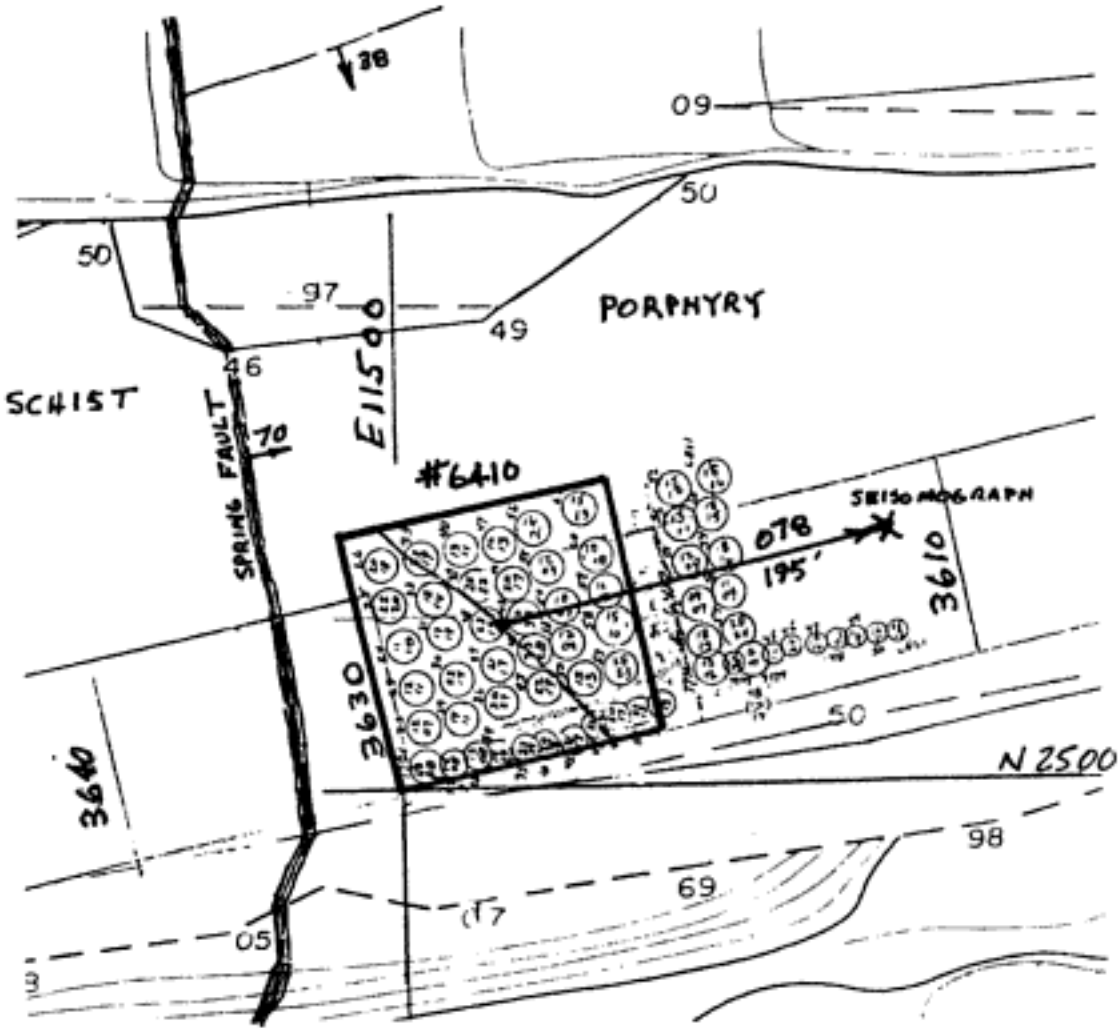

b. Blast Data

Delay	Time	No. of Holes	Wt. Powder Other Than ANFO	Wt. ANFO	ANFO Equiv. Total Wt.	Slope Distance	Scaled Distance
1	0 MS	2	—	800	800	195	6.89
2	25 MS	6	—	2400	2400	195	3.98
3	50 MS	10	—	3950	3950	195	3.10
4	75 MS	8	—	3000	3000	195	3.56
5	100 MS	4	—	1500	1500	195	5.04
	MS						
	MS						
	MS						
	MS						
	MS						
	Total:	30	—	11,650	11,650		

Figure 10.57. Typical data collection from a test blast (Savely, 1986).

BLAST MONITORING

PIT JB 3600 DATE 2/18/93 TIME 5:10 OPERATORS Kastner Anderson

BLAST No. 6410 ROCK TYPE Qmp PHOTOS No

SEISMOGRAPH SPRENGJETHER VS-1200 GAIN 1 ÷ 10 = .1

BLAST COORD. N. 2580 E. 11550 ELEV. 3635 195'

ACCELEROMETER N. 2622 E. 11740 ELEV. 3650 AZ to SOURCE 078

RECORD

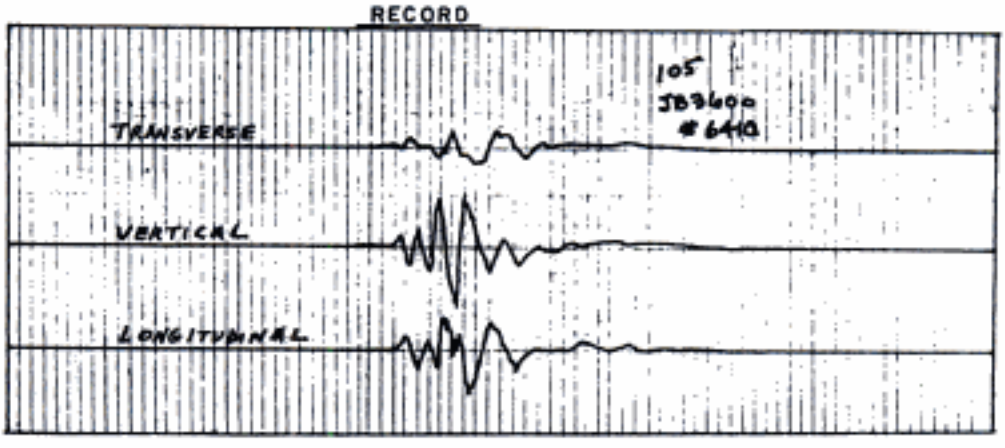

PEAK PARTICLE VELOCITY

	INDIVIDUAL MAX		NET MAX	
	TRACE AMP (in)	VELOCITY (in/sec)	TRACE AMP (in)	VELOCITY (in/sec)
Transverse	.12	1.2	.08	.8
Vertical	.42	4.2	.30	3.0
Longitudinal	.30	3.0	.30	3.0
Net Velocity		5.30 in/sec		4.32 in/sec

Figure 10.57. Continued.

Figure 10.58 shows a summary velocity-scaled distance figure for porphyry with the 46 data points. The best fit curve is

$$V = 31.88\left(\frac{R}{W^{1/2}}\right)^{-1.51} \text{ (in/sec)} \tag{10.52a}$$

$$V = 810\left(\frac{R}{W^{1/2}}\right)^{-1.51} \text{ (mm/sec)} \tag{10.52b}$$

With this information, a new set of design curves was prepared (Fig. 10.59). The modified design as shown in Figure 10.60 was recommended to

– Provide more efficient charging by eliminating the time consuming and labor intensive decking.

Hidden page

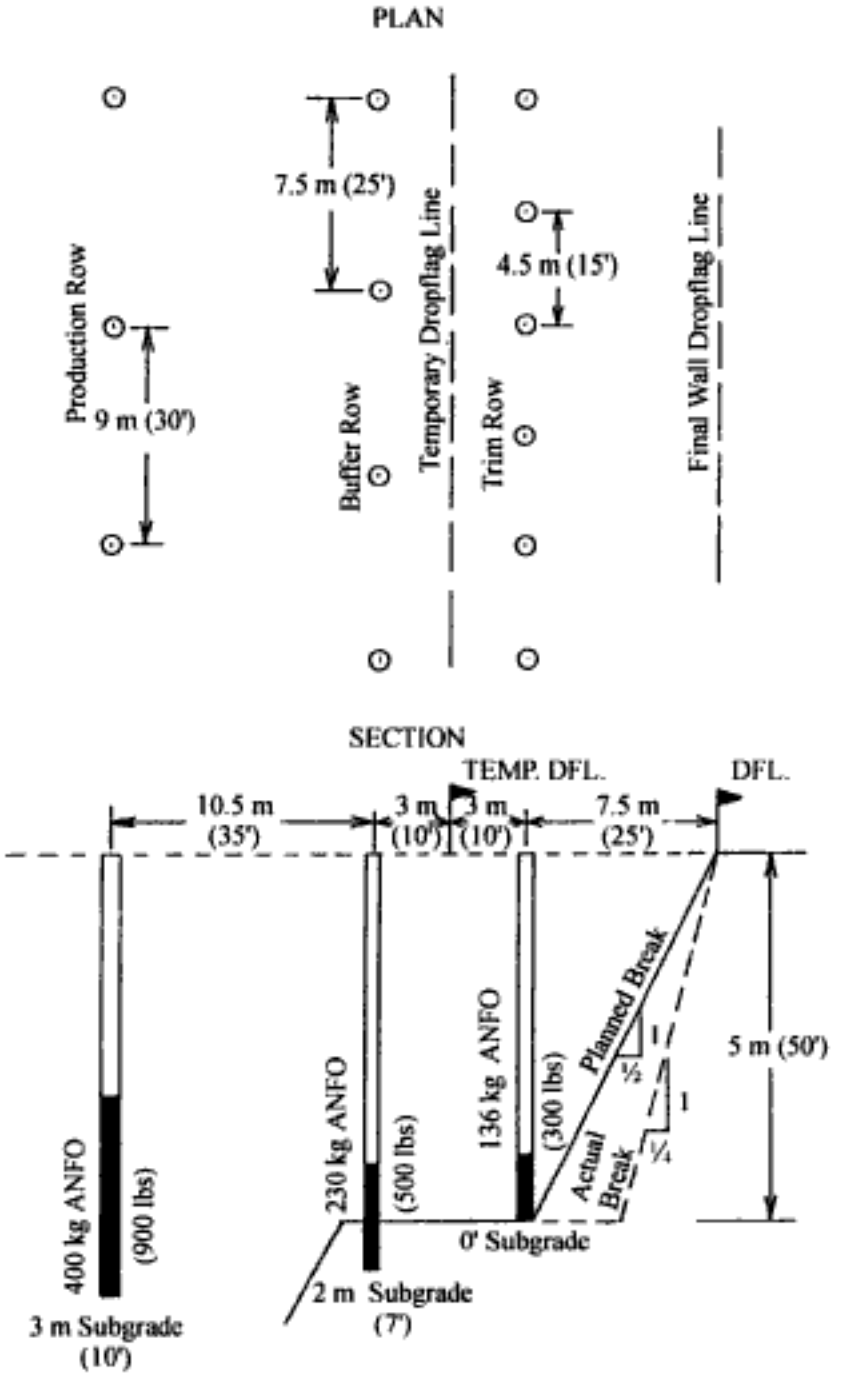

Figure 10.60. The modified design (Savely, 1986).

– Eliminate the hard toe problem.

An increase in blast damage (back break) was expected. The results were

– More back break. The overbreak at the toe was 12 ft. The final bench face angle was 75°.

– Poorer fragmentation. Due to the elimination of the upper deck charges, larger rock blocks came from the upper portion of the blast.

– The position of the buffer row was bad because future bench crests were broken.

– The hard toe problem continued.

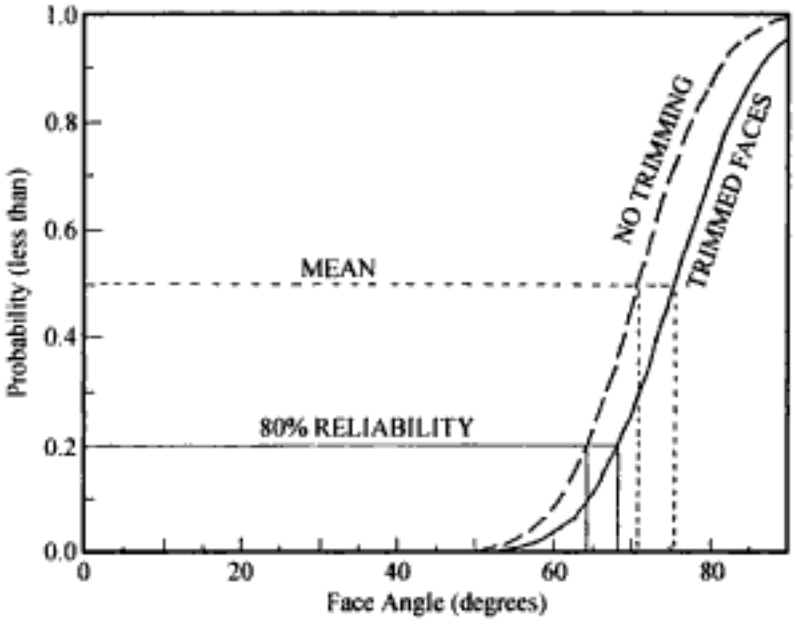

Figure 10.61. Distribution of the face angles with and without trimming (Savely, 1986).

One of the problems in this type of design involves deciding how far from the trim hole position the actual bench face will break. A very limited evaluation suggested that under the highly confined conditions present at the toe, the limiting particle velocity was of the order of 75 in/sec (1900 mm/sec). At the crest, the first approximation for the limiting velocity is 1000 mm/sec. (40 in/sec).

The reason for the hard digging toe was that as shown in Figure 10.61, the average slope angle was not 63° as assumed by rather 70° for the untrimmed bench faces and 75° for those trimmed. In trying to reach the flagged crests, the shovels were digging unfragmented material.

Step 5. The new design shown in Figure 10.62 was proposed.

– The designed distance from the toe of the trim hole was selected as 7 ft. With the 75° face, this gives a crest distance of 20 ft.

– The decks were reinstated. Two larger decks rather than the 3 smaller ones used in Design 1 were chosen.

– The buffer row was moved so that it did not fall within the crest of the future underlying bench. The subgrade drilling was reduced.

The results of the blasting were

– The hard toe was eliminated

– The backbreak seemed to follow the design line closely

– The deck charging improved the distribution near the wall and gave good fragmentation.

An important observation was that better results were achieved when the buffer row was blasted and loaded out prior to shooting the trim row. The maximum distance from the temporary crest to the collar of the trim hole should be 15 ft (4.5 m).

The deck charges were shot as shown in Figure 10.63. When the production, buffer and trim rows were shot together even with delays between rows, the back break was worse.

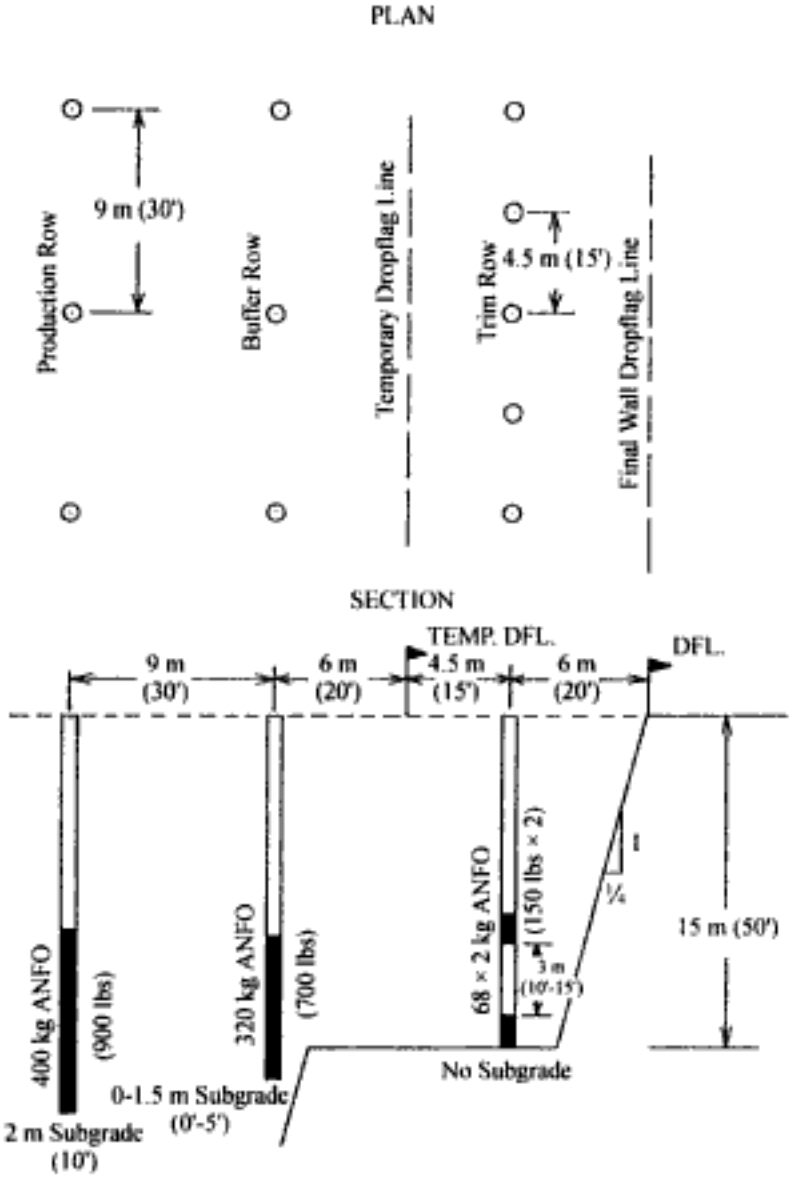

Figure 10.62. The final design (Savely, 1986).

Step 6. The process is repeated in the different rock types/structures making up the pit. At Inspiration there are three major rock types with their characteristics given in Table 10.12. The resulting velocity-scaled distance equations for the other rock types are given in Table 10.13. The design limiting peak particle velocities are given in Table 10.14.

10.4.4 *The CSM approach*

The Swedish approach to perimeter design is an extremely useful one. There are however a number of problems involved with the development and use of empirical propagation equations of the form

$$V = K\, W^{\alpha} R^{\beta} \tag{10.53}$$

where K = constant, W = source charge weight, R = distance from the source, α = empirically determined constant, β = empirically determined constant.

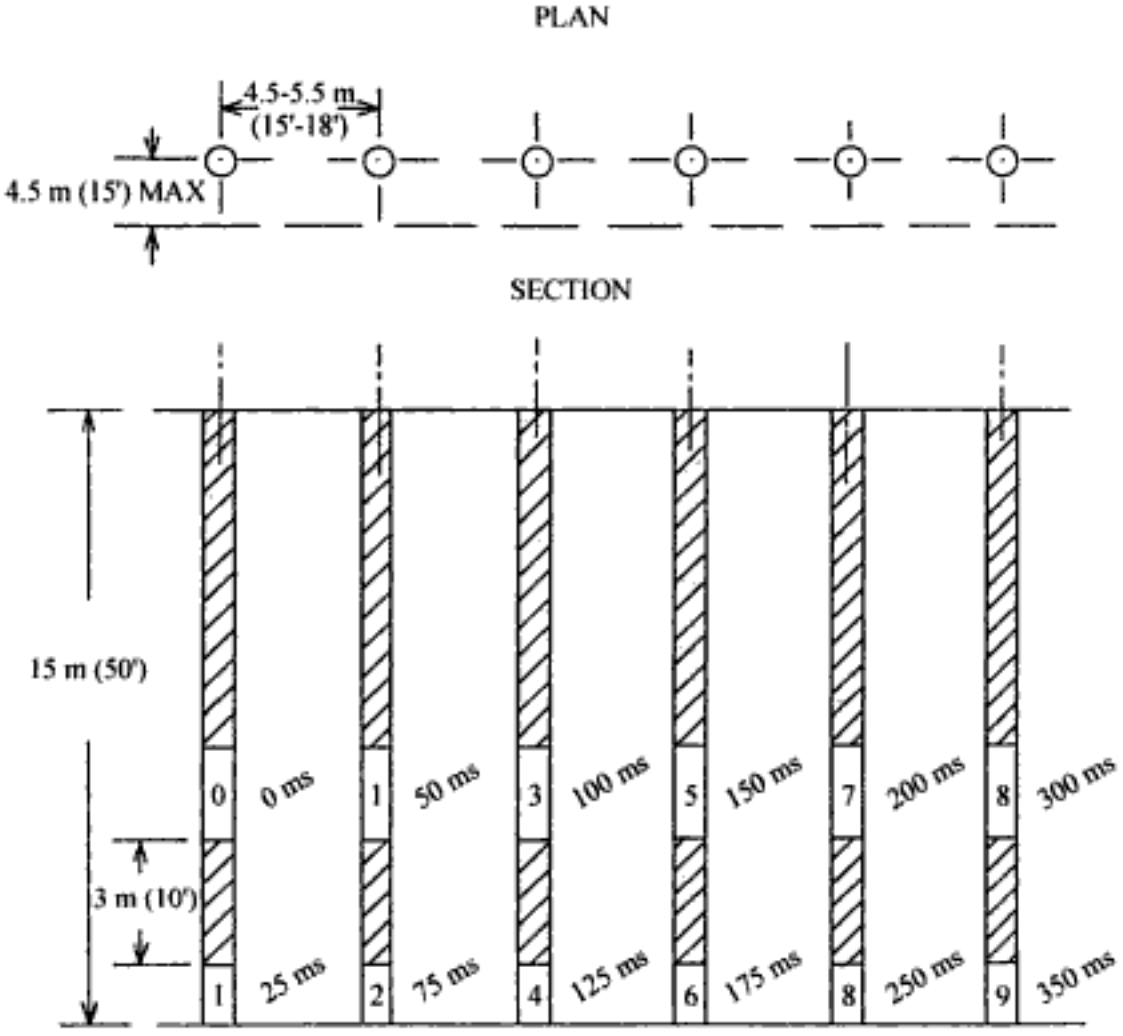

Figure 10.63. The delay pattern used for the trim row (Savely, 1986).

Table 10.12. Characteristics of the Inspiration rock types.

Porphyry	– Hard, brittle and intensely fractured
	– Typically the blasted rock would have 80 percent of rock fragments less than 5 cm (2 in.) size. The maximum size block would be about 30 to 60 cm (1 to 2 ft).
	– Back break is controlled by joints and faults
	– In some areas the porphyry can be loaded by shovels without blasting but blasting makes loading more efficient
Schist	– Variable in hardness and fracture intensity
	– Most of the schist is foliated
	– The blasted rock tends to be more coarse than the porphyry. Typically 60 percent is more coarse than 5 cm (2 in.). The maximum size is about 120 cm (4 ft).
	– The schist seems to absorb energy but back break is often extensive. It follows major structure or foliation.
	– Is generally associated with the more severe slope instabilities
Dacite	– Massive and competent
	– Usually over 50 percent of the rock blocks are greater than 30 cm (1 ft) in diameter. Maximum size blocks are 300 cm (10 ft).
	– At hole spacings greater than 20 ft (6 m) large blocks will occur and secondary blasting is required.

Table 10.13. Results of blast monitoring.

Data	Number of blasts	Slope of log-log regression curve	Intercept at unity scaled distance mm/sec (in/sec)	
Porphyry	46	–1.51	810	(32)
Schist	14	–1.10	398	(16)
Dacite	10	–2.02	2240	(88)

Table 10.14. Criteria for observable blast damage. After Savely (1986).

Observation	Conclusion	Limiting peak particle velocity mm/sec (in/sec) Porphyry		Schist		Dacite	
Occasional falling of loose rocks from bench faces.	No damage.	127	(5)	51	(2)	635	(25)
Partially loosened rock falls from faces that would have remained in place if not blasted.	Possible damage, but probably acceptable.	381	(15)	254	(10)	1270	(50)
Portions of bench face fall, loosened. rock falls, some fracture in bench level	Minor blast damage.	635	(25)	381	(15)	1905	(75)
Backbreak extends into toe, crest of future benches heavily fractured, noticeable increase in fracture intensity on bench and in face, loose rock blocks in face, cratering near bench toe, heaved ground and offset on structure.	Blast damage.	> 635	(> 25)	>381	(> 15)	> 1905	(> 75)

A few of these problems will be listed below:

1. A number of field tests must be run to determine the needed values for K, α and β.

2. The units in which K is to be expressed are variable. When $W = R = 1$, the units of K are those of velocity. For other values, the units of K depend upon α and β.

3. As noted by Holmberg and Persson (1979) when one gets close to the charge, the travel distances from different parts of the charge to the point of interest are quite different. They have shown one way of how this can be taken into account. Their procedure involves assuming that the contributions from the different elemental charges making up the total charge arrive at the point of interest at the same time. This is not true for two reasons:

a) there is a finite detonation velocity along the charge column. For an end initiated 3 m long explosive column having a VOD of 5000m/sec the time delay along the column is

$$\Delta t = \frac{5}{5000} = 1 \times 10^{-3} \text{ sec}$$

b) The waves generated by the explosive travel at the speed of sound in the medium. Thus the longer travel paths require a greater amount of time to traverse than do the shorter paths.

A related problem is that the angle of approach of the wave from the elemental charge to the observation point is not taken into account. It should be a vector addition of the arriving amplitudes and not a straight addition.

4. The use of total explosive weight (W) or even the charge concentration per unit charge length (q) does not take into account certain special but important conditions such as decoupled charges.

5. In the Swedish approach the particle velocities corresponding to the extent of the damage zone must be determined using the same curves used eventually for design. By doing this the problems described above are largely removed. There is a problem, however, if one tries to break this chain and obtain the critical particle velocities by some other technique, for example by laboratory testing.

To overcome these objections, a different approach is required. The one described here was developed at the Colorado School of Mines (Hustrulid et al. 1992) at the end of the 1980s and hence the name CSM approach. A more detailed description of this and related approaches such as described by Plewman and Starfield (1965), Starfield (1966, 1967, 1968) and Harries (1983) are discussed in detail in Chapter 16. The approach is built on the use of the expression for the particle velocity arising from the detonation of a spherical charge in an infinite, isotropic and homogeneous medium as presented by Favreau (1969)

$$V(r,t) = e^{\frac{-\alpha^2 t}{\rho c b}}\left[\frac{Pb^2 c}{\alpha\beta R^2} - \frac{\alpha Pb}{\beta\rho cR}\sin\frac{\alpha\beta t}{\rho cb} + \frac{Pb}{\rho cR}\cos\frac{\alpha\beta t}{\rho cb}\right] \tag{10.54}$$

$$\alpha^2 = \frac{2(1-2\nu)\rho c^2 + 3(1-\nu)\gamma P}{2(1-\nu)} \tag{10.55}$$

$$\beta^2 = \frac{2\rho c^2 - 3(1-\nu)\gamma P}{2(1-\nu)} \tag{10.56}$$

where t = time, ρ = rock density (kg/m^3), c = compressional wave velocity in rock (m/sec), b = original spherical cavity radius (m), P = explosion pressure (Pa), ν = Poissons ratio for the rock, γ = ratio of the specific heats of the explosion gases, R = distance of the observation point from the charge center (m), τ = retarded time (sec) = $t - (R - b)/c$.

To use Equation (10.54) the following must hold:

$$2\rho\ c^2 > 3(1-\nu)\,\gamma\,P$$

which is true for most rock-explosive combinations. For the interested reader Favreau (1969) has presented the appropriate equations for the other cases as well.

Most blasting operations today use cylindrical charges and to apply this propagation equation, the cylindrical charge is first divided into a series of elemental charges each of which will be modelled as a spherical charge (Fig. 10.64). To have equivalent volumes of the explosive represented by the spheres, the radius of the sphere is chosen such that the volume of the sphere is the volume of of the cylinder whose length is the diameter of the sphere (Harries, 1983). By this procedure the overall length of the cylindrical charge and the set of spheres remains the same. Thus if the radius of the sphere is b and the radius of the cylinder is r_c, then

$$b = 1.2247\ t_c \tag{10.57}$$

The particle velocity produced at Point A (R = 5 m) by one spherical charge of radius

$$b = 0.0503 \text{ m}$$

will be considered.

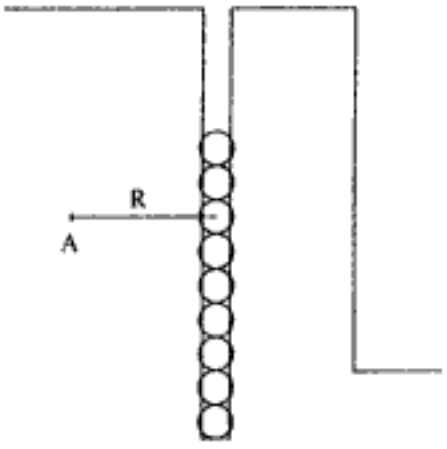

Figure 10.64. Simulation of a cylindrical charge by equivalent spheres.

The rather typical explosive-hardrock characteristics assumed are:

Explosive

$P = 2360 \times 10^6$ Pa

$\gamma = 1.67$

Rock (granite)

$\rho = 2630$ kg/m^3

$c = 5550$ m/sec

$\nu = 0.451$

From the particle velocity versus time curve shown in Figure 10.65, the peak velocity is about 1.6 m/sec at retarded time zero, i.e. just when the strain wave produced by this charge initially reaches this point. From the peak value, the velocity rapidly dies off before oscillating about zero. The initial pulse is of very short duration (about 16 microseconds in this case). The duration is insensitive to changes in R.

The distance (d) between adjacent charge centers in this example is

$$d = 2b = 0.106 \text{ m}$$

Assuming that the detonation velocity (VOD) of the explosive is 5500 m/sec, the time delay (Δt) between detonations is

$$\Delta t = \frac{d}{VOD} = 0.1006/5500 = 18.3 \times 10^{-6} \text{ secs}$$

The overall peak particle velocity at Point A is obtained by summing in time the overall contributions from the single elemental charges. Figures 10.66 and 10.67 show the effects of superimposing the particle velocities from two adjacent spherical charges for 380 mm and 150 mm diameter holes, respectively. The same explosive-rock characteristics used above are assumed and the distance from the charge center is 5 m. As can be seen, due to the short duration of the peak velocity pulse and the relatively long time between arrivals there is little overlap. The maximum peak particle velocity is that produced by the element closest to the point of interest (multiple elemental charges need not in this end initiation example be considered). The peak particle velocity occurs at

$$\tau = 0 \text{ sec}$$

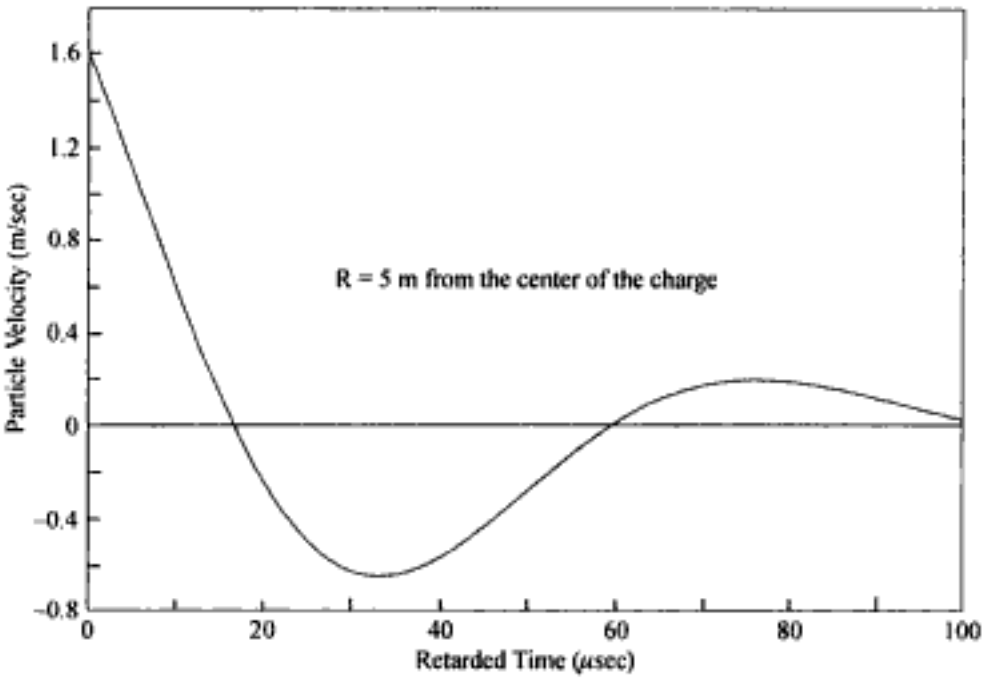

Figure 10.65. Particle velocity as a function of retarded time. Bennett (1991a, b), Hustrulid et al. (1992).

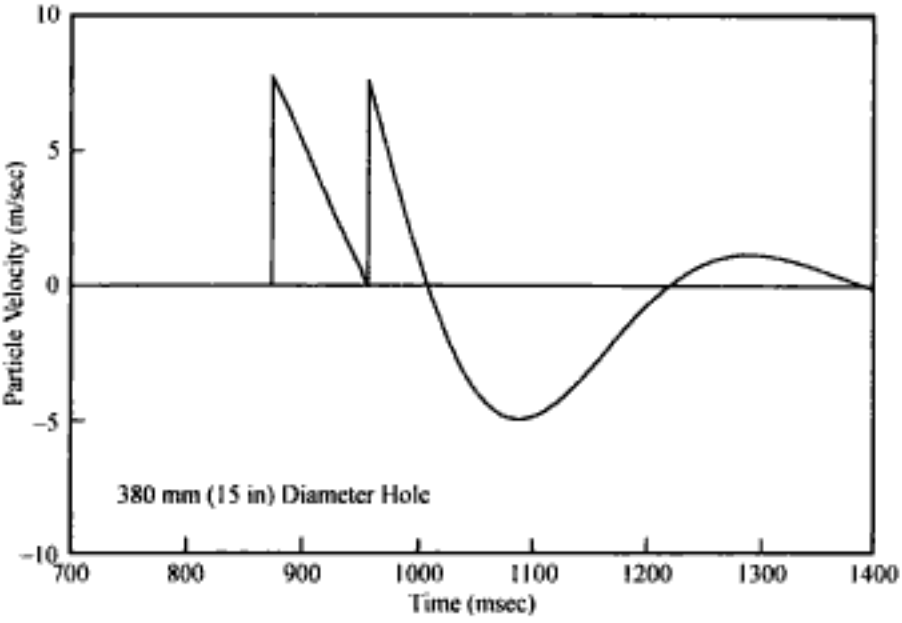

Figure 10.66. Effect of overlapping on the peak particle velocity-time curve for the 380 mm (15 in) diameter holes. Bennett (1991a, b), Hustrulid et al. (1992).

This means that

$$e^{-\frac{\alpha^2\tau}{\rho c b}} = 1 \tag{10.58}$$

and

$$\sin\frac{\alpha\beta\tau}{\rho c b} = 0 \tag{10.59}$$

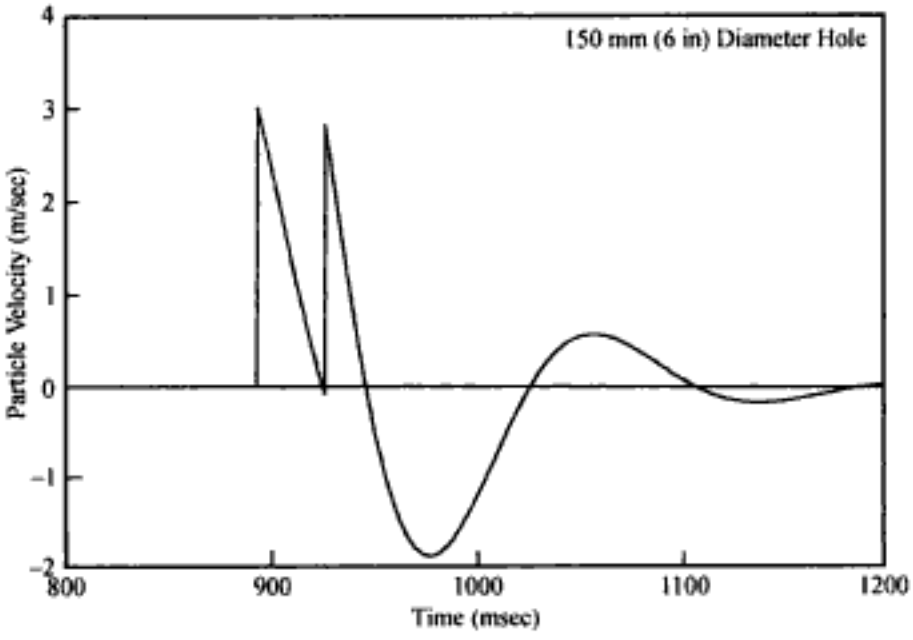

Figure 10.67. Effect of overlapping on the peak particle velocity-time curve for the 150 mm (6 in) diameter holes. Bennett (1991a, b), Hustrulid et al. (1992).

and

$$\cos\frac{\alpha\beta\tau}{\rho c b} = 1 \tag{10.60}$$

The particle velocity propagation equation (Equation 10.50) for the spherical charges simplifies to

$$V(\text{peak}) = \frac{Pb}{\rho c R} \tag{10.61}$$

For cylindrical blastholes this becomes

$$V(\text{peak}) = \frac{1.2247\,Pr}{\rho c R} \tag{10.62}$$

where r = radius of the cylindrical hole (m).

An example of the use of this predictor equation is shown in Figure 10.68, which includes borehole diameters of 170 mm (6.75 ins) to 380 mm (15 ins) commonly found in surface mining operations. The parameters which have been used are

$P = 2000 \times 10^6$ Pa
$\rho = 2650$ kg/m^3
$c = 5500$ m/sec

These curves can be easily transformed for other choices of parameter values simply by multiplying by the appropriate scaling factor (see Eq. 10.61).

The design procedure involving these curves is exactly the same as has been discussed by Holmberg & Persson (1979). In the development of the curves the pressure (P) used is appropriate for ANFO (and related explosives) when the hole diameters are completely filled with explosive. There are many perimeter blasting situations when the hole cross-section is not completely filled with explosive. These can be easily included in the proposed technique.

Hidden page

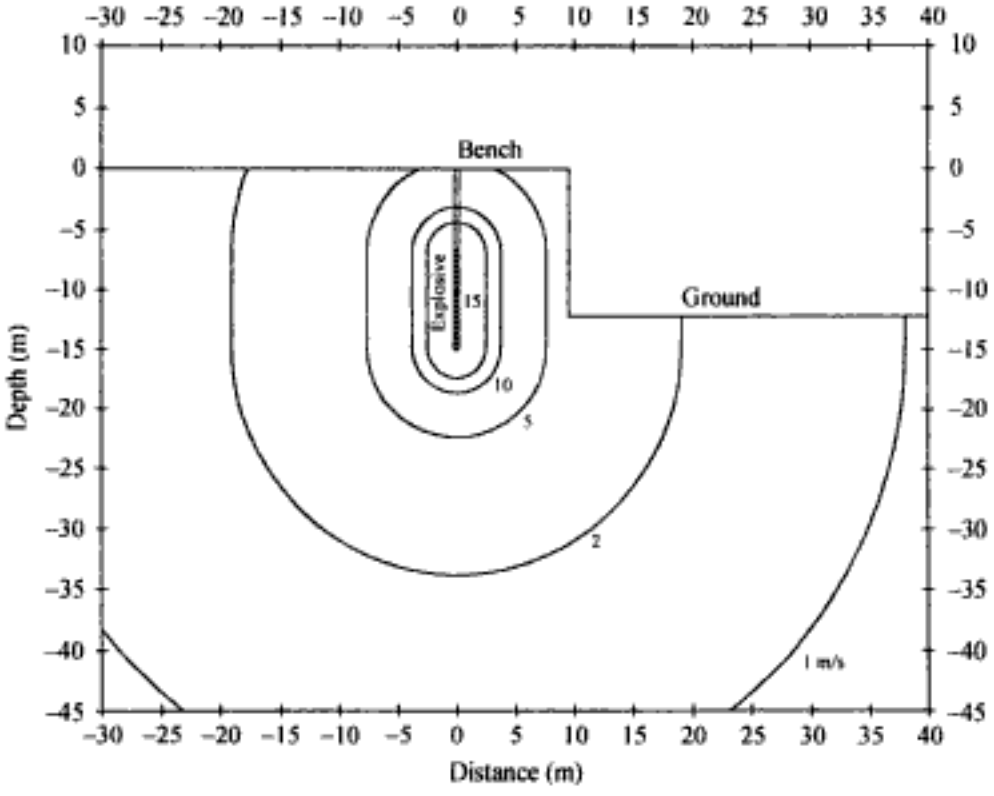

Figure 10.69. Iso-velocity contours for a fully charged 380 mm diameter hole. Bennett (1991a, b), Hustrulid et al. (1992).

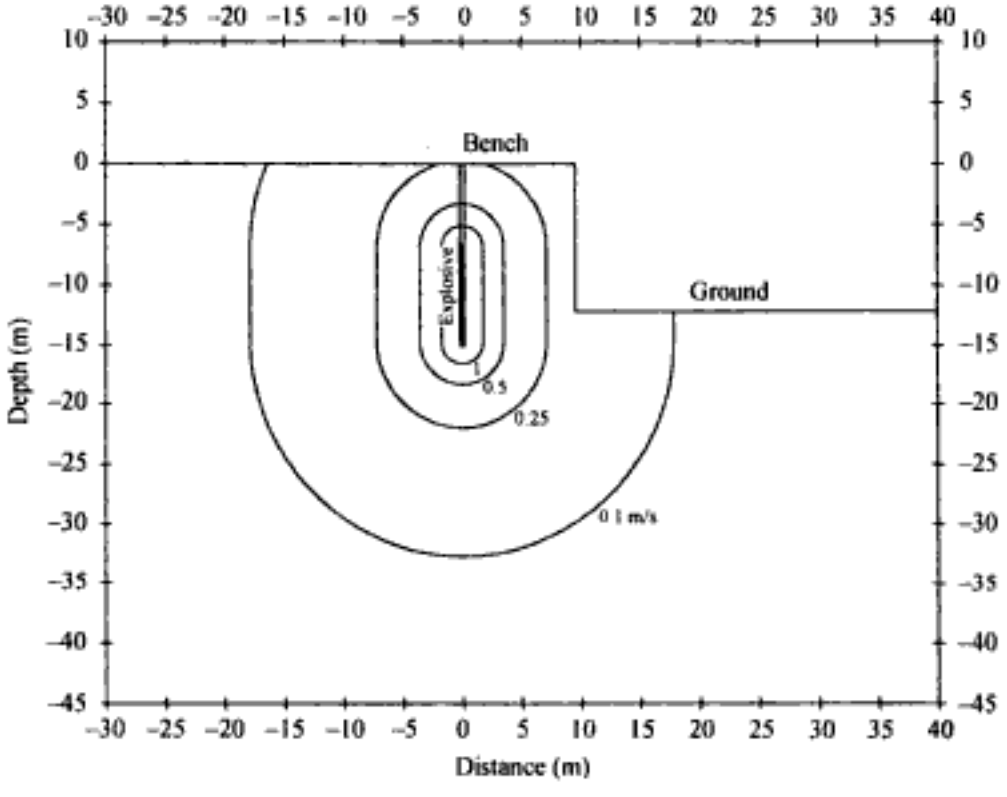

Figure 10.70. Iso-velocity contours for a de-coupled (150 mm diameter) charge in a 380 mm diameter hole. Bennett (1991a, b), Hustrulid et al. (1992).

The explosive has the following characteristics

$P = 2630 \times 10^6$ Pa

$\gamma = 1.67$

In the first case (Fig. 10.69) the hole is filled with explosive. In the second case (Fig. 10.70) a 150 mm (6 in) diameter tube has been placed in the borehole and filled with explosive. The rock mass properties are assumed to be

$\rho = 2360$ kg/m^3

$c = 5550$ m/sec

As can be seen, there is a major difference in the velocity profiles. With the use of plastic tubes, even large holes can produce acceptable damage zones. Figure 10.71 shows a comparison between the peak particle velocities as a function of R as calculated using the CSM and Swedish approaches for the fully-coupled case when

$q = 6.8$ kg/m

$P = 2360 \times 10^6$ Pa

$D = 0.102$ mm

$\rho = 2630$ kg/m^3

$c = 5550$ m/sec

At a distance of $R = 3.2$ m, the two yield the same result. For distances closer to the charge, the Swedish approach gives higher values probably due to the fact that the velocities from all of the incremental charges are added together. For distances greater that 3.2 m, the CSM technique yields higher values than the Swedish approach due to the different powers of R ($1/R$ versus $1/R^{1.51}$). If the velocity limit of 1m/sec is selected, the damage zone radii are:

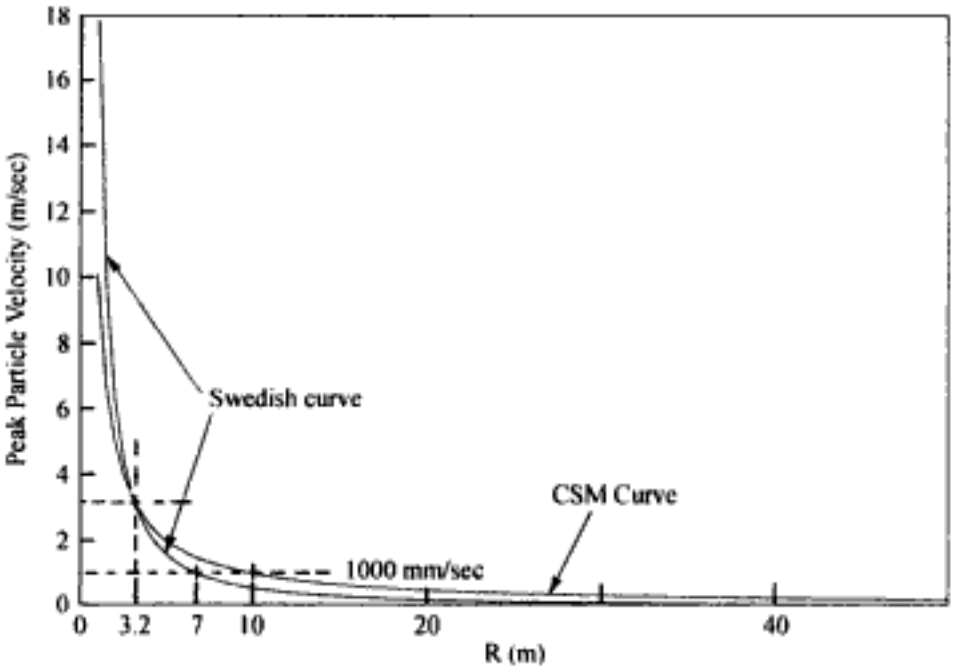

Figure 10.71. Comparison of the peak particle velocity-radial distance curves obtained using the CSM and the Swedish approaches.

CSM approach: $R \approx 10$ m
Swedish approach: $R \approx 7$ m

The Favreau particle velocity equation applies for waves travelling in an elastic medium. This means that the decay in amplitude with distance travelled is simply due to geometrical spreading. Attenuation due to geometrical spreading is due to a decrease in energy density as the waves propagating from the explosion encounter larger volumes of rock. There are three main types of waves which may be generated by a blast. These are body waves travelling within a semi infinite medium, body waves travelling along the surface and Rayleigh waves (Ewing, et al, 1957). Each type will attenuate in a different manner. For a homogeneous, isotropic, linearly elastic medium, the decrease in vibration velocity amplitude with distance is given by

– $1/R$ for body waves within a semi-infinite medium,
– $1/R^2$ for body waves travelling along the surface,
– $1/R^{0.5}$ for Rayleigh waves.

Since on the whole, rock masses are not homogeneous, isotropic, or elastic, geometrical spreading does not account for all of the attenuation seen in the particle velocity amplitude. Energy losses may be attributed to many inelastic mechanisms (Ghosh & Daemen, 1983):

– Matrix inelasticity,
– Fluid flow,
– Dissipation in a fully saturated rock because of the relative motion of the frame with respect to the fluid inclusions,
– Shearing flow of the fluid layer,
– Partial saturation effects,
– Enhanced intercrack flow,
– Stress induced diffusion of absorbed volatiles,
– Systems undergoing phase changes,
– Scattering from small pores and large irregularities,
– Selective reflection from thin beds.

Barkan (1962) has suggested that inelastic attenuation can be modelled by an experimental decay function of the form

$$D_f = e^{-IR} \tag{10.64}$$

where I = inelasticity coefficient.

Introducing this factor, the peak particle velocity equation becomes

$$V = \frac{Pbe^{-I(R-b)}}{\rho cR} \tag{10.65}$$

The quantity $R - b$ has been used instead of R since at the wall of the hole, $R = b$, the inelastic attenuation must be zero.

The value of the factor I can be determined by plotting the quantity $V \times R$ as a function of $(R - b)$ on semi-log paper. The slope of the curve is equal to the coefficient I. This procedure is described in detail in Chapter 14.

Application to the Aitik Mine

The steepness of the slopes which can be created and maintained at the Aitik Mine in Northern Sweden is of major importance. Unwanted blast damage results in flatter bench

face angles and the need to leave wider safety benches. The overall slope angles are thereby reduced and stripping requirements increased. This translates into smaller mineable reserves, a reduced mine life and higher costs per ton. A number of different blasting studies (see for example Section 10.4.2) have been conducted at Aitik the objective of which was to develop blast design rules leading to steeper final overall slopes. Some of the published blasting results have been reanalyzed using the present approach. In the first test series the explosive Reolit A6 was used in 250 mm diameter holes. Peak particle velocity measurements were made at distances of 13.2, 27.0 and 49.0 m from the charge. The following values are assumed to apply for the explosive:

Explosive = Reolit A6,

$\rho_{ex} = 1.45$ g/cm^3

$VOD = 4800$ m/sec (in-hole measurement)

$P_{DET} = 8360$ MPa

$P_e = 4180$ MPa

$q = 74.2$ kg/m (hole diameter of 251 mm)

For the rock it is assumed that

$\rho = 2.64$ g/cm^3

$c = 4000$ m/sec

The measured (vertical) peak particle velocities made by Holmberg & Persson (1978b) were

Distance (m)	*PPV* (m/sec)
13.2	1.520
27.0	0.693
49.0	0.130

These are plotted in Figure 10.72. Using Equation (10.65) one finds that the predicted *PPV* versus scaled distance relationship assuming no attenuation is given by

$$V_{max} = \frac{P_e b}{\rho c R} = \frac{4180 \times 10^6 b}{(2640)(4000)R} = 396\frac{b}{R} \tag{10.66}$$

The relationship between b and the hole diameter r is

$$b = 1.2247\, r$$

and hence

$$b = 1.2247\,(0.251)/2 = 0.154 \text{ m}$$

Equation (10.66) becomes

$$V_{max} = \frac{60.87}{R} \tag{10.67}$$

This curve has been superimposed upon Figure 10.72. As can be seen the predicted values of *PPV* assuming no attenuation are considerably higher than those measured. The theoretical expression for *PPV* versus scaled distance including the attenuation term

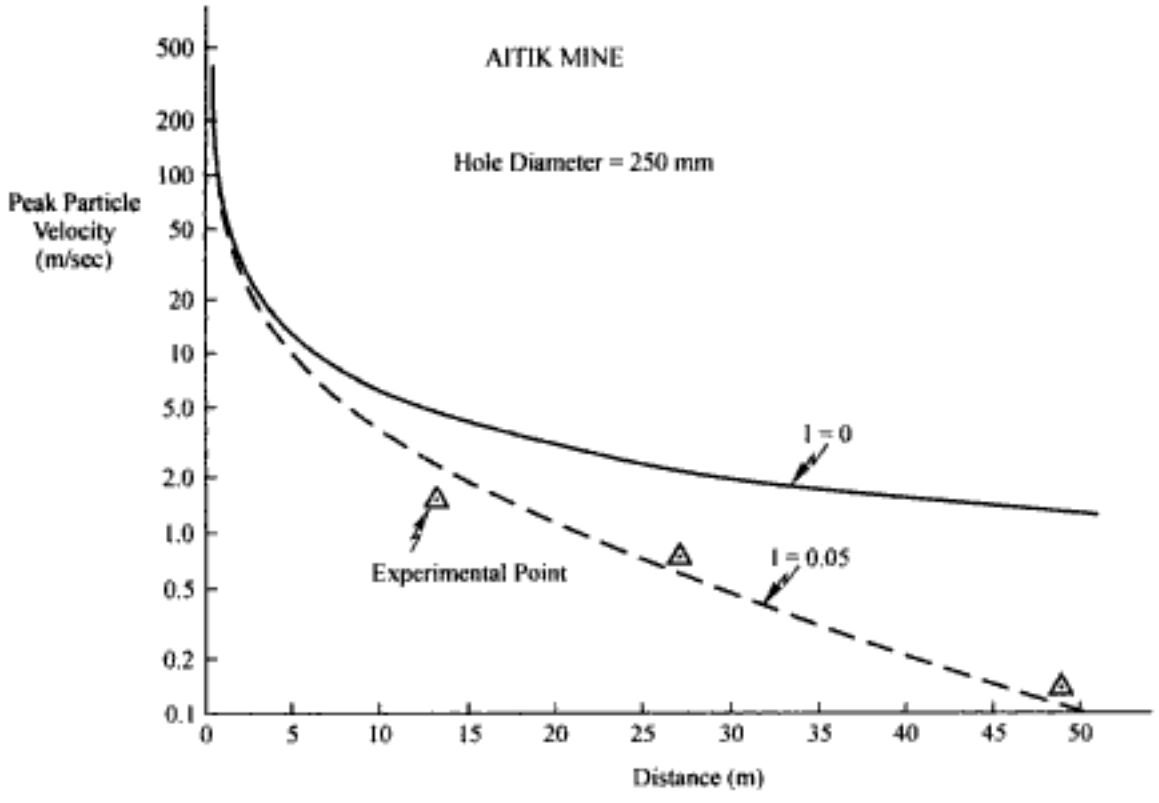

Figure 10.72. The peak particle velocity versus distance curves for the Aitik mine (250 mm diameter holes).

$$V_{max} = \frac{P_e b}{\rho c R} e^{-I(R-b)} = \frac{60.87}{R} e^{-I(R-b)} \tag{10.68}$$

was now applied. The attenuation factor 'I' was varied until the curve passed approximately through the measured points. In this case the resulting value was found to be

$$I = 0.05/\text{m}$$

The predictive expression becomes

$$V_{max} = \frac{60.87}{R} e^{-0.05(R-b)} \tag{10.69}$$

It is observed that the measurement at the distance of 13.2 m lies slightly below the curve.

A second set of experiments were performed using Reolit 10 in 171 mm diameter production holes. A summary of the important parameters are:

Explosive = Reolit 10

$\rho_{ex} = 1.45$ g/cm^3

$VOD = 5000$ m/sec (ideal)

$= 4800$ m/sec (estimated for in hole conditions)

$P_{DET} = 5800$ MPa

$P_e = 2900$ MPa

$q = 34.4$ kg/m (hole diameter of 171 mm)

The peak particle measurements made by Holmberg & Persson (1978b) revealed that

Distance (m)	PPV (m/sec)
8.5	1.442
13.9	0.562
26.9	0.283

These are plotted in Figure 10.73. Using Equation (10.65) one finds that the predicted PPV versus scaled distance relationship assuming no attenuation is given by

$$V_{max} = \frac{P_e b}{\rho c R} = \frac{2900 \times 10^6 b}{(2640)(4000)R} = 275\frac{b}{R} \tag{10.70}$$

The relationship between b and the hole diameter r is

$$b = 1.2247\, r$$

and hence

$$b = 1.2247\ (0.171)/2 = 0.105 \text{ m}$$

Equation (10.70) becomes

$$V_{max} = \frac{28.84}{R} \tag{10.71}$$

This curve has been superimposed upon Figure 10.73. As can be seen the predicted values of *PPV* assuming no attenuation are considerably higher than those measured. The theoretical expression for *PPV* versus scaled distance including the attenuation term

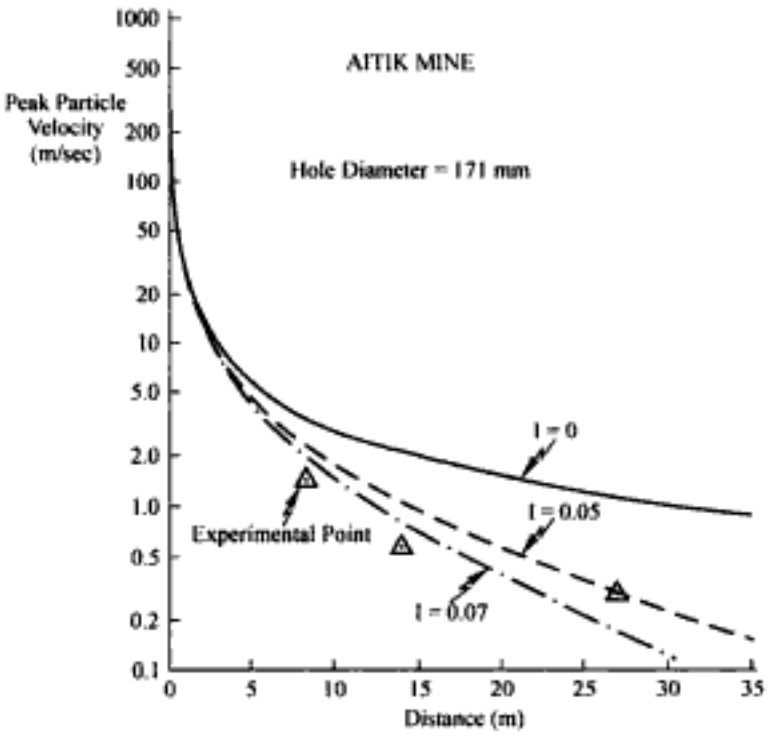

Figure 10.73. Peak particle velocity versus distance curves for the Aitik Mine (171 mm diameter holes).

$$V_{max} = \frac{P_e b}{\rho c R} e^{-I(R-b)} = \frac{28.84}{R} e^{-I(R-b)} \tag{10.72}$$

was now applied. The attenuation factor 'I' was varied until the curve passed approximately through the measured points. In this case the resulting value was also found to be

$$I \cong 0.05/\text{m}$$

The predictive expression becomes

$$V_{max} = \frac{28.84}{R} e^{-0.05(R-b)} \tag{10.73}$$

It is observed that the measurement at the distance of 13.9 m lies below the predicted curve. The appropriate value in this case is

$$I = 0.07/\text{m}$$

In continuing the analysis it will be assumed that $I = 0.05$ adequately describes both sets of experimental results.

In the first set of experiments, that involving the 251 mm diameter production holes, disturbance assessment was done by coring and through the use of extensometers. Damage is considered to have occurred when the number of cracks measured after the shot is greater than before the shot. Holmberg & Persson (1978b) concluded that

– There were great difficulties in determining 'new' fractures in this jointed rock,
– With the possible exception of the zone within a two meter distance from the blasthole, the number of cracks which result from the blasting is small,
– There were obvious differences before and after blasting in the 0-10 m zone,
– There is a 50% probability of damage extending to 22.5 m from the hole,
– There is only a 5% probability that the damage extends beyond 32 m.

One can then translate these observations into the following practical limits

Crushed zone = 2 m,
Fractured zone = 10 m,
Influenced zone = 22.5 m.

When comparing these dimensions to the radius of the sphere 'b' (b = 0.154 m) one finds that

Crushed zone: R/b = 13,
Fractured zone: R/b = 65,
Influenced zone: R/b = 146.

Vovk et al. (1974) have presented the results of a series of experiments (a detailed discussion of these experiments is included in Chapter 21) in which concentrated (spherical) charges of TNT were used in large blocks of granite, limestone and concrete. Prior to blasting, diamond drilling was done in the blocks. The number of cores, their length and the fissure orientation was determined. After blasting the new fissure pattern was determined. By comparing the fissure networks before and after blasting, the induced fracture pattern could be determined. The distance at which the core yield is equal to that before the explosion is taken as the limit of fissure propagation. The rock properties are given in Table 10.15. After blasting, the following three damage zone radii were determined

– Crushing (R_{cr}),

– Radial fissures (R_{fi}),
– Induced fracturing (R_{fr}),

and the ratios of these radii with the charge radius (b) formed. The results are given in Table 10.16.

In comparing the values determined from the Holmberg & Persson (1978b) experiments to the results of the Russian experiments for granite

R/b (crushing) = 11 → 14
R/b (radial fissures) = 25
R/b (induced fracturing) = 54 → 69

it is seen that the crushing zones are similar in extent. The zone of induced fracturing (Russian) corresponds approximately to the Holmberg & Persson fractured zone. The Russians did not have a category corresponding to the influenced zone.

The different damage limits have been superimposed on Figure 10.74. As can be seen, the crushed zone at 2 m corresponds to a peak particle velocity of about 27.5 m/sec. The fractured zone at 10 m corresponds to a value of about 3.7 m/sec. If the influenced zone extends to 22.5 m, the peak particle velocity is about 0.9 m/sec.

However as was noted in Section 10.4.2, the damage assessment hole was drilled at about 45° to the direction of the blasted face. The corrected damage zone dimensions become

Crushed zone = 1.4 m; R/b = 9
Fractured zone = 7 m; R/b = 46
Influenced zone = 16 m; R/b = 104

instead of, respectively, 2 m, 10 m and 22.5 m. These new limits have been plotted on Figure 10.75. The corresponding peak particle velocity limits are:

Table 10.15. Rock properties in the Russian blasting tests (Vovk et al., 1974).

Rock type	Description	Density (gm/cm^3)	Wave velocity (m/sec)	Compressive strength (MPa)	Elastic modulus (GPa)	Poisson's ratio
Granite	gray-green, coarse-grained	2.60	5720	154	29.4	0.22
Limestone	shelly, recrystallized	1.90	3220	9	2.2	0.30
Concrete		2.07	3660	26	14.4	0.25

Table 10.16. Results of the Russian blasting tests (Vovk et al., 1974).

Rock	Charge		Crushing		Radial fissures		Induced fracturing	
	Wt (gm)	Radius (m)	R_{cr} (cm)	R_{cr}/b	R_{fr} (cm)	R_{fr}/b	R_{fi} (cm)	R_{fi}/b
Concrete	120	0.0262	26-34	10-13	63	24	135	52
Granite	120	0.0262	29-37	11-14	68	25	140-180	54-69
Limestone	200	0.0310	25	8	62	20	120-150	39-48
	180	0.0298	27-36	9-12	72	24	134	45
	180	0.0298	24-30	8-10	63	21	108-180	36-60

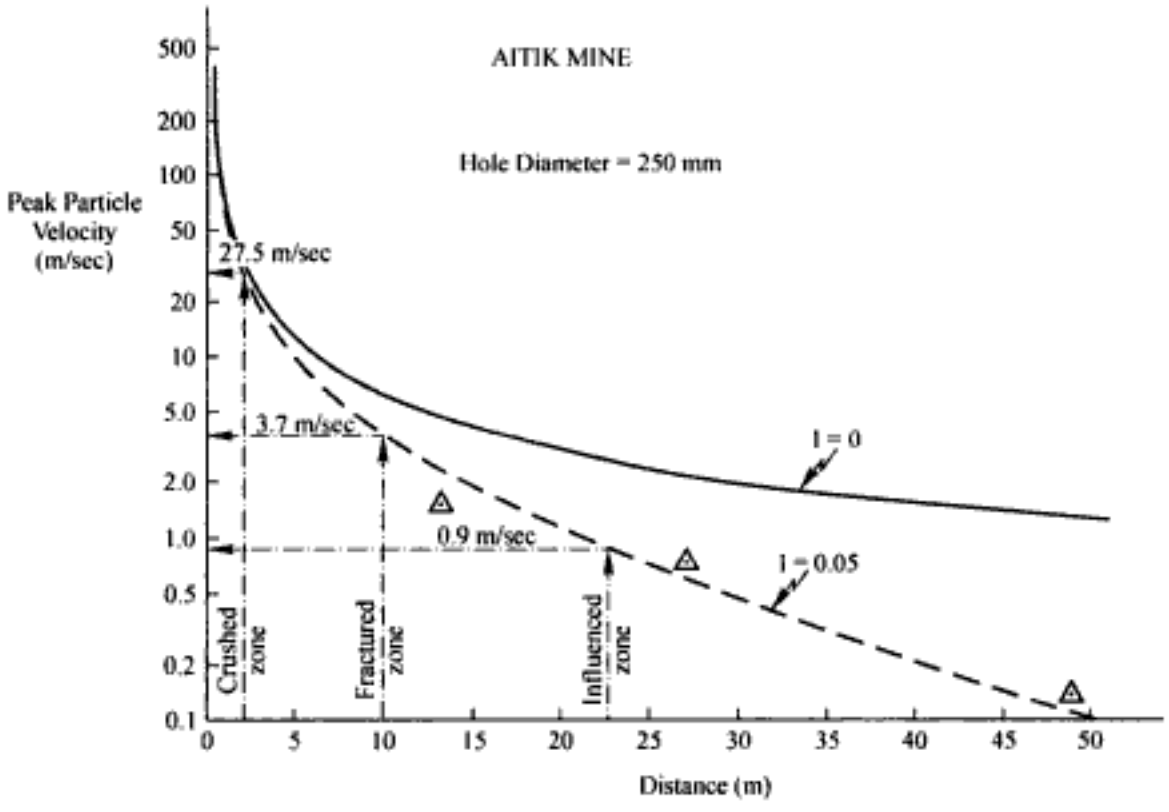

Figure 10.74. Peak particle velocity versus distance curves for the Aitik Mine (250 mm diameter holes).

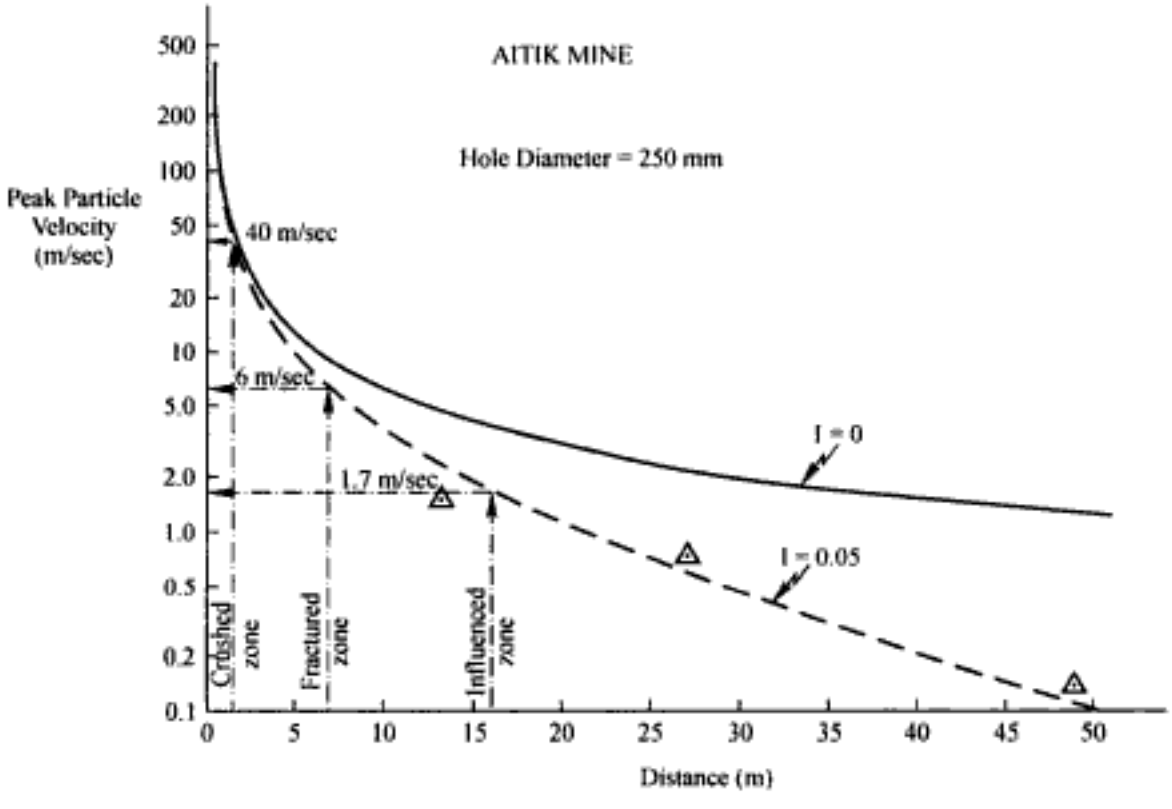

Figure 10.75. Peak particle velocity versus distance curves for the Aitik Mine (250 mm diameter holes) with the damage limits added.

Crushed zone = 40 m/sec
Fractured zone = 6 m/sec
Influenced zone = 1.7 m/sec

If one now applies these same limits to the 171 mm diameter hole one finds that (Fig. 10.76)

Crushed zone = 0.7 m
Fractured zone = 4 m
Influenced zone = 10 m

These corresponds to

Crushed zone: $R/b = 7$
Fractured zone: $R/b = 38$
Influenced zone: $R/b = 96$

There was, unfortunately, no diamond drilling done and hence no possibility to confirm whether these predictions are correct or not. In any case the technique, as described, allows the simulation of a number of explosive combinations and blast geometries with the possibility of identifying those which might improve slope conditions. The simplified application of the CSM approach as discussed here does have some limitations. These are discussed in some detail in Chapter 16.

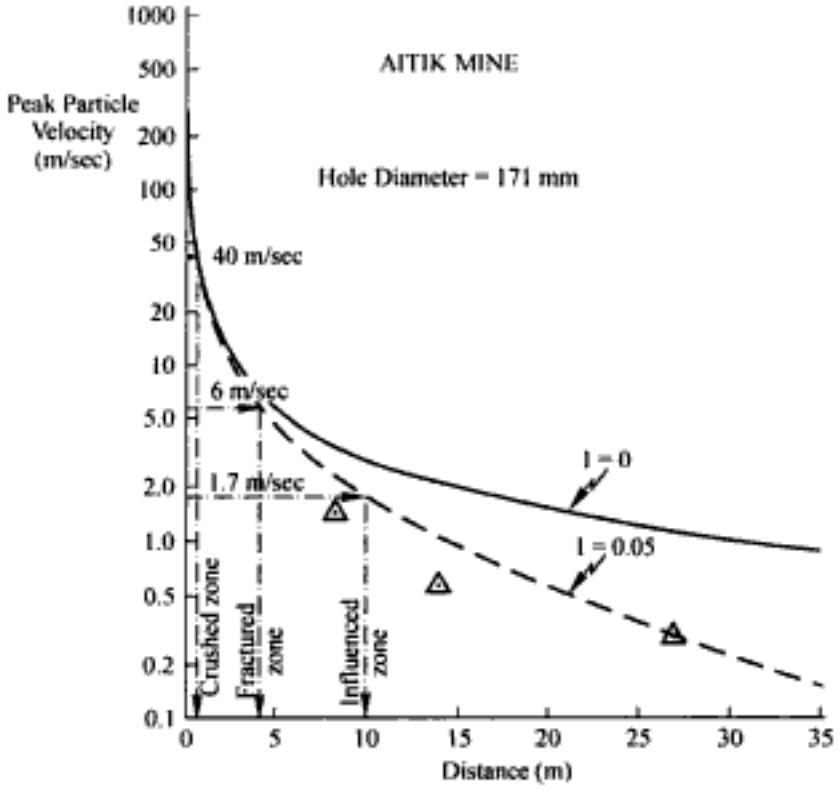

Figure 10.76. Peak particle velocity versus distance curves for the Aitik Mine (171 mm diameter holes) with the damage limits added.

REFERENCES AND BIBLIOGRAPHY

AECI Explosives and Chemicals Limited. 1978. Perimeter Blasting – General Background. *Explosives Today.* 2(13): September.

AECI Explosives and Chemicals Limited. 1978. Perimeter blasting techniques. *Explosives Today.* 2(14): December.

Aimone, C.T. 1985. Near borehole fracture and fragmentation studies in copper porphyries. *Proceedings of the 11th Conference on Explosives and Blasting Technique (Mini Symp). SEE.* pp. 118-129.

Anderson, D.A. & J.W. Reil 1988. Measuring fragmentation efficiency of a blast using ground vibration. *Proceedings of the 14th Conference on Explosives and Blasting Technique (4th Mini-Symp.). SEE.* pp. 60-72.

Andersson, P. 1994. The Damage Zone During Tunnel Driving. *Proceedings of a Seminar held in October 1992. SveBeFo Rapport 8.* 125pp. In Swedish.

Anonymous. 1977. Perimeter Blasting. Chapter 7 of the Pit Slope Manual. CANMET Report 77-14. Energy, Mines and Resources Canada, 555 Booth Street, Ottawa, Canada. 82pp.

Asby, J.P. 1980. Production blasting and the development of open pit slopes. *Proceedings of the 6th Conference SEE.* pp. 291-311.

Atlas Powder Company.1987. *Explosives and Rock Blasting.* Maple Press. 662pp.

Atlas Powder Company. *Kleen-Kut Explosives.*

Atlas Powder Company. Airdek: *A new system for safer, affordable highwall control.*

Attewell, P.B. 1963. *Dynamic fracturing of rocks.* Part 1 (pp. 203-210, May) Part 2 (pp. 248-252, June), Part 3 (pp. 289-294, July). Colliery Engineering. 40(471): 203-210, 40(472): 248-252, 40(473): 289-294.

Attewell, P.B. & D. Brentnall 1964. Attenuation measurements in rocks in the frequency range 12 kc/s to 51 kc/s and in the temperature range 100k to 115k. *Proceedings 6th US Symposium on Rock Mechanics* (G.B. Clark, ed.), Rolla, Mo. pp. 330-357.

Avey, L. 1990. Pre-split economics and practice at Gold Fields Operating Co. – Chimney Creek Mine. *Explosives Engineering.* 8(1): 32-35.

Baranov, E.G. & V.A. Kovalenko 1976. Effect of the detonation parameters of explosives on the explosion energy distribution of a borehole charge. *Soviet Mining Science.* 12: 665-669.

Barnes, J.J. 1988. Presplitting techniques with large diameter blastholes in western coal. *Proceedings of the 14th Conference on Explosives and Blasting Technique. SEE.* pp. 218-229.

Bauer, A. 1982. Wall Control blasting in open pits. CIM Special Volume 30. *Rock Breaking and Mechanical Excavation* (P. Baumgartner, ed). pp. 3-10.

Bauer, A. & D. Frantzos 1987. Finite element modelling of presplit blasting using measured pressure-time curves. *Proceedings of the 13th Conference on Explosives and Blasting Technique (3rd Mini-Symp.). SEE.* pp. 41-55.

Bennett, R. 1991a. Computer evaluation of the Favreau equations. Sept. Unpublished report. Colo School of Mines, Golden.

Bennett, R. 1991b. A new theoretically based particle velocity predictor. Dec. Unpublished report. Colo School of Mines, Golden.

Borovikov, V.A. 1976. The influence of an annular air space between a charge and the borehole wall on the stress wave. *Soviet Mining Science.* 12: 493-498.

Brown, C.C. & J. Bigando 1972. Presplit and Smooth-wall blasting in La Cananea Pit. *Mining Engineering.* 24(9): 50-52.

Bussey, J. & D.G. Borg 1988. Pre-splitting with the new airdeck technique. *Proceedings of the 14th Conference on Explosives and Blasting Technique. SEE.* pp. 197-217.

Butkovich, T.R. & J.R. Hearst 1976. Prediction and determination of explosive-induced fracture. *Proceedings of the 2nd Conference on Explosives and Blasting Technique. SEE.* pp. 301-339.

Calder, P.N. 1977. Perimeter Blasting. Chapter 7. *CANMET Pit Slopes Manual.* Queens Printer, Ottawa.

Calder, P.N. & J.N. Tuomi. 1980. Control blasting at Sherman Mine. *Proceedings of the 6th Conference on Explosives and Blasting Technique. SEE.* pp. 312-330.

Calder, P.N. & R.J. Jackson 1981. Revised Perimeter Blasting Chapter. *CANMET Pit Slopes Manual.*

Calder, P.N & A. Bauer 1983. Pre-split design for open-pit and underground mines. *Proc. 5th Int. Soc. of Rock Mech, Melbourne.* 2: E185-E190.

Carlevato, H.G. 1967. Controlled blasting. *Pit & Quarry.* 60(8): 115-120, 125, 133.

Chenier, R., J. McManus & J. Currie 1985. Controlled blasting practice at Cominco Copper Division's Valley Mine. *CIM Bulletin.* 78(July): 69-72.

Chertkov, V.Y. 1985. Relationship of zones of buckling, crushing, fragmentation and radial fracturing with critical microfracturing. *Soviet Mining Science.* 21: 381-384.

Chiappetta, R.F. 1994. Presplitting techniques for conventional, air deck and dimension stone applications. *Proceedings of the 5th High-Tech Seminar on Blasting Technology, Instrumentation and Explosives Applications. New Orleans, Louisiana (July 9-14). Blasting Analysis International,* Inc. pp. 339-407.

Chironis, N.P. 1991. Double airdecks cushion presplitting of highwalls. *Coal.* 96(4): 56-59.

Chironis, N.P. 1991. Innovations in surface mine blasting. *Coal.* 96(7): 37-42.

Crosby, W.A. & A. Bauer 1982. Wall control blasting in open pits. *Mining Engineering.* 34(2): 155-158.

de Bremaecker, J., R.H. Godson & J.S. Watkins 1966. Attenuation measurements in the field. *Geophysics,* 31: 562-569.

Davids, T. & B.J.J. Botha 1994. The application of mid-column air decks in full scale production blasts. *Proceedings of the 5th High-Tech Seminar on Blasting Technology, Instrumentation and Explosives Applications. New Orleans, Louisiana (July 9-14). Blasting Analysis International,* Inc. pp. 437-457.

Devine, F.J., R.H. Beck. A.V.C. Meyer & W.I. Duvall 1965. Vibration levels transmitted across a presplit fracture. *USBM RI 6695.* 29p.

Drukovanyi, M.F., V.M. Komir, N.I. Myachina, S.N. Rodak & E.A. Semenyuk 1974. Effect of the charge diameter and type of explosive on the size of the overcrushing zone during an explosion. *Soviet Mining Science.* 10: 500-506.

Drukovanyi, M.F., V.S. Kravtsov, Y.E. Chernyavskii, V.V. Shelenok, N.P. Reva & S.N. Zverkov 1977. Calculation of fracture zones created by exploding cylindrical charges in ledge rocks. *Soviet Mining Science.* 13: 292-295.

E.I. DuPont de Nemours and Co. DuPont *Blasters' Handbook.* 1977 Edition. Wilmington, Del. 494 pp.

Favreau, R.F. 1969. Generation of strain waves in rock by an explosion in a spherical cavity. *Journal of Geophysical Research,* 74: 4267-4280.

Fauquier, G.P. 1983. Trim blasting and double benching for steeper slopes and competent walls at PMC. *E&MJ.* 184(4): 46-52.

Feshchenko, A.A. & M.I. Shuifer 1974. Reducing the destructive action of an explosion. *Soviet Mining Science.* 10: 37-41.

Field, J.E. & A. Ladegaard-Pedersen 1969. Controlled fracture growth in rock blasting. Report DL 1969: 8 Swedish Detonic Research Foundation

Field, J.E. & A. Ladegaard-Pedersen 1969. The importance of the reflected shock wave in rock blasting. Report No. DL 1969: 7, Swedish Detonic Research Foundation and also in 1970 *Int. J. Rock Mech Min Sci.* 7: 213-226.

Gribanova, L.P., N.I. Dyadechkin, V.A. Gavrik. T.M. Tkachenko & V.N. Vasilev 1975. Influence of certain parameters on the seismic action and quality index of blasting. *Soviet Mining Science.* 11: 39-43.

Hagan, T.N. 1977. Overbreak control blasting techniques. Chapter 11 in *Australian Mineral Foundation's Drilling and Blasting Technology* Course, Adelaide, May. 62pp.

Hagan, T.N. 1977. Good delay timing-prerequisite of efficient bench blasts. Proc. *Australas. Inst. Min. Metall.,* (263): 47-54.

Hagan, T.N. 1979. Designing primary blasts for increased slope stability. *Proc. 4th Int. Rock Mech Congr. Montreux,* Switzerland. Vol 1, pp. 657-664.

Hagan, T.N. 1981. Designing primary blasts for increased slope stability. *Proceedings, Workshop Course 153/81. Drilling and Blasting in Open Pits and Quarries.* Australian Mineral Foundation. Brisbane 30 Mar-3 April pp. 1-17.

Hagan, T.N. & J.K. Mercer 1983. Safe and Efficient Blasting in Open Pit Mining. Proceedings of a *workshop held by ICI Australian Operations Pty Ltd at Karratha.* 23-25 November.

Harries, G. 1983. The modelling of long cylindrical charges of explosives. Proceedings of the 1st Int. Symp. On Rock Fragmentation by Blasting, Luleå, Sweden. pp. 419-438

Heinen, R.H. 1976. The use of seismic measurements to determine the blastibility of rock. *Proceedings of the 2nd Conference on Explosives and Blasting SEE.* pp. 234-248.

Hendron, A.J., Jr. & L.L. Oriard 1972. Specifications for controlled blasting in civil engineering projects. *Proc 1st North American Rapid Excavation and Tunneling Conference, SME,* Littleton, Colorado, vol 2, pp. 1585-1609.

Holmberg, R & Krauland 1977. Evaluation of the fracture frequency before and after blasting with 250 mm holes at Aitik. Swedish Detonic Research Foundation Report DS 1977: 12. 36pp. In Swedish.

Holmberg, R. & P.A. Persson 1978a. The Swedish approach to contour blasting. *Proceedings of the 4th Conference on Explosives and Blasting Technique. SEE.* pp. 113-127.

Holmberg, R. & P.A. Persson 1978b. Ground vibration measurements during blasting in the vicinity of Boliden AB's Aitik Mine. Report DS 1978: 1. Swedish Detonic Research Foundation. In Swedish. 26 pp.

Holmberg, R. 1981. Evaluation of blast damage at the Leveaniemi Open Pit. Swedish Detonic Research Foundation Report DS 1981: 65pp. In Swedish.

Holmberg, R. & K. Maki 1982. Case examples of blasting damage and its influence on slope stability. *Proceedings of the 3rd Int. Conf. on Stability in Surface Mining* (C. Brawner, ed.). Vancouver. AIME(SME), NY. pp. 773-793.

Holmberg, R., Larsson, B. & C. Sjöberg 1984. Improved stability through optimized rock blasting. Swedish Detonic Research Foundation Report DS 1984: 2: 17pp.

Holmberg, R. 1997. Private communication.

Hustrulid, W.,R. Bennett, F. Ashland & M. Lenjani 1992. A new method for predicting the extent of the blast damaged zone. *Proceedings of the Sprangteknisk Konferens, Nitro Nobel, Goteberg-Kiel,* Jan 15-16. 55pp.

Hustrulid, W. 1994. The 'practical' blast damage zone in drift driving at the Kiruna Mine. Proceedings of the Seminar 'Skadezon vid Tunneldrivning' (Per Andersson, ed.). Swedish Rock Engineering Research Foundation. Report 8. Stockholm. pp. 75-125.

Huttagosol, P. 1989. Comparative study of spherical strain wave models. *Proceedings, 1st CSM Student Symposium on Rock Blasting,* Dec. pp. 134-148.

Ionin, A.A., V.P. Belyatskii & V.A. Artemov 1976. Experimental determination of the bulk velocity in the near zone for long charges detonated in rocks. *Soviet Mining Science.* 12: 657-659.

Ito, I. & K. Sassa 1962. On the detonation pressure produced at the inner surface of a charge hole. *Proceedings, Int Symp. on Mining Research* (G.B. Clark, ed.). Pergamon Press, New York. pp. 103-124.

Ito, I., K. Sassa, C. Tanimoto & K. Katsuyama 1970. Rock breakage by smooth blasting. *Proceedings of the Second Congress of the Int. Society for Rock Mech., Beograd.* pp. 53-57.

Jinnerot, M. & H. Nilsson. 1998. Experimental study of peak particle velocity and the extent of the damage zone in drift driving. MSc Thesis. Chalmers Institute of Technology, Gothenburg, Sweden. In Swedish.

Jordaan, A.J. & H.L. Graham 1986. Wall control blasting at Donkerpoort. *The planning and operation of Open Pit and Strip Mines* (J.P. Deetlefs, ed.) Johannesburg, SAIMM.

Jordan, D.W. 1962. The stress wave from a finite cylindrical explosive source. *J. Math. Mech.* 11: 503-552.

Jurmu, J.J. & W.B. Lee 1986. Wall control at Michigan iron ore mines. *Proceedings of the 12th Conference on Explosives and Blasting Technique. SEE.* pp. 116-127.

Khanukaev, A.N. & V.P. Belyatskii 1975. The close-range zone in rock blasting. *Soviet Mining Science.* 11: 154-158.

Konya, C.J. 1987. Controlling backbreak with proper borehole timing. *Proceedings of the 13th Conference on Explosives and Blasting Technique. SEE.* pp. 49-59.

Konya, C.J., R.Britton & S. Lukovic 1987. Charge decoupling and its effect on energy release and transmission for one dynamite and water gel explosive. *Proceedings of the 13th Conference on Explosives and Blasting Technique (3rd Mini-Symp.) SEE.* pp. 14-25.

Konya, C.J. 1980. Pre-split blasting: theory and practice. Presented at the AIME Annual Meeting in Las Vegas, Nev. Feb 24-28. Preprint No. 80-97.

Konya, C.J., R. Britton & S. Lukovic Removing some of the mystery from pre-split blasting. *Explosives Engineering.* pp. 20-22.

Koryavov, V.P., V.M. Kuznetsov. V.I. Kulikov & L.D. Livshits 1982. Influence of the prestressed state of a medium on the fracturing effect of an explosion. *Soviet Mining Science.* 18: 251-256.

Kutuzov, B.N. & Y.K. Krasnov 1982. Breaking action of contour charges. *Soviet Mining Science.* 18: 243-248.

Lenjani, M.Z. 1991. Damage criterion for blasting. Unpublished paper Colorado School of Mines, Golden, Colo. 21pp.

Lundborg, N., Holmberg, R. & P.A. Persson 1978. The dependence of ground vibrations on distance and charge size. Report R11:78. Byggforskning. In Swedish.

McKenzie, C.K., G.P. Stacey & M.T. Gladwin 1982. Ultrasonic characteristics of a rock mass. *Int J. Rock Mech Min Sci & Geomech. Abstr,* 19: 25-30.

McKown, A.F. 1984. Some aspects of design and evaluation of perimeter control blasting in fractured and weathered rock. *Proceedings of the 10th Conference on Explosives and Blasting Technique. SEE.* pp. 120-151.

Maki, K. & B. Niklasson 1982. Damage to the remaining rock during the blasting tests in sedimentary limestone. Swedish Detonic Research Foundation Report DS 1982: 9: 42 pp. In Swedish.

Morriss, P. 1981. Final wall blasting practices at Hammersley Iron's Tom Price Pit. *Proceedings, Workshop Course 153/81. Drilling and Blasting in Open Pits and Quarries.* Australian Mineral Foundation. Brisbane 30 Mar– 3April pp. 35-55.

Mosinets, V.N. 1966. Mechanism of rock breaking by blasting in relation to its fracturing and elastic constants. *Soviet Mining Science.* 2(5): 492-499.

Mosinets, V.N. & V.V. Korostovenko 1975. Formation of stress and fracture zones when solid rock is blasted using charges of various types. *Soviet Mining Science.* 12(2): 163-166.

Ouchterlony, F., Sjöberg, C. & B.A. Jonsson 1993. Blast damage predictions from vibration measurements at the SKB underground laboratories at ÄspÖ in Sweden. *Proceedings, 9th Annual Symp on Explosives and Blasting Research. ISEE.* pp. 189-197.

Oriard, L.L. 1972. Blasting effects and their control in open pit mining. Chapter 13 in Geotechnical Practice for Stability in Open Pit Mining (*Proceedings of the second Int. Conf. On Stability in Open Pit Mining,* Vancouver B.C., Canada, Nov 1-2, 1971 edited by C.O. Brawner and V. Milligan. SME of AIME, New York pp 197-222.

Oriard, L.L. 1982. Influence of blasting on slope stability; state-of-the-Art. Ch.4 *Proc. 3rd Int. Conf. on Stability in Open Pit Mining.* Vancouver, B.C. AIME, New York, pp 43-87.

Oriard, L.L. 1989. Scale of effects in evaluating vibration damage potential. *Proceedings of the 15th Conference on Explosives and Blasting Technique. SEE.* pp. 161-176.

Oriard, L.L. 1992. Near-source attenuation of seismic waves from spatially distributed sources. *Explosives Engineering.* 10(3): 18-28.

Paine, R.S, D.K. Holmes & H.E. Clark 1961. Presplit blasting at the Niagara power project. *The Explosives Engineer. May-June.* pp. 72-93.

Paine, R.S., D.K. Holmes & H.E. Clark. Controlling overbreak by presplitting. 1962. *Proceedings, Int Symp. on Mining Research* (G.B. Clark, ed.). Pergamon Press, New York. pp. 179-209.

Persson P.A., Holmberg, R. & G. Persson 1977. The gentle blasting of slopes in open pits. Report DS 1976: 4. Swedish Detonic Research Foundation. 12 pp. In Swedish.

Persson, P-A. 1990. Fragmentation mechanics. *Proceedings, Third Int. Symp. Rock Fragmentation by Blasting* (FRAGBLAST '90), Brisbane, Australia. Aug 26-31. pp. 101-108.

Plakhotnyi, P.I., K.N. Tkachuk & V.A. Dorovskii 1973. The stress and fracture fields caused by contour blasting. *Soviet Mining Science.* 9: 648-499.

Plewman, R.P. & A.M. Starfield. 1965. The effect of finite velocities of detonation and propagation on the strain pulses induced in rock by linear charges. JSAIMM 65(Oct.): 77-96.

Porter, D.D. 1971. A Role of Borehole Pressure in Blasting: The Formation of Cracks. PhD Thesis. Univ of Minnesota, 158pp.

Porter, D.D. & C. Fairhurst 1971. A study of crack propagation produced by sustained borehole pressure in blasting. Dynamic Rock Mechanics (G.B. Clark, ed.). *Proceedings of the 12th US Rock Mechanics Symp. AIME,* NY pp. 497-515.

Ratan, S. & B.B. Dhar 1976. Controlled blasting in rock excavation projects-a review. *Mining Magazine.* 134(1): 25-32.

Redpath, B.B. & T.E. Ricketts 1987. An improved scaling procedure for close-in blast motions. *Proceedings of the 13th Conference on Explosives and Blasting Technique (3rd Mini-Symp.). SEE.* pp. 118-131.

Repin, N.Y. & I. A. Panachev 1970. A method of determining the depth of the zone of fracture of the solid rock during blasting operations. *Soviet Mining Science.* 6: 92-94.

Revey, G.F. 1989. Controlled blasting in underground applications. Prepared for Atlas Underground Seminar. Atlas Powder Company. pp13.

Reznik, Y.I. & I.M. Kovler 1983. Approximate computation od the boundaries of the crack-formation zone on detonating a system of similar explosive charges. *Soviet Mining Science.* 19: 498-502.

Rinehart, J.S. 1960. On Fractures Caused by Explosions and Impacts. *Quarterly of the Colo.School of Mines.* vol 55, no 4. Oct. 155 pp.

Sher, E.N. 1975. Estimating the crushing action of a long charge in a brittle medium. *Soviet Mining Science.* 11: 81-84.

Siebert, H. & G. Raitt. 1965. Development of rock slopes in metamorphic rocks by controlled slope holes. *Proceedings of the 7th US Symp on Rock Mech.,* Penn State University. 2:242-252.

Savely, J.P. 1986. Designing a final blast to improve stability. Preprint No. 86-50. Presented at the SME Annual Meeting in New Orleans, Louisiana Mar 2-6, 19pp.

Siskind, D.E. & R.R Fumanti 1974. Blast-produced fractures in Lithonia granite. *USBM RI 7901.* 38pp.

Spivak, A.A & V.M. Tsvetkov 1974. Blasting in a solid medium of the rock type. *Soviet Mining Science.* 10: 496-499.

Stacey, F.D., M.T. Gladwin, B. McKavanagh, A.T. Linde & L.M. Hastle 1975. Anelastic damping of acoustic and seismic pulses. *Geophysical Surveys.* 2: 133-151.

Stacey, P.F. 1994. The impact of blasting on pit slope stability. *Proceedings of the 5th High-Tech Seminar on Blasting Technology, Instrumentation and Explosives Applications. New Orleans, Louisiana* (July 9-14). Blasting Analysis International, Inc. pp. 511-521.

Starfield, A.M. 1966. Strain wave theory in rock blasting. Chapter 23. *Proceedings of the 8th U.S. Rock Mechanics Symposium*, Univ. of Minnesota, pp. 538-549.

Starfield, A.M. 1967. The value of theory in blasting design. *Proceedings, 28th Annual Mining Symposium and the 40th Annual Meeting of the Minnesota Section AIME.* Jan 16-18 Duluth, Minnesota. pp. 197-202.

Starfield, A.M. & J.M. Pugliese 1968. Compression waves generated in rock by cylindrical explosive changes: A comparison between a computer model and field measurements. *Int. J. of Rock Mech. and Min. Sci* 5(1): 65-77.

Stepanov, Y.U. 1975. Maximum fracture zone in solid rock due to explosion of two parallel cylindrical charges. *Soviet Mining Science.* 11: 672-674.

Tomashev, G.S. 1976. A mathematical-probabilistic model of blasting damage in fissured block-structured medium. *Soviet Mining Science.* 11: 651-656.

Torrance, A.C., S.B. Richardson & N.T. Moxon 1989. Fragmentation control through the attenuation of explosively produced shock waves. *Proceedings of the 15th Conference on Explosives and Blasting Technique (5th Mini-Symp). SEE.* pp. 151-162.

Tregubov, B.G., E.P. Taran, Y.A. Balagur & N.E. Trufakin 1982. Experimental investigation of a contained explosion of elongated charges. *Soviet Mining Science.* 18: 532-538.

Vovk, A.A., A.V. Mikhalyuk & I.V. Belinskli 1974. Development of fracture zones in rocks during camouflet blasting. *Soviet Mining Science.* 10: 383-387.

Walsh, S.F. 1988. San Manuel Oxide Pit Blasting. Preprint Number 88-107. Presented at the SME Annual Meeting in Phoenix, AZ Jan 25-28. pp. 7.

Worsey, P.N. & Q. Chen 1986. The effect of rock strength on perimeter blasting and the 'blastibility' of massive rock. *Proceedings of the 12th Conference on Explosives and Blasting Technique (Mini-Symp). SEE.* pp. 118-131.

Worsey, P.N. & S. Qu 1987. Effect of joint separation and filling on pre-split blasting. *Proceedings of the 13th Conference on Explosives and Blasting Technique (3rd Mini-Symp.). SEE.* pp. 26-40.

Worth, I.R. 1981. Perimeter blasting at Panguna. *Proceedings, Workshop Course 153/81. Drilling and Blasting in Open Pits and Quarries. Australian Mineral Foundation. Brisbane 30 Mar-3 April.* pp. 167-195.

Yang, R., W.F. Bawden, S. Talebi & P. Rocque 1993. An integrated technique for vibration monitoring adjacent to a blast hole. *CIM Bulletin.* 86 (July-August): 46-52.

Hidden page

Index

Hidden page

The invention of black powder, the first of the explosives, is attributed to the Chinese in about the 4th century. Brought to Europe by the Barbarians in the 13th century, its first use in hard rock mining was reported in the early 17th century. The invention of dynamite by Alfred Nobel in 1867 opened up enormous new possibilities fo rthe mining industry. Both black powder and dynamite were essential ingredients when the age of large-scale open pit mining began at the end of he 19th century on the Mesabi Range in Northern Minnesota. The well-fragemented iron ore was loaded by steam shovel directly into trains to begin the long voyage to the eastern steel mills. Today the largest of the world's open pit mines removes nearly one million tons of drilled and blasted rock per day. With the deepest of these openings now approaching 1000m, plans are being made for pits nearly one mile in depth. In removing the rock, the walls of the opening created in the earth's surface must generally be as steep as possible and remain stable over many years. The challenge for the blasting/fragmentation engineer is to remove the desired rock with the desired degree of fragmentation as inexpensively as possible while leaving the remaining rock, that forming the walls, in pristine conditions. This is, needless to say, a formidable task involving a delicate balance of planning, production and geomechanics inputs so that the overall fragmentation plan is optimal. Blasting Principles for Open Pit Mining is intended to assist the fragmentation engineer in meeting this challenge.

The book is designed to serve as both a textbook and a reference book describing the principles involved in hard rock blasting as applied to surface excavations, in general, and open pit mines, in particular.

Blasting Principles for Open Pit Mining has been written in two parts and published in two corresponding volumes. Volume 1 entitled 'General Design Concepts' is intended to introduce the reader to the basic engineering concepts and the building blocks that make up a blast design. Volume 2 entitled 'Theoretical Foundations' is intended to provide the reader additional depth and breadth for better understanding some of the fundamental concepts involved in rock blasting. The material contained and the presentation form should make it of value to practicing mining, civil, and construction engineers involved in surface rock excavation as well. The contained material should provide a basis for engineers to improve (a) their blasting operations as well as (b) their ability to understand the content and potential application of blasting papers appearing in the technical literature.

The focus has been on presenting the principles involved in explosive rock excavation in as logical and easily understood way as possible. A large number of examples are included to illustrate the application of the principles.

ISBN 9054104589

Photograph: Kennecott Utah Copper Corporation